

Award Number:
DAMD17-00-2-0008

TITLE:

Human Metabolism and Interactions of Deployment-Related
Chemicals

PRINCIPAL INVESTIGATOR:

Ernest Hodgson PhD, Alan A. Brimfield PhD, Joyce E. Goldstein
(through April 2003), Randy L. Rose, PhD deceased, Co-PI through
May 2006), Andrew D. Wallace (June 2006-2008).

CONTRACTING ORGANIZATION:

North Carolina State University
Raleigh, NC 27695-7514

REPORT DATE:

August 2008

TYPE OF REPORT:

Final Addendum

PREPARED FOR: U.S. Army Medical Research and Materiel Command
Fort Detrick, Maryland 21702-5012

DISTRIBUTION STATEMENT:

Approved for public release; distribution unlimited

The views, opinions and/or findings contained in this report are
those of the author(s) and should not be construed as an official
Department of the Army position, policy or decision unless so
designated by other documentation.

REPORT DOCUMENTATION PAGE

Form Approved
OMB No. 0704-0188

Public reporting burden for this collection of information is estimated to average 1 hour per response, including the time for reviewing instructions, searching existing data sources, gathering and maintaining the data needed, and completing and reviewing this collection of information. Send comments regarding this burden estimate or any other aspect of this collection of information, including suggestions for reducing this burden to Department of Defense, Washington Headquarters Services, Directorate for Information Operations and Reports (0704-0188), 1215 Jefferson Davis Highway, Suite 1204, Arlington, VA 22202-4302. Respondents should be aware that notwithstanding any other provision of law, no person shall be subject to any penalty for failing to comply with a collection of information if it does not display a currently valid OMB control number. **PLEASE DO NOT RETURN YOUR FORM TO THE ABOVE ADDRESS.**

1. REPORT DATE (DD-MM-YYYY) 01/08/2008		2. REPORT TYPE Final Addendum		3. DATES COVERED (From - To) 2 Jul 2003 – 1 Jul 2008	
4. TITLE AND SUBTITLE Human Metabolism and Interactions of Deployment-Related Chemicals Cancer Treatment				5a. CONTRACT NUMBER	
				5b. GRANT NUMBER DAMD17-00-2-0008	
				5c. PROGRAM ELEMENT NUMBER	
6. AUTHOR(S) Principal Investigator, Ernest Hodgson, PhD Co-Investigators, Alan A. Brimfield, Joyce E. Goldstein (through April 2003), Randy L. Rose, (deceased, Co-PI through May, 2006), Andrew D. Wallace(June 06-08) E-Mail:				5d. PROJECT NUMBER	
				5e. TASK NUMBER	
				5f. WORK UNIT NUMBER	
7. PERFORMING ORGANIZATION NAME(S) AND ADDRESS(ES) North Carolina State University Raleigh, NC 27695-7514				8. PERFORMING ORGANIZATION REPORT NUMBER	
9. SPONSORING / MONITORING AGENCY NAME(S) AND ADDRESS(ES) U.S. Army Medical Research and Materiel Command Fort Detrick, Maryland 21702-5012				10. SPONSOR/MONITOR'S ACRONYM(S)	
				11. SPONSOR/MONITOR'S REPORT NUMBER(S)	
12. DISTRIBUTION / AVAILABILITY STATEMENT Approved for Public Release; Distribution Unlimited					
13. SUPPLEMENTARY NOTES					
14. ABSTRACT Methods were developed for the investigation of the in vitro metabolism of deployment-related chemicals in humans. These studies utilized recombinant human enzymes, human liver cell fractions and isolated human hepatocytes. The metabolism of chlorpyrifos, DEET, permethrin, pyridostigmine bromide, sulfur mustard, naphthalene and nonane as well as a number of their metabolites and related chemicals was investigated. For the most part these were the first investigations of the metabolism of these chemicals in humans. Metabolic interactions, including inhibition of the metabolism of xenobiotics and endogenous metabolites such as testosterone and estradio were also examined. The potency of organophosphorus chemicals such as chlorpyrifos in the inhibition CYP-dependent monooxygenase reactions was, in many cases, dramatic and a cause for concern as was the ability of chlorpyrifos oxon to inhibit permethrin metabolism. The potential for interactions based on induction and on a combination of induction and cytotoxicity were demonstrated in the case of pyrethroids, DEET and chlorpyrifos in experiments utilizing human hepatocytes. Interactions involving JP-8 jet fuel components such as nonane and naphthalene were of interest because of the expected exposure scenarios and since the fuel itself appeared to function both as an inhibitor and as an inducer in human in vitro experiments. Preliminary genotyping experiments were conducted on two small sample sets of DNA from veterans of the first Gulf War. All of the above permitted a number of conclusions concerning human health risk analysis and possible populations and individuals at increased risk from chemical exposure. A number of recommendations were made concerning risk analysis specific to military needs and to research activities that should have a high priority in that regard.					
15. SUBJECT TERMS No subject terms provided.					
16. SECURITY CLASSIFICATION OF:			17. LIMITATION OF ABSTRACT	18. NUMBER OF PAGES	19a. NAME OF RESPONSIBLE PERSON
a. REPORT	b. ABSTRACT	c. THIS PAGE			19b. TELEPHONE NUMBER (include area code)
U	U	U	UU	310	USAMRMC

Table of Contents

4. INTRODUCTION	6
5. BODY OF THE REPORT	7
5.1. Chemicals	7
5.2. Specific Aims	7
5.3. Report Format	8
5.4. Analytical Methods	9
5.4.1 Chlorpyrifos	9
5.4.2 DEET	9
5.4.3 Permethrin	9
5.4.4 Pyridostigmine bromide	10
5.4.5 Sulfur Mustard and its Degradation Products ...	10
5.4.6 Testosterone	10
5.4.7 Estradiol	11
5.4.8 Naphthalene	11
5.4.9 Nonane	12
5.4.10 Additional Analytical Methods	13
5.5. Metabolism of Specific Deployment-Related Chemicals .	13
5.5.1 Chlorpyrifos	13
5.5.2 DEET	14
5.5.3 Permethrin	14
5.5.4 Pyridostigmine bromide	14
5.5.5 Sulfur mustard	15
5.5.6 Naphthalene	17
5.5.7 Nonane	17
5.5.8 Carbaryl	17
5.5.9 Endosulfan	18
5.9.10 Fipronil	18
5.6. Interactions Based on Inhibition	19
5.6.1 Inhibition of metabolism of other xenobiotics, etc.	19
5.6.2 Inhibition of metabolism of endogenous metabolites,	22
5.7. Interactions Based on Activation	24
5.8. Interactions Based on Induction	24
5.8.1 In Mice	24
5.8.2 Induction in Mice by Sulfur Mustard, etc.....	25
5.8.3 In Human Hepatocytes	27
5.8.4 Microarrays	28
5.9. Interactions Based on Induction and Cytotoxicity	29
5.9.1 Fipronil	29

5.9.2	Pyrethroids	29
5.9.3	Chlorpyrifos and DEET	30
5.9.4	JP-8	31
5.10.	Genotyping	31
5.11.	Evaluation of Relevance of Human Studies to Risk Analysis of Deployment-Related Chemicals	31
6.	KEY RESEARCH ACCOMPLISHMENTS	33
7.	REPORTABLE OUTCOMES	34
7.1.	Publications	34
7.2.	Presentations	36
8.	CONCLUSIONS AND RECOMMENDATIONS	40
8.1.	Conclusions	40
8.2.	Recommendations	41
9.	REFERENCES	41
10.	PERSONNEL PAID ON DAMD17-00-2-0008	46
10.	APPENDICES	47

4. INTRODUCTION

Award History. The initial award entitled “Human Metabolism and Interactions of Deployment-Related Chemicals” was initiated with a start date of 18 January 2000, for a three year period, received a supplemental award for the purchase of an HPLC and associated supplies and was scheduled to end 17 January 2003. The life of the award was extended by a four year supplement, retitled “Further Studies on the Human Metabolism of Deployment-Related Chemicals” and was then scheduled to end 1 August 2007. A no-cost extension was approved establishing a new termination date of 1 August 2008. This final report covers the entire period 18 January 2000 through 1 August 2008.

Chemicals used during deployments, and particularly interactions between such chemicals, are frequently cited as possible causative agents in deployment-related illnesses. However, definitive evidence for or against such a role is usually lacking. This is due primarily to the fact that toxicity is generally assessed using surrogate animals, usually rodents, and such studies assume relevance only when they can be extrapolated with confidence to humans. When these studies were initiated there little or nothing was known about the human metabolism of deployment-related chemicals or, in fact, the human metabolism of most occupational chemicals.

The military need for information on human health risk from chemicals was clear. In several recent conflicts, poorly defined aggregations of health effects (most recently Gulf War Related Illness) had been attributed to chemicals or to interactions between two or more chemicals (Haley and Kurt, 1997). Thus the need existed both to determine whether previous health effects were indeed chemical-related and also to minimize future problems. Following the Gulf War a number of veterans reported a variety of illnesses which may have been the result of abnormal chemical exposures. Some studies of these veterans concluded that significant correlations between perceived illnesses and chemical exposure existed (Haley and Kurt, 1997).

The toxicity of a chemical is not a single defining event. Rather, it is the end point of a cascade of events that starts with exposure and ends with the expression of a toxic endpoint. Intermediate steps include absorption, distribution, metabolism, distribution of metabolites, excretion and/or interaction with cellular macromolecules, followed by overt toxicity or repair. Although interactions can occur at any of these loci, two are of critical importance, interaction of reactive metabolites with cellular macromolecules such as DNA, RNA, proteins and/or cell membranes, and metabolism. Metabolism is of importance inasmuch as chemicals may be metabolically detoxified or activated to products more toxic than the parent compound. Phase I metabolism generally results in the introduction of a reactive group into the molecule, a reactive group that is subsequently conjugated with an endogenous compound during Phase II metabolism. Phase I and Phase II reactions are catalyzed by a group of enzymes known collectively as xenobiotic-metabolizing enzymes (XMEs). The most important Phase I enzymes are the isoforms of cytochrome P450 (CYP) and the flavin-containing monooxygenase (FMO) (Smart and Hodgson, 2008). Furthermore, since XMEs have broad and often overlapping substrate specificities, metabolism is a probable locus for chemical interactions and for effects on the metabolism of endogenous substrates.

Since these metabolic activities are frequently species, organ, enzyme, isoform and polymorphism specific, human studies using recombinant enzymes, subcellular preparations and/or cultured cells are essential to bridge the gap between studies in surrogate animals and those in humans, resulting in improvement of human health risk assessment, as follows:

- a. Identification of human XMEs, their isoforms and polymorphic forms involved in activation and/or detoxication;
- b. Identification of reactive metabolites produced by human XMEs;
- c. Identification of interactions between chemicals at the metabolic level;
- d. Evaluation of the variation between individuals and identification of individuals and subpopulations at increased risk;
- e. Providing mechanistic insight into the results of epidemiological studies;
- f. Overall improvement of the process of human health risk assessment with particular reference to deployment-related chemicals and deployment-related exposures.

The human studies reported herein are at the level of metabolism and metabolic interactions. In the broad sense such interactions can result from inhibition, induction and/or cytotoxicity.

During the course of these studies we have published a number of minireviews and one full length review of important aspects of these and other studies carried out in our laboratories and elsewhere (Hodgson and Rose, 2005, 2006, 2007a, 2007b). An update of the full length review (Hodgson et al., 2009) is currently in preparation.

5. BODY OF THE REPORT

5.1. Chemicals

The initial chemicals to be tested (years 1 through 3) were chlorpyrifos, diethyl toluamide (DEET), permethrin, pyridostigmine bromide, sulfur mustard and related chemicals as appropriate. Chemicals to be tested through the duration of the supplement (years 4 through 7) were: chlorpyrifos; DEET; permethrin; pyridostigmine bromide; sulfur mustard plus jet fuel components such as naphthalene and nonane as well as related chemicals as appropriate.

5.2 Specific Aims

The initial specific aims were as follows:

Year 1.

1. Development of new HPLC methods or validation and/or modification of existing methods for analysis of all of the test compounds and their metabolites.
2. Determination of substrate specificity of recombinant human CYP and FMO isoforms relative to the test compounds.
3. Initiate induction experiments with mice.
4. Determine the importance of the plasma pyridostigmine bromide esterase and the soluble cysteine oxidase in the human metabolism of the test chemicals.

Year 2.

1. Kinetic analysis of all substrates and isoforms active in their metabolism.
2. Determination the metabolism of the test chemicals in a bank of human microsomes prephenotyped with prototype chemicals of each of the human CYP isoforms.

3. Determine the effect of inhibitors of specific human CYP isoforms on metabolism of the test chemicals by human liver microsomes.
4. Determination of the inhibitory potential of all test compounds relative to: a) the metabolism of other test compounds; b) the metabolism of other known xenobiotic substrates of human CYPs; c) the metabolism of endogenous substrates (eg testosterone).
5. Continue induction experiments with mice.

Year 3.

1. Complete induction experiments with mice.
2. Carry out selected synergism or potentiation experiments as indicated by the results obtained from the above experiments.
3. Re-evaluate the relevance to humans of published findings from experiments carried out using experimental animals.
4. Define protocols for the evaluation of deployment-related chemicals and their interactions that makes maximum use of human data combined with the most appropriate animal models.

Specific aims added for years 4 – 7 [supplement years 1 – 4]

Year 4 (supplement year 1)

1. Complete metabolic studies of individual chemicals already under investigation.
2. Initiate metabolic studies of additional chemicals.
3. Initiate studies of metabolism by human hepatocytes.

Year 5 (supplement year 2)

1. Complete metabolic studies of additional chemicals.
2. Complete metabolic studies in human hepatocytes.
3. Initiate studies of interactions in human hepatocytes.
4. Process application to NCSU IRB for genotyping studies.

Year 6 (supplement year 3)

1. Continuation of human hepatocyte interaction studies.
2. Development of methods for genotyping human samples utilizing buccal cell samples. Since this is a completely non-invasive procedure, using mouthwash samples, approval is expected.
3. Genotyping of small number of samples (c. 20 local volunteers) for evaluation of methods.
4. Develop collaboration to obtain military samples for genotyping.

Year 7 (supplement year 4)

1. Completion of human hepatocyte interaction studies.
2. Genotyping a statistically significant, representative number of deployment-related samples
3. Reevaluate methods for use of human studies in risk assessment, with particular reference to past and anticipated military exposures.

5.3 Report Format

All but one of the objectives (year 7, #2) (see later for current status) have been met or exceeded. Over the extended period of this award the annual accomplishments often overlap from year to year. Moreover, the emphases and approaches may be slightly modified in the light of experience. That being the case, a more logical and more readable format has been adopted

although, in the interests of accountability, the relationship of the sections in this format to the objectives above is indicated.

5.4. Analytical methods (year 1, aim 1, year 4, aim 2).

5.4.1. Chlorpyrifos:

The HPLC method we developed for the analysis of chlorpyrifos and its metabolites is described, in detail, in Tang et al., 2001 and Dai et al., 2001. Briefly, the method use a system consisting of two Shimadzu (Kyoto, Japan) pumps, (LC-10AT), a Shimadzu auto-detector (SIL-10AD VP), and a Waters (Milford, MA) 486 tunable absorbance detector. The mobile phase for pump A was 10% acetonitrile, 89% water and 1% phosphoric acid, whereas that for pump B was 99% acetonitrile and 1% phosphoric acid. A gradient system was initiated at 20% pump B and increased to 100% pump B in 20 minutes. The flow rate was 1 ml/min. Metabolites were separated by a C₁₈ column (Luna 5 μ , 150 x 3 mm) (Phenomenex, Rancho Palos Verdes, CA) and detected at 230 nm. Using this system the retention times for TCP, chlorpyrifos oxon, and CPS were 8.5, 12 and 17 minutes respectively. The limits of detection for CPO and TCP were 0.03 and 0.04 μ M respectively, at an injection volume of 15 μ l. Concentrations of metabolites were obtained by extrapolation of peak height from a standard curve and $K_{m_{app}}$ and $V_{max_{app}}$ were obtained from a Hanes-Woolf plot (Segal, 1975).

This method has proven most useful, resulting initially in the two peer-reviewed papers referenced above, in subsequent published studies referenced later in this report and is currently in use in this and other laboratories.

Chlorpyrifos studies were initiated, in part, utilizing funds made available by the North Carolina Environmental Trust Fund.

5.4.2 DEET (diethyl-*m*-toluimide):

The method developed for the analysis of DEET and its metabolites (*N*-ethyl-*m*-toluamide (ET) and *N, N*-diethyl-*m*-hydroxymethylbenzamide (BALC) utilized the same Shimadzu HPLC system (Kyoto, Japan), and the same column, as that used for chlorpyrifos. It is described in detail in Usmani et al., 2002.

5.4.3 Permethrin:

The HPLC method for the separation and quantitation of permethrin and its metabolites has been utilized in the published study of the in vitro metabolism of permethrin by human enzymes and their isoforms (Choi et al., 2002). Since substantial revisions in the procedure were found to be necessary due to poor resolution of phenoxybenzoic acid we conducted extensive studies to optimize the procedure with respect to run time, detection wavelength and pH for resolution of each metabolite. These are summarized in Choi et al., (2002).

The optimal conditions for separation and resolution of permethrin and its metabolites involved the use of a gradient system. Two solvents (solvent A: 90% acetonitrile and 10% H₂O, solvent B: 100% H₂O adjusted to pH 1.7 with 85% phosphoric acid) were used for gradient elution (flow

rate: 1ml/min). The HPLC gradient system reliably resolved and detected the two permethrin isomers and three major metabolites, phenoxybenzyl alcohol, phenoxybenzoic acid and phenoxybenzaldehyde; 230 nm was the most appropriate detection wavelength.

Since phenoxybenzoic acid is ionized at a neutral pH, the effect of mobile phase pH on the protonation of this and other metabolites was determined. As the protonation of phenoxybenzoic acid proceeded with increasing hydrogen ion concentration in the mobile phase, a separate peak of phenoxybenzoic acid gradually became distinguishable, forming a clearly identifiable peak at a mobile phase pH of 1.7.

5.4.4. Pyridostigmine bromide:

A reverse phase high pressure liquid chromatography (HPLC) method was developed for the separation and detection of pyridostigmine bromide and its potential metabolites based on the HPLC method of Leo (1997). The Shimadzu HPLC system (Kyoto, Japan) used in this study consisted of 2 pumps (LC-10AT VP) a Shimadzu auto injector (SIL-10AD VP), and a Shimadzu UV/VIS detector (SPD-10A VP). All system components were controlled through the Shimadzu powerline firmware. Data was collected via a Shimadzu system controller (SCL-10A VP) and analyzed using CLASS-VP 7.0 software. The mobile phase consisted of 5% methanol, 5% acetonitrile, 0.1% triethylamine, and 89.9% ammonium acetate buffer, pH 4.0 (adjusted with acetic acid) running at 1.0 ml/min. Metabolites were separated by a Synergi Max column (Synergi 4 μ , 150 x 4.60 mm, Phenomenex, Rancho Palos Verdes, CA) and detected at 260 nm.

5.4.5. Sulfur Mustard and its Degradation Products:

However, HPLC methods did not offer a useful chromophore that would make them applicable to the analysis of sulfur mustard (2,2'-bis chloroethylsulfide) metabolites, specifically thiodiglycol (TDG). In aqueous medium mustard undergoes intramolecular rearrangement and hydrolysis to form 2,2'-bis hydroxyethylsulfide (thiodiglycol, TDG), a dihydric alcohol. TDG is able to inhibit protein phosphatase activity in cytosolic preparations but not the pure enzymes. Therefore, we investigated possible metabolic activation and demonstrated the facile metabolism of TDG by alcohol dehydrogenase (ADH) from horse liver and from cloned human ADH isoforms by monitoring NAD reduction spectrophotometrically. That technique, however, provides little direct information about intermediates and products. Recently, ADH has been investigated using proton NMR. The NMR technique was used to determine the ultimate fate of TDG acted upon by horse liver ADH. The work was performed on a Varian Unity Inova 600 MHz NMR. Aqueous samples were prepared in 0.1 M NaPO₄, pH 7.5 containing 10% D₂O (v/v). Spectra were obtained at $37 \pm 0.1^\circ$ C every 8 min for the first 6 hours and every 30 min thereafter. A typical run lasted 10.5 hours. Analysis of the data showed the appearance over time of a singlet at 3.19 ppm representing two equivalent methylene protons indicating that TDG is oxidized to 2-hydroxyethyl thioacetic acid. Integration of the peaks in successive spectra provided concentrations of the individual components of the reaction mixture, allowing, when plotted, evaluation of kinetic and stoichiometric relationships among the substrates and products.

5.4.6 Testosterone

An improved HPLC Method for the separation of testosterone and its metabolites was developed based on the method of Purdon and Lehman-McKeeman (1997). Metabolites were analyzed using a Shimadzu HPLC system (Kyoto, Japan). The Shimadzu HPLC system (Kyoto, Japan) used in this study consisted of pump (LC-10AT VP), a solvent proportioning valve (FCV-10AL VP), a degasser (DUG-14A), a Shimadzu auto injector (SIL-10AD VP), and a Shimadzu UV/VIS detector (SPD-10A VP). Data was collected via a Shimadzu system controller (SCL-10A VP) and analyzed using CLASS-VP 7.0 software. The mobile phase for pump A was 5% tetrahydrofuran, 95% water, and for pump B 100% methanol. A linear system was employed in the following manner: 0-6 min (30%B), 6-50 min (30-60% B), 50-55 min (60-90% B), 55-57 min (90% B), 57-58 min (90-30%B), and 58-60 min (30% B). The flow rate was 0.5 ml/min. Metabolites were separated by a C18 column (Luna 5 μ , 150 x 3 mm, Phenomenex, Rancho Palos Verdes, CA) and detected at 247 nm. The method has been used in a study of testosterone metabolism and its inhibition by the test chemicals (Usmani et al., 2003).

5.4.7. Estradiol

Analysis of 2-OHE₂ and 6 β -hydroxytestosterone by HPLC. Analysis of the E₂ metabolite 2-OHE₂ was performed with an HPLC system coupled with in-line UV detection as described previously (Suchar et al., 1995). The HPLC system (Usmani et al., 2006) consisted of a Waters 2690 separation module and a Waters UV photodiode array detector (model 2996). All system components were controlled through the Waters powerline firmware. Data was collected via a Waters system controller and analyzed using Waters Empower software. The solvent system for separation of E₂ and 2-OHE₂ consisted of acetonitrile (solvent A), 0.1% acetic acid in water (solvent B), and 0.1% acetic acid in methanol (solvent C). The solvent gradient (solvent A/solvent B/solvent C) used for eluting E₂ and 2-OHE₂ was as follows: 8 min of isocratic at 16:68:16, 7 min of a concave gradient (curve number 9) to 18:64:18, 13 min of a concave gradient (curve number 8) to 20:59:21, 10 min of a convex gradient (curve number 2) to 22:57:21, 13 min of a concave gradient (curve number 8) to 58:21:21, followed by a 0.1 min step to 92:5:3 and a 3.9 min isocratic period at 92:5:3. The gradient was returned to the initial condition (16:68:16) for 2 min and held for 3 min before analyzing the next sample. The flow rate was 1.2 ml/min. E₂ and 2-OHE₂ were separated by an Ultracarb 5 ODS column (150 x 4.6 mm, Phenomenex, Rancho Palos Verdes, CA) at 30°C and detected at 280 nm. The limits of detection for 2-OHE₂ was approximately 0.04 μ M. Concentrations of 2-OHE₂ were obtained from the chromatographic peak area from a standard curve (0.15 μ M – 20.0 μ M). A

5.4.8 Naphthalene

Analysis of Metabolites by HPLC (Cho et al., 2006). The generation of metabolites was analyzed using a Waters 2695 HPLC system equipped with a 2996 Photodiode Array (PDA) detector (Milford, MA). This HPLC system was equipped with a degasser and an autoinjector, and data were collected and analyzed using Waters Empower software version 5.00. The solution for pump A was composed of 3% tetrahydrofuran, 0.2% O-phosphorus acid (85%) and 96.8% water, and for pump B 100% acetonitrile. The gradient in the mobile phase was designed as follows: 0 to 2 min. (20% B), 2 to 22 min. (gradient to 80% B), 22 to 25 min. (80% B), and 25 to 30 min. (gradient to 20% B). The flow rate was 1.0 ml/min. Metabolites were separated by a reversed phase C₁₂ column (Synergi 4 μ Max-RP, 250 x 4.6 mm, Phenomenex, Torrance, CA)

and detected using a PDA detector operated from 190 to 350 nm. Optimal wavelengths for 1-naphthol, 2-naphthol, *trans*-1,2-dihydro-1,2-naphthalenediol, 1,4-naphthoquinone, 1,7-dihydroxynaphthalene and 2,6-dihydroxynaphthalene were selected as 232.7, 225.6, 262.2, 251.6, 239.8, and 228 nm, respectively. Standards of metabolites were prepared in acetonitrile and 50 μ l of standard or sample was injected into the HPLC system.

Sample Preparation for GC/MS Analysis. Naphthalene (300 μ M) was incubated in a total volume of 500 μ l 100 mM potassium phosphate buffer containing 3.3 mM MgCl₂ (pH 7.4) with pHLM (0.96 mg/ml) and the NADPH generating system mentioned above for 10 minutes at 37°C after 5-minute preincubation. Immediately after incubation, sample tubes were centrifuged at 15,000 rpm (21,000 g) for 5 minutes and 470 μ l of supernatant from each tube was transferred into a fresh tube. 100 μ l Dichloromethane (DCM) was added to the fresh tube containing supernatant, and each tube was vigorously shaken for 1 minute. The lower (DCM) layer was then collected for analysis after the tubes were centrifuged at 5,000 rpm for 3.5 minutes. This extraction process with DCM was performed three more times, and the supernatants were combined for the GC/MS analysis.

Analysis of Metabolites by GC/MS. The generation of naphthalene metabolites by pHLM was confirmed by analysis with an Agilent GC/MS system equipped with 6890 GC and 5973 Mass Selective Detector (Palo Alto, CA). A 30-meter capillary column with 0.25-mm nominal diameter (Restek Rtx-5MS, Bellefonte, PA) was used for the analyses with an injection volume of 2 μ l and a constant flow of helium gas (1 ml/min. carrier gas). The oven temperature was programmed as follows: initially 40°C with a 1-min. hold, increased to 100°C at a rate of 25°C/min., followed by an increase to 300°C at a rate of 10°C/min. followed by a 10-min. hold. The total running time was 33.4 minutes and electron impact was used for the ionization of metabolites.

These analyses were performed as a confirmatory process for the HPLC analysis for the production of primary metabolites of naphthalene metabolism by human liver microsomes. Throughout the GC/MS analyses, naphthalene, 1-naphthol, and *trans*-1,2-dihydro-1,2-naphthalenediol were detected at retention times of 7.7, 11.6, and 12.0, respectively, and their fragmentation patterns were compared with those of standards. Detection of 2-naphthol was not successful in these analyses probably due to the combination of its low level of production and potential loss during the extraction process.

5.4.9 Nonane

The GC/FID system used for the analysis of nonane and its metabolites (Edwards et al., 2005) consisted of a Hewlett Packard (currently Agilent Technologies) 7673 auto injector, 5890 Series II GC system, RESTEK RTX[®]-1701 column (30 m, 0.25 mm i.d.) and a flame ionization detector (FID). The injection port and detection temperatures were set at 250 °C and 280 °C, respectively. The oven temperature was programmed to rise from 40 °C to 80 °C at a rate of 6 °C/min, from 80 °C to 120 °C at a rate of 3 °C/min, followed by a rate of 15 °C/min until a temperature of 270 °C was reached. Helium was used as a carrier gas at a flow rate of 1 ml/min. Nonane, 2-nonanone and 2-nonanol were measured at 7.5, 18.1 and 18.5 min and their method

detection limits were 0.071, 0.069 and 0.096 μM , respectively. The linear range ($r^2 > 0.99$) of the assay was 1-100 μM for a 2 μl injection.

5.4.10 Additional Analytical Methods

Methods were also developed for studies of chemicals (atrazine, carbaryl, endosulfan and fipronil) supported by other funds, usually by adaptation of the methods either developed for the above chemicals or by adaptation of methods found in the literature. Some of the results are included briefly in appropriate sections of this report because of their interactions with the test chemicals or their use as model substrates. In either case they fall under the “related chemicals as appropriate” approved in the original award.

5.5. Metabolism of Specific Deployment-Related Chemicals (year 1, aims 2 and 4, year 2, aims 1 and 2, year 4, aims 1 and 2, year 5, aim 1).

5.5.1. Chlorpyrifos

The studies of human chlorpyrifos metabolism have been published (Tang et al., 2001). These are the most complete in vitro human metabolism studies of an organophosphorus xenobiotic published to date and, as detailed below, have important implications for possible interactions and for the definition of individuals and sub-populations at increased risk.

This latter point is further exemplified by the studies of variants of human CYP3A4, an isoform active in both the activation and detoxication of chlorpyrifos (Dai et al., 2001). It is known that the expression of this isoform, often the most abundant CYP isoform in human liver can, nevertheless, vary as much as 40-fold between individuals. In the current studies several new polymorphic variants of CYP3A4 have been identified, sequenced, expressed and characterized. These variants differ from the wild type in their frequency in different populations and in their ability to metabolize chlorpyrifos. Similarly, variants of CYP2C19 showed decreased ability to metabolize chlorpyrifos (Tang et al., 2001).

Chlorpyrifos metabolism in human hepatocytes. The metabolism of chlorpyrifos (CPS) and chlorpyrifos oxon (CPO) by human hepatocytes and human liver S9 fractions was investigated using LC-MS/MS (Choi et al., 2006). CYP-dependent and phase II-related products were determined following incubation with CPS and CPO. The CYP-related products, 3, 5, 6-trichloro-2-pyridinol (TCP), diethyl thiophosphate (DETP) and dealkylated CPS were found following CPS treatment and dealkylated CPO following CPO treatment. Diethyl phosphate (DEP) was not identified due to its high polarity and lack of retention with the chromatographic conditions employed. Phase II-related conjugates, including O- and S- glucuronides as well as 11 GSH-derived metabolites were identified in CPS-treated human hepatocytes, although the O-sulfate of TCP conjugate was found only when human liver S9 fractions were used as the enzyme source. The O-glucuronide of TCP was also identified in CPO-treated hepatocytes. CPS and CPO were identified using HPLC-UV after CPS metabolism by the human liver S9 fraction. However, CPO was not found following treatment of human hepatocytes with either CPS or CPO. These results suggest that human liver plays an important role in detoxification, rather than activation, of CPS.

5.5.2. DEET

The studies of the oxidative metabolism of the insect repellent *N,N*-diethyl-*m*-toluamide (DEET) by pooled human liver microsomes (HLM), rat liver microsomes (RLM), and mouse liver microsomes (MLM) have been published (Usmani et al., 2002). DEET is metabolized by CYPs leading to the production of a ring methyl oxidation product, *N,N*-diethyl-*m*-hydroxymethylbenzamide (BALC) and an *N*-deethylated product, *N*-ethyl-*m*-toluamide (ET). Both the affinities and intrinsic clearance of HLM for ring hydroxylation are greater than those for *N*-deethylation. Among 15 cDNA-expressed CYP enzymes examined, CYP1A2, 2B6, 2D6*1 (Val₃₇₄), and 2E1 metabolized DEET to the BALC metabolite while CYP3A4, 3A5, 2A6, and 2C19 produced the ET metabolite. CYP2B6 is the principal CYP involved in the metabolism of DEET to its major BALC metabolite while CYP2C19 had the greatest activity for the formation of the ET metabolite. Use of phenotyped HLM demonstrated that individuals with high levels of CYP2B6, 3A4, 2C19, and 2A6 have the greatest potential to metabolize DEET. Mice treated with DEET demonstrated induced levels of the CYP2B family, increased hydroxylation, and a 2.4 fold increase in the metabolism of chlorpyrifos to chlorpyrifos-oxon, a potent anticholinesterase. Preincubation of human CYP2B6 with chlorpyrifos completely inhibited the metabolism of DEET. Preincubation of human or rodent microsomes with chlorpyrifos, permethrin, and pyridostigmine bromide, alone or in combination, can lead to either stimulation or inhibition of DEET metabolism.

5.5.3. Permethrin

Permethrin is a pyrethroid insecticide used in agriculture, public health and in military deployments, for control of disease vectors and nuisance insects. Because of this use pattern it was important to understand the basic enzymatic pathways for its metabolism in humans as a preliminary to the study of interactions with implications for human health. In these studies we determined that trans-permethrin is metabolized by human liver fractions, producing phenoxybenzyl alcohol by hydrolysis and subsequently phenoxybenzoic acid. Alcohol and aldehyde dehydrogenases were identified as the enzymes responsible for the metabolism of phenoxybenzyl alcohol to phenoxybenzoic acid, with phenoxybenzaldehyde as an intermediate. Cis-permethrin was not significantly metabolized by human liver fractions and CYP isoforms were not involved either in the hydrolysis of trans-permethrin or in the oxidation of phenoxybenzyl alcohol to phenoxybenzoic acid. Purified alcohol dehydrogenase isoforms oxidized phenoxybenzyl alcohol to phenoxybenzyl aldehyde. Purified aldehyde dehydrogenase was responsible for the formation of phenoxybenzoic acid from phenoxybenzyl aldehyde. These studies are described in detail in Choi et al., (2002).

5.5.4 Pyridostigmine bromide

Pyridostigmine bromide metabolism activity assays were performed by incubation of 50 mM pyridostigmine bromide with pooled human liver microsomes, pooled human liver cytosol, pooled human liver S9, rat liver microsomes, rat liver cytosol, and rat serum for 60 min. The microsomal protein concentrations used in the assays were 1.0 mg/ml in 100 mM Tris-HCl

buffer (pH 7.4 at 37°C) containing 5 mM MgCl₂ and 3 mM EDTA. Reactions were stopped by the addition of methanol followed by centrifugation at 15,000 rpm. The supernatant was analyzed for pyridostigmine bromide metabolites by HPLC.

The data indicate that pyridostigmine bromide is not metabolized by pooled human liver microsomes, rat liver microsomes, pooled human liver cytosol, rat liver cytosol, pooled human liver S9, or rat serum. An earlier study by Leo et al., (1977) provided evidence that pyridostigmine bromide is not metabolized in humans and specifically that it is not a substrate for human CYPs 1A1, 2C9, 2E1, 2D6 and 3A4. This is confirmed and extended by our results.

5.5.5 Sulfur mustard

Thiodiglycol Oxidation by Alcohol Dehydrogenase: Cytosolic preparations made with the microsomes were evaluated for alcohol dehydrogenase activity using ethanol and thiodiglycol (TDG). These preparations readily metabolized TDG as measured spectrophotometrically by following the change in OD at 340 nm as described by Dudley et al. (2000). However, there was no difference among the thiodiglycol or mustard treated animals that would indicate induction as a function of treatment. Attempts to evaluate the actual metabolic products arising from the action of purified human recombinant alcohol dehydrogenase isoforms on TDG using NMR (Brimfield et al., 2002) were unsuccessful possibly due to the presence of large quantities of glycerol present in the purified enzyme preparations or to protein denaturation during removal of the glycerol by column chromatography.

Subsequent studies, using the NMR technique described above indicated that the oxidation of TDG by horse liver ADH occurs via a two-step process in which TDG remains in the active site while two moles of NAD are sequentially reduced. There was no release of the intermediate aldehyde as evidenced by the absence of a signal from an aldehydic proton at low field, nor was the monoacid a substrate for further oxidation by ADH. The structure of the product was confirmed by synthesis. Additional metabolism work awaits the availability of quantities of the cloned human isoforms. The protein (serine/threonine) phosphatase inhibiting properties of 2-hydroxyethyl thioacetic acid are under investigation with samples of the pure enzymes.

TDG, the hydrolysis product of the chemical warfare agent sulfur mustard, has been implicated in the toxicity of sulfur mustard through the inhibition of protein phosphatases in mouse liver cytosol. The absence of any inhibitory activity when TDG was present in assays of pure enzymes, however, led us to investigate (Brimfield et al., 2006) the possibility for metabolic activation of TDG to inhibitory compound(s) by cytosolic enzymes. We have successfully shown that mammalian alcohol dehydrogenases rapidly oxidize TDG *in vitro*, but the classic spectrophotometric techniques for following this reaction provided no specific information on the identity of TDG intermediates and products. The use of proton NMR to monitor the oxidative reaction with structural confirmation by independent synthesis allowed us to establish the ultimate product, 2-hydroxyethylthioacetic acid, and to identify an intermediate equilibrium mixture consisting of 2-hydroxyethylthioacetaldehyde, 2-hydroxyethylthioacetaldehyde hydrate and the cyclic 1,4-oxathian-2-ol. The intermediate nature of this mixture was determined

spectrophotometrically when it was shown to drive the production of NADH when added to ADH and NAD.

During the last twenty years it has been the prevailing opinion among many who study sulfur mustard (2,2'-bis-chloroethyl sulfide) toxicity that tissue damage arises from the alkylation and cross linking of chromatin in affected tissues driven by sulfonium ion formation. That theory led to the conclusion that monofunctional mustards such as chloroethylethyl sulfide (CEES) and chloroethylmethyl sulfide (CEMS) could not act via the same mechanism as sulfur mustard because they lacked the capacity to cross link DNA and, therefore, could not serve as model compounds for the study of mustard toxicity. Current work from our laboratory (Brimfield and Mancebo, 2007, 2008, Brimfield et al., 2008), however, indicates that the toxicity of mustards is a consequence of free radicals arising from enzymatic reduction of the immonium and sulfonium ions which form as intermediates in the hydrolysis of nitrogen and sulfur mustards, respectively.

Studies using pure NADPH-CYP reductase (Novak and Brimfield, 2006), microsomes and cytochrome c and EPR with spin trapping indicated interaction of mustard and the flavoenzyme reductases of the microsomal electron transport system. We investigated the hypothesis that the reduction of sulfur mustard-related sulfonium ions by electrons from NADPH-cytochrome P450 reductase resulted in free radical production. "Onium" species such as the pyridonium ions of paraquat and diphenyl iodonium accept an electron from NADPH-cytochrome P450 reductase to form a free radical. We hypothesized that sulfonium ions of sulfur mustard would behave in a similar manner. To document radical production using electron spin resonance (EPR) spectrometry an *in vitro* system consisting NADPH (2.4 mM), cytochrome c from bovine heart (0.21 mM), recombinant human NADPH-cytochrome P450 reductase (0.016 μ M), sulfur mustard (4.0 mM) and the spin trap 4-POBN (α -[4-pyridyl-1-oxide]-N-*tert*-butylnitron) (1.03 M) in 0.1 M KPO₄ buffer, pH 7.5 containing 250 mM NaCl was utilized. The reaction was started by adding the enzyme solution to a tube containing the other materials at room temperature, mixing and transferring the mixture to a 0.25 mL flat cell. Repeated scans of the sample on a Bruker ESP 300E EPR spectrometer produced a triplet of doublets having fine splitting constants of N=15.44 G and H= 2.85 G. Instrument settings were: modulation amplitude, 1.000 G; time constant, 327.68 ms; and sweep width, 100.00 G. This outcome was indicative of alkyl radical production and supported the hypothesis that free radicals are produced when mustard-related sulfonium ions are reduced by NADPH-cytochrome P450 reductase.

The primary biochemical lesion concept has been used as a framework to guide experimentation in the study of the vesicant action of sulfur mustard. That work has led to the discovery of sulfur mustard-related protein phosphatase inhibition, the identification of thiodiglycol as a previously unknown substrate for mammalian alcohol dehydrogenases and the identification of previously unreported sulfur mustard metabolites. However, those results seem to fall into the category of downstream effects in the cascade of toxicity rather than its cause. Building on the success in reducing mustard toxicity of Dr. Thomas Sawyer in Canada and Dr. Uri Wormser in Israel, Dr Brimfield's group, as illustrated above recently revisited the problem with an investigation of the interaction of mustard derived sulfonium ions with purine nucleotide-driven flavoenzyme reductases. The results thus far have been exciting with broad implications for the toxicology of sulfur mustard.

5.5.6. Naphthalene

The polycyclic aromatic hydrocarbon naphthalene is an environmental pollutant, a component of jet fuel and, since 2000, has been reclassified as a potential human carcinogen. Few studies of the *in vitro* human metabolism of naphthalene are available and these focus on lung metabolism. The current studies (Cho et al., 2006) were performed to characterize naphthalene metabolism by human cytochromes P450 (CYP). Naphthalene metabolites from pooled human liver microsomes (pHLM) were *trans*-1,2-dihydro-1,2-naphthalenediol (dihydrodiol), 1-naphthol, and 2-naphthol. Metabolite production generated K_m s of 23, 40, and 116 μ M and V_{max} s of 2860, 268, and 22 pmol/mg protein/min., respectively. CYP isoform screening of naphthalene metabolism identified CYP1A2 as the most efficient isoform for producing dihydrodiol and 1-naphthol and CYP3A4 as the most effective for 2-naphthol production. Metabolism of the primary metabolites of naphthalene was also studied to identify secondary metabolites. While 2-naphthol was readily metabolized by pHLM to produce 2,6- and 1,7-dihydroxynaphthalene, dihydrodiol and 1-naphthol were inefficient substrates for pHLM. A series of human CYP isoforms was used to further explore the metabolism of dihydrodiol and 1-naphthol. 1,4-naphthoquinone and four minor unknown metabolites from 1-naphthol were observed, and 1A2 and 2D6*1 were identified as the most active isoforms for the production of 1,4-naphthoquinone. Dihydrodiol was metabolized by CYP isoforms to three minor unidentified metabolites with CYP3A4 and CYP2A6 having the greatest activity toward this substrate. The metabolism of dihydrodiol by CYP isoforms was lower than that of 1-naphthol. These studies identify primary and secondary metabolites of naphthalene produced by pHLM and CYP isoforms. The dihydrodiol is a potential biomarker of human exposure to naphthalene.

5.5.7. Nonane

Nonane, a component of jet-propulsion fuel JP-8 as well as other kerosene-based fuels is metabolized (Edwards et al., 2005) to 2-nonanol and 2-nonanone by pooled human liver microsomes. CYP isoforms 1A2, 2B6 and 2E1 metabolize nonane to 2-nonanol, whereas alcohol dehydrogenase, CYPs 2B6 and 2E1 metabolize 2-nonanol to 2-nonanone.

5.5.8. Carbaryl

The initial studies of carbaryl metabolism were not supported by this award. Their inclusion, however, is necessary since, as part of this award, it was shown that carbaryl metabolism was inhibited by a deployment-related chemical, chlorpyrifos. In the initial studies we characterized the *in vitro* human metabolism of the carbaryl, and identified the isoforms responsible for the production of the three major oxidative metabolites.

Carbaryl is a widely used anticholinesterase carbamate insecticide. Although previous studies have demonstrated that carbaryl can be metabolized by CYP, the identification and characterization of CYP isoforms involved in metabolism have not been described either in humans or in experimental animals. The *in vitro* metabolic activities of

human liver microsomes (HLM) and human CYP isoforms toward carbaryl were investigated in this study (Tang et al., 2002). The three major metabolites, i.e. 5-hydroxycarbaryl, 4-hydroxycarbaryl and carbaryl methylol, were identified after incubation of carbaryl with HLM or individual CYP isoforms and analysis by HPLC. Most of the 16 human CYP isoforms studied showed some metabolic activity toward carbaryl. CYP1A1 and 1A2 had the greatest ability to form 5-hydroxycarbaryl, while CYP3A4 and CYP1A1 were the most active in generation of 4-hydroxycarbaryl. The production of carbaryl methylol was primarily the result of metabolism by CYP2B6. Differential activities toward carbaryl were observed among five selected individual HLM samples with the largest difference occurring in the production of carbaryl methylol. It is clear, therefore, that carbaryl metabolism in humans and its interaction with other chemicals is reflected by the concentration of CYP isoforms in HLM and their activities in the metabolic pathways

Of relevance to this report, however, is the observation that chlorpyrifos is a potent inhibitor of carbaryl metabolism [section 5.6.1 of this report].

5.5.9. Endosulfan.

These studies (Casabar et al., 2006) were not supported by this award. Their inclusion, however, is necessary to establish a complete picture of the critical importance of *in vitro* human in human health risk analysis.

Endosulfan- α is metabolized to a single metabolite, endosulfan sulfate, in pooled human liver microsomes ($K_m = 9.8 \mu\text{M}$, $V_{max} = 178.5 \text{ pmol/mg/min}$). With the use of recombinant cytochrome P450 (rCYP) isoforms, we identified CYP2B6 ($K_m = 16.2 \mu\text{M}$, $V_{max} = 11.4 \text{ nmol/nmol CYP/min}$) and CYP3A4 ($K_m = 14.4 \mu\text{M}$, $V_{max} = 1.3 \text{ nmol/nmol CYP/min}$) as the primary enzymes catalyzing the metabolism of endosulfan- α , although CYP2B6 had an 8-fold higher intrinsic clearance rate ($CL_{int} = 0.70 \mu\text{L/min/pmol CYP}$) than CYP3A4 ($CL_{int} = 0.09 \mu\text{L/min/pmol CYP}$). Using 16 individual human liver microsomes (HLM), a strong correlation was observed with endosulfan sulfate formation and S-mephenytoin N-demethylase activity of CYP2B6 ($r^2 = 0.79$) while a moderate correlation with testosterone 6 β -hydroxylase activity of CYP3A4 ($r^2 = 0.54$) was observed. Ticlopidine (5 μM), a potent CYP2B6 inhibitor, and ketoconazole (10 μM), a selective CYP3A4 inhibitor, together inhibited approximately 90% of endosulfan- α metabolism in HLMs. Using six HLM samples, the percent total normalized rate (% TNR) was calculated to estimate the contribution of each CYP in the total metabolism of endosulfan- α . In five of the six HLMs used, the percent inhibition (% I) with ticlopidine and ketoconazole in the same incubation correlated with the combined % TNRs for CYP2B6 and CYP3A4. This study shows that endosulfan- α is metabolized by HLMs to a single metabolite, endosulfan sulfate, and that it has potential use, in combination with inhibitors, as an *in vitro* probe for CYP2B6 and 3A4 catalytic activities.

5.5.10. Fipronil.

These studies (Tang et al., 2004) were not supported by this award. Their inclusion, however, is necessary since fipronil is a model substrate for human hepatocyte studies on interactions based

on both induction and cytotoxicity. Thus they are necessary to establish a complete picture of the importance of in vitro human in human health risk analysis of deployment-related chemicals.

Fipronil (5-amino-1-[2,6-dichloro-4-(trifluoromethyl)phenyl]-4-[(trifluoromethyl)sulfinyl]-1*H*-pyrazole-3-carbonitrile) is a highly active, broad spectrum insecticide from the phenyl pyrazole family, which targets the γ -amino butyric acid (GABA) receptor. This study was designed to investigate in vitro human metabolism and possible metabolic interactions of fipronil. Fipronil was incubated with liver micromes or CYP isoforms. HPLC was used for metabolite identification and quantification. Fipronil sulfone was the predominant metabolite via CYP oxidation. The K_m and V_{max} values for human liver microsomes (HLM) are 27.2 μM and 0.11 nmol/mg protein/min, respectively; for rat liver microsomes (RLM) the K_m and V_{max} are 19.9 μM and 0.39 nmol/mg protein/min, respectively. CYP3A4 is the major isoform responsible for fipronil oxidation in humans while CYP2C19 is considerably less active. Other human CYP isoforms have minimal or no activity toward fipronil. The presence of cytochrome b_5 is essential for CYP3A4 to manifest high activity toward fipronil. Two μM ketoconazole inhibits 70-80% of the HLM activity toward fipronil. Oxidative activity toward fipronil in 19 single-donor HLMs correlated well with their ability to oxidize testosterone. The interactions of fipronil and other CYP3A4 substrates, such as testosterone and diazepam, were also investigated. Fipronil metabolism was activated by testosterone in HLM but not in CYP3A4 Supersomes®.

5.6. **Interactions Based on Inhibition** (year 2, aim 3).

5.6.1. Inhibition of metabolism of other xenobiotics, including other deployment related chemicals (year 2, aim 4).

Chlorpyrifos inhibition of carbaryl metabolism. . Co-incubations of carbaryl and chlorpyrifos in HLM greatly inhibited carbaryl metabolism. The ability of HLM to metabolize carbaryl was also reduced by preincubation of HLM with chlorpyrifos. Chlorpyrifos inhibited the generation of carbaryl methylol, catalyzed predominately by CYP2B6, more than other pathways, correlating with an earlier observation that chlorpyrifos is metabolized to its oxon primarily by CYP2B6.

Table 1. Inhibition of carbaryl metabolism by pre-incubation of pooled human liver microsomes with chlorpyrifos.

pre-incubation time (min)	% inhibition of 5-hydroxy carbaryl formation	%inhibition of 4-hydroxy carbaryl formation	% inhibition of N-methylol carbaryl formation
5	0	6	52
15	14	37	69
30	43	56	80

Note: 1) Final concentrations for chlorpyrifos were 50 μM , carbaryl 500 μM , and microsomal protein 1 mg in 500 μl reaction volume. Incubation time with carbaryl was 15 min.

Table 2. Inhibition of carbaryl metabolism by pre-incubation of human CYP2B6 with chlorpyrifos.

pre-incubation time (min)	% inhibition of 5-hydroxy carbaryl formation	% inhibition of 4-hydroxy carbaryl formation	% inhibition of N-methylol carbaryl formation
5	100	100	100
15	100	100	100
30	100	100	100

Note: 1) Final concentrations for chlorpyrifos were 50 μ M, carbaryl 500 μ M, and 22.73 pmol CYP2B6 in 500 μ l reaction volume. Incubation time with carbaryl was 15 min.

Table 3. Inhibition of carbaryl metabolism by pre-incubation of human CYP3A4 with chlorpyrifos.

pre-incubation time (min)	% inhibition of 5-hydroxy carbaryl formation	% inhibition of 4-hydroxy carbaryl formation	% inhibition of N-methylol carbaryl formation
0	96	94	86
5	89	92	93
30	99	95	100

Note: 1) Final concentrations for chlorpyrifos were 50 μ M, carbaryl 500 μ M, and 25 pmol CYP3A4 in 500 μ l reaction volume. Incubation time with carbaryl was 15 min.

Chlorpyrifos inhibition of DEET metabolism

As discussed in the manuscript on DEET (Usmani et al., 2002), chlorpyrifos is also an inhibitor of the metabolism of DEET by human liver microsomes. Preincubation of HLM with chlorpyrifos inhibited DEET oxidation while preincubation of CYP2B6 with chlorpyrifos and an equimolar (100 μ M) completely inhibited DEET oxidation.

Chlorpyrifos inhibition of fipronil and nonane metabolism.

Based on our previous studies, it has been established that chlorpyrifos, fipronil and nonane can all be metabolized by human liver microsomes (HLM) and a number of CYP isoforms. However, metabolic interactions between these three substrates had not been described. To fill this data gap the effect of either co-incubation or pre-incubation of chlorpyrifos with HLM or CYP isoforms with either fipronil or nonane as substrate was investigated (Joo et al., 2007). In both co- and pre-incubation experiments chlorpyrifos significantly inhibited the metabolism of fipronil or nonane by HLM although chlorpyrifos inhibited the metabolism of fipronil more effectively than that of nonane. Chlorpyrifos significantly inhibited the metabolism of fipronil by CYP3A4 as well as

the metabolism of nonane by CYP2B6. In both cases pre-incubation with CPS caused greater inhibition than co-incubation, suggesting that the inhibition is mechanism based.

Inhibitory effects of nonane and JP-8 jet fuel.

Nonane and 2-nonanol showed no significant effect on the metabolism of testosterone, estradiol or DEET, but did inhibit carbaryl metabolism (Edwards et al., 2005). JP-8 showed modest inhibition of testosterone, estradiol and carbaryl metabolism, but had a more significant effect on the metabolism of DEET. JP-8 was shown to inhibit CYPs 1A2 and 2B6 mediated metabolism of DEET, suggesting that at least some of the components might be metabolized by CYPs 1A2 and/or 2B6.

Inhibition of permethrin metabolism

This section is a summary of our findings on inhibition of permethrin hydrolysis (Choi et al., 2004).

Chlorpyrifos oxon (CFO) inhibition of *trans*-permethrin hydrolysis. *Trans*-permethrin hydrolysis in human liver fractions was inhibited more effectively by CFO than by carbaryl. In given assay conditions, IC₅₀s of CFO in human liver cytosolic and microsomal fractions were 35 nM and 60 nM, respectively. Above 60 nM (cytosol) or 150 nM (microsomes) levels, *trans*-permethrin hydrolysis was completely inhibited by CFO.

When the cytosolic fraction was pre-incubated for 5 min with 32 nM CFO, the V_{max} value was significantly reduced from 0.92 nmole/mg/min to 0.38 nmole/mg/min while K_m values stayed within 95% of confidence interval. Five minutes pre-incubation with 80 nM CFO in the microsomal fraction resulted in a significant decrease in V_{max} value (8.45 to 4.60) with an insignificant drop in K_m values. The same pattern of kinetic parameter changes, decreased V_{max} with no changes in K_m, were found in both fractions and based on this observation, non-competitive or irreversible type of inhibition was assumed for CFO in human liver fractions. The inhibition constant (*K_i*), an indicator of inhibitor affinity to target enzyme was calculated for CFO from V_{max} and K_m values. They were 21.39 nM for the cytosolic fraction and 95.00 nM in the microsomal fraction, respectively. These values were approximately one hundred times lower than those for carbaryl, indicating a higher inhibitory potential of CFO.

The parent compound, chlorpyrifos was not inhibitory but co-incubation with an NADPH regenerating system and the microsomal fraction led to inhibitory effects confirming that CFO, the reactive metabolite of chlorpyrifos, is the chemical responsible for the inhibition. In the assay to further clarify whether CFO inhibition of permethrin hydrolysis is non-competitive or irreversible, no hydrolysis products were produced up to 30 µg level indicating that the human liver esterases involved in *trans*-permethrin hydrolysis are irreversibly inhibited by CFO.

Carbaryl inhibition of trans-permethrin hydrolysis.

The most noticeable difference between carbaryl and CFO inhibition was that *trans*-permethrin hydrolysis in either the microsomal and the cytosolic fractions was not completely inhibited by a wide range of carbaryl concentrations. This observation had led to an assumption that the esterases involved in *trans*-permethrin hydrolysis in both the microsomal and the cytosolic fractions are composed of at least two different entities, which have different susceptibility to carbaryl inhibition.

These studies demonstrate that there are potentially important interactions between permethrin and chlorpyrifos in humans. Chlorpyrifos, which has been used in military deployments in conjunction with permethrin, is a very potent inhibitor of *trans*-permethrin hydrolysis after metabolic activation to CFO. This observation implies that co-exposure to chlorpyrifos might potentiate the toxicity of permethrin by deactivating the metabolic detoxification pathway for permethrin. Other deployment related compounds, an insect repellent (N,N-diethyl-*m*-toluamide) a nerve gas prophylactic (pyridostigmine bromide) did not cause inhibition of *trans*-permethrin hydrolysis regardless of the presence of an NADPH regeneration system. CFO completely inhibited *trans*-permethrin hydrolysis in both human liver fractions with very low K_i values indicating that B-esterases are responsible for *trans*-permethrin hydrolysis in human liver fractions. Compared to CFO the parent compound, chlorpyrifos and the other major chlorpyrifos metabolite (3,5,6-trichloro-2-pyridinol) showed minimal levels of inhibition in either fraction. The observation that pre-incubation with NADPH in the microsomal fraction substantially increased chlorpyrifos inhibition capability confirmed that CFO is the chemical species responsible for the inhibition of *trans*-permethrin hydrolysis.

The mechanism of CFO inhibition is *trans*-esterification, forming a strong covalent bond between the oxon and the alcohol functional group of a serine residue in the active site of the esterase. With endogenous substrates, a transient bond is formed in place of the covalent bond and readily cleaved by deacylation (Chambers, 1992). The observed inhibition kinetics (reduced V_{max} and constant K_m) and the irreversible nature of inhibition strongly implies that the inhibition of the human liver esterases hydrolyzing permethrin is mediated by the same mechanism.

Carbaryl, on the other hand, shows typical non-competitive inhibition. This result is in accord with the fact that carbamate compounds are reversible and less persistent inhibitors compared to organophosphorus compounds, and that carbamate compounds can be hydrolyzed by esterases. This also explains why K_i values for carbaryl are two orders of magnitude higher than those for CFO. It is also important that carbaryl does not completely inhibit permethrin hydrolysis even at high concentrations. Incomplete inhibition at high concentrations of carbaryl suggests that there are multiple hydrolytic enzymes involved in *trans*-permethrin hydrolysis, a finding that was not revealed by CFO inhibition. It is deduced that in *trans*-permethrin hydrolysis in human liver fractions, at least two species (or groups) of B-esterases are involved, both sensitive to CFO

5.6.2. Inhibition of the Metabolism of Endogenous Metabolites.

Inhibition of testosterone metabolism.

One of the possible mechanisms for toxic effects on human health is the inhibition of the metabolism of endogenous metabolites, particularly metabolites with significant effects on physiological processes or control mechanisms, such as hormones. Since there have been no such studies utilizing human materials we felt it important to gain insight into the potential for this mechanism in humans by conducting some initial experiments on the effects of deployment-related chemicals on the metabolism of testosterone by human oxidative enzymes (Usmani et al., 2003).

CYP-dependent monooxygenases are not only major catalysts involved in the metabolism of xenobiotics but also in the oxidative metabolism of endogenous substrates such as testosterone. Major testosterone metabolites formed by human liver microsomes include 6 β -hydroxytestosterone, 2 β -hydroxytestosterone and 15 β -hydroxytestosterone. Utilizing the HPLC method developed (described above) a screen of 16 cDNA expressed human CYPs demonstrated that 94% of all testosterone metabolites are produced by members of the CYP3A subfamily with 6 β -testosterone accounting for 84% of all testosterone metabolites. While similar K_m values were observed with HLM, regardless of which metabolite is measured, V_{max} and Cl_{int} were much higher for 6 β -testosterone than for any other metabolite.

Preincubation of human liver microsomes with a variety of ligands, including the deployment-related test chemicals used throughout this project, resulted in varying levels of inhibition or activation of testosterone metabolism. The greatest inhibition of testosterone metabolism in human liver microsomes was seen following preincubation with organophosphorus compounds, including chlorpyrifos, phorate and fonofos, with up to 80% inhibition of the formation of several metabolites, including 6 β -testosterone. Preincubation of CYP3A4 with chlorpyrifos, but not chlorpyrifos oxon, resulted in 98% inhibition of testosterone metabolism. Kinetic analysis indicated that chlorpyrifos is one of the most potent inhibitors of testosterone metabolite to be discovered to date and that phorate and fonofos were also potent inhibitors. In all cases the inhibition is noncompetitive and irreversible. Conversely, preincubation of CYP3A4 with pyridostigmine bromide increased the metabolism of testosterone. Preincubation of aromatase (CYP19) with the test chemicals had no effect on the production of the endogenous estrogen, 17 β -estradiol. Details of the methodology, kinetic constants, etc., are to be found in Usmani et al., 2003.

Inhibition of estradiol metabolism.

CYPs are major catalysts in metabolism of xenobiotics and endogenous substrates such as estradiol (E_2). It has previously been shown that E_2 is predominantly metabolized in humans by CYP1A2 and 3A4 with 2-hydroxyestradiol (2-OHE $_2$) the major metabolite. This study (Usmani et al., 2006) examined effects of deployment-related and other chemicals on E_2 metabolism by human liver microsomes (HLM) and individual CYP isoforms. Kinetic studies using HLM, CYP3A4, and CYP1A2 demonstrated similar affinities (K_m) for E_2 with respect to 2-OHE $_2$ production. V_{max} and Cl_{int} values for HLM are 0.32 nmol/min/mg protein and 7.5 μ l/min/ mg protein, those for CYP3A4 are 6.9 nmol/min/nmole CYP and 291 μ l/min/ nmol CYP and those for CYP1A2 are 17.4 nmol/min/nmole CYP and 633 μ l/min/ nmol CYP. Phenotyped HLM use

demonstrated that individuals with high levels of CYP1A2 and CYP3A4 have the greatest potential to metabolize E₂. Preincubation of HLM with a variety of chemicals, including those used in military deployments, resulted in varying levels of inhibition of E₂ metabolism. The greatest inhibition was observed with organophosphorus compounds, including chlorpyrifos and fonofos, with up to 80% inhibition for 2-OHE₂ production. Carbaryl, a carbamate pesticide, and naphthalene, a jet fuel component, inhibited ca. 40% of E₂ metabolism. Preincubation of CYP1A2 with chlorpyrifos, fonofos, carbaryl, or naphthalene resulted in 96, 59, 84, and 87% inhibition of E₂ metabolism, respectively. Preincubation of CYP3A4 with chlorpyrifos, fonofos, deltamethrin or permethrin resulted in 94, 87, 58 and 37% inhibition of E₂ metabolism. Chlorpyrifos inhibition of E₂ metabolism was shown to be irreversible.

5.7. Interactions Based on Activation (year 3, aim 2,
[add details from Usmani TST paper]

Chlorpyrifos-oxon (CPO), a metabolite of chlorpyrifos, is a potent inhibitor of acetylcholinesterase and, although the neurotoxicological impact of this organophosphorus compound has been broadly studied both in vitro and in vivo, there are few studies of metabolic interactions of CPO with other xenobiotics. CPO significantly activated (Cho et al., 2007) the production of 1-naphthol (5-fold), 2-naphthol (10-fold), trans-1,2-dihydro-1,2-naphthalenediol (1.5-fold), and 1,4-naphthoquinone from naphthalene by human liver microsomes (HLM). It was further demonstrated that the production of naphthalene metabolites by CYP2C8, 2C9*¹, 2C19, 2D6*¹, 3A4, 3A5, and 3A7 was activated by CPO, while the production of naphthalene metabolites by CYP1A1, 1A2, 1B1, and 2B6 was inhibited by CPO. CPO inhibited CYP1A2 production of naphthalene metabolites, while activating their production by CYP3A4. Similarly, CPO inhibited the production of N,N-diethyl-m-hydroxymethylbenzamide (BALC) from DEET by human liver microsomes, but activated the production of N-ethyl-m-toluamide (ET) from this substrate. CYP2B6, the most efficient isoform for BALC production, was inhibited by CPO while CYP3A4, the most efficient isoform for ET production, was activated by CPO. CPO inhibited CYP2B6 production of both BALC and ET from DEET, but activated CYP3A4 production of ET, while inhibiting CYP3A4 BALC production. CPO appears to facilitate the binding of naphthalene to CYP3A4. This metabolic activation is independent of cytochrome b₅, suggesting that activation of CYP3A4 by CPO is associated with a conformational change of the isoform rather than facilitating electron transfer. Other less marked activations have also been seen in the course of these studies, for example, preincubation of CYP3A4 with pyridostigmine bromide increases the metabolism of testosterone. In general, while activation is uncommon, when it is observed it is generally when the primary substrate is metabolized by CYP3A4.

5.8. Interactions Based on Induction.

5.8.1. Induction in Mice (year 1, aim 3, year 2, aim 5, year 3, aim 1).

Adult male CD-1 mice, 28-30 grams, were obtained from Charles River Laboratories and acclimated for 4 days. Doses for pyridostigmine bromide, trans- and cis-permethrin, and chlorpyrifos were selected such that the highest administered dose did not exceed doses known to produce physiological effects. The doses administered by intraperitoneal injection for each of three days were as follows: pyridostigmine bromide (0.1, 0.5, and 1 mg/kg/day) in 100 µl

water, *trans*-permethrin (1, 10, and 100 mg/kg/day) in 100 µl corn oil, *cis*-permethrin (1, 10, and 20 mg/kg/day) in 100 µl corn oil, chlorpyrifos (0.1, 1, and 10 mg/kg/day) in 100 µl corn oil. Doses approximating LD₁₀ values for phenobarbital (80 mg/kg/day) in 100 µl water or 3-methylcholanthrene (20 mg/kg/day) in 100 µl corn oil were also administered intraperitoneally, to separate groups of mice, daily for 3 days. Controls were given corn oil only or water.

Microsomes were prepared from livers of fed mice on the fourth day according to the method of Cook and Hodgson (1983). Total CYP content was determined by the CO-difference spectrum method of Omura and Sato (1964). Protein concentration was determined using the BioRad protein assay with bovine serum albumin (BSA) as standard (Bradford, 1976).

The following substrates were used as indicators of the activities for the following isozymes: ethoxyresorufin O-deethylation (EROD) and methoxyresorufin O-demethylation (MROD) for Cyp1A1/2 (Burke and Mayer, 1974; Nerurkar et al., 1993), and pentoxyresorufin O-dealkylation (PROD) for Cyp2B10 (Lubet et al., 1985). Assays were conducted as described by Pohl and Fouts (1980). Product formation for EROD, MROD and PROD activities were determined spectrofluorimetrically (RF-5301PC Personal Fluorescence spectrophotometer, Shimadzu, Kyoto, Japan) by comparison with a standard curve generated with resorufin.

Mice treated with Phenobarbital, 3-methylcholanthrene, or varying concentrations of pyridostigmine bromide, *trans*-permethrin, *cis*-permethrin, and chlorpyrifos showed no significant differences in liver weight. PB treated mouse liver microsomes showed significantly higher P450 content than control or pyridostigmine bromide, *trans*-permethrin, *cis*-permethrin, and chlorpyrifos treated mouse liver microsomes. No significant differences were observed in P450 content between control and pyridostigmine bromide, *trans*-permethrin, *cis*-permethrin, and chlorpyrifos treated mouse liver microsomes. Mice treated with varying concentrations of pyridostigmine bromide, *trans*-permethrin, *cis*-permethrin, and chlorpyrifos exhibited no significant levels of induction toward EROD, MROD, and PROD. Phenobarbital treatment as a positive control significantly induced PROD activity (12-fold). In a similar manner, treatment with 3-methylcholanthrene also resulted in significant induction of MROD (8-fold) and EROD (28-fold) as expected.

5.8.2. Induction in Mice by Sulfur Mustard and its Degradation Products.

The first test of induction of mice with thiodiglycol was a range finding experiment with 5 mice per dose level using ip injections of 5, 10, and 20% of an LD₅₀ dose daily for three days followed by liver microsome preparation on the fourth day and freezing of the microsomes at high protein concentration in phosphate buffer containing 0.25 M sucrose (Sabourin et al., 1984). The animals exhibited no signs of discomfort at the doses employed. There was evidence of liver hypertrophy even at the highest dose.

Subsequent induction studies in mice with thiodiglycol and sulfur mustard were carried out to identify the possible participation of cytochromes P450 in their metabolism as well as the metabolism of other xenobiotics. Adult CD1 males 31 – 32 g were obtained from Charles River Laboratories, acclimated for 10 days, grouped to give equivalent average weights and dosed ip with thiodiglycol in saline and with sulfur mustard in corn oil at 5 mice per group. Treatments

were administered based on average group weights. Treatment levels using sulfur mustard were vehicle control, 5% LD50 (100 μ l at 0.25 mg/ml), 10% LD50 (100 μ l at 0.5 mg/ml), and 20% LD50 (100 μ l at 1.0 mg/ml). Dosage was based on published mouse ip LD50s for sulfur mustard of 7.7 mg/kg (McMaster and Hogeboom, 1942) to 19 mg/kg (Friedberg et al., 1983).

The mouse LD50 for thiodiglycol is 5.3 g/kg (Anslow et al., 1948). It was administered using ip saline injected animals (250 μ l/mouse) as controls and 5% LD50 (75 μ l at 120 mg/ml), 10% LD50 (150 μ l at 120 mg/ml) and 20% LD50 (280 μ l at 120 mg/ml). The animals received injections for three days and were euthanized on day four. Liver microsomes were prepared and stored as described in Sabourin et al., 1984. Liver cytosolic preparations (thiodiglycol induced animals) were prepared as outlined in Dudley et al. (2000). Protein determinations were carried out using the Bradford method (1976). CYP levels were measured by CO difference spectrum as outlined by Omura and Sato (1964)(Table 6).

CYP isoforms present in the mouse microsomal preparations were analyzed by Western blot as described in Emoto et al., (2000), using commercially available antibodies (BD Gentest, Woburn, MA) with specificity for rat CYPs that have been shown to cross react with their mouse counterparts. Microsomes from the thiodiglycol and sulfur mustard treated animals and untreated controls were tested for the presence of CYP 3A2, 2B1/2B2, 2E1, 2C11, 2C13, 2C6, 1A1, 1A2, 1B1 and 4A1/4A3. Samples consisted of aliquots of the treated and control microsomal preparations and mouse "Supersome" standards.

Enzymatic activity toward isoform specific substrates was tested in microsomes from thiodiglycol and sulfur mustard treated animals. Neither catechol formation from *p*-nitrophenol hydroxylase activity nor pentoxyresorufin-O-dealkylation in microsome from treated animals showed any significance difference from untreated controls. These data were generated using the method outlined in literature from BD Gentest (Woburn, MA) which is based on the published spectrophotometric (Beckman DU 70, Beckman Instruments, Palo Alto, CA) method of Koop (1986) for *p*-nitrophenol hydroxylation or the method of Pohl and Fouts (1980) for pentoxyresorufin-O-dealkylation.

Tables 4 and 5 show the effect of thiodiglycol or sulfur mustard on total CYP or on specific CYP isoforms. Although minor differences could be seen they were not consistent in magnitude nor, in most cases, dose-related. The general conclusion from the above experiments is that thiodiglycol and sulfur mustard do not appear to be inducers of CYP isoforms in mice.

Table 4. Total CYP Concentrations in Thiodiglycol and Sulfur Mustard Induced Mouse Liver Microsomes.

Thiodiglycol Induction	
Control	0.23 nmol/mg protein
5% LD50	0.31 nmol/mg protein
10% LD50	0.37 nmol/mg protein
20% LD 50	0.47 nmol/mg protein

Sulfur Mustard Induction

Control	0.22 nmol/mg protein
5% LD50	could not be determined
10% LD50	0.20 nmol/mg protein
20% LD50	0.19 nmol/mg protein

Table 5. Identification of CYP Isoforms in Microsomes from Thiodiglycol and Sulfur Mustard Treated CD1 Mice.

Thiodiglycol Induction	3a2	2b1/2b2	2e1	2c11/2c13	2c6	1a1	1a2	1b1	4a
Control	++	faint	+++	+++	+++	+	faint	faint	++
5% LD50	++	+	+++	++	++	+	faint	faint	++
10% LD50	++	++	+++	++	+	faint	-	faint	++
20% LD50	++	++	+++	++	+	faint	-	faint	++

Mustard Induction	3a2	2b1/2b2	2e1	2c11/2c13	2c6	1a1	1a2	1b1	4a
Control	+++	++	++	+	--	--	faint	faint	+
5% LD50	++	++	++	+	--	--	faint	faint	faint
10% LD50	++	++	++	+	--	--	faint	faint	+
20% LD50	+	++	++	+	--	--	faint	--	++

5.8.3. In Human Hepatocytes (year 4, aim3, year 5, aim 2 and 3, year 6, aim 1, year 7, aim 1).

Although many aspects of pesticide and drug metabolism can be easily studied using human liver microsomal and cytosolic preparations, it is not possible to study the inducing effects of xenobiotic exposure using these systems. Many drugs are known to induce the metabolism of other co-administered drugs as well as to induce their own metabolism, prompting pharmaceutical companies to conduct elaborate screening protocols to verify the lack of potential harmful interactions between new drug candidates prior to releasing drugs to the marketplace. Since the liver is the primary organ of drug metabolism, use of primary cultures of human hepatocytes is one of the best methods for the study of potential interactions of drugs or other xenobiotics. Human hepatocyte cultures have been demonstrated to retain many aspects of liver function; including CYP-mediated oxidation of drugs and CYP induction (Li et al., 1997).

The branched DNA (bDNA) assay is a technique which allows for quantitative determinations of messenger RNA levels from hepatocyte tissues permitting the simultaneous evaluation at the level of mRNA of the genes selected. Experience with the bDNA assay through collaboration with Dr. N. Cherrington (University of Arizona) has demonstrated the utility of this assay to quantitate levels of induction following treatment of hepatocytes with several inducers including some deployment-related chemicals.

The bDNA assay, as explained by Hartley and Klaassen (2000) resembles the well established enzyme linked immunosorbent assay (ELISA) in principle, but uses multi-oligonucleotides not only to capture the mRNA of interest, but also links it to an enzyme which produces a chemiluminescent signal on addition of substrate. The primary value of the bDNA assay lies in its ability to assess the differential expression of a chosen set of genes in response to a chemical stimulus. For a targeted gene sequence, such as a series of metabolizing enzymes, one total RNA sample may be split among several different probe sets for quantitative analysis. Gene expression for many genes can therefore be monitored simultaneously in parallel wells. Results are reproducible and reflect other assays routinely used to monitor gene expression including Northern blot analysis, in situ hybridization, quantitative PCR, etc., although this method is rapidly being replaced by microarray techniques.

Preliminary assays conducted with human hepatocytes in combination with the bDNA assay suggest that several CYP isoforms are induced by permethrin, chlorpyrifos and DEET. Chlorpyrifos was surprisingly efficient in its induction of CYP1A1, 1A2 and 2B6. Other isoforms induced by chlorpyrifos include 2A6 and possibly 3A4. Our previous determinations of metabolic activity by CYPs had demonstrated that CYP2B6 was involved in the activation of chlorpyrifos to chlorpyrifos oxon. Data with mice had also suggested that Cyp2b10, the mouse phenobarbital inducible isoform analogous to CYP2B6, was also inducible by chlorpyrifos. It is of interest that permethrin also strongly induced CYP2B6 and CYP2A6. Neither of these enzymes had been implicated in permethrin metabolism using microsomes and the purified CYP isoforms.

Data acquired examining CYP3A4 induction using western blot analysis has demonstrated that the most effective induction of CYP3A4 was with rifampicin (an established CYP3A4 inducer) and DEET. This data was also corroborated with testosterone metabolism data using hepatocyte S9 preparations which had been exposed to rifampicin, permethrin, chlorpyrifos and DEET. A similar western blot of CYP1A1 activity did not provide confirming evidence for protein induction by chlorpyrifos as might have been expected based upon the bDNA assays performed. It is not yet known if the absence of correlation is the result of protein destabilization (a possibility since chlorpyrifos acts as a suicide inhibitor) or whether in sufficient time between mRNA induction and protein synthesis might explain the result. Permethrin also strongly induced CYP2B6 along with CYP2A6.

Use of human hepatocytes for induction studies is also sponsored, in part, by a grant from NIOSH.

5.8.4. Microarrays.

Since microarrays were (and are) the next logical step in the induction experiments we attempted to examine the effect of chlorpyrifos and JP-8 jet fuel on human hepatocytes by this technique. Unfortunately, it was not possible to bring these experiments to a timely conclusion. *Note that the funds that would have been used to complete these experiments are to be returned at award closure.*

5.9. Interactions Based on Induction and Cytotoxicity.

5.9.1. Fipronil

Recent studies (Das et al., 2006) have demonstrated the potential of pesticides to either inhibit or induce xenobiotic metabolizing enzymes in humans. Exposure of human hepatocytes to doses of fipronil (5-amino-1-[2,6-dichloro-4-(trifluoromethyl)phenyl]-4-[(trifluoromethyl) sulfinyl] -1H-pyrazole-3-carbonitrile) ranging from 0.1 to 25 μM resulted in a dose dependent increase in CYP1A1 mRNA expression (3.5 to ~55-fold) as measured by the branched DNA assay. In a similar manner, CYP3A4 mRNA expression was also induced (10 to 30-fold), although at the higher doses induction returned to near control levels. CYP2B6 and 3A5 were also induced by fipronil, although at lower levels (2 to 3-fold). Confirmation of bDNA results were sought through western blotting and/or enzyme activity assays. Western blots using CYP3A4 antibody demonstrated a dose responsive increase from 0.5 to 1 μM followed by decreasing responses at higher concentrations. Similar increases and decreases were observed in CYP3A4-specific activity levels as measured using 6 β -hydroxytestosterone formation following incubation with testosterone. Likewise, activity levels for a CYP1A1-specific substrate, luciferin CEE, demonstrated that CYP1A1 enzyme activities were maximally induced by 1 μM fipronil followed by dramatically declining activity measurements at 10 and 25 μM . Cytotoxic effects of fipronil and fipronil sulfone were examined using the adenylate kinase and the trypan blue exclusion assays in HepG2 cells and human hepatocytes. The results indicate both that HepG2 cells and primary human hepatocytes are sensitive to the cytotoxic effects of fipronil. The maximum induction of adenylate kinase was c. 3-fold greater than the respective controls in HepG2 and 6 – 10-fold in the case of primary hepatocytes. A significant time- and dose-dependent induction of adenylate kinase activity in HepG2 cells was noted from 0.1 to 12.5 μM fipronil followed by decreasing activities at 25 and 50 μM . For fipronil sulfone, cytotoxic effects increased throughout the dose range. The trypan blue assay indicated that cytotoxic effects contributing to an increase of greater than 10% of control values was indicated at doses above 12.5 μM . However, fipronil sulfone induced cytotoxic effects at lower doses. The possibility that cytotoxic effects were due to apoptosis was indicated by significant time- and dose-dependent induction of caspase-3/7 activity in both HepG2 cells and human hepatocytes. Fipronil mediated activation of caspase-3/7 in concurrence with compromised ATP production and viability are attributed to apoptotic cell death.

5.9.2. Pyrethroids

The pyrethroids deltamethrin, α -cyano type II pyrethroid [(S)- α -cyano-3-phenoxybenzyl-cis-(1R,3R)-3(2,2-dibromovinyl+++)(2,2-dimethyl-cyclopropane-carboxylate)], and permethrin, (3-(2,2-dichloroethenyl)-2,2-dimethylcyclopropanecarboxylic acid (3-phenoxyphenyl) methyl ester) are highly active insecticides due to their bio-efficacy, the latter being used in military

deployments. Their toxicity is mediated by interference with nerve membrane sodium channels, GABA-receptor ionophore complexes and neurotransmitters. Like certain other insecticides pyrethroids are capable of inducing CYP2B1/2B2 and CYP1A1 and P450 content in the rat liver. The objective of this study (Das et al., 2008a, in press) was to evaluate the potentials of deltamethrin and permethrin mediated cytotoxicity and possible induction of CYP isoforms in human hepatocytes. Permethrin and deltamethrin showed dose-dependent effects on adenylate kinase activity in human HepG2 cells, in which 50 and 100 μM dose, respectively, induced about 3- and highest 5-fold, and plateaued at 200 μM dose. Permethrin and deltamethrin likewise induced adenylate kinase activity in human hepatocytes. Approximately 3-fold induction was noted at 200 μM deltamethrin and ~4-fold induction was noted at 100 μM permethrin, the induction reduced at 200 μM . Cytotoxicity at 15-to-25% and 15-to-20%, respectively was noted following 48 to 72 h exposure to 100 and 200 μM deltamethrin and permethrin in HepG2 cells. Dose-dependent induction of caspase-3/7 by deltamethrin was initiated at 12.5 μM and peaked at 100 to 200 μM after 72 h. Permethrin on the other hand showed induction of caspase-3/7 at 3.125 μM , peaked at 100 μM while plateaued at 200 μM after 72 h exposure. Maximal induction was about 2.5-fold by either pyrethroids following 72 h exposure. Positive control inducer actinomycin D induced caspase-3/7 about 5-7 fold whereas specific inhibitor Z-DEVD-FMK completely abrogated the deltamethrin and permethrin induced caspase-3/7 activity. At 100 μM deltamethrin 2-3 fold induction of CYP1A1 and CYP2B6 mRNA was observed while ~25-fold induction of CYP3A4 isoform was noted. Permethrin mediated CYP induction was much less potent, up to 4-fold or less for CYP1A1, CYP3A4, CYP3A5, CYP2B6 and CYP2A6. However, the variability in CYP mRNA induction was extensive causing difficulty in evaluation the induction potential of either pyrethroid. To determine possible mechanism(s) of CYP induction due to pyrethroids, the HepG2 cell line was transiently transfected with CYP3A4-luciferase reporter plasmid and either null expression plasmid or with a pregnane X receptor (PXR) expression plasmid. PXR is expressed in the liver and its ability to act as a transcription factor is activated by binding to compounds. Pyrethroid induction of CYP3A4 promoter activity was found to be approximately 5-fold for deltamethrin and 4 – 10-fold for permethrin. The induction of CYP3A4 promoter activity by pyrethroids was found to be dependent on PXR expression, suggesting these compounds bind and activate PXR. Overall, either pyrethroid showed mild induction of major CYPs including CYP1A1, CYP2B6 and CYP3A4 but also caused cytotoxicity in human hepatocytes.

5.9.3. Chlorpyrifos and DEET

Xenobiotics, including drugs and environmental chemicals can influence CYP levels by altering the transcription of CYP genes. To minimize potential interactions between deployment-related chemicals it is important to evaluate their potential to induce CYP isoforms and to cause cytotoxicity in humans. The present study (Das et al., 2008b, in press) was designed to examine chlorpyrifos and DEET mediated induction of CYP isoforms and also to characterize their potential cytotoxic effects on primary human hepatocytes. DEET significantly induced CYP3A4, CYP2B6, CYP2A6 and CYP1A2 mRNA expression while chlorpyrifos induced CYP1A1, CYP1A2 and CYP3A4 mRNA, and to a lesser extent, CYP1B1 and CYP2B6 mRNA in primary human hepatocytes. Chlorpyrifos and DEET also mediated the expression of CYP isoform(s) particularly CYP3A4, CYP2B6 and CYP1A1 as evidenced by CYP3A4-specific protein expression, testosterone metabolism and CYP1A1-specific activity assays. DEET is a mild,

while chlorpyrifos is a relatively potent, inducer of adenylate kinase and caspase-3/7, an indicator of apoptosis, while inducing 15-20% and 25-30% cell death, respectively. In transient transfection assays induction of CYP3A4 promoter activity by chlorpyrifos was seen to increase in a dose-dependent manner. Induction by chlorpyrifos was seen when either PXR or the constitutive androstane receptor isoform 3 (CAR-3) was co-expressed suggesting that both receptors may play a role in 3A4 induction. Therefore, DEET and chlorpyrifos mediated induction of CYP mRNA and functional CYP isoforms together with their cytotoxic potential in human hepatocytes suggests that exposure to chlorpyrifos and/or DEET should be considered in human health impact analysis.

5.9.4. JP-8

Preliminary experiments in human hepatocytes had suggested that JP-8 could induce CYP3A4 protein expression. To investigate the receptors involved in enhanced CYP3A4 promoter activity, transient transfection assays were carried out by co-expressing PXR in HepG2 cells and CAR in Cos1 cells. CYP3A4 promoter activity was induced 8-fold by 0.1% JP-8 in the presence of CAR and 10-fold in the presence of PXR. These findings suggest that components in JP-8 may bind and activate these important receptors that regulate key human enzymes responsible for xenobiotic and endogenous substrate metabolism.

5.10. Genotyping (year 5, aim 4, year 6, aims 2, 3 and 4, year 7, aim 2).

Unfortunately, it was difficult to obtain samples collected from veterans of the first Gulf War, either because few samples were collected or investigators were reluctant to provide samples for this purpose. However, Dr Oksana Lockridge, of the University of Nebraska, very generously made available all of her samples. They consisted of two sets, one derived from self-diagnosed veterans, the other from veterans would had reported their symptoms to a physician.

DNA was extracted from the whole blood samples using a commercially available kit. DNA samples were amplified using Taqman Genotyping Master Mix and the following Taqman SNP genotyping assays; C_25986767_70 (CYP2C19*2, rs4244285), C_7817765_60 (CYP2B6*6, rs3745274) and C__11170747_20 (AhR 1661G>A, rs2066853). Reagents were supplied by Applied Biosystems (Foster City, CA). Reactions were run on a Mastercycler (Eppendorf, Westbury, NY) and read on a 7300 RT PCR system (Applied Biosystems). DNA free controls and positive controls for each genotype were used for each run.

Treated separately, neither data set showed any significant differences between exposed veterans and controls for any of the three polymorphisms. When combined, however, the polymorphism in the Ah-receptor gene approached the level of significance. While this cannot be taken as a definitive finding, it does indicate that further studies in this area would be potentially important. *As with the microarray studies referred to above, funds that would have been used to complete these experiments are to be returned at award closure.*

5.11. Evaluation of the Relevance of Human studies to Risk Analysis of Deployment-Related Chemicals (year 3, aims 3 and 4, year 7, aim 3).

a. Significance of XME isoform distribution.

Phenotyping of liver microsomes from individual livers shows a wide variation in the expression of different CYP isoforms and that this variation has dramatic effects on the metabolism of the test chemicals. This is clearly evident in our studies of chlorpyrifos metabolism, as well as DEET, naphthalene, nonane, endosulfan, fipronil and carbaryl. It may also be inferred from our studies on human permethrin metabolism that variations in expression of alcohol and aldehyde dehydrogenases will have similar effects on permethrin metabolism. Since the expression of XMEs can depend not only on the genotype of the individual but also on induction, such factors as co-exposure to other toxicants and/or to clinical drugs will be of significance in the assessment of risk from deployment-related chemicals.

b. Significance of polymorphisms in human XME genes.

Polymorphisms have been identified in human XMEs, particularly in CYP isoforms but also in enzymes of interest in the current studies, such as alcohol dehydrogenase and aldehyde dehydrogenase. These heritable variants of normal or wild-type genes usually express proteins of lower activity and individuals expressing these variant enzymes will have a reduced ability to metabolize any xenobiotic metabolized by that isoform. This is clear in our studies on chlorpyrifos and other chemicals, as indicated above. Thus, the genetic constitution as well as the chemical milieu will not only determine the outcome of a particular exposure but will determine who is at greater or lesser risk. These polymorphisms in XMEs are not associated with particular ethnic groups but are seen in small percentages of individuals from all ethnic groups. This is illustrated by studies carried out in the laboratory of a collaborator, (J. A. Goldstein (NIEHS), personal communication) in which polymorphic forms of CYP3A5 are shown to have very different abilities to oxidize testosterone and the drug, nifedipine, but occur in all ethnic groups examined.

c. Interactions based on XME inhibition.

As indicated above there are numerous interactions between the chemicals of interest in this study that are based on the inhibition, by one chemical, of the metabolism of another. For example, chlorpyrifos is a potent inhibitor of DEET, carbaryl and testosterone metabolism. Since the mechanism of this inhibition is almost certainly due to the formation of highly reactive sulfur during the oxidative desulfuration of chlorpyrifos followed by the interaction of this sulfur with the heme iron of CYP, this interaction will occur in the presence of chlorpyrifos whenever another chemical is metabolized by a CYP isoform that carries out the desulfuration reaction. It will also be a general interaction of any organophosphorus compound that has a P=S group in the molecule and our studies have shown that, although chlorpyrifos is the most potent of these inhibitors, other organophosphorus chemicals act in the same way. Other interactions noted are the inhibition of permethrin metabolism by chlorpyrifos oxon and by carbaryl.

d. Interactions based on XME activation. This is exemplified by our studies of the effect of chlorpyrifos oxon on human metabolism of naphthalene which was significant but may be of limited broader significance since the number of other examples of activation seen in our studies was small. Nevertheless, activation should not be ignored in risk analysis of deployment-related chemicals.

d. Interactions based on XME induction.

Since until recently it was necessary to measure induction in experimental animals and extrapolate possible effects to humans, it is difficult to assess the importance of this source of interaction in humans. However, we have recently establishing procedures for measuring induction by deployment-related chemicals in human hepatocytes (see above) and it is clear that this may be a source of interactions that needs much further examination.

e. Interactions based on both XME induction and cytotoxicity.

Our recent studies in this regard all point in the direction of a dose-dependent linkage between these two phenomena, with induction of XMEs at lower doses than those required to induce cytotoxicity. That being the case, exposure scenarios must become an important part of risk analysis of deployment-related chemicals.

e. Identification of individuals and populations at increased risk.

Identification of individuals at increased risk will depend on knowledge of their genotype with respect to XMEs, as well as knowledge of the other chemicals expected to be used during a particular circumstance and clinical drugs prescribed for the individual. Using these results and appropriate paradigms it will be possible to avoid individual or simultaneous exposures that might result in increased toxicity.

6. KEY RESEARCH ACCOMPLISHMENTS

👉 Analytical methods developed for the test compounds, chlorpyrifos, DEET, permethrin, pyridostigmine bromide, naphthalene, nonane and their metabolites as well as sulfur mustard metabolites, testosterone and estradiol have been made available and have been utilized in carrying out the extensive experiments described in this report. The most complete description to date of the human metabolism of an organophosphorus toxicant, chlorpyrifos has been carried out and published. Additional studies of human CYP3A4 polymorphisms involved in detoxication and activation of chlorpyrifos, have also been published.

👉 The first description of DEET metabolism by human enzymes has been accomplished and published, including identification of the CYP isoforms involved in the production of the two principal metabolites. Induction of XMEs by DEET and inhibition of DEET metabolism is also reported.

- ☞ A detailed outline of the human metabolism of permethrin has been developed and published. Monooxygenases do not appear to be involved, metabolism being initiated by hydrolysis, followed by metabolism of the resultant alcohol to the aldehyde by alcohol dehydrogenase and then to the acid by aldehyde dehydrogenase. This pathway has been confirmed by the use of purified human enzymes.
- ☞ In further studies of human metabolism of permethrin we have shown that chlorpyrifos oxon, the principal reactive metabolite of chlorpyrifos, is an inhibitor of permethrin hydrolysis in human liver preparations and that carbaryl, while less potent than chlorpyrifos, is also an inhibitor of this hydrolysis.
- ☞ It has become clear that chlorpyrifos and, by implication, other organophosphorus compounds, are potent inhibitors of the metabolism of other xenobiotics. Chlorpyrifos is shown to be a potent inhibitor of the human metabolism of DEET and the insecticide carbaryl.
- ☞ We have shown that chlorpyrifos and other organophosphorus chemicals are also potent inhibitors of the metabolism of testosterone and estradiol by human liver microsomes and by human CYP3A4.
- ☞ Studies of induction of XMEs based on the use of human hepatocytes, indicate that this technique is of importance in the investigation of metabolic interactions based on induction and providing human data for risk analysis.
- ☞ Studies of induction and cytotoxicity of deployment-related chemicals utilizing human hepatocytes indicate a dose-dependent linkage between these two phenomena.
- ☞ Preliminary genotyping studies suggesting a link between a polymorphism in the Ah-receptor gene and reported symptoms of Gulf War- Related Illness show the need for systematic studies in this area.
- ☞ As a result of all of the studies carried out, it is now possible to construct an overall inclusive picture of the possible metabolic interactions of a subset of deployment-related chemicals that is based, for the first time, on human studies. It will now be possible, based on this beginning, to expand this to include more chemicals and, perhaps of most importance, to predict possible interactions from chemicals proposed for future use.

7. REPORTABLE OUTCOMES

7.1 Publications.

Brimfield, A.A., A. M. Mancebo, R.P. Mason, J.J. Jiang, A.G.Siraki and M.J. Novak. 2008. Free Radical Production from the Interaction of 2-Chloroethyl Vesicants (Mustard Gas) with

Pyridine Nucleotide Driven Flavoprotein Electron Transport Systems. Submitted to Toxicol. App. Pharmacol.

Brimfield, A. A., M. J. Novak and E. Hodgson. 2006. Thioglycol, the hydrolysis product of sulfur mustard: analysis of in vitro biotransformation by mammalian alcohol dehydrogenase using nuclear magnetic resonance. Toxicol. Appl. Pharmacol. 213:207-215.

Casabar, R. C. T., A. A. Wallace, E. Hodgson and R. L. Rose. 2006. Metabolism of endosulfan-alpha by human liver microsomes and its utility as a simultaneous in vitro probe for CYP2B6 and CYP3A4. Drug Metabol. Disp. 34: 1779-1785.

Cho, T. M., R. L. Rose, and E. Hodgson. 2006. In vitro metabolism of naphthalene by human liver microsomal cytochrome P450 enzymes. Drug Metabol. Disp. 34: 176-183.

Cho, T. M., Rose, R. L. and Hodgson E. (2007) The effect of chlorpyrifos-oxon and other xenobiotics on the human cytochrome P450-dependent metabolism of naphthalene and DEET. Drug Metabol. Drug Interact. 22: 235-262.

Choi, J., Rose, R. L., and Hodgson, E. (2002). In vitro human metabolism of permethrin: the role of human alcohol and aldehyde dehydrogenases. Pesticide Biochem. Physiol. 73:117-128.

Choi, J., Hodgson, E. and Rose, R. L., 2004. Inhibition of trans-permethrin hydrolysis in human liver fractions by chlorpyrifos oxon and carbaryl. Drug Metabol. Drug Intereact. 20: 233-246.

Choi, K., H. Joo, R. L. Rose and E. Hodgson. Metabolism of chlorpyrifos and chlorpyrifos oxon by human hepatocytes. J. Biochem. Mol. Toxicol. 20:279-291.

Dai, D., Tang J., Rose, R. L., Hodgson, E., Bienstock, R. J., Mohrenweiser, H. W. and Goldstein, J. A. (2001). Identification of variants of CYP3A4 and characterization of their abilities to metabolize testosterone and chlorpyrifos. J. Pharmacol. Exptl. Therap. 299:825-831.

Das, P. C., Y. Cao, N. Cherrington, E. Hodgson and R.L. Rose. Fipronil induces CYP isoforms in human hepatocytes. Chemico-Biological Interactions. 164: 200-214.

Das, P. C., Cao, Y., Rose, R. L., Cherrington and Hodgson, E. Enzyme induction and cytotoxicity in human hepatocytes by chlorpyrifos and N,N-diethyl-m-toluamide (DEET). Drug Metabol. Drug Interact. **In press.**

Das, P. C., Streit, T. M., Cao, Y., Rose, R. L., Cherrington, N. Ross, M. K., Wallace, A. D. and Hodgson, E. Pyrethroids: cytotoxicity and induction of CYP isoforms in human hepatocytes. Drug Metabol. Drug Interact. **In press.**

Edwards, J. E., Rose, R. L. and Hodgson, E. 2005. The metabolism of nonane, a JP-8 jet fuel component, by human liver microsomes, P450 isoforms and alcohol dehydrogenase and inhibition of human P450 isoforms by JP-8. 2005. Chem.-Biol. Interact. 151:203-211.

Hodgson, E. and Rose, R. L. 2005. Human metabolism and metabolic interactions of deployment-related chemicals. *Drug Metabol. Rev.* 37:1-39.

Joo, H., Choi, K., Rose, R. L. and Hodgson, E. (2007) Inhibition of fipronil and n-nonane metabolism in human liver microsomes and human cytochrome P450 (CYP) isoforms by chlorpyrifos. *J. Biochem. Mol. Toxicol.* 21:76-80.

Lee, S. J., Usmani, K. A., Chanas, B., Ghanayem, B., Xi, T., Hodgson, E., Mohrenweiser, H. W and Goldstein, J. A., 2003. Genetic findings and functional studies of human CYP3A5 single nucleotide polymorphisms in different ethnic groups. *Pharmacogenetics* 13: 461-472.

Novak, M.J and A.A.Brimfield 2006. NMR Analysis of Thiodiglycol Oxidation by Mammalian Alcohol Dehydrogenase. *Current Protocols in Toxicology*, 4.20.1 – 4.20.13. .

Tang, J., Cao, Y., Rose, R. L., Brimfield, A. A., Dai, D., Goldstein, J. A. and Hodgson, E. (2001) Metabolism of chlorpyrifos by human cytochrome P450 isoforms and human, mouse and rat liver microsomes. *Drug Metabol. Disp.* 29:1201-1204.

Tang, J. Y. Cao, R. L. Rose and E. Hodgson. (2002). In vitro metabolism of carbaryl by human cytochrome P450 and its inhibition by chlorpyrifos. *Chem.-Biol. Interact.* 141:229-241.

Tang, J., Usmani, K. A., Hodgson, E. and Rose R. L. 2004 In vitro metabolism of fipronil by human and rat cytochrome P450 and its interactions with testosterone and diazepam. *Chem.-Biol. Interact.* 147: 319-329.

Usmani, K. A., Rose, R. L., Goldstein, J. A., Taylor, W. G., Brimfield, A. A. and Hodgson, E. (2002). In vitro human metabolism and interactions of the repellent, N,N-diethyl-m-toluamide (DEET). *Drug Metabol. Disp.* 30:289-294.

Usmani, K. A., Rose, R. L. and Hodgson, E. (2003). Inhibition and activation of the human liver and human cytochrome P450 3A4 metabolism of testosterone by deployment-related chemicals. *Drug. Metabol. Disp.* 31:384-391.

Usmani, K. A., T. M. Cho, R. L. Rose and E. Hodgson. 2006. Inhibition of the human liver microsomal and human cytochrome P450 1A2 and 3A4 metabolism of estradiol by deployment-related and other chemicals. *Drug Metabol. Disp.* 34:1606-1614.

7.2 **Presentations.**

Brimfield, A.A., J.R. Smith and M.J. Novak. 2000. Identification of Oxidation Products Produced by Mammalian Alcohol Dehydrogenase from Thiodiglycol *In Vitro*. Abstract # 232. Annual Meeting SOT. Philadelphia, PA. March 11-23.

Brimfield, A.A. 2000. Progress in Understanding the Mechanism of Vesication by Sulfur Mustard. Invited presentation , Chemical and Biological Defence Establishment, Porton Down, Salisbury, Wiltshire, November 23-25.

Tang, J. Y. Cao, S. Coleman, R. L. Rose, J. A. Goldstein, and E. Hodgson. In vitro metabolism of chlorpyrifos by human liver microsomes and human cytochrome P450 isoforms. International Society for the Study of Xenobiotics, 2000.

Tang, J., Cao, Y., Rose, R. L., Brimfield, A. A., Goldstein, J. A. and Hodgson, E. 2001. Metabolic activity of human cytochrome P450 isoforms toward chlorpyrifos. *The Toxicologist* 60: Abstract 242. SOT, San Francisco, 2001.

Usmani, K.A., R.L. Rose, J.A. Goldstein, and E. Hodgson. Metabolism of diethyl toluamide (DEET) by pooled human liver microsomes and human cytochrome P450 isoforms. Conference on Illnesses Among Gulf War Veterans: A Decade of Scientific Research. Alexandria, VA. Jan. 24-26, 2001.

J. Tang, Y. Cao, R.L. Rose, A.A. Brimfield, J.A. Goldstein, and E. Hodgson. Differential activities of chlorpyrifos metabolism in human liver microsomes and cytochrome P450 isoforms. Conference on Illnesses Among Gulf War Veterans: A Decade of Scientific Research. Alexandria, VA. Jan. 24-26, 2001.

Rose, R.L., N.J. Cherrington, J. Tang, Y. Cao, D.P. Hartley, C.D. Klaassen, and E. Hodgson. Induction of CYP isoforms by pesticides and DEET as monitored by the bDNA assay. *The Toxicologist* 66:599, 2002.

Usmani, K. A., Rose, R. L., Goldstein, J. A., Taylor, W. G., Brimfield, A. A. and Hodgson, E. Metabolism of diethyl toluamide (DEET) by human, mouse and rat liver microsomes, human cytochrome P450 isoforms, and interactions with other Gulf War chemicals. *Bioscience 2002 Medical Defense Review*.

Choi, J., Rose, R. L. and Hodgson, E. Permethrin: analytical method and human metabolism. *Bioscience 2002 Medical Defense Review*.

Usmani, K.A., R.L. Rose, J.A. Goldstein, W.G. Taylor, A.A. Brimfield and E. Hodgson. In vitro metabolism of diethyl toluamide (DEET) by human, mouse, and rat liver microsomes, human cytochrome P450 isoforms, and interaction of DEET with chlorpyrifos. *The Toxicologist* 66:1130 (2002).

Tang, J., Y. Cao, R.L. Rose, and E. Hodgson. In vitro metabolism of carbaryl by human liver microsomes and human cytochrome P450 isoforms. *The Toxicologist* 66:1125 (2002).

Choi, J. R.L. Rose, and E. Hodgson. An HPLC method for the determination of major permethrin metabolites and permethrin metabolism in human liver. *The Toxicologist* 66:1565, 2002.

Usmani, K.A., R.L. Rose, and E. Hodgson. Effects of various chemicals on metabolism of testosterone by human liver microsomes and human cytochrome P450 3A4. International Society for the Study of Xenobiotics. Orlando, FL. October 27 - 31, 2002.

Brimfield, A.A., D.A. Sartori and M.J. Novak. 2002. Thiodiglycol Metabolism by Alcohol Dehydrogenase Using NMR: Two Step Oxidation Produces 2-Hydroxy- ethylthioacetic Acid and 2 Moles of NADH. Toxicological Sci. 66(1S): 230 SOT Nashville, TN.

J. Choi, R. L. Rose, and E. Hodgson. Chlorpyrifos oxon and carbaryl inhibition of trans-permethrin hydrolysis in human liver. Society of Toxicology Annual Meeting, Salt Lake City, March, 2003.

J. Tang, K. A. Usmani, E. Hodgson and R. L. Rose. In vitro study of fipronil metabolism and its metabolic interaction with testosterone. ISSX, Providence RI. Drug Metabol. Disp. 35:361. 2003.

Brimfield, A.A. 2004. Sulfur Mustard: Searching for the Primary Biochemical Lesion. U.S. Army Medical Research Institute of Chemical Defense Bioscience Review, Hunt Valley Maryland, June 7-12.

K. A. Usmani, R. L. Rose and E. Hodgson. Effects of deployment-related chemicals on metabolism of estradiol by human liver microsomes , CYP3A4 and CYP1A2. Abstract 312, 7th International ISSX Meeting. 2004.

J. E. Edwards, R. L. Rose and E. Hodgson. In vitro metabolism of nonane by human liver microsomes and cytochrome P450 isoforms. Abstract 313, 7th International ISSX Meeting. 2004.

J. Tang, A. Usmani, E. Hodgson, R.L. Rose. Study of metabolic interactions of fipronil and some CYP3A4 substrates. 43rd Annual Meeting of the Society of Toxicology, Baltimore, MD, March 21-25, 2004.

Brimfield, A.A. and E. Hodgson. 2005. Observations on the Interaction of Sulfur Mustard with Cytochrome P450 Annual Meeting SOT, New Orleans, March 6 to 10.

Cho, T.M., R.L. Rose, and E. Hodgson. Human naphthalene metabolism. Society of Toxicology, 44th Annual Meeting, New Orleans, LA. March 6-10, 2005.

Usmani, K.A., R.L. Rose and E. Hodgson. Inhibition of the human liver microsomal and human cytochrome P450 1A2 and 3A4 metabolism of estradiol by deployment-related chemicals. Society of Toxicology, 44th Annual Meeting, New Orleans, LA. March 6-10, 2005.

Cho, T.M., R.L. Rose and E. Hodgson. Activation and inhibition of naphthalene and N,N-diethyl-m-toluamide (DEET) metabolism in human liver microsomes and cytochrome P450 isoforms by chlorpyrifos-oxon. International Society for the Study of Xenobiotics, Maui, HI. October, 2005. Drug Metab. Rev. 37:461.

P. C. Das, N. Cherrington, Y. Cao, E. Hodgson and R. L. Rose. Fipronil induces CYP3A4, CYP2B6 and CYP1A2 gene expression and apoptosis in human hepatocytes. Annual Meeting, Society of Toxicology. San Diego CA. 2006.

A.M. Mancebo and A.A. Brimfield. 2006. Interaction of Sulfur Mustard with NADPH-Cytochrome P450 Reductase and Various Cytochrome P450 Isoforms. Annual Meeting SOT, San Diego, CA, March 5-9.

Brimfield, A.A., M.J. Novak, B.S. Gallagher, A.M. Mancebo and C.M. Arroyo. 2006 The Detection of Free Radical Formation from the Interaction of Sulfur Mustard with NADPH-Cytochrome P450 Reductase. Annual Meeting SOT, San Diego, CA. March 5-9.

Brimfield, A.A., M.J. Novak, B.S. Gallagher, A.M. Mancebo and C.M. Arroyo. 2006 The Detection of Free Radical Formation from the Interaction of Sulfur Mustard with NADPH-Cytochrome P450 Reductase. Annual Meeting SOT, San Diego, CA. March 5-9.

T. M. Cho, R. L. Rose and E. Hodgson. Modification of cytochrome P450 3A4 metabolism of naphthalene and 17 β -estradiol by organophosphorus compounds. Annual Meeting. Society of Toxicology. Charlotte NC. 2007.

H. Joo, K. Chopi, R. L. Rose and E. Hodgson. Inhibition of the human metabolism of fipronil and nonane chlorpyrifos. Annual Meeting. Society of Toxicology. Charlotte NC. 2007.

P. C. Das, E. Hodgson, Y. Cao, N. Cherrington and R. L. Rose. Cytotoxicity and CYP modulation in deltamethrin and permethrin treated human hepatocytes. Annual Meeting. Society of Toxicology. Charlotte NC. 2007.

K. Choi, E. Hodgson, H. Joo and R. L. Rose. Metabolism of chlorpyrifos by human hepatocytes.. Annual Meeting. Society of Toxicology. Charlotte NC. 2007.

A.A. Brimfield and A.M. Mancebo. 2007. Monofunctional Mustards Form Free Radicals when Enzymatically Reduced Making them Useful as Model Compounds for Mechanistic Study and Drug Screening. Annual Meeting SOT. Charlotte, NC. March 25 to 29.

R. C. Casabar, P. C. Das, G. DeKrey, C. S. Gardiner, E. Hodgson, R. L. Rose and A. D. Wallace. Endosulfan-alpha induces CYP2B6 and CYP3A4 by activating the pregnane X receptor (PXR). Annual Meeting. Society of Toxicology. Charlotte NC. 2007.

A.A. Brimfield and A.M. Mancebo. 2008. Thioredoxin Reductase Reduces Sulfur Mustard *In Vitro* to Yield Carbon-based Free Radicals. Annual Meeting SOT. Seattle, WA. March 16 to 20.

8. CONCLUSIONS AND RECOMMENDATIONS

8.1 Conclusions

HPLC analytical methods for chlorpyrifos, DEET, permethrin, pyridostigmine and their metabolites, sulfur mustard metabolites, and testosterone have been brought on line and have been used in several metabolic studies. The human cytochrome P450 isoforms metabolizing chlorpyrifos and DEET have been identified and include forms known to be inducible and forms known to be polymorphic. It has been established that pyridostigmine and permethrin are not significant substrates for human monooxygenases. While pyridostigmine does not appear to be readily metabolized, permethrin has been shown to be metabolized, in humans, through a series of reactions involving hydrolytic enzymes, followed by alcohol dehydrogenase and aldehyde dehydrogenase. Specific purified isoforms of human alcohol and aldehyde dehydrogenases have been shown to be active in these reactions. The reactive metabolite of chlorpyrifos, chlorpyrifos oxon, is a potent inhibitor of permethrin hydrolysis while carbaryl is a less potent inhibitor of this reaction. Chlorpyrifos is shown to be a potent inhibitor of DEET metabolism, the metabolism of the insecticide, carbaryl, and is a potent inhibitor of the metabolism of testosterone and estradiol. It is clear that chlorpyrifos and other organophosphorus compounds, may be significant both in health related interactions between different deployment- related chemicals and in the determination of sub-populations and individuals at increased risk from anticholinergic chemicals.

Even within this very small subset of deployment-related chemicals, essentially all interact with at least one other or with an endogenous metabolite at the metabolic level: chlorpyrifos inhibits the metabolism of DEET, testosterone and carbaryl; chlorpyrifos oxon, the principal reactive metabolite of chlorpyrifos, inhibits the hydrolysis of permethrin; DEET is an inducer of XMEs in human hepatocytes. The potential for interactions is obvious and it should also be noted that essentially all of the XMEs involved are polymorphic and several are inducible, making human variation, both genotypic and phenotypic, important in the expression of toxicity of toxicity.

These studies permit more confident extrapolation of past and future animal studies to humans and have permitted identification of interactions not apparent from animal studies. Perhaps even more important, they open the way to molecular genetic studies that will permit identification of human sub-populations at greater risk from specific xenobiotic toxicants and will produce specific analytic methodologies for assessment of future exposures.

It is now apparent that induction studies previously requiring the use of experimental animals may be accomplished directly with human materials. We continue to explore the possibility that newer techniques that maintain the capacity for induction in cultured human hepatocytes combined with microarray techniques for determination of gene expression and repression may substitute for the proposed animal studies. Our studies indicate that this is a viable approach, that should be used, in lieu of hepatocytes from experimental animals, in risk analysis of deployment-related chemicals.

It is also apparent that genotyping studies will also be invaluable in the determination of sub-populations and individuals at increased risk from deployment-related chemicals and their interactions.

8.2. Recommendations

- a. In view of the special needs of military deployments and their different exposure scenarios it is recommended that formal risk analysis be carried out for all deployment-related chemicals, including not only those used for vector control (pesticides and repellants) but also industrial chemicals such as fuels, lubricants, etc.
- b. It is also recommended that, to improve the quality of these analyses, increased emphasis be placed on human studies.
- c. The U. S. Army should consider carrying out, or supporting, genotyping and microarray studies.

9. REFERENCES

- Anslow, W.P., D.A. Karnofsky, B.J. Jager and H.W. Smith. 1948. The Intravenous, Subcutaneous and Cutaneous Toxicity of *bis* (\exists -Chloroethyl) Sulfide (Mustard Gas) and of Various Derivatives. *J. Pharmacol. Exp. Therap.* 93: 1-9.
- Assaf, P., J. Katzhendler and A.I. Haj-Yehia. 2000. 2-(4-Carboxyphenyl)-6-N,N-diethylaminobenzofuran: a useful reagent for the sensitive determination of alcohols by high-performance liquid chromatography with fluorimetric detection. *J. Chromatog. A.* 869:243-250.
- Bast G.E., Taeschner, D., Kampffmeyer, H.G. 1997. *Arch. Toxicol.* 71:179.
- Bradford, M. M. 1976. A rapid and sensitive method for quantification of microgram quantities of protein utilizing the principle of protein-dye binding. *Anal. Biochem.* 72: 248-254.
- Brimfield, A.A., J.R. Smith and M.J. Novak. 2000. Identification of Oxidation Products Produced by Mammalian Alcohol Dehydrogenase from Thiodiglycol *In Vitro*. Abstract # 232. Annual Meeting SOT. Philadelphia, PA. March 11-23.
- Brimfield, A.A. 2000. Progress in Understanding the Mechanism of Vesication by Sulfur Mustard. Invited presentation , Chemical and Biological Defence Establishment, Porton Down, Salisbury, Wiltshire, November 23-25.
- Brimfield, A.A. and E. Hodgson. 2005. Observations on the Interaction of Sulfur Mustard with Cytochrome P450 Annual Meeting SOT, New Orleans, March 6 to 10.
- Brimfield, A. A. and A.M. Mancebo. 2007. Monofunctional Mustards Form Free Radicals when Enzymatically Reduced Making them Useful as Model Compounds for Mechanistic Study and Drug Screening. Annual Meeting SOT. Charlotte, NC. March 25 to 29.

Brimfield, A. A. and A.M. Mancebo. 2008. Thioredoxin Reductase Reduces Sulfur Mustard *In Vitro* to Yield Carbon-based Free Radicals. Annual Meeting SOT. Seattle, WA. March 16 to 20.

Brimfield, A.A., A. M. Mancebo, R.P. Mason, J.J. Jiang, A.G.Siraki and M.J. Novak. 2008. Free Radical Production from the Interaction of 2-Chloroethyl Vesicants (Mustard Gas) with Pyridine Nucleotide Driven Flavoprotein Electron Transport Systems. Submitted to Toxicol. App. Pharmacol.

Brimfield, A.A., M.J. Novak, B.S. Gallagher, A.M. Mancebo and C.M. Arroyo. 2006 The Detection of Free Radical Formation from the Interaction of Sulfur Mustard with NADPH-Cytochrome P450 Reductase. Annual Meeting SOT, San Diego, CA. March 5-9.

Brimfield, A.A., D.A. Sartori and M.J. Novak. 2002. Thiodiglycol Metabolism by Alcohol Dehydrogenase Using NMR: Two Step Oxidation Produces 2-Hydroxy-ethylthioacetic Acid and 2 Moles of NADH. Toxicological Sci. 66(1S): 230 SOT Nashville, TN.

Brimfield, A.A. 2004. Sulfur Mustard: Searching for the Primary Biochemical Lesion. U.S. Army Medical Research Institute of Chemical Defense Bioscience Review, Hunt Valley Maryland, June 7-12.

Brimfield, A.A., M.J. Novak, B.S. Gallagher, A.M. Mancebo and C.M. Arroyo. 2006 The Detection of Free Radical Formation from the Interaction of Sulfur Mustard with NADPH-Cytochrome P450 Reductase. Annual Meeting SOT, San Diego, CA. March 5-9.

Brimfield, A. A., M. J. Novak and E. Hodgson. 2006. Thioglycol, the hydrolysis product of sulfur mustard: analysis of in vitro biotransformation by mammalian alcohol dehydrogenase using nuclear magnetic resonance. Toxicol. Appl. Pharmacol. 213:207-215.

Burke, M. D. and Mayer, R. T. 1974. Ethoxyresorufin: direct fluorimetric assay of a microsomal O-dealkylation which is preferentially inducible by 3-methylcholanthrene. Drug Metabol. Disp. 2: 583- 588.

Casabar, R. C. T., A. A. Wallace, E. Hodgson and R. L. Rose. 2006. Metabolism of endosulfan-alpha by human liver microsomes and its utility as a simultaneous in vitro probe for CYP2B6 and CYP3A4. Drug Metabol. Disp. 34: 1779-1785.

Chen C.S. and Yoshida A. 1991. Enzymatic aproperties of the protein encoded by newly cloned human alcohol dehydrogenase ADH6 gene. *Biochemical and Biophysical Research Communication* 181:743-747.

Cho, T. M., R. L. Rose, and E. Hodgson. 2006. In vitro metabolism of naphthalene by human liver microsomal cytochrome P450 enzymes. Drug Metabol. Disp. 34: 176-183.

- Cho, T. M., Rose, R. L. and Hodgson E. 2007. The effect of chlorpyrifos-oxon and other xenobiotics on the human cytochrome P450-dependent metabolism of naphthalene and DEET. *Drug Metabol. Drug Interact.* 22: 235-262.
- Choi, J., Hodgson, E. and Rose, R. L., 2004. Inhibition of trans-permethrin hydrolysis in human liver fractions by chlorpyrifos oxon and carbaryl. *Drug Metabol. Drug Intereact.* 20: 233-246.
- Choi, J., Rose, R. L., and Hodgson, E. 2002. In vitro human metabolism of permethrin: the role of human alcohol and aldehyde dehydrogenases. *Pesticide Biochem. Physiol.* 73:117-128.
- Choi, K., H. Joo, R. L. Rose and E. Hodgson. 2006. Metabolism of chlorpyrifos and chlorpyrifos oxon by human hepatocytes. *J. Biochem. Mol. Toxicol.* 20:279-291.
- Cook, J.C. and E. Hodgson. 1983. Induction of cytochrome P450 by methylenedioxyphenyl compounds: Importance of the methylene carbon. *Toxicol. Appl. Pharmacol.* 68:131-139.
- Dai, D., Tang J., Rose, R. L., Hodgson, E., Bienstock, R. J., Mohrenweiser, H. W. and Goldstein, J. A. 2001. Identification of variants of CYP3A4 and characterization of their abilities to metabolize testosterone and chlorpyrifos. *J. Pharmacol. Exptl. Therap.* 299:825-831.
- Das, P. C., Y. Cao, N. Cherrington, E. Hodgson and R.L. Rose. 2006. Fipronil induces CYP isoforms in human hepatocytes. *Chemico-Biological Interactions.* 164: 200-214.
- Das, P. C., Cao, Y., Rose, R. L., Cherrington and Hodgson, E. 2008. Enzyme induction and cytotoxicity in human hepatocytes by chlorpyrifos and N,N-diethyl-m-toluamide (DEET). *Drug Metabol. Drug Interact.* **In press.**
- Das, P. C., Streit, T. M., Cao, Y., Rose, R. L., Cherrington, N. Ross, M. K., Wallace, A. D. and Hodgson, E. 2008. Pyrethroids: cytotoxicity and induction of CYP isoforms in human hepatocytes. *Drug Metabol. Drug Interact.* **In press.**
- Dudley, B.F., A.A. Brimfield and G.W. Winston. 2000. Oxidation of Thiodiglycol by Alcohol Dehydrogenase: Comparison of Human Isoenzymes. *J. Biochem. Molec. Toxicol.* 14: 244-251.
- Edwards, J. E., Rose, R. L. and Hodgson, E. 2005. The metabolism of nonane, a JP-8 jet fuel component, by human liver microsomes, P450 isoforms and alcohol dehydrogenase and inhibition of human P450 isoforms by JP-8. 2005. *Chem.-Biol. Interact.* 151:203-211.
- Emoto, C., H. Yamazaki, S. Yamasaki, N. Shimada, M. Nakajima and T. Yokoi. 2000. Characterization of Cytochrome P450 Enzymes Involved in Drug Oxidations in Mouse Intestinal Microsomes. *Xenobiotica.* 30: 943-953.
- Friedberg, K.D., K Mengel and E. Schlick. 1983. The Action of Azimexone on the Cells of the Hematopoietic System in Mice, Especially After Damage with X-Rays. *Radiat. Environ. Biophys.* 22: 117-131.

GraphPad software version 1.03, San Diego CA USA.

Haley, R. W. and Kurt, T. L. 1997. Self-reported exposure to neurotoxic chemical combinations in the Gulf War – a cross sectional epidemiological study. *J. Amer. Med. Assoc.* 277: 231-237.

Hartley, D. P. and Klaassen, C. D. 2000. Detection of chemical-induced differential expression of rat hepatic cytochrome P450 transcripts using branched signal amplification technology. *Drug Metabol. Disp.* 28: 608-616.

Hodgson, E. and Rose, R. L. 2005. Human metabolism and metabolic interactions of deployment-related chemicals. *Drug Metabol. Rev.* 37:1-39.

Hodgson, E. and Rose R. L. 2006. Organophosphorus chemicals: potent inhibitors of the human metabolism of steroid hormones and xenobiotics. *Drug. Metabol. Rev.* 38: 149-162.

Hodgson, E. and Rose, R. L. 2007a. The importance of cytochrome P450 2B6 (CYP2B6) in the human metabolism of environmental chemicals. *Pharmacol. Therap.* 113:420-428.

Hodgson, E. and Rose, R. L. 2007b. Human metabolic interactions of environmental chemicals. *J. Biochem. Mol. Toxicol.* 21:182-186.

Hodgson, E. Wallace, A. D and Brimfield, A. A. 2009. Human metabolism and metabolic interactions of deployment-related chemicals: *in preparation* for submission to *Drug Metabol. Rev.*

Hurley T.D., Steinmetz C.G., Xie P. and Yang Z.N. 1997. In *Enzymology and Molecular Biology of Carbonyl Metabolism 6* edited by Weiner H, Lindahl R, Crabb D.W. and Flynn T.G. Plenum Press, New York. pp291-302.

Joo, H., Choi, K., Rose, R. L. and Hodgson, E. 2007. Inhibition of fipronil and n-nonane metabolism in human liver microsomes and human cytochrome P450 (CYP) isoforms by chlorpyrifos. *J. Biochem. Mol. Toxicol.* 21:76-80.

Koop, D. R. 1986. Hydroxylation of p-nitrophenol by rabbit ethanol-inducible cytochrome P450_{3A}. *Mol. Pharmacol.* 29: 399-404.

Lee, S. J., Usmani, K. A., Chanas, B., Ghanayem, B., Xi, T., Hodgson, E., Mohrenweiser, H. W and Goldstein, J. A., 2003. Genetic findings and functional studies of human CYP3A5 single nucleotide polymorphisms in different ethnic groups. *Pharmacogenetics* 13: 461-472.

Leo, K. U. 1997. Metabolism of proposed nerve agent pretreatment, pyridostigmine bromine. Walter Reed Army Institute of Research Report No. NTIS/AD-A323 848/2. Available from NTIS at 800 553-6847, Washington DC.

- Li, A. P., Maurel, P., Gomez-Lechon, M. J., Cheng, L. C. and Jurima-Romet, M. 1997. Preclinical evaluation of drug-drug interaction potential: present status of the application of primary human hepatocytes in the evaluation of cytochrome P450 induction. *Chem. Biol. Interact.* 107: 5-16.
- Lubet, R. A., Mayer, R. T., Cameron, J. W., Nims, R. W., Burke, M. D., Wold, T. and Guengerich, F. P. 1985. Dealkylation of pentoxyresorufin: a rapid and sensitive assay for measuring induction of cytochrome(s) P450 by Phenobarbital and other xenobiotics in the rat. *Arch. Biochem. Biophys.* 238: 43-48.
- Mancebo, A. M. and A.A. Brimfield. 2006. Interaction of Sulfur Mustard with NADPH-Cytochrome P450 Reductase and Various Cytochrome P450 Isoforms. Annual Meeting SOT, San Diego, CA, March 5-9.
- McMaster, P.D. and G. Hogeboom. 1942. The Toxicity of DH for Mice. Monthly report of NDRC Contract B4-C, The Rockefeller Institute, August 28.
- Nerurkar, P. V., Park, S. S., Thomas, P. E., Nims, R. W. and Lubet, R. A. 1993. Methoxyresorufin and benzyloxyresorufin – substrates preferentially metabolized by cytochrome P4501A2 and cytochrome P450 2B, respectively, in rat and mouse. *Biochem. Pharmacol.* 46: 933-943.
- Novak, M.J and A.A.Brimfield 2006. NMR Analysis of Thiodiglycol Oxidation by Mammalian Alcohol Dehydrogenase. *Current Protocols in Toxicology*, 4.20.1 – 4.20.13.
- Omura, T. and Sato, R. 1964. The carbon-monoxide binding pigment of liver microsomes. II. Solubilization, purification and properties. *J. Biol. Chem.* 239: 2379-2385.
- Pohl, R. J. and Fouts, J. R. 1980. A rapid method for assaying the metabolism of 7-ethoxyresorufin by microsomal subcellular fractions. *Anal. Biochem.* 107: 150-155.
- Purdon, M. P. and Lehman-McKeeman, L. D. 1997. Improved high-performance liquid chromatographic procedure for the separation and quantification of hydroxytestosterone metabolites. *J. Pharmacol. Toxicol. Methods* 37:67-73.
- Sabourin, P. J., Smyser, B. P. and Hodgson, E. 1984. Purification of the flavin-containing monooxygenase from mouse and pig liver microsomes. *Int. J. Biochem.* 16: 713-720.
- Segal, I. H., 1975. *Biochemical Calculations*. John Wiley and Sons. New York.
- Smart, R. C. and Hodgson, E. (eds). 2008. *Molecular and Biochemical Toxicology*. 4th edition. John Wiley and Sons. Hoboken, New Jersey.

Stone C.L, Bosron W.F. and Dunn M.F. 1993. Amino acid substitutions at position 47 of $\beta_1\beta_1$ and $\beta_2\beta_2$ human and alcohol dehydrogenases affect hydridetransfer and coenzyme dissociation rate constants. *The Journal of Biological Chemistry*. 268:892-899.

Suchar LA, Chang RL, Rosen RT, Lech J and Conney AH 1995. High-performance liquid chromatography separation of hydroxylated estradiol metabolites: formation of estradiol metabolites by liver microsomes from male and female rats. *J Pharmacol Exp Ther* **272**:197-206.

Tang, J., Cao, Y., Rose, R. L., Brimfield, A. A., Goldstein, J. A. and Hodgson, E. 2001. Metabolic activity of human cytochrome P450 isoforms toward chlorpyrifos. *The Toxicologist* 60: Abstract 242. SOT, San Francisco, 2001.

Tang, J. Y. Cao, R. L. Rose and E. Hodgson. (2002). In vitro metabolism of carbaryl by human cytochrome P450 and its inhibition by chlorpyrifos. *Chem.-Biol. Interact.* 141:229-241.

Tang, J., Usmani, K. A., Hodgson, E. and Rose R. L. 2004. In vitro metabolism of fipronil by human and rat cytochrome P450 and its interactions with testosterone and diazepam. *Chem.-Biol. Interact.* 147: 319-329.

Usmani, K. A., Rose, R. L., Goldstein, J. A., Taylor, W. G., Brimfield, A. A. and Hodgson, E. 2002. In vitro human metabolism and interactions of the repellent, N,N-diethyl-m-toluamide (DEET). *Drug Metabol. Disp.* 30:289-294.

Usmani, K. A., Rose, R. L. and Hodgson, E. 2003. Inhibition and activation of the human liver and human cytochrome P450 3A4 metabolism of testosterone by deployment-related chemicals. *Drug. Metabol. Disp.* 31:384-391.

K. A. Usmani, T. M. Cho, R. L. Rose and E. Hodgson. 2006. Inhibition of the human liver microsomal and human cytochrome P450 1A2 and 3A4 metabolism of estradiol by deployment-related and other chemicals. *Drug Metabol. Disp.* 34:1606-1614.

Wagner F.W., Burger A.R. and Vallee B.L 1983. Kinetic properties of human liver alcohol dehydrogenase: oxidation of alcohols by class I isoenzymes. *Biochemistry* 22:1857-1863.

10. Personnel Paid on DAMD17-00-2-0008

1999 – 2000 Hodgson, Ernest
 Rose, Randy L.
 Usmani, K. A.

2000 – 2001 Choi, Jonghoon
 Hodgson, Ernest
 Rose, Randy L.
 Usmani, K. A.

- 2001 – 2002 Choi, Jonghoon
Hodgson, Ernest
Rose, Randy L.
Usmani, K. A.
- 2002 - 2003 Hodgson, Ernest
Rose, Randy L.
Usmani, K. A.
- 2003 – 2004 Cho, Taehyeon Matthew
Edwards, Jeffrey
Hodgson, Ernest
Tang, Jun
Usmani, K. A.
- 2004– 2005 Cho, T.M.
Choi, K.
Das, K. P.
Edwards, J.
Usmani, K. A.
- 2005 – 2006 Cao, Yan
Cho, T. M.
Choi, K.
- 2006 – 2007 Cao, Yan
Cho, T. M.
Choi, K.
Hodgson, E.
Joo, H.
- 2007 – 2008 Cao, Yan
Choi, K.
Das, P.
Hodgson, E.
Joo, H.
- 2008 – 2009 One month (July, 2008) only.
Cao, Yan
Choi, K.
Croom, E.
Das, P.
Hodgson, E.

11. APPENDICES

Appendix 1.

Das, P. C., Streit, T. M., Cao, Y., Rose, R. L., Cherrington, N. Ross, M. K., Wallace, A. D. and Hodgson, E. 2008. Pyrethroids: cytotoxicity and induction of CYP isoforms in human hepatocytes. *Drug Metabol. Drug Interact.* **In press.**
DAMD17-00-2-008 At1.pdf

Appendix 2.

Das, P. C., Cao, Y., Rose, R. L., Cherrington and Hodgson, E. 2008. Enzyme induction and cytotoxicity in human hepatocytes by chlorpyrifos and N,N-diethyl-m-toluamide (DEET). *Drug Metabol. Drug Interact.* **In press.**
DAMD17-00-2-0008 At2.pdf

Appendix 3.

Cho, T. M., Rose, R. L. and Hodgson E. (2007) The effect of chlorpyrifos-oxon and other xenobiotics on the human cytochrome P450-dependent metabolism of naphthalene and DEET. *Drug Metabol. Drug Interact.* 22: 235-262.
DAMD17-00-2-0008 At3.pdf

Appendix 4.

Choi, J., Rose, R. L., and Hodgson, E. (2002). In vitro human metabolism of permethrin: the role of human alcohol and aldehyde dehydrogenases. *Pesticide Biochem. Physiol.* 74:117-128.
DAMD17-00-2-0008 At4.pdf

Appendix 5.

Usmani, K. A., Rose, R. L., Goldstein, J. A., Taylor, W. G., Brimfield, A. A. and Hodgson, E. (2002). In vitro human metabolism and interactions of the repellent, N,N-diethyl-m-toluamide (DEET). *Drug Metabol. Disp.* 30:289-294.
DAMD17-00-2-0008 At5.pdf

Appendix 6.

Usmani, K. A., Rose, R. L. and Hodgson, E. (2003). Inhibition and activation of the human liver and human cytochrome P450 3A4 metabolism of testosterone by deployment-related chemicals. *Drug. Metabol. Disp.* 31:384-391.
DAMD17-00-2-0008 At 6.pdf

Appendix 7.

Usmani, K. A., T. M. Cho, R. L. Rose and E. Hodgson. 2006. Inhibition of the human liver microsomal and human cytochrome P450 1A2 and 3A4 metabolism of estradiol by deployment-related and other chemicals. *Drug Metabol. Disp.* 34:1606-1614.
DAMD17-00-2-0008 At7.pdf

Appendix 8.

Tang, J., Cao, Y., Rose, R. L., Brimfield, A. A., Dai, D., Goldstein, J. A. and Hodgson, E. (2001) Metabolism of chlorpyrifos by human cytochrome P450 isoforms and human, mouse and rat liver microsomes. *Drug Metabol. Disp.* 29:1201-1204.

DAMD17-00-2-0008 At8.pdf

Appendix 9.

Casabar, R. C. T., A. A. Wallace, E. Hodgson and R. L. Rose. 2006. Metabolism of endosulfan-alpha by human liver microsomes and its utility as a simultaneous in vitro probe for CYP2B6 and CYP3A4. *Drug Metabol. Disp.* 34: 1779-1785.

DAMD17-00-2-0008 At9.pdf

Appendix 10.

Cho, T. M., R. L. Rose, and E. Hodgson. 2006. In vitro metabolism of naphthalene by human liver microsomal cytochrome P450 enzymes. *Drug Metabol. Disp.* 34: 176-183.

DAMD17-00-2-0008 At10.pdf

Appendix 11.

Hodgson, E. and Rose, R. L. 2005. Human metabolism and metabolic interactions of deployment-related chemicals. *Drug Metabol. Rev.* 37:1-39.

DAMD-00-2-0008 At11.pdf

Appendix 12.

Brimfield, A. A., M. J. Novak and E. Hodgson. 2006. Thioglycol, the hydrolysis product of sulfur mustard: analysis of in vitro biotransformation by mammalian alcohol dehydrogenase using nuclear magnetic resonance. *Toxicol. Appl. Pharmacol.* 213:207-215.

DAMD17-00-2-0008 At12.pdf

Appendix 13.

Choi, K., H. Joo, R. L. Rose and E. Hodgson. Metabolism of chlorpyrifos and chlorpyrifos oxon by human hepatocytes. *J. Biochem. Mol. Toxicol.* 20:279-291.

DAMD17-00-2-0008 At13.pdf

Appendix 14.

Joo, H., Choi, K., Rose, R. L. and Hodgson, E. (2007) Inhibition of fipronil and n-nonane metabolism in human liver microsomes and human cytochrome P450 (CYP) isoforms by chlorpyrifos. *J. Biochem. Mol. Toxicol.* 21:76-80.

DAMD17-00-2-0008 At14.pdf

Appendix 15.

Dai, D., Tang J., Rose, R. L., Hodgson, E., Bienstock, R. J., Mohrenweiser, H. W. and Goldstein, J. A. (2001). Identification of variants of CYP3A4 and characterization of their abilities to metabolize testosterone and chlorpyrifos. *J. Pharmacol. Exptl. Therap.* 299:825-831.

DAMD17-00-2-0008 At15.pdf

Appendix 17.

Edwards, J. E., Rose, R. L. and Hodgson, E. 2005. The metabolism of nonane, a JP-8 jet fuel component, by human liver microsomes, P450 isoforms and alcohol dehydrogenase and inhibition of human P450 isoforms by JP-8. 2005. *Chem.-Biol. Interact.* 151:203-211.

DAMD17-00-2-0008 At17.pdf

Appendix 18.

Tang, J. Y. Cao, R. L. Rose and E. Hodgson. (2002). In vitro metabolism of carbaryl by human cytochrome P450 and its inhibition by chlorpyrifos. *Chem.-Biol. Interact.* 141:229-241.

DAMD17-00-2-0008 At18.pdf

Appendix 19.

Tang, J., Usmani, K. A., Hodgson, E. and Rose R. L. 2004 In vitro metabolism of fipronil by human and rat cytochrome P450 and its interactions with testosterone and diazepam. *Chem.-Biol. Interact.* 147: 319-329.

DAMD17-00-2-0008 At19.pdf

Pyrethroids: Cytotoxicity and Induction of CYP Isoforms in Human Hepatocytes¹

Parikshit C. Das, Timothy M. Streit², Yan Cao, Randy L. Rose[†], Nathan Cherrington³, Matthew
K. Ross², Andrew D. Wallace and Ernest Hodgson*

Department of Environmental and Molecular Toxicology, Campus Box 7633, North Carolina
State University, Raleigh, NC 27695;

¹This work was presented, in part, at the Annual Meeting & ToxExpo, Society of Toxicology,
Charlotte, NC, March 25-29, 2007.

²Center for Environmental Health Sciences, Department of Basic Sciences, College of
Veterinary Medicine, Mississippi State University, Mississippi State, MS 39762;

³Department of Pharmacy, University of Arizona, Tucson, AZ 85721, USA;

[†]Deceased

***Corresponding author:** Dr. Ernest Hodgson, Department of Environmental and Molecular
Toxicology, Mail Box 7633, North Carolina State University, Raleigh, NC 27695-7633, USA.
Telephone: +1 919 515 5295; fax: +1 919 513 1012; E-mail address: ernest_hodgson@ncsu.edu

Short title: Pyrethroid Cytotoxicity and CYP Induction in Human Hepatocytes

Key words: CYP isoforms, cytotoxicity; deltamethrin; HepG2 cells; human hepatocytes; induction; permethrin; PXR/SXR,

Abbreviations:

AK - Adenylate kinase; bDNA - branched DNA; CYP - cytochrome P450; PKC - protein kinase C; PXR or SXR - pregnane X receptor or steroid and xenobiotic receptor;

ABSTRACT

Deltamethrin, [(S)- α -cyano-3-phenoxybenzyl-cis-(1R, 3R)-3(2,2-dibromovinyl) (2,2-dimethylcyclopropane-carboxylate)], and permethrin, (3-(2, 2-dichloroethenyl) -2, 2-dimethylcyclopropanecarboxylic acid (3-phenoxyphenyl) methyl ester) are pyrethroid insecticides used in agriculture, public health and military deployments. Pyrethroids known to be are capable of inducing cytochrome P450 (CYP) 2B1/2B2, CYP1A1 and overall CYP content in rat liver. The objectives of this study were to evaluate the potential of deltamethrin and permethrin to cause cytotoxicity and to induce CYP isoforms in human hepatocytes. Permethrin and deltamethrin showed dose-dependent effects on adenylate kinase activity in HepG2 cells, in which 50 and 100 μ M doses, respectively, induced a 3-5-fold increase in activity, and also induced adenylate kinase activity in primary human hepatocytes. An approximately 3-fold induction was noted at 200 μ M deltamethrin and a 4-fold induction at 100 μ M permethrin. Cytotoxicity was noted in HepG2 cells following 48 to 72 h exposure to 100 or 200 μ M deltamethrin and permethrin, respectively. Dose-dependent induction of caspase-3/7 was initiated by 12.5 μ M deltamethrin or by 3.125 μ M permethrin. Actinomycin D, a positive control for induction of caspase 3/7, induced caspase-3/7 an effect completely abrogated by the specific inhibitor Z-DEVD-FMK. At 100 μ M deltamethrin 2-3 fold induction of CYP1A1 and CYP2B6 mRNA was observed while, at the same time an ~25-fold induction of CYP3A4 was noted. Permethrin mediated CYP induction was much less potent, 4-fold or less for CYP1A1, CYP3A4, CYP3A5, CYP2B6 and CYP2A6. It has also been shown that these pyrethroids are ligands for the pregnane X receptor (PXR).

INTRODUCTION

Photostable synthetic pyrethroids were discovered in the 1970s /1/ and are widely used in agriculture, forestry, horticulture and public health, as well as in the textile industry and military deployments /2,3/. Pyrethroids are good substitutes for organochlorine, organophosphate and carbamate insecticides and are classified as safe due to their lower persistence and comparatively lower mammalian toxicity /2,4,5,6,7/.

Due to their lipophilicity pyrethroids are absorbed through the gastrointestinal and respiratory tracts and are preferentially distributed into lipid-rich body fat and nerve tissues /2/. Only a few cases of acute toxicity have been reported in occupationally exposed human subjects /8/. Permethrin shows estrogen and progesterone activities in human endometrial and breast cancer cells /9/.

Metabolism studies in humans have been limited to the detection of primary pyrethroid metabolites in blood or urine /10 – 12/. The urinary levels of the deltamethrin metabolite 3-phenoxybenzoic acid are similar or higher in children than in adults in exposed populations /13,14/. *cis*-Permethrin is poorly metabolized by human liver fractions although the *trans*-isomer is readily metabolized, initially by both soluble and microsomal esterases, followed by alcohol and aldehyde dehydrogenases /15/. This metabolic difference between *trans*- and *cis*- pyrethroids correlates with the greater toxicity of *cis*-isomers /2/. Covalent binding of deltamethrin to hepatic microsomal proteins suggests CYP-mediated metabolism of deltamethrin /16/. Different CYP isoforms, including CYP2B1/2B2 and CYP1A1/2, are involved in deltamethrin hydroxylation /17/. Pyrethroids cause a slight induction of CYP2B1, CYP2B2, CYP1A1 and total CYP content in rat liver /17,18/. Moreover, permethrin was shown to be an inducer of CYP2B1 in isolated rat hepatocytes /19/. Recent studies have shown that permethrin, cypermethrin and fenvalerate are ligands of the pregnane X receptor (PXR) /20,21/. The aims of the present study were to evaluate

the potential of deltamethrin and permethrin to cause their two most important hepatic effects, namely cytotoxicity and induction of CYP isoforms.

MATERIALS AND METHODS

Chemicals and Reagents. Deltamethrin [(S)- α -cyano-3-phenoxybenzyl-cis-(1R, 3R)-3(2, 2-dibromovinyl)3+ (2, 2-dimethyl-cyclopropane-carboxylate)] and permethrin [3-phenoxybenzyl (\pm)-cis, trans-3-(2,2-dichlorovinyl)-2,2-dimethyl-cyclopropane-1-carboxylate] were purchased from Chem Service (West Chester, PA) and Accu Standard, Inc. (New Haven, CT), respectively. Williams E culture medium and medium supplements, dexamethasone and insulin, were obtained from BioWhittaker (Walkersville, MD). EME Medium without L-glutamine and phenol red, non-essential amino acid solution, L-glutamine solution, and other cell culture related products were purchased from Mediatech Inc (Herndon, VA). Certified fetal bovine serum, trypsin-EDTA solution and HBSS buffers were obtained from GIBCO Invitrogen Corporation (Carlsbad, CA). Tissue culture flasks, 6-well, 24-well, 48-well, and 96-well culture plates and other tissue culture related products were purchased from Fisher Scientific Inc. (Pittsburgh, PA). FuGene 6, the renilla expression vector (pRL-TK), and the Dual Luciferase reporter assay system were obtained from Promega (Madison, WI). The PXR expression plasmid, pCDG1-SXR, was kindly provided by Dr. R. Evans (Salk Institute). pGL3-CYP3A4 (-7830 Δ 7208_364)/22/, which contains the firefly luciferase reporter gene under control by the CYP3A4 proximal and distal promoter, was generously provided by Dr. O. Burk (Dr. Margarete Fischer-Bosch Institute of Clinical Pharmacology, Germany). The ToxiLightTM assay kit was purchased from Cambrex Bio Science Rockland, Inc. (Rockland, ME). Caspase-GloTM-3/7 Assay kit was purchased from Promega Corporation (Madison, WI). Actinomycin D and Z-DEVD-FMK are products of Alexis Biochemicals supplied by AXXORA, LLC (San Diego, CA). Rifampicin,

phenobarbital, 3-methylcholanthrene and all other chemicals, unless specified otherwise, were purchased from Sigma-Aldrich Chemical Company (St. Louis, MO). Rabbit polyclonal anti-CYP2B6 antibodies and mouse monoclonal anti-CYP3A4 antibodies were purchased from BD Biosciences (Bedford, MA) and R & D Systems, Inc. (Minneapolis, MN), respectively. All chemicals, reagents and biological wastes were disposed of according to NCSU guidelines.

Human Hepatocyte Primary Culture. Primary cultures of adult human hepatocytes were obtained from ADMET Technologies (Durham, NC). Hepatocytes were plated at 9×10^6 cells/plate subdivided into equal numbers in all wells of culture plates coated with Type I collagen and overlaid with matrigel. The viability of cells at plating was greater than 84% as measured by the trypan blue exclusion method. Fresh hepatocytes were cultured in Williams medium E supplemented with 10^{-7} M dexamethasone, 10^{-7} M insulin, 100 U/ml penicillin G, 100 μ g/ml streptomycin and 10% FBS. The cultures were maintained in a humidified incubator at 5% CO₂ / 95% air at 37°C for 48 h prior to the initiation of treatment.

Human Hepatoma HepG2 Cell Line. Human hepatoma HepG2 cells were cultured in EME supplemented with 10% fetal bovine serum (FBS), penicillin (100 U/mL), streptomycin (100 μ g/mL), sodium pyruvate (1 mM), non-essential amino acids (0.1 mM) and L-glutamine (2 mM). Cells were maintained in a humidified atmosphere containing 5% CO₂ / 95% air at 37°C and were sub-cultured every 4-5 days. The initial culture was designated as passage number 1 and all experiments were performed using cells within the first 10 passages to minimize the inter-experimental variability and to maximize the intra-experimental data reproducibility.

Cell culture-based luciferase reporter gene assay. The HepG2 cells were transfected with 3 plasmids, a PXR expression vector, a plasmid containing the luciferase reporter gene, and a plasmid containing the renilla luciferase gene, the latter as a transfection efficiency control. Transfection of HepG2 cells was performed based on a recently published method describing the dual-luciferase assay in the HepG2 cell line /23/. Briefly, HepG2 cells were seeded into a 12-well plate at a density of ~500 000 cells/well. One day post-seeding, the cells (~50-80% confluent) were co-transfected with pGL3-CYP3A4, pCDG1-SXR, and pRL-TK plasmids for 24 h. The transfection reagent FuGene 6 and plasmid DNA were mixed and incubated together according to the manufacturer's protocol. Transfection solutions per well consisted of the pGL3-CYP3A4, pCDG1-SXR, and pRL-TK plasmids in the amounts of 360, 90, and 10 ng, respectively, along with 540 ng sonicated salmon sperm DNA to reach a total DNA amount of 1 µg. In select cases, HepG2 cells were mock transfected with PXR expression vector.

Treatment of Human Primary Hepatocytes and HepG2 Cells. Human hepatoma HepG2 cells were plated at 2×10^4 cells/well in 96-well plates and treated with vehicle (DMSO), phenobarbital (100 µM) and actinomycin D (1 µM) (positive controls), and increasing concentrations of permethrin (25 - 200 µM) or deltamethrin (12.5 - 200 µM) for 24, 48 and 72 h. For the caspase-3/7 assay, HepG2 cells were treated with permethrin or deltamethrin (3 - 200 µM) for the same duration.

Fresh human hepatocytes seeded at 1.875×10^5 cells/well in 48-well plates were used for ToxiLight and Caspase-3/7 assays following exposure to vehicle controls, positive controls such as phenobarbital (100 µM) and actinomycin D (1 µM), inhibitor Z-DEVD-FMK (0.05 µM), permethrin (3 - 200 µM) or deltamethrin (12.5 - 200 µM) for 24, 48, and 72 h. Again, fresh human hepatocytes were seeded at 1.5×10^6 cells/well of 6-well plate and at 3.75×10^5 cells/well

of 24-well plate. Primary hepatocytes were exposed for 72 h to vehicle, inducing agents such as rifampicin (10 μ M) or 3-methyl cholanthrene (10 μ M), and increasing concentrations of permethrin (5 - 100 μ M) or deltamethrin (10 - 100 μ M) for the branched DNA (bDNA) and Western blot analyses, and for the CYP1A1 and CYP3A4 enzyme activity assays.

Transfected HepG2 cells were treated for 24 h with fresh medium containing 10 μ M of the following compounds: rifampicin, deltamethrin, permethrin or cypermethrin in the first set of experiment, and 10 μ M of the following compounds: rifampicin, bioresmethrin, trans-permethrin, cis/trans (50/50) permethrin, cis-permethrin, cypermethrin, cyhalothrin, or esfenvalerate in the second set of experiments. The amount of vehicle DMSO in the medium was always 0.1% (v/v).

Sample Preparation. Culture supernatant was collected from 96-well and 48-well plates for use in the ToxiLight assay, while a mixture of both culture medium and cells was used for the caspase-3/7 assay. Cells in 96-well plates were harvested as suspensions using 2-5 μ l trypsin-EDTA for the trypan blue exclusion assay. Cells were harvested using a cell scraper and pooled in Eppendorf tubes for extraction of protein and total RNA, respectively. Following centrifugation at 5000 g for 3 min the supernatant was discarded. The cells were re-suspended in 75 μ l chilled CYP storage buffer (0.1 M potassium phosphate buffer with 0.1 mM EDTA, pH 7.5) and sonicated twice for 30 s. S9 fraction was obtained by centrifuging the homogenate at 9000 g for 15 minutes. Following treatment of transfected HepG2 cells, the culture medium was removed and the cells were washed twice with PBS prior to being lysed with 250 μ l of passive lysis buffer (Promega). Lysates were stored at -20° C until the luciferase activity assays were performed. Following treatment, the culture medium was removed and the cells were washed

twice with PBS prior to being lysed with 250 µl of passive lysis buffer (Promega). Lysates were stored at -20° C until the luciferase activity assays were performed.

Cell Viability and/or Cytotoxicity Assay. Cell viability was assessed using cell suspensions in isotonic culture medium by the trypan blue exclusion assay. Specifically, 100 µl of 0.4% trypan blue in PBS, pH 7.4, was added into 900 µl of cell suspension. Ten µl of this mixture was placed on the hemocytometer and more than 100 cells per field were examined to determine the percentage of dead versus viable cells.

Adenylate Kinase Assay. ToxiLight™ bioassay is a non-destructive luciferase-based bioluminescence cytotoxicity assay used to measure toxicity in mammalian primary cells and cell lines in culture. This assay quantitatively measures the release of adenylate kinase into the culture medium. The emitted luminescence intensity expressed as the RLU (relative luminescence unit) value is linearly related to the adenylate kinase activity released into the medium. The assay was performed according to the manufacturer's protocol (Lonza Rockland, Inc., Rockland, ME). Measurements at different time points are cumulative from the zero time point.

Caspase-3/7 Assay. Caspase-Glo™-3/7 assay is a homogeneous luciferase based bioluminescence assay that quantitatively measures caspase-3/7 activities using a luminometer. Intensity of the luminescence produced by luciferase is proportional to the amount of caspase-3/7 activity present in the sample mixture. The assay was performed according to the manufacturer's protocol (Tech. Bull. No.323, Promega Corporation, Madison, WI).

Branched DNA (bDNA) Assay. The bDNA assay is a measure of mRNA induction /24,25/. Oligonucleotide probe sets specific for human CYP1A1, CYP1A2, CYP3A4, CYP3A5, CYP2B6, CYP2D6, CYP2A6 and glyceraldehyde phosphate dehydrogenase were a generous gift from Xenotech LLC (Olathe, Kansas). Reagents required for RNA analysis (i.e., lysis buffer, amplifier/label probe buffer and substrate solution) were supplied in the QuantiGene Discover kit (Genospectra, Fremont, CA). Expression levels were analyzed as described by Hartley and Klaassen /24/. Briefly, specific oligonucleotide probe sets were diluted in lysis buffer. Cell lysate was vortexed and 20 μ L was added to each well of a 96-well plate containing capture hybridization buffer (0.05 M HEPES sodium salt, 0.05 M HEPES free acid, 0.037 M lithium lauryl sulfate, 0.5 % [v/v] Micr-O-protect, 8 mM EDTA, 0.3 % [w/v] nucleic acid blocking agent) and 50 μ L diluted probe set (50, 100, and 200 fmol/ μ L for capture, blocker, and label probes, respectively). RNA was allowed to hybridize to each probe set containing all probes for a given transcript (blocker probes, capture probes, and label probes) overnight at 53°C. Subsequent hybridization and post-hybridization wash steps were carried out according to the manufacturer's instructions, and luminescence was measured with the Quantiplex 320 bDNA Luminometer (Bayer Diagnostics) interfaced with Quantiplex Data Management Software Version 5.02 (Bayer Diagnostics) for analysis of luminescence from 96-well plates. CYP expression data was normalized with respect to glyceraldehyde phosphate dehydrogenase levels and expressed as induction relative to controls.

Gel Electrophoresis, Immunodetection and Quantification. A 7.5% sodium dodecyl sulfate-polyacrylamide gel electrophoresis (SDS-PAGE) was used to resolve microsomal proteins based on the method of Laemmli /26/. Proteins from the gel were electrophoretically transferred to a nitrocellulose membrane at constant voltage (100 V) for 1 hour, and stained with Ponceau S for

verification of transfer. The blots were blocked in 1% nonfat dry milk for 12 h and incubated in primary monoclonal anti-human CYP3A4 antibody and secondary anti-mouse IgG antibody conjugated to alkaline phosphatase. Specific protein bands were visualized in BCIP/NBT. The intensities of the bands on a film were measured using densitometry and data expressed on a quantitative scale.

Dual-Luciferase Assay. To measure the firefly luciferase activity of the lysates, 30 μ l of luciferase assay reagent II (Promega) was mixed with 5 μ l of lysate and luminescence was measured using a TD-20/20 luminometer (Turner Designs). The firefly luciferase reaction was quenched by the addition of 30 μ l of Stop and Glo reagent (Promega) followed by detection of luminescence derived from the renilla luciferase activity. Firefly luciferase activity was normalized to the renilla activity in each sample. Two and three independent transfections were performed with triplicate treatments for each compound for first and second set of experiments (n=6 & n= 9), respectively. Induction relative to the DMSO control was averaged for each compound.

Statistical Analysis. Data are summarized and expressed as the mean \pm SE by using Microsoft Excel spread sheet and Sigma Plot graphics program (Chicago, IL, USA). The significant differences between control and treated data sets were determined using Student's t-test.

RESULTS

Effect of Deltamethrin and Permethrin on Adenylate Kinase Activity in HepG2 Cells and Human Hepatocytes. The induction and subsequent release of adenylate kinase into the culture medium is an indicator of cytotoxic damage to cells. Permethrin and deltamethrin had a dose-

dependent effect on the release of adenylate kinase activity from cultured human HepG2 cells, where 50 and 100 μM doses caused the highest release, ~3- and 5-fold, respectively. At the highest (200 μM) dose of either pyrethroid adenylate kinase release was somewhat lower (Figure 1A, B). Permethrin and deltamethrin also induce adenylate kinase in human primary hepatocytes in a time- and dose-dependent manner, a ~3 fold induction being noted at the highest (200 μM) dose of deltamethrin, and a ~4 fold induction at the 100 μM dose. 200 μM permethrin caused reduced activity (Figure 2A, B).

Toxicity of Deltamethrin and Permethrin in HepG2 Cells. The trypan blue assay was used to correlate adenylate kinase activity with cell cytotoxicity caused by permethrin and deltamethrin. The data showed 15 to 25% cytotoxicity after 48 to 72 h exposure to 100 or 200 μM deltamethrin, and 15 to 20% cell death at 100 or 200 μM permethrin in HepG2 cells (Figure 3A, B).

Effect of Deltamethrin and Permethrin on Caspase-3/7 Activity in HepG2 Cells and Human Hepatocytes. Induction of activated caspase-3/7 is an indicator of cellular apoptosis. In order to characterize whether pyrethroid-mediated cell death was triggered through this known apoptotic pathway, cultured human HepG2 cells were exposed to increasing doses of deltamethrin and permethrin (0 - 200 μM) for 24, 48 and 72 h and caspase-3/7 activity was measured. A dose-dependent increase in the induction of activated caspase-3/7 was noted from the lowest dose of 3.125 μM to a maximum at 12.5 to 50 μM , approaching a plateau or decreasing at 200 μM after 72 h. Approximately 2-3-fold activation was noted for both chemicals at 72 h (Figure 4A, B). Primary cultures of human hepatocytes were also exposed to increasing doses of deltamethrin and permethrin for up to 72 h. A single dose of a known inducer such as actinomycin D (1 μM)

and the well known caspase-3/7 inhibitor Z-DEVD-FMK (0.05 μ M) served as positive controls. Deltamethrin showed ~2-fold induction at 100 and 200 μ M, while permethrin showed a 1.5-2-fold induction in caspase-3/7 at 25-100 μ M decreasing at 200 μ M from 48 to 72 h in primary hepatocytes (Figure 5A, B). Actinomycin D induced caspase-3/7 about 5-7 fold whereas Z-DEVD-FMK abrogated the pyrethroid-induced caspase-3/7 activity (data not shown).

Effect of Deltamethrin and Permethrin on CYP Isoform mRNA Transcripts in Human

Hepatocytes. In order to determine effects on CYP gene expression, primary human hepatocytes were exposed to 100 μ M of deltamethrin or permethrin for 72 h. The data showed induction of mRNA expression of CYP1A1, CYP3A4 and CYP2B6 isoforms. 2-3-fold induction of CYP1A1 and CYP2B6 was noted while ~25-fold induction of CYP3A4 was noted with deltamethrin (Figure 6A). However, substantial variability among individuals, as yet unexplained, was noted in the induction of CYP isoform mRNAs. Permethrin-mediated CYP isoform induction was less potent. Up to 4-fold induction was noted for CYP1A1, CYP3A4, CYP3A5, CYP2B6 and CYP2A6 mRNA (Figure 6B). Permethrin also showed substantial variability in CYP induction.

Effect of Deltamethrin and Permethrin on CYP3A4 Protein in Human Hepatocytes

In order to verify the potential of deltamethrin and permethrin to induce CYP3A4-specific protein expression, Western blot analysis was performed and CYP3A4-specific protein was measured semi-quantitatively in primary human hepatocytes following treatment with deltamethrin (0 - 100 μ M) or permethrin (0 - 100 μ M) for 72 h. Even though induction was shown to be dose-dependent, inter-individual variability in induction reduced the significance of the CYP3A4 protein expression findings (Figure 7A, B).

Effect of Deltamethrin and Permethrin on Nuclear Receptor PXR in Transiently Transfected

HepG2 cells. To determine whether the induction of CYP mRNA following deltamethrin or permethrin treatments is mediated via a PXR mechanism, a dual-luciferase assay was performed using HepG2 cells. Co-transfected cells were treated with 10 μ M deltamethrin, 10 μ M permethrin or 10 μ M rifampicin along with other pyrethroids and sham controls with DMSO (final concentration, 0.1% v/v) for 24 h. Induction profiles for rifampicin, deltamethrin, cypermethrin and DMSO treated controls, along with the appropriate PXR-mock transfection treatments are shown in Figure 8A. Similarly, induction profiles for another set of pyrethroids (rifampicin, bioresmethrin, trans-, cis/trans- and cis-permethrin, cypermethrin, deltamethrin, cyhalothrin, esfenvalerate and DMSO) are shown in Figure 8B. As expected, the rifampicin positive control exhibited a PXR-dependent induction of luciferase following activation of the CYP3A4 promoter. PXR-dependence was verified by the lack of rifampicin-mediated induction when the PXR expression vector was absent. Likewise, the pyrethroids exhibited PXR-dependent induction. Except for bioresmethrin, the various pyrethroids tested were shown to induce CYP3A4 promoter activity by several-fold. This study demonstrates that deltamethrin and permethrin can activate CYP3A4 promoter activity by acting as potent PXR ligands. Specifically, deltamethrin treated cells exhibited an ~5-fold increase and permethrin treated cells showed approximately 4-10 fold increase in luciferase activity as compared to the vehicle treated control.

DISCUSSION

Because of the widespread use of pyrethroids this study was designed to examine the potential toxicity and metabolic impact of pyrethroids on human liver cells. Deltamethrin, an α -cyano type II pyrethroid, induced adenylate kinase activity both in human hepatoma HepG2 cells

and primary hepatocytes. Activated adenylate kinase can trigger ATP synthesis, which in turn may enhance the hydrolysis of phosphoinositide to generate inositol phosphates and diacylglycerol that trigger the mobilization of intracellular $[Ca^{2+}]$ and activation of protein kinase C. Pyrethroids have been reported to activate the protein kinase C / phosphoinositol pathway in rat brain tissue /27/. Deltamethrin or permethrin may thus trigger ATP formation through a cascade of second messenger signaling mechanisms to activate PKC, which are involved in the cellular regulation of programmed cell death or apoptosis /28/.

Caspases are also involved in the initiation and transduction of apoptotic signals /29,30/. Pyrethroids induce oxidative stress and alter antioxidant systems in rat tissues /31,32,33/. Formation of oxidative metabolites causes release of cytochrome c and other polypeptides that bind to the apoptotic protease activating factor-1, causing ATP- or dATP-dependent binding to the prodomain of procaspase-9 /34/. The proteolytic activity of procaspase-9 initiates a protease cascade /35,36/, resulting in activation of caspases-3/7. Short and long term exposure to deltamethrin stimulates lipid peroxidation in mice /37/, and induces neurodegeneration and apoptotic cell death in rats /38/. In the present study exposure of human hepatoma HepG2 and primary hepatocytes to deltamethrin (up to 100 μ M) significantly induced caspase-3/7 activity, while permethrin induced activity at all doses (3.12 to 200 μ M). Pyrethroid-mediated caspase-3/7 induction may occur via mitochondrial oxidative stress (see above).

Pyrethroids such as deltamethrin appear to impact kinase and phosphatase – mediated signal transduction pathways. For example, in astrocytes deltamethrin can inhibit the Ca^{2+} /calmodulin-dependent phosphatase, calcineurin /39/. Deltamethrin-mediated enhancement of ATP-induced intracellular Ca^{2+} release via the inositol-1, 4, 5-phosphate receptor (IP_3R) is regulated by calcineurin-mediated dephosphorylation in COS-7 cells /40,41,42/. In endothelial cells, deltamethrin acts as an inhibitor of PP2B /43,44,45,46/. Pyrethroids have estrogenic and

antiprogestogenic effects in human tumor cells /9,47/ and pyrethroid metabolites are capable of interacting with the estrogen receptor /48/.

Signaling pathways involving PKC repress PXR activity by altering the PXR-co-factor protein complex in mouse hepatocytes /49/. Recent studies have demonstrated that various pesticides are capable of activating hPXR, although permethrin has a lower affinity for hPXR than the positive control rifampicin /21/. Activated hPXR forms a heterodimer with the retinoid X receptor (RXR), this complex interacting with a xenobiotic-responsive element found in the promoter regions of genes that regulate multiple drug-metabolizing genes /50/, including CYP3A4 and CYP2B6 /51 – 54/. Permethrin elicits the most pronounced induction of CYP2B1 and CYP3A1 mRNA and these effects occurred at the transcriptional level /19/. In our study, pyrethroids elicited mixed effects on CYP-encoded mRNA expression. In general, deltamethrin and permethrin exhibited low inducibility of CYP-specific mRNA and the effects were extremely variable for different CYPs. The induction of CYP-isoforms CYP1A, CYP3A4 and CYP2B6 by deltamethrin and permethrin in human hepatocytes may be due to variable effects on transcription signaling mechanisms. Much of the variation is due, presumably, to interindividual variation in transcription factor levels between hepatocyte donors /55/. Further research is necessary to resolve this question.

Similar to previous work /20,51,54/, rifampicin exhibited a PXR dependent induction of luciferase activity by activation of the CYP3A4 promoter. This study further demonstrated that deltamethrin and permethrin are potent PXR agonists. Specifically, deltamethrin treated cells exhibited 5-15-fold and permethrin 4-10-fold increases in CYP3A4 promoter activity compared to vehicle treated cells. We have demonstrated for the first time that deltamethrin and permethrin are ligands of PXR. Trans-permethrin showed lesser induction of luciferase activity compared to deltamethrin and cis-permethrin, corroborating recent findings /21/. Thus, deltamethrin and

permethrin acting as PXR ligands, are capable of triggering CYP-specific transcription and translation. CYP3A4 is the most abundant and important CYP isoform in human liver, has broad substrate specificity and metabolizes ~60% of clinical drugs and other chemicals /56,57/. CYP2B6 is also important in pesticide metabolism /58/ thus changes in functional CYP3A4 and CYP2B6 expression by deltamethrin and permethrin may have implications for human health risk assessment.

It is important to note that although pyrethroids have been in use as alternatives to organochlorine, organophosphate and carbamate insecticides and are believed to be only mildly toxic to mammals, they are not free from adverse effects /59/. Pyrethroids are transmitted through breast milk /60/ and possess antiandrogenic and antiestrogenic activity /61,62/. Pyrethroids moderately induce CYP1B1/2B2 and CYP1A1 which are directly involved in xenobiotic metabolism, including the bioactivation of carcinogens in a variety of cell types. As discussed above, pyrethroid-mediated induction of mitochondrial oxidative stress, apoptotic cell death and the potential to affect hormonal and immune suppression have been shown in a number of in vitro and in vivo mammalian studies. Deltamethrin and permethrin can act as ligands for PXR and show moderate effects on the major metabolic enzymes, and they induce apoptotic cytotoxicity in human hepatocytes. Overall, our findings further emphasize that pyrethroid insecticides may impact human health and require further analysis and assessment.

Acknowledgements:

This publication was supported by Grant/Cooperative Agreement Number 5 U50 OH007551-05 from CDC - NIOSH. Its contents are solely the responsibility of the authors and do not necessarily represent the official views of Centers for Disease Control (CDC). The authors acknowledge the help of Edward L. Croom with the transfection studies.

REFERENCES

1. Elliot, M., Farnham, A. W., Janes, N. F., Needham, P. H., Pulman, D. A. Synthetic insecticide with a new order of activity. *Nature (London)*. 1974; 248: 710-711.
2. Soderlund, D. M., Clark, J. M., Sheets, L. P., Mullin, L. S., Piccirillo, V. J., Sargent D, Stevens, J. T., Weiner, M. L. Mechanisms of pyrethroid neurotoxicity: implications for cumulative risk assessment. *Toxicology*. 2002; 171: 3-59.
3. Institute of Medicine, Gulf War and Health, Volume 1: Depleted Uranium, Pyridostigmine Bromide, Sarin, Vaccines; and Volume 2: Insecticides and Solvents. Institute of Medicine, National Academy Press, Washington, DC. 2003.
4. Vijverberg, H. P. M., van den Bercken, J. Neurotoxicological effects and the mode of action of pyrethroid insecticides. *CRC Rev. Toxicol*. 1990; 21: 105-126.
5. Ray, D. E., Fry, J. R. A reassessment of the neurotoxicity of pyrethroid insecticides. *Pharmacol. Ther*. 2006; 111: 174-193.
6. Schultz, M. W., Gomez, M., Hansen, R. C., Mills, J., Menter, A., Rodgers, H., Judson, F. N., Mertz, G., Handsfield, H. H. Comparative study of 5% permethrin cream and 1% lindane lotion for the treatment of scabies. *Arch. Dermatol*. 1990; 126: 167-170. Comment in: 126, 966-967.
7. Tomalik-Scharte, D., Lazar, A., Meins, J., Bastian, B., Ihrig, M., Wachall, B., Jetter, A., Tantcheva-Poor, I., Mahrle, G., Fuhr, U. Dermal absorption of permethrin following topical administration. *Eur. J. Clin. Pharmacol*. 2005; 61: 399-404.
8. Chen, S. Y., Zhang, Z. W., He, F. S., Yao, P. P., Wu, Y. Q., Sun, J. X., Liu, L. H., Li, Q. G. An epidemiological study on occupational acute pyrethroid poisoning in cotton farmers. *Br. J. Ind. Med*. 1991; 48: 77-81.

9. Garey, J., and Wolff, M. S. Estrogenic and antiprogestagenic activities of pyrethroid insecticides. *Biochem. Biophys. Res. Commun.* 1998; 251: 855-859.
10. Asakawa, F., Jitsunari, F., Miki, K., Choi, J., Takeda, N., Kitamado, T., Suna, S., Manabe, Y. Agricultural worker exposure to and absorption of permethrin applied to cabbage. *Bull. Environ. Toxicol.* 1996; 56: 42-49.
11. Leng, G., Kuhn, K. H., Idel, H. Biological monitoring of pyrethroids in blood and pyrethroid metabolites in urine: applications and limitations. *Sci. Total Environ.* 1997; 199: 173-181.
12. Hardt, J., Angerer, J. Biological monitoring of workers after the application of insecticidal pyrethroids. *Int. Arch. Occup. Environ. Health.* 2003; 76: 492-498.
13. Heudorf, U., and Angerer, J. Metabolites of pyrethroid insecticides in urine specimens: Current exposure in urban population in Germany. *Environ. Health Perspect.* 2001; 109: 213-217.
14. Yáñez, L., Ortiz-Perez, D., Batres, L. E., Borja-Aburto, V. H., Diaz-Barriga, F. Levels of dichlorodiphenyltrichloroethane and deltamethrin in humans and environmental samples in malarious areas of Mexico. 2002; *Environ. Res. Sect. A88*: 174-181.
15. Choi, J., Rose, R. L., Hodgson, E. In vitro human metabolism of permethrin: the role of human alcohol and aldehyde dehydrogenases. *Pestic. Biochem. Physiol.* 2002; 73: 117-128.
16. Catinot, R., Hoellinger, H., Sonnier, M., Do, C-T., Pichon, J., Nguyen, H. N. In vitro covalent binding of the pyrethroids cismethrin, cypermethrin and deltamethrin to rat liver homogenate and microsomes. *Arch. Toxicol.* 1989; 63: 214-220.
17. Dayal, M., Parmar, D., Dhawan, A., Dwivedi, U. N., Doehmer, J., Seth, P. K. Induction of rat brain and liver cytochrome P450 1A1/1A2 and 2B1/2B2 isoenzymes by deltamethrin. *Environ. Toxicol. Pharmacol.* 1999; 7: 169-178.

18. Krechniak, J., and Wrzesniowska, K. Effect of pyrethroid insecticides on hepatic microsomal enzymes in rats. *Environ. Res.* 1991; 55: 129-134.
19. Heder, A. F., Hirsch-Ernst, K. I., Bauer, D., Kahl, G. F., Desel, H. Induction of cytochrome P450 2B1 by pyrethroids in primary rat hepatocyte cultures. *Biochem. Pharmacol.* 2001; 62: 71-79.
20. Lemaire, G., Sousa, G., and Rahmani, R. A PXR reporter gene assay in a stable cell culture system: CYP3A4 and CYP2B6 induction by pesticides. *Biochem. Pharmacol.* 2004; 68: 2347-2358.
21. Lemaire, G., Mnif, W., Pascussi, J. M., Pillon, A., Rabenoelina, F., Fenet, H., Gomez, E., Casellas, C., Nicolas, J. C., Cavailles, V., Duchesne, M. J., Balaguer, P. Identification of new human PXR ligands among pesticides using a stable reporter cell system. *Toxicol. Sci.* 2006; 91: 501-509.
22. Hustert, E., Zibat, A., Presecan-Siedel, E., Eiselt, R., Mueller, R., Fuss, C., Brehm, I., Brinkmann, U., Eichelbaum, M., Wojnowski, L. and Burk, O. Natural protein variants of the pregnane X receptor with altered transactivation activity toward CYP3A4. *Drug. Metab. Disp.* 2001; 29: 1454-1459.
23. Chang, T. K. H., and Waxman, D. J. Pregnane X receptor-mediated transcription. *Methods in Enzymology.* 2005; 400: 588-598.
24. Hartley, D. P., and Klaassen, C. D. Detection of chemical-induced differential expression of rat hepatic cytochrome P450 mRNA transcripts using branched signal amplification technology. *Drug Metab. Dispos.* 2000; 28: 608-616.
25. Rose, R. L., Tang, J., Choi, J., Cao, Y., Usmani, A., Cherrington, N., Hodgson, E. Pesticide metabolism in humans, including polymorphisms. *Scand J. Work Environ. Health.* 2005; 31: suppl 1, 156-163.

26. Laemmli, U. K. Cleavage of structural proteins during the assembly of the head of bacteriophage T4. *Nature*. 1970; 227: 680-685.
27. Enan, E., Matsumura, F. Activation of phosphoinositide/protein kinase C pathway in rat brain tissue by pyrethroids. *Biochem. Pharmacol.* 1993; 45: 703-710.
28. Lucas, M., and Sanchez-Margalet, V. Review: Protein kinase C involvement in apoptosis. *Gen. Pharmac.* 1995; 26: 881-887.
29. Earnshaw, W. C., Martins, L. M., and Kaufmann, S. H. Mammalian caspases: structure, activation, substrates, and functions during apoptosis. *Annu. Rev. Biochem.* 1999; 68: 383-424.
30. Nunez, G., Benedict, M., Hu, Y., and Inohara, N. Caspases: the proteases of the apoptotic pathway. *Oncogene*. 1998; 17: 3237-3245.
31. Gupta, A. Effect of pyrethroid-based liquid mosquito repellent inhalation on the blood-brain barrier function and oxidative damage in selected organs of developing rats. *J. Appl. Toxicol.* 1999; 19: 67-72.
32. Kale, M., Rathore, N., John, S., Bhatnagar, D. Lipid peroxidative damage on pyrethroid exposure and alterations in antioxidant status in rat erythrocytes: a possible involvement of reactive oxygen species. *Toxicol. Lett.* 1999; 105: 197-205.
33. Giray, B., Gurbay, A., Hincal, F. Cypermethrin-induced oxidative stress in rat brain and liver is prevented by vitamin E or allopurinol. *Toxicol. Lett.* 2001; 118: 139-146.
34. Li, P., Nijhawan, D., Budihardjo, I., Srinivasula, S. M., Ahmad, M., Alnemri, E. S., and Wang, X. Cytochrome c and dATP-dependent formation of Apaf-1/caspase-9 complex initiates an apoptotic protease cascade. *Cell*. 1997; 91: 479-489.
35. Srinivasula, S. M., Ahmad, M., Fernandes-Alnemri, T., and Alnemri, E. S. Autoactivation of procaspase-9 by Apaf-1-mediated oligomerization. *Mol. Cell*. 1998; 1: 949-957.

36. Rodriguez, J., and Lazebnik, Y. Caspase-9 and APAF-1 form an active holoenzyme. *Genes Dev.* 1999; 13: 3179-3184.
37. Yarsan, E., Bilgili, A., Kanbur, M. Effects of deltamethrin on lipid peroxidation in mice. *Vet. Human Toxicol.* 2002; 44: 73-75.
38. Wu, A., Ren, T., Hu, Q., Liu, Y. Deltamethrin induces altered expression of P53, Bax and Bcl-2 in rat brain. *Neurosci. Lett.* 2000; 284: 29-32.
39. Matsuda, T., Takuma, K., Asano, S., Kishida, Y., Nakamura, H., Mori, K., Maeda, S., Baba, A., Involvement of calcineurin in Ca²⁺ paradox-like injury of cultured rat astrocytes. *J. Neurochem.* 1998; 70: 2004-2011.
40. Bandyopadhyay, A., Shin, D. W., Kim, D. H. Regulation of TP-induced calcium release in COS-7 cells by calcineurin. *Biochem. J.* 2000; 348 Pt-1: 173-181.
41. Enan, E., Pinkerton, K. E., Peake, J., Matsumura, F. Deltamethrin-induced thymus atrophy in male Balb/c mice. *Biochem. Pharmacol.* 1996; 51: 447-454.
42. Taylor, B. K., Stoops, T. D., Everett, A. D. Protein phosphates inhibitors arrest cell cycle and reduce branching morphogenesis in fetal rat lung cultures. *Am. J. Physiol. Lung Cell Mol. Physiol.* 2000; 278: L1062-L1070.
43. Verin, A. D., Cooke, C., Herenyiova, M., Patterson, C. E., Garcia, J. G. Role of Ca²⁺/calmodulin-dependent phosphatase 2B in thrombin-induced endothelial cell contractile responses. *Am. J. Physiol.* 1998; 275(4Pt 1): L788-L799.
44. Schreiber, S. I., Crabtree, G. R. The mechanism of action of cyclosporine A and FK506. *Immunol. Today.* 1992; 13: 136-142.
45. Galat, A. Peptidylproline cis-trans-isomerases: immunophilins. *Eur. J. Biochem.* 1993; 216: 689-707.

46. Enan, E., Matsumura, F. Specific inhibition of calcineurin by type II synthetic pyrethroid insecticides. *Biochem. Pharmacol.* 1992; 43: 1777-1784.
47. Kim, I. Y., Han, S. Y., Kang, T. S., Lee, B. M., Choi, K. S., Moon, H. J., Kim, T. S., Kang, I. H., Kwack, S. J., Moon, A., Ahn, M. Y., Kim, H. S. Pyrethroid insecticides, fenvalerate and permethrin, inhibit progesterone-induced alkaline phosphatase activity in T47D human breast cancer cells. *J. Toxicol. Environ. Health A.* 2005; 68: 2175-2186.
48. McCarthy, A. R., Thomson, B. M., Shaw, I. C., Abell, A. D. Estrogenicity of pyrethroid insecticide metabolites. *J. Environ. Monit.* 2006; 8: 197-202.
49. Ding, X., Staudinger, J. L. Repression of PXR-mediated induction of hepatic CYP3A gene expression by protein kinase C. *Biochem. Pharmacol.* 2005; 69: 867-873.
50. Geick, A., Eichelbaum, M., Burk, O. Nuclear receptor response elements mediate induction of intestinal MDR1 by rifampin. *J. Biol. Chem.* 2001; 276: 14581-14587.
51. Bertilsson, G., Heidrich, J., Svesson, K., Asman, M., Jendeberg, L., Sydow-Backman, M., Ohlsson R., Postlind H., Blomquist P., Berkenstam. Identification of a human nuclear receptor defines a new signaling pathway for CYP3A induction. *Proc. Natl. Acad. Sci. USA.* 1998; 95: 12208-12213.
52. Blumberg, B., Sabbagh, Jr., W., Juguilon, H., Bolado, Jr., J., van Meter, C. M., Ono, E. S., Evans, R. M. SXR, a novel steroid and xenobiotic-sensing nuclear receptor. *Genes Dev.* 1998; 12: 3195-3205.
53. Kliewer, S. A., Moore, J. T., Wade, L., Staudinger, J. L., Watson, M. A., Jones, S. A., McKee, D. D., Oliver, B. B., Willson, T. M., Zetterstrom, R. H., Perimann, T., Lehmann, J. M. An orphan nuclear receptor activated by pregnanes defines a novel steroid signaling pathway. *Cell.* 1998; 92: 73-82.

54. Lehman, J. M., McKee, D. D., Watson, M. A., Willson, T. M., Moore, J. T., Kliewer, S. A. The human orphan nuclear receptor PXR is activated by compounds that regulate CYP3A4 gene expression and cause drug interactions. *J. Clin. Invest.* 1998; 102: 1016-1023.
55. Hamzeiy, H., Bombail, V., Plant, N., Gibson, G., Goldferb, P. Transcriptional regulation of cytochrome P4503A4 gene expression: effects of inherited mutations in the 5`-flanking region. *Xenobiotica.* 2003; 33: 1085-1095.
56. Guengerich, F. P. Role of cytochrome P450 enzymes in drug-drug interactions. *Adv. Pharmacol.* 1997; 43: 7-35.
57. Szklarz, G. D., and Halpert, J. R. Molecular basis of P450 inhibition and activation: implications for drug development and drug therapy. *Drug Metab. Dispos.* 1998; 26: 1179-1184.
58. Hodgson, E. and Rose, R. L. The importance of P450 2B6 (CYP2B6) in the human metabolism of environmental chemicals. *Pharmacol. Therap.* 2007; 113: 420-428.
59. Miyamoto, J., Kaneko, H., Tsuji, R., and Okuno, Y. Pyrethroids, nerve poisons: how their risks to human should be assessed. *Toxicol. Lett.* 1995; 82: 933-940.
60. Bouwman, H., Sereda, B., Meinhardt, H. M. Simultaneous presence of DDT and pyrethroid residues in human breast milk from a malaria endemic area in South Africa. *Environ Pollut.* 2006; 144(3): 902-917..
61. Sun, H., Xu, X. L., Xu, L. C., Song, L., Hong, X., Chen, J. F., Cui, L. B., Wang, X. R., Antiandrogenic activity of pyrethroid pesticides and their metabolite in reporter gene assay. *Chemosphere. Online.* 2006.
62. Usmani, K. A., Cho, T. M., Rose, R. L., Hodgson, E. Inhibition of the human liver microsomal and human cytochrome P450 1A2 and 3A4 metabolism of estradiol by deployment-related and other chemicals. *Drug Metab. Dispos.* 2006; 34: 1606-1614.

FIGURE LEGENDS

Figure 1A and 1B: Dose- and time- dependent effect of deltamethrin (Figure 1A) and permethrin (Figure 1B) on the adenylate kinase activity of HepG2 cells. Cultured HepG2 cells were exposed to increasing concentrations of deltamethrin (0, 12.5, 25, 50, 100 and 200 μM) or permethrin (0, 25, 50, 100 and 200 μM) for 24, 48 and 72 h and adenylate kinase activity was measured using the ToxiLight assay kit. Each bar represents the RLU value mean of 9 determinations from 3 independent experiments for HepG2 cells the error bar represents the standard error of the mean.

Figure 2A and 2B: Dose- and time- dependent effect of deltamethrin (Figure 2A) or permethrin (Figure 2B) on the adenylate kinase activity of primary cultures of human hepatic cells. Cultured hepatocytes were exposed to increasing concentrations of deltamethrin (0, 12.5, 25, 50, 100 and 200 μM) or permethrin (0, 3.125, 6.25, 25, 50, 100 and 200 μM) for 24, 48 and 72 h and adenylate kinase activity was measured using the ToxiLight assay kit. Each bar represents the RLU value mean of 6 to 8 determinations from 2 individuals the error bar represents the standard error of the mean.

Figure 3A and 3B: Dose- and time- dependent effect of deltamethrin (Figure 3A) or permethrin (Figure 3B) on human hepatoma HepG2 cell viability. Cultured HepG2 cells were exposed to increasing concentrations of deltamethrin (0, 12.5, 25, 50, 100 and 200 μM) and permethrin (0, 25, 50, 100 and 200 μM) for 24, 48 and 72 h and cell viability was assessed by the Trypan blue assay and expressed as % cytotoxicity. Each bar represents the value derived from counting 150 to 200 cells in each treated sample.

Figure 4A and 4B: Dose and time dependent effects of deltamethrin (Figure 4A) and permethrin (Figure 4B) on caspase-3/7 activity in human hepatoma HepG2 cells. Cultured HepG2 cells were exposed to various concentrations (0, 3.125, 6.25, 12.5, 25, 50, 100 and 200

μM) of deltamethrin or permethrin along with actinomycin D ($1 \mu\text{M}$), an inducer of apoptosis, and the caspase-3/7 specific inhibitor Z-DEVD-FMK ($0.05 \mu\text{M}$) for 24, 48 and 72 h and caspase-3/7 activity was quantitatively measured by Caspase-Glo®-3/7 assay kit. Each bar represents the mean of RLU value of 2 independent experiments, 3-4 well determinations per group per experiment and error bars are the standard error of the mean.

Figure 5A and 5B: Dose and time dependent effect of deltamethrin (Figure 5A) or permethrin (Figure 5B) on caspase-3/7 activity in human primary hepatocytes. Primary cultures of hepatocytes were exposed to various concentrations of deltamethrin (0, 12.5, 25, 50, 100 and 200 μM) or permethrin (0, 3.12, 6.25, 12.5, 25, 50, 100 and 200 μM) along with Actinomycin D ($1 \mu\text{M}$), an inducer of apoptosis, or the caspase-3/7 specific inhibitor Z-DEVD-FMK ($0.05 \mu\text{M}$) for 24, 48 and 72 h and caspase-3/7 activity was quantitatively measured using a Caspase-Glo®-3/7 assay kit. Each bar represents the mean of RLU value from 6 determinations (2 individuals, 3 wells each) and error bars are the standard error of the mean.

Figure 6A and 6B: Effect of deltamethrin (Figure 6A) or permethrin (Figure 6B) on the expression of mRNA transcripts of different CYP isoforms in human hepatocytes. Freshly prepared human hepatocytes from different individuals were exposed to $100 \mu\text{M}$ deltamethrin and permethrin, respectively for 72 h and mRNA transcripts were measured by the bDNA assay. Each bar represents the mean mRNA value of each isoform from 6 determinations (2 individuals, 3 wells each) and the error bars are the standard error of the mean. Appropriate positive controls were included in the experiment. The absence of an error bar indicates a single determination.

Figure 7A and 7B: Dose-response effect of deltamethrin (Figure 7A) or permethrin (Figure 7B) on CYP3A4 protein in fresh human hepatocytes. Freshly prepared donor human hepatocytes from different individuals were exposed to increasing concentrations of (0, 10, 25 and $100 \mu\text{M}$)

deltamethrin and (0, 5, 50 and 100 μM) permethrin for 72 h and CYP3A4 protein was determined by Western Blot analysis from hepatocytes from 2 - 4 individuals donors. The graph represents the mean of semi-quantitative densitometric data at different doses. Error bars are the standard error of the mean.

Figure 8A and 8B: Effect of deltamethrin, permethrin, and few other pyrethroids (Figure 8A and 8B) on induction of CYP3A4 promoter luciferase activity in dual-transfection HepG2 cells. Dual-transfection HepG2 cells were treated with variety of pyrethroids including deltamethrin (50 μM), permethrin (50 μM), and cypermethrin (50 μM) (Figure 8A), as well as bioresmethrin (10 μM), trans-, 50/50 cis/trans-, and cis-permethrin (10 μM each), cypermethrin (10 μM), deltamethrin (10 μM), cyhalothrin (10 μM), and esfenvalerate (10 μM) (Figure 8B) for 24 h and luciferase activity was determined by Dual-Luciferase assay from five independent experiments (two and three experiments, respectively, for each set of data). The graph represents the mean \pm SE (where $n = 6$ and $n = 9$ for 8A and 8B, respectively) of relative induction of luciferase activity data at different doses.

Figure 1

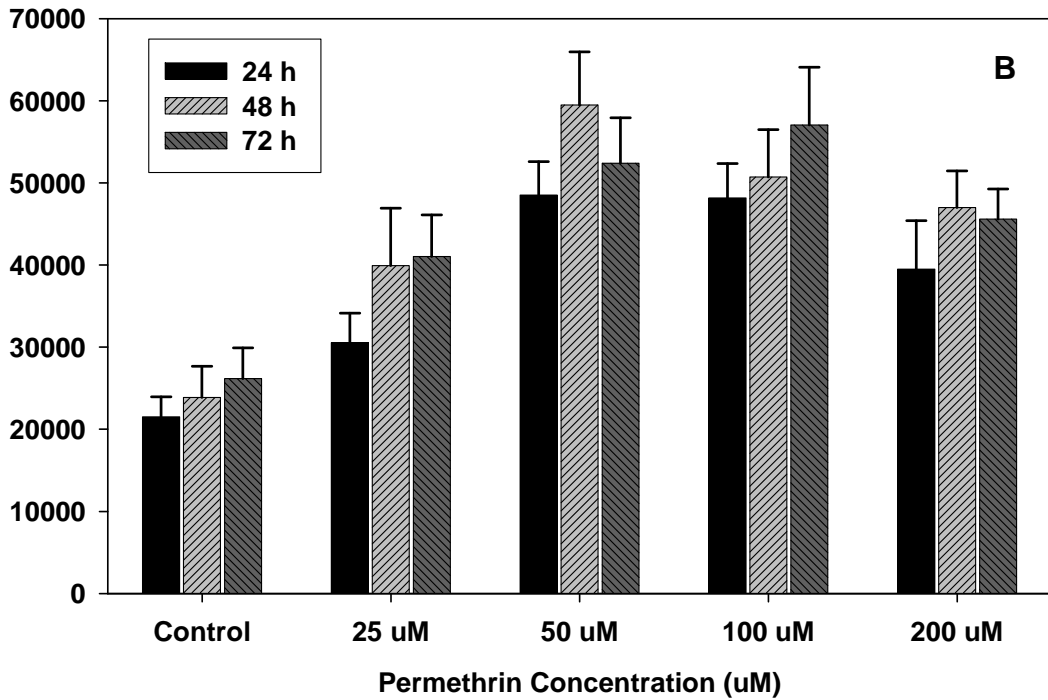
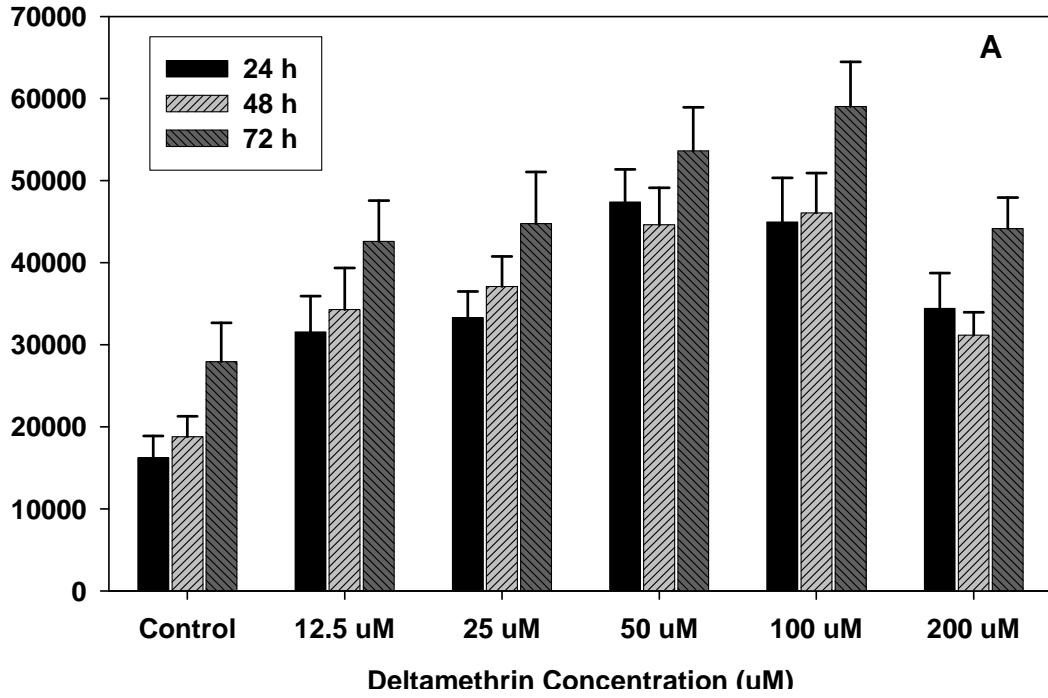


Figure 2

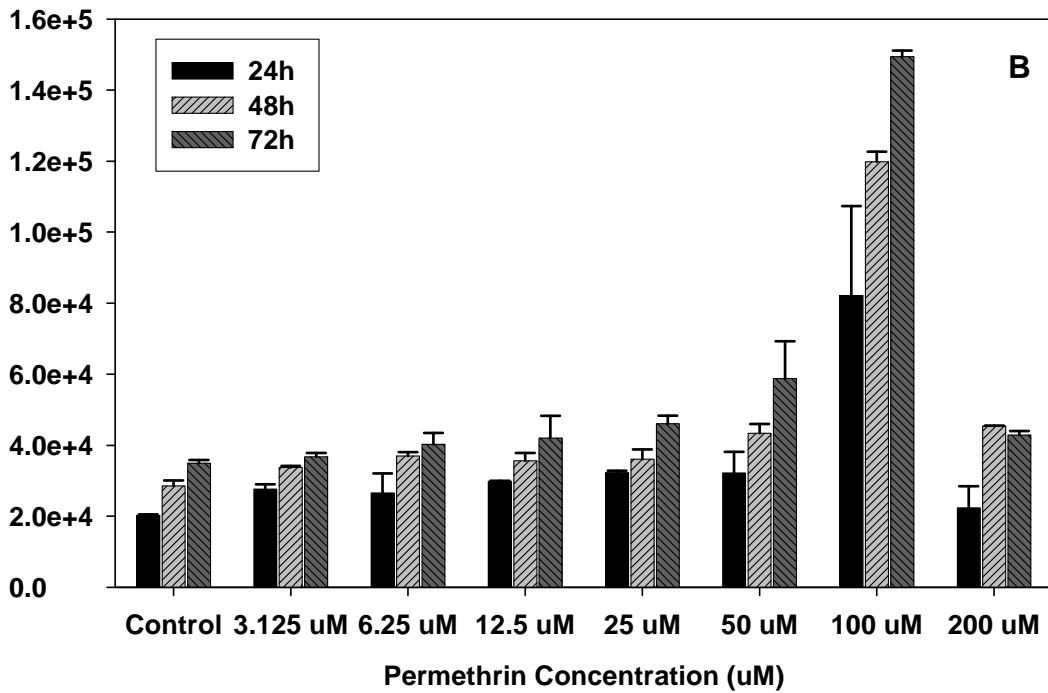
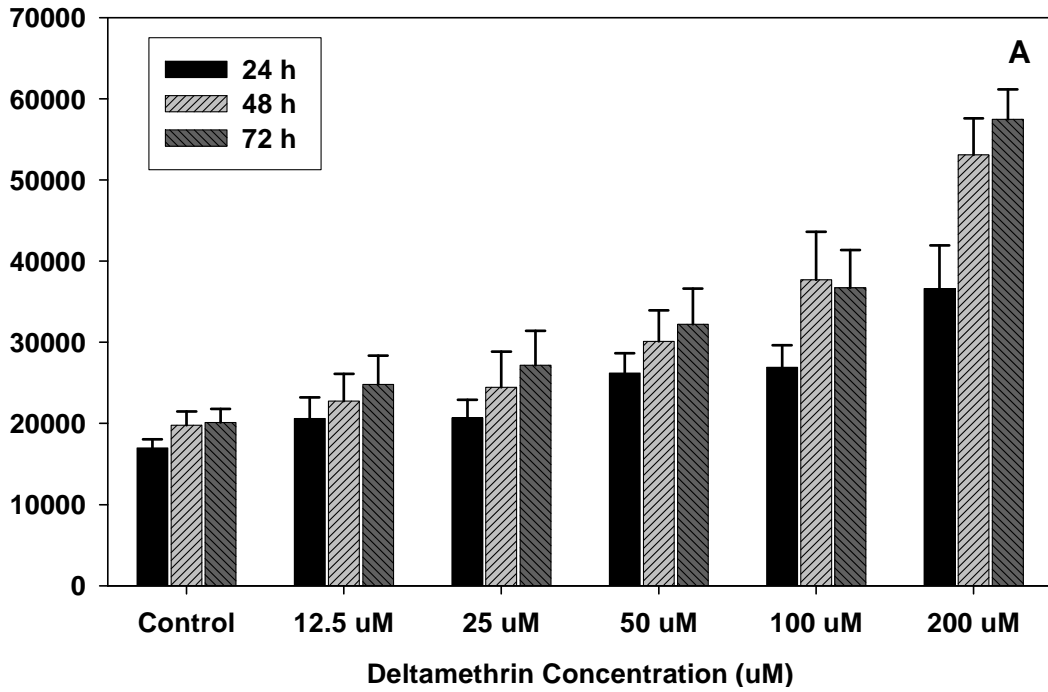


Figure 3

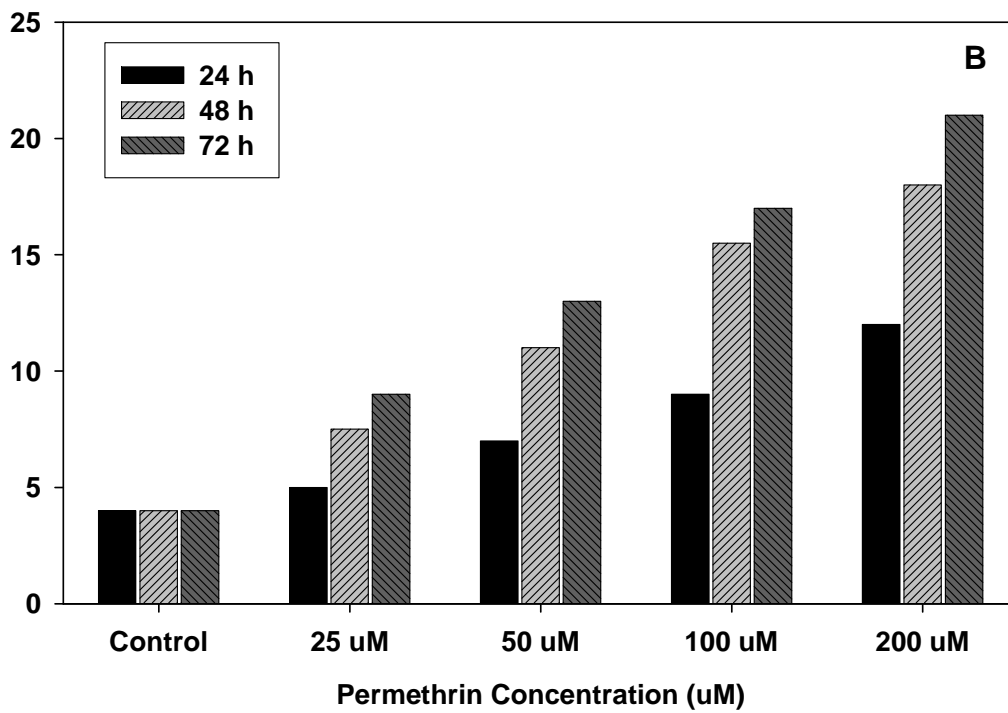
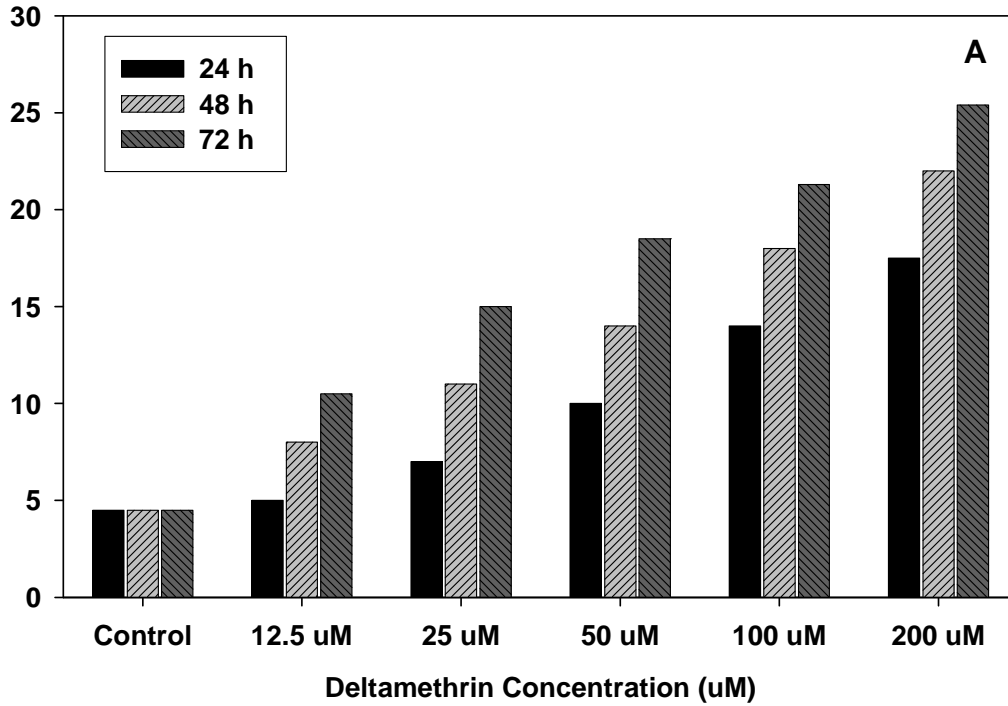


Figure 4

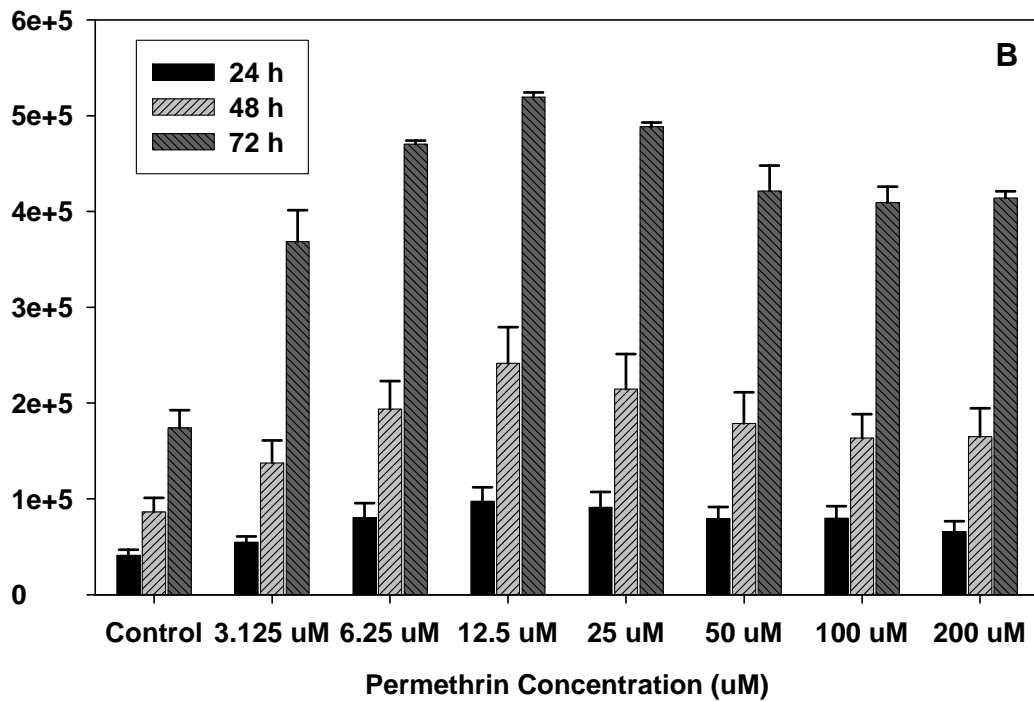
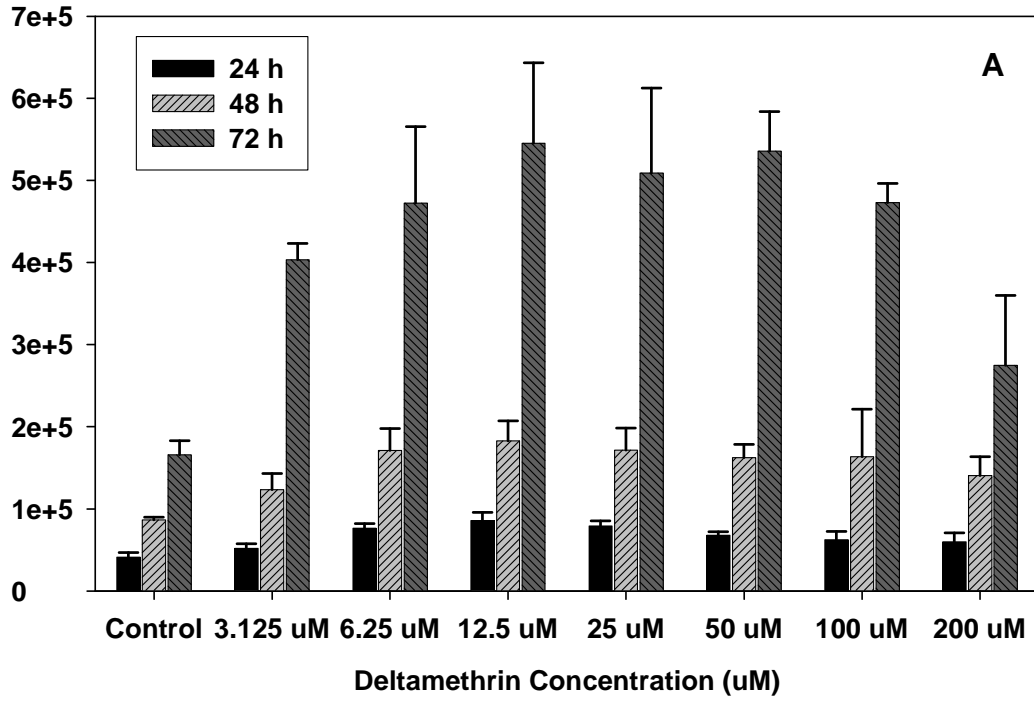


Figure 5

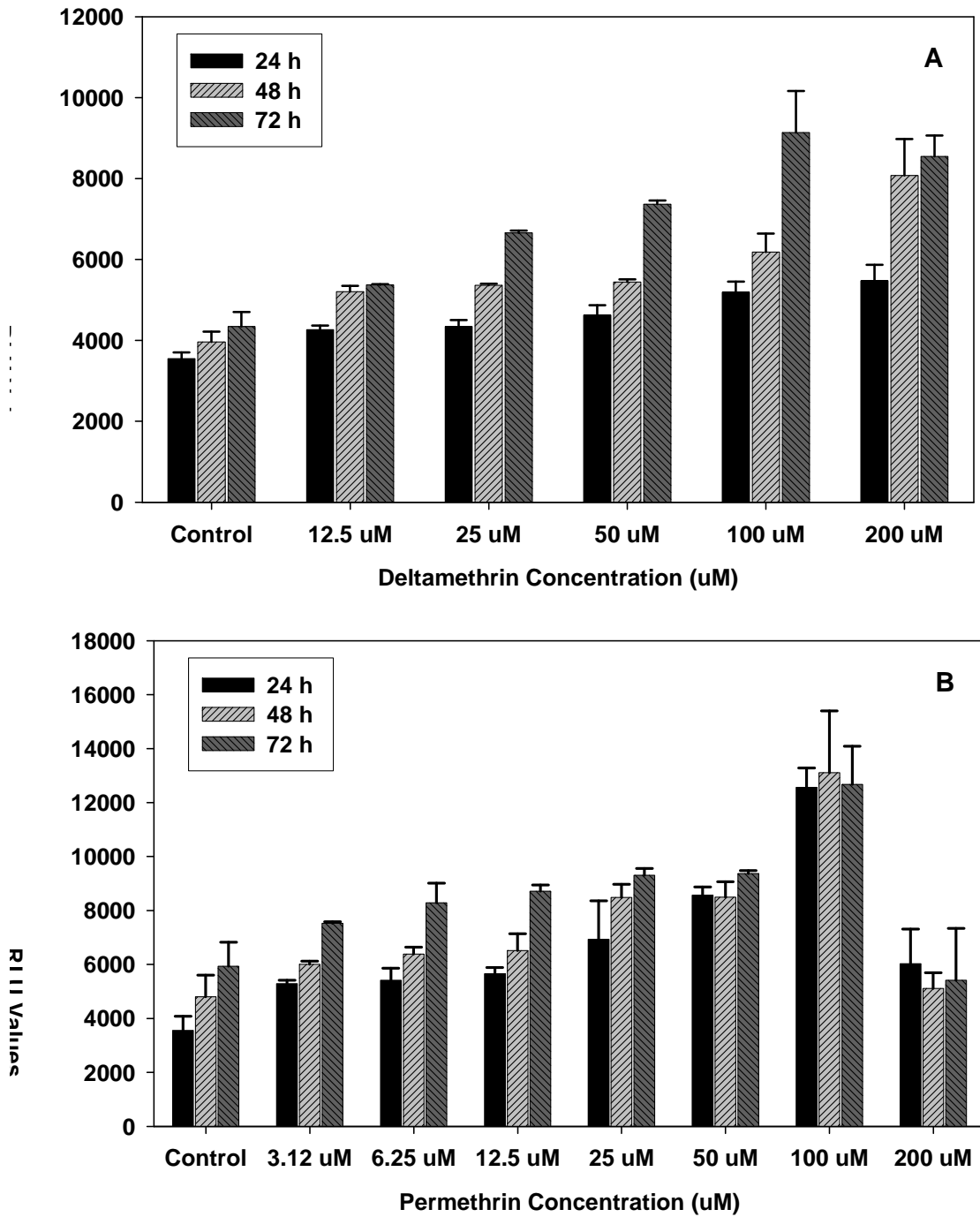


Figure 6

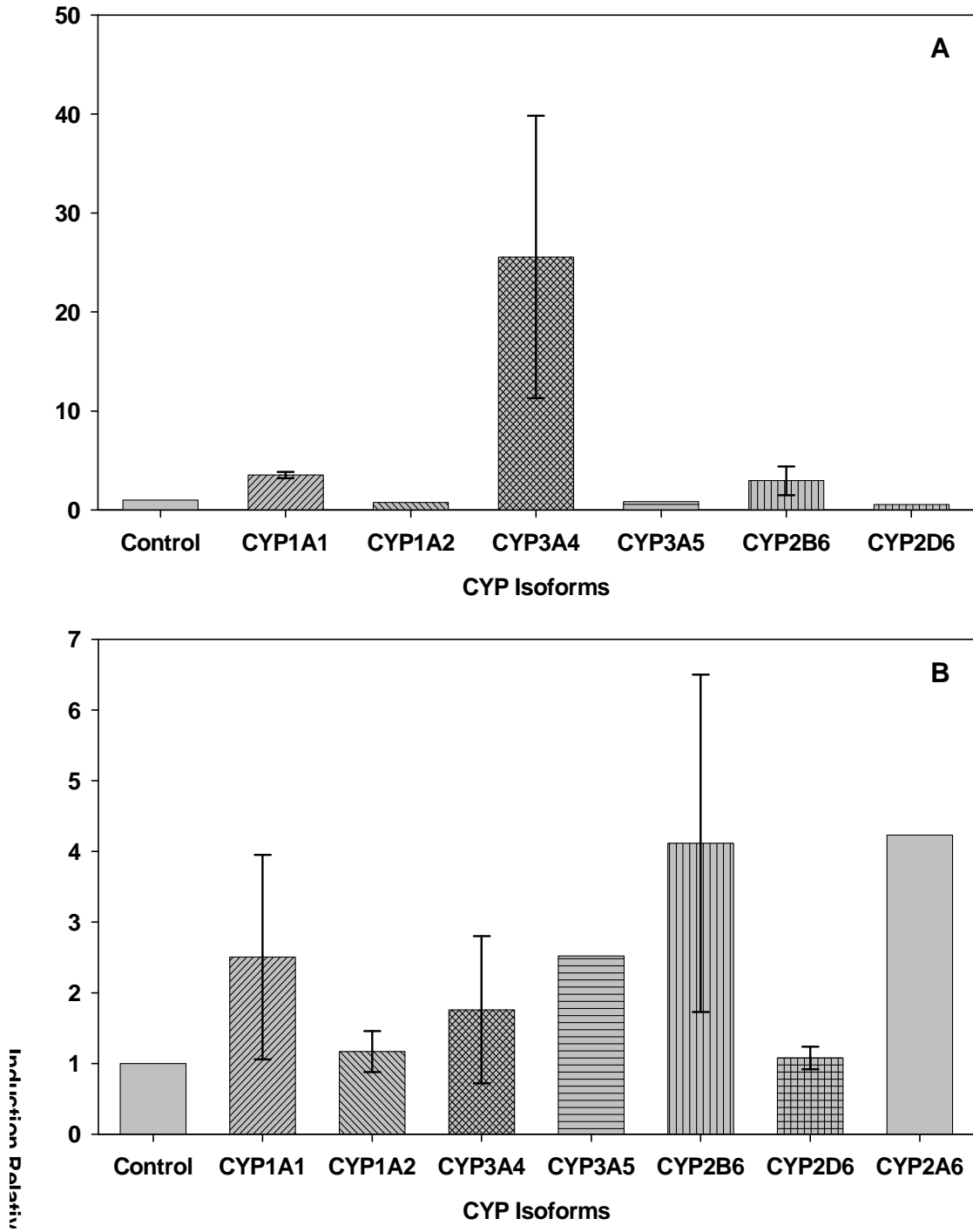


Figure 7

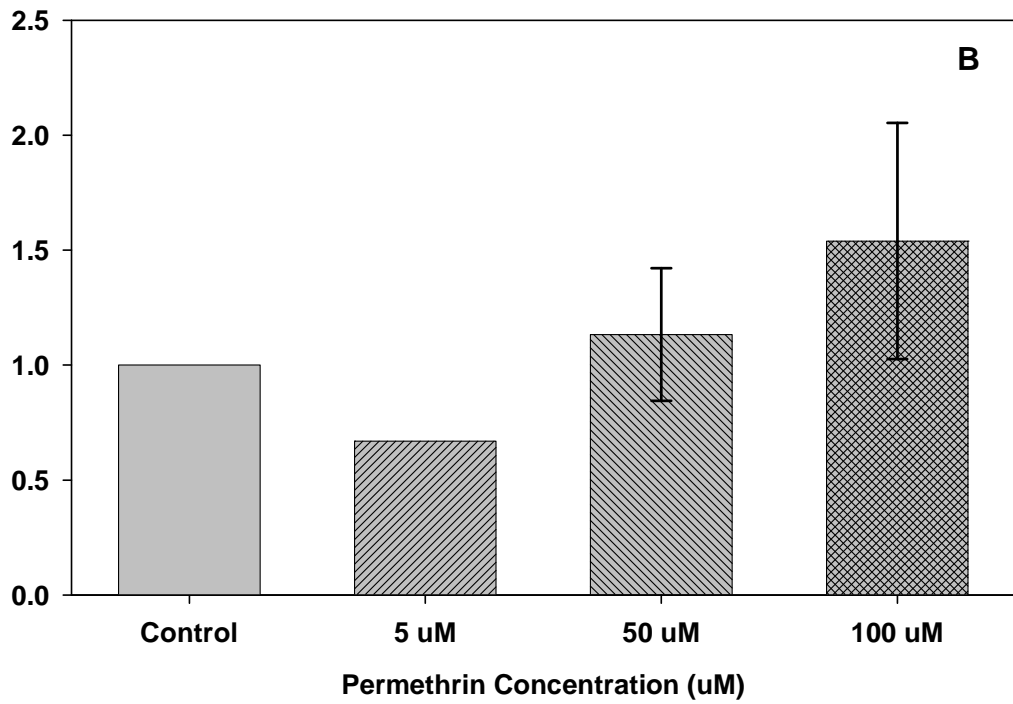
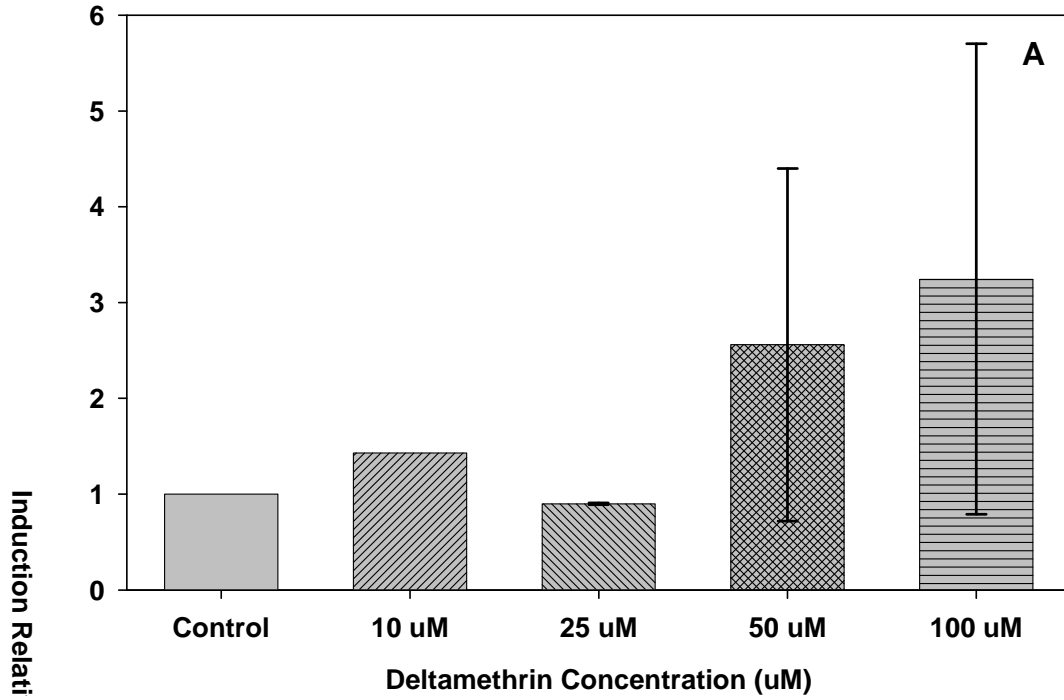
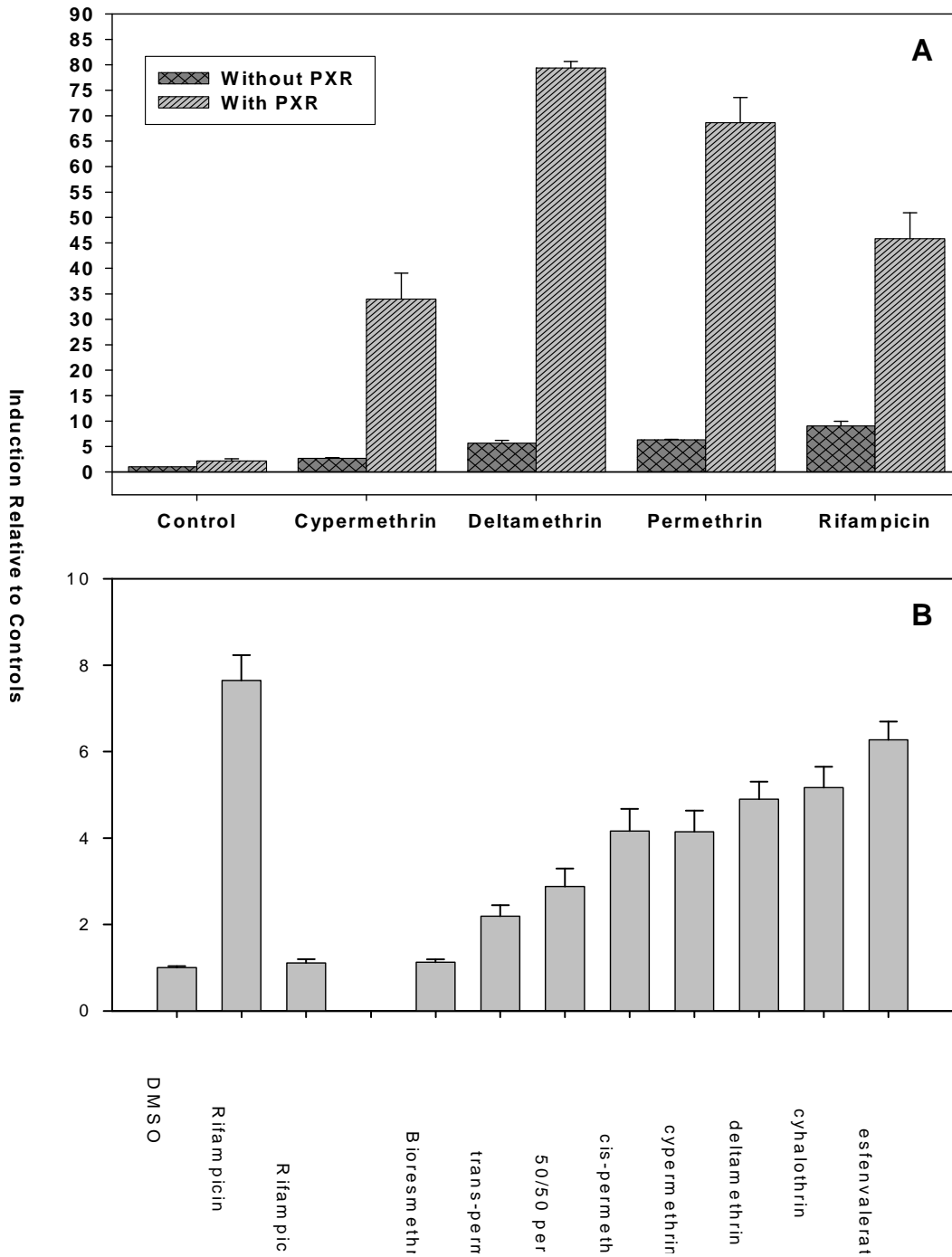


Figure 8



Enzyme Induction and Cytotoxicity in Human Hepatocytes by Chlorpyrifos and N, N-Diethyl-m-Toluamide (DEET)

Parikshit C. Das, Yan Cao, Randy L. Rose[†], Nathan Cherrington¹ and Ernest Hodgson*

Department of Environmental and Molecular Toxicology, Mail Box 7633, North Carolina State University, Raleigh, NC 27695-7633, USA; [†]deceased; ¹Department of Pharmacy, University of Arizona, Tucson, AZ 85721-0207, USA

***Corresponding author:** Dr. Ernest Hodgson, Department of Environmental and Molecular Toxicology, Mail Box 7633, North Carolina State University, Raleigh, NC 27695-7633, USA. Telephone: +1 919 515 5295; fax: +1 919 513 1012; E-mail address: ernest_hodgson@ncsu.edu

Acknowledgements:

This publication was supported by Grant/Cooperative Agreement Number 5 U50 OH007551-05 from CDC - NIOSH. Its contents are solely the responsibility of the authors and do not necessarily represent the official views of Centers for Disease Control (CDC).

Short title: CYP Induction by Chlorpyrifos and DEET in Human Hepatocytes

Key words: Chlorpyrifos; DEET; Human Hepatocytes; CYP Isoforms; Cytotoxicity

=====

Abbreviations

AK: Adenylate Kinase; Apaf-1: Apoptotic protease activating factor-1; DEET: N, N-diethyl-m-toluamide; E₂:17 β -estradiol; PXR: Pregnane X Receptor; RXR: Retinoid X Receptor; XRE: Xenobiotic Responsive Element.

ABSTRACT

Xenobiotics, including drugs and environmental chemicals can influence cytochrome P450 (CYP) levels by altering the transcription of CYP genes. To minimize potential drug-pesticide and pesticide-pesticide interactions it is important to evaluate the potential of pesticides to induce CYP isoforms and to cause cytotoxicity in humans. The present study was designed to examine chlorpyrifos and DEET mediated induction of CYP isoforms and also to characterize their potential cytotoxic effects on primary human hepatocytes. DEET significantly induced CYP3A4, CYP2B6, CYP2A6 and CYP1A2 mRNA expression while chlorpyrifos induced CYP1A1, CYP1A2 and CYP3A4 mRNA, and to a lesser extent, CYP1B1 and CYP2B6 mRNA in primary human hepatocytes. Chlorpyrifos and DEET also mediated the expression of CYP isoform(s) particularly CYP3A4, CYP2B6 and CYP1A1 as evidenced by CYP3A4-specific protein expression, testosterone metabolism and CYP1A1-specific activity assays. DEET is a mild, while chlorpyrifos is a relatively potent, inducer of adenylate kinase and caspase-3/7, an indicator of apoptosis, while inducing 15-20% and 25-30% cell death, respectively. Therefore, DEET and chlorpyrifos mediated induction of CYP mRNA and functional CYP isoforms together with their cytotoxic potential in human hepatocytes suggests that exposure to chlorpyrifos and/or DEET should be considered in human health impact analysis.

INTRODUCTION

DEET (N, N-diethyl-m-toluamide) was developed in 1946 and registered as a repellent for insects and other arthropods in 1957 /1-4/. Many products containing 10 to 100% DEET are sold annually, and ~75 million people in the U.S. use DEET-containing products on an annual basis /3, 5/. There is anecdotal evidence that DEET can cause a number of toxic symptoms /1, 5-8/ but these effects appear to be rare. DEET metabolism has been studied in vivo in a variety of animals /9-11/. N-dealkylation, ring hydroxylation and ring dealkylation of DEET occur in rat liver microsomes /12, 13/, while limited in vivo studies have been performed in human volunteers /14/. In vitro human studies indicated the involvement of CYP2B6 and CYP1A2 in DEET metabolism /15/.

Chlorpyrifos [O, O-diethyl-O-(3, 5, 6-trichloro-2-pyridinyl)-phosphorothioate] is a widely used organophosphorus pesticide in agricultural, military and other applications. After metabolic activation to its oxon, it is a potent acetylcholinesterase inhibitor and manifests a variety of pathological symptoms /16/. During development the chlorpyrifos metabolite is concentrated in peripheral tissues, especially in the liver (Hunter et al.1998), affects hepatic adenylyl cyclase signal transduction at a sub-threshold level for systemic toxicity (17, 18), and can be hepatotoxic at higher doses (19). In vivo, the toxicity of chlorpyrifos can be further impacted by the status of the human polymorphic enzyme PON1, and also from the release of reactive sulfur during oxon formation /20, 21/. However, toxicity is primarily determined by CYP-mediated chlorpyrifos-oxon formation /22/. Chlorpyrifos metabolism has been studied in variety of animals /23/ and is metabolized in vitro by human liver microsomes and CYP isoforms, particularly CYP2B6 /24/.

Interaction of Gulf War related chemicals produced greater than additive toxicity in rats and mice /25/ and a correlation has been suggested between Gulf War illnesses and use of pesticides and repellants, including DEET and chlorpyrifos /26, 27/. Recent in vitro studies have demonstrated human metabolism of DEET and chlorpyrifos and their interactions with each other, with other chemicals and with endogenous neurochemicals and hormones /15, 28-31/. DEET increased the biotransformation of chlorpyrifos to chlorpyrifos-oxon, while on the other hand, chlorpyrifos completely inhibits CYP-mediated metabolism of DEET. However, no studies have been performed to delineate their capability for CYP isoform induction or cytotoxicity in human hepatocytes. Recent studies raise the possibility that pesticide mediated inhibition of drug and hormone metabolism pose a health risk to humans /29-36/. However, there have been only limited studies of pesticide-mediated CYP induction in humans /37, 38/. Thus, the present study was designed to examine chlorpyrifos and DEET mediated induction of metabolic CYP enzymes and cytotoxicity in primary human hepatocytes.

MATERIALS AND METHODS

Chemicals and Reagents

DEET (N, N-diethyl-m-toluamide) and chlorpyrifos [O, O-diethyl-O-(3, 5, 6-trichloro-2-pyridinyl)-phosphorothioate] were purchased from Chem Service (West Chester, PA). Williams E culture medium and the medium supplements dexamethasone and insulin were obtained from Bio-Whittaker (Walkersville, MD). EME Medium without L-glutamine and phenol red, non-essential amino acid solution, L-glutamine solution, and other cell culture related products were purchased from Media-tech, Inc (Herndon, VA). Certified fetal bovine serum, trypsin-EDTA

solution and HBSS buffers were obtained from GIBCO InVitrogen Corporation (Carlsbad, CA). Tissue culture flasks and culture plates along with other tissue culture related products were purchased from Fisher Scientific, Inc. (Pittsburgh, PA). The ToxiLight™ BioAssay Kit was purchased from Lonza, (Rockland, ME). Caspase-Glo™-3/7 Assay Kit was purchased from Promega Corporation (Madison, WI). Actinomycin D and Z-DEVD-FMK were products of Alexis Biochemicals and supplied by AXXORA, LLC (San Diego, CA). Rifampicin, phenobarbital and all other chemicals, unless specified otherwise, were purchased from Sigma-Aldrich Chemical Company (St. Louis, MO). Monoclonal anti-human CYP3A4 from mice were purchased from BD Biosciences (Bedford, MA) and R & D Systems (Minneapolis, MN), respectively. All chemical, reagent and biohazard wastes were disposed of according to the safety protocols of NCSU.

Human Hepatocyte Culture:

The details of maintaining human hepatoma HepG2 culture in our laboratory, their viability and experimental use were previously described /37, 38/. Primary cultures of human hepatocytes were purchased from ADMET Technologies (Durham, NC). Verification of viability by the trypan blue exclusion assay was also described previously /37, 38/.

Hepatocyte and HepG2 cell treatment

For measuring adenylate kinase release and performing the trypan blue exclusion assays human hepatoma HepG2 cells were treated with 0 - 250 µM DEET or chlorpyrifos for 24, 48 or 72 h. Similarly, HepG2 cells were exposed to 0 - 250 µM DEET or chlorpyrifos for 24, 48 or 72 h for assaying caspase-3/7 activity. Primary cultures of human hepatocytes, approximately 1.5×10^6

cells per well in 6-well plates, were treated in culture medium for 72 h with 100 μM DEET or chlorpyrifos for measuring quantitative mRNA expression of CYP isoforms. Primary hepatocytes in 6-well plates were treated for 72 h with 0 - 100 μM DEET or chlorpyrifos for semiquantitative measurement of immunoreactive CYP2B6 and CYP3A4 protein expression. Human hepatocytes, 3×10^5 , in 24-well tissue culture plates were exposed to 50 or 100 μM DEET or chlorpyrifos for 72 h before the DEET or chlorpyrifos-containing medium was replaced with fresh medium. Medium containing testosterone was then added into the wells and incubated for 30 min. before measuring the formation of 6 β -OH testosterone. Human hepatocytes in 48-well tissue culture plates, 1.5×10^5 cells per well in 1 mL medium, were exposed for 72 h to inducing agents, including 3-methyl cholanthrene (3-MC) (10 μM), rifampicin (Rif) (10 μM) or phenobarbital (PB) (100 μM), and increasing concentrations (0 - 100 μM) of chlorpyrifos along with a solvent control for CYP1A1 activity assay. Similarly, hepatocytes were also treated with increasing concentrations (0 - 200 μM) of chlorpyrifos for 24, 48 or 72 h for quantitative determination of adenylate kinase and caspase-3/7 activity. In all experiments inducers such as 3-MC, Rif or β -naphthoflavone were used as positive controls.

Hepatocyte Sample Preparation

Appropriate samples were prepared for the following assays which have been previously described in detail /37, 38/.

Branched DNA (bDNA) Assay

Changes in the expression of CYP isoform mRNA in human hepatocytes following treatment with DEET or chlorpyrifos was measured quantitatively using the branched DNA (bDNA) assay as described previously /38, 39/.

Western blot analysis

Gel electrophoresis, immunodetection and quantification: 7.5% sodium dodecyl sulfate-polyacrylamide gel electrophoresis (SDS-PAGE) was used to resolve microsomal proteins as described by Laemmli /40/. The details of the subsequent steps have also been described previously /38/.

CYP1A1 and CYP3A4 Metabolic Activity Assays

Primary cultures of human hepatocytes in 24 well culture plates were treated for 72 h with increasing concentrations of chlorpyrifos or DEET at 37°C having the chlorpyrifos or DEET-containing media changed every 24 h. Chlorpyrifos-treated hepatocytes were used for the determination of CYP1A1 and CYP3A4 activity while DEET treated hepatocytes were used for CYP3A4 activity assay. The determination of CYP1A1 and CYP3A4 activity was performed according to the manufacturer's protocol (Promega Corporation, Madison, WI). Other details have already been described /38/. The details of the measurement of testosterone metabolism have also been described /29, 38/.

Cell Viability and Cytotoxicity Assay

Following completion of treatment, cells were harvested as a cell suspension in isotonic culture medium and viability was assessed by the trypan blue exclusion method using a hemocytometer (Hausser Scientific, Horsham, PA) as described previously /38/.

ToxiLight BioAssay

The toxic effects of chlorpyrifos and DEET have also been measured using the ToxiLight™ BioAssay Kit, a non-destructive luciferase-based bioluminescence cytotoxicity assay. This quantitatively measures the release of adenylate kinase, a marker of toxicity, into the culture medium. The emitted light intensity expressed as relative luminescence unit (RLU) value is linearly related to the adenylate kinase activity. The assay was performed according to the manufacturer's protocol (Lonza, Rockland, ME) and as described previously /38/.

Caspase-3/7 Assay

Caspase-3/7 is a well known marker for apoptotic cell death. The activity of caspase-3/7 was measured using a luminometer and a Caspase-Glo™-3/7 Assay kit. Luminescence produced by luciferase as RLU value is proportional to the amount of caspase-3/7 activity present in the sample. The assay was performed according to the manufacturer's protocol (Tech. Bull. No 323, Promega Corporation, Madison, WI) and the details described previously /38/.

Statistical Analysis

The data were summarized and expressed as the mean \pm SE by using Microsoft Excel spreadsheet and Sigma Plot graphics programs (Chicago, IL, USA). The significant differences

between control and treated data sets were determined by using analysis of variance and student's t-test.

RESULTS

Effect of DEET and Chlorpyrifos on CYP Isoform mRNA transcription in human hepatocytes

The data show DEET substantially induced CYP mRNAs, approximately 8- fold for CYP1A1 and CYP2B6, while 4-, 10- and 6-fold induction relative to control was noted for CYP1A2, CYP3A4, and CYP2A6, respectively. However, CYP1A1 induction was variable and very little induction of the CYP3A5 isoform was noted (Figure 1A). Chlorpyrifos showed ~25-fold induction of CYP1A1, and 8-, 6-, and 4-fold induction of CYP1A2, CYP3A4, and CYP1B1, respectively, relative to control. A low level of induction was noted for CYP2B6 while no induction of CYP2A6 was apparent (Figure 1B).

Effect of DEET and chlorpyrifos on CYP3A4 and CYP1A1 functional protein expression in human hepatocytes

To confirm DEET and chlorpyrifos mediated translation of CYP3A4 mRNA transcripts into protein expression, treated human hepatocytes were examined by Western blotting. Both DEET and chlorpyrifos dose-dependently increased CYP3A4 protein expression, reaching a maximum of 4-5 fold relative to control at higher doses with some variability (Figure 2A and 2B).

Verification of functional CYP3A4 protein induced in primary hepatocytes by DEET and chlorpyrifos was probed using testosterone as a substrate. CYP3A4 activity was normalized to total cell protein, and 6 β -hydroxytestosterone production essentially mirrored expression levels

of immunoreactive proteins. However, the degree of testosterone metabolism was 4.5 to 6-fold at 50-100 μM chlorpyrifos while 2.5 to 3-fold at 50-100 μM DEET relative to controls (Figure 3). Induction of CYP1A1 mRNA expression was ~25-fold with 100 μM chlorpyrifos in contrast to that of DEET where it was ~7-fold with some degree of variability relative to their respective controls (Figure 1). In order to verify the functional activity of induced CYP mRNA, CYP1A1 activity was measured in treated human hepatocytes and the data normalized to total cell protein. CYP1A1 activity exhibited greater than 2-fold induction but at much lower dose of (1 μM) of chlorpyrifos which tapered off at higher concentrations (Figure 4), while CYP1A1 showed very little activity with DEET (data not shown).

Effect of DEET and chlorpyrifos on adenylate kinase activity in human hepatocytes

Adenylate kinase, a determinant of cellular toxicity, was determined. DEET and chlorpyrifos both showed a dose-dependent effect on the release of adenylate kinase activity in HepG2 cells, where 50, 100 and 250 μM DEET induced increased release of 2.5-to-3.5 fold relative to control (Figure 5A). Similarly, chlorpyrifos at 25 and 50 μM induced a 2-3 fold increase, however, the release of adenylate kinase plateaued at 100 and 200 μM chlorpyrifos (Figure 5B). Likewise, in primary human hepatocytes both DEET and chlorpyrifos dose-dependently induced adenylate kinase, which peaked at 100 μM DEET and 12.5-to-25 μM chlorpyrifos, respectively with plateaus at higher doses at 24 h. A pattern similar to that of 24 h but with a higher response was noted at longer time points, 48 and 72 h (Figure 6A and 6B).

Toxicity of DEET and chlorpyrifos in HepG2 Cells

In order to ascertain the degree of cell cytotoxicity relative to the release of adenylate kinase the trypan blue exclusion assay was performed on HepG2 cells. 15 to 20 % cell death was noted following 48 to 72 h exposure at 100 and 250 μM DEET (Figure 7A) while dose- and time-dependent cytotoxic effects of chlorpyrifos were also noted. Initial signs of cytotoxicity were noted at 25 μM reaching approximately 35% at 200 μM chlorpyrifos (Figure 7B).

Effect of DEET and chlorpyrifos on caspase-3/7 activity in HepG2 cells and human hepatocytes

For initial characterization of cell death the activity of caspase-3/7 was determined. Induction of activated caspase-3/7 is one of the last cascade steps and an identifiable landmark of the cellular apoptotic process. Apparently, DEET and chlorpyrifos have only a minor effect in inducing caspase-3/7 activity in both HepG2 cells and primary human hepatocytes. 2 to 2.5-fold induction was noted at 50 and 100 μM DEET at 72 h (Figure 8A, B), while a dose-dependent increase in induction of activated caspase-3/7 was noted at 3.12 μM which peaked at 12.5-25 μM chlorpyrifos in both cell types at 72 h (Figure 8C, D).

DISCUSSION

DEET and chlorpyrifos are interacting chemicals used, among other pesticides, in the first Gulf War, and recently studied in in vitro human hepatic system(s) in our laboratory. Chlorpyrifos, which completely inhibits DEET metabolism, also inhibits not only the metabolism of a variety of other xenobiotics but also the metabolism of steroid hormones /41, 42/. Studies using human liver microsomes revealed that DEET and chlorpyrifos-oxon stimulate the production of

testosterone metabolites /29/. In the rat DEET also increased the metabolism of testosterone /43/. In vitro human studies indicated involvement of several CYPs in DEET and chlorpyrifos metabolism /29, 41/. Studies with rat and human hepatocytes indicated that various pesticides are capable of inducing many metabolic enzymes /44, 45/. However, induction of CYPs and cytotoxicity of chlorpyrifos and DEET have yet to be characterized in human hepatocytes. Our recent study indicated that CYP induction may not have a mechanistic relationship with insecticide cytotoxicity /38/. In the present study, DEET significantly induced mRNA expression of CYP3A, CYP2B, CYP2A and CYP1A2; while chlorpyrifos induced CYP1A1, CYP1A2, CYP3A4, and to a lesser extent CYP1B and CYP2B in primary human hepatocytes. Since CYP3A and CYP2B may be co-regulated as a result of activation of the human pregnane X receptor (hPXR) and CYP1A is regulated by aromatic hydrocarbon receptor (AhR), variations in CYP gene expressions may be due to the interactions of pesticides and the regulatory elements involved in induction of these CYP isoforms /46-48/.

CYP3A4 is the major enzyme among human CYPs which, along with CYP2B6 and CYP1A1, plays a predominant role in the metabolism of clinical drugs, and numerous other xenobiotics and endogenous substrates /29, 49, 50/. Chlorpyrifos and DEET mediate mRNA expression of CYP isoform(s) particularly CYP3A4, CYP2B6 and CYP1A1 and this has been supported by the demonstration of their translation into functional proteins as evidenced by the data on CYP3A-specific protein expression, testosterone metabolism and CYP1A1-specific activity assays. Previous evidence indicated that pesticide mediated CYP-induction has significant impact on drug/pesticide, hormone/pesticide and pesticide/pesticide interactions /29, 38, 41/, suggesting

that DEET and / or chlorpyrifos exposure may disrupt drug-, pesticide- or hormone- metabolism and thus cause concern for human health effects.

Chlorpyrifos is a potent acetylcholinesterase inhibitor well known for its neurotoxicity in various rodent neuronal cell systems in vitro and in vivo. This has led to increasing concern and restricted use /51, 52/. Chlorpyrifos induced apoptotic cell death in human monocytes in vitro at somewhat higher doses than those used in the present study /53/. Although DEET is considered a relatively benign chemical, anecdotal reports involving heavy and excessive exposure indicate a variety of possible toxic side effects /1, 5/. The mode of action of DEET cytotoxicity is mostly unknown. The cellular signaling mechanisms of DEET and chlorpyrifos mediated cytotoxicity potential have not been characterized in human hepatocytes, the primary site of metabolism. In the present study, DEET at moderately high doses and chlorpyrifos at much lower doses induced adenylate kinase release, an indicator of cytotoxicity. The release of adenylate kinase was lower at a higher dose(s) of DEET and chlorpyrifos. While at highest doses (200-250 μ M) of DEET and chlorpyrifos the levels of cytotoxicity were 15-20% and 25-30%, respectively; and this was semi-quantitatively substantiated by the trypan blue exclusion assay data. Both DEET and chlorpyrifos are capable of potentially inducing major metabolic enzymes at the lower doses while causing cytotoxic effects at higher doses, thus these pesticides may have an impact on human health.

Previous studies indicated that concurrent application of DEET and permethrin induce urinary excretion of 3-nitrotyrosine and 8-hydroxy-2'-deoxyguanosine, markers of DNA damage and oxidative stress, and mitochondrial cytochrome c release in rat /54/. Initiation of programmed

cell death (apoptosis) is evidenced by the release of mitochondrial cytochrome c activity, activation of caspases, elevation of 8-hydroxy-2-deoxyguanosine levels, increased levels of 3-nitrotyrosine, and alterations of p53 gene expression /55/. Genotoxic effects of DEET were reported in primary human nasal mucosal cells /56/. Chlorpyrifos mediated apoptosis was indicated by staining with Annexin-V, activation of caspase-3 and DNA fragmentation in the human monocyte U937 cell line /53/. In the present study, DEET is a mild, while chlorpyrifos is a relatively potent, inducer of adenylate kinase and caspase-3/7, indicators of apoptotic cell death. Thus, in rodent and humans, both DEET and chlorpyrifos induced apoptotic cell death in hepatocytes.

Like chlorpyrifos, DEET can induce mRNA and functional protein of the major and important CYP isoforms in the human hepatocytes. Whether this functional CYP induction has any correlation with the induction of cytotoxic effects cannot be ascertained from this study. Both DEET and chlorpyrifos at higher dose levels induce functional CYPs and exert cytotoxic effects in human hepatocytes. Recent in vitro studies have demonstrated an induction profile in CYP mRNA in rat intestine and liver slices by known inducers is very similar when compared to that in vivo /57, 58/. Therefore, DEET and chlorpyrifos mediated induction in functional CYP along with their cytotoxicity via apoptosis in human hepatocytes suggests that high-level short-term exposure to chlorpyrifos and DEET alone or in combination may have significant health impact in humans, which may warrants further risk analysis and assessment.

REFERENCES

1. Robbins PJ and Cherniack MG (1986): Review of the biodistribution and toxicity of the insect repellent N, N-diethyl-m-toluamide (DEET). *J Toxicol Environ Health* 18: 503-525.
2. Brown M and Hebert AA (1997): Insect repellents: An overview. *J Am Acad Dermal.* 36: 243-249.
3. U.S. EPA (1998): Prevention, Pesticides and Toxic Substances. Registration eligibility decision (RED): DEET. <http://cfpub.epa.gov/oppref/rereg/status.cfm?show=rereg>. Pp. 2-9.
4. Coosemans M and Guillet P (1999): Individual protection against mosquito bites. *Med Maladies Infect.* 29 (suppl.): 390S-396S.
5. Veltri JC, Osimitz TG, Bradford DC, and Page BC (1994): Retrospective analysis of calls to poison control centers resulting from exposure to the insect repellent N, N-diethyl-m-toluamide (DEET) from 1985 to 1989. *Clin Toxicol.* 32: 1-16.
6. Bell JW, Veltri JC, and Page BC (2002): Human exposures to N, N-diethyl-m-toluamide insect repellents reported to the American Association of Poison Control Centers 1993-1997. *Intern J Toxicol.* 21, 341-352.
7. Abdel-Rahman A, Shetty AK, and Abou-Donia MB (2001): Subchronic dermal application of N, N-diethyl-m-toluamide (DEET) and permethrin to adult rats, alone or in combination, cause diffuse neuronal cell death and cytoskeletal abnormalities in the cerebral cortex and the hippocampus, and Purkinje neuron loss in the cerebellum. *Exp Neurol.* 172, 153-171.
8. Abdel-Rahman A, Dechkovskaia AM, Goldstein LB, Bullman SH, Khan W, EL-Masry EM, Abou-Donia MB (2004): Neurological deficits induced by malathion, DEET, and permethrin, alone or in combination in adult rats. *J Toxicol Environ Health, Pt. A.* 67, 331-356.
9. Taylor WG, Danielson TJ, Spooner RW, and Goldstein LR (1994): Pharmacokinetic assessment of the dermal absorption of N, N-diethyl-m-toluamide (DEET) in cattle. *Drug Metab Dispos.* 22: 106-112.
10. Schoenig GP, Hartnagel RE, Osimitz TG, and Llanso S (1996): Absorption, distribution, metabolism, and excretion of N, N-diethyl-m-toluamide in the rat. *Drug Metab Dispos.* 24: 156-163.
11. Qui H, Jun HW, and Tao J (1997): Pharmacokinetics of insect repellent N,N-diethyl-m-toluamide in beagle dogs following intravenous and topical routes of administration. *J Pharm Sci.* 86: 514-516.
12. Taylor WG (1986): Metabolism of N, N-diethyl-meta-toluamide by rat liver microsomes. *Drug Metab Dispos.* 14: 532-539.

13. Constantino L and Iley J (1999): Microsomal metabolism of N,N-diethyl-m-toluamide (DEET, DET): The extended network of metabolites. *Xenobiotica* 29: 409-416.
14. Seliem S, Hartnagel RE, Osimitz TG, Gabriel KL and Schoening GP (1995): Absorption, metabolism, and excretion of N, N-diethyl-m-toluamide following dermal application to human volunteers. *Fundam Appl Toxicol.* 2: 95-100.
15. Usamani KA, Rose RL, Goldstein JA, Taylor WG, Brimfield AA, and Hodgson E (2002): In vitro human metabolism and interactions of repellent N,N-diethyl-M- toluamide. *Drug Metab Dispos* 30, 289-294.
16. Echobicon DJ (2001): Toxic effects of pesticides. In: Klaassen CD, ed. Cassarett and Doull's *Toxicology: the Basic Science of Poisons*. 6th. ed. New York: McGraw-Hill, pp. 763-810.
17. Song X, Seidler FJ, Saleh JL, Zhang J, Padilla S, Slotkin TA (1997): Cellular mechanisms for developmental toxicity of chlorpyrifos: targeting the adenylyl cyclase signaling cascade. *Toxicol Appl Pharmacol* 145, 158-174.
18. Auman JT, Seidler FJ, Slotkin TA (2000): Neonatal chlorpyrifos exposure targets multiple proteins governing the hepatic adenylyl cyclase signaling cascade: implications for neurotoxicity. *Dev Brain Res* 121, 19-27.
19. Goel A, Chauhan DP, Dhawan DK (2000): Protective effects of zinc in chlorpyrifos induced hepatotoxicity: a biochemical and trace elemental study. *Biol Trace Elem Res* 74, 171-183.
20. Li WF, Costa LG, Richter RJ, Hagen T, Shih DM, Tward A, Lulis AJ, Furlong CE (2000): Catalytic efficiency determines the in vivo efficiency of PON1 for detoxifying organophosphorus compounds. *Pharmacogenetics* 10, 767-779.
21. Neal RA (1980): Microsomal metabolism of thiono-sulfur compounds: Mechanisms and toxicological significance. *Rev Biochem Toxicol.* 2, 131-171.
22. Levi PE, Hodgson E (1985): Oxidation of pesticides by purified cytochrome P450 isozymes from the mouse liver. *Toxicol Lett.* 24, 221-228.
23. Sultatos LG (1991): Metabolic activation of the organophosphorus insecticides chlorpyrifos and fenitrothion by perfused rat liver. *Toxicology* 68, 1-9.
24. Tang J, Cao Y, Rose RL, Brimfield AA, Dai D, Goldstein JA, Hodgson E (2001): Metabolism of chlorpyrifos by human cytochrome P450 isoforms and human, mouse, and rat liver microsomes. *Drug Metab Dispos.* 29, 1201-1204.
25. Cheney LA, Rockhold RW, Wineman RW, and Hume AS (1999): Anticonvulsant-resistant seizures following pyridostigmine bromide (PB) and N, N-diethyl-m-toluamide (DEET). *Toxicol. Sci.* 49, 306-311.

26. Bolton HT (1995): Use and safety of pesticides (repellents) in Persian Gulf. Presentation to the Department of Veterans' Affairs: Update on Health Consequences of Persian Gulf Service. Baltimore, MD.
27. Jamal GA (1998): Gulf War syndrome – a model for the complexity of biological and environmental interaction with human health. *Adverse Drug React Toxic Rev.* 17, 1-17.
28. Tang J, Rose RL, Hodgson E (2002): In vitro metabolism of carbaryl by human cytochrome P450 and its inhibition by chlorpyrifos. *Chem-Biol Inter.* 141, 229-241.
29. Usmani KA, Rose RL, and Hodgson E (2003): Inhibition and activation of the human liver microsomal and human cytochrome P450 3A4 metabolism of testosterone by deployment-related chemicals. *Drug Metab Dispos.* 31, 384-391.
30. Usmani KA, Rose RL, Hodgson E (2006): Inhibition of the human liver microsomal and human cytochrome P450 1A2 and 3A4 metabolism of estradiol by deployment-related chemicals. *Drug Metab Dispos.* 34, 1606-1614.
31. Yager JD (2000): Endogenous estrogens as carcinogens through metabolic activation. *J Natl Cancer Inst Monographs* 27, 67-73.
32. Rogan EG, Badawi AF, Devanesan PD, Meza JL, Edney JA, West WW, Higginbotham SM, and Cavalieri EL (2003): Relative imbalances in estrogen metabolism and conjugation in breast tissue of women with carcinoma: potential biomarkers of susceptibility to cancer. *Carcinogenesis* 24, 697-702.
33. Cavalieri EL, Stack DE, Devanesan PD, Todorovic R, Dwivedy I, Higginbotham S, Johansson SL, Patil KD, Gross ML, Gooden JK, Ramanathan R, Cerny RL, Rogan EG (1997): Molecular origin of cancer: catechol estrogen-3,4-quinones as endogenous tumor initiators. *Proc. Natl. Acad. Sci. USA* 94, 10937-10942.
34. Cavalieri EL, Devanesan P, Bosland MC, Badawi AF, and Rogan EG (2002): Catechol estrogen metabolites and conjugates in different regions of the prostate of Noble rats treated with 4-hydroxyestradiol: implications for estrogen-induced initiation of prostate cancer. *Carcinogenesis* 23, 329-333.
35. Tang J., Usmani KA, Hodgson E., Rose RL. (2004): In vitro metabolism of fipronil by human and rat cytochrome P450 and its interactions with testosterone and diazepam. *Chemico-Biological Interactions* 147, 319-329.
36. Di Consiglio E, Meneguz A, Testai E (2005): Organophosphorothionate pesticides inhibit the bioactivation of imipramine by human hepatic cytochrome P450s. *Toxicol. Appl. Pharmacol.* 205, 237-246.

37. Das PC, Streit TM, Cao Y, Rose RL, Cherrington N, Ross, MK, Wallace AW, and Hodgson E (2008): Pyrethroids: Cytotoxicity and Induction of CYP Isoforms in Human Hepatocytes. (in press).
38. Das PC, Cao Y, Cherrington N, Hodgson E, Rose RL (2006): Fipronil induces CYP isoforms and cytotoxicity in human hepatocytes. *Chemico-Biological Interactions* 164, 200-214.
39. Hartley DP, Klaassen CD (2000): Detection of chemical-induced differential expression of rat hepatic cytochrome P450 mRNA transcripts using branched DNA signal amplification technology. *Drug Metab. Dispos.* 28, 608-616.
40. Laemmli U (1970): Cleavage of structural proteins during the assembly of the head bacteriophage T4. *Nature* 227, 680-685.
41. Choi J, Hodgson E, Rose RL (2004): Inhibition of trans-permethrin hydrolysis in human liver fractions by chlorpyrifos oxon and carbaryl. *Drug Metabol Drug Interact.* 20, 233-246.
42. Hodgson E, Rose RL (2005): Human metabolism and metabolic interactions of deployment-related chemicals. *Drug Metab Rev.* 37, 1-39.
43. Abu-Qare AW, Abou-Donia MB (2001): DEET (N, N-diethyl-m-toluamide) alone and in combination with permethrin increased urinary excretion of 6 β -hydroxycortisol in rats, a marker of hepatic CYP3A induction. *J Toxicol Environ Health A.* 64, 373-384.
44. Ledirac N, Delescluse C, de Sousa G, Pralavorio M, Lesca P, Amichot M, Berge JB, and Rahman R. (1997): Carbaryl induces CYP1A1 gene expression in HepG2 and HaCaT cells but is not a ligand of the human hepatic Ah receptor. *Toxicol Appl Pharmacol.* 144, 177-182.
45. Rose RL, Tang J, Choi J, Cao Y, Usmani A, Cherrington N, Hodgson E (2005): Pesticide metabolism in humans, including polymorphisms. *Scand J Work Environ Health* 31, suppl 1, 156-163.
46. Kopponen P, Torronen R, Maki-Paakkanen J, von Wright A, Karenlapi S (1994): Comparison of CYP1A1 induction and genotoxicity in vitro as indicators of potentially harmful effects of environmental samples. *Arch Toxicol.* 68, 167-173.
47. Bertilsson G, Heidrich J, Svesson K, Asman M, Jendeberg L, Sydow-Backman M, Ohlsson R, Postlind H, Blomquist P, Berkenstam A (1998): Identification of a human nuclear receptor defines a new signaling pathway for CYP3A induction. *Proc Natl Acad Sci USA* 95, 12208-12213.
48. Goodwin B, Moore LB, Stoltz CM, McKee DD, Kliewer SA (2001): Regulation of the human CYP2B6 gene by the nuclear pregnane X receptor. *Mol Pharmacol* 60, 427-431.

49. Waxman DJ, Lapenson DP, Aoyama T, Gelboin HV, Gonzalez FJ, and Korzekwa K (1991): Steroid hormone hydroxylase specificities of eleven cDNA-expressed human cytochrome P450s. *Arch Biochem Biophys* 290, 160-166.
50. Yamazaki H and Shimada T (1997): Progesterone and testosterone hydroxylation by cytochrome P-450 2C19, 2C9, and 3A4 in human liver microsomes. *Arch Biochem Biophys* 364, 161-169.
51. Meyer A, Seidler FJ and Slotkin TA (2004): Developmental effects of chlorpyrifos extend beyond neurotoxicity: critical periods for immediate and delayed-onset effects on cardiac and hepatic cell signaling. *Environ Health Perspect.* 112, 170-178.
52. Slotkin TA, Seidler FJ (2007): Comparative developmental neurotoxicity of organophosphates in vivo: transcriptional responses of pathways for brain cell development, cell signaling, cytotoxicity and neurotransmitter systems. *Brain Res Bull.* 72, 232-274.
53. Abu-Qare AW, Abou-Donia MB (2003): Combined exposure to DEET (N, N-diethyl-m-toluamide) and permethrin: pharmacokinetics and toxicological effects. *J Toxicol Environ Health B Crit Rev.* 6, 41-53.
54. Abu-Qare AW and Abou-Donia MB (2001): Biomarkers of apoptosis: Release of cytochrome c, activation of caspase-3, induction of 8-hydroxy-2-deoxyguanosine, increased 3-nitrotyrosine, and alteration of p53 gene. *J Toxicol Environ Health B* 4: 313-332.
55. Tisch M, Schmezer P, Faulde M, Groh A, Maier H (2002): Genotoxicity studies on permethrin, DEET and diazinon in primary human nasal mucosal cells. *Eur Arch Otorhinolaryngol.* 259, 150-153.
56. Nakadai A, Li Q, Kawada T (2006): Chlorpyrifos induces apoptosis in human monocyte cell line U937. *Toxicology* 224, 202-209.
57. Meredith C, Scott MP, Renwick AB, Price RJ, Lake BG (2003): Studies on the induction of rat hepatic CYP1A, CYP2B, CYP3A and CYP4A subfamily form mRNAs in vivo and in vitro using precision-cut rat liver slices. *Xenobiotica* 33, 511-527.
58. Martignoni M, de Kanter R, Grossi P, Mahnke A, Saturno G, Monshouwer M (2004): An in vivo and in vitro comparison of CYP induction in rat liver and intestine using slices and quantitative RT-PCR. *Chem-Bio Int.* 151, 1-11.

FIGURE LEGENDS

Figure 1A and 1B: Effect of DEET (1A) and chlorpyrifos (1B) on the expression of mRNA transcripts of different CYP isoforms in human hepatocytes. Freshly prepared human hepatocytes from four individuals were exposed to 100 μ M of DEET and chlorpyrifos, respectively for 72 h and mRNA transcripts were quantitatively measured by the bDNA assay. Each bar represents the mean mRNA value of each isoform from 1 to 4 individuals per group and error bars are the standard error mean in human hepatocytes. Appropriate positive controls were included in the experiment and absence of an error bar indicates a single determination.

Figure 2A and 2B: Dose-response effect of DEET (2A) and chlorpyrifos (2B) on the CYP3A4 protein in fresh human hepatocytes. Freshly prepared human hepatocytes from five individuals were exposed to increasing concentrations of (0, 10, 50 and 100 μ M) DEET and (0, 10, 50 and 100 μ M) chlorpyrifos for 72 h and CYP3A4 protein was determined by Western Blot analysis. The graph represents the mean of semi-quantitative densitometric data and error bars are the standard error of the mean at different doses.

Figure 3: Dose-response effect of DEET and chlorpyrifos on CYP3A4 activity/function in primary culture of human hepatocytes. Freshly prepared human hepatocytes were exposed to two doses each (50 and 100 μ M) of DEET and chlorpyrifos for 72 h. CYP3A4 mediated metabolism of testosterone was assayed in these treated human hepatocytes by measuring 6 β -(OH)-testosterone production, where the mean control value was 470 ± 251 pmol/mg protein/min. The bar at each dose represents the mean of induction of 6 β -(OH)-testosterone production relative to control and the error bar is the standard error of the mean, where n=3.

Figure 4: Dose-response effect of chlorpyrifos on CYP1A1 activity in primary human hepatocytes. Primary cultures of human hepatocytes were exposed to doses of chlorpyrifos for 72 h and CYP1A1 activity was measured according to the manufacturer's protocol. Activity was expressed as relative luminescence units (RLU), each bar represents the mean where n=2, triplicate determinations were performed from each individual.

Figure 5A and 5B: Dose- and time- dependent effect of DEET (5A) and chlorpyrifos (5B) on the adenylate kinase activity in HepG2 cells. HepG2 cells were exposed to increasing concentrations of DEET (0, 25, 50, 100 and 250 μM) or chlorpyrifos (0, 25, 50, 100 and 200 μM) for 24, 48 and 72 h and adenylate kinase activity was measured using the ToxiLight Bioassay kit. Each bar represents the mean relative luminescence unit (RLU) value of 9 determinations from 3 independent experiments using HepG2 cells. The error bar represents the standard error of the mean. The data are based on triplicate experiments.

Figure 6A and 6B: Dose- and time- dependent effect of DEET (6A) or chlorpyrifos (6B) on the adenylate kinase activity of primary cultures of human hepatocytes. Cultures of primary human hepatocytes were exposed to increasing concentrations of DEET (0, 1, 3.12, 12.5, 50, 100 and 200 μM) or chlorpyrifos (0, 1, 3.12, 12.5, 25, 50 and 100 μM) for 24, 48 and 72 h and then adenylate kinase activity was measured using the ToxiLight Bioassay kit. Each bar represents the relative luminescence unit (RLU) value mean of 6 determinations from 2 individuals. The error bar represents the standard error of the mean and the data are based on triplicate experiment.

Figure 7A and 7B: Dose- and time- dependent effect of DEET (7A) or chlorpyrifos (7B) on human hepatoma HepG2 cell viability. Cultures of HepG2 cells were exposed to increasing concentrations of DEET (0, 25, 50, 100 and 250 μM) and chlorpyrifos (0, 25, 50, 100 and 200 μM) for 24, 48 and 72 h and cell viability was semi-quantitatively assessed by the trypan blue exclusion assay and expressed as % cytotoxicity. Each bar represents the value derived from counting >100 and up to 200 cells in each treated sample.

Figure 8A to 8D: Dose- and time- dependent effects of DEET (8A and 8B) and chlorpyrifos (8C and 8D) on caspase-3/7 activity in human hepatoma HepG2 cells and in primary human hepatocytes, respectively. Cultured HepG2 cells and primary human hepatocytes were exposed to various concentrations (0, 1, 3.12, 6.25, 12.5, 25, 50, 100 and 250 μM) of DEET or chlorpyrifos (0, 1, 3.12, 6.25, 12.5, 25, 50, 100 and 200 μM) along with (not shown) β -naphthoflavone (20 μM), rifampicin (10 μM) and actinomycin D (1 μM), inducers of caspase-3/7, and the caspase-3/7 specific inhibitor Z-DEVD-FMK (0.05 μM) for 24, 48 and 72 h.

Caspase-3/7 activity was quantitatively measured by Caspase-Glo®-3/7 assay kit. Each bar represents the mean of relative luminescence unit (RLU) value of 2-3 independent experiments for HepG2 cells and 2 individuals for primary human hepatocytes. Three to 4 well determinations per group per experiment were performed and error bars are the standard error of the mean.

Figure 1

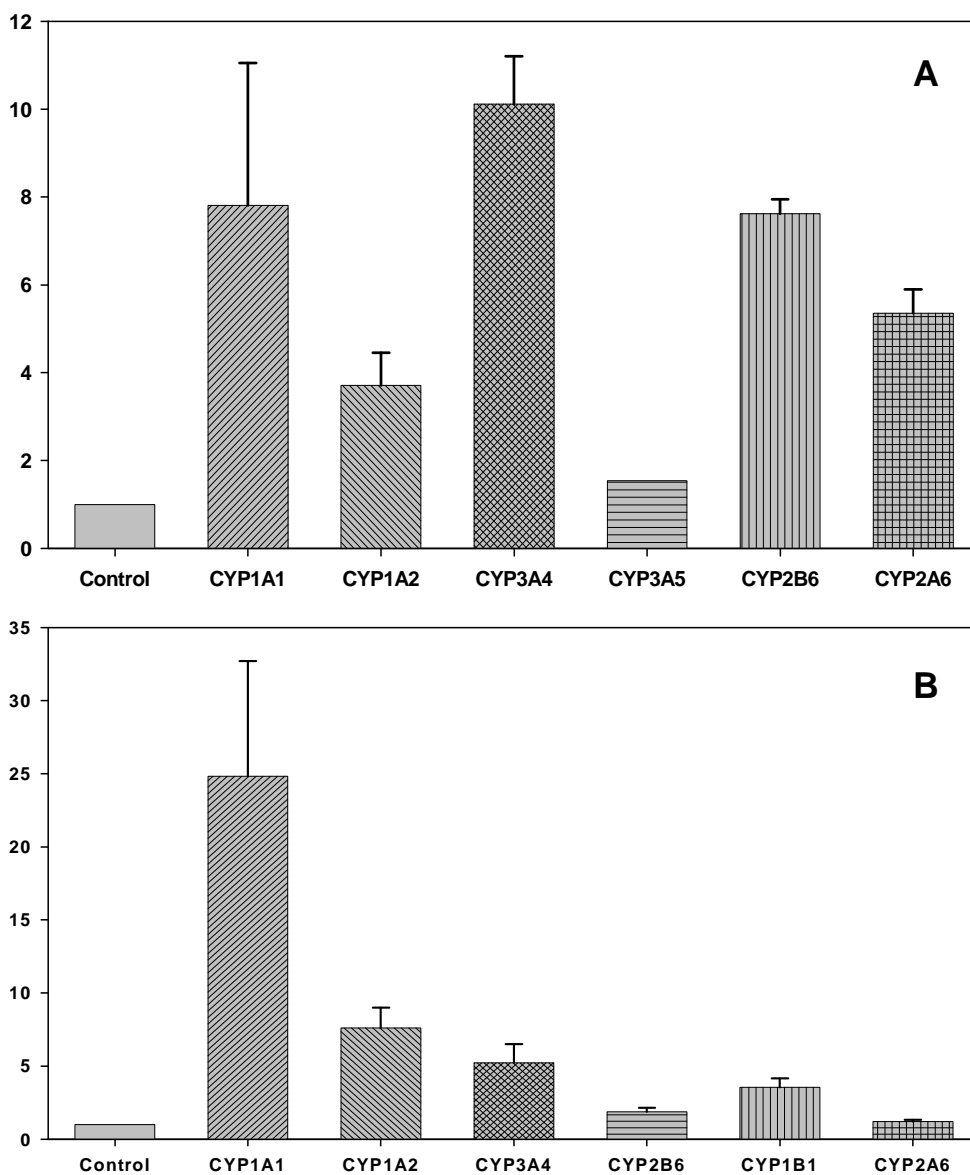


Figure 2

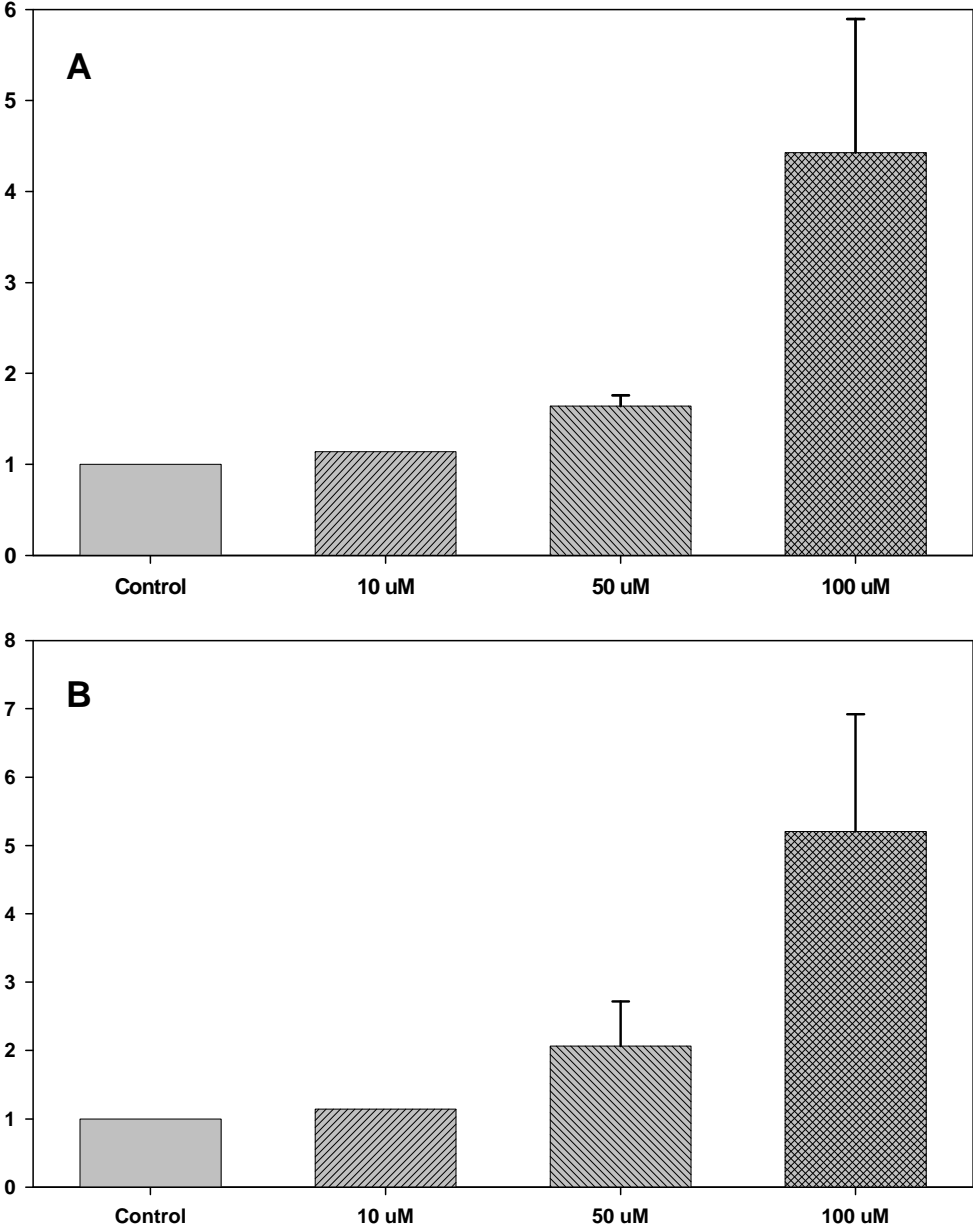


Figure 3

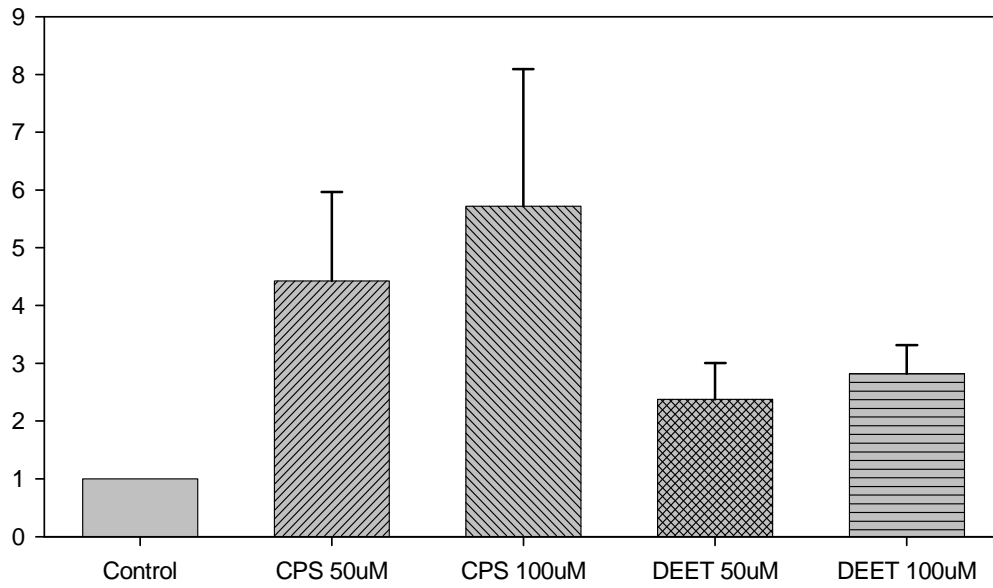


Figure 4

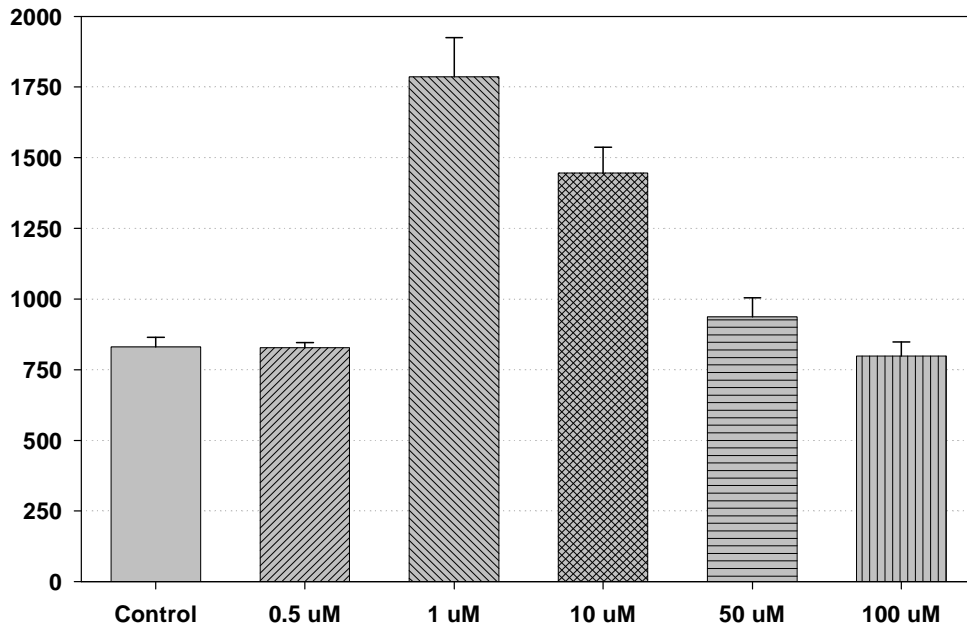


Figure 5

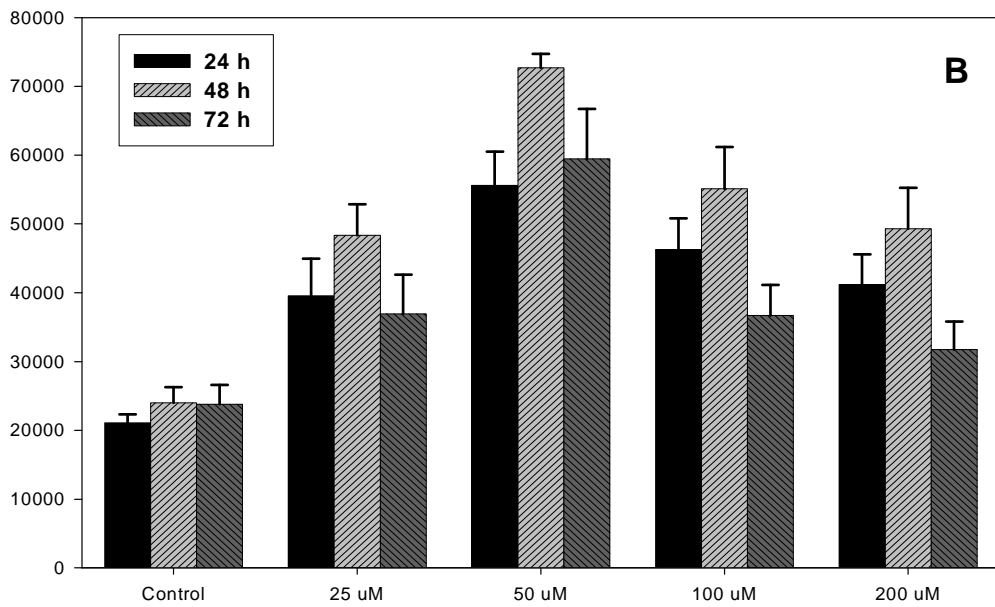
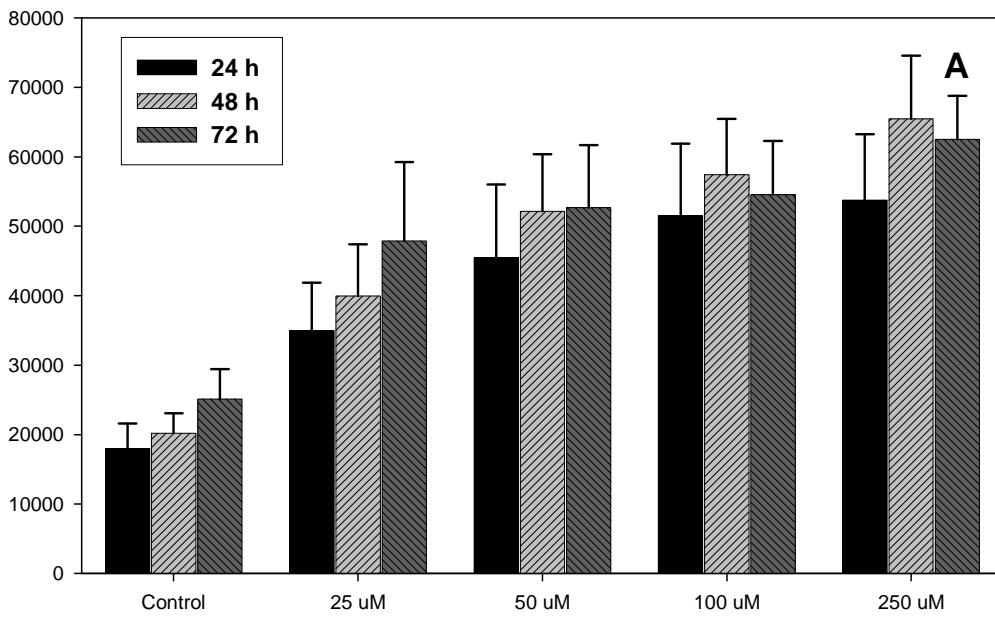


Figure 6

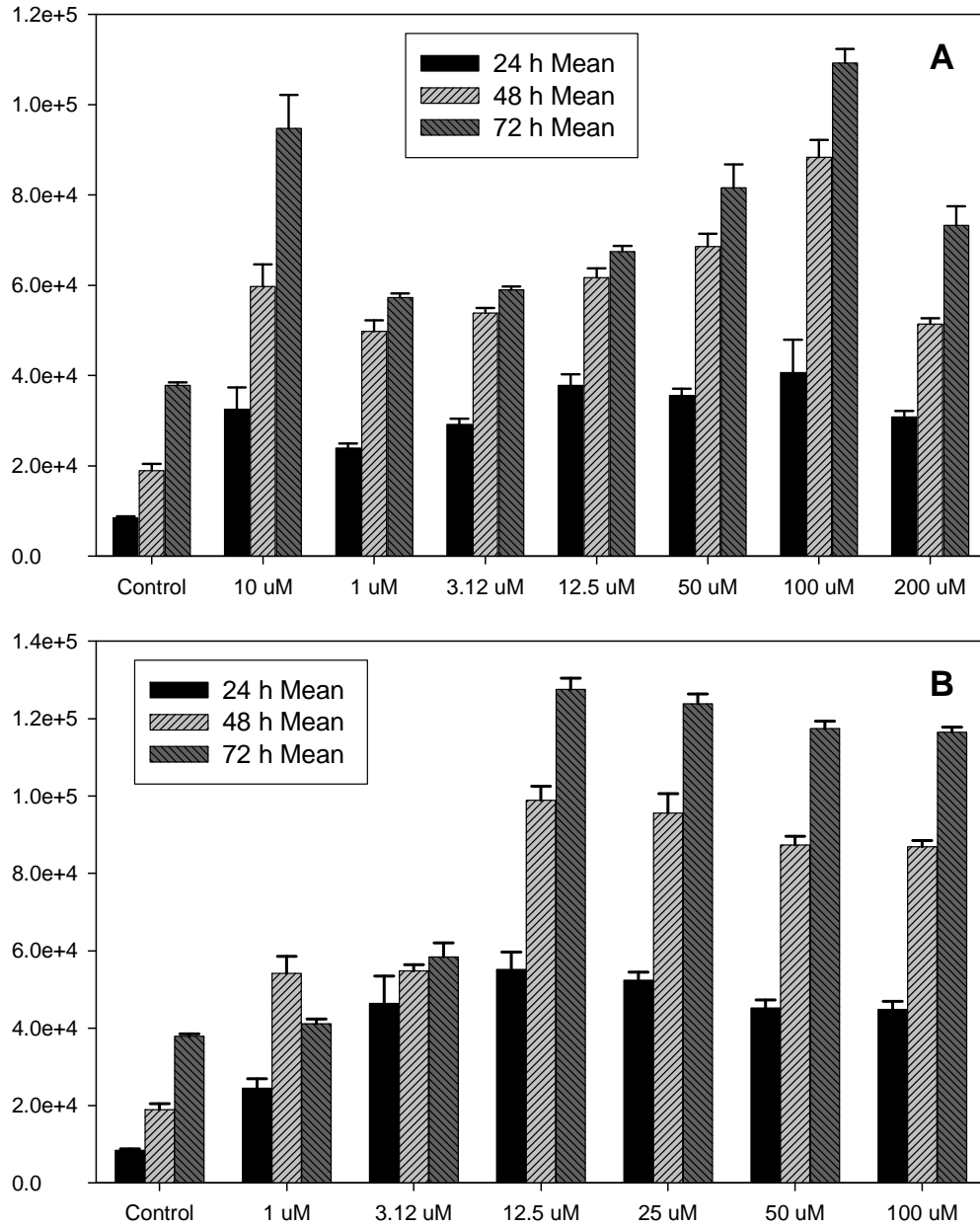


Figure 7

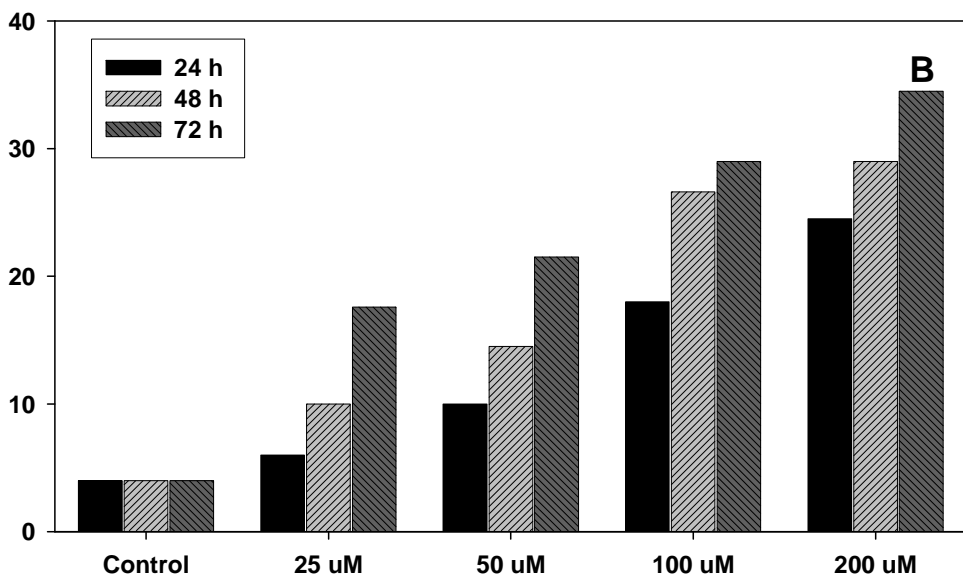
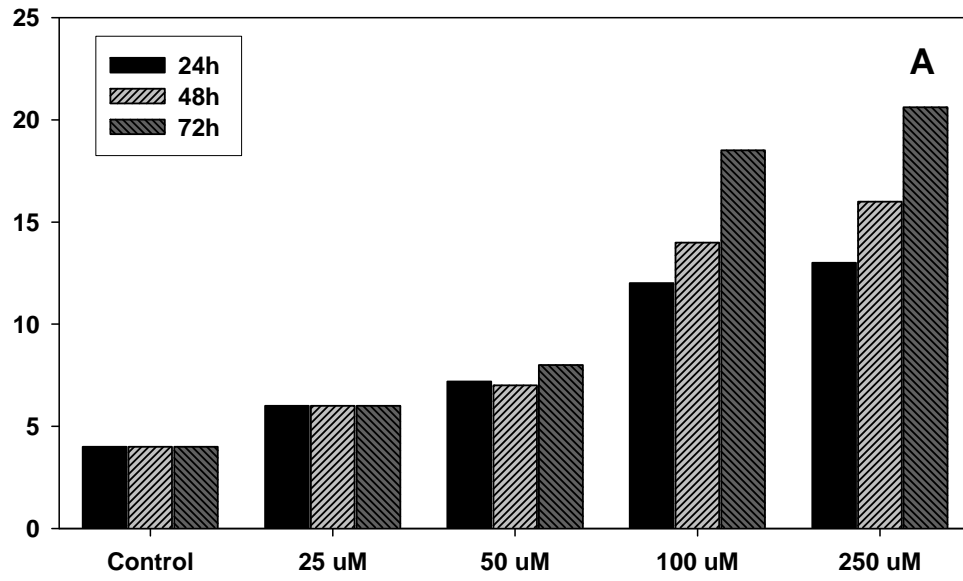
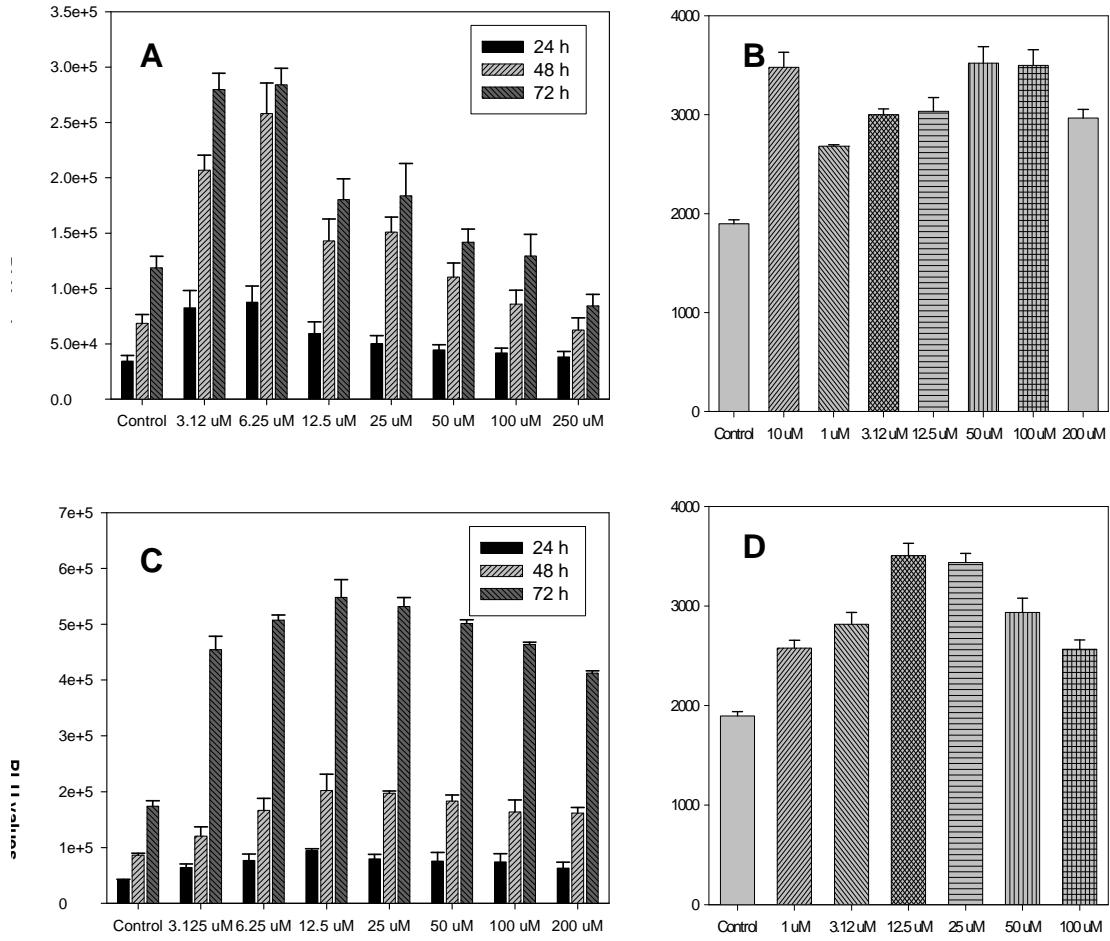


Figure 8



The Effect of Chlorpyrifos-oxon and Other Xenobiotics on the Human Cytochrome P450
- Dependent Metabolism of Naphthalene and DEET

Taehyeon M. Cho¹, Randy L. Rose² and Ernest Hodgson³

Department of Environmental and Molecular Toxicology
North Carolina State University
Raleigh, North Carolina, USA

¹Current address: U. S. Navy Environmental Health Center, Portsmouth, Virginia, USA

²Deceased, Dr. Rose died in a tragic accident on May 23rd, 2006

³Corresponding Author

Dr. Ernest Hodgson

Department of Environmental and Molecular Toxicology

Campus Box 7633

North Carolina State University

Raleigh North Carolina 27695-7633 USA

Tel: 919-515-5295

Fax: 919-513-1012

Email: ernest_hodgson@ncsu.edu

Running Head: Effect of chlorpyrifos-oxon on naphthalene and DEET metabolism

Keywords: Activation; chlorpyrifos; chlorpyrifos-oxon; CYP3A4; human CYP isoforms; inhibition; naphthalene; DEET.

Abstract

Chlorpyrifos-oxon (CPO), a metabolite of chlorpyrifos, is a potent inhibitor of acetylcholinesterase and, although the neurotoxicological impact of this organophosphorus compound has been broadly studied both *in vitro* and *in vivo*, there are few studies of metabolic interactions of CPO with other xenobiotics. CPO significantly activated the production of 1-naphthol (5-fold), 2-naphthol (10-fold), trans-1,2-dihydro-1,2-naphthalenediol (1.5-fold), and 1,4-naphthoquinone from naphthalene by human liver microsomes (HLM). It was further demonstrated that the production of naphthalene metabolites by CYP2C8, 2C9*¹, 2C19, 2D6*¹, 3A4, 3A5, and 3A7 was activated by CPO, while the production of naphthalene metabolites by CYP1A1, 1A2, 1B1, and 2B6 was inhibited by CPO. CPO inhibited CYP1A2 production of naphthalene metabolites, while activating their production by CYP3A4. Similarly, CPO inhibited the production of N,N-diethyl-m-hydroxymethylbenzamide (BALC) from DEET by human liver microsomes, but activated the production of N-ethyl-m-toluamide (ET) from this substrate. CYP2B6, the most efficient isoform for BALC production, was inhibited by CPO while CYP3A4, the most efficient isoform for ET production, was activated by CPO. CPO inhibited CYP2B6 production of both BALC and ET from DEET, but activated CYP3A4 production of ET, while inhibiting CYP3A4 BALC production. CPO appears to facilitate the binding of naphthalene to CYP3A4. This metabolic activation is independent of cytochrome b₅, suggesting that activation of CYP3A4 by CPO is associated with a conformational change of the isoform rather than facilitating electron transfer.

Introduction

Cytochrome P450 (CYP) monooxygenases are the most important enzymes in the metabolism of xenobiotics, including clinical drugs and environmental chemicals as well as endogenous compounds, such as steroids, bile acids, fatty acids, eicosanoids, fat-soluble vitamins /1/. Among fifty-seven CYP isoforms known in humans, fifteen are involved in the metabolism of xenobiotics while the function of thirteen is unknown /2/. Metabolism of a xenobiotic by these CYP enzymes can lead to either activation or detoxication of the parent chemical /3, 4/.

Although *in vivo* studies of metabolism in animal models, including rodents, produce scientifically important data, xenobiotic metabolism in such surrogate animals frequently deviates from metabolism in humans /reviewed in 5,6/. The metabolism of rodent CYP3A and CYP2D are particularly discrepant from those of human CYP3A4 and CYP2D6, respectively, the latter being collectively involved in the metabolism of more than 70% of clinical drugs /5, 6, 7/. *In vitro* metabolic studies have significant advantages for the study of human metabolism of xenobiotics, the determination of kinetic parameters, metabolic efficiency, contributions of individual CYP isoforms and intrinsic clearance rates facilitating *in vitro-in vivo* correlations /8/. For studies of either xenobiotic-xenobiotic metabolic interactions or CYP allosterism, *in vitro* models are more advantageous than *in vivo* models /9/.

Naphthalene, a component of fossil fuels, as well as products for household and industrial use /10/, is metabolized to 1-naphthol, 2-naphthol, and *trans*-1,2-dihydro-1,2-naphthalenediol by pooled human liver microsomes and individually expressed human

CYP isoforms /11/. 1-Naphthol is further metabolized to 1,4-naphthoquinone and 2-naphthol to 2,6- and 1,7-dihydroxynaphthalene, respectively /11/.

N,N-Diethyl-*m*-toluamide (DEET), the active ingredient in most insect repellents, is metabolized to *N,N*-diethyl-*m*-hydroxymethylbenzamide (BALC) and *N*-ethyl-*m*-toluamide (ET) by liver microsomes of human, rat, or mouse, as well as individually expressed human CYP isoforms /12/.

Xenobiotic-associated changes in metabolic activity of human CYP isoforms have frequently been observed. Both ketoconazole and chlorpyrifos inhibit 3-hydroxycarbofuran formation from carbofuran by human liver microsomes /13/ while *in vitro* metabolism of carbaryl by human CYP enzymes is inhibited by chlorpyrifos /14/. Although activation of CYP enzymes by xenobiotics is less frequently encountered and less well understood than inhibition, in some cases the metabolic activity of these enzymes is significantly enhanced by xenobiotics. Enhancement by acetone of the hepatic microsomal *p*-hydroxylation of aniline was first reported in 1968 /15/. Flavone and 7,8-benzoflavone both stimulate benzo[*a*]pyrene metabolism by rabbit CYPs, the extent of the stimulation depending on the type of CYP obtained from rabbit liver microsomes /16/. 6 β -Hydroxylation of testosterone by human CYP3A4 is significantly increased by preincubation of the enzyme with pyridostigmine bromide /17/.

The objectives of the current studies were to identify the public health and agriculture-related chemicals most effective in influencing the metabolic activity of human liver microsomes toward naphthalene, to investigate metabolic interactions between naphthalene or DEET and chlorpyrifos-oxon (CPO), to identify the most efficient human CYP isoforms relative to activation or inhibition of naphthalene or DEET

metabolism by chlorpyrifos-oxon, to investigate the role of CPO in the activation and inhibition of human oxidative metabolism of naphthalene, and to investigate the mechanism of activation of CYP3A4-mediated naphthalene metabolism.

Materials and Methods

Chemicals. Naphthalene, 1-naphthol, 2-naphthol, 1,4-naphthoquinone and dodecane (DD) were purchased from Sigma-Aldrich (St. Louis, MO). *trans*-1,2-Dihydro-1,2-naphthalenediol was a generous gift from Dr. Alan R. Buckpitt (University of California, Davis, CA). Chlorpyrifos (CPS), chlorpyrifos-oxon (CPO), permethrin (PM), carbaryl (CB), *N,N*-diethyl-*m*-toluamide (DEET), and pyridostigmine bromide (PB) were purchased from ChemService (West Chester, PA). *N,N*-Diethyl-*m*-hydroxymethylbenzamide (BALC) and *N*-ethyl-*m*-toluamide (ET) were generous gifts from Dr. Wesley G. Taylor (Saskatoon Research Center, Saskatoon, Canada). Acetonitrile and tetrahydrofuran were purchased from Fisher Scientific (Pittsburgh, PA).

Human Liver Microsomes and Human Cytochrome P450 Isoforms. Pooled human liver microsomes (pHLM) and human CYP isoforms expressed in baculovirus infected insect (*Autographa californica*) cells (BTI-TN-5B1-4) as follows: CYP1A1, 1A2, 1B1, 2A6, 2B6, 2C8, 2C9*¹(Arg₁₁₄), 2C18, 2C19, 2D6*¹(Val₃₇₄), 2E1, 3A4, 3A5, 3A7, 4A11, were purchased from the BD Gentest (Woburn, MA).

***In vitro* Metabolic Interactions of Xenobiotics with Naphthalene Metabolism Mediated by Pooled Human Liver Microsomes or CYP1A2.** Naphthalene metabolism mediated by pHLM or CYP1A2 was tested after pre-incubation of the enzyme with 40 μM of the individual chemicals, such as chlorpyrifos (CPS), chlorpyrifos-oxon (CPO), permethrin (PM), carbaryl (CB), *N,N*-diethyl-*m*-toluamide (DEET), pyridostigmine bromide (PB), or dodecane (DD) followed by the addition of 40 μM naphthalene. These assays were performed with an NADPH-generating system (0.25 mM NADP, 2.5 mM glucose 6-phosphate and 2 U/ml glucose 6-phosphate dehydrogenase) in 100 mM

potassium phosphate buffer containing 3.3 mM MgCl₂ (pH 7.4). After each xenobiotic (40 μM) was preincubated with pHLM (0.48 mg/ml) or CYP1A2 (40 pmol/ml) at 37°C for 5 minutes, naphthalene metabolism was initiated by the addition of naphthalene (40 μM) followed by incubation at 37°C for 10 minutes. For controls, the same incubation was carried out in the absence of the NADPH-generating system.

Naphthalene Metabolism by pHLM, CYP1A2, or CYP3A4 after Pre-incubation with Chlorpyrifos-oxon (CPO). After preliminary screening of the metabolic interaction of naphthalene with seven individual chemicals, CPO was chosen for further investigation of its metabolic influence on naphthalene metabolism. After a series of CPO concentrations (0 to 600 μM) were pre-incubated with pHLM (0.48 mg/ml), CYP1A2 (40 pmol/ml), or CYP3A4 (40 pmol/ml) in an NADPH-generating system (0.25 mM NADP, 2.5 mM glucose 6-phosphate and 2 U/ml glucose 6-phosphate dehydrogenase) in 100 mM potassium phosphate buffer containing 3.3 mM MgCl₂ (pH 7.4) at 37°C for 5 minutes, naphthalene metabolism was initiated by the addition of the substrate (40 μM) and incubated at 37°C for 10 minutes. Additionally, pHLM was pre-incubated with the same concentrations of CPS or a 1:1 mixture of CPO and CPS (0 to 600 μM) before being incubated with 40 μM naphthalene as described above. For controls, the same incubation was carried out without the NADPH-generating system.

***In vitro* Screening for Activation or Inhibition of Human Cytochrome P450 Isoform-mediated Naphthalene Metabolism by CPO.** Modulation of the metabolic activity of the fifteen human CYP isoforms (40 pmol/ml) listed above for naphthalene (40 μM) by CPO (160 μM) was determined. The enzymatic assays were performed in the same manner as stated above. Generation of each metabolite mediated by individual

CYP isoforms was compared. Sf9 insect cell microsomes from wild type baculovirus infected cells (BD Gentest, Woburn, MA) were used as controls for these assays.

Kinetics of Naphthalene Metabolism by CYP3A4 in the Presence of CPO With or Without Cytochrome b₅. To investigate the mechanism of activation of naphthalene metabolism by CYP3A4, the kinetics of the reaction were studied in the presence of CPO (0, 5, or 80 μ M). CYP3A4, coexpressed with cytochrome b₅, was preincubated with CPO at 37°C for 5 minutes, followed by the addition of naphthalene (0 to 500 μ M) to initiate the reaction, which was then continued for 10 minutes. The kinetic parameters (V_{\max} and K_m) for naphthalene metabolism by CYP3A4 preincubated with three different concentrations of CPO were calculated as stated below. The production ratios of the major metabolites, 1-naphthol and 2-naphthol, produced by CYP isoforms preincubated in the three different concentrations of CPO were calculated to determine whether preincubation with CPO can influence the production of those metabolites from naphthalene 1,2-epoxide.

To examine whether electron transfer from cytochrome b₅ was involved in this metabolic activation of naphthalene in CYP3A4 coexpressed with cytochrome b₅, an additional experiment was carried out as follows; CYP3A4, not coexpressed with cytochrome b₅, was preincubated with CPO (0 to 600 μ M) at 37°C for 5 minutes, followed by the addition of naphthalene (100 μ M) to initiate a 10 minute metabolic reaction. The pattern of naphthalene metabolic activation in CYP3A4 without cytochrome b₅ was compared with the metabolism in CYP3A4 coexpressed with cytochrome b₅ as described above.

Effect of Pre-incubation with Chlorpyrifos-oxon (CPO) on DEET

Metabolism by pHLM. After CPO (0 to 600 μ M) was pre-incubated with pHLM (0.48 mg/ml) and an NADPH-generating system (0.25 mM NADP, 2.5 mM glucose 6-phosphate and 2 U/ml glucose 6-phosphate dehydrogenase) in 100 mM potassium phosphate buffer containing 3.3 mM $MgCl_2$ (pH 7.4) at 37°C for 5 minutes, DEET metabolism was initiated by the addition of the substrate (100 μ M) and incubated at 37°C for 20 minutes. For controls, DEET and pHLM pre-incubated with CPO were incubated in the same buffer system but without the NADPH-generating system.

CPO (40 μ M)-associated modulation of the metabolic activity of the human CYP isoforms (40 pmol/ml) toward DEET (40 μ M) metabolism was determined, the CYP isoforms being selected based on a previous study /12/. The enzymatic assays were performed in a same manner as above. Generation of each metabolite mediated by the individual CYP isoforms was compared. Sf9 insect cell microsomes from wild type baculovirus infected cells (BD Gentest, Woburn, MA) were used as controls for these assays.

Metabolism of DEET (100 μ M) by CYP2B6 or CYP3A4 in the presence of CPO was further characterized in order to determine the effect of preincubation of each isoform with CPO (0 to 600 μ M) at 37°C for 5 minutes. The enzymatic assays of DEET with each CYP isoform (40 pmol/ml) were performed in a same manner as stated above. For controls, DEET and the CYP isoform pre-incubated with CPO were incubated in the same buffer system but without the NADPH-generating system.

All assay reactions were terminated by addition of an equal volume (250 μ l) of acetonitrile and vortexing. After a 5-minute centrifugation at 15,000 rpm (21,000 g), the

supernatant was collected for metabolite characterization using an HPLC system. No metabolites were detected in controls in which the NADPH-generating system was absent.

Analysis of Metabolites by HPLC. The generation of metabolites was analyzed using a Waters 2695 HPLC system equipped with a 2996 Photodiode Array (PDA) detector (Milford, MA). This HPLC system was equipped with a degasser and an autoinjector, and data were collected and analyzed using Waters Empower software, version 5.00. The solution for pump A was 3% tetrahydrofuran, 0.2% O-phosphorus acid (85%) and 96.8% water, and for pump B 100% acetonitrile. The gradient in the mobile phase was as follows: 0 to 2 min. (20% B), 2 to 22 min. (gradient to 80% B), 22 to 25 min. (80% B), and 25 to 30 min. (gradient to 20% B). The flow rate was 1.0 ml/min. Metabolites were separated by a reversed phase C₁₂ column (Synergi 4 μ Max-RP, 250 \times 4.6 mm, Phenomenex, Torrance, CA) and detected using a PDA detector operated from 190 to 350 nm. Optimal wavelengths for 1-naphthol, 2-naphthol, *trans*-1,2-dihydro-1,2-naphthalenediol, 1,4-naphthoquinone, BALC, and ET were selected as 232.7, 225.6, 262.2, 251.6, 231.5 and 231.5 nm, respectively. Standards of metabolites were prepared in acetonitrile and 50 μ l of standard or sample was injected into the HPLC system.

Data Analysis and Statistics. The apparent V_{max} and K_m were calculated using a nonlinear regression curve fitted to the Michaelis-Menton equation. The coefficients of determination (R²), a measure of how well a regression model describes the data, were greater than 0.95. Data means were obtained by at least three determinations and the data show the mean and the S.E. The percentages of total normalized rate (%TNR) were determined as described previously /18/. The nominal specific contents of individual

CYP proteins in native human livers (10 donors) used for calculating the %TNR were obtained from BD Gentest (2003 product catalog) except for the contents of CYP2C8 and CYP2C18, which were from Rodrigues (1999) /18/.

Statistical significance of the data was determined with one-way ANOVA followed by the Tukey's multiple comparisons when three or more data sets need to be compared with one another, and by the Dunnett's comparisons when data sets need to be compared to their corresponding control. Student's t test was also applied to compare data with their corresponding controls in the CYP screening assays.

Results

As a preliminary test, 40 μM of the test chemicals (carbaryl, chlorpyrifos, chlorpyrifos-oxon, DEET, dodecane, permethrin and pyridostigmine bromide) were pre-incubated with pHLM followed by the same concentration of naphthalene and incubated under the conditions stated in the methods section. While most chemicals did not affect 1- or 2-naphthol production from naphthalene by pHLM, their production was significantly enhanced by CPO (Fig. 1). However, CPO did not affect dihydrodiol production under these conditions while CPS or CB significantly reduced the production of dihydrodiol (Fig. 1). In another preliminary test, CYP1A2 was utilized to screen the most effective chemicals for their effects on naphthalene metabolism. In contrast to pHLM-mediated naphthalene metabolism, CPO significantly reduced the metabolic activity of CYP1A2 for the production of three naphthalene metabolites (Fig. 2). While CPS significantly reduced the activity of CYP1A2 for the production of 2-naphthol and dihydrodiol in naphthalene metabolism, DEET significantly enhanced the production of 1- and 2-naphthol (Fig. 2).

Metabolite production in pHLM-associated naphthalene metabolism in the presence of varying concentrations of CPO, CPS, or 1:1 CPO/CPS mixture was examined. The production of 1-naphthol (5.5 fold), 2-naphthol (10 fold), and dihydrodiol (1.6 fold) was significantly increased by pre-incubation with CPO (Fig. 3). CPS did not increase the production of any metabolite at most concentrations; rather it decreased 1-naphthol production at the two lowest concentrations (20 and 40 μM) of CPS and increased it slightly at the highest (600 μM) (Fig. 3, A). The production of dihydrodiol was significantly inhibited by CPS (Fig. 3, C). The 1:1 mixture of CPO and CPS caused

reduced activation for the production of metabolites compared to CPO alone. CPO significantly increased production of naphthalene metabolites in human pHLM at the most concentrations of the chemicals (Fig. 3, A, B, and C). The production of 1,4-naphthoquinone was also significantly enhanced by pre-incubation with CPO (Fig. 3, D). The amounts of metabolites produced were dihydrodiol > 1-naphthol > 2-naphthol > 1,4-naphthoquinone.

To investigate which human CYP isoforms are activated or inhibited by CPO for naphthalene metabolism, a screening assay of CYP isoforms for naphthalene metabolism was performed in the presence or absence of CPO. The production of 1-naphthol by CYP1A1, 1A2, 1B1, and 2B6 was inhibited by CPO, while CYP2C8, 2C9*¹, 2C19, 2D6*¹, 3A4, 3A5, and 3A7 were activated for 1-naphthol production by CPO (Fig. 4, A). Similar patterns of inhibition and activation were observed for 2-naphthol and dihydrodiol production (Fig. 4, B and C).

The percentages of total normalized rate (%TNR) for the production of naphthalene metabolites in individual CYP isoforms preincubated without or with 160 μ M CPO are shown in table 1. CYP isoforms including CYP1A2, 2A6, and 2B6 showed decreased %TNR, while those including CYP2C19 and 3A4 demonstrated increased %TNR values for the production of three naphthalene metabolites (Table 1).

To examine how much the metabolic activity of CYP1A2 for naphthalene is inhibited by CPO, a study of the metabolism of 40 μ M naphthalene was performed with CYP1A2 pre-incubated with varying concentrations of CPO. CPO significantly reduced the production of three metabolites, 1-naphthol, 2-naphthol, and dihydrodiol in a dose-dependant manner (Fig. 5). The highest dose (160 μ M) of CPO reduced CYP1A2-

mediated 1-naphthol and 2-naphthol production by 82% and 97%, respectively (Fig. 5, A and B). Doses of 120 μM CPO and higher abolished the production of dihydrodiol (Fig. 5, C).

To investigate how much the metabolic activity of CYP3A4 for naphthalene is activated by CPO, a study of the metabolism of 40 μM naphthalene was performed using CYP3A4 pre-incubated with varying concentrations of CPO. Metabolic activity of CYP3A4 for naphthalene was significantly activated by CPO in a dose-dependant manner (Fig. 6). The production of 1-naphthol and 2-naphthol was significantly enhanced by CPO up to 9 fold and 4.6 fold compared to the corresponding controls (Fig. 6, A and B). Concentrations of CPO as low as 5 μM significantly enhanced the production of dihydrodiol mediated by CYP3A4 (Fig. 6, C). The production of 1,4-naphthoquinone in naphthalene metabolism was also increased by the pre-incubation of CYP3A4 with CPO (Fig. 6, D).

To investigate the mechanism of CPO activation of naphthalene metabolism by CYP3A4, naphthalene kinetics studies were performed in the presence and absence of CPO (5 and 80 μM) (Fig. 7). CPO activated the production of the major metabolites, 1-naphthol and 2-naphthol, by CYP3A4 in a dose-dependant manner (Fig 7, A and B). The apparent K_m values for both metabolites were significantly reduced by pre-incubation of CYP3A4 with CPO and V_{max} values were significantly increased by CPO in a dose-dependant manner (Fig. 7, C and D). The production of 1-naphthol was more accelerated than that of 2-naphthol as the concentration of CPO was increased. The production of 1-naphthol was 5.15 ± 0.07 (CPO 0 μM), 7.86 ± 0.07 (CPO 5 μM), and 10.88 ± 0.33 (CPO 80 μM) times as much as the one of 2-naphthol based on the V_{max} values. The

acceleration of 1-naphthol over 2-naphthol production by CPO in a dose dependent manner shows significant differences from one another.

To investigate whether cytochrome b₅ is involved in this activation of naphthalene metabolism by CYP3A4, naphthalene metabolism by CYP3A4 coexpressed with and without cytochrome b₅ was observed using varying concentrations of CPO. The control velocity of naphthalene metabolism is lower in CYP3A4 without cytochrome b₅ compared to CYP3A4 with cytochrome b₅, but the degree of activation by CPO in a dose dependant manner is similar to the naphthalene metabolism in CYP3A4 coexpressed with cytochrome b₅.

Metabolic activity of pHLM for DEET metabolism in the presence of varying concentrations of CPO was also investigated. While the production of ET was significantly increased 4.7 fold by CPO, the production of BALC was decreased 4 fold by this chemical in a dose-dependant manner (Fig 8).

To investigate which human CYP isoforms among those chosen are activated or inhibited by CPO for DEET metabolism, a screening assay of CYP isoforms for DEET metabolism was performed in the absence and presence of CPO. CYP1A2, 2B6, and 2C19 were significantly inhibited for the production of BALC by CPO, while metabolic activity of other isoforms for BALC was not significantly affected by this chemical (Fig. 9A). CYP3A4 and 3A5 were significantly activated by CPO for the production of ET, while production of ET by CYP2B6 was inhibited (Fig. 9B).

To investigate the inhibition and activation of metabolic activity of CYP isoforms (CYP2B6 and 3A4) by CPO for the production of metabolites in DEET metabolism, each isoform was pre-incubated with CPO and the metabolism of DEET subsequently added

was observed. Both ET and BALC production from CYP2B6-mediated DEET metabolism was significantly decreased by CPO in a dose-dependant manner (Fig. 10A and 10B). While the production of BALC was significantly reduced by CPO, the production of ET was increased by CPO up to 80 μ M and declined to 80% of the maximum velocity (Fig. 10C and 10D).

Discussion

This study investigated xenobiotic-associated stimulation or inhibition of naphthalene or DEET metabolism by human CYP isoforms. Metabolic inhibition of metabolism by CYP isoforms by xenobiotics other than the substrate is frequently observed and has been extensively studied, but stimulation of substrate metabolism is less well understood. Several human CYP isoforms including members of 3A subfamily were stimulated by CPO for naphthalene metabolism, showing a similar pattern for the production of each metabolite, and DEET metabolism by pHLM and CYP3A4 preincubated with CPO showed a biphasic response; increased production of ET and decreased production of BALC.

In contrast to CPO, CPS, the parent chemical of CPO, inhibited naphthalene metabolism in pHLM and this inhibition is believed to be correlated with reactive sulfur dissociated from the parent chemical /19,20-22/. The 1:1 mixture of CPS and CPO caused relatively reduced stimulation of naphthalene metabolism. This observation indicates that, in all probability, CPS and CPO bind to CYP isoforms and microsomal epoxide hydrolase competitively at the binding sites. CPO appeared to have stimulatory effects on naphthalene metabolism by human CYP isoforms as well as epoxide hydrolase.

CPO inhibited naphthalene metabolism by CYP1A1, CYP1A2, CYP1B1, and CYP2B6 while stimulating the metabolism of naphthalene by CYPs of the subfamilies 2C, 3A, and CYP2D6*¹ with CYP3A4 being the most significantly affected isoform (Fig. 4). Calculation of the percentages of total normalized rate (%TNR) based on these CYP isoform screening assays is an integrated method to carry out in vitro CYP reaction

phenotyping /18/. Through this analysis it appeared that the major portion of naphthalene metabolism by pHLM preincubated with CPO is attributable to the metabolic contribution of CYP3A4. In contrast to CYP3A4, the contribution of CYP1A2 and 2B6 to naphthalene metabolism was significantly reduced or abolished following preincubation with CPO (Table 1). This example indicates that multiple xenobiotic exposures can cause modifications in the contributions of different CYPs to the overall metabolism of a substrate.

While CYP1A2 isoform metabolism of naphthalene is inhibited by CPO (Fig. 5), CYP3A4 metabolism of the substrate is stimulated by CPO (Fig. 6). Coincidentally, α -naphthoflavone inhibited CYP1A2 metabolism of flavonoids /23/ and stimulated CYP3A4 metabolism of midazolam /24/. These different effects of xenobiotics on CYP1A2 and CYP3A4 are probably related to the characteristics of active sites; size, shape, and hydrophobicity /25/. The hydrophobic cleft as well as the entire active site in CYP1A2 is presumably smaller than those in CYP3A4 /25/. The active site of CYP1A2 occupied by CPO is unlikely to have enough space for naphthalene, resulting in the inhibition of CYP1A2 metabolism of naphthalene by CPO, either competitively or noncompetitively. Unlike other CYP isoforms, some CYP isoforms, including CYP3A4, are considered to have multiple binding sites and their active site is large enough to hold more than one substrate /26-30/.

The causes of activation or stimulation of CYP isoform metabolism of xenobiotics may include facilitation of electron transfer from cytochrome b_5 /31/, interaction of CYP and CYP reductase /32/, and/or conformational changes upon binding of substrates or effectors /33/. When the metabolic activity of CYP isoforms is

stimulated by the enhanced interaction of CYP and the CYP reductase, V_{\max} values are enhanced, but K_m values for the substrates do not generally change. For instance, 7,8-benzoflavone (or α -naphthoflavone) and flavone stimulate rabbit liver microsomal metabolism of benzo[a]pyrene and show an enhanced V_{\max} value but the K_m value of the substrate is not changed /32/, indicating that electron transport from the reductase to CYPs is facilitated. Cytochrome b_5 has a role to transport electron to some CYPs /34/, and may also be involved in allosteric stimulation of CYPs with a role in conformational changes /35,36/. Conformational changes of CYP enzymes by effectors have been also reported [24,37]. Striking shifts of substrates toward the heme iron of CYP isoforms upon the binding with the effectors have been observed /24,37/.

Stimulation of the metabolism of several CYP isoform substrates, such as naphthalene or DEET, was observed in these studies. Among those CYP isoforms, stimulation of CYP3A4 activity by CPO was most distinctive, and this stimulation was further characterized (Figs. 6, 7, 8, 10). The current observation of increased V_{\max} and decreased K_m values (indicating increased affinity of the substrate) for naphthalene metabolism by CYP3A4 preincubated with CPO is similar to a previous report that dapsona produces stimulation of CYP2C9 metabolism of flurbiprofen, which was interpreted as being caused by a shift of the substrate closer to the heme iron of CYP2C9 /37/. The observation that the substrate affinity of naphthalene with CYP3A4 is significantly enhanced by the presence of CPO, indicates that electron transfer from CYP reductase or cytochrome b_5 to CYP3A4 isoform is not likely to be involved. CPO also stimulated naphthalene metabolism of CYP3A4 without cytochrome b_5 . This observation indicates that the stimulation of substrate metabolism in CYP3A4 by CPO is independent

of the presence of cytochrome b₅. Therefore, this stimulation appears to be related to conformational change of CYP3A4 upon preincubating with CPO, possibly bringing the substrate closer to the heme iron of the enzyme, improving binding affinity, and facilitating reaction velocity. Topological alterations of the active site of CYP3A4 are also supported by the increased ratios of 1-naphthol to 2-naphthol production from naphthalene metabolism, indicating a changed position of the bound substrate in the active site. This increased value of the ratio of 1-naphthol to 2-naphthol production additionally indicates that the production of 1-naphthol and 2-naphthol from the chemically unstable intermediate, naphthalene-1,2-epoxide may, at least in part, be influenced by the enzyme environment /11/ in addition to the generation due to the spontaneous, nonenzymatic rearrangement /10,38,39/. The regio-selectivity shown in the data of DEET metabolism in pHLM (Fig. 8) or CYP3A4 (Fig 10, C and D) preincubated with CPO, namely increased ET and decreased BALC production, supports that the hypothesis the topological characteristics of substrate at the active site of the enzyme are changed upon CPO binding. This stimulatory activity of CYP3A4 due to preincubation of the enzyme with CPO appears to be substrate-dependent because the stimulation pattern of DEET metabolism by CYP3A4 is different from that of naphthalene metabolism. While production of all metabolites was enhanced in the case of naphthalene metabolism, in the case of DEET production of one metabolite was stimulated with the other being inhibited by CPO.

In summary, metabolic interactions of naphthalene and DEET with CPO in human CYP isoforms were studied. CPO, unlike its parent chemical CPS, stimulated the metabolism of naphthalene and DEET by several human CYP isoform. Naphthalene

metabolism was inhibited in CYP1A1, 1A2, 1B1, and 2B6 by CPO, but stimulated in CYP subfamilies of 2C, 3A, and CYP2D6*¹ by the same effector. Metabolic modification by CPO caused CYP3A4 to be the most contributory isoform for naphthalene metabolism. DEET metabolism in pHLM preincubated with CPO showed a biphasic mode; increased ET production and decreased BALC production. CYP1A2, 2B6, and 2C19 were inhibited by CPO for BALC production, while CYP3A4 and 3A5 were stimulated by this effector for ET production. Thus stimulation of CYP3A4 activity by CPO appears to be substrate dependent. The stimulation of CYP3A4 metabolism of naphthalene by CPO appears to be associated with conformational changes of the active site on the binding of CPO, and to be independent of cytochrome b₅.

Acknowledgments

We thank Dr. Alan R. Buckpitt (University of California, Davis, CA) for the generous gift of *trans*-1,2-dihydro-1,2-naphthalenediol. We also thank Dr. Wesley G. Taylor (Saskatoon Research Center, Saskatoon, Canada) for the generous gifts of *N,N*-diethyl-*m*-hydroxymethylbenamide (BALC) and *N*-ethyl-*m*-toluamide (ET). This research was supported by a grant from the U.S. Army (DAMD 17-00-2-008).

References

1. Guengerich FP. Cytochromes P450, drugs, and diseases, *Mol. Interv.* 2003; 3: 194-204.
2. Guengerich FP, Wu Z, Bartleson CJ. Function of human cytochrome P450s: Characterization of the orphans, *Biochem. Biophys. Res. Commun.* 2005; 338: 465-469.
3. Tang J, Cao Y, Rose RL, Brimfield AA, Dai D, Goldstein JA, Hodgson E. Metabolism of chlorpyrifos by human cytochrome P450 isoforms and human, mouse, and rat liver microsomes, *Drug Metab. Dispos.* 2001; 29: 1201-1204.
4. Boocock DJ, Brown K, Gibbs AH, Sanchez E, Turteltaub KW, White INH. Identification of human CYP forms involved in the activation of tamoxifen and irreversible binding to DNA, *Carcinogenesis* 2002; 23: 1897-1901.
5. Gonzalez FJ, Yu A. Cytochrome P450 and xenobiotic receptor humanized mice, *Annu. Rev. Pharmacol. Toxicol.* 2006; 46: 41-64.
6. Bogaards JJ, Bertrand M, Jackson P, Oudshoorn MJ, Weaver RJ, vanBladeren PJ, Walther B. Determining the best animal model for human cytochrome P450 activities: a comparison of mouse, rat, rabbit, dog, micropig, monkey and man, *Xenobiotica* 2000; 30: 1131-1152.
7. Guengerich FP. Comparisons of catalytic selectivity of cytochrome P450 subfamily enzymes from different species, *Chem. Biol. Interact.* 1997; 106: 161-182.
8. Tracy TS, Hummel MA, Modeling kinetic data from in vitro drug metabolism enzyme experiments, *Drug Metab. Rev.* 2004; 36: 231-242.
9. Atkins WM. Implications of the allosteric kinetics of cytochrome P450s, *Drug Discov. Today*, 2004; 9: 478-484.

10. Preuss R, Angerer J, Drexler H. Naphthalene-an environmental and occupational toxicant, *Int. Arch. Occup. Environ. Health.* 2003; 76: 556-576.
11. Cho TM, Rose RL, Hodgson E, *In Vitro* Metabolism of naphthalene by human liver microsomal cytochrome P450 enzymes, *Drug Metab. Dispos.* 2006; 34: 176-183.
12. Usmani KA, Rose RL, Goldstein JA, Taylor WG, Brimfield AA, Hodgson E. *In vitro* human metabolism and interactions of repellent *N,N*-diethyl-*m*-toluamide, *Drug Metab. Dispos.* 2002; 30: 289-294.
13. Usmani KA, Hodgson E, Rose RL. *In vitro* metabolism of carbofuran by human, mouse, and rat cytochrome P450 and interactions with chlorpyrifos, testosterone, and estradiol, *Chem. Biol. Interact.* 2004; 150: 221-232.
14. Tang J, Cao Y, Rose RL, Hodgson E. *In vitro* metabolism of carbaryl by human cytochrome P450 and its inhibition by chlorpyrifos, *Chem. Biol. Interact.* 2002; 141: 229-241.
15. Anders MW, Acetone enhancement of microsomal aniline para-hydroxylase activity, *Arch. Biochem. Biophys.* 1968; 126: 269-275.
16. Huang M, Johnson EF, Muller-Eberhard U, Koop DR, Coon MJ, Conney AH, Specificity in the activation and inhibition by flavonoids of benzo[a]pyrene hydroxylation by cytochrome P-450 isozymes from rabbit liver microsomes, *J. Biol. Chem.* 1981; 256: 10897-10901.
17. Usmani KA, Rose RL, Hodgson E, Inhibition and activation of the human liver microsomal and human cytochrome P450 3A4 metabolism of testosterone by deployment-related chemicals, *Drug Metab. Dispos.* 2003; 31: 384-391.

18. Rodrigues AD. Integrated cytochrome P450 reaction phenotyping, attempting to bridge the gap between cDNA-expressed cytochromes P450 and native human liver microsomes, *Biochem. Pharmacol.* 1999; 57: 465-480.
19. Norman BJ, Poore RE, Neal RA. Studies of the binding of sulfur released in the mixed-function oxidase-catalyzed metabolism of diethyl *p*-nitrophenyl phosphorothionate (parathion) to diethyl *p*-nitrophenyl phosphate (paraoxon), *Biochem. Pharmacol.* 1974; 23: 1733-1744.
20. Halpert J, Hammond D, Neal RA, Inactivation of purified rat liver cytochrome P-450 during the metabolism of parathion (diethyl *p*-nitrophenyl phosphorothionate), *J. Biol. Chem.* 1980; 255: 1080-1089.
21. Neal RA, Halpert J, Toxicology of thiono-sulfur compounds, *Ann. Rev. Pharmacol. Toxicol.* 1982; 22: 321-339.
22. Butler AM, Murray M. Biotransformation of parathion in human liver: participation of CYP3A4 and its inactivation during microsomal parathion oxidation, *J. Pharmacol. Exp. Ther.* 1997; 280: 966-973.
23. Breinholt VM, Offord EA, Brouwer C, Nielsen SE, Brøsen K, Friedberg T. In vitro investigation of cytochrome P450-mediated metabolism of dietary flavonoids, *Food Chem. Toxicol.* 2002; 40: 609-616.
24. Cameron MD, Wen B, Allen KE, Roberts AG, Schuman JT, Campbell AP, Kunze KL, Nelson SD, Cooperative binding of midazolam with testosterone and α -naphthoflavone within the CYP3A4 active site: a NMR T_1 paramagnetic relaxation study, *Biochemistry* 2005; 44: 14143-14151.

25. Lewis DFV, Lake BG, Dickins M. Quantitative structure-activity relationships within a homologous series of 7-alkoxyresorufins exhibiting activity towards CYP1A and CYP2B enzymes: molecular modelling studies on key members of the resorufin series with CYP2C5-derived models of human CYP1A1, CYP1A2, CYP2B6 and CYP3A4, *Xenobiotica* 2004; 34: 501-513.
26. Yano JK, Wester MR, Schoch GA, Griffin KJ, Stout CD, Johnson EF. The structure of human microsomal cytochrome P450 3A4 determined by X-ray crystallography to 2.05-Å resolution, *J. Biol. Chem.* 2004; 279: 38091-38094.
27. Tanaka T, Okuda T, Yamamoto Y. Characterization of the CYP3A4 active site by homology modeling, *Chem. Pharm. Bull.* 2004; 52: 830-835.
28. Galetin A, Clarke SE, Houston JB. Multisite kinetic analysis of interactions between prototypical CYP3A4 subgroup substrates: midazolam, testosterone, and nifedipine, *Drug Metab. Dispos.* 2003; 31: 1108-1116.
29. Korzekwa KR, Krishnamachary N, Shou M, Ogai A, Parise RA, Rettie AE, Gonzalez FJ, Tracy TS. Evaluation of atypical cytochrome P450 kinetics with two-substrate models: evidence that multiple substrates can simultaneously bind to cytochrome P450 active sites, *Biochemistry* 1998; 37: 4137-4147.
30. Shou M, Grogan J, Mancewicz JA, Krausz KW, Gonzalez FJ, Gelboin HV, Korzekwa KA. Activation of CYP3A4: evidence for the simultaneous binding of two substrates in a cytochrome P450 active site, *Biochemistry* 1994; 33: 6450-6455.
31. Lee CA, Manyike PT, Thummel KE, Nelson SD, Slattery JT. Mechanism of cytochrome P450 activation by caffeine and 7,8-benzoflavone in rat liver microsomes, *Drug Metab. Dispos.* 1997; 25: 1150-1156.

32. Huang M-T, Chang RL, Fortner JG, Conney AH. Studies on the mechanism of activation of microsomal benzo[a]pyrene hydroxylation by flavonoids, *J. Biol. Chem.* 1981; 256: 6829-6836.
33. Ueng Y-F, Kuwabara T, Chun Y-J, Guengerich FP. Cooperativity in oxidations catalyzed by cytochrome P450 3A4, *Biochemistry* 1997; 36: 370-381.
34. Porter TD. The roles of cytochrome b₅ in cytochrome P450 reactions, *J. Biochem. Mol. Toxicol.* 2002; 16: 311-316.
35. Auchus RJ, Lee TC, Miller WL, Cytochrome b₅ augments the 17,20-lyase activity of human P450c17 without direct electron transfer, *J. Biol. Chem.* 1998; 273: 3158-3165.
36. Yamazaki H, Nakamura M, Komatsu T, Ohyama K, Hatanaka N, Asahi S, Shimada N, Guengerich FP, Shimada T, Nakajima M, Yokoi T. Roles of NADPH-P450 reductase and apo- and holo-cytochrome b₅ on xenobiotic oxidations catalyzed by 12 recombinant human cytochrome P450s expressed in membranes of *Escherichia coli*, *Protein Expr. Purif.* 2002; 24: 329-337.
37. Hummel MA, Gannett PM, Aguilar JS, Tracy TS. Effector-mediated alteration of substrate orientation in cytochrome P450 2C9, *Biochemistry* 2004; 43: 7207-7214.
38. van Bladeren PJ, Vyas KP, Sayer JM, Ryan DE, Thomas PE, Levin W, Jerina DM. Stereoselectivity of cytochrome P-450c in the formation of naphthalene and anthracene 1,2-oxides, *J. Biol. Chem.* 1984; 259: 8966-8973.
39. Buckpitt A, Boland B, Isbell M, Morin D, Shultz M, Baldwin R, Chan K, Karlsson A, Lin C, Taff A, West J, Fanucchi M, van Winkle L, Plopper C. Naphthalene-induced respiratory tract toxicity: metabolic mechanisms of toxicity, *Drug Metab. Rev.* 2002; 34: 791-820.

Figure Legends

Fig. 1. Naphthalene (40 μ M) metabolism by pHLM, which has been pre-incubated with other xenobiotics (40 μ M). Each chemical is abbreviated as stated in the materials and methods section. Production of 1-naphthol (A), 2-naphthol (B), or *trans*-dihydrodiol (C) is shown. The asterisk indicates a significant difference compared to the corresponding control ($p < 0.05$).

Fig. 2. Naphthalene (40 μ M) metabolism by CYP1A2, which has been pre-incubated with other xenobiotics (40 μ M). Each chemical is abbreviated as stated in the materials and methods section. Production of 1-naphthol (A), 2-naphthol (B), or *trans*-dihydrodiol (C) is shown. The asterisk indicates a significant difference compared to the corresponding control ($p < 0.05$).

Fig. 3. Naphthalene (40 μ M) metabolism by pHLM, which has been pre-incubated with CPO, CPS, or their 1:1 mixture, respectively. Production of 1-naphthol (A), 2-naphthol (B), *trans*-dihydrodiol (C), or 1,4-naphthoquinone (D) is shown. * and ‡, indicate significant increases or decreases in the production of each metabolite compared to the corresponding control ($p < 0.05$).

Fig. 4. Activation and inhibition of naphthalene (40 μ M) metabolism by various human CYP isoforms, which have been pre-incubated with CPO (160 μ M). Production of 1-naphthol (A), 2-naphthol (B), or *trans*-dihydrodiol (C) is shown. The asterisk indicates significant difference compared to the corresponding control ($p < 0.05$).

Fig. 5. CPO inhibition of naphthalene (40 μ M) metabolism by human CYP1A2. Production of 1-naphthol (A), 2-naphthol (B), or *trans*-dihydrodiol (C) is shown.

Fig. 6. CPO activation of naphthalene (40 μ M) metabolism by human CYP3A4.

Production of 1-naphthol (A), 2-naphthol (B), *trans*-dihydrodiol (C), or 1,4-naphthoquinone (D) is shown.

Fig. 7. Kinetics of naphthalene metabolism in the presence of three different concentrations of CPO. Both (A) and (B) present production of 1-naphthol and 2-naphthol, respectively. Kinetic parameters, K_m and V_{max} , of 1-naphthol (C) and 2-naphthol (D) production are shown. The letters, a or b, indicates a significant difference compared to their corresponding controls (CPO 0 μ M), and different letter indicates statistical difference in V_{max} between those data (C and D) ($p < 0.05$).

Fig. 8. Activation and inhibition of DEET (100 μ M) metabolism by pHLM, which has been pre-incubated with CPO.

Fig. 9. Inhibition and activation of DEET (40 μ M) metabolism by human CYP isoforms, pre-incubated with CPO (40 μ M). Production of BALC (A) or ET (B) is shown. The asterisk indicates a significant difference compared to the corresponding control ($p < 0.05$).

Fig. 10. CPO inhibition and activation of DEET (100 μ M) metabolism by human CYP2B6 (A and B) or CYP3A4 (C and D). Production of ET (A) or BALC (B) in CYP2B6, and ET (C) or BALC (D) in CYP3A4 is shown.

Table 1. The total percentage normalized rate (%TNR) of naphthalene metabolites of individual CYP isoforms preincubated with or without 160 μ M CPO, and the specific content of each CYP protein in human liver microsomes.

CYP Isoform	% TNR						Mean content of CYP¶ (pmol CYP/mg Prot.)
	1-Naphthol		2-Naphthol		Dihydrodiol		
	Control	CPO 160 μ M	Control	CPO 160 μ M	Control	CPO 160 μ M	
1A1	ND	ND	ND	ND	ND	ND	NA
1A2	23.4	2.0 (\downarrow 11.7)	7.5	0.0 (\downarrow)	34.7	0.0 (\downarrow)	55
1B1	ND	ND	ND	ND	ND	0.0	NA
2A6	10.8	5.3 (\downarrow 2.0)	3.3	1.2 (\downarrow 2.8)	44.5	22.0 (\downarrow 2.0)	52
2B6	11.7	1.2 (\downarrow 9.8)	5.0	0.3 (\downarrow 16.7)	6.3	0.0 (\downarrow)	21
2C8†	0.5	2.1 (\uparrow 4.2)	0.0	0.3 (\uparrow)	0.0	0.0	64
2C9* ¹	1.1	1.5 (\uparrow 1.4)	0.0	0.1 (\uparrow)	0.0	0.0	76
2C18†	0.01	0.01	0.0	0.0	0.0	0.0	2.5
2C19	8.9	10.6 (\uparrow 1.2)	2.3	5.1 (\uparrow 2.2)	7.1	15.7 (\uparrow 2.2)	39
2D6* ¹	1.3	1.3	0.1	0.3 (\uparrow 3.0)	2.4	2.9 (\uparrow 1.2)	12
2E1	18.2	8.3 (\downarrow 2.2)	3.8	1.4 (\downarrow 2.7)	0.0	0.0	52
3A4	24.1	67.4 (\uparrow 2.8)	77.9	91.1 (\uparrow 1.2)	5.1	59.5 (\uparrow 11.7)	133
3A5	0.01	0.2 (\uparrow 20.0)	0.0	0.2 (\uparrow)	0.0	0.0	1.2
3A7	ND	ND	ND	ND	0.0	ND	NA
4A11	0.0	0.0	0.0	0.0	0.0	0.0	NA

¶ Mean content data were obtained from the BD Gentest (2003).

† Mean content data for 2C8 and 2C18 were obtained from Rodrigues (1999) [18].

ND indicates not determined. NA indicates not available.

The numbers in parentheses are the decreased (\downarrow) or increased (\uparrow) percentages ($\times 100$) compared to their corresponding controls.



ACADEMIC
PRESS

Available online at www.sciencedirect.com

SCIENCE @ DIRECT®

Pesticide Biochemistry and Physiology 73 (2002) 117–128

PESTICIDE
Biochemistry & Physiology

www.elsevier.com/locate/ypest

In vitro human metabolism of permethrin: the role of human alcohol and aldehyde dehydrogenases

Jonghoon Choi, Randy L. Rose, and Ernest Hodgson*

Department of Environmental and Molecular Toxicology, Campus Box 7633, North Carolina State University, Raleigh, NC 27695-7633, USA

Received 7 June 2002; accepted 11 December 2002

Abstract

Permethrin is a pyrethroid insecticide widely used in agriculture and public health. It has been suggested that permethrin may interact with other chemicals used during military deployments and, as a result, be a potential cause of Gulf War Related Illness. To determine the causal relationship between permethrin and human health effects, the basic enzymatic pathway of permethrin metabolism in humans should be understood. In the present study we report that *trans*-permethrin is metabolized in human liver fractions, producing phenoxybenzyl alcohol (PBOH) and phenoxybenzoic acid (PBCOOH). We identified human alcohol (ADH) and aldehyde dehydrogenases (ALDH) as the enzymes involved in the oxidation of phenoxybenzyl alcohol, the permethrin hydrolysis product, to phenoxybenzoic acid by way of phenoxybenzaldehyde (PBCHO). *Cis*-permethrin was not significantly metabolized in human liver fractions. Cytochrome P450 isoforms were not involved either in the hydrolysis of *trans*-permethrin or in the oxidation of PBOH to PBCOOH. Purified ADH isozymes oxidized PBOH to PBCHO and PBOH was a preferred substrate to ethyl alcohol. Purified ALDH was responsible for PBCHO oxidation to PBCOOH with similar substrate affinity to a previously known substrate, benzyl alcohol. Based on these observations, it appears that PBOH is oxidized to PBCHO by ADH and subsequently to PBCOOH by ALDH, although PBCHO does not accumulate during microsomal incubation. In order to analyze permethrin and its metabolites, previous HPLC-UV methods had to be re-validated and modified. The resulting refined HPLC-UV method is described in detail.

© 2003 Elsevier Science (USA). All rights reserved.

Keywords: Permethrin; Permethrin metabolism; Human alcohol dehydrogenase; Human aldehyde dehydrogenase

1. Introduction

Permethrin (3-phenoxy-benzyl (\pm) *cis/trans*-3-(2,2-dichlorovinyl)-2,2-dimethylcyclopropane-1-carboxylate) is a widely used photo-stable

synthetic pyrethroid insecticide acting as a neurotoxin [1]. Permethrin is not acutely toxic to mammals since it is rapidly hydrolyzed [2,3]. However it is known that permethrin causes some toxic symptoms at high oral doses [4].

Recent controversies over the nature and the potential causes of Gulf War Related Illnesses have indicated potential roles for various chemicals used for military personnel [5,6]. In addition

* Corresponding author. Fax: +1-919-513-1012.

E-mail address: ernest_hodgson@ncsu.edu (E. Hodgson).

to permethrin these chemicals include pyridostigmine bromide, *N,N*-diethyl-*m*-toluamide and chlorpyrifos. Interaction of permethrin with pyridostigmine bromide and *N,N*-diethyl-*m*-toluamide has been suggested as a potential cause of Gulf War Related Illnesses [6,7]. In a recent study on human metabolism of *N,N*-diethyl-*m*-toluamide, it was found that there are potential chemical interactions among deployment related chemicals through enzymatic induction and inhibition [8]. Also, there have been indications that permethrin metabolites (phenoxybenzyl alcohol, PBOH and phenoxybenzaldehyde, PBCHO) can be more cytotoxic [9] and have more potential as estrogenic agents [10] than the parent compound. To determine the causal relationship between potential chemical exposure and human health effects, it is important to define basic metabolic pathways and to identify the enzymes involved in humans.

Even though the importance of the liver in xenobiotic metabolism is well recognized, no permethrin metabolism studies based on human liver tissue or human liver microsomes have been reported. Previous studies of human permethrin metabolism have mainly focused on the detection of primary metabolites such as *cis/trans*-3-(2,2-dichlorovinyl)-2,2-dimethylcyclopropane-1-carboxylate (DCCA), PBOH, and phenoxybenzoic acid (PBCOOH) in either human blood or urine samples [11–13] and no reports are available on the identification of the enzymes involved in permethrin metabolism in humans.

Permethrin metabolites found in rodents indicate that the parent permethrin is hydrolyzed to DCCA and PBOH with further oxidation of PBOH to PBCOOH [14]. These basic metabolites are subject to further oxidative hydroxylation and conjugation. We are interested in delineating human enzymatic pathways involved in the metabolic transformation of permethrin and its hydrolysis products and here we report that, based on human liver fractions and purified human dehydrogenases, PBOH is oxidized to PBCHO by alcohol dehydrogenase (ADH) and then to PBCOOH by aldehyde dehydrogenase (ALDH). The further metabolism of the other hydrolysis product, DCCA, will be the subject of subsequent studies. Regarding the HPLC analysis method for permethrin and its metabolites, we revalidated and modified previously used methods. We report, as a part of human permethrin metabolism study, an efficient HPLC-UV method that can separate five compounds (two permethrin

isomers, PBOH, PBCHO, and PBCOOH) with emphasis on the optimal detection wavelength and a proper mobile phase pH range for an ionizable metabolite (PBCOOH).

2. Methods

2.1. Chemicals, human liver fractions, and human CYPs

Cis-permethrin (98% purity), PBOH (98% purity), and PBCOOH (99% purity) were purchased from Chem Service (West Chester, PA). *Trans*-permethrin (98.1% purity) and PBCHO (98% purity) were purchased from Sigma (St. Louis, MO). HPLC grade acetonitrile and water were purchased from Fisher Scientific (Fair Lawn, NJ). All other chemicals, if not specified, were purchased from Sigma (St. Louis, MO). Pooled human liver microsomes and cytosol were purchased from Gentest Biosciences (Woburn, MA). Microsomal and cytosolic fractions were derived from the same batch of 13 pooled human liver samples. Human CYP 1A1, 1A2, 1B1, 2A6, 2C8, 2C9, 2C18, 2C19, 2E1, 3A4, 3A5, 3A7, and 4A11 Supersomes expressed in a baculovirus expression system were purchased from Gentest Biosciences (Woburn, MA).

2.2. HPLC method development

Permethrin isomers (*trans* and *cis*) and three major metabolites (PBOH, PBCHO, and PBCOOH) were analyzed using a Shimadzu HPLC system (Kyoto, Japan) consisting of a pump (LC-10AT VP), a solvent proportioning valve (FCV-10AL VP), a degasser (DGU-14A), a controller (SCL-10A VP), and an auto injector (SIL-10AD VP). Permethrin isomers and metabolites were separated on Phenomenex (Torrance, CA) Luna column (reverse phase C18, 5 μ m, 150 \times 3.0 mm) and detected using a Shimadzu SPD-10AV VP UV-VIS detector. Two solvents (solvent A: 90% acetonitrile and 10% H₂O, solvent B: 100% H₂O adjusted to pH 1.7 with 85% phosphoric acid) were used for gradient elution (flow rate: 1 ml/min). The gradient system (linear increase) was initiated with 50% of solvent A and 50% of solvent B reaching 75% of solvent A at 6 min and 100% of solvent A at 7 min. One hundred percent of solvent A was maintained for 4 min and then reduced to 50% at 12 min, which was kept for 4 min to prepare the column for

initial conditions. The chromatographic analysis was conducted at ambient temperature.

A series of dilutions prepared in Tris (0.1 M, pH 7.5)/acetonitrile (1:1, v/v) from a concentrated mixture of five compounds were used to construct a standard curve based on peak areas. In order to find the optimal detection wavelength, standard curves for permethrin isomers and metabolites were constructed at four previously used wavelengths (210, 230, 254, and 270 nm). *Trans*-permethrin and two metabolites were identified by comparing retention times with analytical standards. For each compound, the lowest detectable concentration was determined as the detection limit assuming a signal-to-noise ratio of 3:1. The lowest concentration of each compound generating reproducible and predictable peak area was determined as the limit of quantitation. For this study, the solvent B pH was set at 1.7.

Among the compounds analyzed, PBCOOH is ionized at neutral pH. For consistent peak identification and quantification, ionization should be suppressed. In order to characterize the effect of mobile phase pH on the protonation of PBCOOH, the metabolites were analyzed at several different mobile phase pH levels. The mobile phase pH was adjusted by increasing the hydrogen ion concentration in solvent B (pH levels of 1.7, 2.3, 3.2, and 8.0) with 85% phosphoric acid. The eluted compounds were detected at 230 nm.

2.3. Permethrin metabolism in human liver fractions and CYPs

Trans-permethrin was incubated with human liver fractions. A reaction mixture of 500 μ l in 0.1 M Tris buffer (pH 7.5) contained 0.5 mg of cytosolic or microsomal protein, 10 μ l of *trans*-permethrin stock solution (10 mM in acetonitrile), 25 μ l of NADPH regenerating system solution A, and 10 μ l of NADPH generation system solution B. For CYP isoform incubations 25 pmol in 500 μ l of reaction buffer (as recommended by Gentest) was used. Solution A of the NADPH regenerating system contained 26.0 mM NADP⁺ and 66 mM of glucose-6-phosphate in phosphate buffer (pH 7.4). Solution B of the NADPH regenerating system contained 40 U/ml of glucose-6-phosphate dehydrogenase in phosphate buffer (pH 7.4). All components except the liver fractions or CYP isoforms were mixed and pre-incubated for 5 min at 37°C. One hundred minute incubations were started when the liver fractions were added to the pre-warmed reaction mixture. After the incuba-

tion was completed, 500 μ l of cold acetonitrile was added to each reaction mixture to stop enzymatic reactions. The reaction mixtures were centrifuged at 20,000g for 5 min using a microcentrifuge. The supernatant was sampled and stored at 4°C until HPLC analysis. The concentration of each compound was calculated based on the standard curve constructed at 230 nm with solvent B, pH 1.7.

2.4. Protein purification

Human ADH isozymes were expressed and purified from *Escherichia coli* (JM105 strain) containing pKK223-3 expression vector (Pharmacia Biotech, Uppsala, Sweden) inserted with human ADH cDNA. The *E. coli* strain was provided by Dr. Brimfield (US Army Medical Research Institute of Chemical Defense). *E. coli* cells were grown in Terrific Broth media (with 50 mg ampicillin/L) and harvested as described previously [15] with some modifications. After inoculation of *E. coli* cells, cells were grown at 37°C until the absorbance reached 0.6–0.8 at 595 nm. Then, isopropylthiogalactoside (1.0 ml of 0.1 M stock per liter media) and ZnSO₄ (0.7 ml of 100 mM stock per liter media) were added to the media and incubation temperature was reduced to room temperature. The cells were cultured for 12–24 h before collection and collected by centrifugation at 4000g for 10 min. Collected cells were disrupted using a sonicator (550 sonic dismembrator, Fisher Scientific, Fair Lawn, NJ) in cell lysis buffer (pH 8.0, 10 mM Tris, 2 mM dithiothreitol (DTT), 0.1 mM ZnSO₄, and 1 mM benzamidine). The cytosolic ADHs enzymes were contained in the supernatant after ultracentrifugation (100,000g for 35 min at 4°C).

ADHs were purified using modifications of methods involving three chromatography columns in sequence as previously described [16]: DEAE-Sephacel CL-6B (Pharmacia Biotech, Uppsala, Sweden), SP-Sephacel Fast Flow (Pharmacia Biotech, Uppsala, Sweden), and Affi-Gel Blue Gel (Bio-Rad, Hercules, CA) columns. For β I and β II purifications, the supernatant was directly applied to the DEAE-Sephacel column. Cell lysis buffer described above was used as an elution buffer at a flow rate of 1.7 ml/min. Active eluent fractions were collected and buffer-exchanged to SP-Sephacel buffer (pH 8.0, 10 mM Hepes, 2 mM DTT, 0.1 mM ZnSO₄, and 1 mM benzamidine) using ultrafiltration tubes (30,000 Da molecular weight cutoff, Centricon, Millipore, Bedford, MA). ADH activity was measured in 100 mM glycine buffer (pH 10.0)

with 2.5 mM NAD^+ and 33 mM ethanol at 25 °C. ADH activity was measured using the absorbance change at 340 nm with a molar extinction coefficient of 6.22 mM/min/cm for NADH. After binding to SP-Sepharose and rinsed with the column buffer, ADH proteins were eluted using a NaCl gradient from 0 to 250 mM prepared in the column buffer. Collected active fractions were buffer-exchanged to Affi-Gel Blue Gel column buffer (pH 7.4, 10 mM sodium phosphate, 0.5 mM DTT, and 0.1 mM ZnSO_4). β ADH proteins strongly bind to Affi-Gel Blue columns and 0.8 M NaCl solution prepared in the column buffer was used to elute bound proteins after a thorough rinsing step. Pooled active fractions were buffer-exchanged to Affi-Gel Blue Gel column buffer and stored at -70 °C with 50% glycerol. Flow rate for Affi-Gel Blue Gel column was 1.0 ml/min. Protein concentration was measured based on the bicinchoninic acid reaction [17].

For α ADH, which has a lower isoelectric point than β ADH isozymes, the pH of the SP-Sepharose elution buffer was lowered to 7.2. All other chromatography procedures were the same as described for β ADH isozymes. For δ ADH, the pH of the SP-Sepharose elution buffer was 6.4 with 77 mM sodium phosphate, 1 mM DTT, 0.1 mM ZnSO_4 , and 1 mM benzamidine. δ ADH from the SP-Sepharose column was eluted using a linear gradient elution starting with 7 mM and ending with 65 mM sodium phosphate buffer (pH 6.4). The Affi-Gel Blue Gel column buffer for δ ADH had the same composition as other isozymes with a lower pH (6.4). δ ADH was eluted from the Affi-Gel Blue Gel column using a linear gradient elution starting with column buffer and ending with 100 mM Tris buffer (pH 8.8). The storage conditions for α and δ isozymes were the same as for the β ADHs. The purity of ADH enzymes was evaluated based on SDS-PAGE with Coomassie blue staining.

Purified human ALDH3A1 was provided by Dr. Alan Townsend (Wake Forest University, School of Medicine). The ALDH3A1 provided had been purified from Chinese hamster lung fibroblast cell line (V79/SD1) stably transfected with ALDH3A1 cDNA containing $\Delta\text{pCEP4}\Delta$ mammalian expression vector [18].

2.5. Enzyme kinetics

Purified ADH isozymes were assayed for PBOH oxidation to PBCHO and K_m/V_{\max} values were calculated based on Michaelis–Menten steady-state kinetics. A series of different concen-

trations of PBOH and ethyl alcohol were prepared in 100 mM glycine buffer (pH 10.0) and mixed with NAD^+ (final concentration 2.5 mM). The reaction mixtures were pre-warmed to 25 °C and the enzymatic reaction was started by adding purified ADH to the reaction mixture. The reaction rate was calculated by spectrophotometric measurement of NADH formation (UV-2101PC, Shimadzu, Kyoto, Japan) at 340 nm (molar extinction coefficient of 6.22 mM/min/cm).

For the ALDH assay a series of different concentrations of PBCHO were prepared in 33 mM sodium pyrophosphate buffer (pH 8.2) and mixed with 1 mM EDTA, 0.1 mM pyrazole (ADH inhibitor) and NAD^+ (final concentration 2.5 mM). The reaction mixtures were pre-warmed to 37 °C and the enzymatic reaction was started by adding purified ALDH to the reaction mixture. As in ADH assay, the reaction rate of PBCHO oxidation to PBCOOH was determined by NADH formation.

In order to determine whether PBOH or PBCHO are oxidized by CYPs, 13 isoforms were incubated, separately, in the presence of NADPH regeneration system with the two compounds. Other conditions were the same as in the *trans*-permethrin incubation. GraphPad [19] program was used for Michaelis–Menten model fitting to estimate K_m and V_{\max} values.

2.6. Statistical analysis

The concentrations of each compound were presented as means \pm 1 standard error of mean (SEM). The number of replicates per treatment was 3. Metabolite production data were analyzed using an analysis of variance (ANOVA) with a subsequent multiple comparison test (all pair-wise differences) using the Tukey method [20]. Statistical tests were performed using S-Plus statistical software [21]. The level of statistical significance for all tests was $p < 0.05$.

3. Results

3.1. Permethrin HPLC analysis

The HPLC analysis method described in Section 2 reliably resolved and detected permethrin isomers and three major metabolites. Using this HPLC method PBOH, PBCHO, PBCOOH, *trans*-permethrin, and *cis*-permethrin were eluted at 3.7, 4.1, 5.9, 10.2, and 10.5 min, respectively.

As shown in Fig. 1, permethrin and its metabolites showed the highest levels of absorption at 210 nm among the four different detection wavelengths previously used in permethrin metabolism studies. The second highest absorption was observed at 230 nm and the compounds showed significantly lower absorption at 254 and 270 nm. While higher absorption was observed at 210 nm, lower detection and quantitation limits were obtained at 230 nm as shown in Table 1. This was due to relatively high levels of background noise at 210 nm.

Mobile phase hydrogen ion concentration clearly affected the resolution of ionizable metabolite (PBCOOH). As shown in Fig. 2, PBCOOH did not form a distinguishable peak at

the solvent B, pH 8.0. As the protonation of PBCOOH proceeded with increasing hydrogen ion concentration in the mobile phase, a separate peak of PBCOOH gradually became distinguishable, forming a clearly identifiable peak at the lowest solvent B, pH 1.7, among the four tested solvent B pHs (Fig. 2). A pH 1.7 for solvent B and a detection wavelength of 230 nm were used for all HPLC analyses in this study.

3.2. *In vitro* human liver metabolism of permethrin

Using the HPLC analysis method developed in this study, the metabolic products of *trans*-permethrin metabolism were profiled after incubating with pooled human liver microsomes and cytosol.

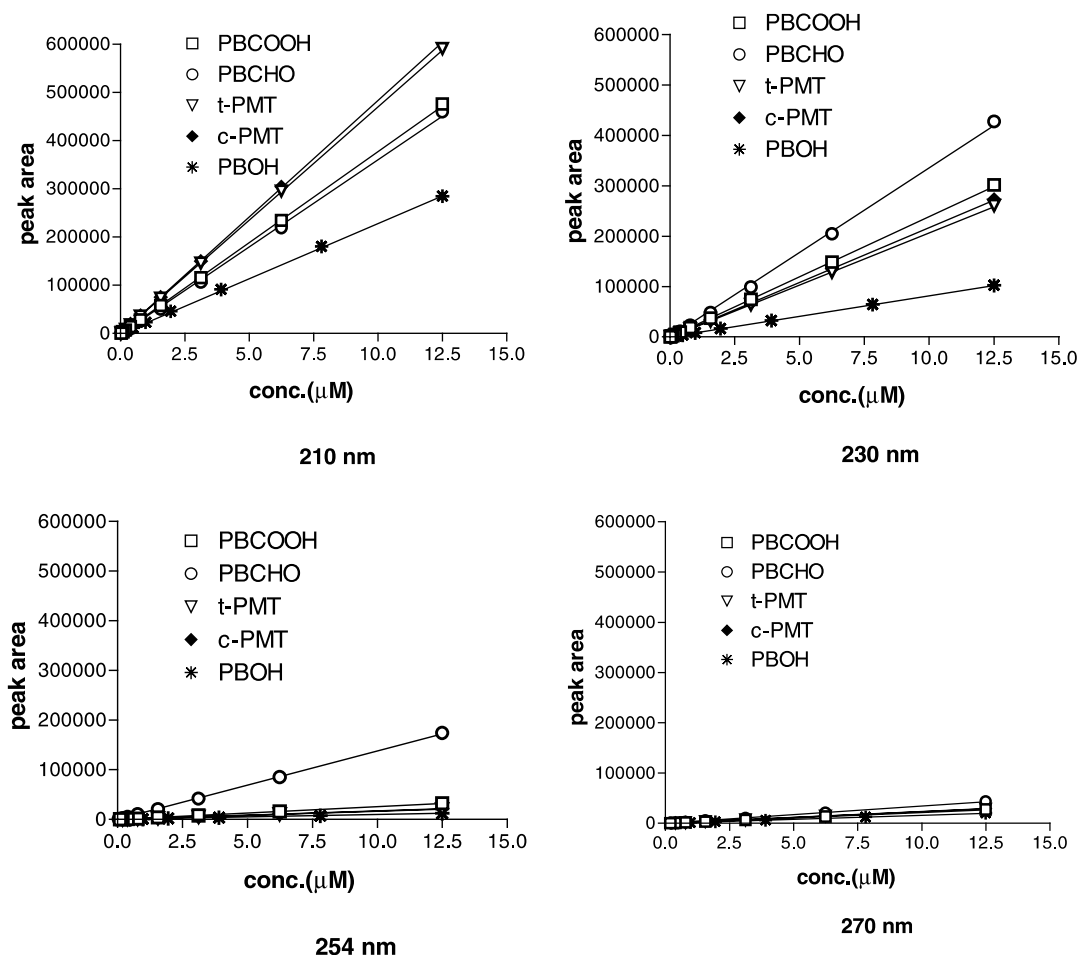


Fig. 1. Standard calibration curves for permethrin isomers and their metabolites at four different wavelengths. t-PMT, *trans*-permethrin; c-PMT, *cis*-permethrin; PBOH, phenoxybenzyl alcohol; PBCHO, phenoxybenzaldehyde; and PBCOOH, phenoxybenzoic acid. Solvent B, pH 1.7.

Table 1

Limits of detection and quantitation for permethrin isomers and their metabolites at different detection wavelengths based on the HPLC method described in Section 2

Wavelength (nm)	Compound	Limit of detection (nM)	Limit of quantitation (nM)
210	PBOH	120	120
	PBCOOH	24	49
	PBCHO	49	98
	t-PMT	24	49
	c-PMT	24	97
230	PBOH	120	120
	PBCOOH	12	12
	PBCHO	12	24
	t-PMT	24	49
	c-PMT	24	49
254	PBOH	490	980
	PBCOOH	98	390
	PBCHO	49	49
	t-PMT	195	390
	c-PMT	195	390
270	PBOH	240	490
	PBCOOH	195	390
	PBCHO	195	195
	t-PMT	390	390
	c-PMT	390	390

t-PMT, *trans*-permethrin; c-PMT, *cis*-permethrin; PBOH, phenoxybenzyl alcohol; PBCHO, phenoxybenzaldehyde; and PBCOOH, phenoxybenzoic acid.

Since no significant *cis*-permethrin metabolism was observed in either cytosolic or microsomal fractions, subsequent metabolism studies focused on *trans*-permethrin metabolism. Fig. 3 shows a typical metabolite profile of human liver microsomal metabolism of *trans*-permethrin. While PBOH and PBCOOH were detected, PBCHO was rarely detected in microsomal incubations. No *trans*-permethrin metabolites were produced in the absence of human liver fractions.

On incubation with the microsomal fraction without an NADPH regenerating system, the sum of the concentration of unmetabolized *trans*-permethrin and the two metabolites equaled 100 μmol (initial *trans*-permethrin concentration) in 500 μl indicating no metabolites other than PBOH and PBCOOH were produced in the incubation. In the remainder of the treatments, the total concentrations were significantly less than 100 μmol (Fig. 4). In these treatments the difference between 100 μmol and the values in Fig. 4 indicated the likelihood that metabolites other than PBOH and PBCOOH were produced. The amount of these unaccounted metabolites was greater in microsomes and cytosol containing the NADPH regenerating system. Fig. 5 shows that

the highest level of overall *trans*-permethrin metabolism occurred in the microsomal fraction with NADPH and NADPH enhanced *trans*-permethrin metabolism in both fractions.

Potential involvement of human CYP isoforms in the hydrolysis of *trans*-permethrin was explored by incubating *trans*-permethrin with CYP isoforms. None of these incubations resulted in detectable products nor did they result in observable loss of the parent *trans*-permethrin (data not shown).

3.3. Phenoxybenzyl alcohol oxidation to phenoxybenzoic acid by purified human alcohol and aldehyde dehydrogenases

All four purified human ADHs readily oxidized PBOH to PBCHO with the lowest K_m observed with β -I ADH and the highest K_m with δ ADH (Table 2). The range of K_m values for PBOH oxidation was two orders of magnitude smaller than that for ethyl alcohol oxidation to acetaldehyde indicating a much higher substrate affinity for PBOH. V_{max} values were relatively close for both substrates. As a result, for all isozymes the catalytic efficiencies (V_{max}/K_m) for PBOH are

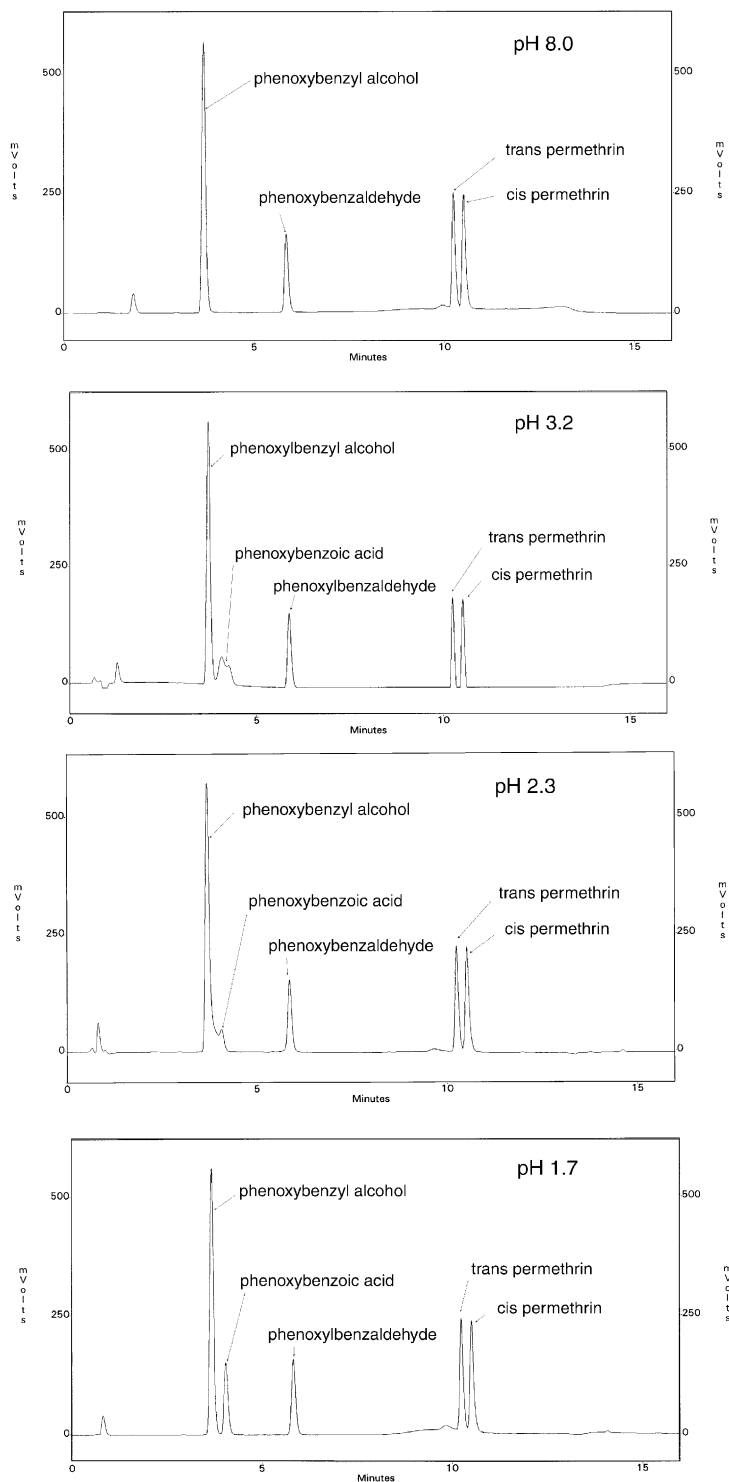


Fig. 2. The effect of pH change in the mobile phase solvent B on the resolution of permethrin isomers and their metabolites. pH was adjusted with 85% phosphoric acid. The compounds were detected at 230 nm.

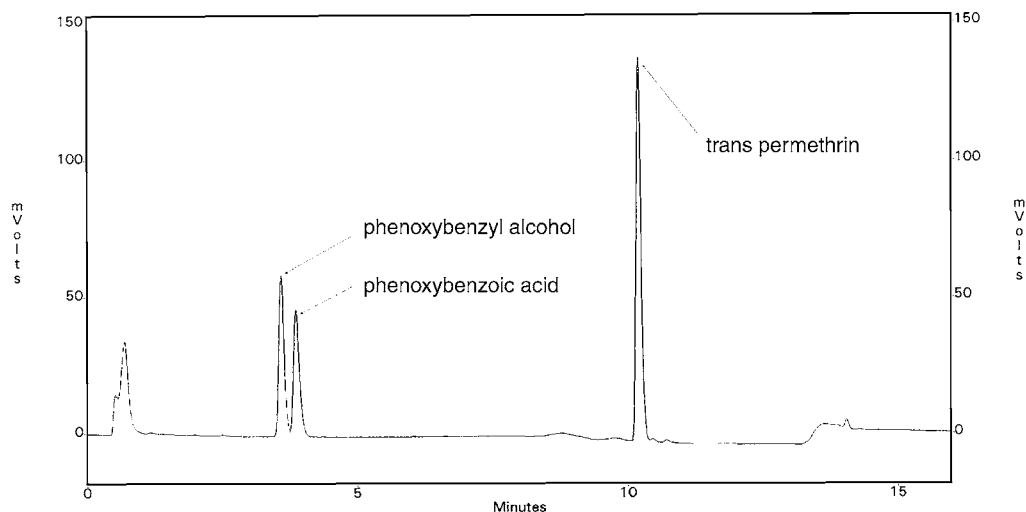


Fig. 3. Metabolite profile of *trans*-permethrin (100 μ M) incubation with pooled human liver microsomal fraction (0.5 mg protein/500 μ l of 0.1 M Tris (pH 7.5) for 100 min at 37 $^{\circ}$ C). Solvent B, pH 1.7, and the compounds were detected at 230 nm.

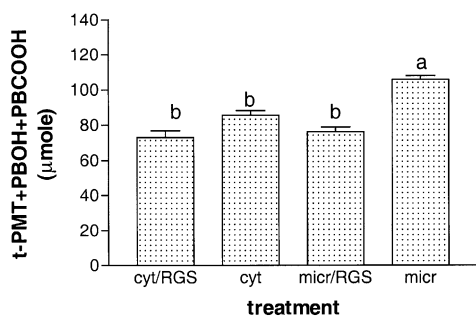


Fig. 4. Sum of *trans*-permethrin and two major metabolites (PBOH and PBCOOH) after incubation with human liver cytosolic and microsomal fractions (500 μ l). cyt/RGS: incubated in human liver cytosol with NADPH regenerating system. cyt: incubated in human liver cytosol without NADPH regenerating system. micr/RGS: incubated in human liver microsomes with NADPH regenerating system. micr: incubated in human liver microsomes without NADPH regenerating system. Values are presented as means + SEM ($n = 3$). A different letter indicates a significant difference ($p < 0.05$) among treatments in ANOVA multiple comparison analysis.

significantly higher than those for ethyl alcohol. In contrast, kinetic parameters and catalytic efficiency for ALDH3A1 toward PBCHO were relatively close to a known ALDH3A1 substrate, benzaldehyde (Table 3). NAD⁺ was required in both ADH and ALDH reactions.

HPLC analysis indicated that PBOH was not oxidized by ALDH3A1 and no PBCOOH was

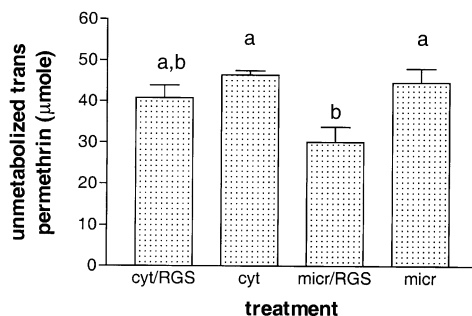


Fig. 5. Amount of unmetabolized *trans*-permethrin after incubation with human liver cytosolic and microsomal fractions (500 μ l). cyt/RGS: incubated in human liver cytosol with NADPH regenerating system. cyt: incubated in human liver cytosol without NADPH regenerating system. micr: incubated in human liver microsomes with NADPH regenerating system. micr: incubated in human liver microsomes without NADPH regenerating system. Values are presented as means + SEM ($n = 3$). A different letter indicates a significant difference ($p < 0.05$) among treatments in ANOVA multiple comparison analysis.

produced from PBOH by ADH isozymes (data not shown). Also, ADHs and ALDH3A1 incubation with *trans/cis*-permethrin did not produce any metabolites indicating ADH/ALDH are not involved in permethrin hydrolysis. Human CYP isoforms are not involved in PBOH oxidation to PBCOOH. Incubation of PBOH and PBCHO with human CYP isoforms with a NADPH

Table 2

Kinetic constants of human alcohol dehydrogenase isoforms for phenoxybenzyl alcohol (PBOH) oxidation to phenoxybenzaldehyde (PBCHO) and ethyl alcohol (EtOH) oxidation

Isozyme	Substrate	K_m (μM) (SE)	V_{max} (nmol/mg/min) (SE)	V_{max}/K_m (min^{-1})
α	PBOH	34 (3)	2765 (68)	82.15
β -I	PBOH	4 (1)	389 (23)	103.46
β -II	PBOH	29 (4)	266 (10)	9.19
δ	PBOH	48 (6)	6452 (203)	134.81
α	EtOH	1570 (180)	3987 (122)	2.54
β -I	EtOH	1120 (160)	541 (21)	0.48
β -II	EtOH	4750 (510)	657 (18)	0.14
δ	EtOH	4060 (330)	7752 (158)	1.91

Table 3

Kinetic constants of human aldehyde dehydrogenase isoform ALDH3A1 for phenoxybenzaldehyde (PBCHO) oxidation to phenoxybenzoic acid (PBCOOH)

Substrate	K_m (μM) (SE)	V_{max} (nmol/mg/min) (SE)	V_{max}/K_m (min^{-1})
Benzaldehyde	148 (58)	2878 (283)	19.45
Phenoxybenzaldehyde	230 (49)	2111 (107)	9.18

regeneration system did not result in detectable products (data not shown).

4. Discussion

The present study is the first report on the characterization of the permethrin metabolic pathway in humans. This study demonstrated that *trans*-permethrin is hydrolyzed and oxidized in human liver cytosol and liver microsomes producing PBOH and PBCOOH. We provide evidence that in human metabolism, PBOH is oxidized to PBCOOH via PBCHO by ADH and ALDH.

Previously described HPLC-UV methods for analysis of permethrin and its metabolites used a variety of wavelength and mobile phase conditions [22–24]. The only previous article reporting a separation method that included all five compounds analyzed in this study was that by Bast et al. [23]. Improvements in mobile phase in this study resulted in decreasing elution time for *cis*-permethrin (the last peak to be eluted) from 25 to 11 min without compromising peak resolution. Mobile phase acidification to protonate PBCOOH (pKa value of 3.95), which is ionized at neutral pH, had also not been described. As shown in Fig. 2, insufficient protonation leads to a broad or missing peak, confounding interpretation of HPLC results. In our gradient scheme, a pH level

below 2 was required for solvent B to achieve reliable protonation of PBCOOH for accurate qualitative and quantitative analysis (Fig. 2).

The central ester linkage in permethrin has been shown to be cleaved in experimental animals by esterases producing PBOH and 3-(2,2-dichlorovinyl)-2,2-dimethylcyclopropane-1-carboxylic acid [14,25]. It was assumed that PBOH is further oxidized to PBCHO and PBCOOH with further hydroxylations and conjugations on these metabolites before excretion. Even though these modifications were presumed to be carried out by Phase I and II enzymes [26], neither the pathways beyond hydrolysis of the ester linkage nor the enzymes involved were identified.

Incubation of *trans*-permethrin with either human liver cytosol or microsomal fractions resulted in the formation of two primary metabolites, PBOH and PBCOOH, indicating that esterases in either cell fraction can cleave the ester bond (Figs. 3 and 4). To date the number of esterases involved in permethrin hydrolysis is not known, and their substrate specificities remain poorly characterized. Soderlund et al. [25] suggested that, based on selective inhibition, *trans/cis*-permethrin hydrolysis is mediated by several esterases with differing substrate specificities and inhibitor sensitivities. In this study *cis*-permethrin was barely hydrolyzed in human liver fractions. Even though previous animal studies have shown that *cis*-permethrin is less prone to hydrolysis

compared to *trans* isomer [14,27], the almost total lack of hydrolysis in human liver fractions implies that human liver esterase specificity or composition is significantly different from animals.

Even though the addition of an NADPH regenerating system facilitated *trans*-permethrin metabolism in both the cytosolic and microsomal fractions, it appears that CYP isozymes are not involved in *trans*-permethrin hydrolysis and subsequent oxidation of PBOH to PBCOOH. This assumption is deduced from the observation that incubation of *trans*-permethrin with 13 individual human CYP isoforms expressed in insect super-somes did not produce PBOH/PBCOOH and the same incubation with PBOH did not produce PBCHO/PBCOOH. In similar studies conducted in our laboratory [8,28,29], the combination of CYP isoforms and the NADPH regeneration system used in this study have demonstrated varying levels of oxidative reactions mediated by CYP isoforms.

It is assumed that in conjunction with conjugation enzymes, CYP isoforms might be involved in hydroxylation and conjugation of permethrin and its metabolites, and likely account for the production of the unaccounted metabolites, which ranges from 0 to 50% of metabolized *trans*-permethrin depending on the presence of the NADPH regenerating system. The products of secondary hydroxylation and subsequent conjugation are believed to be more polar and undetected with the HPLC method used in this study.

Replacement of the NADPH regenerating system with NAD^+ in the liver fractions significantly increased the production of PBCOOH, suggesting that PBOH oxidation is mediated by NAD^+ requiring enzymes and not by CYP isoforms. Also from occasional resolution of small PBCHO peaks on incubation with liver fractions, it was deduced that in the liver fractions PBOH is oxidized to PBCOOH via PBCHO. This postulation was confirmed by the observation that incubating PBOH with purified human ADH isozymes produced PBCHO. In a similar manner, incubation of PBCHO with purified human ALDH produced a PBCOOH peak (data not shown). Incubation of PBOH with ALDH did not produce PBCOOH. These results provide direct evidence that ADH and ALDH are involved in the sequential oxidation of PBOH to PBCOOH via PBCHO.

PBOH is a better substrate than ethyl alcohol (Table 2) for human ADH isoforms. This is in

agreement with previous observations that human ADH isozymes showed higher affinities for alcohols with larger side chains [30,31]. All tested human ADHs were very specific for PBOH oxidation to PBCHO with no significant amount of PBCOOH produced. Also ADHs did not show any enzymatic activities with either *trans*-permethrin or PBCHO.

Human ADH isoforms are a family of dimeric NAD^+ - and zinc-dependent enzymes with nine known different subunits [32]. Human ADH isoforms are involved in the oxidation of ethyl alcohol and various kinds of endogenous alcoholic compounds such as steroid and retinoid metabolites [33,34]. α , β -I, and β -II ADHs are hepatic enzymes while δ ADH is found in the stomach [32]. As implied by the symbolic designations, β isozymes are polymorphic. Most Caucasian populations have β -I ADH, which has a higher affinity for ethyl alcohol, whereas the less efficient β -II ADH is found in 50% of the Asian population [15]. Our results showed that differential enzymatic activity of the β isoforms was more pronounced with PBOH implying that genetically dependent differential permethrin metabolism may have significant physiological ramifications. In this study we have not investigated the interaction between ethyl alcohol and permethrin, but it is plausible that ethyl alcohol consumption might affect permethrin metabolism by ADHs as ethyl alcohol inhibited retinoic acid formation by ADHs [35].

Human ALDHs are a group of enzymes catalyzing the conversion of various aldehydes to the corresponding acids by means of an NAD(P)^+ -dependent reaction. ALDH3A1 is viewed as a cellular protective mechanism and showed high enzymatic activity to aromatic aldehydes such as benzaldehyde [36]. Also ALDH3A1 detoxifies endogenous aldehydes such as the byproducts of lipid peroxidation as well as exogenous aldehyde species such as antineoplastic prodrugs (cyclophosphamide and ifosfamide) [36]. ALDH3A1 is found in stomach tissue (mucosa), and is not constitutively expressed in liver. However, in a rat study it was found that many agents such as 2,3,7,8-tetrachlorodibenzo-*p*-dioxin and 3-methylcholanthrene could induce this isozyme in liver [37]. ALDH3A1 showed slightly higher substrate affinity and higher V_{max} values for benzaldehyde resulting in higher enzymatic efficiency for the compound over PBCHO. ALDH3A1 did not show any enzymatic activities with either *trans*-permethrin or PBOH.

In this study, PBCHO was actively oxidized to PBCOOH in pooled human liver microsomes, which may not contain sufficiently high levels of ALDH3A1. This result implies that ALDH1A1 and ALDH2, which are found mainly in liver tissue and have been demonstrated to possess benzaldehyde metabolic capability [36], were involved in the oxidation. Another possibility is that there are other enzymes with a substrate range overlapping with that of ALDH.

In conclusion we report that *trans*-permethrin is actively hydrolyzed in human liver fractions and that the hydrolysis product of *trans*-permethrin, PBOH, is oxidized to PBCOOH via PBCHO by ADHs and ALDH. In future studies, the effects of active metabolites of other deployment related chemicals (e.g., chlorpyrifos, pyridostigmine bromide, *N,N*-diethyl-*m*-toluamide) on *trans*-permethrin hydrolysis and subsequent metabolite oxidation need to be studied. Also it will be important to assess how the active participation of ADH and ALDH in metabolizing exogenous substrates affects the oxidation of endogenous substrates whose transformation has important physiological functions.

Acknowledgments

These studies were funded, in part, by award number DAMD17-00-2-0008 from the US Army. Authors would like to thank Dr. Alan Brimfield and Dr. Alan Townsend for providing us with transformed *E. coli* strains and purified human aldehyde dehydrogenase.

References

- [1] W.N. Aldridge, An assessment of the toxicological properties of pyrethroids and their neurotoxicity, *Toxicology* 21 (1990) 89.
- [2] F. Cantalamessa, Acute toxicity of two pyrethroids, permethrin and cypermethrin in neonatal and adult rats, *Arch. Toxicol.* 67 (1993) 510.
- [3] J. Ishmael, M.H. Litchfield, Chronic toxicity and carcinogenic evaluation of permethrin in rats and mice, *Fundam. Appl. Toxicol.* 11 (1988) 308.
- [4] S.P. Bradbury, J.R. Coats, Comparative toxicology of the pyrethroid insecticides, *Rev. Environ. Contam. Toxicol.* 108 (1989) 133.
- [5] H.T. Bolton, Use and safety of pesticides (repellents) in Persian Gulf, Presentation to the Department of Veterans' Affairs: Update on Health Consequences of Persian Gulf service, Baltimore, MD, 1995.
- [6] G.A. Jamal, Gulf War Syndrome—a model for the complexity of biological and environmental interaction with human health, *Adverse Drug React. Toxicol. Rev.* 17 (1998) 1.
- [7] Z.X. Shen, Pyridostigmine bromide and Gulf War Syndrome, *Med. Hypotheses* 51 (1998) 235.
- [8] K.A. Usmani, R.L. Rose, J.A. Goldstein, W.G. Taylor, A.A. Brimfield, E. Hodgson, In vitro human metabolism and interactions of repellent *N,N*-diethyl-*m*-toluamide, *Drug Metab. Dispos.* 30 (2002) 289.
- [9] G.W. Stratton, C.T. Corke, Comparative fungitoxicity of the insecticide permethrin and ten degradation products, *Pestic. Sci.* 13 (1982) 679.
- [10] C.R. Tyler, N. Beresford, M. Van der Woning, J.P. Sumpter, K. Thorpe, Metabolism and environmental degradation of pyrethroid insecticides produce compounds with endocrine activities, *Environ. Toxicol. Chem.* 19 (2000) 801.
- [11] F. Asakawa, F. Jitsunari, K. Miki, J. Choi, N. Takeda, T. Kitamado, S. Suna, Y. Manabe, Agricultural worker exposure to and absorption of permethrin applied to cabbage, *Bull. Environ. Toxicol.* 56 (1996) 42.
- [12] J. Angerer, A. Ritter, Determination of metabolites of pyrethroids in human urine using solid phase extraction and gas chromatography-mass spectrometry, *J. Chromatogr.* 695 (1997) 217.
- [13] G. Leng, K.H. Kuhn, H. Idel, Biological monitoring of pyrethroids in blood and pyrethroid metabolites in urine: applications and limitations, *Sci. Total Environ.* 199 (1997) 173.
- [14] L.C. Gaughan, T. Unai, J.E. Casida, Permethrin metabolism in rats, *J. Agric. Food Chem.* 25 (1977) 1.
- [15] C.L. Stone, W.F. Bosron, M.F. Dunn, Amino acid substitutions at position 47 of $\beta_1\beta_1$ and $\beta_2\beta_2$ human and alcohol dehydrogenases affect hydride transfer and coenzyme dissociation rate constants, *J. Biol. Chem.* 268 (1993) 892.
- [16] T.D. Hurley, C.G. Steinmetz, P. Xie, Z.N. Yang, in: H. Weiner, R. Lindahl, D.W. Crabb, T.G. Flynn (Eds.), *Enzymology and Molecular Biology of Carbonyl Metabolism*, vol. 6, Plenum Press, New York, 1997, p. 291.
- [17] P.K. Smith, R.I. Krohn, G.T. Hermanson, A.K. Mallia, F.H. Gartner, M.D. Provenzano, E.K. Fujimoto, B.J. Goeke, B.J. Olson, D.C. Klenk, Measurement of protein using bicinchoninic acid, *Anal. Biochem.* 150 (1985) 76.
- [18] K.D. Bunting, A.J. Townsend, Protection by transfected rat or human class3 aldehyde dehydrogenases against the cytotoxic effects of oxazaphosphorine alkylating agents in hamster V79 cell lines, *J. Biol. Chem.* 271 (1996) 11891.
- [19] GraphPad software version 1.03, San Diego, CA, USA.
- [20] J. Neter, M.H. Kutner, C.J. Nachtsheim, W. Wasserman, *Applied Linear Statistical Models*, fourth ed., Irwin, Chicago, IL, 1996.
- [21] S-Plus 4.0 (1997), Mathsoft, Seattle, WA, USA, 1997.

- [22] S. Lam, E. Grushka, Separation of permethrin and some of its degradation products by high-performance liquid chromatography, *J. Chromatogr.* 154 (1978) 318.
- [23] G.E. Bast, D. Taeschner, H.G. Kampffmeyer, Permethrin absorption not detected in single-pass perfused rabbit ear, and absorption with oxidation of 3-phenoxybenzyl alcohol, *Arch. Toxicol.* 71 (1997) 179.
- [24] R. Manadas, F. Veiga, J.J. Sousa, M.E. Pina, Development and validation of an HPLC method for simultaneous determination of *cis*- and *trans*-permethrin and piperonyl butoxide in pharmaceutical dosage forms, *J. Liq. Chromatogr. Relat. Technol.* 22 (1999) 1867.
- [25] D.W. Soderlund, Y.A.I. Abdel-Aal, D.W. Helmuth, Selective inhibition of separate esterases in rat and mouse liver microsomes hydrolyzing malathion, *trans*-permethrin and *cis*-permethrin, *Pestic. Biochem. Phys.* 17 (1982) 162.
- [26] S.E. Maloney, A. Maule, A.R.W. Smith, Transformation of synthetic pyrethroid insecticides by a thermophilic *Bacillus* sp, *Arch. Microbiol.* 158 (1992) 282.
- [27] M. Elliott, N.F. Janes, D.A. Pulman, L.C. Gaughan, T. Unai, J.E. Casida, Radiosynthesis and metabolism in rats of 1R isomers of the insecticide permethrin, *J. Agric. Food Chem.* 24 (1976) 270–276.
- [28] J. Tang, R.L. Rose, E. Hodgson, Metabolism of chlorpyrifos by human cytochrome P450 isoforms and human, mouse, and rat liver microsomes, *Drug Metab. Dispos.* 29 (2001) 1201–1204.
- [29] J. Tang, R.L. Rose, E. Hodgson, In vitro metabolism of carbaryl by human cytochrome P450 and its inhibition by chlorpyrifos, *Chem.–Biol. Interact.* 141 (2002) 229–241.
- [30] F.W. Wagner, A.R. Burger, B.L. Vallee, Kinetic properties of human liver alcohol dehydrogenase: oxidation of alcohols by class I isoenzymes, *Biochemistry* 22 (1983) 1857.
- [31] C.S. Chen, A. Yoshida, Enzymatic properties of the protein encoded by newly cloned human alcohol dehydrogenase ADH6 gene, *Biochem. Biophys. Res. Commun.* 181 (1991) 743.
- [32] N.Y. Kedishvili, W.F. Bosron, C.L. Stone, T.D. Hurley, C.R. Peggs, H.R. Thomasson, K.M. Popov, L.G. Carr, H.J. Edenberg, T.K. Li, Expression and kinetic characterization of recombinant human stomach alcohol dehydrogenase, *J. Biol. Chem.* 270 (1995) 3625.
- [33] G. Duester, L. Deltour, H.L. Ang, in: H. Weiner, R. Lindahl, D.W. Crabb, T.G. Flynn (Eds.), *Enzymology and Molecular Biology of Carbonyl Metabolism*, vol. 6, Plenum Press, New York, 1997, pp. 357–364.
- [34] F. Strasser, M.N. Huyng, B.V. Plapp, in: H. Weiner, R. Lindahl, D.W. Crabb, T.G. Flynn (Eds.), *Enzymology and Molecular Biology of Carbonyl Metabolism*, vol. 6, Plenum Press, New York, 1997, pp. 313–320.
- [35] G. Duester, in: H. Weiner, R. Lindahl, D.W. Crabb, T.G. Flynn (Eds.), *Enzymology and Molecular Biology of Carbonyl Metabolism*, vol. 7, Plenum Press, New York, 1998, pp. 311–320.
- [36] N.E. Sladek, G.K. Rekha, M.J.C. Lee, H.T. Nagasawa, Inhibition of ALDH3A1-catalyzed oxidation by chlorpropamide analogues, *Chem.–Biol. Interact.* 138 (2001) 201.
- [37] R. Lindahl, Aldehyde dehydrogenases and their role in carcinogenesis, *Crit. Rev. Biochem. Mol. Biol.* 27 (1992) 283.

IN VITRO HUMAN METABOLISM AND INTERACTIONS OF REPELLENT *N,N*-DIETHYL-*m*-TOLUAMIDE

KHAWJA A. USMANI, RANDY L. ROSE, JOYCE A. GOLDSTEIN, WESLEY G. TAYLOR, ALAN A. BRIMFIELD,
AND ERNEST HODGSON

Department of Environmental and Molecular Toxicology, North Carolina State University, Raleigh, North Carolina (K.A.U., R.L.R., E.H.); National Institute of Environmental Health Sciences, Research Triangle Park, North Carolina (J.A.G.); Saskatoon Research Center, Saskatoon, Saskatchewan, Canada (W.G.T.); and United States Army Medical Research Institute of Chemical Defense, Aberdeen Proving Ground, Maryland (A.A.B.)

(Received September 13, 2001; accepted December 4, 2001)

This article is available online at <http://dmd.aspetjournals.org>

ABSTRACT:

Oxidative metabolism of the insect repellent *N,N*-diethyl-*m*-toluamide (DEET) by pooled human liver microsomes (HLM), rat liver microsomes (RLM), and mouse liver microsomes (MLM) was investigated. DEET is metabolized by cytochromes P450 (P450s) leading to the production of a ring methyl oxidation product, *N,N*-diethyl-*m*-hydroxymethylbenzamide (BALC), and an *N*-deethylated product, *N*-ethyl-*m*-toluamide (ET). Both the affinities and intrinsic clearance of HLM for ring hydroxylation are greater than those for *N*-deethylation. Pooled HLM show significantly lower affinities (K_m) than RLM for metabolism of DEET to either of the primary metabolites (BALC and ET). Among 15 cDNA-expressed P450 enzymes examined, CYP1A2, 2B6, 2D6*1 (Val₃₇₄), and 2E1 metabolized DEET to the BALC metabolite, whereas CYP3A4, 3A5, 2A6, and 2C19 produced the ET metabolite. CYP2B6 is the principal cytochrome

P450 involved in the metabolism of DEET to its major BALC metabolite, whereas CYP2C19 had the greatest activity for the formation of the ET metabolite. Use of phenotyped HLMs demonstrated that individuals with high levels of CYP2B6, 3A4, 2C19, and 2A6 have the greatest potential to metabolize DEET. Mice treated with DEET demonstrated induced levels of the CYP2B family, increased hydroxylation, and a 2.4-fold increase in the metabolism of chlorpyrifos to chlorpyrifos-oxon, a potent anticholinesterase. Preincubation of human CYP2B6 with chlorpyrifos completely inhibited the metabolism of DEET. Preincubation of human or rodent microsomes with chlorpyrifos, permethrin, and pyridostigmine bromide alone or in combination can lead to either stimulation or inhibition of DEET metabolism.

N,N-Diethyl-*m*-toluamide, commonly known as DEET¹, is the principle active ingredient in most personal insect repellents worldwide and is highly effective against a broad spectrum of insect pests, including potential disease vectors such as mosquitoes, biting flies, and ticks (including ticks that may carry Lyme disease). DEET was first developed and patented in 1946 by the U.S. Army for use by military personnel and later registered for general public use in 1957 (Schoenig et al., 1999). Every year, approximately one-third of the U.S. population (75,000,000) uses DEET-containing insect repellent

products with DEET concentrations ranging from 10 to 100% in a variety of liquids, lotions, gels, sprays, sticks, and impregnated materials and more than 30 million packages of DEET-containing products are sold annually (Veltri et al., 1994). Approximately 230 products containing DEET are currently registered with the Environmental Protection Agency by about 70 different companies.

DEET is generally considered a benign chemical; however, isolated reports involving heavy and excessive exposure indicate a variety of toxic side effects, including toxic encephalopathy, seizure, acute manic psychosis, cardiovascular toxicity, and dermatitis (Robbins and Cherniack, 1986; Veltri et al., 1994). Because DEET was widely used during the Gulf War, it is one of several chemicals believed to have potential for possible detrimental interactions with other chemicals (Chaney et al., 1997, 1999; Haley and Kurt, 1997; McCain et al., 1997). For example, DEET has been shown to synergize seizures produced by pyridostigmine bromide and vice versa (Chaney et al., 1997, 1999). Subsequent investigations in rats have shown that DEET in combinations with pyridostigmine bromide or permethrin can lead to significant neurobehavioral deficits associated with significant inhibition of brainstem acetylcholinesterase activities (Abou-Donia et al., 2001). Mechanisms of these chemical interactions are currently unknown but may include the ability of one chemical to inhibit and/or induce the metabolism of another chemical. For example, the phosphorothioate organophosphate pesticide chlorpyrifos is capable of

This research was supported by U.S. Army Cooperative Agreement DAMD 17-00-2-0008. Preliminary studies were presented at the Conference on Illnesses among Gulf War Veterans: A Decade of Scientific Research, Alexandria, Virginia, 2001; and part of the studies will be presented at the 41st Society of Toxicology annual meeting in Nashville, TN, 2002.

¹ Abbreviations used are: DEET, *N,N*-diethyl-*m*-toluamide; P450, cytochrome P450; BALC, *N,N*-diethyl-*m*-hydroxymethylbenzamide; ET, *N*-ethyl-*m*-toluamide; HPLC, high-performance liquid chromatography; RLM, rat liver microsomes; MLM, mouse liver microsomes; HLM, human liver microsomes; EROD, *O*-deethylation; MROD, methoxyresorufin *O*-demethylation (MROD); PROD, pentoxyresorufin *O*-dealkylation (PROD); BROD, benzyloxyresorufin *O*-dealkylation.

Address correspondence to: Ernest Hodgson, Department of Environmental and Molecular Toxicology, Box 7633, North Carolina State University, Raleigh, NC 27695. E-mail: ernest_hodgson@ncsu.edu

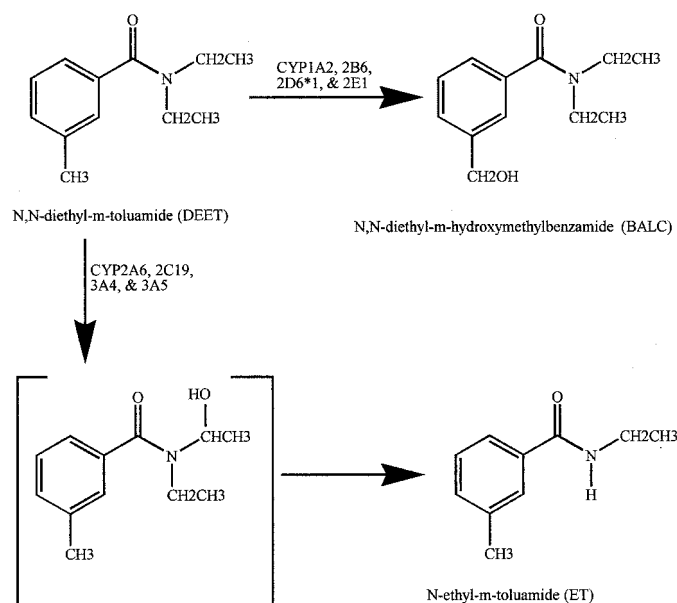


FIG. 1. Primary in vitro metabolites of DEET.

inhibiting metabolism of other chemicals due to its ability to irreversibly inhibit metabolizing enzymes such as cytochromes P450 (P450s) (Butler and Murray, 1997). Thus, an understanding of how DEET is metabolized in humans, the isoforms responsible for such metabolism, and the possible interactions of DEET in metabolism of other chemicals will aid in the evaluation of the possible role that DEET may play in deployment-related illnesses.

The available literature on the pharmacokinetics and metabolism of DEET has been reviewed (Qui et al., 1998). In rat, oxidative metabolism seems to account for most, if not all, of the metabolites derived from DEET. The major metabolites are *N,N*-diethyl-*m*-hydroxymethylbenzamide (BALC) and *N*-ethyl-*m*-toluamide (ET) (Fig. 1), indicating that either the *N*-ethyl or the ring methyl groups can be oxidized (Taylor, 1986; Yeung and Taylor, 1988; Taylor and Spooner, 1990; Schoenig et al., 1996; Constantino and Iley, 1999). These two major and several minor metabolites were characterized in liver microsomes from phenobarbital-pretreated rats (Taylor, 1986; Yeung and Taylor, 1988; Constantino and Iley, 1999). Studies of the metabolism of DEET by human enzymes are lacking. Studies of absorption and metabolism in humans have been conducted only at the level of determining urinary metabolites and suggest that 5 to 8% of topically applied DEET is rapidly absorbed and excreted. As many as six metabolites were recovered from the human urine samples (Selim et al., 1995).

The main objectives of the present study were to identify and quantify the oxidative metabolism of DEET by human liver microsomes and to compare the metabolism of DEET in human liver microsomes with that in rat and mouse liver microsomes. Further objectives were to identify the human P450 isoforms responsible for DEET metabolism, and to investigate potential interactions of DEET with other xenobiotics.

Materials and Methods

Chemicals. DEET, chlorpyrifos, chlorpyrifos-oxon, 3,5,6-trichloro-2-pyridinol, and permethrin (50:50 *cis-trans*) were purchased from ChemService (West Chester, PA). ET and BALC were synthesized as described previously (Taylor, 1986). Pyridostigmine bromide was purchased from Roche Molecular Biochemicals (Indianapolis, IN). HPLC grade acetonitrile and tetrahydrofuran were purchased from Fisher Scientific (Pittsburgh, PA) and Mallinckrodt

Baker, Inc. (Paris, KY), respectively. All other chemicals were purchased, if not specified, from Sigma Chemical (St. Louis, MO).

Rodent Liver Microsome Preparation. Rat liver microsomes (RLM) and mouse liver microsomes (MLM) were prepared from adult male Long Evans rats and adult male CD-1 mice (Charles River Laboratories, Raleigh, NC), respectively, according to the method of Cook and Hodgson (1983). Briefly, immediately after sacrificing the animals, the fresh livers were excised, weighed, minced, and washed with ice-cold homogenized buffer (50 mM potassium phosphate buffer, pH 7.5; 0.1 mM EDTA; 1.15% potassium chloride). Samples were homogenized with a Polytron homogenizer in ice-cold homogenization buffer and centrifuged at 10,000g for 15 min. The supernatant was filtered through glass wool, centrifuged at 100,000g for 1 h, and the microsomal pellet was resuspended in storage buffer (50 mM potassium phosphate, pH 7.5; 0.1 mM EDTA; 0.25 M sucrose). All processes were performed at 0–4°C. The microsomal preparation was aliquoted and stored at –80°C until used.

Total cytochrome P450 content was determined by the CO-difference spectrum method of Omura and Sato (1964). Protein concentration was determined using the Bio-Rad protein assay with bovine serum albumin as standard (Bradford, 1976).

Human Liver Microsomes and Human Cytochrome P450 Isoforms. Pooled human liver microsomes (HLM) (pooled from 10 donors) and human P450 isoforms expressed in baculovirus-infected insect cells (Sf9) (BTI-TN-5B1-4), CYP1A1, 1A2, 2A6, 1B1, 2B6, 2C8, 2C9*1 (Arg₁₁₄), 2C18, 2C19, 2D6*1 (Val₃₇₄), 2E1, 3A4, 3A5, 3A7, and 4A11 were purchased from GENTEST (Woburn, MA). Gender specific HLM (pooled from five male donors or five female donors, respectively) were purchased from GENTEST. Gender specific HLM (pooled from 10 male donors or 10 female donors, respectively) were also purchased from Xenotech (Kansas City, KS). Selected individual human liver microsomes (HG042, HG043, and HG095) were purchased from GENTEST.

In Vitro DEET Metabolism. Enzyme kinetic assays for microsomes were performed by incubation in 1.5-ml microcentrifuge tubes of serial concentrations of DEET (final concentrations 31.24–3000 μM) with microsomes in 20 mM Tris-HCl buffer, pH 8.3 at 37°C, containing 5 mM MgCl₂ (final volume 1.0 ml) for 5 min. Preliminary studies demonstrated that a pH of 8.3 was optimal for the production of DEET metabolites as had previously been reported for metabolites of DEET by rat liver microsomes (Yeung and Taylor, 1988). The microsomal protein concentrations used in assays were 1.5 mg/ml for HLM, RLM, and MLM. After preincubation at 37°C for 5 min, reactions were initiated by the addition of ice-cold microsomes to prewarmed buffer/substrate/cofactors. The final concentration of the NADPH-generating system was 0.25 mM NADP, 2.5 mM glucose 6-phosphate, and 2 U/ml glucose-6-phosphate dehydrogenase. The controls were performed in the absence of the NADPH-generating system. Reactions were terminated by the addition of an equal volume of acetonitrile and vortexing. After 10-min centrifugation at 15,000 rpm in a microcentrifuge, the supernatants were analyzed for BALC and ET concentrations by HPLC as described below.

The initial metabolic activity assays for human P450 isoforms were performed by incubation of DEET (final concentrations 1000 or 3000 μM) with P450 isoforms (final P450 contents 100–200 pmol/ml) for 20 min in P450-specific buffers recommended by the supplier (GENTEST). The controls were performed in the absence of an NADPH-generating system. For CYP1A1, 1A2, 1B1, 2D6*1 (Val₃₇₄), 3A4, 3A5, and 3A7 a 100 mM potassium phosphate buffer with 3.3 mM MgCl₂, pH 7.4, was used. For CYP2B6, 2C8, 2C19, and 2E1 a 50 mM potassium phosphate buffer with 3.3 mM MgCl₂, pH 7.4, was used. For CYP2C9*1 (Arg₁₄₄), 2C18, and 4A11 a 100 mM Tris-HCl buffer with 3.3 mM MgCl₂, pH 7.5, was used. For CYP2A6 a 50 mM Tris-HCl buffer with 3.3 mM MgCl₂, pH 7.5, was used.

Enzyme kinetic assays for human CYP1A2, 2B6, and 2D6*1 (Val₃₇₄) were performed by incubations of serial concentrations of DEET (final concentrations 31.25–1000 μM) (final P450 content 50 pmol) for 10 min in P450-specific buffers recommended by the supplier (GENTEST).

Assays of five pooled male and female HLM purchased from GENTEST and 10 pooled male and female HLM purchased from Xenotech were performed by incubations of DEET (final concentration 1000 μM) with microsomes (final protein concentration 1.5 mg/ml) for 10 min. Similar conditions were used for assays of individual HLM.

TABLE 1

Kinetic parameters for the ring methyl oxidation and *N*-deethylation of DEET by pooled HLM, RLM, MLM, and DEET treated mouse liver microsomes

Means in the same column followed by the same letter are not significantly different ($P < 0.01$). Values are the mean \pm S.E.M. ($n = 3$).

	BALC (Ring Methyl Oxidation)			ET (<i>N</i> -Deethylation)		
	K_m	V_{max}	CL_{int}	K_m	V_{max}	CL_{int}
	μM	nmol/mg protein/min	10^{-6} /mg protein/min	μM	nmol/mg protein/min	10^{-6} /mg protein/min
HLM	67.6 \pm 4.2 ^b	12.9 \pm 1.6 ^{ab}	191.5 \pm 15.4 ^b	842.5 \pm 49.9 ^b	20.5 \pm 3.4 ^a	24.4 \pm 5.1 ^b
RLM	38.3 \pm 0.2 ^a	17.6 \pm 1.2 ^a	461.3 \pm 23.5 ^a	214.3 \pm 26.1 ^a	19.2 \pm 2.8 ^a	89.5 \pm 10.9 ^a
MLM	43.4 \pm 0.6 ^{ab}	6.8 \pm 1.4 ^b	156.8 \pm 23.8 ^b	660.6 \pm 59.5 ^b	14.5 \pm 2.9 ^a	21.7 \pm 3.9 ^b
MLM*	42.6 \pm 13.6 ^{ab}	16.4 \pm 3.4 ^a	385.1 \pm 52.6 ^a	630.9 \pm 128.0 ^b	22.9 \pm 2.9 ^a	38.3 \pm 5.1 ^b

* DEET treated animals LD₁₀ (200 mg/kg/day).

Induction. Adult male CD-1 mice, 28 to 30 g, were obtained from Charles River Laboratories and acclimated for 4 days. Low (2 mg/kg/day), medium (20 mg/kg/day), and high (200 mg/kg/day) doses of DEET in 100 μ l of corn oil were given intraperitoneally daily for 3 days. The dose range for DEET was selected to not exceed a dose known to produce a physiological effect (Chaney et al., 1999). Doses approximating LD₁₀ values for phenobarbital (80 mg/kg/day) in 100 μ l of water or 3-methylcholanthrene (20 mg/kg/day) in 100 μ l of corn oil were also administered intraperitoneally, to separate groups of mice, daily for 3 days. Controls were given corn oil only or water. Microsomes were prepared from livers of fed mice on the 4th day as described above.

The following substrates were used as indicators of the activities for the following isozymes: ethoxyresorufin *O*-deethylation (EROD) and methoxyresorufin *O*-demethylation (MROD) for CYP1A1/2 (Burke and Mayer, 1974; Nerurkar et al., 1993), pentoxyresorufin *O*-dealkylation (PROD) for CYP2B10 (Lubet et al., 1985), and benzyloxyresorufin *O*-dealkylation (BROD) for CYP2B (Nerurkar et al., 1993). Assays were conducted as described by Pohl and Fouts (1980). Briefly, assays were initiated by the addition of an NADPH-regenerating system and incubated for 5 min at 37°C. Product formation for EROD, MROD, PROD, and BROD activities were determined spectrofluorometrically (F-2000 fluorescence spectrophotometer; Hitachi, Tokyo, Japan) by comparison with a standard curve generated with resorufin.

Chlorpyrifos Metabolism. Chlorpyrifos metabolism activity assays were performed by incubation of 100 μ M chlorpyrifos with induced MLM for 5 min. The microsomal protein concentrations used in the assays were 1.0 mg/ml in 100 mM Tris-HCl buffer, pH 7.4 at 37°C, containing 5 mM MgCl₂ and 3 mM EDTA. Reactions were stopped by the addition of acetonitrile followed by centrifugation at 15,000 rpm. The supernatant was analyzed for chlorpyrifos-oxon and 3,5,6-trichloro-2-pyridinol concentrations by HPLC as described by Tang et al. (2001).

Inhibition. The inhibition of human CYP2B6 by chlorpyrifos and chlorpyrifos-oxon were studied by incubating these two compounds (final concentration 100 μ M), CYP2B6 (50 pmol), NADPH-generating system, and 50 mM potassium phosphate buffer with 3.3 mM MgCl₂, pH 7.4, for 5 min at 37°C before adding DEET (final concentration 1000 μ M). The reaction was terminated after an additional 20 min by the addition of an equal volume of acetonitrile. After brief centrifugation the supernatant was analyzed for BALC concentration by HPLC.

To understand possible interactions produced by potential induction of metabolizing enzymes by DEET; effects on DEET metabolism were examined in HLM, MLM, and RLM after preincubations with chlorpyrifos, permethrin, and pyridostigmine bromide either alone or in combination (final concentration 100 μ M). In addition, the effects of these compounds were also examined in some mice that had been induced with phenobarbital (80 mg/kg/day), 3-methylcholanthrene (20 mg/kg/day), or the high dose of DEET (200 mg/kg/day). Microsomes (final protein concentrations 1.5 mg/ml), NADPH-generating system, and 20 mM Tris-HCl buffer with 5 mM MgCl₂, pH 8.3 at 37°C, were incubated for 5 min at 37°C before adding DEET (final concentration 1000 μ M). The reaction was terminated after 10 min by the addition of an equal volume of acetonitrile. After centrifugation at 15,000 rpm, the supernatant was analyzed for BALC and ET concentrations by HPLC.

All assays were conducted in triplicate. The protein concentrations and incubation times used in the assays were found to be in the linear range in

preliminary experiments. No metabolites were detected when incubations were carried out in the absence of an NADPH-generating system.

Analysis of Metabolites by HPLC. Metabolites were analyzed using a Shimadzu HPLC system (Kyoto, Japan). The Shimadzu HPLC system used in this study consisted of two pumps (LC-10AT), a Shimadzu autoinjector (SIL-10AD VP), and a Waters 486 tunable absorbance detector (Waters, Milford, MA). For DEET metabolites, the mobile phase for pump A was 3.5% tetrahydrofuran, 96.5% water; for pump B 100% acetonitrile. A gradient system was used as described by Yeung and Taylor (1988) in the following manner: 0 to 3 min (10% B), 3 to 30 min (10–60% B), 30 to 32 min (60–10% B), and 32 to 35 min (10% B). The flow rate was 1 ml/min. For chlorpyrifos metabolites, the mobile phase for pump A was 10% acetonitrile, 89% H₂O and 1% phosphoric acid; for pump B 99% acetonitrile and 1% phosphoric acid. A gradient system was initiated at 20% pump B and increased to 100% pump B in 20 min. The flow rate was 1 ml/min. Metabolites for DEET and chlorpyrifos were separated by a C₁₈ column (Luna 5 μ m, 150 \times 3 mm; Phenomenex, Rancho Palos Verdes, CA) and detected at 230 nm. Under these conditions the retention times for BALC, ET, and DEET were 2.5, 5, and 11 min, respectively. The limit of detection for the two DEET metabolites was approximately 10 μ M. Concentrations of metabolites were obtained by extrapolation of peak height from a standard curve. K_m and V_{max} were obtained from Lineweaver-Burk plots (1/velocity versus 1/substrate concentration).

Statistics. Significant differences between data sets were determined by one-way analysis of variance and multiple comparisons were performed with the Tukey-Kramer honestly significant different test by using a SAS program (SAS, 1989).

Results

Pooled HLM as well as RLM and MLM showed a much lower K_m (higher affinity) and higher intrinsic clearance for ring hydroxylation (BALC formation) than for *N*-deethylation (ET formation) from DEET (~10-fold differences) (Table 1). HLM also exhibited higher K_m values (lower affinities) than either RLM or MLM. HLM exhibited a lower intrinsic clearance rate [$CL_{int} (V_{max}/K_m)$] for both metabolites than RLM. However, the CL_{int} for MLM was similar to that of HLM. When mice were treated with the high dose (200 mg/kg/day) there was a significant increase in the V_{max} and intrinsic clearance of BALC and ET, indicating that DEET induced its own metabolism.

Among 15 different human P450 isoforms screened, only CYP1A2, 2B6, 2D6*1 (Val₃₇₄), and 2E1 displayed detectable BALC metabolite production (Table 2). The activity of CYP2E1 was significantly less than the activities of the other P450s producing the BALC metabolite. Production of the BALC metabolite was generally much higher than that of the ET metabolite. Isoforms producing detectable amounts of the ET metabolite included CYP3A4, 3A5, 2A6, and 2C19. These isoforms produced no detectable amounts of the BALC metabolite. CYP2C19 showed significantly higher activity than CYP3A4, 3A5, and 2A6. Isoforms CYP1A1, 1B1, 3A7, 2C8, 2C9*1 (Arg₁₄₄), 2C18, and 4A11 were inactive in the production of either metabolite.

Kinetic studies of CYP1A2, 2B6, and 2D6*1 (Val₃₇₄) with respect

TABLE 2

Ring methyl oxidation and *N*-deethylation activities toward DEET in human cytochrome P450 isoforms expressed in baculovirus-infected insect cells

Means in the same column followed by the same letter are not significantly different ($P < 0.01$). Values are the mean \pm S.E.M. ($n = 3$).

	BALC (Ring Methyl Oxidation)	ET (<i>N</i> -Deethylation)
	nmol/nmol isoform/min	
1A2	68.94 \pm 2.64 ^a	Not detected
2B6	69.51 \pm 1.83 ^a	Not detected
2D6*1	56.56 \pm 2.52 ^b	Not detected
2E1	3.34 \pm 0.17 ^c	Not detected
2A6	Not detected	4.55 \pm 0.30 ^a
2C19	Not detected	8.96 \pm 0.82 ^b
3A4	Not detected	5.05 \pm 0.20 ^a
3A5	Not detected	5.81 \pm 0.24 ^a

to the production of the ring methyl oxidation product BALC are shown in Table 3. No significant differences in K_m , V_{max} , and CL_{int} (V_{max}/K_m) in production of the BALC metabolite were observed between CYP1A2 and 2B6. Activity of the CYP2D6 isoform was too low for accurate kinetic determinations. Comparisons of male and female differences in metabolism of DEET were performed using pooled liver microsomes from two different suppliers. Microsomes from GENTEST included five pooled males and females, whereas those from Xenotech included 10 individuals from each gender. In both cases, activity of females in the production of BALC and ET metabolites was greater than that of males; however, due to departure from randomness in the way these pooled samples were prepared the data are insufficient to demonstrate a definitive gender difference (data not shown).

To further determine the importance of CYP2B6 and 1A2 in ring methyl oxidation of DEET and, in addition, the importance of CYP3A4, 2C19, and 2A6 in *N*-deethylation of DEET, liver microsomes from three different individuals possessing varying levels of these isoforms were investigated with respect to their ability to metabolize DEET (Table 4). The individual with high levels of both CYP2B6 and 1A2 (HG042) had significantly greater ability to produce the BALC metabolite than the other two individuals. In contrast, individuals with high levels of CYP1A2 (HG043) or CYP2D6 (HG095) had significantly lower ability to metabolize DEET to the BALC metabolite, indicating the importance of CYP2B6 in formation of this metabolite. The individual with high levels of CYP3A4 and 2A6 but low level of CYP2C19 (HG042) had the highest activity for production of the ET metabolite. The individual (HG043) with the highest level of CYP2C19 but low levels of CYP3A4 and 2A6 had significantly greater ability to produce the ET metabolite than the individual (HG095) with very low levels of these isoforms.

Experiments were conducted to examine the potential of DEET to induce enzymes involved in metabolism. These experiments included the prototypical P450 inducers phenobarbital and 3-methylcholanthrene. Doses of DEET were low, medium, and high (2, 20, and 200 mg/kg/day). As expected, phenobarbital and 3-methylcholanthrene induced P450 content. Phenobarbital induced BROD (5.2-fold) and PROD (30-fold) activities, whereas 3-methylcholanthrene induced EROD (23-fold) and MROD (10.5-fold) activities. No significant levels of induction were observed for the two lower doses of DEET. In contrast, the high dose of DEET produced significant increases in BROD (3.5-fold) and in PROD activities (4.0-fold).

Studies were also conducted to examine the possible effect of DEET, phenobarbital, and 3-methylcholanthrene to induce metabolism of chlorpyrifos in mice. No significant differences were observed in the dearylation of chlorpyrifos with any treatment. However, sig-

TABLE 3

Kinetic parameters for ring methyl oxidation of DEET by human cytochrome P450 isoforms expressed in baculovirus infected insect cells

Means in the same column followed by the same letter are not significantly different ($P < 0.01$). Values are the mean \pm S.E.M. ($n = 3$).

	BALC (Ring Methyl Oxidation)		
	K_m	V_{max}	CL_{int}
	μM	nmol/nmol isoform/min	10^{-6} /nmol isoform/min
CYP2B6	40.2 \pm 1.2 ^a	22.3 \pm 2.1 ^a	552.0 \pm 40.4 ^a
CYP1A2	41.0 \pm 2.0 ^a	24.5 \pm 1.2 ^a	598.7 \pm 39.6 ^a
CYP2D6	>1000		

TABLE 4

Ring methyl oxidation and *N*-deethylation activities toward DEET in individual human liver microsomes

BALC and ET activities are based on 5- and 20-min incubations, respectively. Means in the same column followed by the same letter are not significantly different ($P < 0.01$). Values are the mean \pm S.E.M. ($n = 3$).

	BALC (Ring Methyl Oxidation)	ET (<i>N</i> -Deethylation)
	nmol/mg protein/min	
HG042*	3.30 \pm 0.17 ^a	1.59 \pm 0.03 ^a
HG043*	0.54 \pm 0.03 ^b	1.14 \pm 0.05 ^b
HG095*	0.52 \pm 0.01 ^b	0.63 \pm 0.03 ^c

* Individual human liver microsomes (protein concentration 20 mg/ml). CYP2B6, 2D6, 2E1, 1A2, 3A4, 2C19, and 2A6 activities (picomoles of product per milligram of protein per minute), represented by (*S*)-mephenytoin *N*-demethylase, bufuralol 1'-hydroxylase (amount of activity inhibited by 1 μM quinidine), chlorzoxazone 6-hydroxylase, phenacetin *O*-deethylase, testosterone 6 β -hydroxylase, (*S*)-mephenytoin 4'-hydroxylase, and coumarin 7-hydroxylase catalytic activities, respectively, are 270, 68, 1700, 640, 13,000, 8, and 2300 for HG042 (48-year-old female); 34, 20, 1100, 630, 5600, 700, and 850 for HG043 (23-year-old female); and 12, 160, 1200, 280, 760, 30, and 200 for HG095 (47-year-old female) (data were provided by GENTEST).

nificant increases in chlorpyrifos desulfuration activity were observed with phenobarbital (5.5-fold) and the high dose of DEET (2.8-fold).

The possibility that chlorpyrifos or chlorpyrifos-oxon may inhibit DEET metabolism by human CYP2B6 was investigated by incubating 100 μM concentration of each substrate for 5 min before addition of DEET as a substrate. Chlorpyrifos preincubation resulted in 100% inhibition of the production of the BALC metabolite, whereas for chlorpyrifos-oxon, 58% inhibition was observed.

The effects of chlorpyrifos, permethrin, and pyridostigmine bromide alone or in combination on DEET metabolism were investigated using human, rat, and mouse liver microsomes (Table 5). Preincubation of pooled HLM with permethrin, pyridostigmine bromide, and permethrin + pyridostigmine bromide significantly increased the production of BALC. Preincubation of pooled HLM with chlorpyrifos alone or in combination with any other compound significantly decreased the production of BALC. Preincubation of pooled HLM with chlorpyrifos, permethrin, pyridostigmine bromide alone or in combination showed no significant differences on the production of ET. Generally, preincubation of pooled HLM, RLM, MLM, DEET-treated MLM, phenobarbital-treated MLM, and 3-methylcholanthrene-treated MLM with chlorpyrifos alone or in combination of any other compound significantly inhibited the production of BALC and ET.

Discussion

Despite the extensive use of DEET as an insect repellent worldwide, no in vitro studies have been carried out using human enzymes and none of the rat studies have been at the level of individual isoforms. The mean metabolic intrinsic clearance rates, as estimated by V_{max}/K_m , indicate that RLM metabolize DEET more efficiently than pooled HLM or MLM and that the BALC metabolite is produced more readily than the ET metabolite.

TABLE 5

Effects of chlorpyrifos (CPS), permethrin (PMT), and pyridostigmine bromide (PYB) alone and in combination on DEET metabolism by pooled HLM, RLM, MLM, DEET-treated MLM, phenobarbital (PB)-treated MLM, and 3-methylcholanthrene (3-MC)-treated MLM

DEET High (DH) 200 mg/kg/day, PB 80 mg/kg/day, 3-MC 20 mg/kg/day. Means in the same column followed by the same letter are not significantly different ($P < 0.01$). Values are the mean \pm S.E.M. ($n = 3$).

Treatment	HLM		RLM		MLM (Control)		MLM (DH)		MLM (PB)		MLM (3-MC)	
	BALC	ET	BALC	ET	BALC	ET	BALC	ET	BALC	ET	BALC	ET
Control	1.1 \pm 0.1 ^b	1.5 \pm 0.1 ^a	4.3 \pm 0.1 ^a	3.1 \pm 0.2 ^a	1.3 \pm 0.1 ^a	1.7 \pm 0.3 ^a	2.0 \pm 0.2 ^a	1.9 \pm 0.1 ^a	4.8 \pm 0.3 ^a	4.3 \pm 0.3 ^a	1.3 \pm 0.1 ^a	2.0 \pm 0.1 ^a
CPS	0.3 \pm 0.0 ^c	1.4 \pm 0.0 ^a	1.1 \pm 0.1 ^c	1.6 \pm 0.1 ^{bc}	0.2 \pm 0.0 ^b	0.8 \pm 0.2 ^b	0.3 \pm 0.1 ^b	1.0 \pm 0.0 ^b	1.0 \pm 0.2 ^b	1.6 \pm 0.3 ^b	0.6 \pm 0.1 ^b	1.0 \pm 0.2 ^b
PMT	1.7 \pm 0.1 ^a	1.6 \pm 0.1 ^a	2.2 \pm 0.0 ^b	2.3 \pm 0.1 ^{ac}	0.9 \pm 0.2 ^a	1.4 \pm 0.2 ^a	1.8 \pm 0.4 ^a	2.4 \pm 0.5 ^a	2.5 \pm 0.2 ^c	3.4 \pm 0.3 ^a	0.8 \pm 0.1 ^{bc}	1.7 \pm 0.2 ^a
PYB	1.8 \pm 0.1 ^a	2.1 \pm 0.1 ^a	3.6 \pm 0.2 ^a	3.0 \pm 0.1 ^a	1.2 \pm 0.2 ^a	1.8 \pm 0.2 ^a	2.2 \pm 0.3 ^a	2.8 \pm 0.5 ^a	2.9 \pm 0.3 ^c	3.0 \pm 0.2 ^a	1.2 \pm 0.1 ^{ac}	1.8 \pm 0.1 ^a
CPS + PMT	0.6 \pm 0.0 ^c	1.6 \pm 0.3 ^a	1.1 \pm 0.2 ^c	1.4 \pm 0.0 ^{bc}	0.3 \pm 0.0 ^b	0.8 \pm 0.1 ^b	0.3 \pm 0.0 ^b	0.9 \pm 0.1 ^b	0.4 \pm 0.1 ^b	1.1 \pm 0.1 ^b	0.5 \pm 0.1 ^b	0.7 \pm 0.1 ^b
CPS + PYB	0.4 \pm 0.0 ^c	1.3 \pm 0.1 ^a	1.5 \pm 0.4 ^{bc}	2.0 \pm 0.3 ^c	0.2 \pm 0.0 ^b	0.8 \pm 0.1 ^b	0.2 \pm 0.1 ^b	0.8 \pm 0.2 ^b	0.5 \pm 0.0 ^b	1.3 \pm 0.1 ^b	0.6 \pm 0.0 ^b	0.9 \pm 0.0 ^b
PMT + PYB	1.6 \pm 0.1 ^a	1.6 \pm 0.1 ^a	2.5 \pm 0.1 ^b	2.4 \pm 0.2 ^{ac}	0.9 \pm 0.0 ^a	1.7 \pm 0.2 ^a	1.7 \pm 0.5 ^a	2.4 \pm 0.6 ^a	2.6 \pm 0.2 ^c	3.2 \pm 0.3 ^a	0.6 \pm 0.1 ^b	1.1 \pm 0.1 ^b
CPS + PMT + PYB	0.6 \pm 0.0 ^c	1.4 \pm 0.1 ^a	0.9 \pm 0.1 ^c	1.3 \pm 0.0 ^{bc}	0.2 \pm 0.1 ^b	0.8 \pm 0.1 ^b	0.2 \pm 0.0 ^b	1.0 \pm 0.1 ^b	0.9 \pm 0.2 ^b	1.5 \pm 0.1 ^b	0.3 \pm 0.0 ^a	0.9 \pm 0.1 ^b

A previous study using rat liver microsomes demonstrated a significant gender difference in the metabolism of DEET with males having nearly 3-fold greater metabolizing ability than females (Yeung and Taylor, 1988). Although some pooled female HLM showed significantly higher activities in BALC and ET production from DEET than pooled male HLM the results could not be regarded as definitive as noted above. Further research with large randomly selected pooled male and female HLM or microsomes from individuals is required to better understand possible gender differences in humans.

It is of interest that although eight different isoforms are capable of metabolizing DEET, each isoform produced only one metabolite. Results from individual incubations of DEET with various P450 isoforms suggested that CYP1A2 and 2B6 were highly active in production of the BALC metabolite, whereas CYP3A4, 2C19, and 2A6 were important in the formation of the ET metabolite. Inasmuch as different individuals have varying levels of each of these isoforms, we selected microsomes from individuals possessing widely varying activities of these isoforms to represent contrasting levels of predicted metabolic activity. As expected, the individual with high levels of CYP2B6 and 1A2 had the greatest ability to produce the BALC metabolite. In contrast, individuals possessing high levels of either CYP3A4 or 2C19 had the greatest levels of the ET metabolite production, whereas the individual with the lowest levels of these isoforms had the lowest ET metabolite production. Based on these results it seems reasonable to suggest that individuals, regardless of gender, with varying activities of these P450 isoforms, will be more or less efficient in the metabolism of DEET.

To determine which P450 isoforms were inducible by DEET, substrate-specific assays were conducted using microsomes from DEET-treated mice. DEET treatment did not induce CYP1A1/1A2 as determined from EROD and MROD activity measurement. In contrast, PROD and BROD activities, measures of CYP2B isoform activity, significantly increased in the animals treated with the highest dose of DEET. These induction studies corroborated our results, which indicated that CYP2B6, similar to phenobarbital-induced CYP2B isoforms in rodents (Levi et al., 1988; Fabrizi et al., 1999), is one of the most important P450 isoforms in ring methyl oxidation of DEET and, furthermore, that DEET induces its own metabolism.

Tang et al. (2001) reported that CY2B6 has the highest activity for desulfuration of chlorpyrifos, an activation process. In this study, mice treated intraperitoneally with the highest dose of DEET had significant induction of CYP2B. This induction was demonstrated to result in increased chlorpyrifos desulfuration (2.8-fold), resulting in the production of the activation product, chlorpyrifos oxon. The lower doses of DEET were not effective inducers of CYP2B6. Although these results may imply that DEET could increase organophosphate toxicity, the high levels necessary to produce the effects, combined with the mode of administration, might suggest that risks through epidermal exposures to humans may be minimal. On the other hand, preincubation of chlorpyrifos with CYP2B6 resulted in complete inhibition of DEET metabolism to the BALC metabolite. Thus, chlorpyrifos exposure could inhibit the subsequent metabolism of DEET in humans by inhibiting the isoforms involved in DEET metabolism.

Serious side effects caused by drug-drug interactions have been reported (Guengerich, 1997). Either inhibition or induction can modulate the activity of an enzyme; P450s may exhibit stimulation (positive cooperativity) in the presence of certain xenobiotic compounds (Guengerich, 1997; Szklarz and Halpert, 1998). Our data show stimulation of pooled HLM, wherein conversion of DEET to BALC increased significantly in the presence of permethrin, pyridostigmine bromide, and permethrin + pyridostigmine bromide. However, no stimulation was observed with RLM, MLM, and MLM induced with

DEET, phenobarbital, or 3-methylcholanthrene in the presence of permethrin, pyridostigmine bromide, and permethrin + pyridostigmine bromide. Inhibition in a sense may be considered more serious than enzyme induction because inhibition happens quickly, not taking time to develop, as with induction (Guengerich, 1997). Our data show the inhibition of pooled HLM, RLM, MLM, and MLM induced with DEET, phenobarbital, or 3-methylcholanthrene, wherein conversion of DEET to its metabolites, BALC and ET, decreased significantly in the presence of chlorpyrifos alone or in combination of any other tested compound.

In summary, the present investigation has demonstrated that human liver microsomes appear to have generally lower activities for DEET metabolism than those from rodent livers. A screen of human P450 isoforms demonstrated that different sets of isoforms are responsible for the production of each metabolite (BALC and ET). Individuals with varying levels of activities of these human P450 isoforms, regardless of gender, are more or less active in their metabolism of DEET. DEET induction studies, conducted in mice, demonstrate that exposure could result in the induction of CYP2Bs, resulting in potential interactions with other chemicals such as chlorpyrifos. MLM from DEET-treated mice metabolized chlorpyrifos more readily to chlorpyrifos-oxon, a potent anticholinesterase, than control MLM. Preincubation of chlorpyrifos alone with CYP2B6 completely inhibited the metabolism of DEET, whereas preincubation of microsomes with chlorpyrifos, permethrin, and pyridostigmine bromide alone or in combinations may lead to either stimulation or inhibition of DEET metabolism.

References

- Abou-Donia MB, Goldstein LB, Jones KH, Abdel-Rahman AA, Damodaran TV, Dechkovskaia AM, Bullman SL, Amir BE, and Khan WA (2001) Locomotor and sensorimotor performance deficit in rats following exposure to pyridostigmine bromide, DEET, and permethrin, alone and in combination. *Toxicol Sci* **60**:305–314.
- Bradford MM (1976) A rapid and sensitive method for the quantitation of microgram quantities of protein utilizing the principle of protein-dye binding. *Anal Biochem* **72**:248–254.
- Burke MD and Mayer RT (1974) Ethoxyresorufin: direct fluorometric assay of a microsomal O-dealkylation which is preferentially inducible by 3-methylcholanthrene. *Drug Metab Dispos* **2**:583–588.
- Butler AM and Murray M (1997) Biotransformation of parathion in human liver: participation of CYP3A4 and its inactivation during microsomal parathion oxidation. *J Pharmacol Exp Ther* **280**:966–973.
- Chaney LA, Moss J, Mazingo J, and Hume A (1997) Toxic interactions between pyridostigmine bromide (PB), *N,N*-diethyl-*m*-toluamide (DEET), adrenergic agents and caffeine. *Toxicologist* **36**:21.
- Chaney LA, Rockhold RW, Wineman RW, and Hume AS (1999) Anticonvulsant-resistant seizures following pyridostigmine bromide (PB) and *N,N*-diethyl-*m*-toluamide (DEET). *Toxicol Sci* **49**:306–311.
- Constantino L and Iley J (1999) Microsomal metabolism of *N,N*-diethyl-*m*-toluamide (DEET, DET): the extended network of metabolites. *Xenobiotica* **29**:409–416.
- Cook JC and Hodgson E (1983) Induction of cytochrome P-450 by methylenedioxyphenyl compounds: importance of the methylene carbon. *Toxicol Appl Pharmacol* **68**:131–139.
- Fabrizi L, Gemma S, Testai E, and Vittozzi L (1999) Identification of the cytochrome P450 isoenzymes involved in the metabolism of diazinon in the rat liver. *J Biochem Mol Toxicol* **13**:53–61.
- Guengerich FP (1997) Role of cytochrome P450 enzymes in drug-drug interactions. *Adv Pharmacol* **43**:7–35.
- Levi PE, Hollingworth RM, and Hodgson E (1988) Differences in oxidative dearylation and desulfuration of fenitrothion by cytochrome P-450 isozymes and in the subsequent inhibition of monooxygenase activity. *Pest Biochem Physiol* **32**:224–231.
- Lubet RA, Mary RT, Cameron JW, Nims RW, Burke MD, Wolff T, and Guengerich FP (1985) Dealkylation of pentoxifyresorufin: a rapid and sensitive assay for measuring induction of cytochrome(s) P-450 by phenobarbital and other xenobiotics in the rat. *Arch Biochem Biophys* **283**:43–48.
- Nerurkar PV, Park SS, Thomas PE, Nims RW, and Lubet RA (1993) Methoxyresorufin and benzyloxyresorufin: substrates preferentially metabolized by cytochrome P4501A2 and 2B, respectively, in the rat and mouse. *Biochem Pharmacol* **46**:933–943.
- Omura T and Sato R (1964) The carbon-monoxide binding pigment of liver microsomes. *J Biol Chem* **239**:2370–2378.
- Pohl RA and Fouts JR (1980) A rapid method for assaying the metabolism of 7-ethoxyresorufin by microsomal subcellular fractions. *Anal Biochem* **107**:150–155.
- Qui H, Jun HW, and McCall JW (1998) Pharmacokinetics, formulation, and safety of insect repellent *N,N*-diethyl-3-methylbenzamide (DEET): a review. *J Am Mosquito Control Assoc* **14**:12–27.
- Robbins PJ and Cherniack MC (1986) Review of the biodistribution and toxicity of the insect repellent, *N,N*-diethyl-*m*-toluamide. *J Toxicol Environ Health* **18**:503–525.
- SAS (1989) *JMP User's Guide*. SAS Institute, Cary, NC.
- Selim S, Hartnagel RE Jr, Osimitz TG, Garbriel KL, and Schoenig GP (1995) Absorption, metabolism and excretion of *N,N*-diethyl-*m*-toluamide following dermal application to human volunteers. *Fund Appl Toxicol* **25**:95–100.
- Schoenig GP, Hartnagel RE Jr, Osimitz TG, and Llanso S (1996) Absorption, distribution, metabolism, and excretion of *N,N*-diethyl-*m*-toluamide in the rat. *Drug Metab Dispos* **24**:156–163.
- Schoenig GP, Osimitz TG, Gabriel KL, Hartnagel R, Gill MW, and Goldenthal EI (1999) Evaluation of the chronic toxicity and oncogenicity of *N,N*-diethyl-*m*-toluamide (DEET.) *Toxicol Sci* **47**:99–109.
- Szklarz GD and Halpert JR (1998) Molecular basis of P450 inhibition and activation: implications for drug development and drug therapy. *Drug Metab Dispos* **26**:1179–1184.
- Tang J, Cao Y, Rose RL, Brimfield AA, Dai D, Goldstein JA, and Hodgson E (2001) Metabolism of chlorpyrifos by human cytochrome P450 isoforms and human, mouse and rat liver microsomes. *Drug Metab Dispos* **29**:1201–1204.
- Taylor WG (1986) Metabolism of *N,N*-diethyl-*meta*-toluamide by rat liver microsomes. *Drug Metab Dispos* **14**:532–539.
- Taylor WG and Spooner RW (1990) Identification and gas chromatographic determination of some carboxylic acid metabolites of *N,N*-diethyl-*m*-toluamide in rat urine. *J Agric Food Chem* **38**:1422–1427.
- Veltri JC, Osimitz TG, Bradford DC, and Page BC (1994) Retrospective analysis of calls to poison control centers resulting from exposure to the insect repellent *N,N*-diethyl-*m*-toluamide (DEET) from 1985 to 1989. *Clin Toxicol* **32**:1–16.
- Yeung JM and Taylor WG (1988) Metabolism of *N,N*-diethyl-*m*-toluamide (DEET) by rat liver microsomes from male and female rats. *Drug Metab Dispos* **16**:600–604.

INHIBITION AND ACTIVATION OF THE HUMAN LIVER MICROSOMAL AND HUMAN CYTOCHROME P450 3A4 METABOLISM OF TESTOSTERONE BY DEPLOYMENT-RELATED CHEMICALS

KHAWJA A. USMANI, RANDY L. ROSE, AND ERNEST HODGSON

Department of Environmental and Molecular Toxicology, North Carolina State University, Raleigh, North Carolina

(Received October 16, 2002; accepted December 18, 2002)

This article is available online at <http://dmd.aspetjournals.org>

ABSTRACT:

Cytochrome P450 (P450) enzymes are major catalysts involved in the metabolism of xenobiotics and endogenous substrates such as testosterone (TST). Major TST metabolites formed by human liver microsomes include 6 β -hydroxytestosterone (6 β -OHTST), 2 β -hydroxytestosterone (2 β -OHTST), and 15 β -hydroxytestosterone (15 β -OHTST). A screen of 16 cDNA-expressed human P450 isoforms demonstrated that 94% of all TST metabolites are produced by members of the CYP3A subfamily with 6 β -OHTST accounting for 86% of all TST metabolites. Similar K_m values were observed for production of 6 β -, 2 β -, and 15 β -OHTST with human liver microsomes (HLM) and CYP3A4. However, V_{max} and CL_{int} were significantly higher for 6 β -OHTST than 2 β -OHTST (~18-fold) and 15 β -OHTST (~40-fold). Preincubation of HLM with a variety of ligands, including chemicals used in military deployments, resulted in varying levels of inhibition or activation of TST metabolism. The great-

est inhibition of TST metabolism in HLM was following preincubation with organophosphorus compounds, including chlorpyrifos, phorate, and fonofos, with up to 80% inhibition noticed for several metabolites including 6 β -OHTST. Preincubation of CYP3A4 with chlorpyrifos, but not chlorpyrifos-oxon, resulted in 98% inhibition of TST metabolism. Phorate and fonofos also inhibited the production of most primary metabolites of CYP3A4. Kinetic analysis indicated that chlorpyrifos was one of the most potent inhibitors of major TST metabolites followed by fonofos and phorate. Chlorpyrifos, fonofos, and phorate inhibited major TST metabolites non-competitively and irreversibly. Conversely, preincubation of CYP3A4 with pyridostigmine bromide increased metabolite levels of 6 β -OHTST and 2 β -OHTST. Preincubation of human aromatase (CYP19) with the test chemicals had no effect on the production of the endogenous estrogen, 17 β -estradiol.

The cytochrome P450 (P450¹) monooxygenase system is comprised of a superfamily of heme-containing enzymes, expressed in many mammalian tissues with the highest levels found in liver, and capable of catalyzing the metabolism of a wide range of both endogenous and exogenous substrates (Nelson et al., 1996). Human CYP3A4 is one of the most important and most abundant drug-metabolizing P450 isoforms in human liver microsomes and accounts for approximately 40% of the total P450 in human liver microsomes (Lehmann et al., 1998). CYP3A4 not only metabolizes xenobiotics but is also responsible for the metabolism of endogenous compounds, such as steroid hormones. Human CYP3A4 plays an important role in the metabolism of testosterone (TST), androstenedione (AD), and progesterone (Waxman et al., 1988). Direct and indirect approaches

have been employed to show that isoforms belonging to the CYP3A subfamily are the major contributors to 6 β -hydroxylation of testosterone as well as the production of several minor metabolites (Waxman et al., 1988, 1991; Yamazaki and Shimada, 1997).

In the human male, TST is the major circulating androgen. TST is essential for the development and maintenance of specific reproductive tissues as well as for other characteristic male properties such as control of spermatogenesis, retention of nitrogen, promotion of muscle strength, hair growth, bone density, and many aspects of sexually dimorphic behavior (Nieschlag and Behre, 1998; Wilson et al., 1998). Maintaining hormonal balance relies upon a number of variables including rate of hormone synthesis, interactions among hormones, and rates of secretion, transport, and metabolism. P450s are a major controlling element in the maintenance of proper steroid hormone levels in mammalian systems. Exposure to foreign compounds can exert changes in endocrine function both directly (hormone agonists or antagonists) or indirectly (altering circulating levels of hormones by influencing rates of hormone synthesis or metabolism) that can severely affect steroid hormone action (Wilson and LeBlanc, 1998). Steroids such as TST are hydroxylated by P450 in a regioselective and stereoselective manner (Waxman et al., 1988). It follows that perturbation of the P450 system by xenobiotics may in turn affect the subsequent metabolism and disposition of TST. Perturbations in TST metabolism may affect levels of circulating TST with possible reproductive and other consequences, including further modulation of the expression of some P450 proteins.

This research was supported by US Army Cooperative Agreement DAMD 17-00-2-0008. Part of this study will be presented at the 11th North American ISSX meeting in Orlando, 2002.

¹ Abbreviations used are: P450, cytochrome P450; TST, testosterone; AD, androstenedione; DEET, *N,N*-diethyl-*m*-toluamide; KTST, ketotestosterone; OHAD, hydroxyandrostenedione; HPLC, high-performance liquid chromatography; HLM, human liver microsomes; OHTST, hydroxytestosterone; K_i , inhibition constant; b_5 , cytochrome b_5 .

Address correspondence to: Ernest Hodgson, Department of Environmental and Molecular Toxicology, Box 7633, North Carolina State University, Raleigh, NC 27695. E-mail: ernest_hodgson@ncsu.edu

Following the Gulf War some veterans reported illnesses which may have been the result of chemical exposures. Some studies of these veterans have concluded that significant correlations between perceived illnesses and chemical use exist (Haley and Kurt, 1997). The reported chemical exposures included the insect repellent *N,N*-diethyl-*m*-toluamide (DEET), insecticides such as permethrin and chlorpyrifos to protect against insect borne diseases and the neuroprotective agent pyridostigmine bromide to protect against possible nerve gas attack. It has been reported that chlorpyrifos and DEET are metabolized by human P450s (Tang et al., 2001; Usmani et al., 2002) and that interactions of Gulf War related chemicals can inhibit or induce the P450s involved in their metabolism (Usmani et al., 2002). Other studies have reported that interaction of Gulf War related chemicals could produce greater than additive toxicity in rats and mice (Chaney et al., 1997; McCain et al., 1997), increased neurotoxicity in hens associated with increased inhibition of brain acetylcholinesterase and Neurotoxicity Target Esterase (Abou-Donia et al., 1996a,b), and neurobehavioral deficit associated with significant inhibition of brainstem acetylcholinesterase activities in rats (Abou-Donia et al., 2001). However, no studies have been carried out to examine the induction or inhibition potential of these or related compounds on human P450-mediated metabolism of steroid hormones, such as TST. An understanding of how Gulf War related chemicals affects the metabolism of TST could aid in the evaluation of the possible role that these chemicals may play in deployment-related illnesses.

The main objectives of present study were to identify human liver P450 isoforms responsible for TST metabolism and the products of their activity using an improved HPLC method, to study the effects of various deployment-related chemicals on the metabolism of TST using HLM and CYP3A4, and to study the effects of the test compounds on human aromatase (CYP19).

Materials and Methods

Chemicals. DEET, chlorpyrifos, chlorpyrifos-oxon, phorate, fonofos, deltamethrin, fipronil, imidacloprid, and permethrin (isomeric mix 78% *trans*-20% *cis*) were purchased from Chem Service (West Chester, PA). Pyridostigmine bromide was purchased from Roche Diagnostics (Indianapolis, IN). 6 α -, 15 β -, 15 α -, 7 α -, 6 β -, 16 α -, 16 β -, 2 α -, 2 β -, 11 β -OHTST, 11-ketotestosterone (11-KTST), 11 β -hydroxyandrostenedione (11 β -OHAD), AD, and 4-hydroxyandrostenedione (4-OHAD) were purchased from Steraloids (Newport, RI). HPLC grade water, methanol, acetonitrile, and tetrahydrofuran were purchased from Fisher Scientific (Pittsburgh, PA). TST, 17 β -estradiol, and all other chemicals were purchased, if not specified, from Sigma-Aldrich (St. Louis, MO).

Human Liver Microsomes and Human P450 Isoforms. Pooled human liver microsomes (HLM) (pooled from 21 donors) and human P450 isoforms expressed in baculovirus infected insect cells (Sf9) (BTI-TN-5B1-4), CYP1A1, 1A2, 2B6, 3A4, 3A5, 3A7, 4A11, 2B6, 2C8, 2A6, 2C9*1 (Arg₁₁₄), 2C9*2 (Cys₁₄₄), 2C9*3 (Leu₃₅₉), 2C18, 2C19, 2D6*1 (Val₃₇₄), 2E1, and human aromatase (CYP19) were purchased from BD Gentest Corporation.

In Vitro TST Metabolism. Metabolic activity assays for human P450 isoforms were performed by incubation of TST (final concentrations, 250 μ M) with an NADPH-regenerating system (0.25 mM NADP, 2.5 mM glucose 6-phosphate, and 2 U/ml glucose-6-phosphate dehydrogenase) in specific buffers recommended by the supplier (BD Gentest Corporation). For CYP1A1, 1A2, 2E1, 2C8, 2D6*1 (Val₃₇₄), 3A4, 3A5, 3A7, 2B6, 2C18, 2C19, and an insect cell control, a 100 mM potassium phosphate buffer with 3.3 mM MgCl₂ (pH 7.4) was used. For 2C9*1 (Arg₁₁₄), 2C9*2 (Cys₁₄₄), 2C9*3 (Leu₃₅₉), 4A11, and 2A6, a 100 mM Tris-HCl buffer with 3.3 mM MgCl₂ (pH 7.5) was used. After preincubation at 37°C for 5 min, the reactions were initiated by the addition of ice-cold P450 isoforms (final P450 contents 50 pmol/ml) for 30 min at 37°C. The controls were performed under identical conditions with the insect cell control.

Enzyme kinetic assays for HLM and CYP3A4 were performed by incubation of serial concentrations of TST (final concentrations, 9.375–500 μ M) with

HLM (final protein concentration, 1 mg/ml) or CYP3A4 (final concentration, 50 pmol/ml) in 100 mM potassium phosphate buffer (pH 7.4 at 37°C) containing 3.3 mM MgCl₂. After preincubation at 37°C for 5 min, the reactions were initiated by the addition of ice-cold HLM or CYP3A4 for 10 min.

The effects of test chemicals on TST metabolism were examined in HLM and CYP3A4 after preincubation with test compounds. The HLM (final protein concentration, 1 mg/ml) or CYP3A4 (final concentration, 50 pmol/ml) were incubated with individual test compounds (final concentration, 100 μ M), NADPH-generating system, and 100 mM potassium phosphate buffer with 3.3 mM MgCl₂, pH 7.4, for 5 min at 37°C before adding TST (final concentration, 250 μ M).

Range finding assays were conducted for chlorpyrifos, fonofos, and phorate inhibition of TST major metabolites. Varying concentrations of chlorpyrifos, fonofos, and phorate (0.5–100 μ M) were incubated with CYP3A4 (final concentration, 50 pmol/ml), NADPH-generating system, and 100 mM potassium phosphate buffer with 3.3 mM MgCl₂, pH 7.4, for 5 min at 37°C before adding TST (final concentration, 100 μ M). Reactions were terminated and analyzed as described above. With selected concentration levels based on the range finding assay, the mode of chlorpyrifos, fonofos, and phorate inhibition on TST major metabolites was investigated. For Michaelis-Menten plots, chlorpyrifos (2 μ M), fonofos (5 μ M), and phorate (30 μ M) were incubated with CYP3A4 (final concentration, 50 pmol/ml), NADPH-generating system, and 100 mM potassium phosphate buffer with 3.3 mM MgCl₂, pH 7.4, for 5 min at 37°C before adding TST (final concentration, 9.375–500 μ M).

To demonstrate whether chlorpyrifos inhibition is reversible or irreversible, incubations with and without chlorpyrifos (2 μ M) were conducted with varying concentrations of CYP3A4 (0.78–6.25 pmol), NADPH-generating system, and 100 mM potassium phosphate buffer with 3.3 mM MgCl₂, pH 7.4, for 5 min at 37°C before adding TST (final concentration, 100 μ M).

To determine (inhibition constant) K_i values, chlorpyrifos (1–8 μ M), fonofos (1–25 μ M), and phorate (10–100 μ M) were incubated for 5 min at 37°C with CYP3A4 (final concentration, 50 pmol/ml), NADPH-generating system, and 100 mM potassium phosphate buffer with 3.3 mM MgCl₂, pH 7.4, prior to adding TST (final concentrations, 50, 100, or 200 μ M). K_i values were calculated from Dixon plots.

Since cytochrome b_5 (b_5) is not coexpressed with CYP3A5 as supplied by BD Biosciences (San Jose, CA), a comparison of CYP3A5 metabolism of TST was made using 10 pmol 3A5 with and without addition of 20 pmol b_5 .

Human aromatase (CYP19) catalyzes the conversion of TST to estradiol. To study the effects of the test chemicals on this conversion, test compounds (final concentration, 200 μ M) or a well known competitive inhibitor, 4-OHAD (final concentration, 200 μ M) were incubated with CYP19 (final concentration, 50 pmol/ml), NADPH-generating system, and 100 mM potassium phosphate buffer with 3.3 mM MgCl₂, pH 7.4, for 5 min at 37°C before adding TST (final concentration, 100 μ M). The reaction was terminated after an additional 10 min, and supernatant was analyzed for 17 β -estradiol concentration by HPLC.

All assays were conducted in triplicate. All reactions were terminated by the addition of an equal volume of methanol and vortexing. After 10-min centrif-

TABLE 1

HPLC retention times for testosterone and hydroxylated testosterone metabolites

Common Name	Chemical Name	Retention Time <i>min</i>
6 α -Hydroxytestosterone	4-Androsten-6 α ,17 β -diol-3-one	14.38
15 β -Hydroxytestosterone	4-Androsten-15 β ,17 β -diol-3-one	15.11
15 α -Hydroxytestosterone	4-Androsten-15 α ,17 β -diol-3-one	15.53
7 α -Hydroxytestosterone	4-Androsten-7 α ,17 β -diol-3-one	15.81
6 β -Hydroxytestosterone	4-Androsten-6 β ,17 β -diol-3-one	16.25
16 α -Hydroxytestosterone	4-Androsten-16 α ,17 β -diol-3-one	17.43
11-Ketotestosterone	4-Androsten-17 β -ol-3,11-dione	18.24
16 β -Hydroxytestosterone	4-Androsten-16 β ,17 β -diol-3-one	19.34
11 β -Hydroxyandrostenedione	4-Androsten-11 β -ol-3,17-dione	19.68
2 α -Hydroxytestosterone	4-Androsten-2 α ,17 β -diol-3-one	20.68
2 β -Hydroxytestosterone	4-Androsten-2 β ,17 β -diol-3-one	21.55
11 β -Hydroxytestosterone	4-Androsten-11 β ,17 β -diol-3-one	21.86
Androstenedione	4-Androsten-3,17-dione	24.92
4-Hydroxyandrostenedione	4-Androsten-4-ol-3,17-dione	27.20
Testosterone	4-Androsten-17 β -ol-3-one	28.90

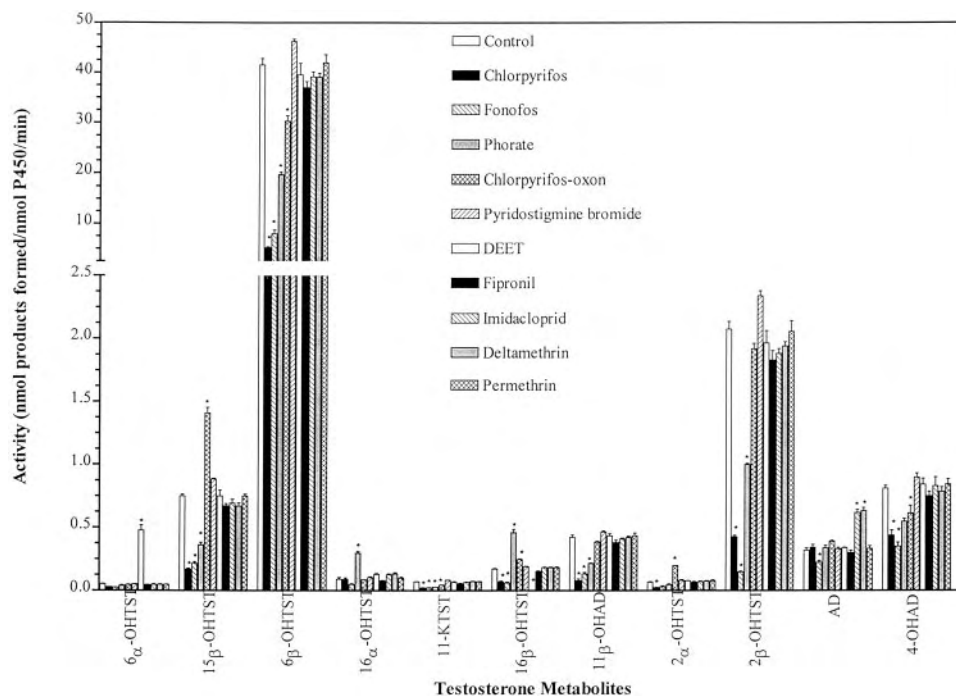


FIG. 1. Effects of deployment-related chemicals on the rate of testosterone metabolism by pooled human liver microsomes.

Specific activities were expressed as nanomole products formed per nanomole P450 per minute. *, statistically significantly different when compared with respective control ($P < 0.01$).

ugation at 15,000 rpm in a microcentrifuge, the supernatants were analyzed for TST metabolite concentrations by HPLC. The protein concentrations and incubation times used in the assays were found to be in the linear range in preliminary experiments. No metabolites were detected when incubations were carried out in the absence of an NADPH-generating system.

Analysis of Metabolites by HPLC. Metabolites were analyzed using a Shimadzu HPLC system (Kyoto, Japan). The Shimadzu HPLC system (Kyoto, Japan) used in this study consisted of one pump (LC-10AT VP), a four-position solvent selection proportioning valve (FCV-10AL VP), a degasser (DUG-14A), a Shimadzu autoinjector (SIL-10AD VP), and a Shimadzu UV/VIS detector (SPD-10AV VP). All system components were controlled through the Shimadzu powerline firmware. Data were collected via a Shimadzu system controller (SCL-10A VP) and analyzed using CLASS-VP 4.3 software. A reverse phase HPLC method was modified based on the HPLC method of Purdon and Lehman-McKeeman (1997), for the separation of TST and its potential metabolites. The mobile phase for pump A was 5% tetrahydrofuran, 95% water, for pump B 100% methanol. A gradient system was employed in the following manner: 0 to 1 min (30% B), 1 to 10 min (30–60%

B), 10 to 22 min (60–65% B), 22 to 28 min (65–80% B), 28 to 30 min (80–90% B), 30 to 32 min (90% B), 32 to 34 min (90–30% B), and 34 to 36 min (30% B). The flow rate was 0.5 ml/min. Metabolites were separated by a Prodigy column [Prodigy 3 μ , 150 \times 4.6 mm, ODS (3), 100A; Phenomenex, Rancho Palos Verdes, CA] and detected at 247 nm. A summary of the retention times of TST and 14 TST metabolites are presented in Table 1. The limits of detection for most of TST metabolites were approximately 0.04 μ M except for 6 β -OHTST (0.15 μ M) and 4-OHAD (0.30 μ M). Standards of TST metabolites were made in methanol and 50- μ l standard or sample injected on HPLC. Concentrations of metabolites were obtained by extrapolation of peak height from a standard curve. Percentages of individual metabolites are expressed on the basis of the total metabolites produced by the isoform or preparation in question.

For 17 β -estradiol, the mobile phase was 60% H₂O and 40% acetonitrile. TST and 17 β -estradiol were eluted isocratically at a flow rate of 1.0 ml/min for 15 min, separated by a Prodigy column [Prodigy 3 μ , 150 \times 4.6 mm, ODS (3), 100A, Phenomenex, Rancho Palos Verdes, CA] and detected at 200 nm. The retention time of 17 β -estradiol and TST was 10.4 and 11.3 min, respectively.

TABLE 2

Testosterone hydroxylation by human cytochrome P450 isoforms expressed in baculovirus-infected insect cells (nanomoles per nanomole isoforms per minute)

Isoforms	6 α -OHTST	15 β -OHTST	6 β -OHTST	16 α -OHTST	11-KT	16 β -OHTST	11 β -OHAD	2 α -OHTST	2 β -OHTST	AD	4-OHAD
1A1	NDA	NDA	3.01 \pm 0.14	NDA	NDA	NDA	NDA	NDA	NDA	NDA	NDA
1A2	NDA	NDA	0.64 \pm 0.02	NDA	NDA	NDA	NDA	NDA	NDA	NDA	NDA
2A6	0.05 \pm 0.00	0.14 \pm 0.01	NDA	NDA	NDA	NDA	NDA	NDA	NDA	0.53 \pm 0.05	NDA
3A4	0.22 \pm 0.02	3.18 \pm 0.11	157.7 \pm 6.00	NDA	1.04 \pm 0.04	0.44 \pm 0.01	1.70 \pm 0.02	0.19 \pm 0.01	7.05 \pm 0.23	0.27 \pm 0.01	2.23 \pm 0.24
3A5	0.11 \pm 0.01	NDA	12.4 \pm 1.57	NDA	NDA	0.08 \pm 0.01	0.14 \pm 0.02	NDA	0.74 \pm 0.10	NDA	NDA
3A7	0.09 \pm 0.01	0.15 \pm 0.02	3.89 \pm 0.34	NDA	0.15 \pm 0.02	0.27 \pm 0.02	0.79 \pm 0.05	3.05 \pm 0.24	0.61 \pm 0.06	0.13 \pm 0.00	NDA
4A11	NDA	NDA	NDA	NDA	NDA	NDA	NDA	NDA	NDA	0.62 \pm 0.01	NDA
2B6	0.05 \pm 0.01	NDA	0.23 \pm 0.01	0.17 \pm 0.00	0.13 \pm 0.03	0.61 \pm 0.12	NDA	NDA	0.03 \pm 0.00	NDA	NDA
2C8	NDA	NDA	NDA	0.38 \pm 0.03	0.14 \pm 0.03	NDA	NDA	NDA	NDA	NDA	NDA
2C9*1	NDA	NDA	NDA	NDA	NDA	0.18 \pm 0.01	NDA	NDA	NDA	NDA	NDA
2C9*2	NDA	NDA	NDA	NDA	NDA	0.11 \pm 0.02	NDA	NDA	NDA	NDA	NDA
2C18	0.05 \pm 0.01	NDA	NDA	NDA	NDA	NDA	NDA	NDA	NDA	NDA	NDA
2C19	0.05 \pm 0.00	NDA	0.43 \pm 0.04	0.15 \pm 0.01	NDA	0.32 \pm 0.05	NDA	NDA	0.04 \pm 0.01	2.53 \pm 0.28	NDA
2E1	NDA	NDA	NDA	NDA	0.15 \pm 0.03	NDA	NDA	NDA	NDA	NDA	NDA
2D6*1	NDA	NDA	1.49 \pm 0.02	NDA	NDA	NDA	NDA	NDA	0.06 \pm 0.00	1.40 \pm 0.08	NDA

NDA, no detectable activity; no metabolite was formed with 2C9*3.

TABLE 3

Kinetic parameters for the production of major testosterone metabolites by human liver microsomes and CYP3A4

Means in the same column followed by the same letter are not significantly different ($P < 0.01$). Values are the mean \pm S.E.M. ($n = 3$).

	Human Liver Microsomes				CYP3A4			
	K_m	V_{max}	CL_{int}	R^2	K_m	V_{max}	CL_{int}	R^2
	μM	nmol/mg protein/min	$\mu l/mg$ protein/min		μM	nmol/nmol 3A4/min	$\mu l/nmol$ 3A4/min	
6 β -OHTST	120.4 \pm 19.4 ^a	36.3 \pm 2.3 ^a	300.0 ^a	0.94	107.7 \pm 12.5 ^a	284.8 \pm 12.5 ^a	2600.0 ^a	0.97
2 β -OHTST	119.2 \pm 18.0 ^a	2.0 \pm 0.1 ^b	20.0 ^b	0.95	122.8 \pm 14.1 ^a	15.7 \pm 0.7 ^b	130.0 ^b	0.98
15 β -OHTST	138.9 \pm 28.2 ^a	0.8 \pm 0.1 ^c	6.0 ^c	0.91	108.7 \pm 16.4 ^a	7.1 \pm 0.4 ^c	70.0 ^c	0.96

The limit of detection for 17 β -estradiol was approximately 0.10 μM . Concentrations of metabolites were obtained by extrapolation of peak height from a standard curve.

Data Analysis and Statistics. The apparent K_m and V_{max} parameters were calculated using nonlinear regression analysis program (Prism, GraphPad software Inc., San Diego, CA), and the K_i values were estimated by nonlinear regression analysis from the Dixon plot (Segel, 1975) using SigmaPlot Enzyme Kinetics Module (Chicago, IL). Significant differences between data sets were determined by one-way analysis of variance, and multiple comparisons were performed with the Dunnett's method using a JMP 4.0.2, SAS program (SAS, 1989).

Results

Four major metabolites were formed after incubation of TST with pooled HLM: 6 β -, 2 β -, 15 β OHTST, and 4-OHAD as well as seven minor metabolites (Fig. 1). Among 16 different human P450 isoforms screened, only 2C9*3 (Leu₃₅₉) had no detectable activity toward TST (Table 2). All other P450 isoforms were active in generating one or more than one TST metabolites, although the extent of metabolism and the ratios of metabolites varied widely among isoforms. In this comparison of metabolite production by equal quantities of each isoform, CYP3A4, 3A5, and 3A7 were most active in TST metabo-

lism among all the P450 isoforms tested (93.5% of the metabolites produced by all isoforms). Among members of the CYP3A subfamily, CYP3A4 produced the highest amount of total TST metabolites (88.5%) compared with 3A5 (6.9%) and 3A7 (4.6%). 6 β -OHTST, the most prominent TST metabolite, mainly produced by the CYP3A subfamily, accounts for 86% of all TST metabolites. Among the CYP3A subfamily, CYP3A4 produced the highest amount of 6 β -OHTST (90.6%) compared with 3A5 (7.1%) and 3A7 (2.2%). Other major TST metabolites formed by CYP3A4 were 15 β -, 2 β -OHTST, and 4-OHAD, whereas 6 α -, 16 β -, 11 β -, 2 α -OHTST, 11-KTST, and AD were minor metabolites. Among the P450 isoforms tested, CYP3A5 and 3A7 were significantly more important in forming the major TST metabolites than most of the others, but their activity was 10- to 20-fold less than that of CYP3A4. Interestingly, CYP3A7 produced 16 times more 2 α -OHTST than CYP3A4. CYP1A1 is involved in the oxidation of TST at the 6 β -position (3.0 nmol/nmol isoform/min), whereas CYP1A2 oxidized TST poorly at the 6 β -position (0.6 nmol/nmol isoform/min). As can be observed in Table 2, the other P450 isoforms tested generally produced small amounts of one or more TST metabolites. CYP2C19 metabolized TST to AD more actively

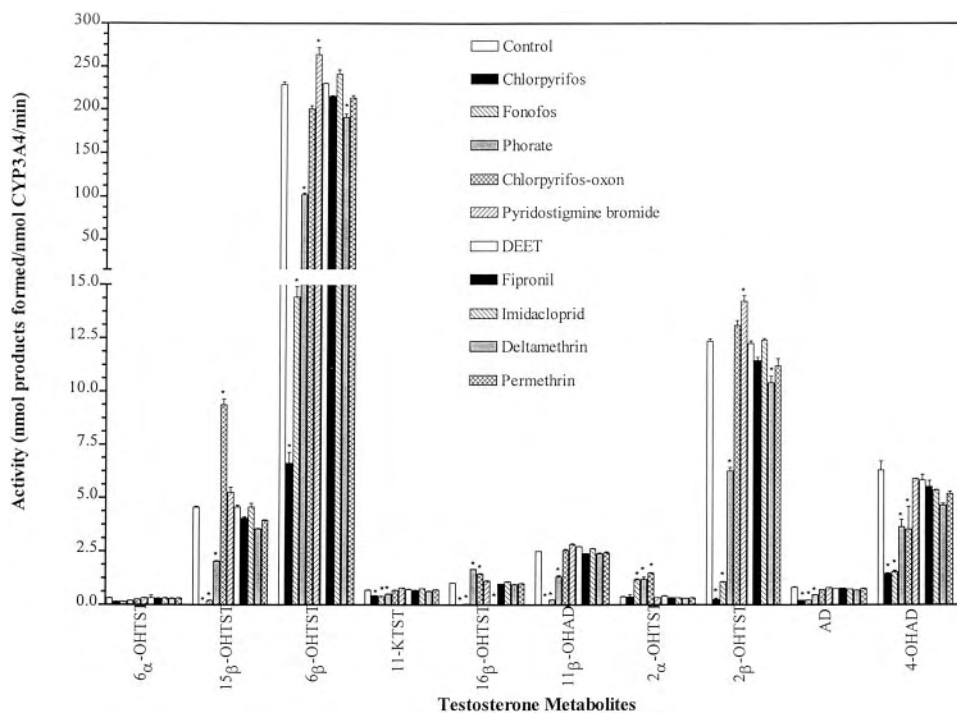


FIG. 2. Effects of deployment-related chemicals on the rate of testosterone metabolism by CYP3A4.

Specific activities were expressed as nanomole products formed per nanomole CYP3A4 per minute. *, statistically significantly different when compared with respective control ($P < 0.01$).

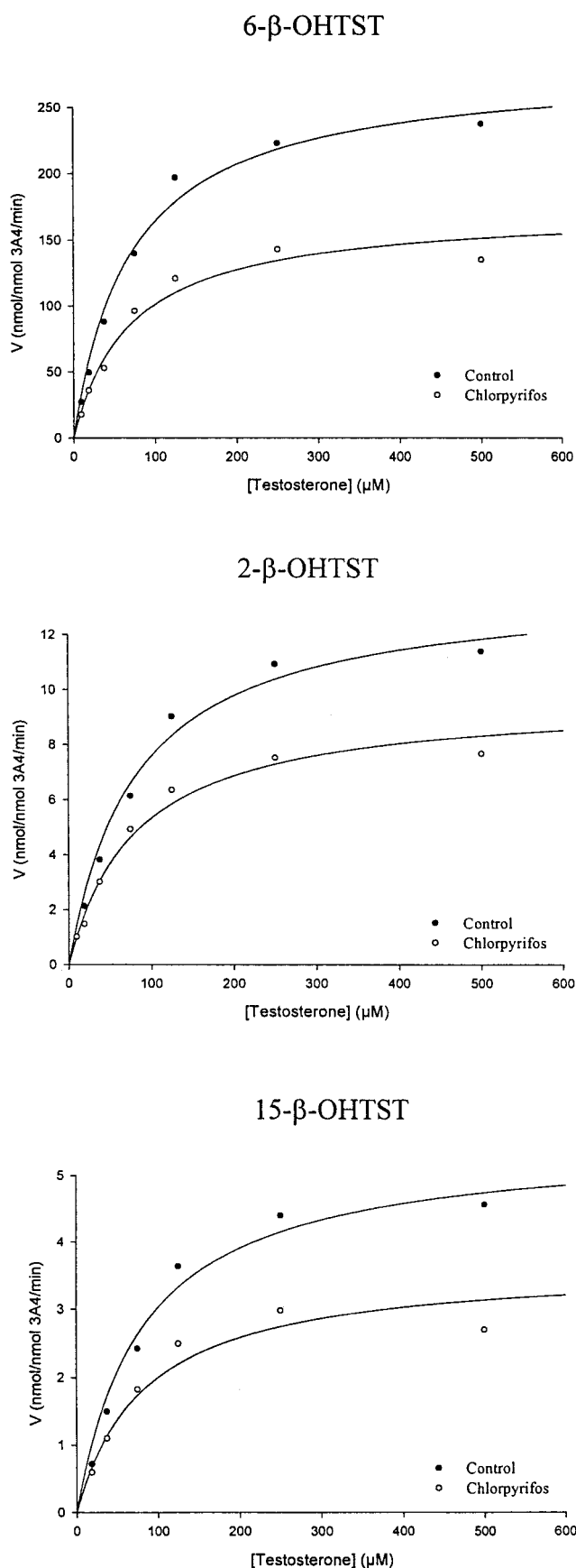


Fig. 3. Representative Michaelis-Menten plots for the inhibition of CYP3A4-mediated testosterone hydroxylation by chlorpyrifos (2 μM).

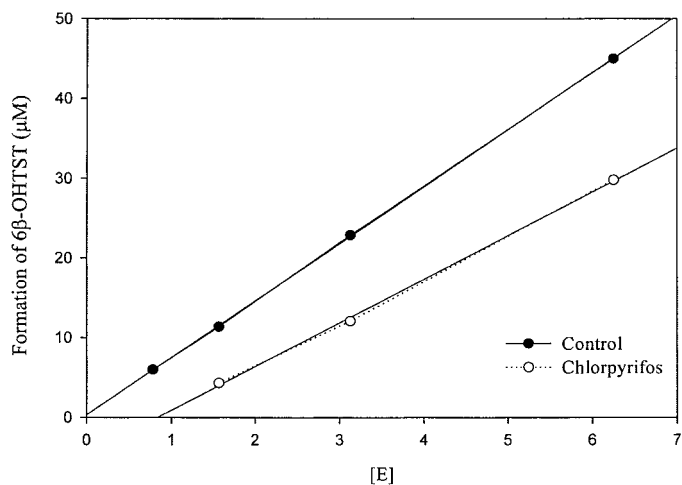


Fig. 4. Representative plot of V_{max} versus amount of enzyme (CYP3A4) added to distinguish between a reversible and an irreversible noncompetitive inhibitor chlorpyrifos (2 μM).

than any other isoform tested, whereas it catalyzed the formation of 6α -, 6β -, 16α -, 16β -, and 2β -OHTST poorly.

HLM and CYP3A4 displayed similar K_m values for 6β -, 2β -, and 15β -OHTST (Table 3). V_{max} and intrinsic clearance rate [Cl_{int} (V_{max}/K_m)] for 6β -OHTST was significantly higher than 2β -OHTST (~ 18 -fold) and 15β -OHTST (~ 40 -fold), respectively.

The effects of various deployment-related chemicals on TST metabolism were investigated by preincubating them with pooled HLM (Fig. 1). Preincubation of pooled HLM with chlorpyrifos, phorate, and fonofos resulted in significant inhibition of 6β -, 2β -, 15β -OHTST, 11 -KTST, 11β -OHAD, and 4 -OHAD. Preincubation of pooled HLM with DEET, chlorpyrifos-oxon, phorate, imidacloprid, and deltamethrin in some cases caused small but significant increases in the production of some TST metabolites by HLM.

Preincubation of CYP3A4 with a variety of chemicals resulted in varying levels of activation and inhibition of TST metabolism (Fig. 2). The greatest inhibition of TST metabolism was observed for the organophosphorus compound chlorpyrifos with up to 98% inhibition of major (6β -, 2β -, 15β -OHTST, and 4 -OHAD) and several minor (11 -KTST, 16β -OHTST, 11β -OHAD, and AD) TST metabolites. However, chlorpyrifos-oxon, an active metabolite of chlorpyrifos, has no inhibitory effect on the major TST metabolites. Two other organophosphorus compounds, phorate and fonofos, also significantly inhibited formation of several TST metabolites including 6β -, 2β -, 15β -OHTST, 11 -KTST, 11β -OHAD, AD, and 4 -OHAD. In contrast, preincubation of CYP3A4 with pyridostigmine bromide resulted in the production of small but significantly greater levels of the 6β - and 2β -OHTST metabolites. Some other TST metabolites were also significantly increased by preincubation of CYP3A4 with chlorpyrifos-oxon, phorate, and fonofos.

To investigate the type of inhibition of CYP3A4 by chlorpyrifos, fonofos, and phorate on major TST metabolites, chlorpyrifos (2 μM), fonofos (5 μM), and phorate (30 μM) were preincubated for 5 min before adding the varying concentrations of TST. Michaelis-Menten plots showed that the V_{max} values were significantly reduced without affecting K_m values, indicative of a noncompetitive inhibition of major TST metabolites by chlorpyrifos (Fig. 3). Similar results were obtained with fonofos and phorate (data were not shown). Further investigation of noncompetitive reversible or nonreversible inhibition data revealed that the inhibition is nonreversible (Fig. 4).

The K_i , an indicator of inhibitor affinity to target enzyme, was calculated by Dixon plot (Table 4; Fig. 5). Chlorpyrifos was the most

TABLE 4

Kinetics parameters for the inhibition of CYP3A4-mediated production of major testosterone metabolites by chlorpyrifos, fonofos, and phorate

Inhibitors	6 β -OHTST		2 β -OHTST		15 β -OHTST	
	K_i	R^2	K_i	R^2	K_i	R^2
Chlorpyrifos	2.0 \pm 0.2	0.99	3.6 \pm 0.3	0.98	3.7 \pm 0.4	0.97
Fonofos	5.8 \pm 0.6	0.98	10.1 \pm 0.7	0.98	6.3 \pm 0.6	0.97
Phorate	34.1 \pm 2.7	0.98	42.9 \pm 4.1	0.98	33.8 \pm 3.6	0.97

potent inhibitor of major TST metabolites with K_i values ranges from 2.0, 3.6, and 3.7 μ M for 6 β -, 2 β -, 15 β -OHTST, respectively. Fonofos was the second best inhibitor with K_i values ranging from 5.8, 10.1, and 6.3 μ M for 6 β -, 2 β -, 15 β -OHTST, respectively. Phorate K_i values ranged from 34.1, 42.9, and 33.8 μ M for 6 β -, 2 β -, 15 β -OHTST, respectively.

We investigated the possibility that b_5 may stimulate CYP3A5 catalytic activity by incubating b_5 (20 pmol) and CYP3A5 (10 pmol), which, in the preparations used, does not have b_5 coexpressed, with 250 μ M of TST for 10 min. Addition of b_5 resulted in a more than 2-fold increase in TST 6 β - and 2 β -OHTST activity.

The possibility that conversion of TST to estradiol, which is catalyzed by aromatase (CYP19), could be inhibited by the test compounds was also investigated. Preincubation of human aromatase (CYP19) with various chemicals (chlorpyrifos, chlorpyrifos-oxon, permethrin, pyridostigmine bromide, DEET, phorate, fonofos, fipronil, imidacloprid, and deltamethrin) had no significant effect on the production of estradiol (data not shown). However, incubation with 4-OHAD, a well known competitive aromatase inhibitor, resulted in 90% inhibition of the aromatase enzyme activity.

Discussion

P450-dependent hydroxylation appears to be a major pathway of oxidative metabolism of TST in mammalian liver. Studies carried out using human P450 isoforms provide further insight into the range of TST hydroxylation reactions that can be catalyzed by human P450 enzymes. Our isoform data corroborates earlier findings (Waxman et al., 1988, 1991; Yamazaki and Shimada, 1997) that CYP3A4 is one of the major isoforms responsible for TST metabolism, and 6 β -OHTST is the major TST metabolite. Greater than 82% of the TST metabolites are formed by CYP3A4, and 87% of the major 6 β -OHTST metabolite is formed by CYP3A4. The mean metabolic intrinsic clearance rates, as estimated by V_{max}/K_m , also indicated that 6 β -OHTST is the major metabolite of TST. Interestingly, CYP3A4 also metabolized TST to 4-OHAD, a potent inhibitor of extrahepatic aromatase (CYP19). It has been reported that 4-OHAD was able to inhibit 90% of the aromatase activity at a concentration of 1 μ M (Mak et al., 1999). The physiological significance or consequence of this reaction is unclear and will require further investigation. Our results indicate that CYP1A1 and 1A2 were able to metabolize TST to 6 β -OHTST, however, activity of CYP1A1 was much higher (4.7-fold) than CYP1A2. Consistent with a previous report (Yamazaki and Shimada, 1997), our data also indicated that CYP2C19 catalyzed oxidation of TST to form AD as a major TST metabolite. However, CYP2C18, which has 81% amino acid sequence identity to CYP2C19, exhibited distinctly poor hydroxylation activity in comparison with CYP2C19. Furthermore, our data indicated that CYP2D6*1, 4A11, and 2A6 metabolized TST to form AD but not as actively as CYP2C19. Guengerich et al. (2002) characterized the affinity of CYP2D6 for testosterone.

Endogenous steroids, such as TST, always exist in vivo, and considerable amounts of these steroids are metabolized by the P450s expressed in the human liver, where foreign compounds are mainly

metabolized. If xenobiotics substantially affect TST metabolism, it may alter the rate of TST metabolism, which may ultimately disrupt TST homeostasis. Preincubation of pooled HLM with organophosphorus compounds, such as chlorpyrifos, phorate, and fonofos, resulted in the extensive inhibition of major and some minor TST

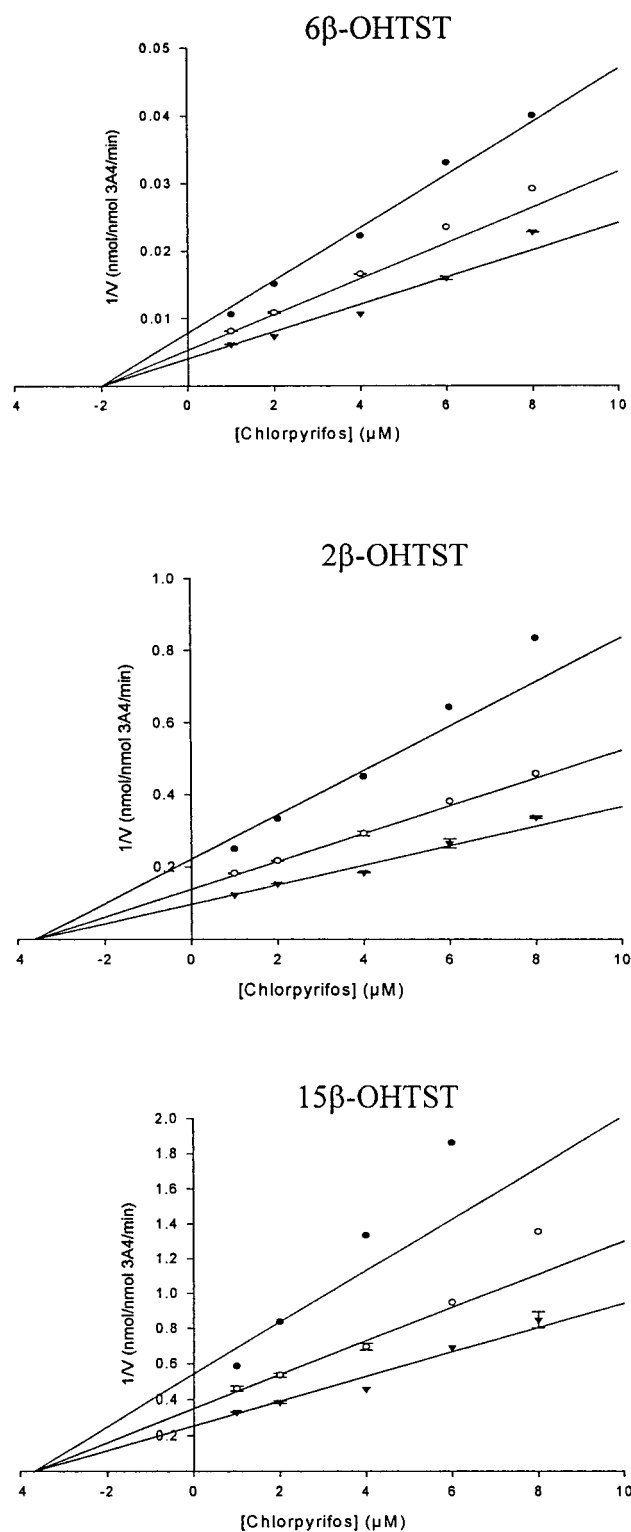


FIG. 5. Representative Dixon plots for the inhibition of CYP3A4-mediated testosterone hydroxylation by chlorpyrifos.

Testosterone concentrations were 50 μ M (\bullet), 100 μ M (\circ), and 200 μ M (\blacktriangledown).

metabolites. Chlorpyrifos, fonofos, and phorate inhibited major TST metabolites noncompetitively and irreversibly, and it is clear that organophosphorus compounds are some of the most potent inhibitors of the CYP3A4-dependent oxidation of TST yet described. Organophosphorus pesticides, such as chlorpyrifos, phorate, and fonofos are activated by a P450-catalyzed desulfuration reaction (Fukuto, 1990). The sulfur atom released from these pesticides in this reaction is highly reactive and is believed to bind immediately to the heme iron of P450 and inhibit its activity (Neal, 1980). On the other hand, enzyme stimulation is a process by which direct addition of one chemical to an enzyme stimulates the rate of reaction of the substrate (Guengerich, 1997). Our data indicated that some compounds, such as pyridostigmine bromide, DEET, chlorpyrifos-oxon, phorate, imidacloprid, and deltamethrin may stimulate the production of some of the TST metabolites.

Several studies, including this, have shown that CYP3A4 is the major P450 involved in the metabolism of TST in human liver microsomes (Waxman et al., 1988, 1991; Yamazaki and Shimada, 1997). Either inhibition or induction can modulate the activity of an enzyme; P450s may exhibit stimulation or inhibition in the presence of certain xenobiotic compounds (Guengerich, 1997; Szklarz and Halpert, 1998). It has been suggested that CYP3A4 is an allosteric enzyme, even though the identity of the allosteric site is not known (Shimada and Guengerich 1989; Lee et al., 1995). In addition, little is known about the active site topology of CYP3A4, although it is generally recognized that the active site of this enzyme has the capacity to accommodate large molecules and even more than one substrate (Shou et al., 1994). Inhibition may, in some interactions, be more serious than enzyme induction since inhibition happens more rapidly, not taking time to develop, as with induction (Guengerich, 1997). Preincubation of CYP3A4 with chlorpyrifos resulted in almost complete inhibition of major TST metabolites. The K_i value indicated that chlorpyrifos is one of the most potent inhibitors yet shown for the production of major TST metabolites. This inhibition was not due to inhibition by the metabolite, chlorpyrifos-oxon, since the latter had no inhibitory effect on the production of the major TST metabolites. Phorate and fonofos also inhibited the production of major and some minor metabolites of TST. The K_i value indicated that fonofos was a much better inhibitor of major TST metabolites than phorate. The possibility exists that inhibition of CYP3A4 may lead to higher levels of TST and may alter hormonal properties. However, in vivo studies are necessary to understand the impact of these changes. Preincubation with pyridostigmine bromide resulted in higher production of 6β - and 2β -OHTST, suggesting stimulation of CYP3A4. Preincubation with chlorpyrifos-oxon, phorate, and fonofos with CYP3A4 also resulted in activation of the production of some TST metabolites. A number of in vivo studies in rodents have shown that organochlorine pesticides increased the overall rate of TST metabolism (Cassidy et al., 1994; Wilson and LeBlanc, 1998; Dai et al., 2001).

Several studies have demonstrated that simultaneous expression of CYP3A4 and P450 reductase in bacterial or baculovirus-based insect cell membranes can produce high catalytic activity for TST 6β -OHTST in the absence of b_5 (Guengerich and Johnson 1997; Shaw et al., 1997), although addition of b_5 to the system can enhance the reaction rates (Yamazaki et al., 1999). In contrast to the CYP3A4 used in these experiments, cytochrome b_5 was not coexpressed in CYP3A5. A comparison of CYP3A5 with and without the addition of exogenous b_5 demonstrated a 2-fold increase in the activity of 6β - and 2β -OHTST in the presence of b_5 .

Human aromatase (CYP19), an extrahepatic P450, catalyzes the conversion of TST via three hydroxylation steps to estradiol. Inhibitors of aromatase currently in use have received considerable attention

as treatments for postmenopausal breast cancer and other estrogen-dependent diseases (Bordie et al., 1999). Endocrine disruptors are hormone mimics that modify hormonal action in humans. Currently, inhibitors of human aromatase have been identified as potential endocrine disruptors or environmental toxicants (Mak et al., 1999). The chemicals used in this study have no significant effect on the activity of aromatase.

In conclusion, the hydroxylation of TST by P450 isoforms indicates important functions for these enzymes other than detoxification of xenobiotics. The present study provided further insight into the range of TST hydroxylation reactions that can be catalyzed by different human P450 isoforms. The deployment-related chemicals used in this study, including pesticides, caused a marked modification of P450-mediated TST metabolism in vitro. Organophosphorus pesticides were very potent inhibitors of the production of the primary metabolites of CYP3A4 and inhibited major TST metabolites noncompetitively and irreversibly. Addition of b_5 to CYP3A5 increased the catalytic activity of this enzyme. Preincubation of the test chemicals had no effect on the production of estradiol from TST.

References

- Abou-Donia MB, Goldstein LB, Jones KH, Abdel-Rehman AA, Damodaran TV, Dechkovskaia AM, Bullman SL, Amir BE, and Khan WA (2001) Locomotor and sensorimotor performance deficit in rats following exposure to pyridostigmine bromide, DEET, and permethrin, alone and in combination. *Toxicol Sci* **60**:305–314.
- Abou-Donia MB, Wilmarth KR, Abdel-Rehman AA, Jensen FK, Oehme FW, and Kurt TL (1996a) Increased neurotoxicity following concurrent exposure to pyridostigmine bromide, DEET, and chlorpyrifos. *Fund Appl Toxicol* **34**:201–222.
- Abou-Donia MB, Wilmarth KR, Jensen FK, Oehme FW, and Kurt TL (1996b) Neurotoxicity resulting from coexposure to pyridostigmine bromide, DEET, and permethrin: implications of Gulf War chemical exposure. *Toxicol Environ Health* **48**:35–56.
- Bordie A, Lu Q, and Long B (1999) Aromatase and its inhibitors. *J Steroid Biochem Mol Biol* **107**:205–210.
- Cassidy RA, Vorhees CV, Minnema DJ, and Hastings L (1994) The effects of chlordane exposure during prenatal and postnatal periods at environmentally relevant levels on sex steroid-mediated behaviors and functions in the rat. *Toxicol Appl Pharmacol* **126**:326–337.
- Chaney LA, Rockhold RW, Mozingo JR, Hume AS, and Moss JI (1997) Potentiation of pyridostigmine bromide toxicity in mice by selected adrenergic agents and caffeine. *Vet Hum Toxicol* **39**:214–219.
- Dai D, Cao Y, Falls G, Levi PE, Hodgson E, and Randy LR (2001) Modulation of mouse P450 isoforms CYP1A2, CYP2B10, CYP2E1, and CYP3A by the environmental chemicals mirex, 2,2-bis (*p*-chlorophenyl)-1,1-dichloroethylene, vinclozolin and flutamide. *Pestic Biochem Physiol* **70**:127–141.
- Fukuto TR (1990) Mechanism of action of organophosphorus and carbamate insecticides. *Environ Health Perspect* **87**:245–254.
- Guengerich FP (1997) Role of cytochrome P450 enzymes in drug-drug interactions. *Adv Pharmacol* **43**:7–35.
- Guengerich FP and Johnson WW (1997) Kinetics of ferric cytochrome P450 reduction by NADPH-cytochrome P450 reductase: rapid reduction in the absence of substrate and variations among cytochrome P450 systems. *Biochemistry* **36**:14,741–14,750.
- Guengerich FP, Miller GP, Hanna IH, Martin MV, Leger S, Black C, Chaurat N, Silva JM, Trimble LA, Yergey JA, and Nicoll-Griffith DA (2002) Diversity in the oxidation of substrates by cytochrome P450 2D6: lack of an obligatory role of aspartate 301–substrate electrostatic bonding. *Biochemistry* **41**:11,025–11,034.
- Haley RW and Kurt TL (1997) Self reported exposure to neurotoxic chemical combinations in the Gulf War: a cross-sectional epidemiological study. *JAMA* **277**:231–237.
- Lee CA, Kadwell SH, Kost TA, and Serabjit-Singh CJ (1995) CYP3A4 expressed by insect cells infected with a recombinant baculovirus containing both CYP3A4 and human NADPH-cytochrome P450 reductase is catalytically similar to human liver microsomal CYP3A4. *Arch Biochem Biophys* **319**:157–167.
- Lehmann JM, McKee DD, Watson MA, Willson TM, Moore JT, and Klierer SA (1998) The human orphan nuclear receptor PXR is activated by compounds that regulate CYP3A4 gene expression and cause drug interactions. *J Clin Invest* **102**:1016–1023.
- Mak P, Cruz FD, and Chen S (1999) A yeast screen system for aromatase inhibitors and ligands for androgen receptor: yeast cells transformed with aromatase and androgen receptor. *Environ Health Perspect* **107**:855–860.
- McCain WF, Lee R, Johnson MS, Whaley JE, Ferguson JW, Beall P, and Leach G (1997) Acute oral toxicity study of pyridostigmine bromide, permethrin and DEET in the laboratory rat. *J Toxicol Environ Health* **50**:113–124.
- Neal RA (1980) Microsomal metabolism of thiono-sulfur compounds: mechanisms and toxicological significance. *Rev Biochem Toxicol* **2**:131–171.
- Nelson DR, Koymans L, Kamataki T, Stegeman JJ, Feyereisen R, Waxman DJ, Waterman MR, Gotoh O, Coon MJ, Estabrook RW, et al. (1996) P450 superfamily: update on new sequences, gene mapping, accession numbers and nomenclature. *Pharmacogenetics* **6**:1–42.
- Nieschlag E and Behre HM (1998) *Testosterone Action Deficiency Substitution*. Springer-Verlag, Berlin Heidelberg, Germany.
- Purdon MP and Lehman-McKeeman D (1997) Improved high-performance liquid chromatography procedure for the separation and quantification of hydroxytestosterone metabolites. *J Pharmacol Toxicol Methods* **37**:67–73.
- SAS (1989) *JMP User's Guide*. SAS Institute, Cary, NC.
- Segel IH (1975) *Biochemical Calculations*. John Wiley and Sons Inc., New York.

- Shaw PM, Hosea NA, Thompson DV, Lenius JM, and Guengerich FP (1997) Reconstitution premixes for assays using purified recombinant human cytochrome P450, NADPH-cytochrome P450 reductase and cytochrome *b*₅. *Arch Biochem Biophys* **348**:107–115.
- Shimada T and Guengerich FP (1989) Evidence for cytochrome P450_{NF}, the nifedipine oxidase, being the principle enzyme involved in the bioactivation of aflatoxins in human liver. *Proc Natl Acad Sci USA* **86**:462–465.
- Shou M, Grogan J, Mancewicz JA, Krausz KW, Gonzalez FJ, Gelboin HV, and Korzekwa KR (1994) Activation of CYP 3A4: Evidence for the simultaneous binding of two substrates in a cytochrome P450 active site. *Biochemistry* **33**:6450–6455.
- Szklarz GD and Halpert JR (1998) Molecular basis of P450 inhibition and activation: implications for drug development and drug therapy. *Drug Metab Dispos* **26**:1179–1184.
- Tang J, Cao Y, Rose RL, Brimfield AA, Dai D, Goldstein JA, and Hodgson E (2001) Metabolism of chlorpyrifos by human cytochrome P450 isoforms and human, mouse and rat liver microsomes. *Drug Metab Dispos* **29**:1201–1204.
- Usmani KA, Rose RL, Goldstein JA, Taylor WG, Brimfield AA, and Hodgson E (2002) In vitro human metabolism and interactions of repellent *N*, *N*-diethyl-*m*-toluamide. *Drug Metab Dispos* **30**:289–294.
- Waxman DJ, Attisano C, Guengerich FP, and Lapenson DP (1988) Human liver microsomal steroid metabolism: identification of the major microsomal steroid hormone 6 β -hydroxylase cytochrome P-450 enzyme. *Arch Biochem Biophys* **263**:424–436.
- Waxman DJ, Lapenson DP, Aoyama T, Gelboin HV, Gonzalez FJ, and Korzekwa K (1991) Steroid hormone hydroxylase specificities of eleven cDNA-expressed human cytochrome P450s. *Arch Biochem Biophys* **290**:160–166.
- Wilson JD, Foster DW, Kronenberg HM, and Larsen PR (1998) *Williams Textbook of Endocrinology*. Saunders, Philadelphia.
- Wilson VS and LeBlanc GA (1998) Endosulfan elevates testosterone biotransformation and clearance in CD-1 mice. *Toxicol Appl Pharmacol* **148**:158–168.
- Yamazaki H, Nakamura M, Nakajima M, Asahi S, Shimada N, Gillam EM, Guengerich J, Shimada T, and Yokoi T (1999) Enhancement of cytochrome P-450 3A4 catalytic activities by cytochrome *b*₅ in bacterial membranes. *Drug Metab Dispos* **27**:999–1004.
- Yamazaki H and Shimada T (1997) Progesterone and testosterone hydroxylation by cytochrome P-450 2C19, 2C9 and 3A4 in human liver microsomes. *Arch Biochem Biophys* **364**:161–169.

Inhibition of the Human Liver Microsomal and Human Cytochrome P450 1A2 and 3A4 Metabolism of Estradiol by Deployment-Related and Other Chemicals

Khawja A. Usmani, Taehyeon M. Cho, Randy L. Rose,¹ and Ernest Hodgson

Arena Pharmaceuticals, Inc., San Diego, California (K.A.U.); and Department of Environmental and Molecular Toxicology, North Carolina State University, Raleigh, North Carolina (T.M.C., R.L.R., E.H.)

Received April 5, 2006; accepted June 16, 2006

ABSTRACT:

Cytochromes P450 (P450s) are major catalysts in the metabolism of xenobiotics and endogenous substrates such as estradiol (E_2). It has previously been shown that E_2 is predominantly metabolized in humans by CYP1A2 and CYP3A4 with 2-hydroxyestradiol (2-OHE₂) the major metabolite. This study examines effects of deployment-related and other chemicals on E_2 metabolism by human liver microsomes (HLM) and individual P450 isoforms. Kinetic studies using HLM, CYP3A4, and CYP1A2 showed similar affinities (K_m) for E_2 with respect to 2-OHE₂ production. V_{max} and CL_{int} values for HLM are 0.32 nmol/min/mg protein and 7.5 μ l/min/mg protein; those for CYP3A4 are 6.9 nmol/min/nmol P450 and 291 μ l/min/nmol P450; and those for CYP1A2 are 17.4 nmol/min/nmol P450 and 633 μ l/min/nmol P450. Phenotyped HLM use showed that individuals with high levels of CYP1A2 and CYP3A4 have the great-

est potential to metabolize E_2 . Preincubation of HLM with a variety of chemicals, including those used in military deployments, resulted in varying levels of inhibition of E_2 metabolism. The greatest inhibition was observed with organophosphorus compounds, including chlorpyrifos and fonofos, with up to 80% inhibition for 2-OHE₂ production. Carbaryl, a carbamate pesticide, and naphthalene, a jet fuel component, inhibited ca. 40% of E_2 metabolism. Preincubation of CYP1A2 with chlorpyrifos, fonofos, carbaryl, or naphthalene resulted in 96, 59, 84, and 87% inhibition of E_2 metabolism, respectively. Preincubation of CYP3A4 with chlorpyrifos, fonofos, deltamethrin, or permethrin resulted in 94, 87, 58, and 37% inhibition of E_2 metabolism. Chlorpyrifos inhibition of E_2 metabolism is shown to be irreversible.

The cytochrome P450 (P450) monooxygenase system is composed of a superfamily of heme-containing enzymes, expressed in many mammalian tissues with the highest levels found in liver, and capable of catalyzing the metabolism of a wide range of both endogenous and exogenous substrates (Nelson et al., 1996). Human CYP3A4 and CYP1A2 are two of the most important and abundant drug-metabolizing P450 isoforms in human liver microsomes (HLM). On average, CYP3A4 and CYP1A2 account for approximately 40 and 13% of the total P450 in HLM, respectively (Shimada et al., 1994; Lehmann et al., 1998). Human CYP3A4 and CYP1A2 not only metabolize xenobiotics but also are responsible for the metabolism of endogenous compounds, such as steroid hormones. Both human CYP1A2 and CYP3A4 are involved in the metabolism of estradiol (E_2) and estrone (Lee et al., 2001, 2003), whereas CYP3A4 plays a predominant role

in the metabolism of testosterone (TST), androstenedione, and progesterone (Waxman et al., 1988; Usmani et al., 2003).

In the human female, E_2 is the most potent primary circulating estrogen of a group of endogenous estrogen steroids that includes estrone and estriol. During female development, E_2 stimulates the growth of female sex organs, regulates and sustains female sexual development and reproductive function, promotes hypertrophy in female breast and male muscle during puberty, initiates the synthesis of specific proteins, and controls fat deposition and distribution in subcutaneous tissues, thereby determining the characteristic female figure. Like TST in males, estrogens are the primary cause of the growth spurt, maturation of long bones, and development of secondary sexual characteristics in females. In the adult, E_2 regulates events during the menstrual cycle (growth of endometrial lining), is important during pregnancy and lactation, and contributes to the maintenance of sexual drive and female personality (Constanti et al., 1998; Wilson et al., 1998). Maintaining hormonal balance relies on a number of variables, including the rate of hormone synthesis, interactions among hormones, and rates of secretion, transport, and metabolism by phase I and phase II enzymes. P450s (phase I) are a major element in the maintenance of proper steroid hormone levels in mammalian systems and are the sole subject of this investigation. Exposure to foreign compounds may exert changes in endocrine function both

This work was supported by U.S. Army Cooperative Agreement DAMD 17-00-2-0008. Parts of the studies were presented at the 7th International ISSX Meeting in Vancouver, Canada, 2004 and the 44th Annual Meeting of the Society of Toxicology in New Orleans, 2005.

¹Deceased. Dr. Rose died in a tragic accident on May 23, 2006.

Article, publication date, and citation information can be found at <http://dmd.aspetjournals.org>.

doi:10.1124/dmd.106.010439.

ABBREVIATIONS: P450, cytochrome P450; HLM, human liver microsome(s); E_2 , estradiol; TST, testosterone; DEET, *N,N*-diethyl-*m*-toluamide; 2-OHE₂, 2-hydroxyestradiol; HPLC, high-performance liquid chromatography; CPS, chlorpyrifos.

directly (hormone agonists or antagonists) or indirectly (altering circulating levels of hormones by influencing rates of hormone synthesis or metabolism) that can severely affect steroid hormone action (Wilson and LeBlanc, 1998). It follows that perturbation of the P450 system by xenobiotics may in turn affect the subsequent metabolism and disposition of E₂. Perturbations in E₂ metabolism may affect levels of circulating E₂ with possible reproductive and other consequences, including further modulation of the expression of some P450 proteins.

The uses of deployment-related chemicals are essential for the health and well being of deployed forces during both peace-keeping and wartime missions. Human hazards associated with chemicals used to protect personnel during peace and wartime are poorly understood because the definition of cause and effect relationships depends on knowledge of the mechanisms of toxic action and interaction in humans. Following the Gulf War, some veterans reported illnesses that might have been the result of chemical exposures. Some studies of these veterans have concluded that significant correlations between perceived illnesses and chemical use exist (Haley and Kurt, 1997). The reported chemical exposures included the insect repellent *N,N*-diethyl-*m*-toluamide (DEET), insecticides such as permethrin and chlorpyrifos used to protect against insect-borne diseases, and the neuroprotective agent pyridostigmine bromide used to protect against possible nerve gas attack. It has been reported that chlorpyrifos and DEET are metabolized by human P450s (Tang et al., 2002; Usmani et al., 2002) and that interactions of deployment-related chemicals can inhibit or induce the P450s involved in their metabolism (Usmani et al., 2002). In a recent study examining the effects of various deployment-related chemicals on TST metabolism, Usmani et al. (2003) reported that organophosphorus pesticides are potent noncompetitive and irreversible inhibitors of TST metabolism caused by CYP3A4 inhibition. Other studies have reported that interaction of Gulf War-related chemicals could produce greater than additive toxicity in rats and mice (Chaney et al., 1997; McCain et al., 1997), increased neurotoxicity in hens associated with increased inhibition of brain acetylcholinesterase and neurotoxicity target esterase (Abou-Donia et al., 1996a,b), and neurobehavioral deficits associated with significant inhibition of brainstem acetylcholinesterase activities in rats (Abou-Donia et al., 2001). Possible detrimental interactions as a result of altered estrogen metabolism have not yet been examined relative to these chemicals, nor have studies been carried out to examine the induction or inhibition by these or related compounds of human P450-mediated metabolism of estrogens, such as E₂.

The objective of the present study was to study the inhibition or activation by various deployment-related chemicals of the metabolism of E₂ by HLM, CYP1A2, and CYP3A4.

Materials and Methods

Chemicals. Chlorpyrifos, fonofos, phorate, DEET, fipronil, imidacloprid, deltamethrin, permethrin, carbofuran, carbaryl, and naphthalene were purchased from ChemService (West Chester, PA). Pyridostigmine bromide was purchased from Roche (Indianapolis, IN). TST, E₂, 2-hydroxyestradiol (2-OHE₂), and 6 β -hydroxytestosterone were purchased from Steraloids (Newport, RI). High-performance liquid chromatography (HPLC) grade water, methanol, acetonitrile, and tetrahydrofuran were purchased from Fisher Scientific (Pittsburgh, PA). All the other chemicals, if not specified, were purchased from Sigma (St. Louis, MO). The structures of all the chemicals tested as inhibitors are shown in Fig. 1.

HLM and Human P450 Isoforms. Pooled HLM (pooled from 21 donors), single-donor HLM, and the human P450 isoforms CYP1A2 and CYP3A4 expressed in baculovirus-infected insect cells (Sf9) (BTI-TN-5B1-4) were purchased from BD Biosciences (Woburn, MA).

Assay Conditions. All the assays were conducted in triplicate, and all the reactions were prewarmed for 5 min at 37°C. All the reactions contained NADPH-regenerating system (0.25 mM NADP, 2.5 mM glucose 6-phosphate, and

2 U/ml glucose-6-phosphate dehydrogenase) and 100 mM potassium phosphate buffer (pH 7.4) containing 5 mM ascorbic acid and 3.3 mM MgCl₂. Final concentrations of HLM were 1 mg/ml, and final concentrations of CYP3A4 and CYP1A2 were 50 pmol/ml. The final reaction volume was 250 μ l, and all the reactions were terminated after 20 min by the addition of 150 μ l of methanol and vortexing. After 5-min centrifugation at 21,000g in a microcentrifuge, the supernatants were analyzed for E₂ metabolite concentrations by HPLC. The protein concentrations and incubation times used in the assays were found to be in the linear range in preliminary experiments. No metabolites were detected when incubations were carried out in the absence of an NADPH-generating system.

In Vitro E₂ Metabolism. Enzyme kinetic assays using HLM or the recombinant isoforms CYP1A2 or CYP3A4 were performed by incubation of serial concentrations of E₂ (final concentrations 3.125–200 μ M) with an NADPH-generating system in potassium phosphate buffer and incubated at 37°C for 5 min. The reactions were initiated by the addition of ice-cold HLM (final protein concentration 1 mg/ml), CYP1A2, or CYP3A4. No measurable lag phase was observed.

To determine the metabolic activities of individual HLM, incubations of E₂ (final concentration 50 μ M) were conducted for 20 min at 37°C using 1 mg protein/ml. To differentiate between the relative concentrations of CYP1A2 and CYP3A4 and the metabolism of E₂ in individual HLM, a specific CYP3A4 inhibitor, ketoconazole (final concentration 2 μ M), was added to the reaction mixture simultaneously with 50 μ M E₂.

Preliminary Inhibition Studies. The effects of test chemicals (chlorpyrifos, fonofos, phorate, DEET, fipronil, imidacloprid, deltamethrin, permethrin, carbofuran, carbaryl, naphthalene, and pyridostigmine bromide) on E₂ metabolism were examined using HLM, CYP1A2, or CYP3A4 after preincubation with the test compounds in otherwise complete mixtures lacking only the substrate E₂. HLM, CYP3A4, or CYP1A2 was incubated with individual test compounds (final concentration 50 μ M) for 5 min at 37°C before adding E₂ (final concentration 50 μ M). All the inhibitors, except pyridostigmine bromide, were added in 2.5 μ l of acetonitrile with an equal volume of acetonitrile being added to the control incubations. Pyridostigmine bromide was added in 2.5 μ l of water. Because of the likelihood that phosphorothioates are metabolized to irreversible P450 inhibitors, preincubation is tested as a variable with these chemicals. Preliminary experiments indicated little or no difference between preincubation and coincubation for other potential inhibitors. Only those chemicals that were capable of greater than 50% inhibition of E₂ metabolism at a concentration of 50 μ M were studied further.

Inhibition Kinetics of Deployment-Related Chemicals on E₂ Metabolism by CYP3A4 and CYP1A2. The chemicals for which IC₅₀ values were below 25 μ M as determined by preliminary incubation studies were analyzed further for inhibitory potential. Range-finding assays were conducted for chlorpyrifos, fonofos, phorate, deltamethrin, and permethrin (0.39–200 μ M) by incubating with CYP3A4 for 5 min at 37°C before adding E₂ (final concentration 50 μ M). The kinetic study of E₂ using varying E₂ concentrations (6.25–100 μ M) was performed using CYP3A4, which was preincubated with chlorpyrifos or fonofos (0.78, 1.56, or 3.125 μ M) for 5 min at 37°C.

For CYP1A2, range-finding assays were conducted for chlorpyrifos and fonofos as described above. Concentrations of chlorpyrifos (0.5 and 2.0 μ M) and fonofos (12.5 and 50.0 μ M) were preincubated with CYP1A2 for 5 min at 37°C before adding E₂ (final concentration 3.125–100 μ M) to measure their inhibition of CYP1A2 metabolism of E₂. In all the inhibition studies involving preincubation with the inhibitor, the NADPH-generating system was present during the preincubation.

Preincubation Time- and Concentration-Dependent Inactivation by Chlorpyrifos of CYP3A4 Metabolism of E₂. These studies were conducted using the same conditions as described in the assay conditions (50 μ M E₂; 20-min incubation at 37°C) but varying concentrations (0, 1, 2, 5, 10, and 50 μ M CPS) and preincubation times (0, 1, 2, 3, 4, and 5 min). The generation of 2-OHE₂ (the major metabolite of E₂) was compared in this assay and conducted in duplicate. Inactivation parameters (k_{inact} and K_I) were estimated as described in previous studies (Silverman, 1995; Heydari et al., 2004). The rate constant for initial inactivation (k_{obs}) at each concentration of inhibitor (CPS) was calculated from the slopes in the regression plots ($-k_{\text{obs}}$) (natural logarithm of remaining activity as percentage of control activity versus preincubation time). The inactivation values (k_{inact} and K_I) were calculated as described in Heydari et al. (2004); $k_{\text{obs}} = k_{\text{inact}} \times [I]/(K_I + [I])$, where $[I]$ is the

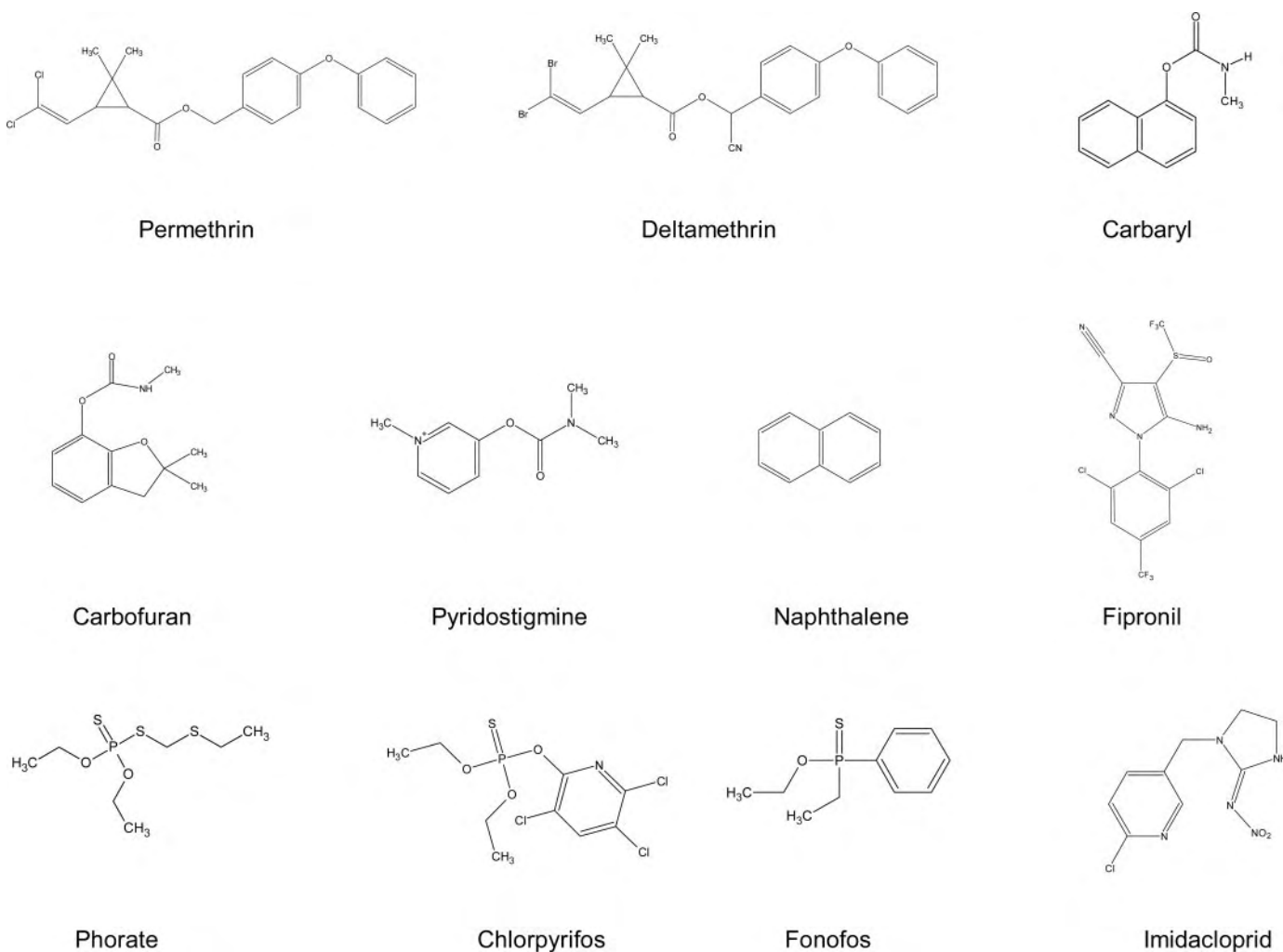


FIG. 1. Structures of all the chemicals tested as inhibitors of estradiol metabolism.

inhibitor concentration, k_{inact} is the maximum rate constant for inactivation, and K_i is the inhibitor concentration that produces half-maximal rate of inactivation.

Inhibition Kinetics of Carbaryl and Its Metabolites on E_2 Metabolism by CYP1A2. Before the K_i (inhibition constant) determination was done, range-finding assays were conducted for the inhibition by carbaryl and its metabolites of the metabolism of E_2 by CYP1A2. Varying concentrations (1.56–50 μM) of carbaryl, 4-hydroxycarbaryl, 5-hydroxycarbaryl, and carbaryl methylol were preincubated or coincubated with CYP1A2. Preincubation experiments with inhibitors were conducted similarly to those described above. For coincubation experiments, carbaryl or its metabolites were incubated with E_2 (final concentration 50 μM). The reactions were initiated by the addition of ice-cold CYP1A2. For Michaelis-Menten plots, carbaryl (6.25 and 12.5 μM), 4-hydroxycarbaryl (6.25 and 12.5 μM), and carbaryl methylol (12.5 and 25 μM) were coincubated with E_2 (final concentration 3.125–100 μM). The reactions were initiated by the addition of ice-cold CYP1A2.

Inhibition Kinetics of Naphthalene and Its Metabolites on E_2 Metabolism by CYP1A2. Before the K_i determination was done, range-finding assays were conducted for the inhibition by naphthalene and its metabolites of the metabolism of E_2 by CYP1A2. Varying concentrations of naphthalene (3.125–25 μM), 1-naphthol (0.78–25 μM), 2-naphthol (25 μM), *trans*-1,2-dihydro-1,2-naphthalenediol (25 μM), 1,2-naphthoquinone (25 μM), 1,4-naphthoquinone (25 μM), and 1,4-dihydroxynaphthalene (25 μM) were preincubated or coincubated with CYP1A2. The preincubation and coincubation experiments with naphthalene and its metabolites were conducted similarly as described above. For Michaelis-Menten plots, naphthalene (1.56, 3.125, and 6.25 μM) was preincubated with CYP1A2 for 5 min at 37°C before adding E_2 (final concentration 3.125–100 μM).

For Michaelis-Menten plots, 1-naphthol (1.56 and 3.125 μM) was coincubated with E_2 (final concentration 3.125–100 μM). The reactions were initiated by the addition of ice-cold CYP1A2.

To show whether 1-naphthol inhibition is reversible or irreversible, incubations with and without 1-naphthol (3.125 μM) were conducted with E_2 (final concentration 50 μM). The reactions were initiated by the addition of varying concentrations of ice-cold CYP1A2 (3.125–12.5 pmol).

Analysis of 2-OHE₂ and 6 β -Hydroxytestosterone by HPLC. Analysis of the E_2 metabolite 2-OHE₂ was performed with an HPLC system coupled with in-line UV detection as described previously (Suchar et al., 1995). The HPLC system consisted of a Waters 2690 separation module and a Waters UV photodiode array detector (model 2996). All the system components were controlled through the Waters Powerline firmware. Data were collected via a Waters system controller and analyzed using Waters Empower software. The solvent system for separation of E_2 and 2-OHE₂ consisted of acetonitrile (solvent A), 0.1% acetic acid in water (solvent B), and 0.1% acetic acid in methanol (solvent C). The solvent gradient (solvent A/solvent B/solvent C) used for eluting E_2 and 2-OHE₂ was as follows: 8 min of isocratic at 16:68:16, 7 min of a concave gradient (curve number 9) to 18:64:18, 13 min of a concave gradient (curve number 8) to 20:59:21, 10 min of a convex gradient (curve number 2) to 22:57:21, 13 min of a concave gradient (curve number 8) to 58:21:21, followed by a 0.1-min step to 92:5:3 and a 3.9-min isocratic period at 92:5:3. The gradient was returned to the initial condition (16:68:16) for 2 min and held for 3 min before analyzing the next sample. The flow rate was 1.2 ml/min. E_2 and 2-OHE₂ were separated by an Ultracarb 5 ODS (octadecylsilane) column (150 \times 4.6 mm, Phenomenex, Rancho Palos Verdes, CA) at 30°C and detected at 280 nm. The limit of detection for 2-OHE₂ was approx-

TABLE 1

Kinetic parameters for 2-hydroxylation of E_2 by pooled HLM, CYP3A4, and CYP1A2

Values are expressed as mean \pm S.E.M. ($n = 3$).

	K_m μM	V_{max} nmol/min/mg protein	V_{max}/K_m $\mu l/min/mg$ protein
HLM	42.8 \pm 9.40	0.32 \pm 0.02	7.5
CYP3A4	23.7 \pm 3.00	6.9 \pm 0.35	291
CYP1A2	27.5 \pm 2.16	17.4 \pm 0.54	633

imately 0.04 μM . Concentrations of 2-OHE₂ were obtained from the chromatographic peak area from a standard curve (0.15–20.0 μM).

TST and its metabolite, 6 β -hydroxytestosterone, were separated using the method described by Usmani et al. (2003). E₂ and its metabolites eluted after 6 β -hydroxytestosterone and TST.

Data Analysis and Statistics. The apparent K_m and V_{max} parameters were calculated using the SigmaPlot Enzyme Kinetics Module for Windows, version 1.1 (SPSS Inc., Chicago, IL). The K_i values were estimated by nonlinear regression analysis by fitting different models of enzyme inhibition to the kinetic data using SigmaPlot Enzyme Kinetics Module for Windows, version 1.1 (SPSS Inc.). The mode of inhibition was established by comparing the statistical results including the r^2 information criterion values of different inhibition models and by selecting the one with the best fit. Furthermore, the mode of inhibition was established by comparing the 95% confidence intervals that did not overlap for K_m and V_{max} values. Significant differences between data sets were determined by Student's t test using SigmaPlot for Windows, version 8.0 (SPSS Inc.).

Results

Enzyme Kinetics. HLM, CYP3A4, and CYP1A2 all displayed similar K_m values for metabolism of E₂ to 2-OHE₂ (Table 1). V_{max} and CL_{int} values for HLM were 0.32 nmol/min/mg protein and 7.5 $\mu l/min/mg$ protein; those for CYP3A4 were 6.9 nmol/nmol P450 and 291 $\mu l/min/nmol$ P450; and those for CYP1A2 were 17.4 nmol/min/nmol P450 and 633 $\mu l/min/nmol$ P450.

E₂ Metabolism in Single-Donor HLM. Incubations of E₂ with individual donor HLM (6 male and 11 female) showed as much as 36-fold variability in metabolism among individuals (Fig. 2). Phenotype data based on metabolic activities of these individuals was used to derive correlations between P450 isoform content and E₂ metabolic activity. CYP3A4 was the isoform with the best correlation ($r^2 = 0.87$). All the other correlations between E₂ hydroxylation activity and

specific P450 isoforms were less than 0.40. To determine the CYP1A2 contribution to E₂ metabolism among individual HLM, ketoconazole (2 μM), a specific CYP3A4 inhibitor, was used to inhibit CYP3A4 activity. Preliminary observations with ketoconazole indicated that 2 μM inhibited less than 5% of CYP1A2 activity (data not shown). In the presence of ketoconazole, variation among individuals was reduced to 12-fold, and the correlation of CYP1A2 with E₂ metabolism increased to 0.81 (Fig. 2).

Inhibition of E₂ Metabolism. The effects of various deployment-related and other chemicals on E₂ (50 μM) metabolism were investigated by preincubating 50 μM concentrations of each chemical with pooled HLM (Fig. 3). The organophosphorus compounds, chlorpyrifos fonofos, and phorate all significantly inhibited E₂ metabolism to 2-OHE₂, although inhibition by chlorpyrifos and fonofos was profound (ca. 80%) compared with phorate (ca. 16.5%). Preincubation of pooled HLM with carbaryl, a carbamate, and naphthalene, a jet fuel component, also resulted in significant inhibition (ca. 40%) of E₂ metabolism to 2-OHE₂. Fipronil, a phenyl pyrazole insecticide, also significantly inhibited E₂ metabolism, although to a lesser degree (ca. 18%).

To further explore the inhibition of E₂ metabolism observed in HLM, assays were also conducted using CYP3A4 and CYP1A2. Preincubation of CYP3A4 with a variety of chemicals resulted in varying levels of activation and inhibition of E₂ metabolism (Fig. 4). E₂ metabolism was significantly inhibited by the organophosphorus compounds chlorpyrifos and fonofos, with up to ca. 90% inhibition of E₂ metabolism to 2-OHE₂. Preincubation of CYP3A4 with the pyrethroids deltamethrin and permethrin resulted in ca. 58 and 37% inhibition of E₂ metabolism to 2-OHE₂, respectively. In contrast, preincubation of CYP3A4 with DEET, an insect repellent, and carbofuran, a carbamate, resulted in the production of small, but not significantly greater, levels of 2-OHE₂.

Similarly, preincubation of CYP1A2 resulted in varying levels of activation and inhibition of E₂ metabolism (Fig. 5). Preincubation of chlorpyrifos and fonofos resulted in ca. 96 and 59% inhibition of E₂ metabolism, respectively. In contrast with CYP3A4, preincubation of CYP1A2 with carbaryl and naphthalene resulted in significant (ca. 85%) inhibition of E₂ metabolism. Some chemicals, such as fipronil and deltamethrin, appeared to produce small, but not significantly higher, levels of 2-OHE₂.

Mechanism of Inhibition. To investigate the type of inhibition of CYP3A4 by chlorpyrifos and fonofos in the production of 2-OHE₂, a

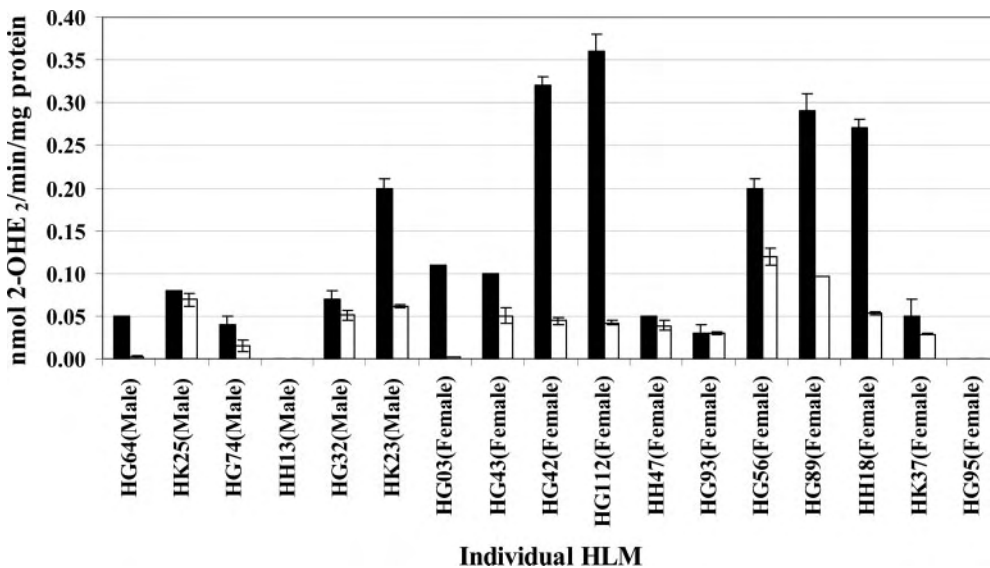


FIG. 2. Metabolism of E₂ to 2-OHE₂ by single-donor HLM in the presence and absence of ketoconazole. Solid bars, no ketoconazole; open bars, 2 μM ketoconazole.

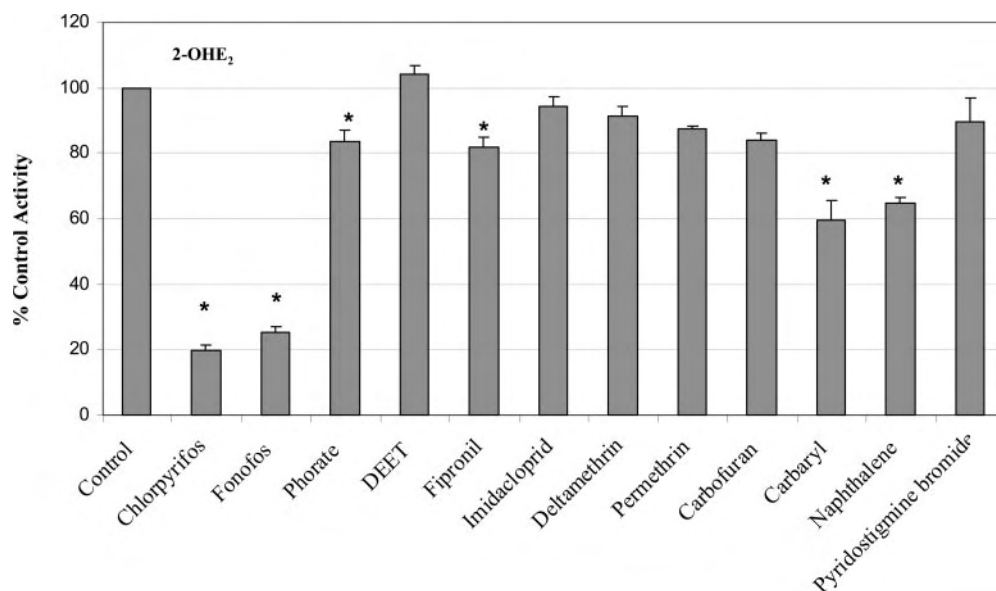


FIG. 3. Effects of deployment-related and other chemicals on E₂ metabolism by pooled HLM. *, statistically significant different when compared with control ($P < 0.01$).

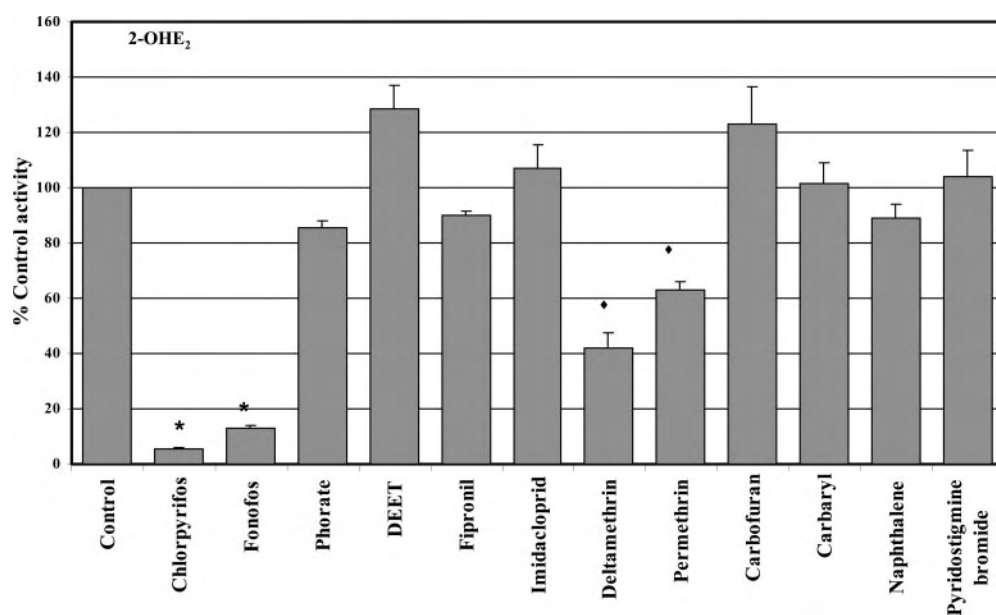


FIG. 4. Effects of deployment-related and other chemicals on E₂ metabolism by CYP3A4. *, statistically significant different when compared with control ($P < 0.01$). ◆, statistically significant different when compared with control ($P < 0.05$).

major E₂ metabolite, different concentrations of chlorpyrifos and fonofos were preincubated for 5 min with CYP3A4 before adding varying concentrations of E₂. Michaelis-Menten plots showed that the V_{max} values were significantly reduced without affecting K_m values, indicative of a noncompetitive inhibition of E₂ metabolism by chlorpyrifos and fonofos (Fig. 6).

In a similar manner, inhibition of CYP1A2 metabolism of E₂ by chlorpyrifos and fonofos involved a 5-min preincubation before the addition of varying concentrations of E₂. As shown for CYP3A4 (Fig. 5), Michaelis-Menten plots for CYP1A2 also indicated noncompetitive inhibition (Fig. 7).

The production of 2-OHE₂ by CYP3A4 was significantly inhibited by CPS in a time- and concentration-dependent manner (Fig. 8A). Inactivation parameters (k_{inact} and K_I) determined for CYP3A4 metabolism of estradiol by CPS were 0.3 min^{-1} and $4.9 \mu\text{M}$, respectively (Fig. 8B). Even at a preincubation of 0', the metabolic activity of CYP3A4 for estradiol was apparently significantly decreased by CPS in a dose-dependent manner, indicating a very rapid initial rate of inhibition.

For IC₅₀ values, varying concentrations of carbaryl and its metabolites were preincubated and coincubated with CYP1A2. Under preincubation conditions but not with coincubation, carbaryl, 4-hydroxycarbaryl, and carbaryl methylol caused small increases in the production of 2-OHE₂ at the low concentrations (1.56, 3.125, and 6.25 μM), whereas at high concentrations (12.5–50 μM) inhibition of E₂ metabolism was observed (data not shown). Under preincubation conditions but not with coincubation, 5-hydroxycarbaryl caused small increases in the production of 2-OHE₂ at all the concentrations (1.56–50 μM) (data not shown). Under coincubation conditions, carbaryl, 4-hydroxycarbaryl, 5-hydroxycarbaryl, and carbaryl methylol all caused inhibition of E₂ metabolism at all the concentrations tested (1.56–50 μM) (data not shown). To determine the K_I value and investigate the type of inhibition of CYP1A2 metabolism of E₂ by carbaryl and its metabolites, different concentrations of carbaryl, 4-hydroxycarbaryl, and carbaryl methylol were coincubated with CYP1A2 and varying concentrations of E₂. Michaelis-Menten plots showed that the V_{max} values were significantly reduced without af-

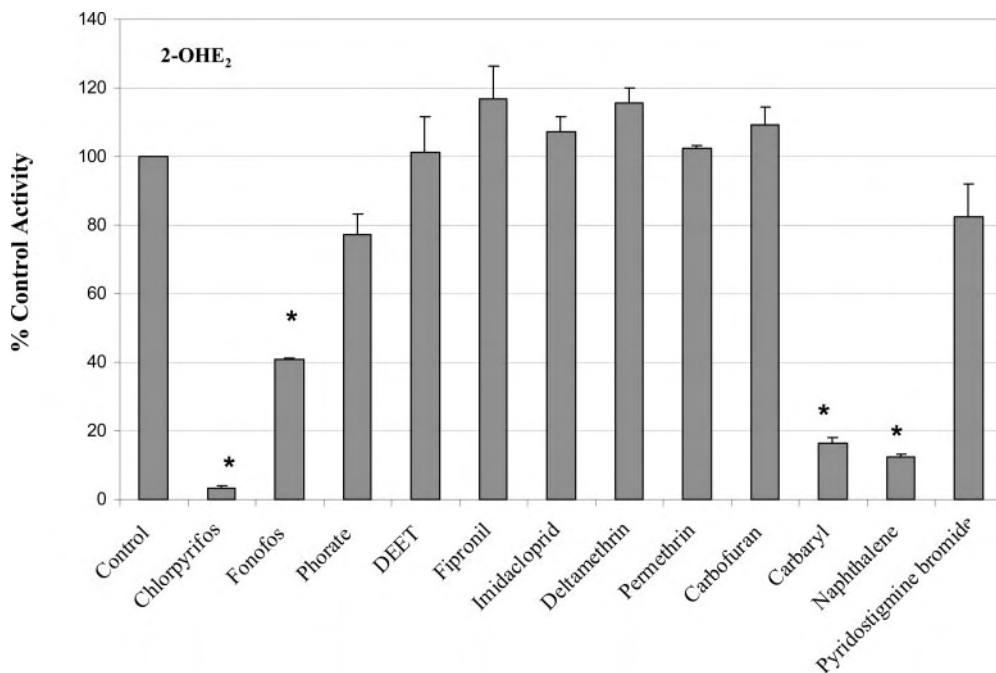


Fig. 5. Effects of deployment-related and other chemicals on E_2 metabolism by CYP1A2. *, statistically significant different when compared with control ($P < 0.01$).

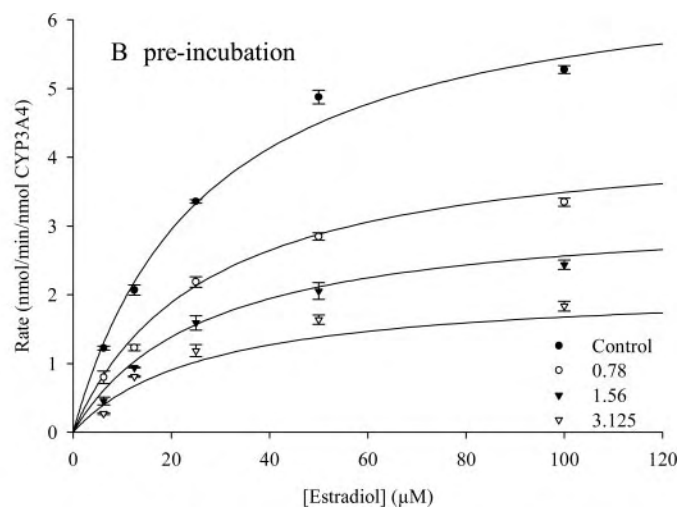
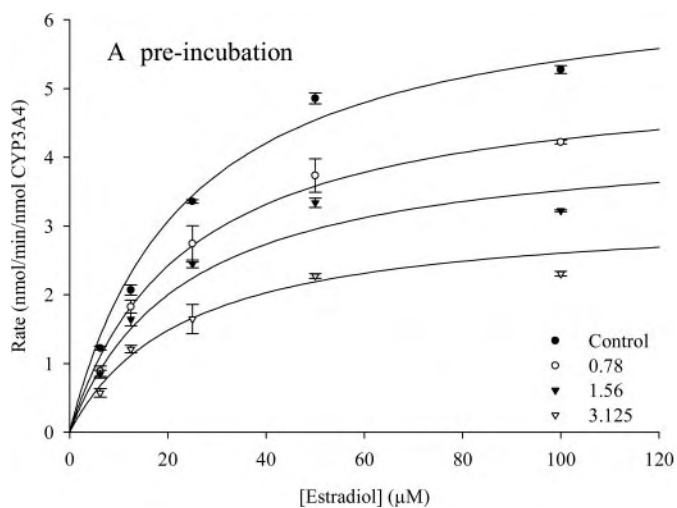


Fig. 6. Michaelis-Menten plots for the inhibition of CYP3A4 mediated E_2 hydroxylation by chlorpyrifos (A) and fonofos (B). Kinetic constants for the uninhibited (no inhibitor present) enzyme are shown in Table 1.

fecting K_m values, indicative of a noncompetitive inhibition of E_2 metabolism by carbaryl and its metabolites (Fig. 9). The inhibition constants (K_i) indicated that carbaryl is the most potent inhibitor of E_2 metabolism with a K_i value of $7.7 \mu\text{M}$; 4-hydroxycarbaryl is the second best inhibitor with a K_i value of $10.2 \mu\text{M}$, whereas carbaryl methylol is a weak inhibitor with a K_i value of $29.0 \mu\text{M}$.

In the determination of IC_{50} values, varying concentrations of naphthalene and its metabolites were preincubated and coincubated with CYP1A2. Preincubation of naphthalene increased the inhibition of E_2 metabolism by nearly 2-fold compared with the coincubation of naphthalene with E_2 , indicating that a reactive metabolite is involved (data not shown). No differences were observed in the IC_{50} values when 1-naphthol was preincubated or coincubated with E_2 (data not shown). 2-Naphthol, 1,2-naphthoquinone, 1,4-naphthoquinone, and 1,4-dihydronaphthalene ($25 \mu\text{M}$) inhibited E_2 ($50 \mu\text{M}$) metabolism ca. 85 to 100%, whereas *trans*-1,2-dihydro-1,2-naphthalenediol had no inhibitory effect on E_2 metabolism (data not shown). To determine

the K_i value and to investigate the type of inhibition of CYP1A2 by naphthalene on E_2 metabolism, naphthalene was preincubated for 5 min with CYP1A2 before adding varying concentrations of E_2 . The Michaelis-Menten plot showed that the V_{max} values were significantly reduced without affecting K_m values, indicative of a noncompetitive inhibition of E_2 metabolism by naphthalene (Fig. 10). To investigate the type of inhibition of CYP1A2 by 1-naphthol on E_2 metabolism, 1-naphthol was coincubated with CYP1A2 and varying concentrations of E_2 . 1-Naphthol, a predominant naphthalene metabolite, was shown to be a noncompetitive inhibitor of E_2 metabolism (Fig. 11). Further investigation of noncompetitive reversible or nonreversible inhibition data revealed that the inhibition of 2-OHE₂ by 1-naphthol is nonreversible (data not shown).

Discussion

P450-dependent hydroxylation is a major pathway of oxidative metabolism of E_2 in mammalian liver. The studies carried out using

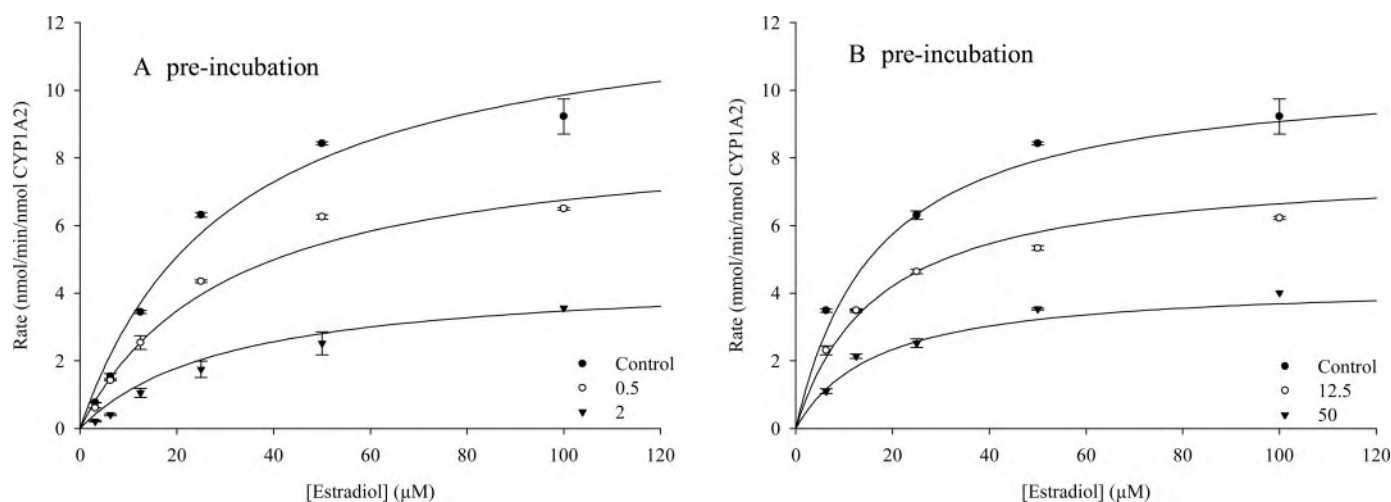


FIG. 7. Michaelis-Menten plots for the inhibition of CYP1A2 mediated E₂ hydroxylation by chlorpyrifos (A) and fonofos (B). Kinetic constants for the uninhibited (no inhibitor present) enzyme are shown in Table 1.

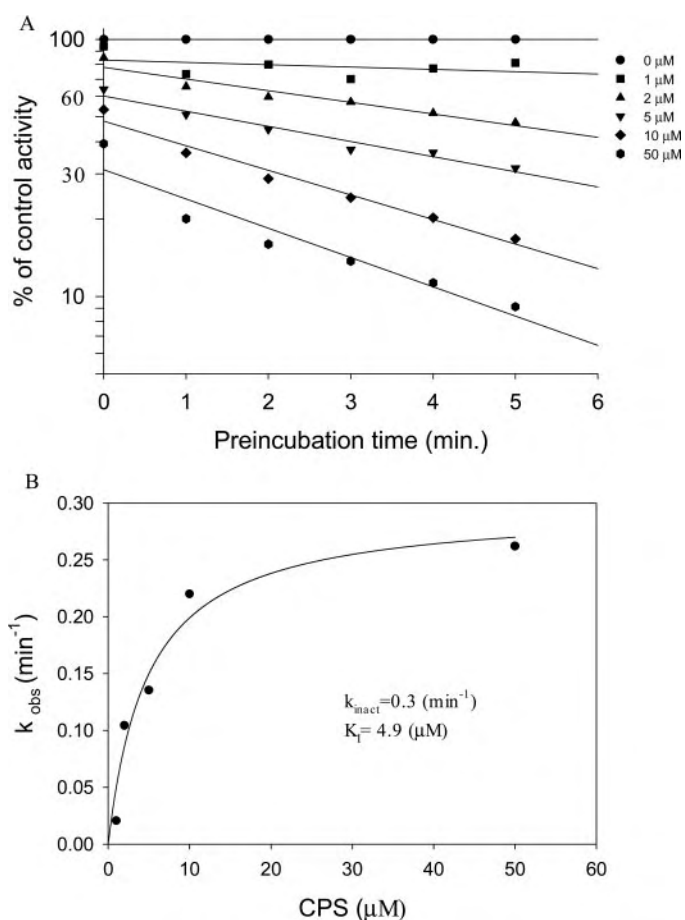


FIG. 8. Time- and concentration-dependent inactivation of CYP3A4 metabolism of E₂ by CPS. A, correlation between preincubation time with various concentrations of CPS and CYP3A4 activity. B, plot of inactivation rate constant as a function of CPS concentration to determine k_{inact} and K_I values.

human P450 isoforms provided further insight into the range of E₂ hydroxylation reactions that can be catalyzed by human P450 enzymes. Human CYP1A2 and CYP3A4 are the major isoforms responsible for E₂ metabolism, and 2-OHE₂ is the major E₂ metabolite, as previously shown (Yamazaki et al., 1998; Lee et al., 2001, 2003). The phenotyped HLM data and the mean metabolic intrinsic clearance

rates, as estimated by V_{max}/K_m , corroborate earlier findings (Yamazaki et al., 1998; Lee et al., 2001, 2003) that both CYP3A4 and CYP1A2 play major roles in the metabolism of E₂ in human liver, and the content of these two P450s in HLM determine which isoform is more important. However, CYP3A4 may play a more important role than CYP1A2 because on average CYP3A4 accounts for approximately 40% of the total P450 in HLM. Our kinetic data presented in this study for CYP1A2 and CYP3A4 are in general agreement with the previous reports showing that CYP1A2 is more active than CYP3A4 in E₂ metabolism (Yamazaki et al., 1998; Badawi et al., 2001).

CYP3A4 is one of the most important and abundant P450 isoforms in human liver and has broad substrate specificity. CYP3A4 not only metabolizes xenobiotics but also is responsible for the metabolism of endogenous compounds such as steroid hormones, including TST and E₂ (Lee et al., 2003; Usmani et al., 2003). Because TST and E₂ are predominantly metabolized by CYP3A4, both can potentially compete for the same catalytic site of CYP3A4. The usual interaction between two different substrates for the same enzyme is competitive inhibition. But because the K_m values for TST and E₂ are different ($K_m = 108$ and $24 \mu\text{M}$ for TST and E₂, respectively), interactions between these substrates may be complicated because of the allosteric characteristics of CYP3A4 (Shimada and Guengerich 1989; Lee et al., 1995; Usmani et al., 2003; Williams et al., 2004). The recent demonstration of a relatively large substrate binding catalytic site by crystal structure elucidation is consistent with the capacity of CYP3A4 to accommodate large molecules and possibly more than one substrate (Yano et al., 2004).

Endogenous steroids, such as E₂, always exist in vivo, and considerable amounts of these steroids are metabolized by the P450s expressed in the human liver, where foreign compounds are mainly metabolized. Because TST and E₂ both have important, and different, effects in vivo, the inhibition of the metabolism of both of these steroid hormones must be considered in detail. If xenobiotics substantially alter enzymes such as CYP3A4 and CYP1A2, they may affect the rate of E₂ metabolism, ultimately disrupting E₂ homeostasis. Preincubation of pooled HLM, CYP3A4, and CYP1A2 with organophosphorus compounds, such as chlorpyrifos and fonofos, resulted in the extensive inhibition of the production of 2-OHE₂, a major E₂ metabolite. Chlorpyrifos and fonofos inhibited 2-OHE₂ formation noncompetitively and are among the most potent inhibitors of the P450-dependent oxidation of E₂ yet described. Organophosphorus pesticides, such as chlorpyrifos and fonofos, are activated by a P450-catalyzed

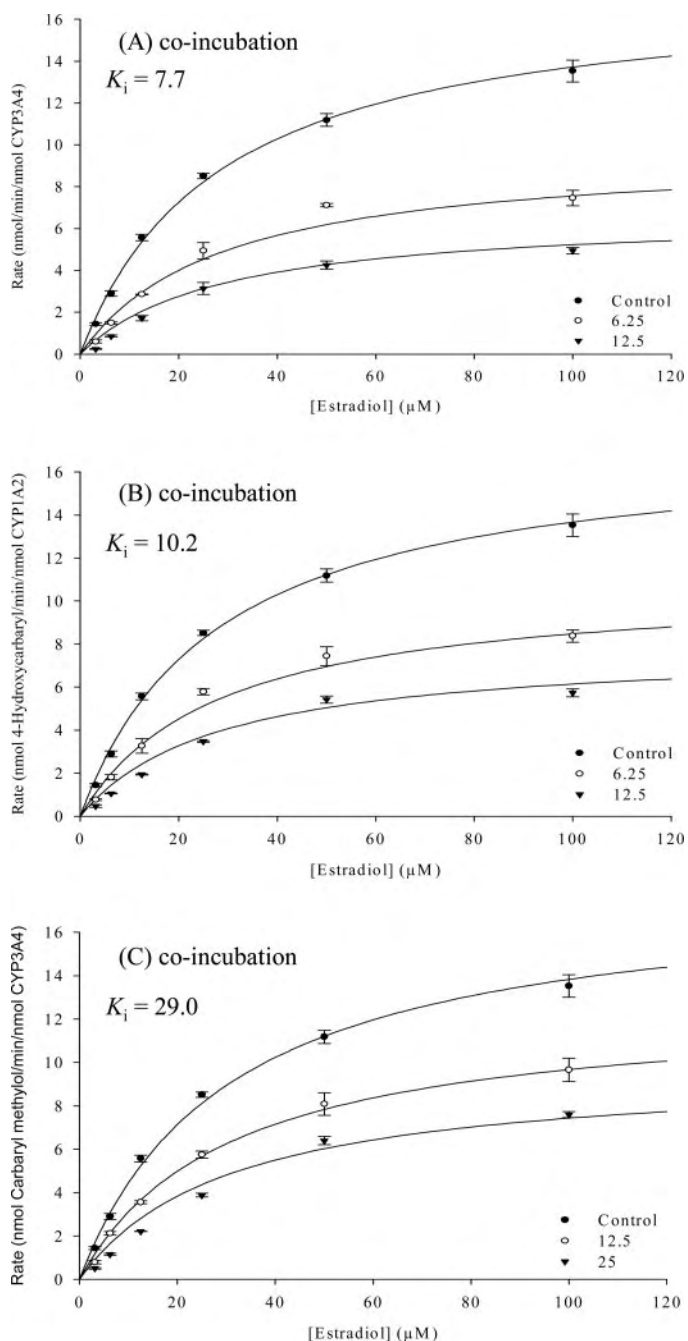


FIG. 9. Michaelis-Menten plots for the inhibition of CYP1A2 mediated E_2 hydroxylation by carbaryl (A), 4-hydroxycarbaryl (B), and carbaryl methylol (C). Kinetic constants for the uninhibited (no inhibitor present) enzyme are shown in Table 1.

desulfuration reaction (Fukuto, 1990). The sulfur atom released from these pesticides in this reaction is highly reactive and is believed to bind immediately to the heme iron of P450 and inhibit its activity (Norman et al., 1974; Halpert et al., 1980; Neal, 1980; Neal and Halpert, 1982; Butler and Murray, 1997). Our previous study showed that organophosphorus pesticides are potent noncompetitive and irreversible inhibitors of TST metabolism by HLM and CYP3A4 (Usmani et al., 2003).

Enzyme activity is often modulated by inhibition or induction, either condition modifying the extent to which xenobiotics or endogenous substrates are metabolized (Guengerich, 1997; Szklarz and Halpert, 1998). Inhibition may, in some interactions, be more serious than enzyme induction because inhibition occurs more rapidly than induction

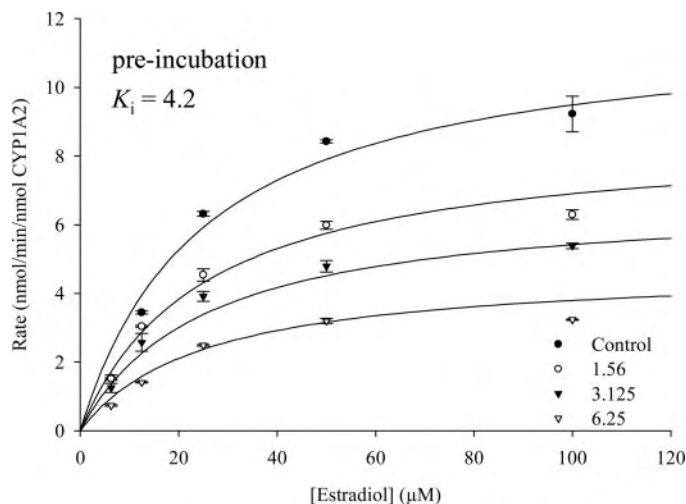


FIG. 10. Michaelis-Menten plot for the inhibition of CYP1A2 mediated E_2 hydroxylation by naphthalene. Kinetic constants for the uninhibited (no inhibitor present) enzyme are shown in Table 1.

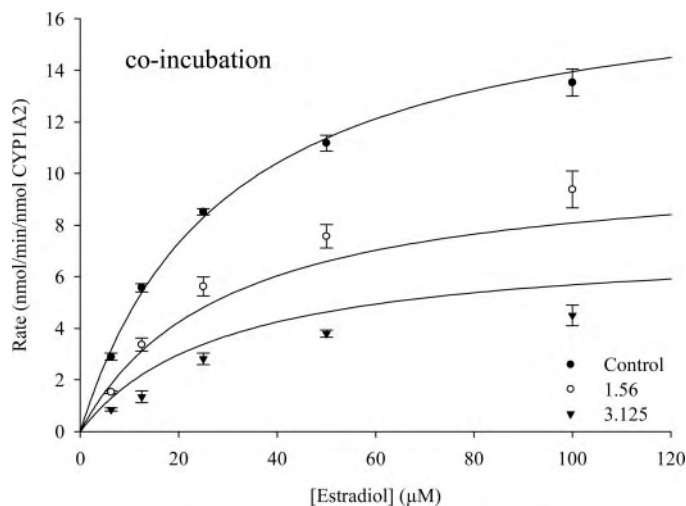


FIG. 11. Michaelis-Menten plot for the inhibition of CYP1A2 mediated E_2 hydroxylation by 1-naphthol.

(Guengerich, 1997). Preincubation of CYP3A4 with chlorpyrifos and fonofos resulted in almost complete inhibition of E_2 metabolism to 2-OHE₂. Preincubation of CYP1A2 with chlorpyrifos resulted in almost complete inhibition of 2-OHE₂ formation, whereas fonofos was not as potent an inhibitor. The kinetics of inactivation of E_2 metabolism by CPS confirms that CPS is a mechanism-based inactivator of CYP3A4 in these studies. Preincubation of CPS in the presence of an NADPH-generating system increased the inhibitory effect in a time- and concentration-dependent manner. The significant reduction of CYP3A4 activity toward E_2 metabolism by CPS at time 0' suggests that the binding affinity of the inhibitor (CPS) is higher than that of the substrate (E_2) with the CYP3A4 isoform and that the initial rate of inhibition is rapid. The relatively low K_i value (high inhibitory potency) of CPS toward CYP3A4 metabolism of E_2 appears to confirm the strong binding affinity of CPS with this isoform. Therefore, the possibility exists that inhibition of CYP3A4 and CYP1A2 by these chemicals could lead to higher levels of E_2 and alter hormonal properties. The in vivo importance of these observations will require further studies.

Carbaryl is a widely used anticholinesterase carbamate insecticide. In an in vitro study, 5-hydroxycarbaryl, 4-hydroxycarbaryl, and carbaryl methylol were identified as the major metabolites of carbaryl produced

by HLM (Tang et al., 2002). P450 isoform data indicated that CYP1A1, CYP1A2, CYP2B6, CYP2C19, and CYP3A4 are the most active isoforms in human metabolism of carbaryl (Tang et al., 2002). In our preliminary inhibition studies, we found that preincubation of pooled HLM and CYP1A2 with carbaryl significantly inhibited E₂ metabolism. Because carbaryl is metabolized by CYP1A2 while also showing significant inhibition of E₂ metabolism, we expected competitive interactions between E₂ and carbaryl or its metabolites. However, carbaryl and its metabolites inhibited formation of 2-OHE₂ noncompetitively in our co-incubation studies. The K_i values indicated that carbaryl and 4-hydroxycarbaryl were much better inhibitors of 2-OHE₂ than carbaryl methylol. Although there is no obvious explanation of the slight activation of E₂ at low concentrations of carbaryl, 4-hydroxycarbaryl, and carbaryl methylol, it may be noted that this is a common phenomenon in the oxidation of TST by HLM (Usmani et al., 2003).

The polycyclic aromatic hydrocarbon naphthalene is an industrial chemical, an environmental pollutant, and a component of jet fuel and has considerable toxicological importance because of widespread human exposure and its potential to form toxic and carcinogenic metabolites in humans (Wilson et al., 1996). We recently showed that CYP1A2 is the most efficient of the 15 different isoforms tested for their ability to metabolize naphthalene to its two major metabolites in HLM, 1-naphthol and 1,2-dihydro-1,2-naphthalenediol (Cho et al., 2006). In this study, preincubations of naphthalene with pooled HLM and CYP1A2 significantly inhibited E₂ metabolism. Because naphthalene is metabolized by CYP1A2 and also significantly inhibited E₂ metabolism, we expected a competitive interaction between E₂ and naphthalene or its metabolite. However, this study showed noncompetitive inhibition of E₂ metabolism. Coincubation of 1-naphthol, a well known cytotoxic metabolite of naphthalene, resulted in noncompetitive and irreversible inhibition of E₂ metabolism.

In conclusion, the hydroxylation of E₂ by CYP3A4 and CYP1A2 isoforms indicates important functions for these enzymes other than detoxification of xenobiotics. The deployment-related and other chemicals used in this study, including pesticides, caused a marked modification of P450-mediated E₂ metabolism in vitro. Organophosphorus pesticides were very potent inhibitors of the production of 2-OHE₂ and inhibited E₂ metabolism noncompetitively. Carbaryl and some of its metabolites inhibited E₂ metabolism noncompetitively. Naphthalene inhibited E₂ metabolism noncompetitively, an effect probably caused by 1-naphthol, a naphthalene metabolite. 1-Naphthol inhibits E₂ metabolism noncompetitively and irreversibly. It should be noted that in vivo toxicokinetic data are not available for these chemicals in humans, and thus the effects noted indicate only the potential for in vivo effects.

References

- Abou-Donia MB, Goldstein LB, Jones KH, Abdel-Rehman AA, Jensen FK, Oehme FW, and Kurt TL (2001) Locomotor and sensorimotor performance deficit in rats following exposure to pyridostigmine bromide, DEET, and permethrin, alone and in combination. *Toxicol Sci* **60**:305–314.
- Abou-Donia MB, Wilmarth KR, Abdel-Rehman AA, Jensen FK, Oehme FW, and Kurt TL (1996a) Increased neurotoxicity following concurrent exposure to pyridostigmine bromide, DEET and chlorpyrifos. *Fund Appl Toxicol* **34**:201–222.
- Abou-Donia MB, Wilmarth KR, Jensen FK, Oehme FW, and Kurt TL (1996b) Neurotoxicity resulting from coexposure to pyridostigmine bromide, DEET and permethrin: implications of Gulf War chemical exposure. *Toxicol Environ Health* **48**:35–56.
- Badawi AF, Cavalieri EL, and Rogan EG (2001) Role of human cytochrome P450 1A1, 1A2, 1B1, and 3A4 in the 2-, 4-, and 16 α -hydroxylation of 17 β -estradiol. *Metabolism* **50**:1001–1003.
- Butler AM and Murray M (1997) Biotransformation of parathion in human liver: participation of CYP3A4 and its inactivation during microsomal parathion oxidation. *J Pharmacol Exp Ther* **280**:966–973.
- Chaney LA, Rockhold RW, Mazingo JR, and Hume AS (1997) Potentiation of pyridostigmine bromide toxicity in mice by selected adrenergic agents and caffeine. *Vet Human Toxicol* **39**:214–219.
- Cho TM, Rose RL, and Hodgson E (2006) In vitro metabolism of naphthalene by human liver microsomal cytochrome P450 enzymes. *Drug Metab Dispos* **34**:176–183.
- Constanti A, Bartke A, and Khardori R (1998) *Basic Endocrinology*. Howard Academic Publishers, Amsterdam.
- Fukuto TR (1990) Mechanism of action of organophosphorus and carbamate insecticides. *Environ Health Perspect* **87**:245–254.
- Guengerich FP (1997) Role of cytochrome P450 enzymes in drug-drug interactions. *Adv Pharmacol* **43**:7–35.
- Haley RW and Kurt TL (1997) Self reported exposure to neurotoxic chemical combinations in the Gulf War: a cross-sectional epidemiological study. *JAMA* **277**:231–237.
- Halpert J, Hammond D, and Neal RA (1980) Inactivation of purified rat liver cytochrome P-450 during the metabolism of parathion (diethyl p-nitrophenyl phosphorothionate). *J Biol Chem* **255**:1080–1089.
- Heydari A, Yeo KR, Lennard MS, Ellis SW, Tucker GT, and Rostami-Hodjegan A (2004) Mechanism-based inactivation of CYP2D6 by methylendioxyamphetamine. Short communication. *Drug Metab Dispos* **32**:1213–1217.
- Lee AJ, Cai XM, Thomas PE, Conney AH, and Zhu BT (2003) Characterization of the oxidative metabolites of 17 β -estradiol and estrone formed by 15 selectively expressed human cytochrome P450 isoforms. *Endocrinology* **144**:3382–3398.
- Lee AJ, Kosh JW, Conney AH, and Zhu BT (2001) Characterization of the NADPH-dependent metabolism of 17 β -estradiol to multiple metabolites by human liver microsomes and selectively expressed human cytochrome P450 3A4 and 3A5. *J Pharmacol Exp Ther* **298**:420–432.
- Lee CA, Kadwell SH, Kost TA, and Serabjit-Singh CJ (1995) CYP 3A4 expressed by insect cells infected with a recombinant baculovirus containing both CYP 3A4 and human NADPH-cytochrome P450 reductase is catalytically similar to human liver microsomal CYP 3A4. *Arch Biochem Biophys* **319**:157–167.
- Lehmann JM, McKee DD, Watson MA, Willson TM, Moore JT, and Klierer SA (1998) The human orphan nuclear receptor PXR is activated by compounds that regulate CYP3A4 gene expression and cause drug interactions. *J Clin Invest* **102**:1016–1023.
- McCain WF, Lee R, Johnson MS, Whaley JE, Ferguson JW, Beall P, and Leach G (1997) Acute oral toxicity study of pyridostigmine bromide, permethrin and DEET in the laboratory rat. *J Toxicol Environ Health* **50**:113–124.
- Neal RA (1980) Microsomal metabolism of thiono-sulfur compounds: mechanisms and toxicological significance. *Rev Biochem Toxicol* **2**:131–171.
- Neal RA and Halpert J (1982) Toxicology of thiono-sulfur compounds. *Ann Rev Pharmacol Toxicol* **22**:321–339.
- Nelson DR, Koymans L, Kamataki T, Stegeman JJ, Feyereisen R, Waxman DJ, Waterman MR, Gotoh O, Coon MJ, Estabrook RW, et al. (1996) P450 superfamily: update on new sequences, gene mapping, accession numbers and nomenclature. *Pharmacogenetics* **6**:1–42.
- Norman BJ, Poore RE, and Neal RA (1974) Studies of the binding of sulfur released in the mixed-function oxidase catalyzed metabolism of diethyl p-nitrophenyl phosphorothionate (parathion) to diethyl p-nitrophenyl phosphate (paraoxon). *Biochem Pharmacol* **23**:1733–1744.
- Shimada T and Guengerich FP (1989) Evidence for cytochrome P450_{NF}, the nifedipine oxidase, being the principle enzyme involved in the bioactivation of aflatoxins in human liver. *Proc Natl Acad Sci USA* **86**:462–465.
- Shimada T, Yamazaki H, Mimura M, Inui Y, and Guengerich FP (1994) Interindividual variations in human liver cytochrome P-450 enzymes involved in the oxidation of drugs, carcinogens and toxic chemicals: studies with liver microsomes of 30 Japanese and 30 Caucasians. *J Pharmacol Exp Ther* **270**:414–423.
- Silverman RB (1995) Mechanism-based enzyme inactivators, in *Enzyme Kinetics and Mechanism, Part D: Developments in Enzyme Dynamics*, vol 249 (Purich DL ed), pp 240–283, Academic Press, London.
- Suchar LA, Chang RL, Rosen RT, Lech J, and Conney AH (1995) High-performance liquid chromatography separation of hydroxylated estradiol metabolites: formation of estradiol metabolites by liver microsomes from male and female rats. *J Pharmacol Exp Ther* **272**:197–206.
- Szklarz GD and Halpert JR (1998) Molecular basis of P450 inhibition and activation: implications for drug development and drug therapy. *Drug Metab Dispos* **26**:1179–1184.
- Tang J, Cao Y, Rose RL, and Hodgson E (2002) In vitro metabolism of carbaryl by human cytochrome P450 and its inhibition by chlorpyrifos. *Chem Biol Interact* **141**:229–241.
- Usmani KA, Rose RL, Goldstein JA, Taylor WG, Brimfield AA, and Hodgson E (2002) In vitro human metabolism and interactions of repellent N,N-diethyl-m-toluamide. *Drug Metab Dispos* **30**:289–294.
- Usmani KA, Rose RL, and Hodgson E (2003) Inhibition and activation of the human liver microsomal and human cytochrome P450 3A4 metabolism of testosterone by deployment-related chemicals. *Drug Metab Dispos* **31**:384–391.
- Waxman DJ, Attisano C, Guengerich FP, and Lapenson DP (1988) Human liver microsomal steroid metabolism: identification of the major microsomal steroid hormone 6 β -hydroxylase cytochrome P-450 enzyme. *Arch Biochem Biophys* **263**:424–436.
- Williams PA, Cosme J, Vinkovic DM, Ward A, Angove HC, Day PJ, Vornhein C, Tickle IJ, and Jhoti H (2004) Crystal structures of human cytochrome P450 3A4 bound to metyrapone and progesterone. *Science (Wash DC)* **305**:683–686.
- Wilson AS, Davis CD, Williams DP, Buckpitt AR, Pirmohamed M, and Park BK (1996) Characterisation of the toxic metabolite(s) of naphthalene. *Toxicology* **114**:233–242.
- Wilson JD, Foster DW, Kronenberg HM, and Larsen JR (1998) *Williams Textbook of Endocrinology*. Saunders, Philadelphia.
- Wilson VS and LeBlanc GA (1998) Endosulfan elevates testosterone biotransformation and clearance in CD-1 mice. *Toxicol Appl Pharmacol* **148**:158–168.
- Yamazaki H, Shaw PM, Guengerich FP, and Shimada T (1998) Roles of cytochromes P450 1A2 and 3A4 in the oxidation of estradiol and estrone in human liver microsomes. *Chem Res Toxicol* **11**:659–665.
- Yano JK, Wester MR, Schoch GA, Griffin KJ, Stout CD, and Johnson EF (2004) The structure of human microsomal cytochrome P450 3A4 determined by X-ray crystallography to 2.05-Å resolution. *J Biol Chem* **279**:38091–38094.

Address correspondence to: Ernest Hodgson, Department of Environmental and Molecular Toxicology, Box 7633, North Carolina State University, Raleigh, NC 27695. E-mail: ernest_hodgson@ncsu.edu

METABOLISM OF CHLORPYRIFOS BY HUMAN CYTOCHROME P450 ISOFORMS AND HUMAN, MOUSE, AND RAT LIVER MICROSOMES

JUN TANG, YAN CAO, RANDY L. ROSE, ALAN A. BRIMFIELD, DIANA DAI, JOYCE A. GOLDSTEIN, AND ERNEST HODGSON

Department of Environmental and Molecular Toxicology, North Carolina State University, Raleigh, North Carolina (J.T., Y.C., R.L.R., E.H.); United States Army Medical Research Institute of Chemical Defense, Aberdeen Proving Ground, Maryland (A.A.B.); and National Institute of Environmental Health Sciences, Research Triangle Park, North Carolina (D.D., J.A.G.)

(Received March 19, 2001; accepted June 8, 2001)

This paper is available online at <http://dmd.aspetjournals.org>

ABSTRACT:

One of the factors determining the toxicity of chlorpyrifos (CPS), an organophosphorus (OP) insecticide, is its biotransformation. CPS can be activated by cytochrome P450 (CYP) through a desulfuration reaction to form chlorpyrifos-oxon (CPO), a potent anticholinesterase. CPS can also be detoxified by CYP through a dearylation reaction. Using pooled human liver microsomes (HLM), a $K_{m_{app}}$ of 30.2 μM and $V_{max_{app}}$ of 0.4 nmol/min/mg of protein was obtained for desulfuration, and a $K_{m_{app}}$ of 14.2 μM and a $V_{max_{app}}$ of 0.7 nmol/min/mg of protein was obtained for dearylation. These activities are lower than those obtained from rat liver microsomes. Gender differences in humans were also observed with female HLM possessing greater activity than male HLM. Use of human CYP isoforms expressed in human lymphoblastoma cells demonstrated

that CYP1A2, 2B6, 2C9*1, 2C19, and 3A4 are involved in CPS metabolism. CYP2B6 has the highest desulfuration activity, whereas dearylation activity is highest for 2C19. CYP3A4 has high activity for both dearylation and desulfuration. The use of phenotyped individual HLM demonstrated that predictions of metabolic activation and/or detoxication could be made based on relative amounts of CYP2B6, 2C19, and 3A4 in the microsomes. Thus, individuals with high CYP2C19 but low 3A4 and 2B6 are more active in dearylation than in desulfuration. Similarly, individuals possessing high levels of CYP2B6 and 3A4 have the greatest potential to form the activation product. These differences between individuals suggest that differential sensitivities to CPS may exist in the human population.

Chlorpyrifos [*O,O*-diethyl-*O*-(3,5,6-trichloro-2-pyridinyl)-phosphorothioate] (CPS¹) is a widely used organophosphorus (OP) insecticide. It has numerous agricultural applications and, until recently, has been used for termite control in foundations and for the control of nuisance insects and disease vectors in homes and during military deployments. The extensive use of CPS inevitably results in human exposure and has the potential to cause toxic effects.

The *in vivo* toxicity of CPS is a result of its bioactivation by cytochrome P450 (CYP)-mediated monooxygenases to a more potent cholinesterase inhibitor, chlorpyrifos-oxon (CPO). This oxidation reaction, which proceeds through a possible phosphooxythiiran intermediate, can result in either a desulfuration reaction that generates the

oxon or a dearylation reaction that degrades the parent compound (Chambers, 1992) (Fig. 1).

Studies of parathion, a related organophosphate, have shown that parathion oxidation is catalyzed by human CYP1A2, 2B6, and 3A4 and that its oxidation is highly correlated to CYP3A4 activity in human liver microsomes (HLM) (Butler and Murray, 1997; Mutch et

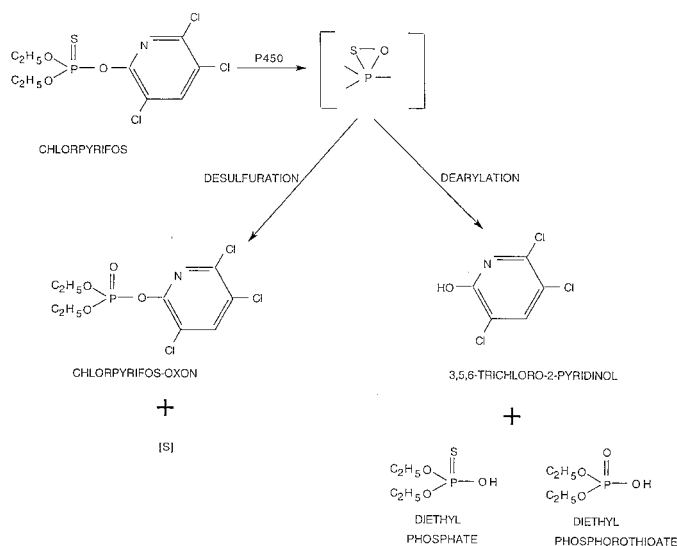


FIG. 1. Cytochrome P450-dependent metabolism of phosphorothioates illustrated with chlorpyrifos.

This work was supported by the North Carolina Department of Agriculture (NCDA) Pesticide Environmental Trust Fund and U.S. Army Cooperative Agreement DAMD 17-00-2-0008. Preliminary studies were presented at the 10th North American International Society for the Study of Xenobiotics (ISSX) meeting in Indianapolis, 2000 and the 40th Society of Toxicology (SOT) annual meeting in San Francisco, 2001.

¹ Abbreviations used are: CPS, chlorpyrifos; CPO, chlorpyrifos-oxon; TCP, 3,5,6-trichloro-2-pyridinol; OP, organophosphorus; HLM, human liver microsomes; RLM, rat liver microsomes; MLM, mouse liver microsomes; CYP, cytochrome P450; HPLC, high-performance liquid chromatography.

Address correspondence to: Dr. Ernest Hodgson, Department of Environmental and Molecular Toxicology, Box 7633, North Carolina State University, Raleigh, NC 27695. E-mail: ernest_hodgson@ncsu.edu

TABLE 1

Dearylation and desulfuration activities toward chlorpyrifos in HLM, RLM, or MLM

Activities are expressed as mean \pm S.E.M. ($n = 3$ determinations), means in RLM (pooled from three male rats) and MLM (pooled from three male mice) significantly different than HLM (pooled from 10 donors) are indicated by * $p < 0.05$ or ** $p < 0.01$.

	Desulfuration			Dearylation		
	$K_{m_{app}}$ μM	$V_{max_{app}}$ nmol/mg protein/min	$V_{max_{app}}/K_{m_{app}}$	$K_{m_{app}}$ μM	$V_{max_{app}}$ nmol/mg protein/min	$V_{max_{app}}/K_{m_{app}}$
HLM	30.2 \pm 1.7	0.4 \pm 0.1	0.01	14.2 \pm 2.2	0.7 \pm 0.1	0.05
RLM	6.1 \pm 1.1**	1.0 \pm 0.2*	0.17	4.8 \pm 1.8*	2.1 \pm 0.4**	0.43
MLM	24.4 \pm 2.4	0.7 \pm 0.1	0.03	14.9 \pm 3.0	2.7 \pm 0.1**	0.18

al., 1999). Other studies using specific chemical inhibitors for human CYP isoforms demonstrated that both CYP2D6 and CYP3A4 were active in the desulfuration of parathion, CPS, and diazinon (Sams et al., 2000).

The present study was designed to 1) determine oxidation activities toward CPS in human, mouse, and rat liver microsomes in the same assay system, 2) identify the human CYP isoforms and CYP polymorphic forms responsible for CPS oxidation, and 3) examine the differences in CPS oxidation activities among liver microsomes from selected individual humans.

Materials and Methods

Chemicals. CPS, CPO, and 3,5,6-trichloro-2-pyridinol (TCP) were purchased from ChemService (West Chester, PA). HPLC grade acetonitrile and methanol were purchased from Fisher Scientific (Fair Lawn, NJ). All other chemicals, if not specified, were purchased from Sigma (St. Louis, MO).

Rodent Liver Microsome Preparation. Rat liver microsomes (RLM) and mouse liver microsomes (MLM) were prepared from adult male Long-Evans rats and adult male CD-1 mice (Charles River Laboratories, Raleigh, NC), respectively, according to the method of Cook and Hodgson (1983). Briefly, immediately after sacrificing the animals, the fresh livers were removed, weighed, minced, and then homogenized with a Polytron homogenizer (Brinkmann Instruments, Westbury, NY) in 50 mM potassium phosphate buffer (pH 7.5) containing 0.1 mM EDTA and 1.15% potassium chloride. The homogenate was centrifuged at 10,000g for 15 min. The supernatant was filtered through glass wool and centrifuged at 100,000g for 1 h. The pellet was resuspended in 50 mM potassium phosphate buffer (pH 7.5) containing 0.1 mM EDTA and 0.25 M sucrose. All processes were performed at 0 to 4°C. The microsomal preparation was aliquoted and stored at $-80^{\circ}C$ until use. Protein concentration was determined using a BCA kit (Pierce, Rockford, IL).

Human Liver Microsomes and Human Cytochrome P450 Isoforms. Pooled HLM (pooled from 10 donors), individual HLM, and human lymphoblast-expressed CYP1A1, 1A2, 2A6, 2B6, 2C8, 2C9*1 (Arg₁₄₄, Ile₃₅₉), 2C9*2 (Cys₁₄₄), 2C19, 2D6*1 (2D6-Val), 2E1, 3A4, and 4A11 were purchased from GENTEST (Woburn, MA). Pooled male and pooled female HLM (pooled from 10 male donors and 10 female donors, respectively) were purchased from Xenotech, LLC (Kansas City, KS). Different mutant alleles of human CYP2C19 were expressed in *Escherichia coli*, according to the method of Luo et al. (1998). NADPH-CYP reductase was obtained from Oxford Biomedical Sciences (Oxford, MI).

In Vitro Chlorpyrifos Metabolism. Enzyme kinetic assays for microsomes were performed by incubation of serial concentrations of CPS (final concentration range, 2–100 μM) with microsomes in 100 mM Tris-HCl buffer (pH 7.4 at 37°C) containing 5 mM MgCl₂ and 3 mM EDTA for 5 min. The microsomal protein concentrations used in assays were 1.5 mg/ml for HLM, 0.5 mg/ml for RLM, and 1 mg/ml for MLM. After preincubation at 37°C for 3 min, reactions were started by the addition of an NADPH-generating system (0.25 mM NADP, 2.5 mM glucose 6-phosphate, and 2 U/ml glucose-6-phosphate dehydrogenase). The controls were identical except for the absence of an NADPH-generating system. Reactions were terminated by adding an equal volume of ice-cold methanol and vortexing. After 5 min of centrifugation at 15,000 rpm in a microcentrifuge, the supernatants were analyzed for CPO and TCP concentrations by HPLC.

Metabolic activity assays for human lymphoblast-expressed CYP isoforms

were performed by incubation of CPS (final concentration, 100 μM) with CYP isoforms (final protein concentration, 0.9 mg/ml; final P450 contents, 23.4–180 pmol/ml) for 20 min in CYP-specific buffers recommended by the supplier (GENTEST). For CYP1A1, 1A2, 2D6, and 3A4, 100 mM potassium phosphate buffer with 3.3 mM MgCl₂ (pH 7.4) was used. For CYP2B6, 2C8, 2C19, and 2E1, 50 mM potassium phosphate buffer with 3.3 mM MgCl₂ (pH 7.4) was used. For CYP2C9*1, 2C9*2, and 4A11, the buffer was 100 mM Tris-HCl buffer with 3.3 mM MgCl₂ (pH 7.5), whereas for CYP2A6, 50 mM Tris-HCl buffer with 3.3 mM MgCl₂ (pH 7.4) was used.

The metabolic activity assays for *E. coli*-expressed human CYP2C19s were performed according to the method of Klose et al. (1998). Briefly, L- α -phosphatidylcholine (0.3 μg /pmol of P450), CYP reductase (4 pmol/pmol of P450), and CYP2C19 (24 pmol) were combined and preincubated at 37°C for 5 min. This mixture then was incubated with 100 μM CPS in 50 mM potassium phosphate buffer with 3.3 mM MgCl₂ (pH 7.4) for 10 min. The reaction was initiated with NADPH-generating system as described previously. Assays of individual HLM (final protein concentration, 1.5 mg/ml) with CPS (final concentration, 100 μM) were described previously.

Analysis of Metabolites by HPLC. The HPLC system used in this study consisted of two Shimadzu (Kyoto, Japan) pumps (LC-10AT), a Shimadzu auto injector (SIL-10AD VP), and a Waters 486 tunable absorbance detector (Milford, MA). The mobile phase for pump A was 10% acetonitrile, 89% water, and 1% phosphoric acid, whereas that for pump B was 99% acetonitrile and 1% phosphoric acid. A gradient system was initiated at 20% pump B and increased to 100% pump B in 20 min. The flow rate was 1 ml/min. Metabolites were separated by a C₁₈ column (Luna 5 μm , 150 \times 3 mm; Phenomenex, Rancho Palos Verdes, CA) and detected at 230 nm. Using this system, the retention times obtained for TCP, CPO, and CPS were 8.5, 12, and 17 min, respectively. The limits of detection for TCP and CPO were 0.03 and 0.04 μM , respectively, at an injection volume of 15 μl . Concentrations of metabolites were obtained by extrapolation of peak height from a standard curve. $K_{m_{app}}$ and $V_{max_{app}}$ were obtained using a Hanes-Woolf plot (Segel, 1975).

Statistics. Significant differences between data sets were determined by one-way analysis of variance, and multiple comparisons were performed with the Tukey-Kramer method using an SAS program (SAS, 1989).

Results

The protein concentrations and incubation times used in the assays were within linear ranges determined in preliminary experiments. No metabolites were detected when incubations were carried out in the absence of an NADPH-generating system.

HLM displayed lower affinity (i.e., higher $K_{m_{app}}$) and lower reaction velocity toward CPS for both desulfuration and dearylation than RLM (Table 1). Compared with HLM, MLM exhibited similar affinities but a higher reaction velocity toward CPS (Table 1). Both RLM and MLM have higher values of clearance terms (V_{max}/K_m) than HLM. Pooled female HLM showed significantly higher metabolic activity toward CPS than pooled male HLM (Table 2).

A screen of several human CYP isoforms demonstrated that CYP1A2, 2B6, 2C9*1, 2C19, and 3A4 were involved in CPS metabolism (Table 3), whereas no oxidation activity toward CPS was detected using CYP1A1, 2A6, 2C8, 2C9*2, 2D6, 2E1, and 4A11. Desulfuration and dearylation activities were greatest for CYP2B6

TABLE 2

Metabolic activities toward chlorpyrifos in pooled male and female HLM

Activities are expressed as mean \pm S.E.M. ($n = 3$ determinations), means in female HLM (pooled from 10 donors) significantly different than male HLM (pooled from 10 donors) are indicated by * $p < 0.05$ or ** $p < 0.01$. Protein concentration and cytochrome P450 content in microsomes are provided by the supplier (XenoTech, LLC).

	Desulfuration		Dearylation	
	nmol/mg protein/ min	nmol/nmol P450/ min	nmol/mg protein/ min	nmol/nmol P450/min
Male	0.24 \pm 0.01	0.54 \pm 0.01	0.47 \pm 0.01	1.05 \pm 0.03
Female	0.56 \pm 0.02**	0.89 \pm 0.02**	0.78 \pm 0.02**	1.23 \pm 0.04*

TABLE 3

Metabolic activities toward chlorpyrifos in human lymphoblast-expressed cytochrome P450 isoforms

Activities are expressed as nanomoles of product per nanomoles of P450 per minute \pm S.E.M. ($n = 3$ determinations).

	Desulfuration*	Dearylation*	Desulfuration/Dearylation
1A2	0.39 \pm 0.06 ^a	0.23 \pm 0.05 ^a	1.70
2B6	1.59 \pm 0.12 ^b	0.47 \pm 0.03 ^a	3.38
2C9	0.32 \pm 0.06 ^a	0.90 \pm 0.10 ^{ab}	0.36
2C19	0.30 \pm 0.08 ^a	2.09 \pm 0.42 ^b	0.14
3A4	0.52 \pm 0.13 ^a	0.79 \pm 0.24 ^{ab}	0.66

* Means in the same column followed by the same letter are not significantly different, $p < 0.01$.

and CYP2C19, respectively. Marked decreases in metabolic activity toward CPS were observed with different polymorphic alleles of CYP2C19 (Table 4).

To determine the variation range of CPS metabolism between individuals, we examined CPS metabolism from five individuals representing contrasting activities of some important CYP isoforms (Table 5). Individuals with high levels of CYP2B6 and 3A4 (HG042 and 112) had high-desulfuration activity; individuals with low levels of CYP2B6 and 3A4 (HG006, 023 and 043) had low-desulfuration activity. The dearylation pathway was more predominant in the individual (HG043) with high-CYP2C19 but low-3A4 levels. No particular increase in either metabolite was observed in the individual (HG023) with high levels of CYP2D6.

Discussion

The metabolic intrinsic clearance rates (V_{\max}/K_m) indicate that liver microsomes from all three species more readily produce a detoxication product (i.e., TCP) than an activation product (i.e., CPO). These observations are similar to previous reports on rodents (Sultatos and Murphy, 1983; Ma and Chambers, 1995). The clearance rates also demonstrate that pooled HLM are less active than RLM and MLM in both desulfuration and dearylation, suggesting that less TCP and CPO are generated in the human liver than in the rodent liver immediately after exposure to CPS.

Consistent with data on other substrates provided by the supplier (XenoTech, LLC) regarding gender differences in CYP activity, pooled female HLM showed higher activities in both desulfuration and dearylation of CPS than pooled male HLM. Note that this gender difference was demonstrated using only one pool of 10 males and 10 females, respectively. It is not known whether this difference would also be true in a larger population. These data contrast with CYP activities in rats because males are more active in CPS desulfuration than females (Chambers and Chambers, 1989; Sultatos, 1991).

Our results show that human lymphoblast-expressed CYP1A2, 2B6, 2C9*1, 2C19, and 3A4 are responsible for both dearylation and desulfuration of CPS, whereas CYP1A1, 2A6, 2C8, 2C9*2, 2D6*1,

TABLE 4

Metabolic activities toward chlorpyrifos in CYP2C19 expressed in E. Coli

Activities are expressed as nanomoles of product per nanomoles of P450 per minute \pm S.E.M. ($n = 3$ determinations). Means in the same column followed by the same letter are not significantly different, $p < 0.01$.

	Desulfuration	Dearylation
	nmol product/nmol P450	
2C19*1B	0.68 \pm 0.03	6.11 \pm 0.28 ^a
2C19*8	not detected	1.66 \pm 0.07 ^b
2C19*6	not detected	0.69 \pm 0.05 ^c
2C19*5	not detected	0.68 \pm 0.06 ^c

TABLE 5

Metabolic activities toward chlorpyrifos in individual human liver microsomes

Activities are expressed as mean \pm S.E.M., ($n = 3-4$ determinations). Individual human liver microsomes (protein concentration, 20 mg/ml). CYP2B6, 2C19, 2D6, and 3A4 activities (pmol/mg of protein/min), represented by (*S*)-mephenytoin *N*-demethylase, (*S*)-mephenytoin 4'-hydroxylase, bufuralol 1'-hydroxylase, and testosterone 6 β -hydroxylase catalytic activities, respectively, are 3.1, 36, not detectable and 2990 for HG006 (16-year-old male), 12.2, 78.1, 160 and 4050 for HG023 (25-year-old male), 140, 3.5, 110 and 14530 for HG042 (48-year-old female), 7.4, 212, 10.6 and 3408 for HG043 (23-year-old female), and 59.1, 260.0, 23 and 17519 for HG112 (2-year-old female) (data were provided by GENTEST).

	Desulfuration*	Dearylation*
	nmol/mg protein/min	
HG006	0.09 \pm 0.01 ^a	0.35 \pm 0.03 ^a
HG023	0.16 \pm 0.01 ^a	0.31 \pm 0.04 ^a
HG042	0.74 \pm 0.10 ^b	0.67 \pm 0.07 ^{ab}
HG043	0.08 \pm 0.01 ^a	0.61 \pm 0.04 ^{ab}
HG112	0.67 \pm 0.08 ^b	0.91 \pm 0.10 ^b

* Means in the same column followed by the same letter are not significantly different, $p < 0.01$.

2E1, and 4A11 did not display detectable activities toward CPS oxidation. These results are similar to those of a parathion metabolism study (Butler and Murray, 1997), where CYP1A2, 2B6, and 3A4 were shown to have high-desulfuration activities toward parathion. CYP2B6 more readily generates the oxon, similar to phenobarbital-induced CYP2B isoforms in rodents (Fabrizi et al., 1999; Levi et al., 1988). CYP2C19 exhibits the greatest dearylation activity and relatively low-desulfuration activity. Genetic polymorphisms have been identified in CYP2C19 (Demorais et al., 1994), and differential metabolic activities toward CPS by different variants of CYP2C19 were observed in this study. Dearylation by the polymorphic CYP2C19 alleles was significantly less than that of the wild-type forms, which could influence the in vivo toxicity of CPS in individuals possessing these alleles.

CYP3A4 is also a highly active, although not the most active, isoform in CPS metabolism. The fact that CYP3A4 is the most abundant CYP isoform in human liver (Shimada et al., 1994) suggests that this isoform plays a significant in vivo role in both desulfuration and dearylation. CYP2C9*1 (Arg₁₄₄) showed some activities in both desulfuration and dearylation of CPS, whereas CYP2C9*2 (Cys₁₄₄), a single amino acid difference, showed no detectable activity toward CPS. CYP2C9*1 and 1A2, although not the most active isoforms for either desulfuration or dearylation, may play a role in vivo. A previous study using specific chemical inhibitors and human lymphoblastoid cell-expressed CYP2D6 suggested that CYP2D6 plays a significant role in desulfuration of parathion, CPS, and diazinon (Sams et al., 2000). Our work with CPS did not reveal any metabolites using human lymphoblast-expressed CYP2D6, nor did HLM with high-CYP2D6 activity (HG023) produce a significant amount of the oxon metabolite.

Potential differences in the human population with respect to CPS metabolism were further examined using different individual HLM.

References

Individuals with varying levels of CYP2B6, 2C19, 2D6, and 3A4 were selected to represent contrasting levels of predicted metabolic activity. Thus, individuals (HG042 and HG112) possessing high levels of CYP2B6 and CYP3A4 would be expected to possess greater ability to form the desulfuration product than those (HG006, HG023, and HG043) with lower levels of these isoforms, as observed (Table 5). Similarly, individuals with greater levels of CYP2C19 or CYP3A4, such as HG042, HG043, and HG112, would also be expected to produce more of the dearylation product than those with significantly lower levels of these isoforms (HG006 and HG023). Because individuals with contrasting levels of CYP2B6 and 3A4 were not available, we were unable to differentiate the extent of their contribution to desulfuration separately. However, based on its content in human liver, CYP3A4 should contribute significantly to both desulfuration and dearylation, as has been previously observed (Butler and Murray, 1997; Mutch et al., 1999; Sams et al., 2000).

Using our selection of five individuals, the variations between individual HLM in desulfuration of CPS were around 8-fold and that for dearylation was 3-fold and would presumably be greater if more samples were examined. For parathion, the difference between individual HLM in dearylation and desulfuration is as great as 10- and 16-fold, respectively (Butler and Murray, 1997; Mutch et al., 1999). Considerations of metabolic differences between individuals should also consider the contributions of esterases, which are also major factors determining the in vivo toxicities of OP compounds (Maxwell et al., 1987; Chambers et al., 1990; Costa et al., 1990).

In conclusion, HLM use the same pathways as RLM and MLM to metabolize CPS, although activities were generally lower in humans than in rodents. From pools of 10 individuals, female HLM displayed a higher activity in CPS metabolism than male HLM. Human lymphoblast-expressed CYP1A2, 2B6, 2C9*1, 2C19, and 3A4 showed oxidation activities toward CPS, whereas no activities were detected for CYP1A1, 2A6, 2C8, 2C9*2, 2D6, 2E1, and 4A11. Although CYP2C19 and 2B6 displayed the greatest dearylation and desulfuration activities, respectively, 3A4 was highly active in both reactions. Activities of CYP2B6, 2C19, and 3A4 greatly affect CPS metabolism in HLM.

- Butler AM and Murray M (1997) Biotransformation of parathion in human liver: participation of CYP3A4 and its inactivation during microsomal parathion oxidation. *J Pharmacol Exp Ther* **280**:966–973.
- Chambers H, Brown B and Chambers JE (1990) Noncatalytic detoxication of six organophosphorus compounds by rat liver homogenates. *Pestic Biochem Physiol* **36**:308–315.
- Chambers HW (1992) Organophosphorus compounds: an overview, in *Organophosphates: Chemistry, Fate, and Effects* (Chambers JE and Levi PE eds) pp 3–17, Academic Press, San Diego, CA.
- Chambers JE and Chambers HW (1989) Oxidative desulfuration of chlorpyrifos, chlorpyrifos-methyl, and leptophos by rat brain and liver. *J Biochem Toxicol* **4**:201–203.
- Cook JC and Hodgson E (1983) Induction of cytochrome P-450 by methylenedioxyphenyl compounds: importance of the methylene carbon. *Toxicol Appl Pharmacol* **68**:131–139.
- Costa LG, McDonald BE, Murphy SD, Omenn GS, Richter RJ, Motulsky AG and Furlong CE (1990) Serum paraoxonase and its influence on paraoxon and chlorpyrifos-oxon toxicity in rats. *Toxicol Appl Pharmacol* **103**:66–76.
- Demorais SMF, Wilkinson GR, Blaisdell J, Nakamura K, Meyer UA and Goldstein JA (1994) The major genetic defect responsible for the polymorphism of S-mephenytoin metabolism in humans. *J Biol Chem* **269**:15419–15422.
- Fabrizi L, Gemma S, Testai E and Vitzozzi L (1999) Identification of the cytochrome P450 isoenzymes involved in the metabolism of diazinon in the rat liver. *J Biochem Mol Toxicol* **13**:53–61.
- Klose TS, Ibeanu GC, Ghanayem BI, Pedersen LG, Li L, Hall SD and Goldstein JA (1998) Identification of residues 286 and 289 as critical for conferring substrate specificity of Human CYP2C9 for diclofenac and ibuprofen. *Arch Biochem Biophys* **357**:240–248.
- Levi PE, Hollingworth RM and Hodgson E (1988) Differences in oxidative dearylation and desulfuration of fenitrothion by cytochrome P-450 isozymes and in the subsequent inhibition of monooxygenase activity. *Pestic Biochem Physiol* **32**:224–231.
- Luo G, Zeldin DC, Blaisdell JA, Hodgson E and Goldstein JA (1998) Cloning and expression of murine CYP2Cs and their ability to metabolize arachidonic acid. *Arch Biochem Biophys* **357**:45–57.
- Ma T and Chambers JE (1995) A kinetic analysis of hepatic microsomal activation of parathion and chlorpyrifos in control and phenobarbital-treated rats. *J Biochem Toxicol* **10**:63–68.
- Maxwell DM, Brecht KM and O'Neill BL (1987) The effect of carboxylesterase inhibition on interspecies differences in soman toxicity. *Toxicol Lett* **39**:35–42.
- Mutch E, Blain PG and Williams FM (1999) The role of metabolism in determining susceptibility to parathion toxicity in man. *Toxicol Lett* **107**:177–187.
- Sams C, Mason HJ and Rawbone R (2000) Evidence for the activation of organophosphate pesticides by cytochromes P450 3A4 and 2D6 in human liver microsomes. *Toxicol Lett* **116**:217–221.
- SAS (1989) *JMP User's Guide*. SAS Institute, Cary, NC.
- Segel IH (1975) *Biochemical Calculations*. John Wiley & Sons, Inc., New York.
- Shimada T, Yamazaki H, Mimura M, Inui Y and Guengerich FP (1994) Interindividual variations in human liver cytochrome P-450 enzymes involved in the oxidation of drugs, carcinogens and toxic chemicals: studies with liver microsomes of 30 Japanese and 30 Caucasians. *J Pharmacol Exp Ther* **270**:414–423.
- Sultatos LG (1991) Metabolic-activation of the organophosphorus insecticides chlorpyrifos and fenitrothion by perfused-rat-liver. *Toxicology* **68**:1–9.
- Sultatos LG and Murphy SD (1983) Kinetic analysis of the microsomal biotransformation of the phosphorothioate insecticides chlorpyrifos and parathion. *Fundam Appl Toxicol* **3**:16–21.

Metabolism of Endosulfan- α by Human Liver Microsomes and Its Utility as a Simultaneous *In Vitro* Probe for CYP2B6 and CYP3A4

Richard C. T. Casabar, Andrew D. Wallace, Ernest Hodgson, and Randy L. Rose¹

Department of Environmental and Molecular Toxicology, North Carolina State University, Raleigh, North Carolina

Received March 31, 2006; accepted July 18, 2006

ABSTRACT:

Endosulfan- α is metabolized to a single metabolite, endosulfan sulfate, in pooled human liver microsomes ($K_m = 9.8 \mu\text{M}$, $V_{\max} = 178.5 \text{ pmol/mg/min}$). With the use of recombinant cytochrome P450 (P450) isoforms, we identified CYP2B6 ($K_m = 16.2 \mu\text{M}$, $V_{\max} = 11.4 \text{ nmol/nmol P450/min}$) and CYP3A4 ($K_m = 14.4 \mu\text{M}$, $V_{\max} = 1.3 \text{ nmol/nmol P450/min}$) as the primary enzymes catalyzing the metabolism of endosulfan- α , although CYP2B6 had an 8-fold higher intrinsic clearance rate ($CL_{\text{int}} = 0.70 \mu\text{l/min/pmol P450}$) than CYP3A4 ($CL_{\text{int}} = 0.09 \mu\text{l/min/pmol P450}$). Using 16 individual human liver microsomes (HLMs), a strong correlation was observed with endosulfan sulfate formation and *S*-mephenytoin *N*-demethylase activity of CYP2B6 ($r^2 = 0.79$), whereas a moderate correlation with testosterone 6 β -hydroxylase activity of CYP3A4 ($r^2 =$

0.54) was observed. Ticlopidine ($5 \mu\text{M}$), a potent CYP2B6 inhibitor, and ketoconazole ($10 \mu\text{M}$), a selective CYP3A4 inhibitor, together inhibited approximately 90% of endosulfan- α metabolism in HLMs. Using six HLM samples, the percentage total normalized rate (% TNR) was calculated to estimate the contribution of each P450 in the total metabolism of endosulfan- α . In five of the six HLMs used, the percentage inhibition with ticlopidine and ketoconazole in the same incubation correlated with the combined % TNRs for CYP2B6 and CYP3A4. This study shows that endosulfan- α is metabolized by HLMs to a single metabolite, endosulfan sulfate, and that it has potential use, in combination with inhibitors, as an *in vitro* probe for CYP2B6 and 3A4 catalytic activities.

Endosulfan is an organochlorine pesticide and a contaminant at toxic superfund sites. It is currently applied as a broad-spectrum insecticide to a variety of vegetables, fruits, cereal grains, and cotton (USEPA, 2002). Endosulfan is sold under the tradename Thiodan and as a mixture of two isomers, namely 70% α - and 30% β -endosulfan (ATSDR, 2000). Endosulfan exposure has been shown to increase rodent liver weights and elevate microsomal enzyme levels (Gupta and Gupta, 1977). In mice, endosulfan exposure resulted in increased testosterone metabolism and clearance (Wilson and LeBlanc, 1998). Studies involving children suggest that long-term environmental exposure to endosulfan causes delayed male sexual maturation and reduced testosterone levels (Saiyed et al., 2003). The mechanism by which endosulfan exerts these effects may involve its ability to activate the human pregnane X receptor and induce the expression levels of cytochrome P450 (P450) enzymes, thereby increasing metabolic rates for steroid hormones.

Before beginning an investigation of endosulfan's possible endo-

This work was supported by National Institute for Occupational Safety and Health Grant OH 07551-ECU. R.C. was a recipient of the Air Force Institute of Technology scholarship. Results were presented at the 13th annual meeting of ISSX in Maui, HI, Oct 23-27, 2005 (*Drug Metab Rev* 37:244).

¹ This article is dedicated in memory of Dr. Randy Rose, who died in a tragic car accident.

Article, publication date, and citation information can be found at <http://dmd.aspetjournals.org>.

doi:10.1124/dmd.106.010199.

crine-disrupting effects, we wished to examine its metabolic pathway in humans. Until recently, there have been no published data on human metabolism of endosulfan or on the possible contributions of P450 isoforms to its metabolism. Based on animal studies, a proposed metabolic pathway for endosulfan was published by the Agency for Toxic Substances and Disease Registry (ATSDR, 2000) and is shown in Fig. 1. A study using cats reported the immediate presence of endosulfan sulfate in the liver following intravenous administration of endosulfan (Khanna et al., 1979). In rats administered a single oral dose of ¹⁴C-endosulfan, the metabolites sulfate, lactone, ether, and diol were detected in their feces 5 days later (Dorough et al., 1978). Analyses of human adipose tissue, placenta, umbilical cord serum, and milk samples demonstrated the presence of parent compound (α - and β -endosulfan) and metabolites endosulfan sulfate, diol, lactone, and ether, although the sulfate was the predominant degradation product (Cerrillo et al., 2005).

The present study determined that endosulfan- α is metabolized to a single metabolite, endosulfan sulfate, in human liver microsomes, and its metabolism is primarily mediated by CYP2B6 (at high efficiency) and CYP3A4 (at low efficiency). CYP2B6 is recognized to be expressed at only 3 to 5% of total P450s in human livers (Gervot et al., 1999; Lang et al., 2001), whereas CYP3A4 is known as the most abundant P450 isoform, expressed at 20 to 60% of total P450s in human liver. The respective levels of CYP2B6 and CYP3A4 in human liver microsomes in combination with their strong affinity to endosulfan- α ($K_m = 16.2$ and $14.4 \mu\text{M}$, respectively) and their corresponding

ABBREVIATIONS: P450, cytochrome P450; rP450, recombinant P450; HLM, human liver microsome; % TNR, percentage total normalized rate; % I, percentage inhibition; ACN, acetonitrile; FMO, flavin-containing monooxygenase; rFMO, recombinant FMO; NR, normalized rate; pHLM, pooled human liver microsome; M-M, Michaelis-Menten; CL_{int} , intrinsic clearance.

clearance rates of endosulfan ($CL_{int} = 0.70$ and $0.09 \mu\text{l}/\text{min}/\text{pmol}$ P450, respectively) presented a unique opportunity of investigating the potential of endosulfan- α to simultaneously probe for the in vitro catalytic activity of both CYP2B6 and 3A4.

Most, if not all, of the information in this communication was presented at the 13th annual ISSX meeting in Maui, HI on October 23 to 27, 2005 (Casabar et al., 2005). Subsequently, after the current communication had been prepared for submission, a manuscript was submitted and published from another laboratory (Lee et al., 2006). Lee et al. (2006) reported on the metabolism of α - and β -endosulfan isomers, whereas the present study only reports on the metabolism of

the α -isomer. Although the results from the two laboratories on metabolism of endosulfan- α are in general agreement, the current communication extends the findings in the development of endosulfan- α as a simultaneous probe for CYP2B6 and 3A4 in human liver microsomes.

Materials and Methods

Chemicals. Endosulfan- α , the predominant isomer (70%) in commercial endosulfan, was used in the study of endosulfan metabolism. Endosulfan- α , endosulfan sulfate, endosulfan diol, endosulfan ether, and endosulfan lactone reference materials were purchased from ChemService (West Chester, PA). Stock solutions of endosulfan- α and metabolites were prepared in acetonitrile (ACN) and stored at -20°C . NADP⁺, glucose 6-phosphate, and glucose-6-phosphate dehydrogenase were purchased from Sigma-Aldrich (St. Louis, MO). High-performance liquid chromatography (HPLC)-grade water, ACN, EDTA, magnesium chloride, Tris, and all other chemicals not specified were purchased from Fisher Scientific (Pittsburgh, PA).

Ticlopidine, a potent mechanism-based chemical inhibitor to CYP2B6 (Richter et al., 2004), and ketoconazole, a selective chemical inhibitor to CYP3A4 (Baldwin et al., 1995) were purchased from Sigma-Aldrich. Stock solutions of ticlopidine were prepared in distilled water and stored at room temperature. Ketoconazole was dissolved in methanol and stock solutions were stored at 4°C .

Human Liver Microsomes (HLMs) and P450 Isoforms. Pooled HLMs (20 mg/ml) and 16 selected individual HLMs (20 mg/ml each) were purchased from BD Biosciences (San Jose, CA). The individual HLMs chosen for this study were representative of the levels of *S*-mephenytoin *N*-demethylase activity of CYP2B6 as follows: Low, HG32, HG95, HH47, HG74, HK37; Mid, HG43, HG93, HH18, HK25, HH101, HG3; and High, HH13, HG89, HG64, HG112, HG42. Human recombinant P450 (rP450) and recombinant flavin monooxygenase (rFMO) isoforms expressed in baculovirus-infected insect cells (Supersomes) were also purchased from BD Biosciences.

Metabolism Assays. Preliminary studies were performed to determine the times and HLM protein concentrations that produced a linear metabolic rate for $50 \mu\text{M}$ endosulfan- α . Endosulfan sulfate formation was linear from 0.05 to 0.25 mg/ml protein and from 5 to 60 min of incubation. The solvent effects of dimethyl sulfoxide, acetone, ACN, methanol, ethanol, and isopropanol at 1% solvent concentration were also tested on endosulfan- α metabolism. There were no differences in the rates of endosulfan sulfate formation among the different solvents, with the exception of isopropanol, which slightly inhibited formation of endosulfan sulfate (data not shown).

Based on the results of initial studies, $20 \mu\text{M}$ endosulfan- α substrate concentration dissolved in ACN, 0.25 mg/ml HLM protein concentration, and 30-min incubation time were used for subsequent metabolism assays, unless

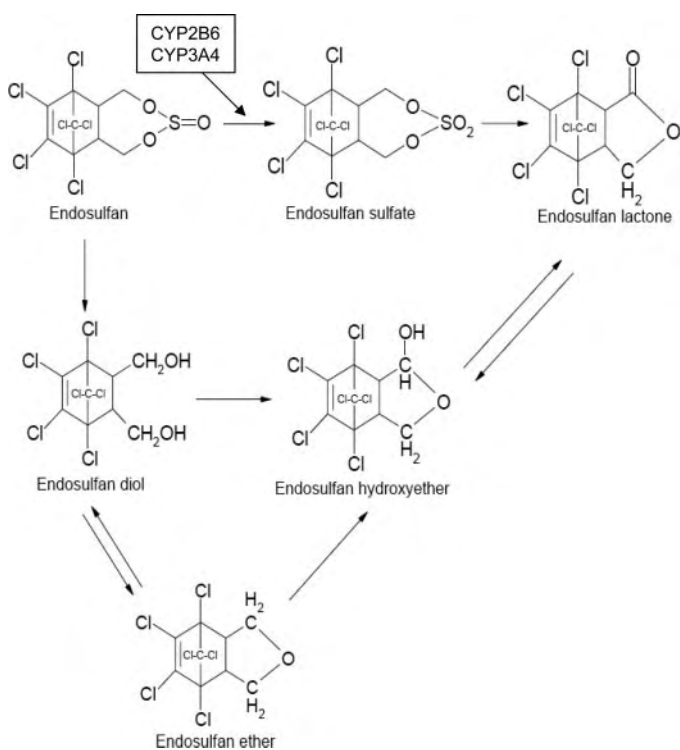


FIG. 1. The proposed metabolic pathway for endosulfan based on animal studies, as published by ATSDR (2000), was modified to show that human CYP2B6 and CYP3A4 primarily catalyze the metabolism of endosulfan- α to endosulfan sulfate, the only metabolite detected in the present study.

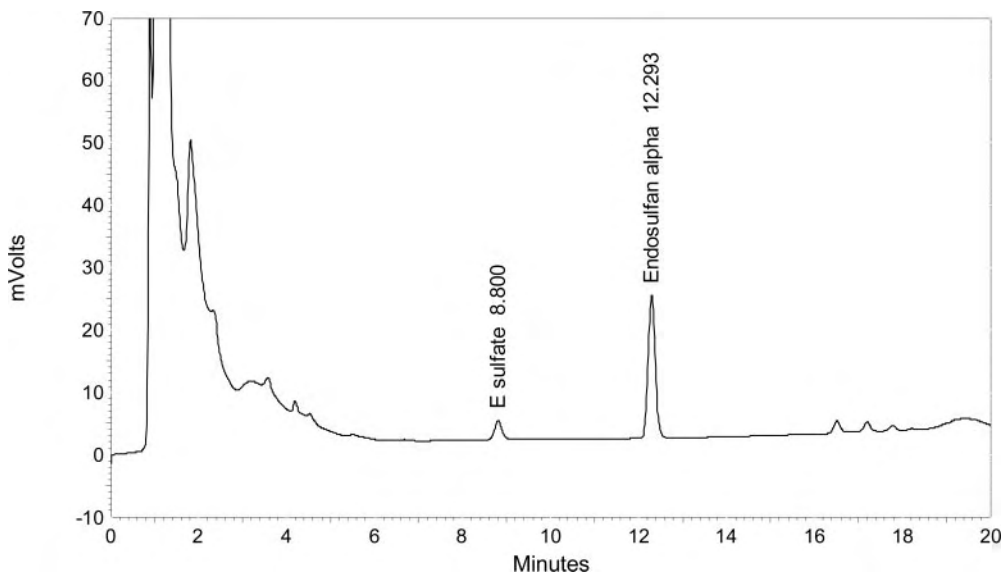


FIG. 2. A representative HPLC chromatogram of endosulfan- α metabolism to endosulfan sulfate, the lone metabolite detected in incubations with HLMs. Endosulfan- α ($50 \mu\text{M}$) was incubated with 0.25 mg/ml HLMs for 20 min. Endosulfan- α and endosulfan sulfate peaks were detected at retention times of 12.29 and 8.80 min, respectively, in a 20-min HPLC run. The three peaks toward the end of the chromatogram were determined to be contributions from HLMs.

otherwise stated. Metabolism assays with HLMs used 100 mM potassium phosphate buffer (pH 7.4). Metabolism with rP450s and rFMOs used the following buffers as recommended by BD Biosciences: 100 mM potassium phosphate (pH 7.4) for CYP1A1, 1A2, 3A4, 3A7, 2D6*1, 3A5, and SF9 insect control; 50 mM potassium phosphate (pH 7.4) for 2B6, 2C8, 2C19, and 2E1; 100 mM Tris (pH 7.4) for 2C9*1, 2C18, and 4A11; 50 mM Tris (pH 7.4) for 2A6; and 50 mM glycine (pH 9.5) for FMOs 1, 3, and 5. All buffers contained 3.3 mM MgCl₂ and 1 mM EDTA.

A preincubation mixture of endosulfan- α (20 μ M), HLMs (0.25 mg/ml) or rP450 isoforms (12.5 pmol), and buffer was prepared in 1.5-ml microcentrifuge tubes. This mixture was preincubated for 3 min at 37°C in a water bath with minimal agitation. NADPH-regenerating system (final concentration of 0.25 mM NADP⁺, 2.5 mM glucose 6-phosphate, and 2 U/ml glucose-6-phosphate dehydrogenase) was added to initiate the reaction. The final assay volume was 250 μ l.

Reactions were carried out for 30 min and terminated with 250 μ l of ice-cold ACN, followed by pulse-vortexing. Samples were centrifuged at 16,000g for 5 min and supernatants were analyzed by HPLC, as described in the HPLC analysis section below.

Inhibition Studies. Protocols for CYP2B6 and CYP3A4 inhibition by ticlopidine and ketoconazole used methods previously established by Richter et al. (2004) and Nomeir et al. (2001), respectively. In the case of ticlopidine, a mechanism-based inhibitor of CYP2B6, a 3-min preincubation at 37°C of ticlopidine (5 μ M) with HLMs (100 μ g) or rP450s (5 pmol) in 50 mM potassium phosphate buffer (with 3.3 mM MgCl₂ and 1 mM EDTA) in combination with an NADPH-regenerating system (final concentration of 0.5 mM NADP⁺, 5 mM glucose 6-phosphate, and 4 U/ml glucose-6-phosphate dehydrogenase) was carried out before the addition of endosulfan- α (20 μ M). In the case of ketoconazole, endosulfan- α (20 μ M) and ketoconazole (10 μ M) were preincubated along with 100 μ g of HLMs or 5 pmol of rP450 in 50 mM potassium phosphate buffer for 3 min at 37°C before the addition of the NADPH-regenerating system (final concentration of 0.25 mM NADP⁺, 2.5 mM glucose 6-phosphate, and 2 U/ml glucose-6-phosphate dehydrogenase). In both cases, final reaction volumes were 250 μ l and reactions were terminated by the addition of 250 μ l of ice-cold ACN and processed as described previously.

HPLC Analysis. Metabolite formation was analyzed with a Shimadzu (Kyoto, Japan) HPLC system consisting of an autoinjector (SIL-10AD VP), two pumps (LC-10AT), and a UV detector (SPD-10A VP). Endosulfan- α and metabolites were separated by a Gemini C18 column, 5 μ m, 100 \times 4.6 mm (Phenomenex, Torrance, CA), and identified with direct injection of reference compounds. The mobile phase for pump A consisted of 99% water and 1% phosphoric acid (pH 2.0) and that for pump B, 100% ACN. The flow rate was 1 ml/min. A gradient methodology was used as follows: 0 to 3 min (60% ACN), 3 to 16 min (60–90% ACN), 16 to 19 min (90–60% ACN), and 19 to 20 min (60% ACN). The injection volume was 50 μ l and solutes were detected at 213 nm. Under these conditions, the retention times for endosulfan- α and endosulfan sulfate were 12.4 and 8.9 min, respectively. Endosulfan- α and endosulfan sulfate peaks were quantified with calibration curves constructed from known concentrations of reference materials. The detection limit for endosulfan sulfate following the U.S. Environmental Protection Agency's method detection limit procedure was 0.04 μ M (CFR, 2006).

Data Analyses. Michaelis-Menten and Eadie-Hofstee plots were generated using the SigmaPlot Enzyme Kinetics Module (Systat Software, Inc., Point Richmond, CA). Enzyme kinetic parameters K_m and V_{max} were determined using nonlinear regression analysis with the SigmaPlot software.

Correlations of endosulfan sulfate formation with each P450-specific catalytic activity or P450 contents were calculated with simple linear regression using the web-based Statcrunch program (www.statcrunch.com). $p < 0.05$ was considered statistically significant.

To estimate the contributions of different P450 isoforms to the metabolism of endosulfan- α , percentage total normalized rates (% TNR) were calculated using the method described by Rodrigues (1999). In brief, metabolite formation rate (pmol/min/pmol rP450) obtained from rP450 metabolism of the compound of interest is multiplied by the immunquantified P450 content (pmol P450/mg) in native human liver microsomes, yielding the "normalized rate" (NR) expressed in pmol/min/mg microsomes. The NRs for each P450 involved in the metabolism of the compound of interest is summed up as the "total normalized rate" (TNR) (Rodrigues, 1999). The % TNR for each P450 was then calculated according to the following equation.

$$\% \text{ TNR} = \frac{\text{NR}}{\text{TNR}} \times 100 = \frac{\text{pmol/min/pmol P450} \times \text{pmol P450/mg}}{\sum (\text{pmol/min/pmol rCYP} \times \text{pmol nP450/mg})} \times 100$$

Results

Metabolism of Endosulfan- α . Endosulfan- α at 50 μ M concentration was metabolized by HLMs to a single metabolite, endosulfan sulfate. Figure 2 shows a representative HPLC chromatogram of this metabolism assay. The retention times for endosulfan- α and endosulfan sulfate were 12.29 and 8.80 min, respectively, in a 20-min HPLC run.

Cytochrome P450 Screening. P450 and FMO contributions to metabolism of endosulfan- α (20 μ M) were investigated using 14 rP450 and 3 rFMO commercially available human isoforms. Recombinant CYP2B6 predominantly mediated the formation of endosulfan sulfate by 8-fold (at 6.9 nmol/min/nmol P450) over the next isoform (CYP3A4) with the next highest metabolite formation rate (at 0.8 nmol/min/nmol P450). CYP2C18, 2C19, 2C9*1, and 3A7 also showed metabolic activity, but at negligible levels (Fig. 3). FMOs had no measurable activity toward endosulfan- α .

Kinetics of Endosulfan- α Metabolism. The kinetic parameters K_m and V_{max} were determined by incubating endosulfan- α (0.78–100 μ M) with pHLM (0.25 mg/ml), rCYP2B6, or rCYP3A4 (12.5 pmol). Calculated apparent K_m , V_{max} , and CL_{int} values are shown in Table 1.

The respective Michaelis-Menten (M-M) and Eadie-Hofstee plots of endosulfan- α metabolism by pHLM, rCYP2B6, and rCYP3A4 are shown in Fig. 4, A to C. The M-M plot show a hyperbolic curve, indicating saturation of metabolite formation over the substrate concentration range used and suggesting that the data obeyed M-M kinetics. The Eadie-Hofstee plots were linear, indicating either involvement of one enzyme or of more than one enzyme with similar affinity (Ward et al., 2003), and with a slight hook at the bottom end of the curve, suggesting allosteric activation (Faucette et al., 2000).

Correlation of Endosulfan Sulfate Formation with Specific P450 Contents and Selective P450 Activities. Endosulfan- α metabolism was conducted in 16 individual HLMs. Correlations between selective P450 activities from these 16 individual HLMs and specific P450 contents (of a subgroup of 8 HLMs with immunquantified P450 contents from BD Biosciences) were

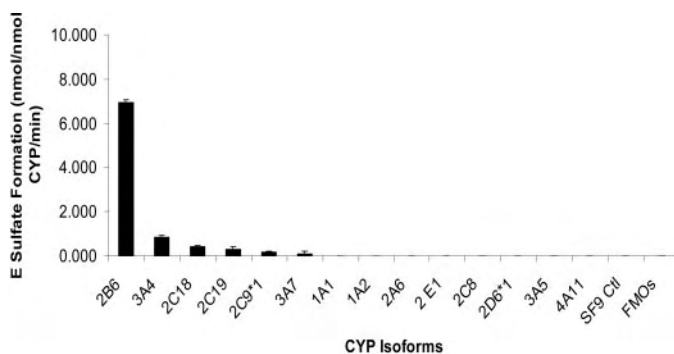


FIG. 3. Rates of endosulfan sulfate formation from endosulfan- α (20 μ M) by 14 rP450 and 3 rFMO isoforms. Data shown are the means of two independent determinations.

TABLE 1

Kinetic parameters of endosulfan- α metabolism in pHLMs, recombinant CYP2B6, and 3A4

HLM or P450	K_m	V_{max}	CL_{int}
	μ M		
pHLM	9.8	178.5 ^a	18.20 ^b
CYP2B6	16.2	11.4 ^c	0.70 ^d
CYP3A4	14.4	1.3	0.09

^a V_{max} expressed in pmol/min/mg protein for pHLM.

^b V_{max} expressed in pmol/min/pmol P450 for CYP2B6 and 3A4.

^c Intrinsic clearance (V_{max}/K_m) expressed in μ l/min/mg protein for pHLMs.

^d Intrinsic clearance (V_{max}/K_m) expressed in μ l/min/pmol P450 for CYP2B6 and 3A4.

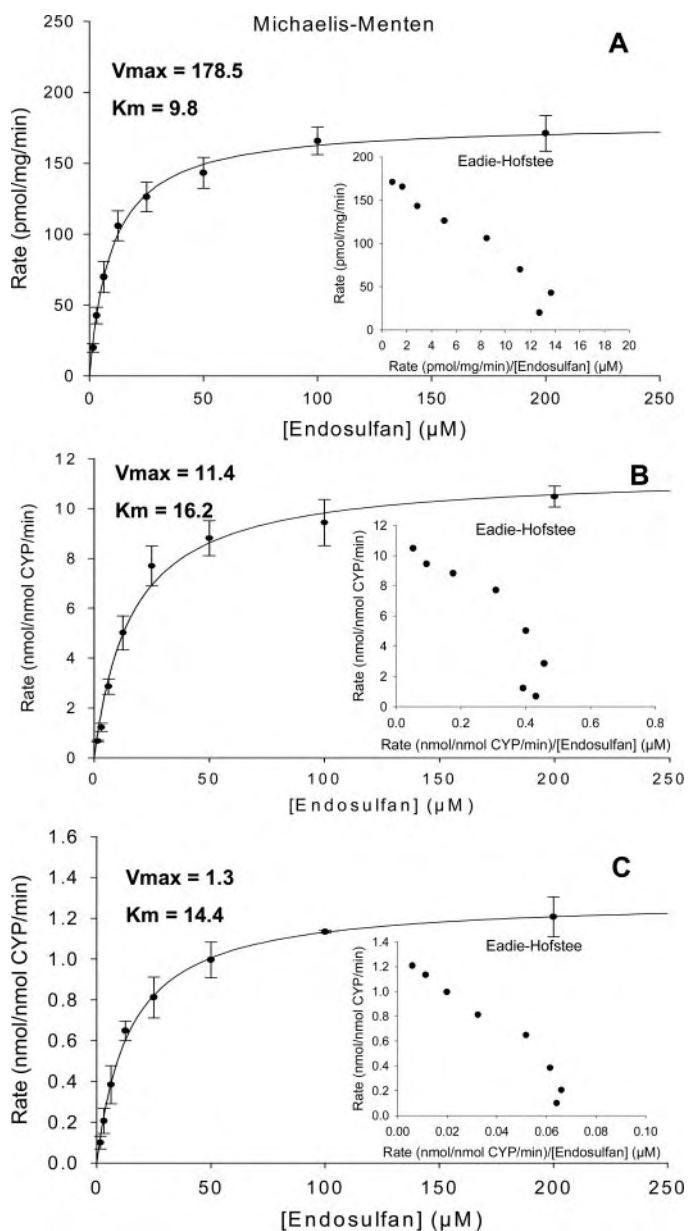


FIG. 4. Velocity of endosulfan sulfate formation versus endosulfan- α concentration in human liver microsomes (A), recombinant CYP2B6 (B), and recombinant CYP3A4 (C). Each point represents the mean of three independent measures.

calculated. A strong correlation was evident between endosulfan sulfate formation and *S*-mephenytoin *N*-demethylase activity of CYP2B6 ($r^2 = 0.79$, $p = 0.0001$). A less significant correlation was found with testosterone 6β -hydroxylase activity of CYP3A4 ($r^2 = 0.54$, $p = 0.001$). Likewise, strong correlations were evident between endosulfan sulfate formation and immunoreactive contents of CYP2B6 ($r^2 = 0.86$, $p = 0.0008$) and 3A4 ($r^2 = 0.81$, $p = 0.002$) (correlation plots shown in Fig. 5, A–D).

No significant correlations were found between endosulfan sulfate formation and diclofenac-4-hydroxylase activity of 2C9 ($r^2 = 0.04$, $p = 0.460$), *S*-mephenytoin 4-hydroxylase activity of 2C19 ($r^2 = 0.01$, $p = 0.743$), and other P450-selective activities (correlation plots not shown). Likewise, no significant correlations were seen with endosulfan sulfate formation and P450 contents of 2C9 ($r^2 = 0.42$, $p = 0.167$), 2C19 ($r^2 = 0.01$, $p = 0.571$), and other P450s. In addition, correlations were calculated for *S*-mephenytoin *N*-demethylase and CYP2B6 content ($r^2 = 0.87$), and testosterone 6β -hydroxylase and CYP3A4 content ($r^2 = 0.97$) in the same subgroup of 8 HLMs (see correlation plots in Fig. 5, E and F).

Inhibition of Endosulfan- α Metabolism by Ticlopidine and Ketoconazole, Selective Chemical Inhibitors for CYP2B6 and 3A4, Respectively. Initially, the optimal concentrations of ticlopidine and ketoconazole needed to obtain maximal inhibition of endosulfan sulfate formation were tested in rCYP2B6 and rCYP3A4. Results of these experiments are shown in Fig. 6, A and B. It was determined that 5 μ M ticlopidine and 10 μ M ketoconazole were optimal for subsequent inhibition studies. Results of inhibition of endosulfan sulfate formation with ticlopidine (5 μ M) and/or ketoconazole (10 μ M) are shown in Table 2. Six individual HLMs were chosen for these studies, based on available immunoreactive P450 contents data supplied by the manufacturer. These individual HLMs also represented various ranges of P450 contents (see Table 3). Inhibition of endosulfan sulfate formation by ketoconazole among the six individuals varied from 9 to 38%, implicating varying levels of CYP3A4 among these individuals. Similarly, the range of CYP2B6 involvement varied from 33 to 80%. The results show that inhibition of endosulfan metabolism with ketoconazole and ticlopidine were generally additive in all six HLMs.

% TNR. % TNR was calculated to verify the percentage inhibition (% I) results from this study (Table 3). % TNR obtained from rP450s can be directly related to % I obtained with native HLMs (Rodrigues, 1999). The % I from the combined incubation with ketoconazole and ticlopidine matched the sum of % TNRs of CYP2B6 and 3A4 in the metabolism of endosulfan- α in five of the six HLMs in this study (see Table 4).

Discussion

In the present study, we found endosulfate sulfate as the only metabolite of endosulfan from incubations with HLMs. In mice exposed to a single dose of 14 C-endosulfan, endosulfan sulfate concentrations were elevated in the liver, intestine, and visceral fat after 24 h (Deema et al., 1966). A study in rats administered a single oral dose of 14 C-endosulfan showed that the endosulfan metabolites diol, sulfate, lactone, and ether were found in the feces 5 days later (Dorough et al., 1978). A recent study, conducted in Spain, in which endosulfan is commonly used identified parent endosulfan and metabolites diol, sulfate, lactone, and ether in adipose tissues, placenta, cord blood, and human milk (Cerrillo et al., 2005). These findings, coupled with results of our study, suggest that the formation of the diol, ether, and lactone metabolites may be the result of metabolic processes beyond those occurring in human liver microsomes.

Our kinetic studies with human liver microsomes as well as with P450 isoforms 2B6 and 3A4 produced monophasic Eadie-Hofstee plots, suggesting that endosulfan- α is metabolized either by one enzyme or by more than one enzyme with similar K_m . A survey of 14 P450 isoforms demonstrated significant metabolism by CYP2B6, followed by 3A4, members of the 2C family, and 3A7. Of these isoforms, CYP2B6 and 3A4 are likely to have the greatest impact based upon activity levels and relative abundance. Although CYP2C18 may be similar to CYP3A4 in its capacity to metabolize endosulfan, it is poorly expressed in human livers (Goldstein, 2001). Our kinetic studies demonstrated that CYP2B6 and CYP3A4 share similar binding affinities (K_m of 16.2 and 14.4 μ M, respectively) but vary significantly in maximum velocity. The resulting difference in clearance of endosulfan sulfate demonstrates that CYP2B6 is 8-fold more efficient than CYP3A4 in catalyzing the metabolism of endosulfan- α (see Table 1). The present study determined the kinetic parameters $K_m = 9.8$ μ M, $V_{max} = 178.5$ pmol/min/mg HLM, and $CL_{int} = 18.2$ μ l/min/mg HLM for endosulfan- α metabolism by human liver microsomes. Lee et al. (2006) reported the following kinetic parameters for endosulfan- α metabolism by HLMs: $K_m = 7.34$ μ M, $V_{max} = 1.48$ pmol/min/pmol P450, $CL_{int} = 0.20$ μ l/min/pmol P450. Although the K_m values obtained by both laboratories are comparable, the V_{max} and CL_{int} are not comparable because of the different methodologies used by each study in calculation of these kinetic parameters. The

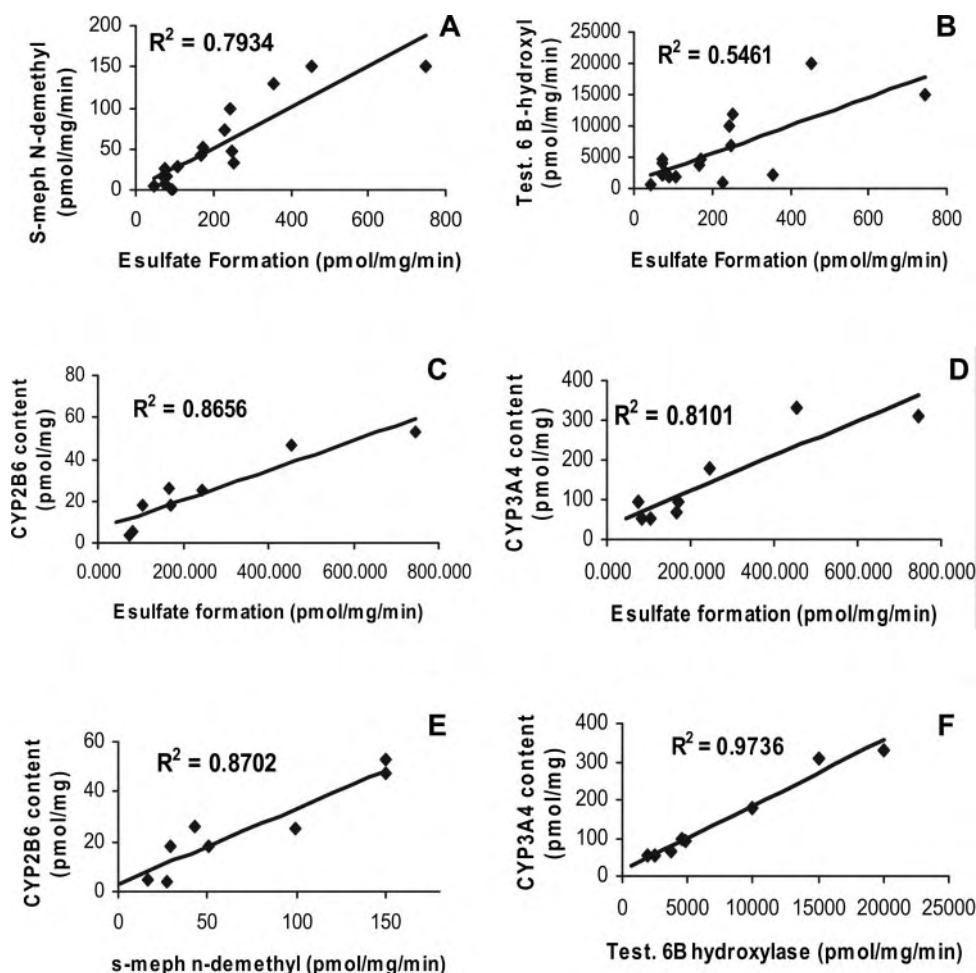


FIG. 5. Correlation plots of endosulfan sulfate formation and selective activities of CYP2B6 (A) and CYP3A4 (B) in 16 individual HLMs or immunoquantified contents of CYP2B6 (C) and CYP3A4 (D) in 8 HLMs. Correlation plots were also generated for *S*-mephenytoin *N*-demethylase and CYP2B6-immunoquantified contents (E) and for testosterone 6 β -hydroxylase and CYP3A4 contents (F) in 8 HLMs. Rates of endosulfan sulfate formation were measured in two independent determinations in each of the HLMs.

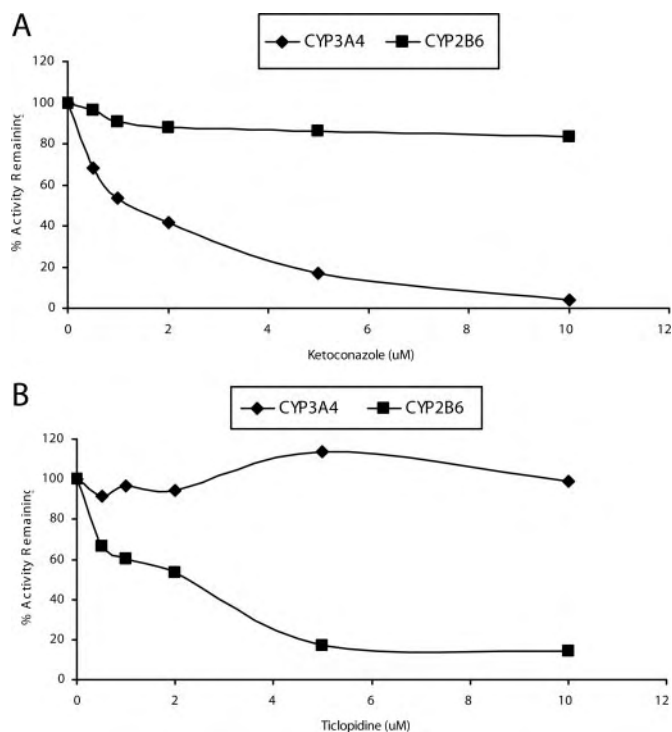


FIG. 6. Inhibition of endosulfan sulfate formation in rCYP2B6 and rCYP3A4 by ketoconazole (0–10 μ M) (A) and ticlopidine (0–10 μ M) (B). Each point represents the mean of two independent measures.

present study used protein content of HLMs, but Lee et al. (2006) used total P450 content in their calculations.

The correlations for CYP2B6 content and rates of *S*-mephenytoin metabolism ($r^2 = 0.87$) and endosulfan- α metabolism ($r^2 = 0.86$) are comparable, indicating that endosulfan- α is an excellent substrate for CYP2B6. However, the correlations for CYP3A4 content and rates of testosterone metabolism ($r^2 = 0.97$) and endosulfan- α metabolism ($r^2 = 0.81$) differ, suggesting that endosulfan- α is only a moderate substrate, in comparison with testosterone, for CYP3A4. The advantage of endosulfan- α is its utility for simultaneous probing of the activity of both CYP2B6 and CYP3A4.

Initial inhibition studies using monoclonal antibodies to CYP2B6 and 3A4 were abandoned because of their poor ability to inhibit endosulfan sulfate formation in the recombinant P450 isoforms (less than 30%; data not shown). This suggests that these monoclonal antibodies, although specific in inhibiting the metabolism of some substrates, may not be optimal inhibitors for endosulfan or other substrates. Hence, we used ticlopidine and ketoconazole, selective chemical inhibitors for CYP2B6 and 3A4, respectively, to characterize the contributions of these isoforms to endosulfan- α metabolism. Because CYP2B6 has been reported to be partially sensitive to ketoconazole at higher concentrations (Baldwin et al., 1995), we tested the effects of different concentrations of ketoconazole on endosulfan sulfate formation by recombinant CYP3A4 and CYP2B6. The present study determined that at the concentrations used in the inhibition of endosulfan sulfate formation (ketoconazole = 10 μ M and ticlopidine = 5 μ M), these inhibitors did not significantly inhibit the activity of the other isoform examined (Fig. 5). It is of interest that in the

TABLE 2

Inhibition of endosulfan sulfate formation in HLMs by ketoconazole and ticlopidine

Inhibitors ketoconazole (KTZ; 10 μ M) and ticlopidine (TCL; 5 μ M) were used alone and combined for metabolism of endosulfan- α in six individual HLMs. Data are means of two independent measurements.

Inhibitor	Percentage Inhibition of Endosulfan Sulfate Formation					
	HG3	HG112	HG42	HG43	HG93	HK23
10 μ M KTZ	23.8 \pm 0.6	20.5 ^a	8.6 \pm 1.5	34.9 \pm 4.7	37.6 \pm 8.8	36.0 \pm 0.2
5 μ M TCL	67.8 \pm 2.6	64.4 \pm 0.5	79.2 \pm 3.0	57.0 \pm 0.4	38.6 \pm 3.3	33.0 \pm 4.8
5 μ M TCL + 10 μ M KTZ	92.3 \pm 0.4	88.0 \pm 1.3	91.5 \pm 2.4	85.2 \pm 0.6	75.6 \pm 6.2	57.0 \pm 0.6

^a No replicate for this measurement due to insufficient HLM HG112 sample.

TABLE 3

Comparison between % TNR and % I in six individual HLMs

% TNR was calculated according to Rodrigues et al. (1999). % I for CYP2B6 was determined with the use of ticlopidine (5 μ M) and that for CYP3A4 with ketoconazole (10 μ M).

HLMs	rP450	Endosulfan Sulfate Formation Rate ^a in rP450	P450 Content ^b in Native HLMs	Normalized Rate	% TNR	% I
HG42	2B6	9.42	53	499.37	64.8	79.3
	2C9	0.34	80	24.12	3.5	N.D.
	2C19	0.32	6	1.89	0.2	N.D.
	3A4	0.78	310	242.73	31.5	8.6
HG112	2B6	9.42	47	442.83	58.8	64.4
	2C9	0.34	87	29.49	3.9	N.D.
	2C19	0.32	72	22.68	3.0	N.D.
	3A4	0.78	330	258.39	34.3	20.5
HG3	2B6	9.42	18	169.60	65.0	67.9
	2C9	0.34	42	14.24	5.04	N.D.
	2C19	0.32	9	2.84	1.1	N.D.
	3A4	0.78	95	74.38	28.5	23.8
HK23	2B6	9.42	7	65.95	42.1	33.0
	2C9	0.34	56	18.98	12.1	N.D.
	2C19	0.32	17	5.36	3.4	N.D.
	3A4	0.78	85	66.56	42.4	36.0
HG43	2B6	9.42	4	37.69	26.3	57.0
	2C9	0.34	51	17.29	12.1	N.D.
	2C19	0.32	47	14.81	10.3	N.D.
	3A4	0.78	94	73.60	51.3	34.9
HG93	2B6	9.42	18	169.60	69.0	38.6
	2C9	0.34	51	17.29	7.3	N.D.
	2C19	0.32	49	15.44	6.7	N.D.
	3A4	0.78	52	40.72	17.0	37.6

N.D., not determined.

^a Rates in pmol/min/pmol rP450.

^b Immunoquantified P450 contents in pmol/min/mg protein.

TABLE 4

Sum of CYP2B6 and 3A4 % TNRs vs. % I with ketoconazole and ticlopidine

Comparison between the sum of % TNRs of CYP2B6 and CYP3A4 in the metabolism of endosulfan- α and % I with ketoconazole and ticlopidine in the same incubation. With the exception of HK23, the other five HLMs had matching % TNR and % I.

HLM	% TNR	% I
HG3	94	92
HG112	93	88
HG42	96	92
HK23	84	57
HG43	78	85
HG93	86	76

six HLMs examined, the combined use of ketoconazole and ticlopidine resulted in inhibition of endosulfan sulfate formation, which was generally similar to the results obtained with each inhibitor alone. For four individuals, the combined inhibition of CYP2B6 and 3A4 yielded values from 85 to 92%, yet two individuals retained significant ability to metabolize endosulfan following inhibition (HK23 and HG93 with 57 and 76% inhibition, respectively). To further explore the possibility that other P450s were involved in metabolism for these individuals, the total normalized rates of metabolism for the P450 isoforms identified by screening efforts were investigated.

The % I from the combined incubation with ketoconazole and

ticlopidine corresponded well with the combined % TNRs of CYP2B6 and 3A4 (Table 4) in the metabolism of endosulfan- α in five of the six HLMs in this study. With HK23, there was a significantly lower percentage inhibition of endosulfan- α metabolism by CYP2B6 (as demonstrated by % I with ticlopidine) compared with the metabolic contribution of CYP2B6 as predicted by % TNR. This decreased inhibition of CYP2B6 activity in HK23 may be due to a CYP2B6 polymorphism. This is supported by a study in which a 26% decrease was seen in *N,N,N'*-triethylene-thiophosphoramidate inactivation of *O*-deethylation of 7-ethoxy-4-(trifluoromethyl)coumarin in mutant CYP2B6 compared with wild-type 2B6 (Bumpus et al., 2005). It is now known that CYP2B6 polymorphisms are common in Caucasians and that CYP2B6 is one of the most polymorphic human P450s (Lang et al., 2001).

A number of substrate probes for CYP2B6 have been reported in the literature, including 7-ethoxy-4-trifluoromethylcoumarin (Code et al., 1997), cyclophosphamide, and ifosfamide (Huang et al., 2000), *S*-mephenytoin (Heyn et al., 1996; Ko et al., 1998), bupropion (Faucette et al., 2000; Hesse et al., 2000), and efavirenz (Ward et al., 2003). The known substrate probes for CYP3A4 include testosterone, midazolam, nifedipine, and erythromycin (Yuan et al., 2002). The use of one substrate to simultaneously probe for the in vitro catalytic activity of CYP2B6 and CYP3A4 would be very advantageous. Based

on the results of our inhibition studies, endosulfan- α appears to be a strong candidate for this role.

In conclusion, endosulfan- α is metabolized to a single metabolite, endosulfan sulfate, by HLMs. This metabolism is primarily mediated by CYP2B6 and CYP3A4. The strategies used to demonstrate this were: 1) endosulfan- α metabolism by rP450s, 2) correlation studies of endosulfan sulfate formation and P450-selective activities or P450 immunoquantified contents in individual HLMs, and 3) inhibition studies using CYP2B6- and CYP3A4-selective chemical inhibitors. In addition, endosulfan- α may be used to simultaneously probe for the in vitro catalytic activities of CYP2B6 and CYP3A4. Finally, endosulfan's endocrine-disrupting effects and mechanisms inducing microsomal enzyme activity are currently under investigation.

Acknowledgments. We thank Ed Croom, Amin Usmani, Yan Cao, Leslie Tompkins, and Beth Cooper for technical assistance.

References

- [ATSDR] Agency for Toxic Substances and Disease Registry (2000) Toxicological Profile for Endosulfan. Agency for Toxic Substances and Disease Registry (ATSDR), U.S. Department of Health and Human Services, Washington, D.C.
- Baldwin SJ, Bloomer JC, Smith GJ, Ayrton AD, Clarke SE, and Chenery RJ (1995) Ketoconazole and sulphaphenazole as the respective selective inhibitors of P4503A and 2C9. *Xenobiotica* **25**:261–270.
- Bumpus NN, Sridar C, Kent UM, and Hollenberg PF (2005) The naturally occurring cytochrome P450 (P450) 2B6 K262R mutant of P450 2B6 exhibits alterations in substrate metabolism and inactivation. *Drug Metab Dispos* **33**:795–802.
- Casabar R, Wallace A, and Rose R (2005) Endosulfan induces cytochrome P450-3A4 and 2B6 through the steroid and xenobiotic receptor (Poster Abstract # 244), in *International Society for the Study of Xenobiotics. Abstracts from 13th ISSX Meeting*, October 23–27, 2005, Maui, HI, pp 141. *Drug Metab Rev* **37**:244.
- Cerrillo I, Granada A, Lopez-Espinosa MJ, Olmos B, Jimenez M, Cano A, Olea N, and Fatima Olea-Serrano M (2005) Endosulfan and its metabolites in fertile women, placenta, cord blood, and human milk. *Environ Res* **98**:233–239.
- [CFR] Code of Federal Regulations (2006) Appendix B to Part 136— Definition and procedure for the determination of the method detection limit—Revision 1.11, Electronic Code of Federal Regulations, Title 40, Feb 2006.
- Code EL, Crespi CL, Penman BW, Gonzalez FJ, Chang TK, and Waxman DJ (1997) Human cytochrome P4502B6: interindividual hepatic expression, substrate specificity, and role in procarcinogen activation. *Drug Metab Dispos* **25**:985–993.
- Deema P, Thompson E, and Ware GW (1966) Metabolism, storage, and excretion of C-14-endosulfan in the mouse. *J Econ Entomol* **59**:546–550.
- Dorough HW, Huhtanen K, Marshall TC, and Bryant HE (1978) Fate of endosulfan in rats and toxicological considerations of apolar metabolites. *Pestic Biochem Physiol* **8**:241–252.
- Faucette SR, Hawke RL, Lecluyse EL, Shord SS, Yan B, Laethem RM, and Lindley CM (2000) Validation of bupropion hydroxylation as a selective marker of human cytochrome P450 2B6 catalytic activity. *Drug Metab Dispos* **28**:1222–1230.
- Gervot L, Rochat B, Gautier JC, Bohnenstengel F, Kroemer H, de Berardinis V, Martin H, Beaune P, and de Waziers I (1999) Human CYP2B6: expression, inducibility and catalytic activities. *Pharmacogenetics* **9**:295–306.
- Goldstein JA (2001) Clinical relevance of genetic polymorphisms in the human CYP2C subfamily. *Br J Clin Pharmacol* **52**:349–355.
- Gupta PK and Gupta RC (1977) Effect of endosulfan pretreatment on organ weights and on pentobarbital hypnosis in rats. *Toxicology* **7**:283–288.
- Hesse LM, Venkatakrishnan K, Court MH, von Moltke LL, Duan SX, Shader RI, and Greenblatt DJ (2000) CYP2B6 mediates the in vitro hydroxylation of bupropion: potential drug interactions with other antidepressants. *Drug Metab Dispos* **28**:1176–1183.
- Heyn H, White RB, and Stevens JC (1996) Catalytic role of cytochrome P4502B6 in the N-demethylation of S-mephenytoin. *Drug Metab Dispos* **24**:948–954.
- Huang Z, Roy P, and Waxman DJ (2000) Role of human liver microsomal CYP3A4 and CYP2B6 in catalyzing N-dechloroethylation of cyclophosphamide and ifosfamide. *Biochem Pharmacol* **59**:961–972.
- Khanna RN, Misra D, Anand M, and Sharma HK (1979) Distribution of endosulfan in cat brain. *Bull Environ Contam Toxicol* **22**:72–79.
- Ko JW, Desta Z, and Flockhart DA (1998) Human N-demethylation of (S)-mephenytoin by cytochrome P450s 2C9 and 2B6. *Drug Metab Dispos* **26**:775–778.
- Lang T, Klein K, Fischer J, Nussler AK, Neuhaus P, Hofmann U, Eichelbaum M, Schwab M, and Zanger UM (2001) Extensive genetic polymorphism in the human CYP2B6 gene with impact on expression and function in human liver. *Pharmacogenetics* **11**:399–415.
- Lee HK, Moon JK, Chang CH, Choi H, Park HW, Park BS, Lee HS, Hwang EC, Lee YD, Liu KH, et al. (2006) Stereoselective metabolism of endosulfan by human liver microsomes and human cytochrome P450 isoforms. *Drug Metab Dispos* **34**:1090–1095.
- Nomeir AA, Ruegg C, Shoemaker M, Favreau LV, Palamanda JR, Silber P, and Lin CC (2001) Inhibition of CYP3A4 in a rapid microtiter plate assay using recombinant enzyme and in human liver microsomes using conventional substrates. *Drug Metab Dispos* **29**:748–753.
- Richter T, Mordt TE, Heinkel G, Pleiss J, Tatzel S, Schwab M, Eichelbaum M, and Zanger UM (2004) Potent mechanism-based inhibition of human CYP2B6 by clopidogrel and ticlopidine. *J Pharmacol Exp Ther* **308**:189–197.
- Rodrigues AD (1999) Integrated cytochrome P450 reaction phenotyping—attempting to bridge the gap between cDNA-expressed cytochromes P450 and native human liver microsomes. *Biochem Pharmacol* **57**:465–480.
- Saiyed H, Dewan A, Bhatnagar V, Shenoy U, Shenoy R, Rajmohan H, Patel K, Kashyap R, Kulkarni P, Rajan B, et al. (2003) Effect of endosulfan on male reproductive development. *Environ Health Perspect* **111**:1958–1962.
- [USEPA] U.S. Environmental Protection Agency (2002) Reregistration Eligibility Decision (R.E.D) for Endosulfan. U.S. Environmental Protection Agency (USEPA), Washington, D.C.
- Ward BA, Gorski JC, Jones DR, Hall SD, Flockhart DA, and Desta Z (2003) The cytochrome P4502B6 (CYP2B6) is the main catalyst of efavirenz primary and secondary metabolism: implication for HIV/AIDS therapy and utility of efavirenz as a substrate marker of CYP2B6 catalytic activity. *J Pharmacol Exp Ther* **306**:287–300.
- Wilson VS and LeBlanc GA (1998) Endosulfan elevates testosterone biotransformation and clearance in CD-1 mice. *Toxicol Appl Pharmacol* **148**:158–168.
- Yuan R, Madani S, Wei XX, Reynolds K, and Huang SM (2002) Evaluation of cytochrome P450 probe substrates commonly used by the pharmaceutical industry to study in vitro drug interactions. *Drug Metab Dispos* **30**:1311–1319.

Address correspondence to: Ernest Hodgson, Department of Environmental and Molecular Toxicology, Box 7633, North Carolina State University, Raleigh, NC 27695. E-mail: ernest_hodgson@ncsu.edu

IN VITRO METABOLISM OF NAPHTHALENE BY HUMAN LIVER MICROSOMAL CYTOCHROME P450 ENZYMES

Taehyeon M. Cho, Randy L. Rose, and Ernest Hodgson

Department of Environmental and Molecular Toxicology, North Carolina State University, Raleigh, North Carolina

Received May 31, 2005; accepted October 19, 2005

ABSTRACT:

The polycyclic aromatic hydrocarbon naphthalene is an environmental pollutant, a component of jet fuel, and, since 2000, has been reclassified as a potential human carcinogen. Few studies of the in vitro human metabolism of naphthalene are available, and these focus primarily on lung metabolism. The current studies were performed to characterize naphthalene metabolism by human cytochromes P450. Naphthalene metabolites from pooled human liver microsomes (pHLMs) were *trans*-1,2-dihydro-1,2-naphthalenediol (dihydrodiol), 1-naphthol, and 2-naphthol. Metabolite production generated K_m values of 23, 40, and 116 μM and V_{max} values of 2860, 268, and 22 pmol/mg protein/min, respectively. P450 isoform screening of naphthalene metabolism identified CYP1A2 as the most efficient isoform for producing dihydrodiol and 1-naphthol, and CYP3A4 as the most effective for 2-naphthol production. Metabolism of the primary metabolites of naphthalene was also

studied to identify secondary metabolites. Whereas 2-naphthol was readily metabolized by pHLMs to produce 2,6- and 1,7-dihydroxynaphthalene, dihydrodiol and 1-naphthol were inefficient substrates for pHLMs. A series of human P450 isoforms was used to further explore the metabolism of dihydrodiol and 1-naphthol. 1,4-Naphthoquinone and four minor unknown metabolites from 1-naphthol were observed, and CYP1A2 and 2D6*1 were identified as the most active isoforms for the production of 1,4-naphthoquinone. Dihydrodiol was metabolized by P450 isoforms to three minor unidentified metabolites with CYP3A4 and CYP2A6 having the greatest activity toward this substrate. The metabolism of dihydrodiol by P450 isoforms was lower than that of 1-naphthol. These studies identify primary and secondary metabolites of naphthalene produced by pHLMs and P450 isoforms.

The polycyclic aromatic hydrocarbon naphthalene is an environmental pollutant, a component of jet fuel, and, since 2000, has been reclassified as a potential human carcinogen (Riviere et al., 1999; White, 1999; McDougal et al., 2000; Preuss et al., 2003). Naphthalene also has been used in the production of phthalate plasticizers and resins, azo dyes, dispersants, and tanning agents in the rubber and leather industries (Preuss et al., 2003). Naphthalene is volatile and is discharged into the environment through incomplete burning of fossil fuels as well as domestic and industrial uses of products containing this chemical.

The toxicity of naphthalene has been studied in vitro and in vivo. In the presence of NADPH and human liver microsomes, 100 μM naphthalene produced significant cytotoxicity in human blood mononuclear leukocytes, but not genotoxicity (Tingle et al., 1993). However, naphthalene has been reclassified as a potential human carcinogen due to evidence of its carcinogenic activity in rats (Preuss et al., 2003). Naphthalene has also been reported to induce oxidative stress, resulting in lipid peroxidation and DNA damage in a cultured macrophage cell line, J774A.1 (Bagchi et al., 1998). Lipid peroxidation in

mitochondria and glutathione decreases in hepatic and brain tissues are observed in naphthalene-dosed rats (Vuchetich et al., 1996). DNA single-strand breaks are caused by naphthalene in hepatic tissues in the same studies (Vuchetich et al., 1996). In addition, the p53 tumor suppressor gene may be related to the toxicity of naphthalene, including enhanced production of superoxide anion and DNA fragmentation (Bagchi et al., 2000). Early stage toxicological indicators of naphthalene exposure in the mouse include perturbation of nonciliated bronchiolar (Clara) epithelial cell membranes, changes of cell ultrastructure, including swollen smooth endoplasmic reticulum and cytoplasmic blebbing, and intracellular glutathione depletion (Van Winkle et al., 1999; Plopper et al., 2001).

Because the toxicity of naphthalene in cell culture and animal models is closely related to the metabolism of the compound, cytochrome P450 (P450) monooxygenases may play an important role in its toxicological effects. High concentrations of naphthalene (>500 μM) cause decreased viability in isolated murine Clara cells, but a P450 inhibitor, piperonyl butoxide, blocks the loss of cell viability on preincubation with Clara cells (Chichester et al., 1994). Naphthalene metabolism to naphthalene 1*R*,2*S*-oxide stereoselectively mediated by CYP2F2 is suggested to be closely related to species-specific and tissue-selective cytotoxicity of this chemical (Buckpitt et al., 1995). Metabolic formation of 1,2- and/or 1,4-naphthoquinone from 1-naphthol may be a direct cause (Stohs et al., 2002) or an intermediate step in the production of naphthoquinone radicals for the toxicity of

This research was supported by a grant from the U.S. Army (DAMD 17-00-2-008). Part of this study was presented at the 44th Annual Meeting of the Society of Toxicology in New Orleans, LA, March 6-10, 2005.

Article, publication date, and citation information can be found at <http://dmd.aspetjournals.org>.

doi:10.1124/dmd.105.005785.

ABBREVIATIONS: P450, cytochrome P450; dihydrodiol, *trans*-1,2-dihydro-1,2-naphthalenediol; pHLM, pooled human liver microsome; mEH, microsomal epoxide hydrolase; HPLC, high performance liquid chromatography; GC/MS, gas chromatography-mass spectrometry; DCM, dichloromethane; %TNR, percentage of total normalized rate; CL_{int} , intrinsic clearance; AUC, area under the curve.

TABLE 1
Metabolism of naphthalene by pooled human liver microsomes

Metabolite	Human Liver Microsomes			
	V_{max}	K_m	$CL_{int} (V_{max}/K_m)$	R^2
	<i>pmol/mg protein/min</i>	μM	$\mu l/mg \text{ protein/min}$	
1-Naphthol	268.2 ± 11.1 ^a	40.2 ± 2.2 ^a	6699 ^a	0.99
2-Naphthol	22.3 ± 0.3 ^b	116.1 ± 9.0 ^b	194 ^a	0.99
Dihydrodiol	2860.2 ± 48.3 ^c	22.9 ± 0.7 ^a	125278 ^b	0.99

^{a,b,c} Means with a different letter in the same column are significantly different ($P < 0.05$). Data shown are the mean ± S.E.M. ($n = 3$).

1-naphthol (Doherty et al., 1984). Susceptibility to naphthalene-induced injury is gender-dependent in the mouse, with female mice producing more dihydrodiol in primary injury sites than male mice (Van Winkle et al., 2002).

The metabolism of naphthalene has been studied primarily in experimental animals (Buckpitt et al., 1984, 1987, 1995, 2002; Buckpitt and Bahnson, 1986; Chichester et al., 1994). Metabolic characterization in humans has been investigated in only a few studies (Buckpitt and Bahnson, 1986; Tingle et al., 1993). Dihydrodiol and three glutathione conjugates are generated by human lung microsomes in the presence of glutathione and glutathione transferases (Buckpitt and Bahnson, 1986). In naphthalene metabolism using human liver microsomes, *trans*-1,2-dihydrodiol and 1-naphthol are generated (Tingle et al., 1993). However, detailed biochemical characterization and identification of the P450 isoforms most responsible for human naphthalene metabolism have not been reported.

In the present studies, we provide the kinetics of naphthalene metabolism by both human liver microsomes and a wide spectrum of human P450 isoforms. The secondary metabolism of naphthalene primary metabolites was also studied to identify metabolic pathways of naphthalene. A new potential biomarker for exposure to naphthalene was suggested by these studies.

Materials and Methods

Chemicals. Naphthalene, 1-naphthol, 2-naphthol, 1,4-naphthoquinone, 2,6-dihydroxynaphthalene, and 1,7-dihydroxynaphthalene were purchased from Sigma-Aldrich (St. Louis, MO). *trans*-1,2-Dihydro-1,2-naphthalenediol was a generous gift from Dr. Alan R. Buckpitt (University of California, Davis, CA). Acetonitrile, tetrahydrofuran, and phosphoric acid were purchased from Fisher Scientific Co. (Pittsburgh, PA).

Human Liver Microsomes and Human Cytochrome P450 Isoforms. Pooled human liver microsomes (pHLMs) and human P450 isoforms expressed in baculovirus-infected insect (*Autographa californica*) cells (BTI-TN-5B1-4) [CYP1A1, 1A2, 1B1, 2A6, 2B6, 2C8, 2C9*1(Arg₁₁₄), 2C18, 2C19, 2D6*1(Val₃₇₄), 2E1, 3A4, 3A5, 3A7, 4A11], and microsomal epoxide hydrolase (mEH) were purchased from BD Gentest (Woburn, MA).

In Vitro Naphthalene Metabolism by Pooled Human Liver Microsomes. Naphthalene metabolism mediated by pHLMs was tested in vitro. These assays were performed with an NADPH-generating system (0.25 mM NADP, 2.5 mM glucose 6-phosphate, and 2 U/ml glucose-6-phosphate dehydrogenase) in 100 mM potassium phosphate buffer containing 3.3 mM MgCl₂ (pH 7.4). After the substrate was preincubated at 37°C for 5 min, the enzymatic reactions were initiated by the addition of ice-cold pHLMs (0.48 mg/ml) and incubated at 37°C for 10 min. Incubated vials were capped to prevent loss of substrate due to volatility. Metabolism of metabolites of naphthalene, 1-naphthol, 2-naphthol, and *trans*-1,2-dihydro-1,2-naphthalenediol, in pHLMs was also studied in the same conditions stated above for investigating the metabolic pathways of naphthalene with a series of substrate concentrations. In addition, 1-naphthol (200 μM) was incubated with a 2-fold higher amount of pHLMs (0.96 mg/ml) and the NADPH-generating system at 37°C for a longer time (30 min) to further examine its metabolism in pHLMs (duplicate). For controls, each substrate was incubated in the same buffer system containing pHLMs without the NADPH-generating system.

In Vitro Screening and Enzyme Kinetics for the Metabolic Activity of Human Cytochrome P450 Isoforms. The metabolic activity of the human P450 isoforms (50 pmol/ml) listed above was determined at a substrate concentration of 300 μM naphthalene. The enzymatic assays were performed in the same manner as above, with a modified incubation time of 15 min. Generation of each metabolite mediated by individual P450 isoforms was compared. Sf9 insect cell microsomes from wild-type baculovirus-infected cells (BD Gentest) were used as a control for these assays.

Based on the screening for metabolic activity of human P450 isoforms, enzyme kinetics of the most efficient isoforms (CYP1A1, 1A2, 2B6, 2E1, and 3A4; 40 pmol/ml) for naphthalene metabolism were also studied using a series of substrate concentrations and an incubation time of 10 min.

The metabolic activity of human P450 isoforms (40 pmol/ml) for 80 μM

1-naphthol or *trans*-1,2-dihydro-1,2-naphthalenediol (dihydrodiol) was also screened. To identify metabolites, the retention time and the spectra of each metabolite were closely compared. A small number of minor metabolites could not be identified in these studies.

Because pooled human liver microsomes generated a higher ratio of *trans*-1,2-dihydro-1,2-naphthalenediol to 1-naphthol than was observed using P450 isoforms, the potential contribution of naturally occurring epoxide hydrolase to the generation of this product was explored using purified CYP1A2. The kinetics of the formation of 1-naphthol, 2-naphthol, and *trans*-1,2-dihydro-1,2-naphthalenediol were examined by incubating various concentrations of naphthalene with CYP1A2 (40 pmol/ml) in the absence or presence of human microsomal epoxide hydrolase (0.2 mg/ml).

To compare the metabolic efficiency of human P450 isoforms for 1-naphthol with that for *trans*-1,2-dihydro-1,2-naphthalenediol, the metabolic activities for two of the most efficient isoforms, based on the isoform screening (CYP1A2 and 2D6*1 for 1-naphthol, and CYP2A6 and 3A4 for *trans*-1,2-dihydro-1,2-naphthalenediol), were compared by measuring residual parent chemical after incubation at 37°C for 15 min. The controls did not include the NADPH-generating system.

All assay reactions were terminated by addition of an equal volume (250 μl) of acetonitrile and vortexing. After a 5-min centrifugation at 15,000 rpm (21,000g), the supernatant was collected for metabolite characterization using an HPLC system. No metabolites were detected in controls from which the NADPH-generating system was absent.

Analysis of Metabolites by HPLC. The generation of metabolites was analyzed using a Waters 2695 HPLC system equipped with a 2996 photodiode array (PDA) detector (Waters, Milford, MA). This HPLC system was equipped with a degasser and an autoinjector, and data were collected and analyzed using Waters Empower software version 5.00. The solution for pump A was composed of 3% tetrahydrofuran, 0.2% *O*-phosphorus acid (85%), and 96.8% water, and for pump B, 100% acetonitrile. The gradient in the mobile phase was designed as follows: 0 to 2 min, 20% B; 2 to 22 min, gradient to 80% B; 22 to 25 min, 80% B; and 25 to 30 min, gradient to 20% B. The flow rate was 1.0 ml/min. Metabolites were separated by a reversed phase C₁₂ column (Synergi 4 μ Max-RP, 250 × 4.6 mm; Phenomenex, Torrance, CA) and detected using a PDA detector operated from 190 to 350 nm. Optimal wavelengths for 1-naphthol, 2-naphthol, *trans*-1,2-dihydro-1,2-naphthalenediol, 1,4-naphthoquinone, 1,7-dihydroxynaphthalene, and 2,6-dihydroxynaphthalene were selected as 232.7, 225.6, 262.2, 251.6, 239.8, and 228 nm, respectively. Standards of metabolites were prepared in acetonitrile, and 50 μl of standard or sample was injected into the HPLC system.

Sample Preparation for GC/MS Analysis. Naphthalene (300 μM) was incubated in a total volume of 500 μl of 100 mM potassium phosphate buffer containing 3.3 mM MgCl₂ (pH 7.4) with pHLMs (0.96 mg/ml) and the NADPH-generating system mentioned above for 10 min at 37°C after 5-min preincubation. Immediately after incubation, sample tubes were centrifuged at 15,000 rpm (21,000g) for 5 min, and 470 μl of supernatant from each tube was transferred into a fresh tube. Dichloromethane (DCM) (100 μl) was added to the fresh tube containing supernatant, and each tube was vigorously shaken for 1 min. The lower (DCM) layer was then collected for analysis after the tubes were centrifuged at 5000 rpm for 3.5 min. This extraction process with DCM was performed three more times, and the supernatants were combined for the GC/MS analysis.

Analysis of Metabolites by GC/MS. The generation of naphthalene metabolites by pHLMs was confirmed by analysis with an Agilent GC/MS system

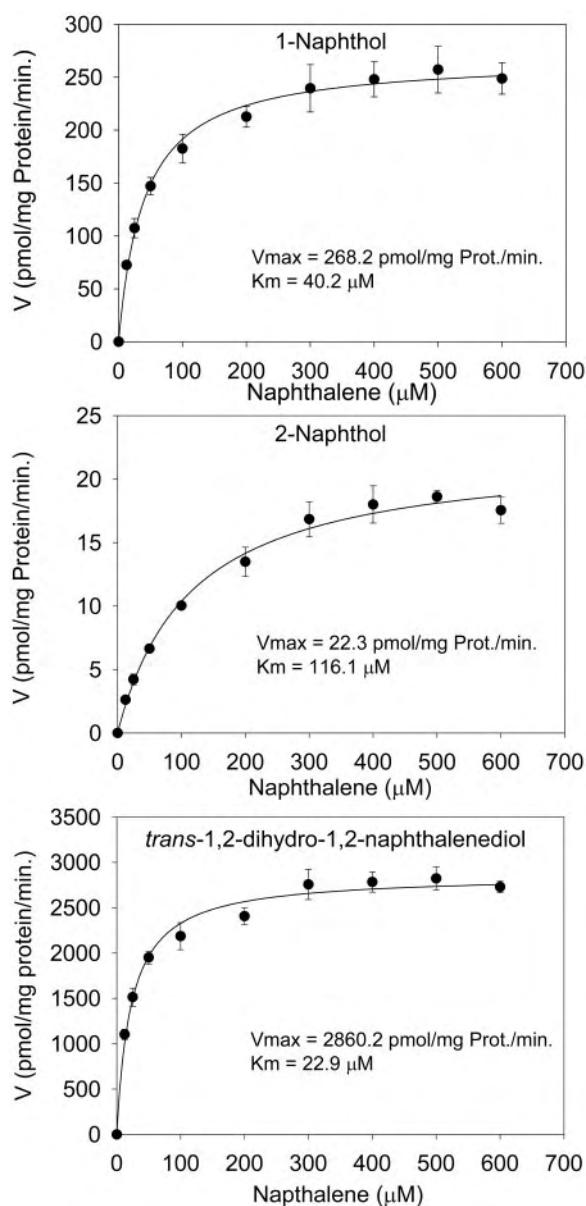


FIG. 1. Naphthalene metabolism by pooled human liver microsomes. Each metabolite was curve-fitted to the Michaelis-Menten equation. Specific activities are expressed as picomoles of product generated per milligram of liver microsomal protein per minute. The data shown are the mean \pm S.E.M. ($n = 3$).

consisting of a 6890 GC and a 5973 Mass Selective Detector (Agilent Technologies, Palo Alto, CA). A 30-m capillary column with a 0.25-mm nominal diameter (Restek Rtx-5MS; Restek, Bellefonte, PA) was used for the analyses with an injection volume of 2 μ l and a constant flow of helium gas (1 ml/min carrier gas). The oven temperature was programmed as follows: initially 40°C with a 1-min hold, increased to 100°C at a rate of 25°C/min, followed by an increase to 300°C at a rate of 10°C/min, followed by a 10-min hold. The total running time was 33.4 min and electron impact was used for the ionization of metabolites.

These analyses were performed as a confirmatory process for the HPLC analysis for the production of primary metabolites of naphthalene metabolism by pHLMs. Throughout the GC/MS analyses, naphthalene, 1-naphthol, and *trans*-1,2-dihydro-1,2-naphthalenediol were detected at retention times of 7.7, 11.6, and 12.0, respectively, and their fragmentation patterns were compared with those of standards. Detection of 2-naphthol was not successful in these analyses, probably due to the combination of its low level of production and potential loss during the extraction process.

Data Analysis and Statistics. The apparent V_{max} and K_m parameters were

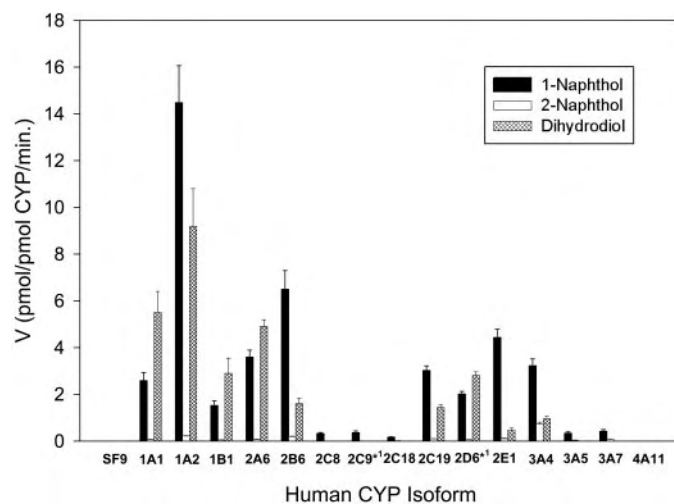


FIG. 2. Human cytochrome P450 isoform activity screening in naphthalene metabolism. Naphthalene (300 μ M) was metabolized by individual P450 isoforms (50 pmol/ml) in a NADPH generating system at 37°C for 15 min. Specific activities are expressed as picomoles of product generated per picomole of P450 isoform per minute. The data shown are the mean \pm S.E.M. ($n = 3$).

calculated using a nonlinear regression curve fitted to the Michaelis-Menten equation. The coefficient of determination (R^2), a measure of how well a regression model describes the data, is shown in the tables. Data means were obtained by at least three determinations. The percentages of total normalized rate (%TNR) were determined as described previously (Rodrigues, 1999). The nominal specific contents of individual P450 proteins in native human livers (10 donors) for calculating the %TNR were obtained from BD Gentest (2003 product catalog) except for the contents of CYP2C8 and CYP2C18, which were from Rodrigues (1999). Statistical significance of the data was determined with one-way analysis of variance followed by Tukey's multiple comparisons.

Results

Three metabolites were detected in metabolism studies of naphthalene by pooled human liver microsomes, 1-naphthol, 2-naphthol, and *trans*-1,2-dihydro-1,2-naphthalenediol (dihydrodiol). As presented in Table 1, dihydrodiol was the most abundant metabolite, followed in order by 1-naphthol and 2-naphthol. The K_m value for dihydrodiol was in the same range as that for 1-naphthol, but the K_m for 2-naphthol was significantly higher than those for the other two metabolites. The intrinsic clearance (CL_{int}) of dihydrodiol was significantly higher than those for 1-naphthol and 2-naphthol (Table 1). The Michaelis-Menten curves and metabolic rates for production of the three naphthalene metabolites are shown in Fig. 1.

Metabolic activities of 15 human P450 isoforms for naphthalene were evaluated (Fig. 2). Among those tested, CYP1A2 was found to be the most efficient for the production of 1-naphthol and dihydrodiol, whereas CYP3A4 was the most efficient for the production of 2-naphthol. The individual isoforms showed varying degrees of efficiency for the production of each metabolite. P450 isoforms such as 2C8, 2C9, 2C18, 3A5, 3A7, and 4A11 showed minimal or no activity for naphthalene metabolism (Fig. 2). CYP1A2 was the only isoform to generate 1,4-naphthoquinone from naphthalene in a detectable amount (data not shown). CYP1A2, 3A4, and 2E1 showed the highest total normalized rates (%TNR) for 1-naphthol and 2-naphthol generated in naphthalene metabolism, and CYP1A2, 2A6, and 3A4 showed the highest %TNR for dihydrodiol (Table 2).

The five most efficient human P450 isoforms for naphthalene metabolism as shown in Fig. 2 were selected to further characterize their metabolic activity for naphthalene. As expected, CYP1A2 was

identified as the most efficient isoform for generating 1-naphthol and dihydrodiol, showing the highest V_{\max} values for these metabolites (Table 3). The V_{\max} and K_m for the production of 1,4-naphthoquinone from naphthalene by this CYP1A2 isoform were 2.3 pmol/pmol/min and 29 μ M, respectively. In general, more 1-naphthol than dihydrodiol was produced from naphthalene by these isoforms, which is in contrast to naphthalene metabolism by pHLMs. CYP2E1 has higher affinity (i.e., lower K_m values) for naphthalene in the production of 1- or 2-naphthol compared with other isoforms. For CL_{int} of 1-naphthol, CYP2E1, 1A2, and 2B6 in that order showed higher values than 3A4 and 1A1. CYP2E1 and 3A4 were higher for the intrinsic clearance of 2-naphthol than other isoforms. CYP3A4 had the highest V_{\max} for the production of 2-naphthol, and CYP2E1 had the lowest K_m , accounting for their greater CL_{int} values observed relative to the other isoforms. The V_{\max} and CL_{int} values of 1A2 and 1A1 were higher for dihydrodiol production than those of the other isoforms (Table 3). Naphthalene metabolism by CYP1A2 produced one unknown minor metabolite (retention time = 14.3 min), for which the area under the curve (AUC) was less than 1% of the total metabolite AUC.

To investigate apparent discrepancies between amounts of dihydro-

diol and 1-naphthol as observed in pHLM- compared with P450 isoform-mediated naphthalene metabolism, naphthalene metabolism by CYP1A2 in the presence of human mEH was studied. These results were compared with the naphthalene metabolism mediated only by CYP1A2 (Table 4; Fig. 3). The production of 1-naphthol and 2-naphthol was significantly reduced in the presence of mEH, whereas the production of dihydrodiol was increased based on V_{\max} and CL_{int} values. K_m values for 1- and 2-naphthol production were significantly increased in the presence of mEH, although the K_m value for dihydrodiol production did not change (Table 4). The significant changes in the catalytic velocities by the addition of mEH are also shown in the fitted curves in Fig. 3.

The secondary metabolism of naphthalene was tested by incubating 1-naphthol, 2-naphthol, or dihydrodiol with either pHLMs or CYP1A2. 1-Naphthol was poorly metabolized by pHLMs with about 11% reduction of parent chemical after metabolism, and four unknown minor metabolites were produced. 2-Naphthol was metabolized to produce 2,6- and 1,7-dihydroxynaphthalene, and two unknown minor metabolites (about 3% based on the AUC). In contrast with pHLMs, however, 1-naphthol was metabolized by CYP1A2 to generate 1,4-naphthoquinone and four unknown metabolites (about 56% based on the AUC). 2-Naphthol metabolism by CYP1A2 also produced the same metabolites as those by pHLMs and three additional unknown metabolites (about 6% based on AUC). More 2,6-dihydroxynaphthalene than 1,7-dihydroxynaphthalene was generated by both pHLMs and CYP1A2. Neither pHLMs nor CYP1A2 metabolized dihydrodiol. Metabolism of 1,4-naphthoquinone by pHLMs resulted in one unknown metabolite without the NADPH-generating system and two unknown metabolites additionally with the system. The incubation of 1,4-naphthoquinone with pHLMs (0.48 mg/ml) for 10 min caused the disappearance of this substrate up to about 38% and 51% in the absence and in the presence of the NADPH-generating system, respectively. The kinetic parameters for this secondary metabolism are shown in Table 5.

To further investigate the unknown metabolites from 1-naphthol or dihydrodiol, and to determine which human P450 isoforms are efficient in secondary metabolism, a series of human P450 isoforms was used for 1-naphthol or dihydrodiol metabolism. 1-Naphthol was metabolized to 1,4-naphthoquinone and four unknown metabolites by most P450 isoforms (Fig. 4). Dihydrodiol metabolism generated three unknown metabolites primarily due to activity of CYP2A6 and 3A4 (data not shown). Based on the total AUC of metabolites for 1-naph-

TABLE 2

The %TNR for naphthalene metabolites by individual P450 isoforms and the specific content of each P450 protein in human liver microsomes

P450 Isoform	%TNR			Mean Content of P450 ^d
	1-Naphthol	2-Naphthol	Dihydrodiol	
	<i>pmol P450/mg protein</i>			
1A1	N.D.	N.D.	N.D.	N.A.
1A2	40.4	9.2	48.8	55
1B1	N.D.	N.D.	N.D.	N.A.
2A6	9.5	3.2	24.7	52
2B6	6.9	3.2	3.3	21
2C8 ^b	1.0	0.0	0.0	64
2C9	1.4	0.0	0.0	76
2C18 ^b	0.02	0.03	0.0	2.5
2C19	6.0	3.0	5.4	39
2D6	1.2	0.5	3.3	12
2E1	11.7	4.3	2.3	52
3A4	21.8	76.5	12.3	133
3A5	0.02	0.03	0.0	1.2
3A7	N.D.	N.D.	0.0	N.A.
4A11	0.0	0.0	0.0	N.A.

N.D., not determined; N.A., not available.

^a Mean content data were obtained from BD Gentest (2003 product catalog).

^b Mean content data for 2C8 and 2C18 were obtained from Rodrigues (1999).

TABLE 3

Metabolism of naphthalene by human CYP isoforms

	P450 Isoform	V_{\max}	K_m	$CL_{\text{int}} (V_{\max}/K_m)$	R^2
		<i>pmol/pmol/min</i>	μ M	μ l/nmol/min	
1-Naphthol	1A1	9.1 \pm 0.6 ^a	111.0 \pm 13.0 ^a	84 ^a	0.99
	1A2	35.8 \pm 4.4 ^b	72.7 \pm 18.5 ^a	522 ^b	0.98
	2B6	20.2 \pm 2.2 ^c	58.6 \pm 10.4 ^{a,b}	361 ^b	0.99
	2E1	8.4 \pm 0.1 ^a	10.1 \pm 0.7 ^b	841 ^c	0.98
	3A4	8.1 \pm 1.0 ^a	60.7 \pm 17.6 ^{a,b}	146 ^a	0.99
2-Naphthol	1A1	0.3 \pm 0.0 ^a	109.5 \pm 25.4 ^a	3 ^a	0.97
	1A2	0.9 \pm 0.0 ^b	116.2 \pm 16.0 ^a	8 ^a	0.99
	2B6	0.8 \pm 0.1 ^{a,b}	93.8 \pm 22.4 ^{a,b}	9 ^a	0.99
	2E1	0.2 \pm 0.0 ^a	9.9 \pm 0.3 ^b	22 ^b	0.95
	3A4	1.6 \pm 0.2 ^c	65.4 \pm 20.3 ^{a,b}	27 ^b	0.99
<i>trans</i> -1,2-Dihydro-1,2-naphthalenediol	1A1	7.4 \pm 0.9 ^a	53.9 \pm 5.9 ^a	140 ^a	0.96
	1A2	7.7 \pm 0.5 ^a	33.5 \pm 8.6 ^a	250 ^b	0.98
	2B6	2.2 \pm 0.2 ^b	49.5 \pm 9.3 ^a	47 ^c	0.99
	2E1	0.4 \pm 0.1 ^b	33.8 \pm 15.0 ^a	14 ^c	0.90
	3A4	1.0 \pm 0.1 ^b	55.8 \pm 13.0 ^a	19 ^c	0.96
1,4-Naphthoquinone	1A2	2.3 \pm 0.0	28.9 \pm 0.9	79	0.95

^{a,b,c} Means with a different letter in the same column are significantly different ($P < 0.05$). Data shown are the mean \pm S.E.M. ($n \geq 3$).

TABLE 4

Metabolism of naphthalene by human CYP1A2 in the presence of human mEH (0.2 mg/ml)

Metabolites	CYP1A2 with mEH (0.2 mg/ml)			
	V_{max}	K_m	$CL_{int} (V_{max}/K_m)$	R^2
	pmol/pmol/min	μM	$\mu L/nmol/min$	
1-Naphthol	$20.2 \pm 1.0^{**}$	$163.5 \pm 14.8^*$	125*	0.99
2-Naphthol	0.6 ± 0.0	$195.7 \pm 17.6^*$	3	0.99
Dihydrodiol	$56.4 \pm 0.9^{**}$	38.5 ± 3.6	1490**	0.99

* and ** $P < 0.05$ and $P < 0.001$, respectively, when compared to their counterparts in the absence of mEH. Data shown are the mean \pm S.E.M. ($n = 3$).

thol or dihydrodiol, the percentage of total normalized rate (%TNR) of their metabolites for each P450 isoform was calculated (Table 6). CYP3A4, 1A2, and 2C19 showed the highest %TNR for 1-naphthol metabolite, and CYP3A4, 2A6, and 2C8 had the highest %TNR for dihydrodiol metabolite (Table 6). Identification of unknown metabolites was not successful because of the lack of potential standards. To investigate which substrate, 1-naphthol or dihydrodiol, is more effectively metabolized by individual P450 isoforms, two isoforms among the most efficient for each substrate, CYP1A2 and 2D6 for 1-naphthol, and 2A6 and 3A4 for dihydrodiol, were selected. Because there were unknown metabolites from this metabolism, substrate disappearance after metabolism by each P450 enzyme was compared for evaluating the metabolic efficiency of each isoform. For 1-naphthol, 16.3 ± 0.5 and $19.6 \pm 1.1\%$ (mean \pm S.E.M.) of the parent chemical were metabolized by 1A2 and 2D6, whereas for dihydrodiol, 0.4 ± 0.1 and $2.7 \pm 0.2\%$ were metabolized by 2A6 and 3A4, respectively.

Discussion

In naphthalene metabolism by pooled human liver microsomes, about 10 times more *trans*-1,2-dihydro-1,2-naphthalenediol (dihydrodiol) was generated than 1-naphthol, and generation of the latter was about 10 times higher than that of 2-naphthol. The observation of the predominant production of the dihydrodiol metabolite in these studies agrees with a previous report, in which about 8.6 times more dihydrodiol was generated than 1-naphthol in human liver microsomes (Tingle et al., 1993). Whereas the previous studies of human naphthalene metabolism were performed with microsomes obtained from a limited number of organ donors [1–6; individual human lung microsomes, or pHLMs or pooled human lung microsomes] (Buckpitt and Bahnsen, 1986; Tingle et al., 1993; Wilson et al., 1996), the human liver microsomes used in these studies were commercially prepared from organs donated from as many as 46 people. Therefore, the potential bias caused by individual variation was significantly reduced in the current studies. Although the generation of 2-naphthol in naphthalene metabolism has been known, the observation of 2-naphthol generation by human liver microsomes has not been previously reported. The predominant generation of the *trans*- form of dihydrodiol is probably related to the catalytic mechanism of human epoxide hydrolase (Morisseau and Hammock, 2005).

The P450 isoform screen in the current studies revealed the most efficient isoforms for producing naphthalene metabolites. Although there have been a few metabolic studies of naphthalene using human microsomes (Buckpitt and Bahnsen, 1986; Tingle et al., 1993; Wilson et al., 1996), naphthalene metabolism using a series of individual human P450 isoforms has not been previously studied. CYP1A2 was identified as the most effective isoform for naphthalene metabolism. Total P450 protein content of the 1A2 isoform in human liver ranges from approximately 8 to 13% (Shimada et al., 1994; Rodrigues, 1999). Using the mean specific protein contents of P450 isoforms

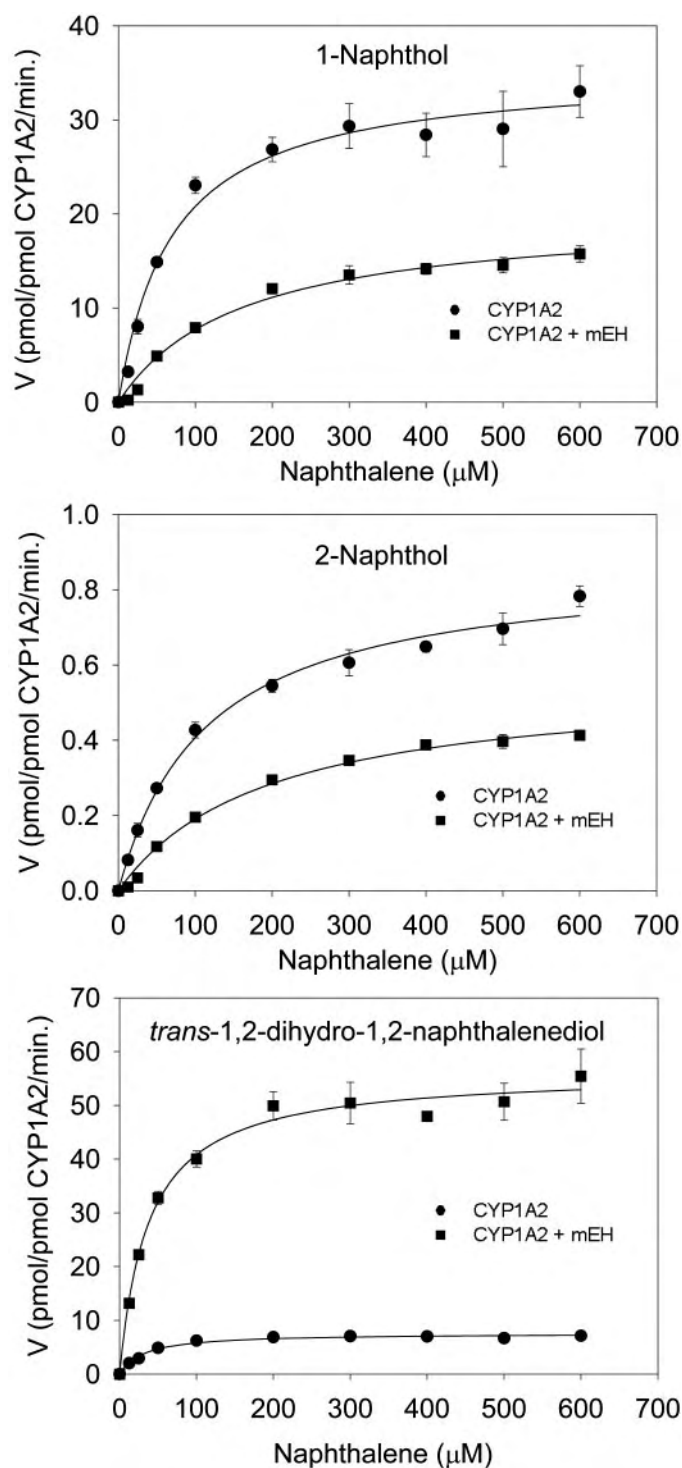


Fig. 3. Naphthalene metabolism by CYP1A2 isoform in the presence of human microsomal epoxide hydrolase (0.2 mg/ml). These data are compared with those of naphthalene metabolism by CYP1A2 only. Specific activities are expressed as picomoles of product generated per picomole of CYP1A2 isoform per minute. The data shown are the mean \pm S.E.M. ($n = 3$).

obtained from BD Gentest (2003 product catalog) and Rodrigues (1999), the calculated %TNR of CYP1A2 demonstrates its important role in naphthalene metabolism in human liver along with CYP3A4, 2E1, and 2A6. Although CYP3A4 showed generally lower metabolic activity toward naphthalene than CYP1A2 (Table 3; Fig. 2), the %TNR of CYP3A4 was approximately 50 and 25% of those for

TABLE 5

Metabolism of 1-naphthol and 2-naphthol by pooled human liver microsomes (pHLM) or CYP1A2

Data shown are the mean \pm S.E.M. ($n = 3$).

Parent Chemical	Metabolite	V_{max}	K_m	$CL_{int} (V_{max}/K_m)$	R^2
		pmol/mg protein/min	μM	$\mu l/mg$ protein/min	
pHLM					
1-Naphthol	1,4-NapQ	N.D.	N.D.	N.D.	
2-Naphthol	2,6-DiOH	322.6 \pm 25.0	7.0 \pm 1.1	47459	0.98
	1,7-DiOH	132.1 \pm 6.5	12.3 \pm 1.2	10978	0.99
		pmol/pmol 1A2/min	μM	$\mu l/nmol$ 1A2/min	
CYP1A2					
1-Naphthol	1,4-NapQ	10.8 \pm 0.4	28.7 \pm 1.4	378	0.99
2-Naphthol	2,6-DiOH	45.2 \pm 1.3	25.2 \pm 2.0	1805	0.98
	1,7-DiOH	6.4 \pm 0.3	43.2 \pm 4.1	149	0.97

1,4-NapQ, 1,4-naphthoquinone; 2,6-DiOH, 2,6-dihydroxynaphthalene; 1,7-DiOH, 1,7-dihydroxynaphthalene; N.D., not determined.

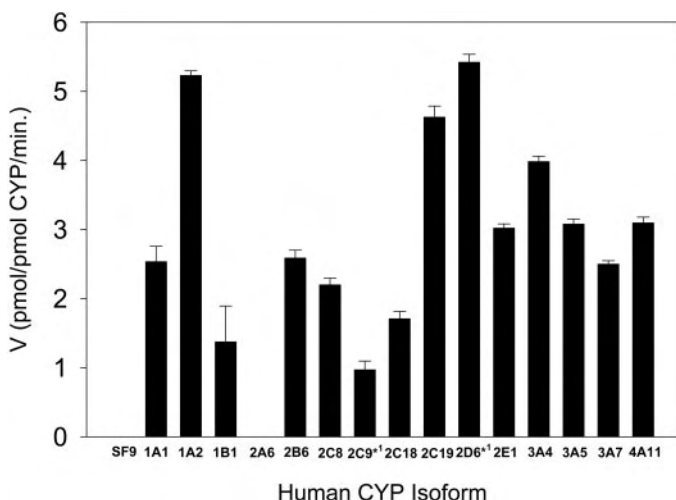


FIG. 4. Human cytochrome P450 isoform activity screening by the production of 1,4-naphthoquinone in 1-naphthol metabolism. 1-Naphthol (80 μM) was metabolized by individual P450 isoforms (40 pmol/ml) in a NADPH generating system at 37°C for 15 min. Specific activities are expressed as picomoles of product generated per picomole of P450 isoform per minute. The data shown are the mean \pm S.E.M. ($n = 3$).

CYP1A2 for 1-naphthol and dihydrodiol generation, respectively, because it had the highest abundance in the human liver microsomes (Table 2). Furthermore, CYP3A4 was the dominant isoform for 2-naphthol formation, not only in the absolute generation of this metabolite but also in the %TNR value, showing that about three fourths of 2-naphthol formed from naphthalene in human liver is associated with CYP3A4. It is known that formation of 1-naphthol and 2-naphthol can be achieved by spontaneous, nonenzymatic rearrangement from the chemically unstable intermediate, naphthalene-1,2-epoxide (Van Bladeren et al., 1984; Buckpitt et al., 2002; Preuss et al., 2003). In the current studies, however, the P450 isoforms tested showed various metabolite ratios produced from naphthalene. These results lead to the conclusion that the production of 1-naphthol and 2-naphthol may be, at least in part, either enzymatic or influenced by the enzyme environment.

Kinetic parameters were obtained for the five P450 isoforms showing the most efficient metabolism of naphthalene. In contrast to naphthalene metabolism in pHLMs, more 1-naphthol was produced by several P450 isoforms than was 2-naphthol or dihydrodiol. In pHLMs, dihydrodiol formation was higher than that of either 1- or 2-naphthol. Epoxide hydrolase is generally known to be involved in the production of dihydrodiol from naphthalene epoxide. Naphthalene assays with a mixture of CYP1A2 and human microsomal epoxide

TABLE 6

The %TNR for 1-naphthol or trans-1,2-dihydro-1,2-naphthalenediol (dihydrodiol) metabolites by individual human P450 isoforms and the specific content of each P450 protein in native human liver microsomes

The %TNR values for metabolites of 1-naphthol or dihydrodiol were calculated with the total area of metabolites.

P450 Isoform	%TNR		Mean Content of P450 ^a
	1-Naphthol	Dihydrodiol	
			pmol P450/mg protein
1A1	N.D.	N.D.	N.A.
1A2	19.5	0.0	55
1B1	N.D.	0.0	N.A.
2A6	0.4	17.0	52
2B6	7.5	2.3	21
2C8 ^b	5.6	14.0	64
2C9	1.9	6.3	76
2C18 ^b	0.2	0.02	2.5
2C19	9.9	3.1	39
2D6	4.5	0.01	12
2E1	7.1	1.2	52
3A4	43.3	56.2	133
3A5	0.2	0.01	1.2
3A7	N.D.	N.D.	N.A.
4A11	N.D.	N.D.	N.A.

N.D., not determined; N.A., not available.

^a Mean content data were obtained from BD Gentest (2003 product catalog).^b Mean content data for 2C8 and 2C18 were obtained from Rodrigues (1999).

hydrolase showed that microsomal epoxide hydrolase in pHLMs contributes to the higher production of dihydrodiol. Epoxide hydrolase may not be the sole contributor to conversion of naphthalene-1,2-epoxide into the dihydrodiol, because individually expressed P450 isoforms also produced the dihydrodiol metabolite from naphthalene, possibly by nonenzymatic hydrolysis. However, because individual isoforms vary in the production of the dihydrodiol, the possibility exists for P450 involvement directly or indirectly in this transformation into dihydrodiol.

In the secondary metabolism of naphthalene, primary metabolites from naphthalene were used as substrates, and their metabolic reactions in pHLMs and P450 isoforms were investigated. Although 1-naphthol is readily metabolized by most P450 isoforms, this substance is a less favorable substrate for pHLMs than its parent chemical, naphthalene; 1-naphthol metabolism in pHLMs did not produce 1,4-naphthoquinone. In contrast to our results with pooled HLMs, individual P450 isoforms, including 1A2 and 2D6, were effective in metabolizing 1-naphthol to produce 1,4-naphthoquinone and unknown metabolites. 1,4-Naphthoquinone appears more effective as a substrate for pHLMs than its parent chemical, 1-naphthol. The significant reduction of 1,4-naphthoquinone in pHLMs may also be

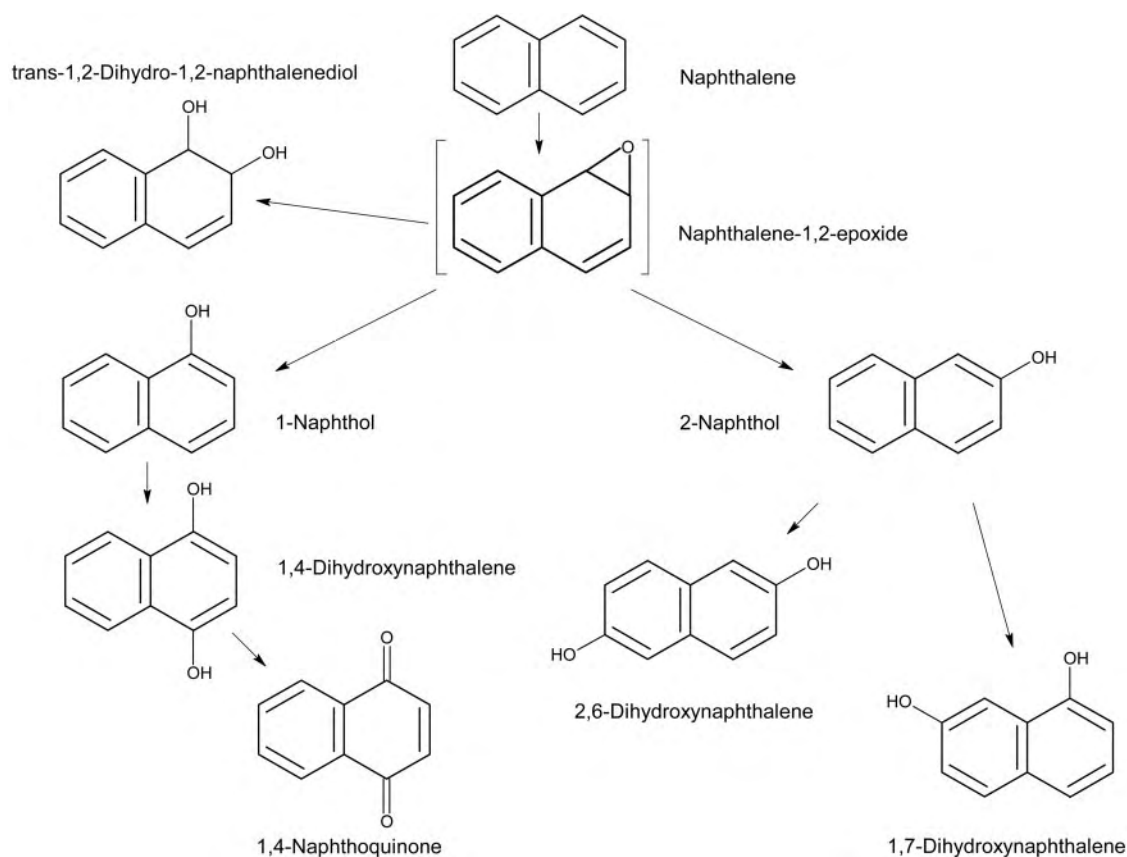


Fig. 5. Partial metabolic pathway of naphthalene by human liver microsomal cytochrome P450 enzymes.

associated with either its metabolism by enzymes other than P450 isoforms, or covalent binding of metabolites derived from metabolism of naphthols to microsomal protein fraction (Hesse and Mezger, 1979), or both.

In a different way from 1-naphthol, 2-naphthol was readily metabolized by pHLMs and CYP1A2. More abundant production of 2,6- rather than 1,7-dihydroxynaphthalene from 2-naphthol indicates that hydroxylation at the carbon 6 position is kinetically more favorable than at the carbon 8 position after carbon 2 is hydroxylated. The product hydroxylated at carbons 2 and 8 is also named 1,7-dihydroxynaphthalene. Metabolism of 2-naphthol by pHLMs, which was more active than that of 1-naphthol and dihydrodiol, may be a factor influencing the higher apparent K_m value for 2-naphthol production from naphthalene than those for 1-naphthol or dihydrodiol production in the metabolic system mediated by pHLMs.

trans-1,2-Dihydro-1,2-naphthalenediol (dihydrodiol) was not readily metabolized by either pHLMs or CYP1A2. Dihydrodiol is known to be converted into 1,2-dihydroxynaphthalene by dihydrodiol dehydrogenase and 1,2-naphthoquinone by further oxidation or 1,2-dihydroxy-3,4-epoxy-1,2,3,4-tetrahydronaphthalene by P450 (Penning et al., 1999; Buckpitt et al., 2002). However, neither 1,2-naphthoquinone nor 1,2-dihydroxy-3,4-epoxy-1,2,3,4-tetrahydronaphthalene was identified in this study. Because dihydrodiol dehydrogenase is a cytosolic enzyme, the absence of this enzyme in liver microsomes may explain why 1,2-naphthoquinone was not detected in the current study. Naphthalene metabolites, such as naphthols and dihydrodiol, can be further transformed into conjugation products with glucuronide/sulfate (Preuss et al., 2003), and epoxide can conjugate with glutathione (Smart and Buckpitt, 1983; Buckpitt et al., 1987; Preuss et al., 2003),

and this is further transformed into mercapturic acid conjugate (Pakenham et al., 2002).

As the major metabolites, naphthols can be used as biomarkers for exposure to naphthalene. 1-Naphthol and 2-naphthol are detected in urine of Wistar rats administered naphthalene intraperitoneally (Elovaara et al., 2003). However, these naphthols have also been detected in cases of exposure to environmental polycyclic aromatic hydrocarbons in humans and animals. A study of the urinary naphthol content in Japanese male workers, for instance, suggests that 1- and 2-naphthol can be used as biomarkers for exposure to airborne polycyclic aromatic hydrocarbons (Yang et al., 1999). In addition, personal preferences in lifestyle, including smoking, can provide significant variation in urinary naphthol content (Lee et al., 2001), and 1-naphthol is also generated as a metabolite when humans are exposed to the insecticide, carbaryl (Shealy et al., 1997). Furthermore, in the present studies, these naphthols were more readily metabolized by P450 isoforms than was dihydrodiol. Therefore, dihydrodiol can be a potential biomarker for exposure to naphthalene in humans due to the abundant generation and less effective conversion in human liver metabolism. The amount of dihydrodiol formed from naphthalene in mouse lung or liver microsomes in the presence of cytosolic proteins is not changed much over the range of 0 to 2 mg of cytosolic protein concentration (Buckpitt et al., 1984). This observation indicates that cytosolic enzymes may have minimal effects in the formation of dihydrodiol from naphthalene and in the conversion into downstream metabolites.

In summary, human naphthalene metabolism was extensively studied. The metabolic pathway of naphthalene by human liver microsomes and P450 isoforms is shown in Fig. 5. Naphthalene metabolism in pooled human liver microsomes produced *trans*-1,2-dihydro-1,2-

naphthalenediol, 1-naphthol, and 2-naphthol in order of production. The most efficient and important isoforms in human naphthalene metabolism were identified through human P450 isoform screening. Based on the total normalized rates (%TNR), CYP1A2, 3A4, 2E1, and 2A6 are considered to be the most important isoforms in human liver naphthalene metabolism. In these studies, the secondary metabolism of naphthalene was investigated using the primary metabolites as substrates for pHLM and P450 isozymes. CYP1A2 and 2D6, and CYP2A6 and 3A4 were identified as the most efficient isoforms for metabolizing 1-naphthol and dihydrodiol, respectively. Based on the protein contents in human liver, CYP3A4, 1A2, and 2C19 are considered the important isoforms for 1-naphthol metabolism, and CYP3A4, 2A6, and 2C8 were important for dihydrodiol. Because dihydrodiol was less favorable for metabolism by P450 isoforms than naphthalene or other primary metabolites, this metabolite has potential as a biomarker for human exposure to naphthalene.

Acknowledgments. We thank Dr. Alan R. Buckpitt (University of California, Davis, CA) for the generous gift of *trans*-1,2-dihydro-1,2-naphthalenediol. We also thank Peter Lazaro for technical assistance in the GC/MS analysis.

References

- Bagchi D, Balmoori J, Bagchi M, Ye X, Williams CB, and Stohs SJ (2000) Role of p53 tumor suppressor gene in the toxicity of TCDD, endrin, naphthalene and chromium (VI) in liver and brain tissues of mice. *Free Radic Biol Med* **28**:895–903.
- Bagchi M, Bagchi D, Balmoori J, Ye X, and Stohs SJ (1998) Naphthalene-induced oxidative stress and DNA damage in cultured macrophage J774A. 1 cells. *Free Radic Biol Med* **25**:137–143.
- Buckpitt A, Boland B, Isbell M, Morin D, Shultz M, Baldwin R, Chan K, Karlsson A, Lin C, Taff A, et al. (2002) Naphthalen-induced respiratory tract toxicity: metabolic mechanisms of toxicity. *Drug Metab Rev* **34**:791–820.
- Buckpitt A, Chang AM, Weir A, Van Winkle L, Duan X, Philpot R, and Plopper C (1995) Relationship of cytochrome P450 activity to Clara cell cytotoxicity. IV. Metabolism of naphthalene and naphthalene oxide in microdissected airways from mice, rats and hamsters. *Mol Pharmacol* **47**:74–81.
- Buckpitt AR and Bahnson LS (1986) Naphthalene metabolism by human lung microsomal enzymes. *Toxicology* **41**:333–341.
- Buckpitt AR, Bahnson LS, and Franklin RB (1984) Hepatic and pulmonary microsomal metabolism of naphthalene to glutathione adducts: factors affecting the relative rates of conjugate formation. *J Pharmacol Exp Ther* **231**:291–300.
- Buckpitt AR, Castagnoli N, Nelson SD, Jones AD, and Bahnson LS (1987) Stereoselectivity of naphthalene epoxidation by mouse, rat, and hamster pulmonary, hepatic and renal microsomal enzymes. *Drug Metab Dispos* **15**:491–498.
- Chichester CH, Buckpitt AR, Chang A, and Plopper CG (1994) Metabolism and cytotoxicity of naphthalene and its metabolites in isolated murine Clara cells. *Mol Pharmacol* **45**:664–672.
- Doherty MD, Cohen GM, and Smith MT (1984) Mechanisms of toxic injury to isolated hepatocytes by 1-naphthol. *Biochem Pharmacol* **33**:543–549.
- Elovaara E, Väänänen V, and Mikkola J (2003) Simultaneous analysis of naphthols, phenanthrols and 1-hydroxypyrene in urine as biomarkers of polycyclic aromatic hydrocarbon exposure: intraindividual variance in the urinary metabolite excretion profiles caused by intervention with β -naphthoflavone induction in the rat. *Arch Toxicol* **77**:183–193.
- Hesse S and Mezger M (1979) Involvement of phenolic metabolites in the irreversible protein-binding of aromatic hydrocarbons: reactive metabolites of [14 C]naphthalene and [14 C]1-naphthol formed by rat liver microsomes. *Mol Pharmacol* **16**:667–675.
- Lee C-Y, Lee J-Y, Kang J-W, and Kim H (2001) Effects of genetic polymorphisms of CYP1A1, CYP2E1, GSTM1 and GSTT1 on the urinary levels of 1-hydroxypyrene and 2-naphthol in aircraft maintenance workers. *Toxicol Lett* **123**:115–124.
- McDougal JN, Pollard DL, Weisman W, Garrett CM, and Miller TE (2000) Assessment of skin absorption and penetration of JP-8 jet fuel and its components. *Toxicol Sci* **55**:247–255.
- Morisseau C and Hammock BD (2005) Epoxide hydrolases: mechanisms, inhibitor designs and biological roles. *Annu Rev Pharmacol Toxicol* **45**:311–333.
- Pakenham G, Lango J, Buonarati M, Morin D, and Buckpitt A (2002) Urinary naphthalene mercapturates as biomarkers of exposure and stereoselectivity of naphthalene epoxidation. *Drug Metab Dispos* **30**:247–253.
- Penning TM, Burczynski ME, Hung C-F, McCoull KD, Palackal NT, and Tsuruda LS (1999) Dihydrodiol dehydrogenases and polycyclic aromatic hydrocarbon activation: generation of reactive and redox active o-quinones. *Chem Res Toxicol* **12**:1–18.
- Plopper CG, Van Winkle LS, Fanucci MV, Malburg SRC, Nishio SJ, Chang A, and Buckpitt AR (2001) Early events in naphthalene-induced acute Clara cell toxicity II. Comparison of glutathione depletion and histopathology by airway location. *Am J Respir Cell Mol Biol* **24**:272–281.
- Preuss R, Angerer J, and Drexler H (2003) Naphthalene—an environmental and occupational toxicant. *Int Arch Occup Environ Health* **76**:556–576.
- Riviere JE, Brooks JD, Monteiro-Riviere NA, Budsaba K, and Smith CE (1999) Dermal absorption and distribution of topically dosed jet fuels Jet-A, JP-8 and JP-8(100). *Toxicol Appl Pharmacol* **160**:60–75.
- Rodrigues AD (1999) Integrated cytochrome P450 reaction phenotyping. Attempting to bridge the gap between cDNA-expressed cytochromes P450 and native human liver microsomes. *Biochem Pharmacol* **57**:465–480.
- Shealy DB, Barr JR, Ashley DL, Patterson DG Jr, Camann DE, and Bond AE (1997) Correlation of environmental carbaryl measurements with serum and urinary 1-naphthol measurements in a farmer applicator and his family. *Environ Health Perspect* **105**:510–513.
- Shimada T, Yamazaki H, Mimura M, Inui Y, and Guengerich FP (1994) Interindividual variations in human liver cytochrome P-450 enzymes involved in the oxidation of drugs, carcinogens and toxic chemicals: studies with liver microsomes of 30 Japanese and 30 Caucasians. *J Pharmacol Exp Ther* **270**:414–423.
- Smart G and Buckpitt AR (1983) Formation of reactive naphthalene metabolites by target vs non-target tissue microsomes: methods for the separation of three glutathione adducts. *Biochem Pharmacol* **32**:943–946.
- Stohs SJ, Ohia S, and Bagchi D (2002) Naphthalene toxicity and antioxidant nutrients. *Toxicology* **180**:97–105.
- Tingle MD, Pirmohamed M, Templeton E, Wilson AS, Madden S, Kitteringham NR, and Park BK (1993) An investigation of the formation of cytotoxic, genotoxic, protein-reactive and stable metabolites from naphthalene by human liver microsomes. *Biochem Pharmacol* **46**:1529–1538.
- Van Bladeren PJ, Vyas KP, Sayer JM, Ryan DE, Thomas PE, Levin W, and Jerina DM (1984) Stereoselectivity of cytochrome P-450c in the formation of naphthalene and anthracene 1,2-oxides. *J Biol Chem* **259**:8966–8973.
- Van Winkle LS, Gunderson AD, Shimizu JA, Baker GL, and Brown CD (2002) Gender differences in naphthalene metabolism and naphthalene-induced acute lung injury. *Am J Physiol* **282**:L1122–L1134.
- Van Winkle LS, Johnson ZA, Nishio SJ, Brown CD, and Plopper CG (1999) Early events in naphthalene-induced acute Clara cell toxicity. Comparison of membrane permeability and ultrastructure. *Am J Respir Cell Mol Biol* **21**:44–53.
- Vuchetich PJ, Bagchi D, Bagchi M, Hassoun EA, Tang L, and Stohs SJ (1996) Naphthalene-induced oxidative stress in rats and the protective effects of vitamin E succinate. *Free Radic Biol Med* **21**:577–590.
- White RD (1999) Refining and blending of aviation turbine fuels. *Drug Chem Toxicol* **22**:143–153.
- Wilson AS, Davis CD, Williams DP, Buckpitt AR, Pirmohamed M, and Park BK (1996) Characterization of the toxic metabolite(s) of naphthalene. *Toxicology* **114**:233–242.
- Yang M, Koga M, Katoh T, and Kawamoto T (1999) A study for the proper application of urinary naphthols, new biomarkers for airborne polycyclic aromatic hydrocarbons. *Arch Environ Contam Toxicol* **36**:99–108.

Address correspondence to: Dr. Ernest Hodgson, Department of Environmental and Molecular Toxicology, Mail Box 7633, North Carolina State University, Raleigh, NC 27695-7633. E-mail: ernest_hodgson@ncsu.edu

HUMAN METABOLISM AND METABOLIC INTERACTIONS OF DEPLOYMENT-RELATED CHEMICALS

Ernest Hodgson and Randy L. Rose

Department of Environmental and Molecular Toxicology, North Carolina State University, Raleigh, North Carolina, USA

It has been suggested that chemicals and, more specifically, chemical interactions, are involved as causative agents in deployment-related illnesses. Unfortunately, this hypothesis has proven difficult to test, because toxicological investigations of deployment-related chemicals are usually carried out on surrogate animals and are difficult to extrapolate to humans. Other parts of the problem, such as the definition of variation within human populations and the development of methods for designating groups or individuals at significantly greater risk, cannot be carried out on surrogate animals, and the data must be derived from humans. The relatively recent availability of human cell fractions, such as microsomes, cytosol, etc., human cells such as primary hepatocytes, recombinant human enzymes, and their isoforms and polymorphic variants has enabled a significant start to be made in developing the human data needed. These initial studies have examined the human metabolism by cytochrome P450, other phase I enzymes, and their isoforms and, in some cases, their polymorphic variants of compounds such as chlorpyrifos, carbaryl, DEET, permethrin, and pyridostigmine bromide, and, to a lesser extent, other chemicals from the same chemical and use classes, including solvents, jet fuel components, and sulfur mustard metabolites. A number of interactions at the metabolic level have been described both with respect to other xenobiotics and to endogenous metabolites. Probably the most dramatic have been seen in the ability of chlorpyrifos to inhibit not only the metabolism of other xenobiotics such as carbaryl and DEET but also to inhibit the metabolism of steroid hormones.

Key Words: Alcohol dehydrogenase; Aldehyde dehydrogenase; Carbamates; Chemical warfare agents; Cytochrome P450; Deployment-related chemicals; Jet fuel components; Metabolic interactions; Metabolism; Organophosphorus compounds; Pyrethroids; Repellents; Xenobiotic-metabolizing enzymes.

INTRODUCTION

Chemicals used during military deployments, and particularly interactions between such chemicals, are frequently cited as possible causative agents in deployment-related illnesses. Unfortunately, definitive evidence for or against such a role is lacking. In part, this is related to the fact that investigations of deployment-related chemicals carried out in experimental animals assume relevance only when they can be extrapolated with confidence to humans. As most exogenous chemicals can be substrates, inhibitors, and/or

Address correspondence to Ernest Hodgson, Department of Environmental and Molecular Toxicology, Box 7633, North Carolina State University, Raleigh, NC 27695, USA; Fax: (919) 513-1012; E-mail: ernest_hodgson@ncsu.edu

inducers of xenobiotic-metabolizing enzymes (XMEs), these enzymes are an important potential locus for interactions. In fact, human XMEs often differ dramatically from those of experimental animals, rendering such extrapolations of little value. Based on animal studies, large uncertainty factors, usually undefined and therefore used as default values, must be employed in any numerical estimate of risk. Under these circumstances, it is difficult to be certain that the best estimate of human health risk is being used. At the same time, it must be understood that many studies of toxic mechanisms can only be carried out using surrogate animals. Recent advances in molecular biology have made available techniques that are helpful in the integration of animal and human studies in toxicology and risk assessment, in particular, the use of genetic knockout and humanized mice, and have thus added new dimensions to animal studies.

Certain aspects essential in risk analysis of chemicals can only be examined in human studies. They include the determination of variation within the human population, which is highly outbred. Little of value can be learned about human variation by the use of inbred experimental animals. Many XMEs are polymorphic, and the distribution of polymorphic variants varies between population subgroups and individuals, potentially putting some individuals and subpopulations at greater or lesser risk than others.

The military need for information on human health risk from chemicals is clear. In several recent conflicts, poorly defined aggregations of health effects (most recently, Gulf War related illness) have been attributed to chemicals or to interactions between two or more chemicals (Haley and Kurt, 1997). Thus the need exists both to determine whether previous health effects are indeed chemical-related and to minimize future problems. Following the Gulf War a number of veterans reported a variety of illnesses which may have been the result of abnormal chemical exposures. Some studies of these veterans have concluded that significant correlations between perceived illnesses and chemical use exist (Haley and Kurt, 1997).

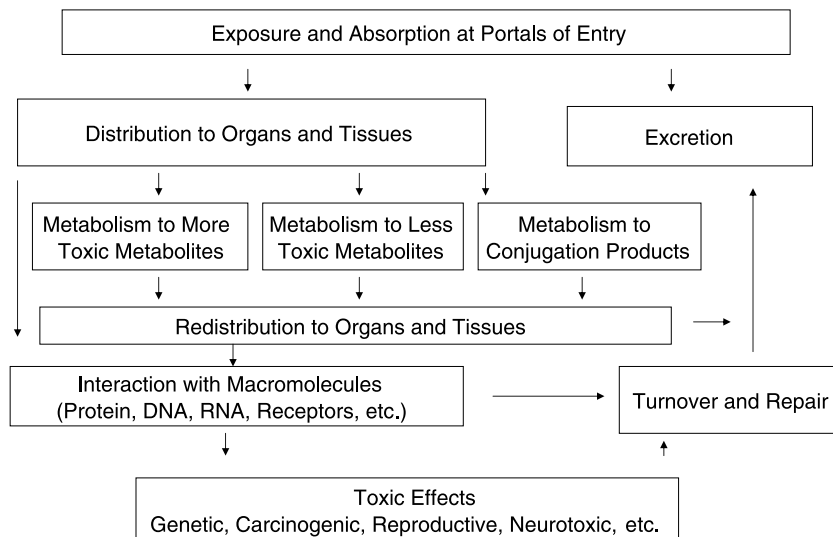


Figure 1. Mode of toxic action: a cascade of events.

Toxicity is the endpoint of a cascade of events that starts with exposure and ends with the expression of a toxic endpoint (Fig. 1). Intermediate steps include absorption, distribution, metabolism, distribution of metabolites, excretion, and/or interaction with cellular macromolecules followed by overt toxicity or repair. Although interactions can occur at any of these loci, metabolism is of critical importance, inasmuch as chemicals may be metabolically detoxified or activated to products more toxic than the parent compound. Phase I metabolism generally results in the introduction of a reactive group into the molecule, a reactive group that is subsequently conjugated with an endogenous compound during phase II metabolism. The most important phase I enzymes are the isoforms of cytochrome P450 (CYP) and the flavin-containing monooxygenase (FMO) (Hodgson and Smart, 2001). Furthermore, because XMEs have broad and often overlapping substrate specificities, metabolism is a probable locus for chemical interactions and for effects on the metabolism of endogenous substrates.

Because these activities are species, enzyme, isoform, and polymorphism specific, human studies using recombinant enzymes, subcellular preparations, and/or cultured cells are essential for the improvement of human health risk assessment, as follows:

- Identification of human XMEs, their isoforms and polymorphic forms involved in activation and/or detoxication
- Identification of reactive metabolites produced by human XMEs
- Identification of interactions between chemicals at the metabolic level
- Evaluation of the variation between individuals and identification of individuals and subpopulations at increased risk
- Provision of mechanistic insight into the results of epidemiological studies
- Overall improvement of the process of human health risk assessment with particular reference to deployment-related chemicals and deployment-related exposures

During the last few years, human subcellular preparations and recombinant enzymes have become readily available, and many new sensitive methods for the identification and quantitation of metabolites have been developed. Furthermore, noninvasive methods for the collection of human DNA combined with methods for high throughput genotyping make population studies possible.

Recent studies, as described below, have examined the role of specific human XMEs on the metabolism of a subset of chemicals important in military deployments. Carbaryl, chlorpyrifos, diethyl toluamide (DEET), permethrin, pyridostigmine bromide, sulfur mustard and its degradation products, and other chemicals of interest have been tested as substrates and inhibitors of the most important human XMEs, including cytochrome P450s (CYPs), flavin-containing monooxygenases (FMOs), alcohol and aldehyde dehydrogenases, and esterases (Choi et al., 2002, 2004; Dai et al., 2001; Tang et al., 2001, 2002; Usmani et al., 2002, 2003). A database on phase I enzymes and the metabolism of chemicals used in agriculture and public health was recently updated (Hodgson, 2003). Most XMEs exist as a number of isoforms, and these isoforms may have a number of polymorphic variants. Thus, it is important to know the relative abundance of these forms as well as their kinetic properties, because an enzyme with high activity may, *in vivo*, be less important than one with somewhat lower activity but with high abundance. The ability of these chemicals to act as inhibitors or enhancers of physiological (endogenous) substrates may also be of importance to the health of

exposed individuals, and effects on testosterone metabolism have been described. The potential of deployment-related chemicals to act as XME inducers has been studied to some extent in experimental animals, but studies are being initiated using human hepatocytes.

It is difficult to know exactly how many chemicals may be defined as deployment-related. Given the complexity of the noncombat deployment environment, with its wide array of public health and industrial chemicals as well as such combat-related chemicals as chemical warfare agents and combustion products, many variants of a list are possible. However, a useful starting point is the list provided in volumes 1 and 2 of "Gulf War and Health" (Institute of Medicine, 2003). To date, almost all studies of human *in vitro* xenobiotic metabolism and metabolic interactions have been carried out on clinical drugs, with few, if any, on insecticides, repellents, solvents, and industrial chemicals.

The relevance of these approaches to other occupational exposures in public health, industrial health, and agriculture is obvious, and the results should enable findings from animal studies to be extrapolated to humans with greater confidence. The results will also permit the identification of metabolic interactions specific to humans and permit the identification of populations at risk. Because the same XMEs are involved in the metabolism of clinical drugs and the xenobiotics of interest in deployments and elsewhere, interactions with clinical drugs are an aspect of considerable importance, unfortunately, an aspect that has not yet been addressed.

INSECTICIDES

Chlorpyrifos and Related Organophosphorus Insecticides

Introduction. Organophosphorus insecticides, including chlorpyrifos, are commonly used to control disease vectors as well as household and agricultural pests. They are potent inhibitors of acetylcholinesterase (AChE), resulting in a variety of symptoms including increased secretion, hyperactivity, and eventually death by respiratory failure (Echobicon, 2001). Many are organophosphorothioates, weak anticholinesterase inhibitors that are activated to their oxons, potent acetylcholinesterase inhibitors, by CYP catalyzed desulfuration. The resultant oxons are three or more orders of magnitude more potent as AChE inhibitors than the parent chemicals. Given these large differences in potency, the traces of oxons found as impurities in the parent compounds can have significant toxicological consequences (Yuknavage et al., 1997), and the effect of this oxon contamination will be impacted by the status of the individual relative to PON1 polymorphic forms (Li et al., 2000). The same enzymes involved in organophosphate activation are also important in the detoxication process. Thus, the ratio of activation to detoxication is dependent upon the individual CYP isoforms present in the tissue at a given time and will determine the amount of oxon available to cause toxicity (Levi and Hodgson, 1985).

Of the 11 insecticides shipped to the Gulf War (Institute of Medicine, 2003), five are organophosphorus chemicals. Three, chlorpyrifos, diazinon, and malathion, are phosphorothioates, containing the P=S group that are activated to their oxons by various CYP isoforms. Two others, azamethiphos and dichlorvos contain the P=O group and are potent AChE inhibitors without metabolic activation. Of these five insecticides, in terms of its use, chlorpyrifos is the most important as a deployment-related chemical.

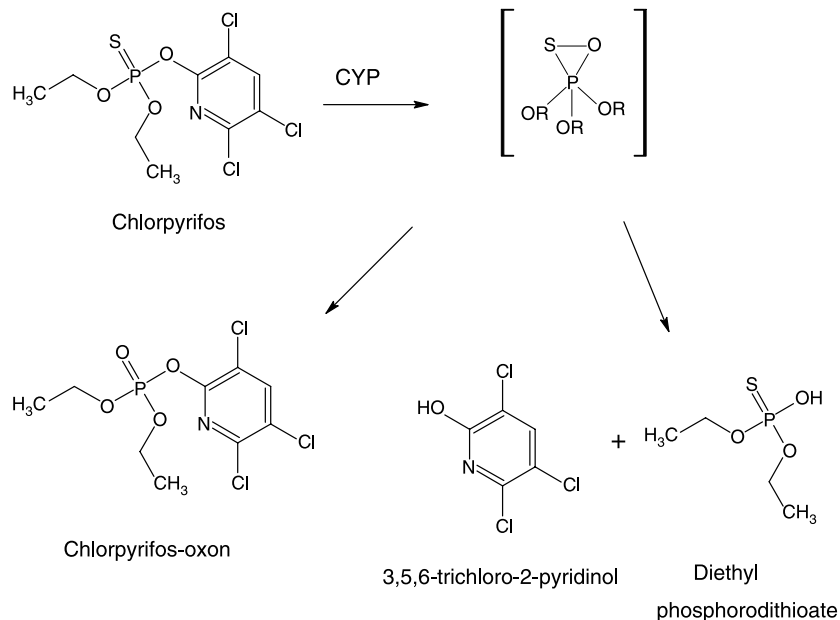


Figure 2. Metabolism of chlorpyrifos by human liver microsomes.

Numerous studies have been conducted in experimental animals [see Sultatos (1991) for references] on the metabolism of organophosphorus pesticides, including chlorpyrifos. Chlorpyrifos is metabolized to the oxon, and both chlorpyrifos and its oxon are rapidly hydrolyzed to 3,5,6-trichloro-2-pyridinol (3,5,6-TCP) (Fig. 2). In humans, low doses of chlorpyrifos are completely metabolized and subsequently eliminated in the urine as 3,5,6-TCP or glucuronide conjugates of 3,5,6-TCP (Nolan et al., 1984). Although under these circumstances, inhibition of AChE may not be apparent, interactions with esterases other than AChE, currently of unknown significance, may occur. Other metabolites may include deethylated chlorpyrifos (*O*-ethyl trichloropyridyl phosphorothioate) as well as glutathione conjugates.

Although the liver appears to play a primary role in metabolism, resulting in a net activation of chlorpyrifos, extrahepatic tissue activation may be important in its ultimate toxicity. Although female rats produce less chlorpyrifos oxon in liver perfusion studies than do males, females are more susceptible to chlorpyrifos. This indicates that the rate of oxon production by the liver cannot adequately explain differences observed in the acute toxicities of these pesticides (Sultatos, 1991).

Organophosphorus insecticides are readily metabolized by cytochrome P450 (Fig. 2). Oxidative metabolism can result in both intoxication as a result of desulfuration or detoxication by several pathways. Esterase metabolism of organophosphates is also an important mechanism of detoxication. A human polymorphic enzyme (PON1), an esterase that hydrolyzes the oxon, in one form (Arg-192) hydrolyzes paraoxon rapidly, while the other form (Gln-192) hydrolyzes paraoxon more slowly. However, the Gln-192 form rapidly hydrolyzes sarin, soman, and diazoxon in contrast with the Arg-192 form. Because the amount of PON1 is also highly variable in humans, the combination of genetic isoforms and the amount of enzyme may affect individual susceptibility to

organophosphates (Furlong et al., 1998). It has long been known that, as a result of the release of highly reactive sulfur, CYP is inhibited during oxon formation (Neal, 1980), and it was demonstrated more recently, in vivo, that chlorpyrifos is a CYP inhibitor when administered at a rate of 50 mg/kg to rats (Vodela and Dalvi, 1995).

Individual variation and the effect of polymorphisms are discussed below. It is clear, however, that there is considerable potential for differential sensitivity to chlorpyrifos to exist in the human population.

Subcellular preparations. Studies of in vitro human chlorpyrifos metabolism (Tang et al., 2001) demonstrate that pooled human liver microsomes, although effective in both desulfuration and oxidative dearylation, are less active toward this substrate than either rat or mouse microsomes. These species differences are illustrated by differences in the intrinsic clearance values (V_{max}/K_m) that have been determined for the more toxic oxon as well as the detoxication product, 3,5,6-TCP. In rats, the intrinsic clearance value for the oxon is 17-fold greater than in humans, while in mice, the intrinsic clearance for this product is only threefold greater. However, rats also have an enhanced ability to produce the detoxication products, as reflected by an eightfold greater intrinsic clearance value for the dearylation product than humans, while mice, again, show a threefold difference compared to humans for this value. Pooled human female liver microsomes were somewhat more active in chlorpyrifos metabolism than were pooled male liver microsomes.

In addition to chlorpyrifos, a number of other organophosphorus insecticides, including diazinon and parathion, are metabolized via both desulfuration and dearylation by pooled liver microsomes [see Hodgson (2003) for references].

Xenobiotic-metabolizing enzymes. Tang et al. (2001) also showed that the ability of human liver microsomes to detoxify chlorpyrifos and to activate it to its oxon was due to CYP isoforms 1A2, 2B6, 2C9, 2C19, and 3A4. The ratio of activation to detoxication varied between CYP isoforms, the ratios of desulfuration to dearylation ranged between 3.38 for the isoform most active in desulfuration (2B6) to 0.14 for the isoform least active in desulfuration (2C19). All of these isoforms are polymorphic and inducible, and thus, the potential for variation between individuals is high. More recently, Buratti et al. (2003) showed by correlation analysis that human CYP2B6 and CYP3A4 are most active in oxon production from a number of organophosphorus insecticides, including chlorpyrifos. The same CYP isoforms active in chlorpyrifos oxidation are also known to be active in the metabolism of diazinon and parathion [see Hodgson (2003) for references].

Polymorphic variants. Polymorphic variants of several of the CYP isoforms active in chlorpyrifos metabolism have been examined. Of three CYP2C19 polymorphisms (Tang et al., 2001), all had reduced ability for dearylation, while no desulfuration activity could be detected.

The variability of polymorphic variants is further exemplified by studies of variants of human CYP3A4, an isoform active in both the activation and detoxication of chlorpyrifos (Dai et al., 2001). It is known that the expression of this isoform, often the most abundant CYP isoform in human liver, can, nevertheless, vary as much as 40-fold between individuals. In these studies, several new polymorphic variants of CYP3A4 were identified, sequenced, expressed, and characterized. These variants differ from the wild type in their frequency in different populations and in their ability to metabolize chlorpyrifos. Of four CYP3A4 polymorphisms examined, two had desulfuration and

dearylation activities similar to the wild type, one appeared to be defective in both activities, and the fourth was significantly more active.

CYP2B6 polymorphisms are also being examined (J. A. Goldstein, personal communication, 2004). Results to date indicate that several polymorphic variants do not differ significantly from the wild type in their ability to metabolize chlorpyrifos.

Individual livers. Potential differences in chlorpyrifos metabolism in the human population based on differences in hepatic enzymes were examined (Tang et al., 2001) using microsomes from five individual livers. Individuals with varying levels of CYP2B6, 2C19, 2D6, and 3A4 were selected to represent contrasting levels of predictable metabolic activity. Thus, as was observed, individuals with higher levels of CYP2B6 and CYP3A4 would be expected to show higher levels of desulfuration than those with lower levels of these isoforms. CYP3A4 should contribute to both desulfuration and dearylation, but, because microsomes from livers with contrasting levels of CYP2B6 and 3A4 were not available, the extent of their separate contributions to desulfuration could not be estimated. However, based on these results and those of others using parathion as a substrate (Butler and Murray, 1997; Mutch et al., 1999; Sams et al., 2000), CYP3A4 should contribute significantly to both desulfuration and dearylation. Even with a number as small as five, the variation in desulfuration activity was fivefold and that for dearylation was threefold. For parathion, the variation was 16- and 10-fold, respectively (Butler and Murray, 1997; Mutch et al., 1999). Mutch et al. (1999) demonstrated that the activation of parathion to paraoxon varied among individuals by as much as 16-fold, while the detoxication rate varied by only threefold.

Considerations of metabolic differences between individuals should also include the contributions of esterases, which, from animal studies, are known to be major factors in determining the in vivo toxicity of organophosphorus insecticides (Chambers et al., 1990; Costa et al., 1990; Maxwell et al., 1987). Unfortunately, with the exception of paraoxonase, the human esterases involved in organophosphorus insecticide metabolism have not been investigated. It is of interest (Li et al., 2000) with regard to the detoxication of diazoxon that only the level of PON1 is important, whereas for chlorpyrifos oxon, the status of the PON1 polymorphic forms as well as the level is also important, with the PON1R192 alloform providing significantly more protection than the PON1Q192 alloform. At the same time, neither alloform appears to be significant in protecting against a paraoxon exposure (Li et al., 2000).

Permethrin and Related Pyrethroids

Introduction. Of the 11 insecticides shipped to the Gulf War (Institute of Medicine, 2003), only two are pyrethroids, permethrin and d-phenothrin. Of these, permethrin is more important.

Permethrin, 3-phenoxybenzyl (\pm)-*cis, trans*-3-(2,2-dichlorovinyl)-2,2-dimethylcyclopropane-1-carboxylate, is a synthetic pyrethroid commonly used as an insecticide, including use in military deployments. The discovery of the first photostable pyrethroid, permethrin (Elliott, 1976; Elliott et al., 1973), revolutionized the use of pyrethroids as a class. Since its discovery, this class of insecticide has become one of the mainstays of chemical control due to high insecticidal efficacy, low mammalian toxicity, and lack of environmental persistence.

Permethrin has been extensively studied with respect to its toxicological properties (Ishmael and Litchfield, 1988; Litchfield, 1985; Metker et al., 1978). At high doses, permethrin produces a syndrome characterized by aggressive sparring, increased sensitivity to external stimuli, and a fine tremor that progresses to whole body tremor and prostration (Verschoyle and Barnes, 1972). At low doses, a dose-dependent decrease in locomotor activity and an increase in startle response to acoustic stimuli are observed (Crofton and Reiter, 1988). Bloomquist (1993) provides an overview of electrophysiological effects and interactions of pyrethroid insecticides with biochemical and physiological target sites in mammals and insects.

The low acute mammalian toxicity of permethrin and other pyrethroids is the result of their rapid metabolism and excretion (Elliott et al., 1976; Gaughan et al., 1977; Miyamoto, 1976). The major mammalian metabolite of permethrin, excreted as both free and conjugated forms, is 4'-hydroxy-3-phenoxybenzoic acid. This product, the result of ester hydrolysis, has been demonstrated to be a significant factor in the detoxication of permethrin in adult rats through the use of esterase synergist studies (Cantalamessa, 1993). Other minor metabolites that include hydroxylations at the acidic geminal dimethyl group and at the phenoxy group of the alcohol are the result of oxidative enzymes. Once these oxidations occur, the resulting carboxylic acids and phenols may be conjugated by a variety of conjugating enzymes. These metabolites are quickly excreted and do not persist in the tissues (Elliott et al., 1976; Gaughan et al., 1977).

Prior to recent studies (Choi et al., 2002), studies of permethrin metabolism in humans had been limited to the detection of primary metabolites in blood or urine samples (Angerer and Ritter, 1997; Asakawa et al., 1996; Hardt and Angerer, 2003; Leng et al., 1997). Although providing information as to permethrin persistence and potential routes of metabolism, actual metabolic pathways and specific enzymes involved are not provided by these studies. The more recent studies have demonstrated that while *cis*-permethrin is poorly metabolized by human liver fractions, the *trans* isomer is readily metabolized by both soluble and microsomal esterases (Choi et al., 2002). The resulting phenoxybenzyl alcohol is then readily metabolized to phenoxybenzoic acid by sequential oxidations by alcohol dehydrogenase and aldehyde dehydrogenases (Fig. 3). Although human alcohol and aldehyde dehydrogenases have been studied [e.g., Chen and Yoshida (1991), Stone et al. (1993), Wagner et al. (1983)], prior to these studies, the role of alcohol and aldehyde dehydrogenase enzymes in metabolism of pyrethroids had not been described in either humans or in mammals, although the metabolites detected would have suggested the existence of these metabolic pathways.

Subcellular Preparations. *Trans*-permethrin is metabolized to phenoxybenzyl alcohol and phenoxybenzoic acid in both pooled human liver microsomes and human liver cytosol, while the *cis* isomer does not appear to be metabolized by these preparations. The addition of NADPH to the microsomal preparations was without effect, indicating that the initial step, to phenoxybenzoic alcohol, was a hydrolysis, a finding supported by the observation that cytosol and microsomes produced the same metabolites. As noted below, this hydrolysis can be inhibited by chlorpyrifos oxon and carbaryl. The hypothesis that the metabolism of phenoxybenzyl alcohol to phenoxybenzoic acid was mediated by alcohol dehydrogenase and aldehyde dehydrogenase and that phenoxybenzaldehyde was an intermediate was tested by the use of recombinant human enzymes (Choi et al., 2002).

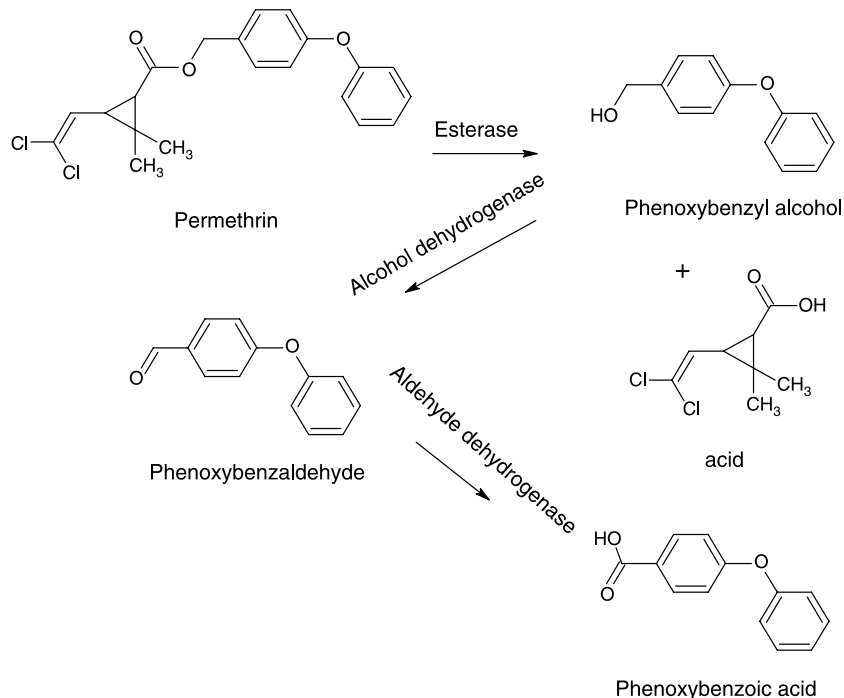


Figure 3. Metabolism of permethrin by human liver microsomes and cytosol.

Xenobiotic-metabolizing enzymes. All four purified recombinant human alcohol dehydrogenases tested metabolized phenoxybenzyl alcohol to phenoxybenzaldehyde with K_m values ranging from 4 to 48 μM . These K_m values are around two orders of magnitude smaller than those for ethanol and catalytic efficiencies, indicating that phenoxybenzyl alcohol is a preferred substrate for this enzyme. Only a single isoform of human aldehyde dehydrogenase (ALDH3A1) was available for these studies (Choi et al., 2002). This isoform catalyzed the metabolism of phenoxybenzaldehyde to phenoxybenzoic acid.

Carbaryl and Related Carbamates

Introduction. Four carbamates are among the insecticides shipped to the Gulf War, carbaryl, bendiocarb, propoxur, and the carbamate oxime, methomyl (Institute of Medicine, 2003). Of these, carbaryl is the one most likely to have been used and is the most important.

Carbaryl, 1-naphthol *N*-methylcarbamate, is a broad-spectrum carbamate insecticide with a variety of agricultural and public health applications. Due to its wide use, humans may be exposed either occupationally or through food and other routes (Cranmer, 1986). The mechanism underlying the toxicity of carbamate pesticides is its action as a cholinesterase inhibitor (Fukuto, 1990). The inhibition of cholinesterase by carbamates is reversible and less persistent than that by organophosphates.

Early studies of carbamate metabolism focused on hydrolysis because of the assumption that the ester linkage was susceptible to esterase attack as well as because of the limitations of the analytical techniques then available (Dorough, 1970). However, the importance of oxidative pathways had been shown earlier with the demonstration of NADPH-dependent metabolic activity toward carbamates in rat liver microsomes (Hodgson and Casida, 1960, 1961). Like many other carbamates, carbaryl can be hydrolyzed by esterases and oxidized by cytochrome P450-mediated monooxygenases (CYP) to form both hydrolysis and hydroxylation products, respectively, that are subject to further conjugation, such as sulfate and glucuronic acid conjugation of 1-naphthol and 4-hydroxycarbaryl (Matsumura, 1975). The major hydroxylation products include 5-hydroxycarbaryl, (5-hydroxy 1-naphthyl *N*-methylcarbamate), 4-hydroxycarbaryl, (4-hydroxy 1-naphthyl *N*-methylcarbamate), and carbaryl methylol, (1-naphthyl *N*-(hydroxymethyl)carbamate) (Dorough and Casida, 1964; Dorough et al., 1963; Strother, 1972; Fig. 4).

Although the contributions of hydrolysis and hydroxylation toward total metabolism of carbaryl have yet to be elucidated, it has been suggested that hydroxylation by CYP is the more important route of carbaryl metabolism (Ehrich et al., 1992; Ward et al., 1988). It has been shown (Ehrich et al., 1992) that chickens have a higher clearance rate for carbaryl than rats, although they have lower carboxylesterase and A-esterase activities, suggesting that these esterases did not contribute to the difference between the

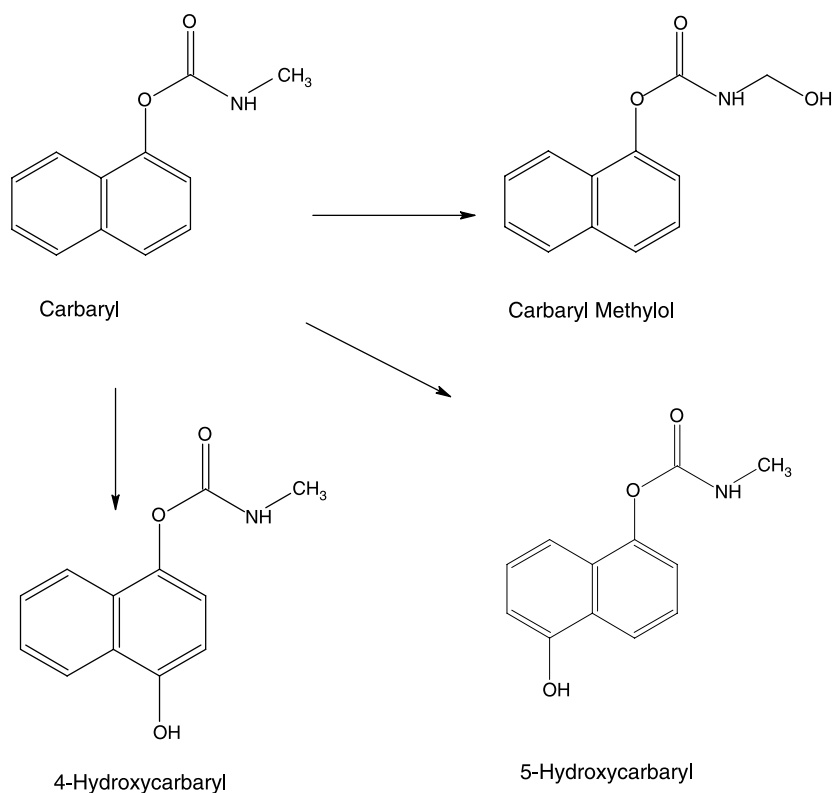


Figure 4. Metabolism of carbaryl by human liver microsomes.

two species. An inhibition study in rats and humans showed that the CYP inhibitor cimetidine reduced the metabolism of carbaryl, again suggesting that CYP plays a major role in carbaryl metabolism (Ward et al., 1988).

Although carbaryl is an anticholinesterase, some hydroxylation products have been shown to be more active than the parent compound. It has been shown (May et al., 1992) that while pretreatment with cimetidine increased the plasma concentration of carbaryl in man, the inhibition of blood cholinesterase activity was reduced, suggesting that cimetidine is blocking the production of active metabolites generated by CYP. 5-Hydroxycarbaryl has been reported to be more toxic than carbaryl (Dorough, 1970; Oonithan and Casida, 1968).

Both carbamate and organophosphorus insecticides are metabolized by CYP (Hodgson and Casida, 1960) and act as anticholinesterases (Fukuto, 1990). It is possible, therefore, that they may interact in metabolic pathways as well as in target sites. One important group of organophosphorus insecticides is the phosphorothionates, such as chlorpyrifos and malathion. Bioactivation of this group by CYP causes suicide inhibition of CYP activity (Neal, 1980), resulting in a reduction of CYP activity. A significant increase in carbaryl toxicity in red-legged partridges following malathion administration has been attributed to inhibition of carbaryl metabolism (Johnston, 1995). Although the hepatic metabolism of carbaryl in humans has been previously investigated *in vitro* (Chin et al., 1974; Strother, 1972), the contributions of individual CYP isoforms to the metabolic pathways had not been elucidated prior to the studies of Tang et al. (2002). Knowledge of the varying contributions of CYP isoforms to carbaryl metabolism should enable better understanding of differences in metabolism among individuals as well as among subpopulations and will provide important information relative to metabolic interactions of carbaryl with other chemicals.

Subcellular preparations. Four metabolites were detected after incubation of carbaryl with pooled human liver microsomes (Tang et al., 2002), namely, 5-hydroxycarbaryl, 4-hydroxycarbaryl, carbaryl methylol, and 1-naphthol. The first three were generated only in the presence of an NADPH-generating system and are, therefore, the products of CYP-mediated reactions. Only very small amounts of 1-naphthol, an hydrolysis product produced in the presence or absence of the NADPH-generating system, were generated in either the microsomal or the cytosolic fractions of human liver. Based on kinetic constants and clearance rates, methylol carbaryl was produced most efficiently and 5-hydroxymethylcarbaryl least efficiently, by liver microsomes.

Xenobiotic-metabolizing enzymes. Of 16 human CYP isoforms tested (Tang et al., 2002), only CYP2D6*10 and CYP4A11 were without detectable activity toward carbaryl. All other isoforms generated all three oxidative metabolites, although the activities and product ratios varied widely among isoforms. The most active isoforms were CYP1A1, 1A2, 2B6, 2C19, and 3A4. Of these, CYP2B6 had the highest activity and produced primarily (almost exclusively) the methylol derivative.

Polymorphic variants. Polymorphic variants of CYP isoforms have not been extensively investigated with respect to carbaryl metabolism. However, CYP2C9*2 is less active than the wild type 2C9, and CYP2D6*10 showed no activity toward carbaryl although 2D6*1 did, producing primarily 5-hydroxycarbaryl (Tang et al., 2002).

Individual livers. Human liver microsomes (Tang et al., 2002) from five selected individuals showed a twofold difference in the generation of either 5-hydroxycarbaryl or 4-hydroxycarbaryl with the activities not correlated with any single CYP isoform. On the other hand, the same microsomes showed a fivefold difference

in the generation of methylol carbaryl, a difference correlated with the level of CYP2B6 activity.

Other Insecticides

Other than those listed above, few other insecticides appear to have been used in military deployments, at least in recent years. An exception is lindane, listed as having been shipped to the Gulf War (Institute of Medicine, 2003).

REPELLENTS

N,N-Diethyl-*m*-Toluamide (DEET)

Introduction. DEET appears to be the only repellent used to any extent in military deployments. Moreover, every year, approximately one-third of the U.S. population, over 75 million people, use DEET-containing products with DEET concentrations ranging from 10 to 100% in a variety of liquids, lotions, gels, sprays, sticks, and impregnated materials, some 30 million packages of DEET-containing products being sold annually (Veltri et al., 1994).

Given this wide use, DEET must be considered safe when applied properly; although there are accounts of side effects, largely anecdotal, that include toxic encephalopathy, seizure, acute manic psychosis, cardiovascular toxicity, and dermatitis. A few cases of death may have resulted from extensive skin absorption (Schoenig et al., 1996). Studies of absorption and metabolism in humans suggest that a small percentage of topically applied DEET is rapidly absorbed (5–8%) and excreted. As many as six major metabolites were recovered from the urine (Selim et al., 1995).

Subcellular preparations. Studies of the oxidative metabolism of the insect repellent *N,N*-diethyl-*m*-toluamide (DEET) have been conducted using pooled human liver microsomes, rat liver microsomes, and mouse liver microsomes. In this first in vitro study of DEET metabolism in humans (Usmani et al., 2002), it was shown that human liver microsomes metabolized DEET primarily to two products, a ring methyl oxidation product, *N,N*-diethyl-*m*-hydroxymethylbenzamide and an *N*-deethylated product, *N*-ethyl-*m*-toluamide (Fig. 5).

Xenobiotic-metabolizing enzymes. Although in vitro studies of DEET metabolism using pooled human liver microsomes showed the production of two metabolites, the production of the ring methyl oxidation product, *N,N*-diethyl-*m*-hydroxymethylbenzamide was approximately 10-fold higher than that of the *N*-deethylated product, *N*-ethyl-*m*-toluamide. Both the affinities and intrinsic clearance of human liver microsomes (HLM) for ring methyl hydroxylation are greater than those for *N*-deethylation. An interesting observation is that the two products are formed by two different sets of CYP isoforms. Among 15 cDNA-expressed CYP enzymes examined, CYP1A2, 2B6, 2D6*1 (Val₃₇₄), and 2E1 metabolized DEET to the ring methyl metabolite, while CYP3A4, 3A5, 2A6, and 2C19 produced the *N*-deethylated metabolite. CYP2B6 is the principal CYP involved in the metabolism of DEET to its major ring methyl oxidation product, while CYP2C19 had the greatest activity for the formation of the *N*-deethylated product (Usmani et al., 2002).

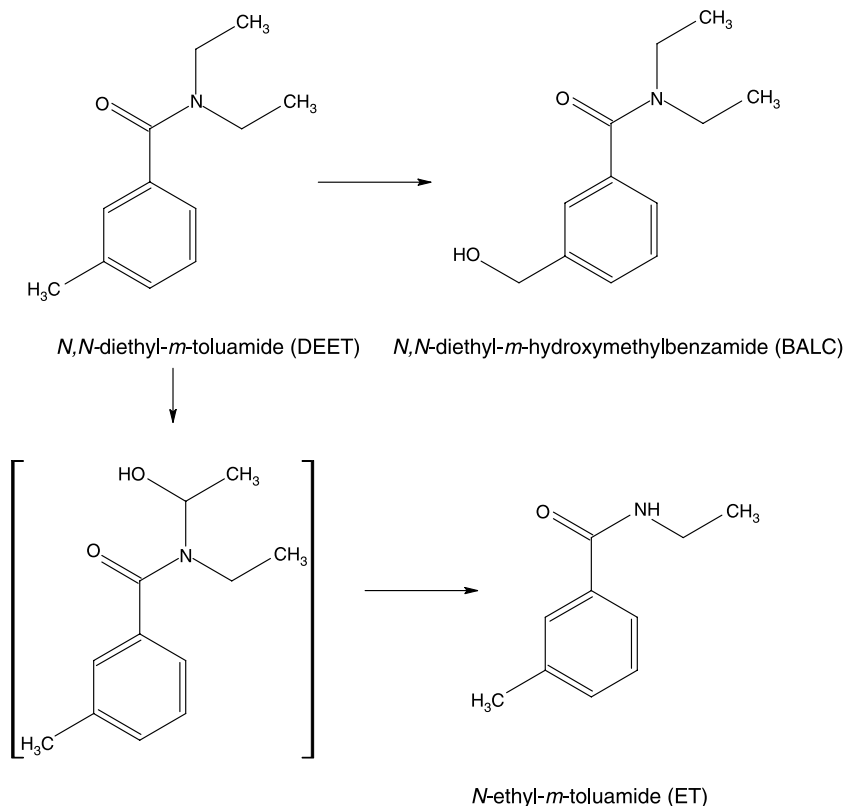


Figure 5. Metabolism of DEET by human liver microsomes.

To summarize, CYPs 1A2, 2B6, 2D6, and 2E1 produced the hydroxymethyl product, and 3A4, 3A5, 2A6, and 2C19 produced the deethylated product with no overlap between the two groups of isoforms, that is to say, there are no isoforms that produce both products. Given the different affinities observed, it is probable that at low substrate concentrations, only the ring methyl hydroxylation is likely to be observed (Usmani et al., 2002).

Individual livers. The use of phenotyped HLM demonstrated that individuals with high levels of CYP2B6, 3A4, 2C19, and 2A6 have the greatest potential to metabolize DEET. Mice treated with DEET demonstrated induced levels of the CYP2B family, increased hydroxylation, and a 2.4-fold increase in the metabolism of chlorpyrifos to chlorpyrifos-oxon, a potent anticholinesterase (Usmani et al., 2002).

SOLVENTS

Although some 53 solvents are listed as being shipped to the Gulf War (Institute of Medicine, 2003), little is known about their human metabolism *in vitro*. Based on industrial experience, many would be regarded as safe in most circumstances, while

others were probably not used extensively. Included in the list are the following; although arranged by functional group, many fall in several categories:

Acids

Acetic acid

Cresylic acid

Alcohols (including glycols)

2-Butoxyethanol

Butyl alcohol

Cyclohexanol

Diethylene glycol

Dipropylene glycol

Ethanol

2-Ethyl butanol

Ethylene glycol

Glycerol

Hexyl alcohol

Hexylene glycol

Isopentyl alcohol

Isopenpropyl alcohol

Methanol

Polyalkylene glycol

Propyl alcohol

Alkanes and Substituted Alkanes

Chloroform

Dichlorofluoromethane

n-Heptane

Methylene chloride (dichloromethane)

Tetrachloroethylene

1,1,1-Trichloroethylene

1,1,2-Trichloro-1,2,2-trifluoroethane

Aldehydes and Ketones

Acetone

Amyl acetate

Cyclohexanone

Ethyl acetate

Isoamyl acetate

1-Methoxy-2-propanol acetate

Methyl ethyl ketone

Methyl isoamyl ketone

Methyl isobutyl ketone

Methyl propyl ketone

Amines

Diethylene triamine

Aromatics

Benzene

Camphor

Cresol

Morpholine

Phenol

Toluene

Xylene

Ethers

Diethylene glycol monobutyl ether

Ethylene glycol monoethyl ether

Ethylene glycol monomethyl ether

Ethyl ether

Phosphorus esters

Tricresyl phosphate

Mixtures

Naphtha

Stoddard solvent

It is clear, from the extensive compilation of Bruckner and Warren (2001), that essentially all populations in any industrialized society are exposed to solvents and vapors and that the many factors that govern exposure, metabolism, and potential metabolic interactions in general are all relevant to solvent exposure. Most of the chemicals listed (Institute of Medicine, 2003) are used in connection with transportation either as solvents, as listed, or as antifreezes or deicers. Their use in specific military applications, such as in military jet planes and fighting vehicles, should not be significantly different from their use in commercial jets, heavy road transport, or earth-moving equipment.

Although few studies of the *in vitro* metabolism of any of the above chemicals have been carried out in humans, most have been investigated in surrogate animals, particularly rodents. It is apparent from these studies that metabolic interactions are possible, indeed probable, in humans. For example, many small, lipophilic molecules are substrates for CYP2E1, a cytochrome P450 isoform found in both hepatic and extrahepatic tissues. It has been shown (Guengerich et al., 1991) that human CYP2E1 metabolized a number of halogenated aromatic and aliphatic hydrocarbons, including several listed above, such as trichloethylene, chloroform, and benzene. It is also known that in individual human liver microsomes, increased ability to metabolize chlorofluorocarbons is correlated with high CYP2E1 levels, and that individuals with chemical exposures (e.g., to ethanol) that increase CYP2E1 levels may be at increased risk from chlorofluorocarbon poisoning (Surbrook and Olson, 1992). In the present context, it is

important to note that oxidation by CYP2E1 may produce reactive metabolites capable of causing cytotoxicity and mutagenicity (Raucy et al., 1993).

Alcohols

In addition to occupational exposure, ethanol is frequently ingested in moderate to excessive amounts. Although the psychomotor effects of ethanol are of prime importance due to their effect on performance of essential tasks, it should be noted that ethanol can have other effects that may be of considerable importance. First, ethanol is metabolized to acetaldehyde, a reactive product, by CYP2E1, but also with the concomitant release of reactive oxygen radicals (Lieber, 1997). Ethanol is also a potent inducer of CYP2E1, possibly increasing the production of reactive intermediates from other substrates (Nakajima et al., 1985). Ethanol is also oxidized by alcohol dehydrogenase (Nakajima et al., 1985), followed by aldehyde dehydrogenase, producing first acetaldehyde and subsequently acetate. As these two enzymes are now known to be important in the metabolism of permethrin in humans (Choi et al., 2002), alcohol–permethrin interactions are possible. The potential utility of physiologically based pharmacokinetic models for the investigation of ethanol interactions is suggested by a recently published pharmacokinetic model for ethanol in humans that incorporates information on isoforms and polymorphisms in human alcohol dehydrogenase (Sultatos et al., 2004).

Methanol is metabolized to formaldehyde by alcohol dehydrogenase in primates or by catalase in rodents. The formaldehyde is further metabolized in both rodents and primates to formate by aldehyde dehydrogenase [see Bruckner and Warren (2001) for details]. Both formaldehyde and formate are toxic. The formate produced is metabolized to carbon dioxide more rapidly in rodents than in primates. Thus, methanol, whether used as a solvent or as a gasoline additive, may be involved in metabolic interactions in humans.

Less is known about the metabolism in experimental animals of the other alcohols listed above, and virtually nothing is known about their metabolism in humans. Given the broad specificity of both CYP isoforms (including CYP2E1) and alcohol and aldehyde dehydrogenases, it seems likely that these enzymes are involved in both surrogate animals and humans and that metabolic interactions with other xenobiotics are possible.

Glycols

These chemicals are widely used as antifreeze agents and deicers as well as for other industrial uses. The widely used ethylene glycol is acutely toxic to humans, toxicity that not infrequently results in death. The involvement of alcohol dehydrogenase may also be a cause of concern for reasons stated above with reference to alcohols. Glycol ethers represent a similar, but somewhat more complex, situation.

Chlorinated Hydrocarbons

Many of these are important solvents, and their metabolism has been studied in experimental animals. Although the pathways differ significantly from one chemical to

another and, in some cases, from one species to another, they usually involve cytochrome P450 isoforms as well as glutathione S-transferases. In both cases, reactive intermediates are common, and the potential for metabolic interactions is high. Although much less is known about their metabolism in humans, in view of the often considerable exposures, they must be a cause for concern.

Aromatic Hydrocarbons

These chemicals, particularly benzene, are important toxicants and may also be involved in metabolic interactions. There is a considerable body of information on the hematopoietic toxicity of benzene to humans (Bruckner and Warren, 2001). Benzene toxicity is more likely to be due to the toxicity of its metabolites than to benzene itself. Some metabolites identified include phenol, catechol, hydroquinone, 1,2,4-trihydroxybenzene, 1-phenylmercapturic acid, and *trans*-muconic acid. Benzene metabolism involves cytochrome P450 and glutathione S-transferase as well as glucuronide and sulfate conjugation pathways (Bruckner and Warren, 2001). Further studies in humans are needed before the extent of such interactions and the risk associated with them becomes clear.

Phosphorus Esters

While most of the concern about phosphorus esters centers around organophosphorus insecticides and chemical warfare agents, there are some lubricants and fuel additives of concern, including tricresyl (tritolyl) phosphate. This chemical has been studied intensively as a cause of organophosphate-induced delayed neuropathy (OPIDN), a human toxic endpoint that, although known earlier, first came to prominence during prohibition in the United States as ginger jake paralysis, caused by the addition of tolyl ester contaminated alcoholic extracts of Jamaican ginger (Echobicon, 2001). Tricresyl phosphate is an important component of jet fuel lubricants that can enter the cabin area through the bleed air when engine seals fail (Winder and Balouet, 2002). Winder and Balouet (2002) stated that the risk of tricresyl phosphate exposure is frequently seriously underestimated.

JET FUEL COMPONENTS

Military personnel may be frequently, even daily, exposed to jet fuels (Pleil et al., 2000), the components of which may be absorbed either through dermal absorption or inhalation. In animal studies, JP-8 jet fuel has been shown to have effects on several organ systems including the liver and skin, as well as the immune, nervous, respiratory, and reproductive systems (Allen et al., 2000, 2001; Cooper and Mattie, 1996; Dudley et al., 2001; Grant et al., 2000; Harris et al., 2000; Kabbar et al., 2001; Kanikkannan et al., 2002; Monteiro-Riviere et al., 2001; Ramos et al., 2002; Rhyne et al., 2002; Ritchie et al., 2001; Robledo et al., 2000; Ullrich and Lyons, 2000). Although not as extensively studied in humans, it is known to cause irritant dermatitis and to have some neurological effects (Smith et al., 1997; Zeiger and Smith, 1998). The toxicology of the jet fuel JP-8 has recently been summarized (National Research Council, 2003).

However, the extent to which jet fuel components are metabolized in humans is not well known, and, therefore, their potential to interact at the metabolic level with other deployment-related chemicals is unknown.

Although not discussed in this review, it should be noted that considerations of the toxicity and metabolism of the components of automotive and other diesel fuels should not be significantly different from those for jet fuel components. Most of the constituents of these fuels are common to all.

Because jet fuels are complex mixtures, it is not possible to use jet fuel itself in studies of the metabolism of jet fuel components. However, jet fuels can be used in preliminary studies in such areas as induction of XMEs or inhibition of the metabolism of either exogenous or endogenous chemicals. Initial studies of metabolism and interaction of components can be carried out using known components representative of different chemical classes. For example, dodecane and naphthalene are JP-8 components that have been used in studies of dermal absorption (Baynes et al., 2000; McDougal et al., 2000; Riviere et al., 1999).

Naphthalene metabolism has been studied in mammalian systems and is known to yield a number of metabolites, including oxidation products and their conjugates (Fig. 6). The initial step appears to be CYP dependent and to yield the arene epoxide, 1,2-naphthalene oxide. 1,2-Naphthalene oxide can spontaneously rearrange to form 1- and 2-naphthol, compounds that can be further hydroxylated to di-, tri-, and tetrahydroxylated products (Horning et al., 1980). Some of these metabolites may be conjugated

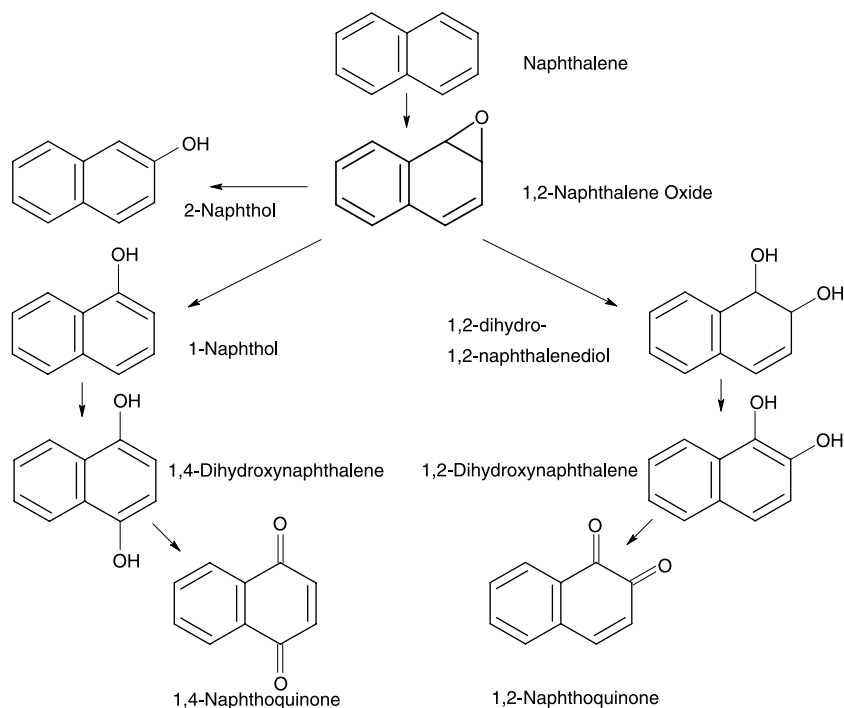


Figure 6. Metabolism of naphthalene by human liver and lung microsomes.

with glutathione, glucuronic acid, or sulfate, with the glutathione conjugates eventually giving rise to mercapturic acids (ATSDR, 1995; Pakenham et al., 2002; USEPA, 1998). An alternative pathway involves the action of epoxide hydrolase on the arene oxide to form 1,2-dihydro-dihydroxynaphthalene, and then, by a series of reactions, 1,2- and 1,4-naphthoquinone are formed (USEPA, 1998).

It is apparent from the small number of human studies that these pathways operate, in whole or in part, in humans. Human lung microsomes exposed in vitro to naphthalene produced dihydro-1,2-naphthalenediol and several of its glutathione derivatives (Buckpitt and Bahnson, 1986; Buckpitt and Richieri, 1984; Buonarati et al., 1990; USEPA, 1998). In human liver microsomes (Tingle et al., 1993), the primary stable metabolite was 1,2-dihydro-1,2-naphthalenediol, while 1-naphthol was a minor product. Earlier urine analyses (Mackell et al., 1951) indicated that both 1,2- and 1,4-naphthoquinone are formed, in vivo, in humans exposed to naphthalene. Few studies appear to have been carried out specifically on CYP, on CYP isoforms, or on their polymorphisms in either humans or experimental animals, although naphthalene was one of the substrates used in a study of atypical kinetics (non-Michaelis-Menton) shown by several human CYP isoforms (Korzekwa et al., 1998). In this study, naphthalene was shown to be metabolized to 1-naphthol by human CYPs 2B6, 2C8, 2C9 3A4, and 3A5 and that the atypical kinetics could be explained by simultaneous binding of more than one substrate to the active site. Other products, known to be produced in humans, were not investigated. However, this mechanism would clearly increase the possibility of interactions at the metabolic level between naphthalene and other CYP substrates.

As it is clear, from the above studies, that humans generate several highly reactive intermediates from naphthalene (the arene oxide as well as naphthoquinones), further investigation of the metabolism of naphthalene (and possibly other polyaromatic jet fuel constituents) in humans and metabolic interactions of naphthalene with other exogenous chemicals and endogenous metabolites is of great importance in the toxicology of deployment-related chemicals. Ongoing studies (Cho et al., 2004) show that several human CYP isoforms produce 1-naphthol, 2-naphthol, and *trans*-dihydroxydihydrodiol naphthalene, the ratio of products varying from one isoform to another.

To date, there appear to have been no studies of dodecane metabolism in humans, although it has been suggested that the dodecane moiety of fatty acids that are substrates for omega-1 hydroxylation by CYP2E1 is involved in binding to the substrate binding site (Adas et al., 1998). Early studies indicated that dodecane, a known cocarcinogen, is an inducer of benzo(a)pyrene metabolism in the isolated, perfused rabbit lung (Warshawsky et al., 1977), raising the possibility of its involvement in metabolic interactions with other chemicals.

Recent studies of nonane metabolism in humans (Edwards et al., 2004a) have indicated that nonane is metabolized to 2-nonanol and 2-nonanone by human liver microsomes, and this activity is due to cytochrome P450, with CYP1A2, -2B6, and -2E1 being the principal isoforms involved. Ongoing studies (Edwards et al., 2004a,b) indicate that 2-nonanol can also be metabolized to 2-nonanone by human alcohol dehydrogenase and that 2-nonanone can be metabolized to the corresponding acid by human aldehyde dehydrogenase.

The risks associated with jet engine lubricants have been mentioned above with regard to tricresyl phosphate, but there may be other chemicals of concern, including *N*-phenyl-1-naphthylamine, a skin sensitizer (Winder and Balouet, 2002).

the monoacid of thiodiglycol (Brimfield et al., 2002). There is a strong likelihood that human isoforms will perform similar oxidative transformations although the reaction has only been followed by nicotine adenine dinucleotide (NAD) reduction up to this point, not by product formation (Dudley et al., 2000).

Induction of cytochrome P450 in mouse liver using 5%, 10%, and 20% of the respective LD50 concentrations of thiodiglycol and sulfur mustard have been carried out (Brimfield, personal communication). The results indicated a dose-related increase in liver levels of P450 after thiodiglycol administration and reduced levels of P450 in the livers of mice treated with sulfur mustard. The apparent reduction of CYP concentration following treatment with sulfur mustard is of interest from the point of view of its potential effect on the metabolism of other compounds involved in coexposure. Sulfur mustard has been reported to alter the activity of several CYP isoforms (Pons et al., 2001). Additionally, sulfur mustard and thiodiglycol have been implicated in the inhibition of protein phosphatase activity (Brimfield, 1995), which is necessary for the induction of CYP2Bs and CYP3Bs in the presence of phenobarbital (Joannard et al., 2000; Kawamura et al., 1999).

Sarin

Little appears to be known of the overall metabolism of sarin and related phosphorus-containing nerve agents such as soman, tabun, and VX (Szynicz and Baskin, 1999), in either experimental animals or humans. However, it appears that, in the rat, the principal route of metabolism is hydrolysis, and that the principal metabolite is an alkylmethylphosphonic acid, isopropylmethylphosphonic acid in the case of sarin (Shih et al., 1994). Metabolism in humans appears to resemble that in rats, and isopropylmethylphosphonic acid has been found in human urine following sarin intoxication (Minami et al., 1997, 1998).

One of the esterases hydrolyzing sarin is paraoxonase (PON1), an enzyme known to be polymorphic in humans (Furlong et al., 1993). The resulting R allozyme (Arg-192) hydrolyzes paraoxon rapidly but has low activity toward nerve agents such as sarin and soman (Davies et al., 1996). The reverse is true of the Q allozyme that has high activity toward soman and low activity toward paraoxon. Thus, individuals with the Q allozyme would be expected to detoxify sarin more rapidly than those with the R allozyme, and the PON1 status may be important in human poisoning, although it has been suggested that the catalytic efficiency of PON1 toward sarin may be inadequate to provide significant *in vivo* protection (Furlong, 2000; Richter and Furlong, 1999). A recent study (Haley et al., 1999) suggested that the R genotype may be a risk factor for illness in Gulf War veterans. Unfortunately, the number of subjects involved was too small to provide any certainty that this was the case.

PROPHYLACTIC DRUGS

Pyridostigmine Bromide

Although the pharmacokinetics of pyridostigmine bromide have been studied (Marino et al., 1998), there are, as yet, no studies that indicate metabolism of this drug in

humans. A study by Leo (1997) provided evidence that pyridostigmine bromide is not metabolized in humans, and specifically, that it is not a substrate for human CYPs 1A1, 2C9, 2E1, 2D6, and 3A4. More recently it has been shown (Usmani et al., 2004) that pyridostigmine bromide is not metabolized by pooled human liver microsomes, rat liver microsomes, pooled human liver cytosol, rat liver cytosol, pooled human liver S9, or rat serum.

METABOLISM-BASED INTERACTIONS

Introduction

Studies of chemical interactions are relatively recent in origin and often provide conflicting data. For example, an acute oral study involving pyridostigmine bromide, permethrin, and DEET in the rat indicated that animals fed combinations of these chemicals at LD16 dose levels suffered greater than additive mortality (McCain et al., 1997). Another study indicating that significant synergistic interactions are possible is that of Chaney et al. (1997), where the lethal effects of pyridostigmine bromide in mice were strongly potentiated by application of other adrenergic drugs (isoproterenol, salbutamol, phentolamine, etc.) or caffeine. (An interesting question raised by this study is whether the interaction is via metabolic perturbations or interactions with the anticholinesterase properties of PB.) Abou-Donia et al. (1996) demonstrated that coadministration of binary or tertiary combinations of pyridostigmine bromide, DEET, and chlorpyrifos to hens resulted in significant increases in neurotoxicity. These increases in neurotoxicity were associated with increases in inhibition of brain acetylcholinesterase and neurotoxicity target esterases.

However, other studies contradict the idea of synergistic interactions. For example, in a study examining chemical uptake into the central nervous system (CNS), application of pyridostigmine bromide was found to reduce tissue levels of permethrin by 30% (Buchholz et al., 1997). Similarly, a study of pesticide absorption through mouse, rat, and pig skin suggests that application of DEET inhibits insecticide absorption for permethrin and carbaryl (Baynes et al., 1997).

Inhibition and Activation of Xenobiotic-Metabolizing Enzymes

Inhibition and activation of xenobiotic substrates

Inhibition and activation of DEET metabolism. The effects on DEET metabolism of chlorpyrifos, permethrin, and pyridostigmine bromide alone or in combination have been investigated in human microsomes (Usmani et al., 2002). The greatest effect shown was the inhibition of the metabolism of DEET to the ring methylol derivative by chlorpyrifos either alone or in combination with any other compound. None of the three compounds tested had any significant inhibitory effect on the production of the *N*-deethylated metabolite. These inhibitory effects were also seen to a greater or lesser extent in microsomes from rat and mouse liver and in microsomes from mice pretreated with DEET, phenobarbital, or 3-methylcholanthrene. Human liver microsomes differed from those from both rats and mice in that pyridostigmine and permethrin, alone or in combination, showed an activation effect for the production of both of the major products of DEET metabolism.

Inhibition of carbaryl metabolism. More recent studies (Tang et al., 2002) indicate that chlorpyrifos inhibited the metabolism of carbaryl by human liver microsomes, preferentially inhibiting the formation of the methylol derivative. This is correlated with the findings first, that the production of this metabolite is primarily the result of CYP2B6 activity and that this is the same isoform that produces the oxon from chlorpyrifos, and second, that CYP isoforms are inhibited during oxon production. This interpretation was confirmed by the results of experiments carried out directly on CYP 2B6.

Inhibition of permethrin metabolism. Because the initial step in the metabolism of *trans*-permethrin in human liver is hydrolysis, it appeared important to test the ability of other chemicals to inhibit this reaction (Choi et al., 2004). Two inhibitors, chlorpyrifos oxon and carbaryl, were examined in some detail.

Trans-permethrin hydrolysis in human liver fractions was inhibited more effectively by chlorpyrifos oxon than by carbaryl. Under similar assay conditions, the IC50s of chlorpyrifos oxon in human liver cytosolic and microsomal fractions were 35 nM and 60 nM, respectively. Above 60 nM (cytosol) or 150 nM (microsomes) levels, *trans*-permethrin hydrolysis was completely inhibited by chlorpyrifos oxon.

When the cytosolic fraction was pre-incubated for 5 min with chlorpyrifos oxon, the V_{max} value was significantly reduced, while K_m values stayed approximately the same. Five minutes preincubation with chlorpyrifos oxon in the microsomal fraction again resulted in a significant decrease in V_{max} value with only an insignificant decrease in K_m . Based on these observations, noncompetitive or irreversible inhibition was assumed for chlorpyrifos oxon inhibition of permethrin hydrolysis in human liver fractions. The inhibition constants (K_i) for chlorpyrifos oxon, an indicator of inhibitor affinity for the target enzyme, were 21 nM for the cytosolic fraction and 95 nM in the microsomal fraction as calculated from V_{max} and K_m values. These values are approximately 100 times lower than those for carbaryl, indicating a higher inhibitory potential of chlorpyrifos oxon.

In range finding assays, carbaryl showed IC50 values of 10 μ M in both microsomal and cytosolic fractions. The most noticeable difference from chlorpyrifos oxon was that *trans*-permethrin hydrolysis in either the microsomal and the cytosolic fractions was not completely inhibited by a wide range of carbaryl concentrations. This observation led to an assumption that the esterases involved in *trans*-permethrin hydrolysis in both the microsomal and the cytosolic fractions are composed of at least two different entities, which have differential susceptibilities to carbaryl and chlorpyrifos oxon inhibition.

K_i values for carbaryl were 2.49 μ M in the cytosolic fraction and 11.08 μ M in the microsomal fraction. In contrast to chlorpyrifos oxon, in the assay to determine the inhibition type, carbaryl appeared to act as a noncompetitive inhibitor.

These studies demonstrate that there are potentially important interactions between permethrin and chlorpyrifos in humans. Chlorpyrifos, which has been used in military deployments in conjunction with permethrin, is a potent inhibitor of *trans*-permethrin hydrolysis after metabolic activation to chlorpyrifos oxon. This observation implies that coexposure to chlorpyrifos might potentiate the toxicity of permethrin by deactivating the metabolic detoxification pathway for permethrin. In a related study, coexposure of a small number of human volunteers to both cyfluthrin and methyl parathion appeared to have significantly increased the half-life of cyfluthrin (Leng et al., 1999). Other deployment-related compounds, an insect repellent (*N,N*-diethyl-*m*-toluamide, DEET) and a nerve gas

prophylactic (pyridostigmine bromide) did not cause the inhibition of *trans*-permethrin hydrolysis, regardless of the presence of an NADPH regeneration system.

Chlorpyrifos oxon completely inhibited *trans*-permethrin hydrolysis in both cytosolic and microsomal human liver fractions with very low K_i values, indicating that B-esterases are responsible for *trans*-permethrin hydrolysis in human liver fractions. Compared to chlorpyrifos oxon, the parent compound, chlorpyrifos and the other major chlorpyrifos metabolite (3,5,6-trichloro-2-pyridinol) showed minimal levels of inhibition in either fraction. The observation that pre-incubation with NADPH in the microsomal fraction substantially increased chlorpyrifos inhibition capability confirmed that chlorpyrifos oxon is the chemical species responsible for the inhibition of *trans*-permethrin hydrolysis.

The mechanism of chlorpyrifos oxon inhibition of esterases is *trans*-esterification, in which a covalent bond is formed between the oxon and the alcohol functional group of a serine residue in the active site of the esterase. With a normal substrate, a transient bond is formed in place of the covalent bond and readily cleaved by deacylation (Chambers et al., 1990). The observed inhibition kinetics (reduced V_{max} and constant K_m) and the irreversible nature of inhibition strongly implies that the inhibition of the human liver esterases hydrolyzing permethrin is mediated by the same mechanism described above.

Carbaryl shows a different pattern of inhibition from chlorpyrifos oxon, typical noncompetitive inhibition. This result is in accord with the fact that carbamate compounds are reversible and less-persistent inhibitors compared to organophosphorus compounds, and that carbamate compounds can be hydrolyzed by esterases. This also explains why K_i values for carbaryl are two orders of magnitude higher than those for chlorpyrifos oxon.

Another important observation is that, in contrast to chlorpyrifos oxon, carbaryl cannot completely inhibit *trans*-permethrin hydrolysis, even at high concentrations. Incomplete inhibition at high concentrations of carbaryl suggests that there are multiple hydrolytic enzymes involved in *trans*-permethrin hydrolysis, a finding that was not revealed by chlorpyrifos oxon inhibition. It is deduced that in *trans*-permethrin hydrolysis in human liver fractions, at least two species (or groups) of B-esterases are involved, both sensitive to chlorpyrifos oxon inhibition but one with higher sensitivity to carbaryl inhibition and the other with lower or no sensitivity to carbaryl.

In conclusion, we reported that in human liver fractions, hydrolysis, the key step in *trans*-permethrin detoxification, is strongly inhibited by chlorpyrifos oxon. The differential inhibition pattern of chlorpyrifos oxon and carbaryl indicates that multiple B-esterases are involved in the hydrolysis of *trans*-permethrin in human liver fractions.

Inhibition of endogenous substrates

Inhibition of testosterone metabolism. Many pesticides are known to have significant endocrine disrupting effects. There are several avenues by which endocrine disruption may occur, including interference with synthesis, secretion, transport, binding, or elimination of natural hormones that are responsible for homeostasis and reproductive development. Although some pesticides are known to interact directly with the hormone receptors, the methods by which many cause endocrine disruption is still poorly understood. It is suspected that many pesticides with endocrine disrupting potential may do this by interfering with the normal hormone synthesis and degradation. In this regard, we have demonstrated in mice that subchronic administration

of some pesticides and polychlorinated biphenyl compounds can significantly increase metabolism of testosterone and estradiol (Gillette et al., 2002). These changes in hormone metabolism as observed in mice were mediated primarily by induction of CYP isoforms by the pesticides.

Cytochrome P450 monooxygenases are not only major catalysts involved in the metabolism of xenobiotics but also in the oxidative metabolism of endogenous substrates such as testosterone. Major testosterone metabolites formed by human liver microsomes include 6 β -hydroxytestosterone, 2 β -hydroxytestosterone, and 15 β -hydroxytestosterone (Fig. 8). A screen of 16 cDNA expressed human CYPs demonstrated (Usmani et al., 2003) that 94% of all testosterone metabolites are produced by members of the CYP3A subfamily, with 6 β -testosterone accounting for 84% of all testosterone metabolites. While similar K_m values were observed with human liver microsomes, regardless of which metabolite is measured, V_{max} and intrinsic clearance are both much higher for 6 β -testosterone than for any other metabolite.

A recent study of effects on endocrine metabolism (Usmani et al., 2003) indicates effects, often dramatic, of deployment-related chemicals on the oxidative metabolism of testosterone. Preincubation of human liver microsomes with a variety of ligands, including the deployment-related test chemicals used throughout this project, resulted in varying levels of inhibition or activation of testosterone metabolism. The greatest inhibition of testosterone metabolism in human liver microsomes was seen following

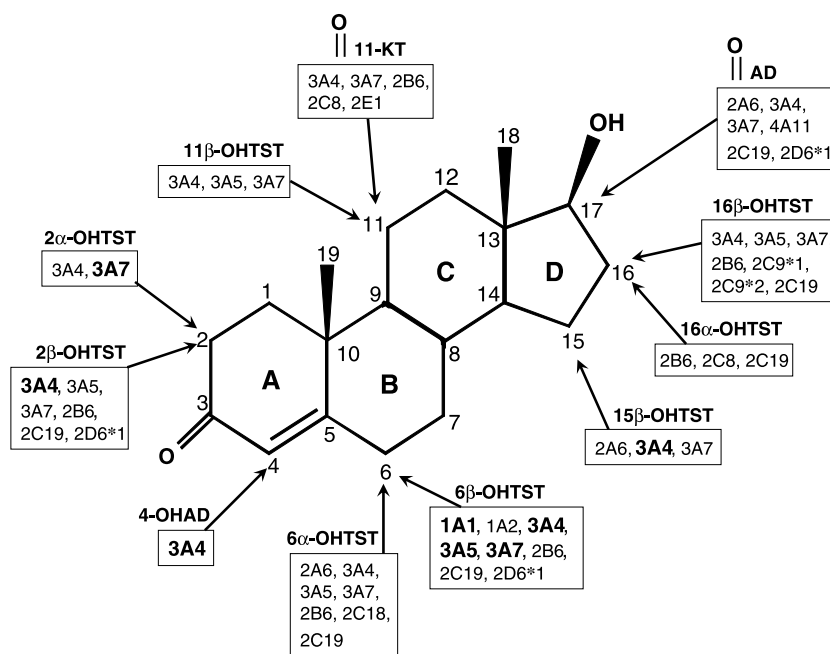


Figure 8. Metabolism of testosterone by human CYP isoforms. Boldface indicates isoforms with either high activity or distinct regioselectivity. The following abbreviations are used: 6 α - or 6 β -OHTST for 6 α - or 6 β -hydroxytestosterone; 15 β -OHTST for 15 β -testosterone; 16 α - or 16 β -OHTST for 16 α - or 16 β -hydroxytestosterone; 11-KT for 11-ketotestosterone; 11 β -OHTST for 11 β -hydroxytestosterone; 2 α - or 2 β -OHTST for 2 α - or 2 β -hydroxytestosterone; AD for androstenedione; 4-OHAD for 4-hydroxyandrostenedione.

preincubation with organophosphorus compounds, including chlorpyrifos, phorate, and fonofos, with up to 80% inhibition of the formation of several metabolites, including 6 β -testosterone. Preincubation of CYP3A4 with chlorpyrifos, but not chlorpyrifos oxon, resulted in 98% inhibition of testosterone metabolism. Kinetic analysis indicated that chlorpyrifos is one of the most potent inhibitors of testosterone metabolism to be discovered to date, and that phorate and fonofos were also potent inhibitors. In all cases, the inhibition is noncompetitive and irreversible. Conversely, preincubation of CYP3A4 with pyridostigime bromide increased the metabolism of testosterone to the 6 β - and 2 β -derivatives. Preincubation of aromatase (CYP19) with the test chemicals had no effect on the production of the endogenous estrogen, 17 β -estradiol. The significance of inhibition of testosterone metabolism *in vivo* in humans has not yet been studied.

Inhibition of estradiol metabolism. To date, similar studies have not been carried out on estradiol metabolism. We are currently carrying out such studies using human preparations and the methods developed during studies involving perturbations of estradiol metabolism by polychlorinated biphenyls (PCBs) in rodents (Gillette et al., 2002)

Induction of Xenobiotic-Metabolizing Enzymes

Although many aspects of pesticide and drug metabolism can be easily studied using human liver microsomal and cytosolic preparations, it is nearly impossible to study the inducing effects of pesticide or drug exposure using these systems. Induction of XMEs requires a complex mechanism that cannot be duplicated *in vitro*. As a consequence, most induction studies in the past have been conducted *in vivo* using experimental animals, generally rodents. While such studies are useful in pointing to the potential of induction to bring about metabolic interactions, definitive findings from human systems are necessary to extrapolate the results to humans with increased confidence. Human hepatocytes represent one possible approach to this dilemma. Their cellular systems are intact, and, at least for some time, they are responsive to XME inducers. Many difficulties remain, however; they can be used only in primary culture, and due to the innate variability of humans, the results are frequently highly variable.

Induction studies in human hepatocytes. Many pesticides and drugs are known to induce the metabolism of other coadministered drugs as well as to induce their own metabolism. The potential of drugs to induce their own metabolism as well as the metabolism of other drugs has prompted many pharmaceutical companies to conduct elaborate screening protocols to verify the lack of potential harmful interactions between new drug candidates prior to releasing drugs to the marketplace. Because the liver is the primary organ of drug metabolism, use of primary cultures of human hepatocytes is one of the best methods for the study of potential drug or pesticide interactions. Human hepatocyte cultures have been demonstrated to retain many aspects of liver function, including CYP-mediated oxidation of drugs and CYP induction (Donato et al., 2000; Li et al., 1997; Robertson et al., 2000).

The branched DNA (bDNA) assay is a new technique that allows for quantitative determinations of messenger RNA (mRNA) levels from hepatocyte tissues. This technique allows for the evaluation of a variety of chosen genes simultaneously at the level of mRNA. Recent experience in our laboratories with the bDNA assay, through collaboration with Dr. N. Cherrington (University of Arizona), has demonstrated the

utility of this assay to quantitate levels of induction following hepatocyte treatment with several inducers, including some pesticides.

The bDNA assay resembles the well-established enzyme-linked immunosorbent assay (ELISA) in principle but uses multioligonucleotides not only to capture the mRNA of interest, but also to link it to an enzyme that produces a chemiluminescent signal on addition of substrate. This technology is thoroughly explained by Hartley and Klaassen (2000). The primary value of the bDNA assay lies in its ability to assess the differential expression of a chosen set of genes in response to a chemical stimulus. For a targeted gene sequence, such as a series of metabolizing enzymes, one total RNA sample may be split among several different probe sets for quantitative analysis. Gene expression for many genes can, therefore, be monitored simultaneously in parallel wells. Results are reproducible and reflect other assays routinely used to monitor gene expression, including Northern blot analysis, *in situ* hybridization, quantitative PCR, etc.

Preliminary assays (Rose and Cherrington, 2004) conducted with human hepatocytes in combination with the bDNA assay suggest that several CYP isoforms are induced by permethrin, chlorpyrifos, and DEET. Chlorpyrifos was surprisingly efficient in its induction of CYP1A1, 1A2, and 2B6. Other isoforms induced by chlorpyrifos include 2A6 and possibly 3A4. Our previous determinations of metabolic activity by CYPs had demonstrated that CYP2B6 was involved in the activation of chlorpyrifos to chlorpyrifos oxon. Data with mice also suggested that CYP2B10, the mouse phenobarbital inducible isoform analogous to CYP2B6, was also inducible by chlorpyrifos. It is of interest that permethrin also strongly induced CYP2B6 and CYP2A6. Neither of these enzymes had been implicated in permethrin metabolism using microsomes and the purified CYP isoforms.

Recently acquired data examining CYP3A4 induction using western blot analysis has demonstrated that the best induction of CYP3A4 was with rifampicin (an established CYP3A4 inducer) and DEET. These data were also corroborated with testosterone metabolism data using hepatocyte S9 preparations that were exposed to rifampicin, permethrin, chlorpyrifos, and DEET. A western blot of CYP1A1 protein did not provide confirming evidence for protein induction by chlorpyrifos as might have been expected based upon the bDNA assays performed. As these results are preliminary, it is not known if the absence of correlation is the result of protein destabilization (a possibility, because chlorpyrifos acts as a suicide inhibitor) or whether insufficient time between mRNA induction and protein synthesis might explain the result. Permethrin also strongly induced CYP2B6 along with CYP2A6.

DISCUSSION

Methodology

The development of new high-performance liquid chromatography (HPLC) methods and/or modification and validation of available methods for analysis of deployment-related chemicals and their metabolites and appropriate endogenous chemicals has greatly facilitated research in this area. Methods include those for chlorpyrifos and its metabolites (Dai et al., 2001; Tang et al., 2001), DEET and its metabolites (Usmani et al., 2002), permethrin and its metabolites (Choi et al., 2002), and pyridostigmine bromide and its potential metabolites (Leo, 1997; Usmani et al., 2004).

The analysis of sulfur mustard and its degradation products has always presented an analytical challenge. Their water solubility and their lack of suitable chromophores in the UV/visible region make them difficult to detect by commonly used techniques at concentrations useful for evaluating enzymatic metabolism. Brimfield et al. (personal communication) are currently having success with a fluorimetric method based on derivatization with 2-(4-carboxyphenyl)-6-*N,N*-diethylaminobenzofuran (Assaf et al., 2000) using a carbodiimide-catalyzed esterification that reacts at the alcoholic hydroxyl groups common to all the oxidative metabolites. Unfortunately, the fluorescent reagent is not commercially available and must be synthesized. Derivative structures are confirmed by HPLC/mass spectroscopy. Separation of the derivatized compounds is readily accomplished using a 150 × 4 mm C18, reverse-phase HPLC column and gradient elution. Detection is by fluorescence with excitation at 387 nm and emission at 537 nm. Sensitivity is in the picogram/microliter range, a level that makes metabolite detection feasible. Thiodiglycol, thiodiglycol sulfoxide, thiodiglycol sulfone, and 2-hydroxyethyl thioacetic acid are easily derivatized with this system. Thiodipropanol is a commercially available, easily derivatized internal standard.

An improved HPLC method for the separation of testosterone and its metabolites has been developed (Usmani et al., 2003) based on the method of Purdon and Lehman-McKeeman (1997) and used in a study of testosterone metabolism and its inhibition by deployment-related chemicals (Usmani et al., 2003).

Significance of Xenobiotic-Metabolizing Enzyme Distribution

Phenotyping of liver microsomes from individual livers shows a wide variation in the expression of different CYP isoforms and that this variation has dramatic effects on the metabolism of the test chemicals. This is clearly evident in our studies of chlorpyrifos metabolism (Dai et al., 2001; Tang et al., 2001) as well as DEET (Usmani et al., 2002) and carbaryl (Tang et al., 2002). It may be inferred from our studies on human permethrin metabolism that variations in expression of alcohol and aldehyde dehydrogenases will have similar effects on permethrin metabolism. Because the expression of XMEs can depend not only on the genotype of the individual but also on induction factors such as coexposure to other toxicants and/or to clinical drugs will be of significance in the assessment of risk from deployment-related chemicals.

The almost 10-fold variation in the production of chlorpyrifos oxon by individual human liver microsomes appears to be related to the levels of expression of CYP2B6, CYP3A4, and CYP2C19 (Dai et al., 2001; Tang et al., 2001). The use of phenotyped human liver microsomes (Usmani et al., 2002) showed that individuals with high CYPs 3A4, 2C19, and 2B6 activities have the greatest potential to metabolize DEET. Similarly, these individual phenotyped microsomes showed differential activity toward carbaryl, an insecticide that is metabolized to three different primary metabolites by human microsomes and human recombinant CYPs (Tang et al., 2002).

Significance of Polymorphisms in Human Xenobiotic-Metabolizing Enzymes

Polymorphisms have been identified in human XMEs, particularly in CYP isoforms but also in enzymes of interest in the current studies, such as alcohol dehydrogenase and

aldehyde dehydrogenase. These heritable variants of normal or wild-type genes usually express proteins of lower activity, and individuals expressing these variant enzymes will have a reduced ability to metabolize any xenobiotic metabolized by that isoform. This is clear in our studies on chlorpyrifos and other chemicals, as indicated above. Thus, the genetic constitution as well as the chemical milieu will not only determine the outcome of a particular exposure but will also determine who is at greater or lesser risk. These polymorphisms in XMEs are not associated with particular ethnic groups but are seen in small percentages of individuals from all ethnic groups, although the gene frequencies may vary from one group to another. This is illustrated by studies carried out in the laboratory of a collaborator, [J. A. Goldstein (NIEHS), personal communication] in which polymorphic forms of CYP3A5 are shown to have very different abilities to oxidize testosterone and the drug, nifedipine, but occur in all ethnic groups examined.

CYP isoforms CYP2C19, 3A4, and 2B6 each have the ability to produce activation or detoxication products from chlorpyrifos, varying significantly in the ratio of the products.

CYP2C19 is one of the isoforms with the greatest potential for detoxication. Three naturally occurring polymorphic alleles of CYP2C19 exhibited markedly reduced ability to detoxify chlorpyrifos, compared to the wild-type enzyme and no ability to produce the oxon (Tang et al., 2001). Individuals carrying these polymorphisms could therefore be at greater risk to chlorpyrifos.

CYP3A4 both activates and detoxifies chlorpyrifos. Four CYP3A4 alleles were tested, one was essentially inactive and one was more active (Dai et al., 2001). Individuals carrying an inactive allele might be more susceptible to chlorpyrifos.

CYP2B6 appeared to be by far the best enzyme at activating chlorpyrifos to the toxic oxon (Tang et al., 2001). Activation in microsomes correlated well with CYP2B6 activity toward other substrates, indicating it is very important in producing the toxic product. Future studies will examine the effect of several newly discovered polymorphic CYP2B6 alleles in man (Goldstein, personal communication).

The use of microsomes with varying CYP3A4, CYP2B6, CYP2C19, CYP2C9, etc., activity (due to induction or polymorphisms in the individuals) is also an excellent way to determine whether particular isozymes are important in toxication/detoxication and whether polymorphisms affect this process. Consideration should also be given to the PON1 status, because, for example, enhanced ability to activate chlorpyrifos combined with low PON1 status could have significant toxicological consequences. This method can also be used to address the role of isoforms and polymorphisms on metabolism of other deployment-related chemicals.

Genotyping Studies

Genotyping studies will be able to address the relative proportions of various CYP alleles for enzymes that are important in metabolism of deployment-related chemicals in representative military populations. These will include the CYP2B6 alleles, CYP2C19 alleles, CYP3A4 alleles, and those for other CYP enzymes identified as vital to the metabolism of these chemicals in man.

In a recent major study (Garcia-Closas et al., 2001) carried out as a preliminary to the Agricultural Health Study (NCI, NIEHS, EPA, etc.) of the use of buccal samples for the collection of genomic DNA, the authors stated "In conclusion, although DNA

isolated from either mouthwash or cytobrush samples collected by mail from adults is adequate for a wide range of PCR-based assays, a single mouthwash sample provides substantially larger samples and higher molecular weight DNA than two cytobrush samples.” As more information is obtained with respect to risks associated with metabolic deficiencies, these samples will be valuable in the testing of hypotheses related to chemical exposure and subsequent health effects.

Interactions Based on Inhibition

As indicated above, there are numerous interactions between the chemicals of interest in this study that are based on the inhibition, by one chemical, of the metabolism of another. For example, chlorpyrifos is a potent inhibitor of DEET, carbaryl, and testosterone metabolism. Because the mechanism of this inhibition is almost certainly due to the formation of highly reactive sulfur during the oxidative desulfuration of chlorpyrifos followed by the interaction of this sulfur with the heme iron of cytochrome P450, this interaction will occur in the presence of chlorpyrifos whenever another chemical is metabolized by a CYP isoform that carries out the desulfuration reaction. It should also be a general interaction of any organophosphorus compound that has a P=S group in the molecule, and our studies have shown that, although chlorpyrifos is the most potent inhibitor, other organophosphorus chemicals act in the same way. Other interactions noted are the inhibition of permethrin metabolism by chlorpyrifos oxon and by carbaryl, presumably by inhibition of the B-esterases involved.

Interactions Based on Induction

Until recently, it was necessary to measure induction in experimental animals and extrapolate possible effects to humans, so it is difficult to assess the importance of this source of interaction in humans. However, we have recently been establishing procedures and baseline conditions for measuring induction in human hepatocytes.

Genotyping and Individuals and Populations at Increased Risk

Identification of individuals at increased risk will depend on a knowledge of their genotype with respect to XMEs, as well as a knowledge of the other chemicals expected to be used during a particular circumstance and clinical drugs prescribed for the individual. Using these results and appropriate paradigms, it will be possible to avoid individual or simultaneous exposures that might result in increased toxicity.

GENERAL CONCLUSIONS

HPLC analytical methods for carbaryl, chlorpyrifos, DEET, permethrin, pyridostigmine and their metabolites, sulfur mustard metabolites, testosterone, estradiol, and other endogenous metabolites have been brought on line in recent years and have been used in a number of human metabolic studies. The human cytochrome P450 isoforms metabolizing carbaryl, chlorpyrifos, and DEET have been identified and include forms known to be inducible and forms known to be polymorphic. It has been established that pyridostigmine and permethrin are not significant substrates for human

monoxygenases. While pyridostigmine does not appear to be readily metabolized, permethrin has been shown to be metabolized, in humans, through a series of reactions involving hydrolytic enzymes, followed by alcohol dehydrogenase and aldehyde dehydrogenase. Specific purified isoforms of human alcohol and aldehyde dehydrogenases have been shown to be active in these reactions. The reactive metabolite of chlorpyrifos, chlorpyrifos oxon, is a potent inhibitor of permethrin hydrolysis, while carbaryl is a less potent inhibitor of this reaction. Chlorpyrifos has been shown to be a potent inhibitor of the metabolism of DEET, carbaryl, and testosterone. It is clear that chlorpyrifos and, by implication, other organophosphorus compounds, may be significant both in health-related interactions between different deployment-related chemicals and in the determination of subpopulations and individuals at increased risk from anticholinergic chemicals.

Even within the very small subset of deployment-related chemicals examined to date, essentially all interact with at least one other or with an endogenous metabolite at the metabolic level: chlorpyrifos inhibits the metabolism of DEET, testosterone, and carbaryl; chlorpyrifos oxon, the principal reactive metabolite of chlorpyrifos, inhibits the hydrolysis of permethrin; and DEET is an inducer of XMEs in human hepatocytes. The potential for interactions is obvious, and it should also be noted that essentially all of the XMEs involved are polymorphic, and several are inducible, making human variation, both genotypic and phenotypic, important in the expression of toxicity. The potential for interactions with clinical drugs is one of great importance, and it is critical that investigations in this area be initiated.

These studies permit more confident extrapolation of past and future animal studies to humans and have permitted identification of interactions not apparent from animal studies. Perhaps even more important, they open the way to molecular genetic studies that will permit identification of human subpopulations at greater risk from specific toxicants, whether from genetic, environmental, or combined considerations, and will produce specific analytic methodologies for assessment of future exposures.

It is becoming increasingly apparent that induction studies previously requiring the use of experimental animals may be accomplished directly with human materials. Newer techniques that maintain the capacity for induction in cultured human hepatocytes combined with microarray techniques for determination of gene expression and repression may substitute for animal studies. Preliminary studies indicate that this is a viable approach that can be used to advantage in lieu of hepatocytes from experimental animals. Thus, it is possible to conclude the following:

- Human XMEs are important loci for toxic interactions of chemicals used in military deployments.
- Such interactions are of importance in the underlying causes of deployment-related illnesses.
- Selection of suitable animal models and extrapolation of animal-derived data to humans requires knowledge of human metabolism.
- Risk assessment for chemicals utilized in future deployments can be improved by the use of human data.
- Individuals and populations at increased risk can be defined by the use of human data on XME levels of expression and polymorphisms.

- Questions of diet and/or clinical drug exposure interactions with deployment-related chemicals can also be addressed by these approaches.
- These studies are of equal significance in industrial health, public health, agriculture, and, indeed, in the human health risk analysis of any group with significant environmental chemical exposure.

ACKNOWLEDGMENTS

Studies carried out in the authors' laboratories were supported in part by grants number DADM17-00-2008 from the U.S. Army and OH07551-ECU from NIOSH.

REFERENCES

- Abou-Donia, M. B., Wilmarth, K. R., AbdelRahman, A. A., Jensen, K. F., Oehme, F. W., Kurt, T. L. (1996). Increased neurotoxicity following concurrent exposure to pyridostigmine bromide, DEET, and chlorpyrifos. *Fundam. Appl. Toxicol.* 34:201–222.
- Adas, F., Berthou, F., Picard, D., Lozac'h, P., Beauge, F., Amet, Y. (1998). Involvement of cytochrome P450 in the (omega-1)-hydroxylation of oleic acid in human and rat liver microsomes. *J. Lipid Res.* 36:1210–1219.
- Allen, D. G., Riviere, J. E., Monteiro-Riviere, N. A. (2000). Identification of early biomarkers of inflammation produced by keratinocytes exposed to jet fuels Jet A, JP-8 and JP8(100). *J. Biochem. Mol. Toxicol.* 14:231–237.
- Allen, D. G., Riviere, J. E., Monteiro-Riviere, N. A. (2001). Cytokine induction as a measure of cutaneous toxicity in primary and immortalized porcine keratinocytes exposed to jet fuels, and their relationship to normal human epidermal keratinocytes. *Toxicol. Lett.* 119:209–217.
- Angerer, J., Ritter, A. (1997). Determination of metabolites of pyrethroids in human urine using solid phase extraction and gas chromatography-mass spectrometry. *J. Chromatogr.* 695:217.
- Asakawa, F., Jitsunari, F., Miki, K., Choi, J., Takeda, N., Kitamado, T., Suna, S., Manabe, Y. (1996). Agricultural worker exposure to and absorption of permethrin applied to cabbage. *Bull. Environ. Toxicol.* 56:42.
- Assaf, P., Katzhendler, J., Haj-Yehia, A. I. (2000). 2-(4-Carboxyphenyl)-6-*N,N*-diethylamino-benzofuran: a useful reagent for the sensitive determination of alcohols by high-performance liquid chromatography with fluorimetric detection. *J. Chromatogr., A* 869:243–250.
- ATSDR. (1995). Toxicological Profile for Naphthalene (Update), ed. *Comparative Biochemistry and Metabolism: Part 2. Naphthalene Lung Toxicity*. Boca Raton, FL: Agency for Toxic Substances and Disease Registry, Department of Health and Human Services, CRC Press.
- Baynes, R. E., Halling, K. B., Riviere, J. E. (1997). The influence of diethyl-*m*-toluamide (DEET) on the percutaneous absorption of permethrin and carbaryl. *Toxicol. Appl. Pharmacol.* 144:332–339.
- Baynes, R. E., Brooks, J. D., Riviere, J. E. (2000). Membrane transport of naphthalene and dodecane in jet fuel mixtures. *Toxicol. Ind. Health* 16:225–238.
- Baynes, R. E., Brooks, J. D., Budsaba, K., Smith, C. E., Riviere, J. E. (2001). Mixture effects of JP-8 additives on the dermal disposition of jet fuel components. *Toxicol. Appl. Pharmacol.* 175:269–281.
- Black, R. M., Read, R. W. (1995). Biological fate of sulfur mustard, 1,1'-thiobis(2-chloroethane): identification of b-lyase metabolites and hydrolysis products in human urine. *Xenobiotica* 25:167–173.
- Black, R. M., Brewster, K., Clarke, R. J., Hambrook, J. L., Harrison, J. M., Howells, D. J. (1992a).

- Biological fate of sulfur mustard, 1,1'-thiobis(2-chloroethane): isolation and identification of urinary metabolites following intraperitoneal administration to rats. *Xenobiotica* 22:405–418.
- Black, R. M., Hambrook, J. L., Howells, D. J., Read, R. W. (1992b). Biological fate of sulfur mustard, 1,1'-thiobis(2-chloroethane): urinary excretion profiles of hydrolysis products and b-lyase metabolites of sulfur mustard after cutaneous application to rats. *J. Anal. Toxicol.* 16:79–84.
- Bloomquist, J. R. (1993). In: Roe, R. M., Kuhr, R. J., eds. *Neuroreceptor Mechanisms in Pyrethroid Mode of Action and Resistance*. Rev. Pestic. Toxicol. Vol. 2. Raleigh, NC: Toxicology Communications.
- Brimfield, A. A. (1995). Possible protein phosphatase inhibition by bis(hydroxyethylsulfide), a hydrolysis product of mustard gas. *Toxicol. Lett.* 78:43–48.
- Brimfield, A. A., Sartori, D. A., Novak, M. J. (2002). Thiodiglycol metabolism by alcohol dehydrogenase using NMR: two-step oxidation produces α -hydroxyethyl thioacetic acid and 2 moles of NADH. *The Toxicologist* 66(1S):230.
- Bruckner, J. V., Warren, D. A. (2001). Toxic effects of solvents and vapors. In: Klaassen, C. D., ed. *Cassarett and Doull's Toxicology: the Basic Science of Poisons*. 6th ed. McGraw-Hill: New York, pp. 869–916.
- Buchholz, B. A., Pawley, N. H., Vogel, J. S., Mauthe, R. J. (1997). Pyrethroid decrease in central nervous system from nerve agent pretreatment. *J. Appl. Toxicol.* 17:231–234.
- Buckpitt, A. R., Bahnson, L. S. (1986). Naphthalene metabolism by human lung microsomal enzymes. *Toxicology* 41:333–341.
- Buckpitt, A. R., Richieri, P. (1984). *Comparative Biochemistry and Metabolism: Part 2. Naphthalene Lung Toxicity*. Wright-Patterson Air Force Base, OH: Air Force Systems Command, Aerospace Medical Division, Air Force Aerospace Medical Research Laboratory. AFAMRL-TR 84-058 (cited in ATSDR, 1995).
- Buonarati, M., Jones, A. D., Buckpitt, A. R. (1990). In vivo metabolism of isomeric naphthalene oxide glutathione conjugates. *Drug Metab. Dispos.* 18:183–189.
- Buratti, F. M., Volpe, M. T., Meneguz, A., Vitozzi, L., Testai, E. (2003). CYP-specific bioactivation of four phosphorothioate pesticides by human liver microsomes. *Toxicol. Appl. Pharmacol.* 186:143–154.
- Butler, A. M., Murray, M. (1997). Biotransformation of parathion in human liver: participation of CYP3A4 and its inactivation during microsomal parathion oxidation. *J. Pharmacol. Exp. Ther.* 280:966–973.
- Cantalamesa, F. (1993). Acute toxicity of 2 pyrethroids, permethrin and cypermethrin in neonatal and adult rats. *Arch. Toxicol.* 67:510–513.
- Chambers, H., Brown, B., Chambers, J. E. (1990). Noncatalytic detoxication of six organophosphorus compounds by rat liver homogenates. *Pestic. Biochem. Physiol.* 36:308–316.
- Chaney, L. A., Rockhold, R. W., Mozingo, J. R., Hume, A. S. (1997). Potentiation of pyridostigmine bromide toxicity in mice by selected adrenergic agents and caffeine. *Vet. Hum. Toxicol.* 39:214–219.
- Chen, C. S., Yoshida, A. (1991). Enzymatic properties of the protein encoded by newly cloned human alcohol dehydrogenase ADH6 gene. *Biochem. Biophys. Res. Commun.* 181:743–747.
- Chin, B. H., Eldridge, J. M., Sullivan, L. J. (1974). Metabolism of carbaryl by selected human tissues using an organ-maintenance technique. *Clin. Toxicol.* 7:37–56.
- Cho, T., Hodgson, E., Rose, R. L. (2004). In vitro human metabolism of naphthalene. unpublished results.
- Choi, J., Rose, R. L., Hodgson, E. (2002). In vitro human metabolism of permethrin: the role of human alcohol and aldehyde dehydrogenases. *Pestic. Biochem. Physiol.* 73:117–128.

- Choi, J., Rose, R. L., Hodgson, R. L. (2004). Chlorpyrifos oxon and carbaryl inhibition of transpermethrin hydrolysis in human liver fractions. *Drug Metab. Drug Interac.* 20: at press.
- Cooper, J. R., Mattie, D. R. (1996). Developmental toxicity of JP-8 fuel in the rat. *J. Appl. Toxicol.* 16:197–200.
- Costa, L. G., McDonald, B. E., Murphy, S. D., Omenn, G. S., Richter, S. J., Motulsky, A. G., Furlong, C. E. (1990). Serum paraoxonase and its influence on paraoxon and chlorpyrifos-oxon toxicity in rats. *Toxicol. Appl. Pharmacol.* 103:66–76.
- Cranmer, M. F. (1986). Carbaryl: a toxicological review and risk analysis. *Neurotoxicology* 7:247–332.
- Crofton, K. M., Reiter, L. W. (1988). The effects of type-I and type-II pyrethroids on motor-activity and the acoustic startle response in the rat. *Fundam. Appl. Toxicol.* 10:624–634.
- Dai, D., Tang, J., Rose, R. L., Hodgson, E., Bienstock, R. J., Mohrenweiser, H. W., Goldstein, J. A. (2001). Identification of variants of CYP3A4 and characterization of their abilities to metabolize testosterone and chlorpyrifos. *J. Pharmacol. Exp. Ther.* 299:825–831.
- Davies, H. G., Richter, R. J., Keifer, M., Broomfield, C. A., Sowalla, J., Furlong, C. A. (1996). The effect of the human serum paraoxonase polymorphism is reversed with diazoxon, somam and sarin. *Nat. Genet.* 14:334–336.
- Donato, M. T., Viitala, P., Rodriguez-Antona, C., Lindfors, A., Castell, J. V., Raunio, H., Gomez-Lechon, M. J., Pelkonen, O. (2000). CYP2A5/CYP2A6 expression in mouse and human hepatocytes treated with various inducers. *Drug Metab. Dispos.* 28:1321–1326.
- Dorough, H. W. (1970). Metabolism of insecticidal methylcarbamates in animals. *J. Agric. Food Chem.* 18:1015–1022.
- Dorough, H. W., Casida, J. E. (1964). Nature of certain carbamate metabolites of the insecticide Sevin. *J. Agric. Food Chem.* 12:294–304.
- Dorough, H. W., Leeling, N. C., Casida, J. E. (1963). Nonhydrolytic pathway in metabolism of *N*-methylcarbamate insecticides. *Science* 140:170–171.
- Dudley, B. F., Brimfield, A. A., Winston, G. M. (2000). Oxidation of thiodiglycol (2,2'-thiobisethanol) by alcohol dehydrogenase: comparison of human isoforms. *J. Biochem. Molec. Toxicol.* 14:244–251.
- Dudley, A. C., Peden-Adams, M. M., EuDaly, J., Pollenz, R. S., Keil, D. E. (2001). An aryl hydrogen receptor independent mechanism of JP-8 jet fuel immunotoxicity in Ah-responsive and Ah-nonresponsive mice. *Toxicol. Sci.* 59:251–259.
- Echobicon, D. J. (2001). Toxic effects of pesticides. In: Klaassen, C. D., ed. *Cassarett and Doull's Toxicology: the Basic Science of Poisons*. 6th ed. New York: McGraw-Hill, pp. 763–810.
- Edwards, J. E., Rose, R. L., Hodgson, E. (2004a). In vitro metabolism of nonane by human liver microsomes and cytochrome P450 isoforms. *Drug Metab. Rev.* (ISSX abstract) in press.
- Edwards, J. E., Rose, R. L., Hodgson, E. (2004b). In vitro human metabolism of nonane. unpublished results.
- Ehrich, M., Correll, L., Strait, J., McCain, W., Wilcke, J. (1992). Toxicity and toxicokinetics of carbaryl in chickens and rats: a comparative study. *J. Toxicol. Environ. Health* 36:411–423.
- Elliott, M. (1976). In: Metcalf, R. L., McKelvey, J. J., Jr., eds. *Insecticides for the Future: Needs and Prospects*. New York: Wiley.
- Elliott, M., Farnham, A. W., Jones, N. F., Needham, P. H., Pulman, D. A., Stevenson, J. H. (1973). A photostable pyrethroid. *Nature* 246:169–170.
- Elliott, M., Janes, N. F., Pulman, D. A., Gaughan, L. C., Unai, T., Casida, J. E. (1976). Radiosynthesis and metabolism in rats of the 1R isomers of the insecticide permethrin. *J. Agric. Food Chem.* 24:270–276.
- Fukuto, T. R. (1990). Mechanism of action of organophosphorus and carbamate insecticides. *Environ. Health Perspect.* 87:245–254.

- Furlong, C. E. (2000). PON1 status and neurologic symptom complexes in Gulf War veterans. *Genome Res.* 10:153–155.
- Furlong, C. E., Costa, L. G., Hassett, C., Richter, R. J., Sundstrom, J. A., Adler, D. A., Disteché, C. M., Omiecinski, C. J., Chapline, C., Crabb, J. W., Humbert, R. (1993). Human and rabbit paraoxonases: purification, cloning, sequencing, mapping and role of polymorphism in organophosphate detoxication. *Chem.-Biol. Interact.* 87:35–48.
- Furlong, C. E., Li, W. F., Costa, L. G., Richter, R. J., Shih, D. M., Lulis, A. J. (1998). Genetically determined susceptibility to organophosphorus insecticides and nerve agents: developing a mouse model for the human PON1 polymorphism. *Neurotoxicology* 19:645–650.
- García-Closas, M., Egan, K., Abruzzo, J., Newcomb, P., Titus-Ernstoff, L., Franklin, T., Bender, P., Beck, J., Le Marchand, L., Lum, A., Alavanja, M., Hayes, R., Rutter, J., Buetow, K., Brinton, L., Rothman, N. (2001). Collection of genomic DNA from adults in epidemiologic studies by buccal cytobrush and mouthwash. *Cancer Epidemiol. Biomark.* 10:687–696.
- Gaughan, L. C., Unai, T., Casida, J. E. (1977). Permethrin metabolism in rats. *J. Agric. Food Chem.* 25:9–17.
- Gillette, J. S., Hansen, L. G., Rose, R. L. (2002). Metabolic effects of episodic polychlorinated biphenyl (PCB) congeners. *Rev. Toxicol.* 4:129–159.
- Grant, G. M., Shaffer, K. M., Kao, W. Y., Stenger, D. A., Pancrazio, J. J. (2000). Investigation of in vitro toxicity of jet fuels JP-8 and Jet A. *Drug Chem. Toxicol.* 23:279–291.
- Guengerich, F. P., Kim, D. H., Iwasaki, M. (1991). Role of human cytochrome P-450 IIE1 in the oxidation of many low molecular weight cancer suspects. *Chem. Res. Toxicol.* 4:168–179.
- Haley, R. W., Kurt, T. L. (1997). Self-reported exposure to neurotoxic chemical combinations in the Gulf War—a cross sectional epidemiologic study. *J. Am. Med. Assoc.* 277:231–237.
- Haley, R. W., Billecke, S., LaDu, B. N. (1999). Association of low PON1 type Q (type A) aryl-esterase activity with neurologic symptom complexes in Gulf War veterans. *Toxicol. Appl. Pharmacol.* 157:227–233.
- Hardt, J., Angerer, J. (2003). Biological monitoring of workers after the application of insecticidal pyrethroids. *Int. Arch. Occup. Environ. Health* 76:492–498.
- Harris, D. T., Sakiestewa, D., Robledo, R. F., Young, R. S., Witten, M. (2000). Effects of short-term JP-8 jet fuel exposure on cell-mediated immunity. *Toxicol. Ind. Health* 16:78–84.
- Hartley, D. P., Klaassen, C. D. (2000). Detection of chemical-induced differential expression of rat hepatic cytochrome P450 mRNA transcripts using branched signal amplification technology. *Drug Metab. Dispos.* 28:608–616.
- Hodgson, E. (2003). In vitro human phase I metabolism of xenobiotics I: pesticides and related compounds used in agriculture and public health, 2003. *J. Biochem. Mol. Toxicol.* 17:201–206.
- Hodgson, E., Casida, J. E. (1960). Biological oxidation of *N,N*-dialkyl carbamates. *Biochim. Biophys. Acta* 42:184–186.
- Hodgson, E., Casida, J. E. (1961). Metabolism of *N,N*-dialkyl carbamates and related compounds by rat liver. *Biochem. Pharmacol.* 8:179–191.
- Hodgson, E., Smart, R. C. (2001). *An Introduction to Biochemical Toxicology*. New York: John Wiley and Sons.
- Horning, M. G., Stillwell, W. G., Griffin, G. W., Tseng, W. S. (1980). Epoxide intermediates in the metabolism of naphthalene in the rat. *Drug Metab. Dispos.* 8:404–414.
- Institute of Medicine. (2003). *Gulf War and Health, Volume 1: Depleted Uranium, Pyridostigmine Bromide, Sarin, Vaccines; and 2: Insecticides and Solvents*. Washington, DC: Institute of Medicine, National Academy Press.
- Ishmael, J., Litchfield, M. H. (1988). Chronic toxicity and carcinogenic evaluation of permethrin in rats and mice. *Fundam. Appl. Toxicol.* 11:308–322.

- Joannard, F., Galisteo, M., Corcos, L., Guillouzo, A., Lagadic-Gossman, D. (2000). Regulation of phenobarbital-induction of CYP2B and CYP3A genes in rat cultured hepatocytes: involvement of several serine/threonine protein kinases and phosphatases. *Cell Biol. Toxicol.* 16:325–337.
- Johnston, G. (1995). The study of interactive effects of pollutants: a biomarker approach. *Sci. Total Environ.* 171:205–212.
- Kabbar, M. B., Rogers, J. V., Gunasekar, P. G., Garrett, C. M., Geiss, K. T., Brinkley, W. W., McDougal, J. N. (2001). Effect of JP-8 jet fuel on molecular and histological parameters related to acute skin irritation. *Toxicol. Appl. Pharmacol.* 175:83–88.
- Kanikkannan, N., Locke, B. R., Singh, M. (2002). Effect of jet fuels on skin morphology and irritation in hairless rats. *Toxicology* 175:35–47.
- Kawamura, A., Yoshida, Y., Kimura, N., Oda, H., Kakinuma, A. (1999). Phosphorylation/dephosphorylation steps are crucial for the induction of CYP2B1 and CYP2B2 gene expression by phenobarbital. *Biochem. Biophys. Res. Commun.* 264:530–536.
- Korzekwa, K. R., Krishnamachary, N., Shou, M., Ogai, A., Parise, R. R., Rettie, A. E., Gonzalez, F. J., Tracy, T. S. (1998). Evaluation of atypical cytochrome P450 kinetics with two-substrate models: evidence that multiple substrates can simultaneously bind to cytochrome P450 active sites. *Biochemistry* 37:4137–4147.
- Leng, G., Kuhn, K. H., Idel, H. (1997). Biological monitoring of pyrethroids in blood and pyrethroid metabolites in urine: applications and limitations. *Sci. Total Environ.* 199:173.
- Leng, G., Lewalter, J., Rohrig, B., Idel, H. (1999). The influence of individual susceptibility in pyrethroid exposure. *Toxicol. Lett.* 107:123–130.
- Leo, K. U. (1997). *Metabolism of Proposed Nerve Agent Pretreatment, Pyridostigmine Bromide*. Walter Reed Army Institute of Research Report No. NTIS/AD-A323 848/2, Available from NTIS at 800-553-6847, Washington DC.
- Levi, P. E., Hodgson, E. (1985). Oxidation of pesticides by purified cytochrome P450 isozymes from the mouse liver. *Toxicol. Lett.* 24:221–228.
- Li, A. P., Maurel, P., Gomez-Lechon, M. J., Cheng, L. C., Jurima-Romet, M. (1997). Preclinical evaluation of drug–drug interaction potential: present status of the application of primary human hepatocytes in the evaluation of cytochrome P450 induction. *Chem.-Biol. Interact.* 107:5–16.
- Li, W. F., Costa, L. G., Richter, R. J., Hagen, T., Shih, D. M., Tward, A., Lulis, A. J., Furlong, C. E. (2000). Catalytic efficiency determines the in vivo efficacy of PON1 for detoxifying organophosphorus compounds. *Pharmacogenetics* 10:767–779.
- Lieber, C. S. (1997). Cytochrome P450E1: its physiological and pathological role. *Physiol. Rev.* 77:515–544.
- Litchfield, M. H. (1985). Toxicity to mammals. In: Leahey, J. P., ed. *The Pyrethroid Insecticides*. London: Taylor & Francis, pp. 99–150.
- Mackell, J. V., Reiders, F., Brieger, H., et al. (1951). Acute hemolytic anemia due to ingestion of naphthalene moth balls I. Clinical aspects. *Pediatrics* 7:722–727.
- Marino, M. T., Schuster, B. G., Brueckner, R. P., Lin, E., Kaminskis, A., Lasseter, K. C. (1998). Population pharmacokinetics and pharmacodynamics of pyridostigmine bromide for prophylaxis against nerve agents in humans. *J. Clin. Pharmacol.* 38:227–235.
- Matsumura, F. (1975). Metabolism of carbamate insecticides. In: Matsumura, F., ed. *Toxicology of Insecticides*. New York: Plenum Press, pp. 228–239.
- Maxwell, D. M., Brecht, K. M., O'Neill, B. L. (1987). The effect of carboxylesterase inhibition on interspecies differences in soman toxicity. *Toxicol. Lett.* 39:35–42.
- May, D. G., Naukam, R. J., Kambam, J. R., Branch, R. A. (1992). Cimetidine–carbaryl interaction in humans: evidence for an active metabolite of carbaryl. *J. Pharmacol. Exp. Ther.* 262:1057–1061.
- McCain, W. C., Lee, R., Johnson, M. S., Whaley, J. E., Ferguson, J. W., Beall, P., Leach, G. (1997).

- Acute oral toxicity study of pyridostigmine bromide, permethrin, and DEET in the laboratory rat. *J. Toxicol. Environ. Health* 50:113–124.
- McDougal, J. N., Pollard, D. L., Weisman, W., Garrett, C. M., Miller, T. E. (2000). Assessment of skin absorption and penetration of JP-8 jet fuel and its components. *Toxicol. Sci.* 55:247–255.
- Metker, L., Angerhofer, R. A., Pope, C. R., Swentzel, K. C. (1978). *Toxicological Evaluation of 3-(Phenoxyphenyl)methyl (±)-cis, trans-3-(2,2-Dichloroethyl)- 2,2-Dimethylcyclopropane Carboxylate (Permethrin)*. Report No. 51-0831-78, U.S. Army Environmental Hygiene Agency.
- Minami, M., Hui, D. M., Katsumata, M., Inagaki, H., Boulet, A. (1997). Method for the analysis of the methylphosphonic acid metabolites of sarin and its ethanol-substituted analogue in urine as applied to the victims of the Tokyo sarin disaster. *J. Chromatogr., B, Biomed. Sci. Appl.* 695(2):237–244.
- Minami, M., Hui, D. M., Wang, Z., Katsumata, M., Inagaki, H., Li, Q., Inuzuka, S., Mashiko, K., Yamamoto, Y., Oosuka, T., Boulet, A., Clement, J. G. (1998). Biological monitoring of metabolites of sarin and its by-products in human urine samples. *J. Toxicol. Sci.* 23(suppl. 2):250–254.
- Miyamoto, J. (1976). Degradation, metabolism, and toxicity of synthetic pyrethroids. *Environ. Health Perspect.* 14:15–28.
- Monteiro-Riviere, N., Inman, A., Riviere, J. (2001). Effects of high-dose and low-dose dermal exposure to Jet A, JP-8 and JP8 (100) jet fuels. *J. Appl. Toxicol.* 21:485–494.
- Mutch, E., Blain, P. G., Williams, F. M. (1999). The role of metabolism in determining parathion toxicity in man. *Toxicol. Lett.* 107:177–187.
- Nakajima, T., Okuyama, S., Yonekura, I., Sato, A. (1985). Effects of ethanol and phenobarbital administration on the metabolism and toxicity of benzene. *Chem.-Biol. Interact.* 55:23–38.
- National Research Council. (2003). *Toxicologic Assessment of Jet-Propulsion Fuel 8*.
- Neal, R. A. (1980). Microsomal metabolism of thiono-sulfur compounds: mechanisms and toxicological significance. *Rev. Biochem. Toxicol.* 2:131–171.
- Nolan, R. J., Rick, D. L., Feshour, N. L., Saunders, J. H. (1984). Chlorpyrifos: pharmacokinetics in human volunteers. *Toxicol. Appl. Pharmacol.* 73:8–15.
- Oonithan, E. S., Casida, J. E. (1968). Oxidation of methyl- and dimethylcarbamate insecticide chemicals by microsomal enzymes and anticholinesterase activity of the metabolites. *J. Agric. Food Chem.* 16:28–44.
- Pakenham, E., Lango, J., Buonarati, M., Morin, D., Buckpitt, A. (2002). Urinary naphthalene mercapturates as biomarkers of exposure and stereoselectivity of naphthalene epoxidation. *Drug Metab. Dispos.* 30:247–253.
- Pleil, J. D., Smith, L. B., Zelnick, S. D. (2000). Personal exposure to JP-8 fuel vapors and exhaust at Air Force bases. *Environ. Health Perspect.* 108:183–192.
- Pons, F., Kalvet, J. H., Haag, M., Raeppl, V., Keravis, T., Frossard, N. (2001). Altered expression of lung cytochrome P450 3A1 after exposure to sulfur mustard. *Pharmacol. Toxicol.* 88:40–44.
- Purdon, M. P., Lehman-McKeeman, L. D. (1997). Improved high-performance liquid chromatographic procedure for the separation and quantification of hydroxytestosterone metabolites. *J. Pharmacol. Toxicol. Methods* 37:67–73.
- Ramos, G., Nghiem, D. X., Walterschied, J. P., Ullrich, S. E. (2002). Dermal application of jet fuel suppresses immune reactions. *Toxicol. Appl. Pharmacol.* 180:136–144.
- Raucy, J. L., Kraner, J. C., Lasker, J. M. (1993). Bioactivation of halogenated hydrocarbons by cytochrome P4502E1. *Crit. Rev. Toxicol.* 23:1–20.
- Rhyne, B. N., Pirone, J. R., Riviere, J. E., Monteiro-Riviere, N. A. (2002). The use of enzyme histochemistry in detecting cutaneous toxicity of three topically applied jet fuel mixtures. *Toxicol. Mech. Methods* 12:17–34.

- Richter, R. J., Furlong, C. E. (1999). Determination of paraoxonase (PON1) status requires more than genotyping. *Pharmacogenetics* 9:745–753.
- Ritchie, G. D., Still, K. R., Alexander, W. K., Nordholm, D. F., Wilson, C. L., Rossi, J., Mattie, D. R. (2001). A review of neurotoxicity risk of selected hydrocarbon fuels. *J. Toxicol. Environ. Health, Part B, Crit. Rev.* 4:223–312.
- Riviere, J. E., Brooks, J. D., Monteiro-Riviere, N. A., Budsaba, K., Smith, C. E. (1999). Dermal absorption and distribution of topically dosed jet fuels Jet-A, JP-8 and JP-8(100). *Toxicol. Appl. Pharmacol.* 160:60–75.
- Robertson, P., Decory, H. H., Madan, A., Parkinson, A. (2000). In vitro inhibition and induction of human hepatic cytochrome P450 enzymes by modafinil. *Drug Metab. Dispos.* 28:664–671.
- Robledo, R. F., Scott Young, R., Lantz, C., Witten, M. (2000). Short-term pulmonary response to inhaled JP-8 jet fuel aerosol in mice. *Toxicol. Pathol.* 28:656–663.
- Rose, R. L., Cherrington, N. (2004). Pesticide induction of xenobiotic-metabolizing enzymes in human hepatocytes. Unpublished results.
- Sams, C., Mason, H. J., Rawbone, R. (2000). Evidence for the activation of organophosphate pesticides by cytochromes P450 3A4 and 2D6 in human liver microsomes. *Toxicol. Lett.* 116:217–221.
- Schoenig, G. P., Hartnagel, R. J. Jr., Osimitz, T. G., Llanso, S. (1996). Absorption, distribution, metabolism and excretion of *N,N*-diethyl-*m*-toluamide in the rat. *Drug Metab. Dispos.* 24:156–163.
- Selim, S., Hartnagel, R. J., Osimitz, T. G., Garbriel, K. L., Schoenig, G. P. (1995). Absorption, excretion and metabolism of *N,N*-diethyl-*m*-toluamide following dermal application to human volunteers. *Fundam. Appl. Toxicol.* 25:95–100.
- Shih, M. L., McMonagle, J. D., Dolzine, D. W., Gresham, V. C. (1994). Metabolite pharmacokinetics of soman, sarin and GF in rats and biological monitoring of exposure to toxic organophosphorus agents. *J. Appl. Toxicol.* 14:195–199.
- Smith, L. B., Bhattacharya, A., Lemasters, G., Succop, P., Puhala, E., Medvedovic, M., Joyce, J. (1997). Effect of chronic low-level exposure to jet fuel on postural balance of U.S. Air Force personnel. *J. Occup. Environ. Med.* 39:623–632.
- Stone, C. L., Bosron, W. F., Dunn, M. F. (1993). Amino acid substitutions at position 47 of $\beta_1\beta_1$ and $\beta_2\beta_2$ human and alcohol dehydrogenases affect hydride transfer and coenzyme dissociation rate constants. *J. Biol. Chem.* 268:892–899.
- Strother, A. (1972). In vitro metabolism of methylcarbamate insecticides by human and rat liver fraction. *Toxicol. Appl. Pharmacol.* 21:112–129.
- Sultatos, L. G. (1991). Metabolic activation of the organophosphorus insecticides chlorpyrifos and fenitrothion by perfused rat liver. *Toxicology* 68:1–9.
- Sultatos, L. G., Pastino, G. M., Rosenfeld, C. A., Flynn, E. J. (2004). Incorporation of the genetic control of alcohol dehydrogenase into a physiologically based pharmacokinetic model for ethanol in humans. *Toxicol. Sci.* 78:20–31.
- Surbrook, S. E., Olson, M. J. (1992). Dominant role of cytochrome P-450 2E1 in human hepatic microsomal oxidation of the CFC-substitute 1,1,1,2-tetrafluoroethane. *Drug Metab. Dispos.* 20:518–524.
- Szinicz, L., Baskin, S. L. (1999). Chemical and biological agents. In: Marquardt, H., Schafer, S. G., McClellan, R. O., Welsch, F., eds. *Toxicology*. New York: Academic Press, pp. 851–877.
- Tang, J., Cao, Y., Rose, R. L., Brimfield, A. A., Dai, D., Goldstein, J. A., Hodgson, E. (2001). Metabolism of chlorpyrifos by human cytochrome P450 isoforms and human, mouse and rat liver microsomes. *Drug Metab. Dispos.* 29:1201–1204.
- Tang, J., Cao, Y., Rose, R. L., Hodgson, E. (2002). In vitro metabolism of carbaryl by human cytochrome P450 and its inhibition by chlorpyrifos. *Chem.-Biol. Interact.* 141:229–241.
- Tingle, M. D., Pirmohamad, M., Templeton, E., et al. (1993). An investigation of the formation of

- cytotoxic, genotoxic, protein-reactive and stable metabolites from naphthalene by human liver microsomes. *Biochem. Pharmacol.* 46:1529–1538.
- Tripathi, D. N., Sugendran, K., Malhotra, R. C., Bhattacharya, A., Dasgupta, S. (1995). Studies on urine and tissues of rats, guinea pigs and mice exposed to sulfur mustard using mass-spectrometry. *J. Biosci.* 20:29–33.
- Ullrich, S. E., Lyons, H. J. (2000). Mechanisms involved in the immunotoxicity induced by dermal application of JP-8 jet fuel. *Toxicol. Sci.* 58:290–298.
- USEPA. (1998). *Toxicological Review of Naphthalene (CAS No. 91-20-3) in Support of Summary Information on the Integrated Risk Information System (IRIS)*. U.S. Environmental Protection Agency.
- Usmani, K. A., Rose, R. L., Goldstein, J. A., Taylor, W. G., Brimfield, A. A., Hodgson, E. (2002). In vitro human metabolism and interactions of the repellent, *N,N*-diethyl-*m*-toluamide (DEET). *Drug Metab. Dispos.* 30:289–294.
- Usmani, K. A., Rose, R. L., Hodgson, E. (2003). Inhibition and activation of the human liver and human cytochrome P450 3A4 metabolism of testosterone by deployment-related chemicals. *Drug Metab. Dispos.* 31:384–391.
- Usmani, K. A., Hodgson, E., Rose, R. L. (2004). In vitro human metabolism of pyridostigmine. unpublished studies.
- Veltri, J. C., Osimitz, T. G., Bradford, D. C., Page, B. C. (1994). Retrospective analysis of calls to poison control centers resulting from exposure to the insect repellent *N,N*-diethyl-*m*-toluamide (DEET) from 1985 to 1989. *Clin. Toxicol.* 32:1–16.
- Verschoyle, R. D., Barnes, J. M. (1972). Toxicity of natural and synthetic pyrethrins to rats. *Pestic. Biochem. Physiol.* 2:308–311.
- Vodela, J. K., Dalvi, R. R. (1995). Comparative toxicological studies of chlorpyrifos in rats and chickens. *Vet. Hum. Toxicol.* 37:1–3.
- Wagner, F. W., Burger, A. R., Vallee, B. L. (1983). Kinetic properties of human liver alcohol dehydrogenase: oxidation of alcohols by class I isoenzymes. *Biochemistry* 22:1857–1863.
- Ward, S. A., May, D. G., Heath, A. J., Branch, R. A. (1988). Carbaryl metabolism is inhibited by cimetidine in the isolated perfused rat liver and in man. *Clin. Toxicol.* 26:269–281.
- Warshawsky, D., Bingham, E., Niemeier, R. M. (1977). The effects of *N*-dodecane on the metabolism and distribution of benzo(a)pyrene in the isolated perfused rabbit lung. *Life Sci.* 27:1827–1837.
- Winder, C., Balouet, J. C. (2002). The toxicity of commercial jet fuels. *Environ. Res.* 89:146–164.
- Yuknavage, K. L., Fenske, R. A., Kalman, D. A., Keifer, M. C., Furlong, C. E. (1997). Simulated dermal contamination with capillary samples and field cholinesterase biomonitoring. *J. Toxicol. Environ. Health* 51:35–55.
- Zeiger, E., Smith, L. (1998). The first international conference on the environmental health and safety of jet fuel. *Environ. Health Perspect.* 106:763–764.

Thiodiglycol, the hydrolysis product of sulfur mustard: Analysis of in vitro biotransformation by mammalian alcohol dehydrogenases using nuclear magnetic resonance[☆]

A.A. Brimfield^{a,*}, Mark J. Novak^b, Ernest Hodgson^c

^a Pharmacology Division, U.S. Army Medical Research Institute of Chemical Defense, 3100 Ricketts Point Rd. Aberdeen Proving Ground/Edgewood Area, MD 21010-5400, USA

^b Department of Chemistry, Florida Institute of Technology, Melbourne, FL 32901, USA

^c Department of Environmental and Molecular Toxicology, North Carolina State University, Raleigh, NC 27695, USA

Received 8 August 2005; revised 17 November 2005; accepted 18 November 2005

Available online 18 January 2006

Abstract

Thiodiglycol (2,2'-bis-hydroxyethylsulfide, TDG), the hydrolysis product of the chemical warfare agent sulfur mustard, has been implicated in the toxicity of sulfur mustard through the inhibition of protein phosphatases in mouse liver cytosol. The absence of any inhibitory activity when TDG was present in assays of pure enzymes, however, led us to investigate the possibility for metabolic activation of TDG to inhibitory compound (s) by cytosolic enzymes. We have successfully shown that mammalian alcohol dehydrogenases (ADH) rapidly oxidize TDG in vitro, but the classic spectrophotometric techniques for following this reaction provided no information on the identity of TDG intermediates and products. The use of proton NMR to monitor the oxidative reaction with structural confirmation by independent synthesis allowed us to establish the ultimate product, 2-hydroxyethylthioacetic acid, and to identify an intermediate equilibrium mixture consisting of 2-hydroxyethylthioacetaldehyde, 2-hydroxyethylthioacetaldehyde hydrate and the cyclic 1,4-oxathian-2-ol. The intermediate nature of this mixture was determined spectrophotometrically when it was shown to drive the production of NADH when added to ADH and NAD.

© 2005 Elsevier Inc. All rights reserved.

Keywords: Sulfur mustard; Thiodiglycol; In vitro metabolism; Alcohol dehydrogenase; NMR

Introduction

Sulfur mustard (2,2'-bis-chloroethylsulfide, Fig. 1A) is a vesicant causing delayed injury to human skin that varies in severity from erythema to massive blistering and necrosis in a dose-dependent manner. The actual mechanism by which this occurs remains unexplained although inflammation certainly plays a role. In aqueous medium, pure sulfur mustard undergoes rearrangement by an S_N1 mechanism to a cyclic sulfonium ion that quickly hydrolyzes (Fig. 2). This process is

repeated, due to the bifunctional nature of the molecule, leading to the final hydrolysis product thiodiglycol (2,2'-bis-hydroxyethylsulfide, TDG, Fig. 1B) a symmetric, water-soluble, liquid primary diol with low vapor pressure (Bartlett and Swain, 1949; Yang et al., 1988). TDG itself is relatively non-toxic (Reddy et al., in press) so its formation has been considered a sulfur mustard detoxification step.

In earlier work (Brimfield, 1995), we showed that TDG inhibited non-alkaline phosphatase-related *p*-nitrophenylphosphate phosphatase (*p*-NPP) activity in mouse liver cytosolic preparations. There was strong circumstantial evidence to indicate a mechanistic relationship between *p*-NPP inhibition by TDG in cytosol and the inhibition of one or more protein (serine/threonine) phosphatases by the natural vesicant cantharidin (Li and Casida, 1992). However, cantharidin also inhibited preparations of pure protein phosphatases 1, 2a and 2b while

[☆] The opinions or assertions herein are the private views of the authors and are not to be construed as official or as reflecting the views of the Army or the Department of Defense.

* Corresponding author. Fax: +1 410 436 8377.

E-mail address: alan.a.brimfield@us.army.mil (A.A. Brimfield).

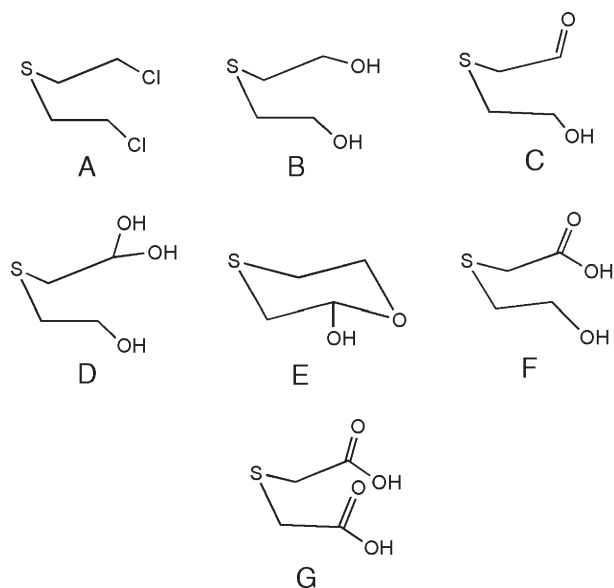


Fig. 1. The structures under discussion: (A) sulfur mustard, 2,2'-bis-chloroethyl sulfide; (B) thiodiglycol, TDG, 2,2'-thiodiethanol; (C) 2-hydroxyethylthioacetaldehyde; (D) 2-hydroxyethylthioacetaldehyde hydrate; (E) 1,4-oxathian-2-ol; (F) 2-hydroxyethylthioacetic acid; (G) thiodiglycolic acid, 2,2'-thio-bis-acetic acid.

TDG did not. That observation led us to investigate the metabolic activation of TDG to a protein phosphatase inhibitor by liver cytosolic enzymes.

When we added TDG to mouse liver cytosol and monitored absorbance at 340 nm, we detected a steady increase in optical density indicating the reduction of NAD. This result, plus the structural resemblance of TDG to ethanol, led us to test alcohol dehydrogenase (alcohol:NAD⁺ oxidoreductase, ADH) as a source of metabolic transformation. We subsequently established kinetic constants for the interaction of TDG with ADH and demonstrated its facile metabolism in pig and human skin cytosol, by ADH from horse liver (Brimfield et al., 1998) and by cloned human isoforms (Dudley et al., 2000).

However, monitoring ADH activity by following the absorbance from NADH production provided no information about the structure of enzymatic intermediates and reaction products. The route of the reaction is transparent to spectrophotometric monitoring (Henehan and Oppenheimer, 1993; Abeles and Lee, 1960). The alternative approach using batch-wise incubations, isolating the products from the reaction mixture and characterizing them by physicochemical means, permits product identification but raises the risk of failure to identify transient low concentration intermediates and yields little insight into the timing of their comings and goings. We needed a system by which we could establish metabolite identity and dynamically monitor product and intermediate appearance and disappearance.

Oppenheimer's work offered such a system (Oppenheimer and Henehan, 1995; Henehan and Oppenheimer, 1993; Henehan et al., 1993, 1995). He developed an ¹H NMR procedure that employed catalytic quantities of ADH and NAD and a lactate dehydrogenase/pyruvate-based NAD regenerating system in

aqueous buffer. The process is made possible by the application of water suppression using the presaturation technique which reduces the large signal from the protons on water in aqueous media and allows the visualization of the comparatively weak signals from compounds of interest (Hore, 1989).

This report presents the results from a study of the enzyme-mediated transformation of TDG by horse liver ADH and several human isoforms in vitro. The use of ¹H NMR, with structural confirmation by synthesis, allowed us to identify intermediates and products produced from TDG as the result of ADH oxidation. In the future, we will test these newly identified metabolites for their ability to inhibit pure protein (serine/threonine) phosphatases and determine whether or not TDG is a factor in the mechanism of sulfur mustard-induced vesication.

Materials and methods

Reagents and supplies. Equine liver alcohol dehydrogenase, lactate dehydrogenase (LDH) from rabbit muscle, sodium pyruvate and β-nicotinamide adenine dinucleotide were purchased from Sigma Chemical Co., St. Louis, MO. Thiodiglycol and thiodiglycolic acid were from Aldrich Chemical Co., Milwaukee, WI, and were used without additional purification. Deuterium oxide (D₂O) was supplied by the ACROS Division of Fisher Scientific, Somerville, NJ. Other chemicals and solvents were reagent grade from standard suppliers.

Human α and β₁ ADH isozymes were the kind gift of Dr. Thomas Hurley, Department of Biochemistry and Molecular Biology, Indiana University School of Medicine. The isozymes were expressed and purified from *Escherichia coli* (JM105 strain) as described in Choi et al. (2002). Glycerol, added to the purified enzyme preparations before freezing, interfered with the collection of NMR data. It was removed and the buffer corrected by passage through a small Sephadex G25 (Pharmacia Fine Chemicals, Uppsala, Sweden) column followed by repeated concentration and resuspension in fresh buffer at 4 °C using Amicon Microcon centrifugal filtration devices (Millipore Corp., Billerica, MA) with a 10,000 molecular weight cut off.

Enzymology. For NMR, each sample consisted of 10 mM TDG, 2.0 mM NAD, 0.15 U of horse liver ADH and an NAD regenerating system consisting of 250 U of lactate dehydrogenase and 100 mM sodium pyruvate dissolved in 0.1 M sodium phosphate buffer, pH 7.5, in a total volume of 500 μl. Deionized water used to prepare the buffer was made 10% by volume with respect to D₂O. All components except ADH were prepared as a mixture and kept at 0 °C. A 480 μl aliquot of the mixture was transferred to a standard 5-mm NMR tube and

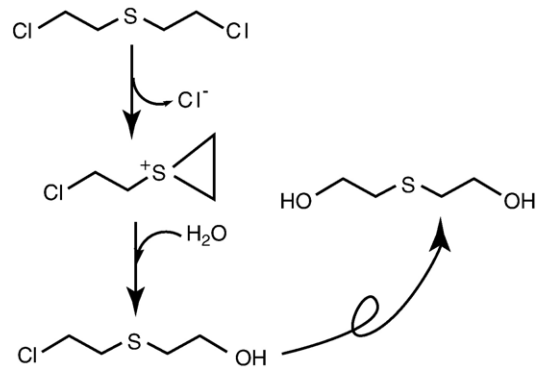


Fig. 2. The rapid S_N1 mediated formation of TDG from sulfur mustard in aqueous medium, via a cyclic sulfonium ion, followed by hydrolysis. The bifunctional nature of the mustard leads to the formation of a symmetrical diol via two cycles of sulfonium ion formation.

brought to 37 °C. The reaction was begun with the addition of 20 μ l of ADH (0.15 U) in buffer at 37 °C. Proton NMR monitoring of the enzymatic reaction was done on a Varian Unity Inova 600 MHz instrument equipped with Varian data analysis software version 6.1C (Varian Instruments, Palo Alto, CA). The probe temperature was maintained at 37 °C. Each time point consisted of 64 scans acquired with a spectral width of 10,000 Hz using 32K data points. A 3.9-s post-acquisition delay was used to allow for full relaxation of the resonances. During monitoring of the enzymatic activity, spectra were collected every 5 to 8 min for up to 16 h.

When recombinant human isoforms were evaluated, activity was normalized to that of the equine enzyme spectrophotometrically by following the increase in optical density at 340 nm using ethanol as a substrate, as described in Dudley et al. (2000), immediately before starting the analysis. The concentration of human isoform was adjusted until the rate was equal to that given by the 0.15 U of horse liver ADH used in the NMR evaluation of that enzyme. This allowed us to base our comparisons on equipotent enzymatic systems.

For spectrophotometric evaluation of ADH activity toward the oxathianol (Fig. 1E), we used a mixture in 0.01 M sodium phosphate buffer, pH 7.5 containing 1.0 mg/ml enzyme, 5.0 mM NAD and 10 mM oxathianol. The reaction was run at 30 °C, and the optical density at 340 nm was measured. NADH produced was determined using an extinction coefficient of 6317 $\text{mol}^{-1} \text{cm}^{-1}$ (McComb et al., 1976).

Organic synthesis. The aldehyde (Fig. 1C) was synthesized in its lactol form (Fig. 1E) in a single step from TDG using a chromium VI-pyridine reagent according to the method of Corey and Schmidt (1979). To 245 mg of CrO_3 stirred in 10 ml of dry CH_2Cl_2 at 0 °C was added 200 μ l of anhydrous pyridine drop wise via syringe. The resulting orange/yellow heterogeneous reaction was allowed to stir at 0 °C for 30 min, whereupon 100 mg of thiodiglycol dissolved in 1.5 ml of dry CH_2Cl_2 was added. After stirring for 1.5 h at 0 °C, the brown heterogeneous reaction mixture was warmed to room temperature, diluted with 30 ml of diethyl ether and filtered through a plug of silica gel with 50 ml of diethyl ether being used to complete the transfer. Removal of the solvent in vacuo yielded the crude product mixture as a light yellow oil. Flash chromatography with a 1:40 methanol/chloroform mobile phase yielded 70 mg (70%) of 1,4-oxathian-2-ol as a colorless oil which solidified upon storage at 4 °C: ^1H NMR, Bruker AMX-360 (Buena Vista, NJ) (CDCl_3 , ppm) 5.04 (1 H, t, $J=2.8$ Hz), 4.28 (1 H, m), 3.87 (1 H, m), 3.59 (1 H, d, $J=7.6$ Hz), 2.86 (1 H, dd, $J=13.2$ Hz, $J=0.8$ Hz), 2.56 (3 H, m); mass spectrum Hewlett-Packard G1800A (Agilent Technologies, Palo Alto, CA) (EI, 70 eV) m/e (relative intensity) $\text{C}_4\text{H}_8\text{O}_2\text{S}$ MW = 120.15, observed, 120.1 (M^+ , 35), 102 (8), 91 (21), 74 (51), 61 (73), 46 (100).

Hydroxyethylthioacetic acid (Fig. 1F), used to confirm the structure of the final metabolic product, was synthesized according to the procedures published by Black et al. (1993) and was isolated as the sodium salt. Spectral characterization gave results consistent with the published values.

Results

NMR using ADH from equine liver

The NMR system performed well as a means for evaluating the disappearance of reactants and the appearance of products with the horse liver enzyme. Fig. 3 clearly shows the peaks of significance for evaluating the dynamics of the reaction. The signals associated with the NAD regenerating system were prominent. The methyl protons contributed by the keto form of pyruvate appear as a singlet at 2.36 ppm and for the hydrated form as a singlet at 1.47 ppm. The methyl protons of lactate appear as a doublet at 1.32 ppm. The quartet at 4.12 ppm represented the single proton on the α carbon of lactate. The complex set of signals from protons on the pyridine nucleotide appears above 6.0 ppm. Their intensity was relatively low consistent with the catalytic concentration (2.0 mM) of NAD.

Although the pyruvate peak appeared apparently unchanged during the course of the incubation because of the high starting concentration (100 mM), side by side comparison of consecutive spectra (Fig. 4) and graphing the integrated data (Fig. 5) showed a reduction in pyruvate concentration consistent with the increase in the concentration of the methyl group of lactate. The stoichiometry of lactate production and pyruvate consumption (20 mM) and for TDG disappearance (10 mM) indicated the reduction of 2 mol of NAD per mole of TDG oxidized (Fig. 5) as one would predict for the twofold oxidation of TDG to TDGA (Fig. 1F).

The signals originating with TDG were also prominent. The signal for the methylene protons on the carbon adjacent to sulfur

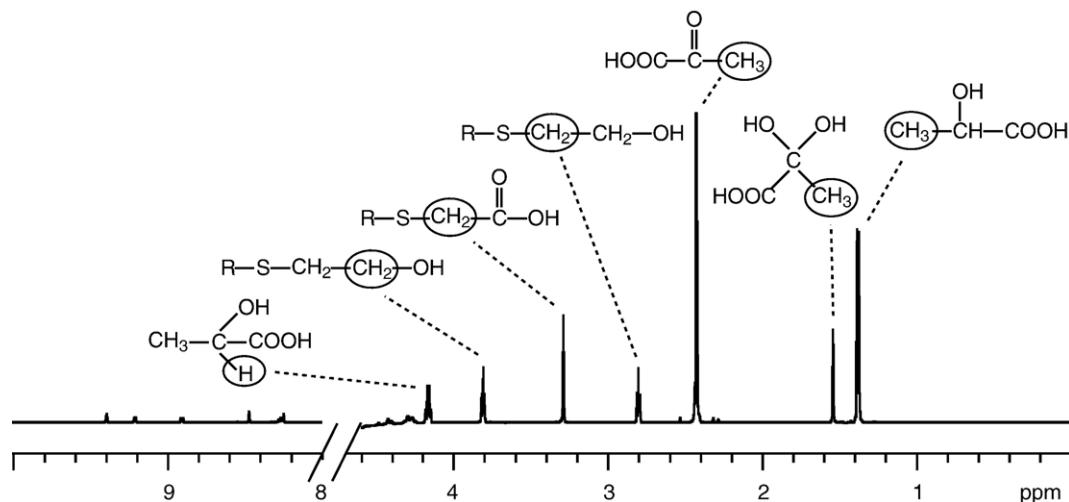


Fig. 3. The complete NMR spectrum produced using horse liver ADH to transform TDG at 602 min of incubation. The resonances arising from the components of the NAD regenerating system appear at 1.40 ppm, the methyl protons of lactate; 1.60 ppm, pyruvate hydrate; 2.42 ppm, pyruvate in the keto form; 4.19 ppm, the single methylene proton of lactate. There are no significant features between 5.0 and 8.0 ppm. The resonances arising from TDG can be seen at 2.78 ppm and 3.78 ppm. The origin of each signal is identified on the structures above. R = HO-CH₂-CH₂-. The signal for the final product, hydroxyethylthioacetic acid, appears at 3.27 ppm. The small peaks above 8.00 ppm are the resonances from protons on NAD.

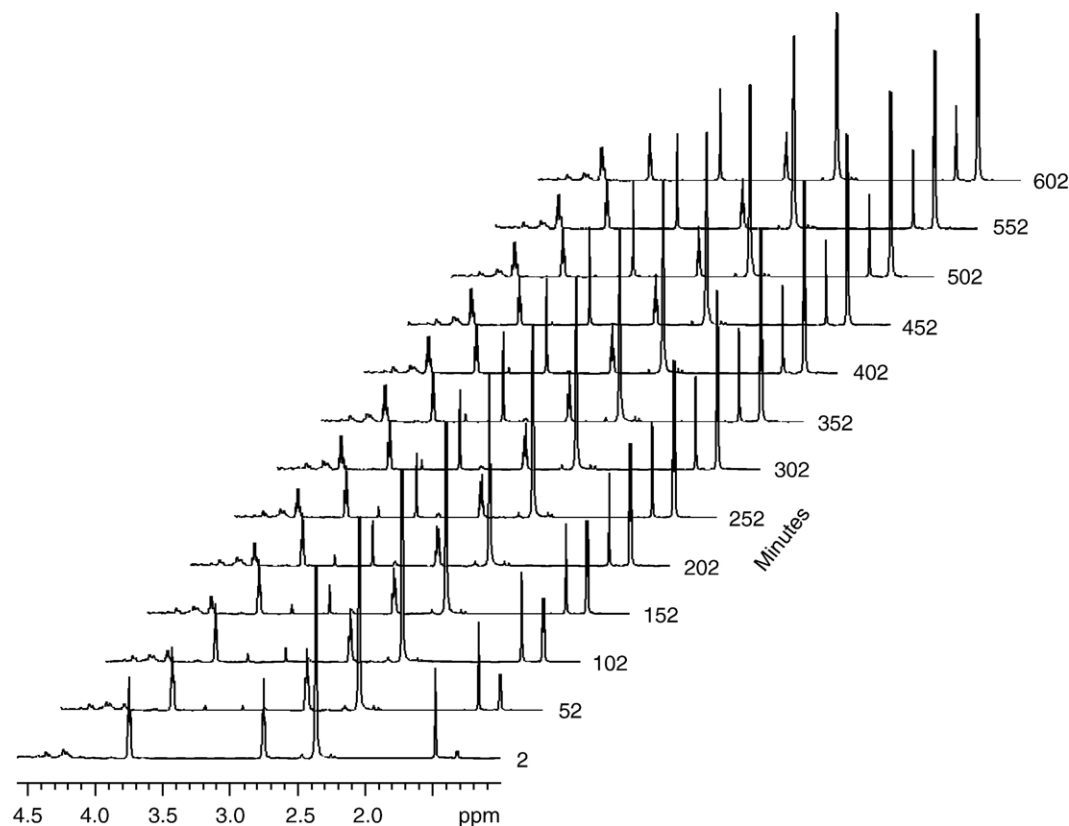


Fig. 4. Sequential spectra of TDG acted upon by equine ADH from 2 to 602 min showing the evolution of lactate via the resonance from the protons of its methyl group (1.44 ppm) and the accumulation of the methylene peak from hydroxyethylthioacetic acid (3.23 ppm) over time. There is 50 min separating each spectrum.

in TDG (triplet, 2.78 ppm, Fig. 3) and the methylene protons on the hydroxyl-containing carbon in TDG (triplet, 3.78 ppm, Fig. 3) were consistent with a standard spectrum of TDG run under identical conditions of temperature, pH and solvent composition (Fig. 6A). The appearance of a new signal at 3.23 ppm (singlet) representing two equivalent methylene protons on a carbon adjacent to a carboxylic acid group indicated the generation of 2-hydroxyethylthioacetic acid (TDGA, Fig. 1F) as a product. The structure was confirmed by comparison with the NMR spectra of TDG (Fig. 6A), thiodiglycolic acid (Fig. 6B) and 2-hydroxyethylthioacetic acid (Fig. 6C) under the conditions employed in the enzyme work. The terminal nature of the acid in the metabolic pathway was determined by substituting it for TDG in the otherwise complete *in vitro* horse liver NMR system and finding no evidence of enzymatic turnover (data not shown).

Our initial assumption was that the signal from a free aldehyde would appear in the 9.0–9.5 ppm range where the signal for an aldehydic proton usually appears. This was not the case in the spectra from our experimental metabolic system. However, the appearance of minor transient signals between 2.64 and 2.75 ppm and 3.9 to 4.0 ppm (Fig. 7) caused us to reexamine that expectation. These minor signals seemed to correspond to a single compound based on peak integrals and 2-dimensional correlation spectroscopy (COSY) which allows one to isolate and identify spin systems associated with each compound in a mixture (data not shown). The chemical shifts and splitting patterns suggested a cyclic compound with a hemiacetalic proton.

A chromium (VI)-mediated oxidation (Corey and Schmidt, 1979) of TDG yielded 1,4-oxathian-2-ol (Fig. 1E) a cyclic hemiacetal. NMR analysis of this synthetic product under conditions of temperature, pH and solvent composition identical to those used to investigate the enzymatic activity (Fig. 8) enabled us to identify a doublet of doublets at 2.66 ppm and a multiplet at 2.72 ppm (Fig. 9A). These corresponded to signals found in the spectra made using the horse liver ADH (Fig. 9B). Further analysis showed that these signals arose from the methylene protons on the carbons adjacent to the sulfur in the oxathianol. The complex splitting pattern in the multiplet arose from the diastereotopic nature of the protons imposed by the rigid structure of the oxathianol ring. Each proton is in a unique electronic environment giving each a different chemical shift. The spectra obtained from the pure compound in aqueous buffer and from the experimental enzymatic mixture after 8 min of incubation are compared in Figs. 9A and B. Comparison clearly indicates the presence of the oxathianol in the experimental sample (Fig. 9B).

A doublet of doublets between 4.96 and 5.00 ppm, which showed up in the aqueous spectrum of the synthetic product and also in the experimental spectra (Figs. 10A and B), is the signal produced by the proton on the hydroxylated carbon of the oxathianol split by the protons on the methylene group adjacent to the sulfur. The presence of this signal in spectra arising both from the metabolic system and from the synthetic product in our aqueous buffer provided additional confirmation for oxathianol as an intermediate in the metabolism of

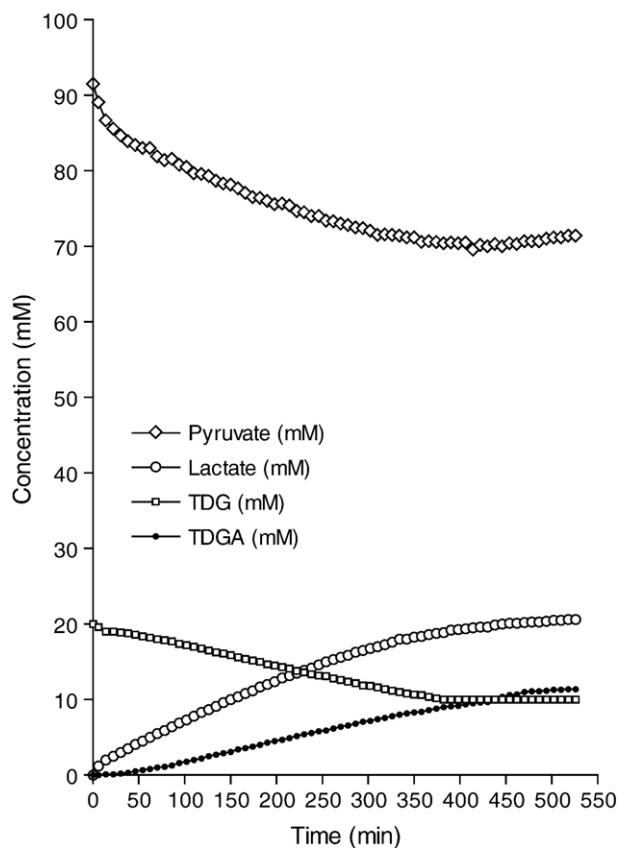


Fig. 5. A kinetic plot generated from sequential spectra based on peak integration illustrates the stoichiometric relationship between the pyruvate to lactate and TDG to TDGA conversions. The actual starting concentration of pyruvate + its hydrate was 100 mM. Approximately 9% of the pyruvate was hydrated so the starting concentration of the keto form was 91 mM. The actual starting concentration of TDG was 10 mM. However, since it is a symmetrical molecule the molarity of each methylene group was actually 20 mM. Since only one hydroxyl group is oxidized per molecule, the molarity of the methylene groups drops from 20 mM to 10 mM.

TDG by ADH. A set of doublets centered around 2.83 ppm in the spectrum of the synthetic oxathianol in buffer (Fig. 8D) arises from the methylene protons on the carbon adjacent to the ring oxygen. In the experimental enzymatic spectra, these signals are obscured by a large peak related to TDG.

NMR analysis of the synthetic product in deuteriochloroform done in conjunction with synthesis (see Materials and methods) indicated only the presence of the oxathianol. In the aqueous medium used for the metabolic spectra, however, the synthetic oxathianol (Fig. 8) exhibited signals not found in the deuteriochloroform spectrum. A minor signal at 9.47 ppm (Fig. 8A), observed after expanding the vertical scale, provided evidence of the free acyclic aldehyde. Triplets at 5.15 ppm (Fig. 8B), 3.73 ppm (Fig. 8C) and 2.87 ppm (Fig. 8D) and a doublet centered around 2.81 ppm (Fig. 8D) provided chemical shifts and splitting patterns consistent with the presence of an acyclic aldehyde hydrate. This conclusion was supported by COSY analysis (data not shown). It appeared that the oxathianol formed an equilibrium mixture with the aldehyde and its hydrate in aqueous medium at pH 7.5.

The presence of the hydrated aldehyde was consistent with the results of Henehan et al. (1993), who identified acetaldehyde hydrate as the actual intermediate in the metabolism of ethanol to acetic acid. That led us to test the oxathiane-2-ol spectrophotometrically to establish whether it acted as a substrate for the ADH by measuring NADH production using the optical density at 340 nm. The equine enzyme oxidized the oxathianol-related mixture, presumably via the hydrated aldehyde component, at 6 nmol NADH/min/U.

NMR using human isoforms

Additionally, we tested the recombinant human α and β_1 isoforms of ADH using the NMR system to test their mechanistic similarity to the horse liver enzyme. TDG seemed to be a poor substrate for human $\beta_1\beta_1$. There was little evidence of peaks attributable to either the aldehyde or the acid even after more than 6 h of incubation. This was consistent with results from our spectrophotometric kinetic studies where the $\beta_1\beta_1$ ADH had the lowest activity toward TDG among the human class I isoforms capable of using TDG as a substrate (Dudley et al., 2000).

When human- α ADH was used in place of the equine enzyme, the singlet at approximately 3.2 ppm, produced by the protons on the methylene group between the sulfur and the carboxyl group of 2-hydroxyethylthioacetic acid, was observed to form over time (Fig. 11). However, the minor peaks observed with the equine ADH (Fig. 7) were not observed at any time with the human α . The only product detected was the 2-hydroxyethylthioacetic acid, suggesting that the human

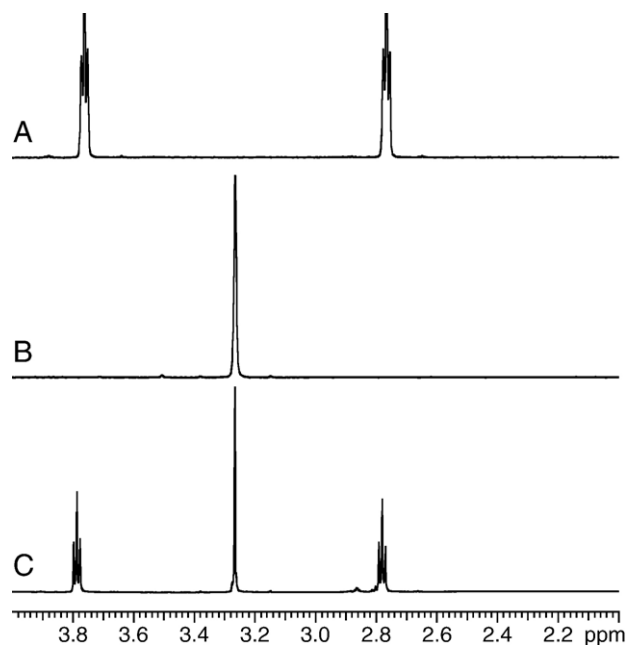


Fig. 6. The spectra of the pure compounds used to illustrate the basis for concluding the peak at 3.27 ppm represented the methylene protons on the carbon adjacent to sulfur in hydroxyethylthioacetic acid. (A) TDG (Fig. 1B); (B) thiodiglycolic acid (Fig. 1G); (C) 2-hydroxyethylthioacetic acid (Fig. 1F). The conditions of solvent and pH used were as outlined in Materials and methods under Enzymology.

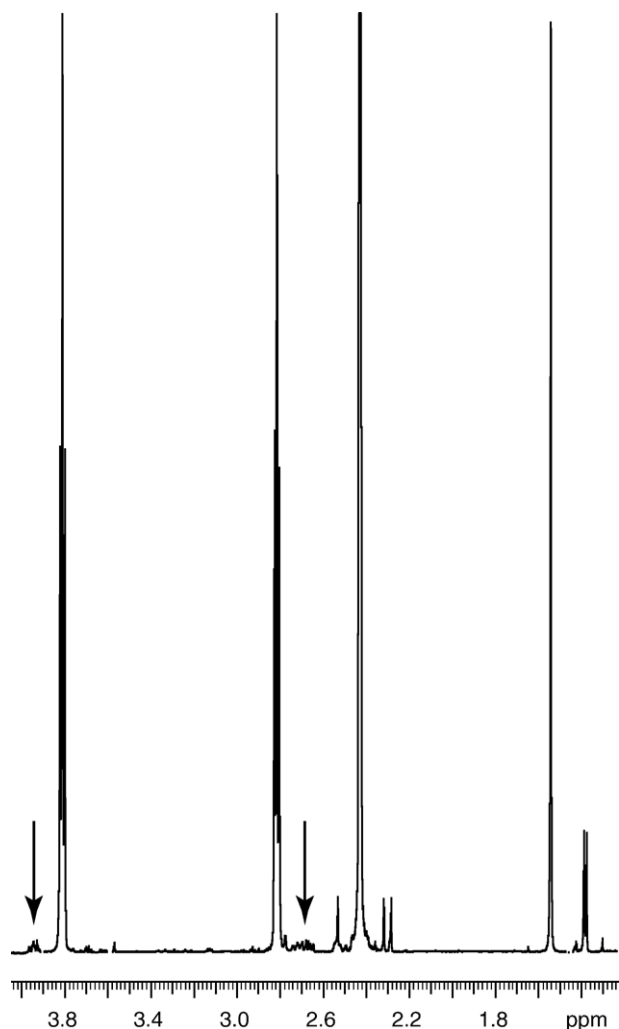


Fig. 7. An expansion of a portion of an experimental spectrum early in the metabolic process to show the location of the minor peaks (arrows) that indicated an intermediate and that were used to interpret the results produced by the analysis of the synthetic oxathianol under the conditions of solvent and pH outlined in Materials and methods under Enzymology.

enzyme, while processing TDG via a pathway similar to that of the horse liver enzyme, may handle the oxathianol with greater facility. When the activities of the equine enzyme and human- α ADH were compared spectrophotometrically under identical conditions (Materials and methods), the human- α ADH metabolized the equilibrium mixture at the rate of 716 nmol NADH/min/U of enzyme. This can be compared with the much lower rate using horse liver enzyme (above), 6 nmol NADH/min/U of enzyme. As with the equine ADH, the use of 2-hydroxyethylthioacetic acid as a potential substrate in the assays using the human α isoform indicated no activity, suggesting that it is the terminal metabolite with the human α enzyme as well.

Discussion

ADH is so inextricably linked with human dietary ethanol that the concept of its action as part of a xenobiotic metabolizing system does not immediately leap to mind. Mammalian ADHs exhibit broad substrate specificity oxidizing most primary and

secondary aliphatic and aromatic alcohols. They function as detoxifiers with the digitalis glycosides (Frey and Vallee, 1979) and permethrin (Choi et al., 2002), for example. They can also act as metabolic activators as in the case of 1,4-dihydroxybutane (Besseman and McCabe, 1972), allyl alcohol (Serafini-Cessi, 1972) and 1,3-difluoro-2-propanol, the rodenticide Gliflor (Menon et al., 2001). It was the metabolic activator function that was of interest to us vis-à-vis TDG, protein phosphatases and their participation in the toxicity sulfur mustard.

The facility with which ADH oxidized TDG (Brimfield et al., 1998), the older literature on ethanol metabolism involving aldehyde dehydrogenase (Dalziel and Dickerson, 1965) and speculation from the literature on in vivo TDG metabolism (Black et al., 1993), raised our expectation for the production of a reactive aldehyde intermediate. However, ADH not only oxidizes alcohols to aldehydes but is also capable of oxidizing aldehydes to the corresponding carboxylic acids with comparable efficiency absent any involvement from other enzymes such as aldehyde dehydrogenase (Oppenheimer and Henehan, 1995; Velonia and Smonou, 2000). This is made possible because in aqueous medium most aliphatic aldehydes exist in equilibrium with their hydrates, structural analogs of secondary alcohols, which are also substrates for ADH (Bell and Evans, 1966).

The process can take two pathways depending on the relative affinities of the aldehyde and NADH for the enzyme active site. When the substrate is a short chain alcohol like ethanol, the product aldehyde is rapidly released into solution from the ADH active site and builds to measurable levels in equilibrium with its hydrate. The aldehyde hydrate, in competition with the alcohol for the ADH-NAD⁺ complex, is oxidized again to give the acid. Evidence for this comes from Oppenheimer's (1995) work with ethanol. He referred to this process as sequential oxidation.

With longer chain alcohols, such as octanol, the affinity of the active site for the aldehyde product is increased (Oppenheimer and Henehan, 1995; Hinson and Neal, 1975). In this sequence, the aldehyde remains in the active site and is hydrated in situ, setting the stage for oxidation of the hydrated aldehyde to the carboxylic acid. Very little of the aldehyde exists free in solution under these circumstances. Oppenheimer and Henehan (1995) referred to this process as didehydrogenation. Sequential oxidation and didehydrogenation probably represent the extremes in a continuum based on substrate structure.

Identification of the oxathianol in equilibrium with the free aldehyde of TDG and its hydrate at very low levels in our NMR reaction mixture plus the spectrophotometric demonstration that the NADH is formed in the presence of ADH, NAD and the equilibrium mixture provides evidence that this mixture is further oxidized by ADH. The demonstration that 2-hydroxyethyl-thioacetic acid is not further metabolized allows us to propose the metabolic scheme shown in Fig. 12. Mechanistically TDG falls toward the didehydrogenation end of Oppenheimer and Henehan's (1995) sequential oxidation–didehydrogenation continuum with both equine liver ADH and the human α enzyme since the free aldehyde and its equilibrium partners are either absent (human α) or present at very low levels (horse liver ADH). The initial step in which TDG (Fig. 12A) is oxidized to its aldehyde (Fig. 12B) is reversible. However, with the NAD being

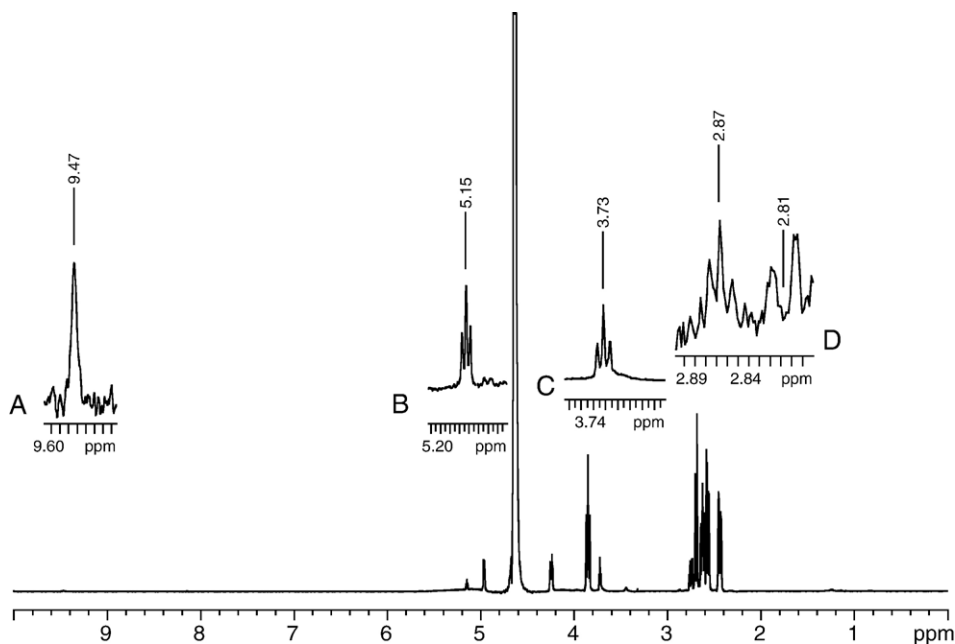


Fig. 8. The NMR spectrum produced by the synthetic oxathianol under the conditions of solvent and pH used to generate the spectra with the horse liver enzyme (see Enzymology in Materials and methods for details). When the vertical axis was expanded, the minor signal at 9.47 ppm (inset A) produced by the aldehydic proton of the free aldehyde became evident. Additional minor signals at 5.15 ppm (inset B) and 3.73 ppm (inset C), a triplet at 2.87 ppm and a doublet of doublets centered around 2.81 ppm (inset D) were consistent with the presence of the acyclic aldehyde hydrate. This indicated that the oxathianol developed into a mixture containing the cyclic compound, the free aldehyde and the hydrated aldehyde when dissolved in buffer.

rapidly regenerated by lactate dehydrogenase, there is insufficient build-up in NADH concentration to drive the reverse reaction in our system. Oppenheimer and Henehan (1995) showed this by following the NAD recycling on a UV spectrophotometer in parallel with the NMR and observing no changes in the A_{340} during the course of the reaction.

The aldehyde exists in equilibrium with its hydrate (Fig. 12C) and the oxathianol (Fig. 12D). The dominant species in the mixture depends on the medium. NMR on the oxathianol dissolved in chloroform during the monitoring of synthesis showed only signals for the cyclic compound. When the solvent was our potassium phosphate buffer, pH 7.5, however, signals

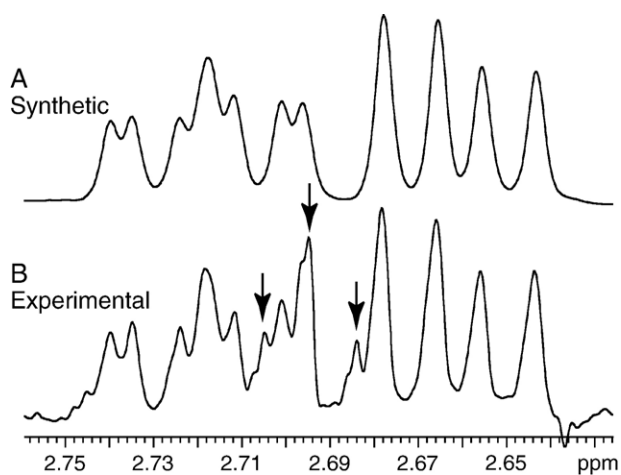


Fig. 9. A comparison of the experimental spectrum with the spectrum generated with the synthetic oxathianol in our experimental buffer provided strong evidence for the oxathianol as a metabolic intermediate. Signals between 2.63 and 2.76 ppm produced by methylene protons on the carbons adjacent to the sulfur of the synthetic oxathianol dissolved in our experimental buffer (A) compared with the actual experimental result produced during the metabolism of TDG by the horse liver enzyme (B). It is evident that these two spectra are identical with the exception of the satellite peaks (arrows) in the experimental spectrum (B) arising from TDG due to coupling with protons on naturally occurring ^{13}C species.

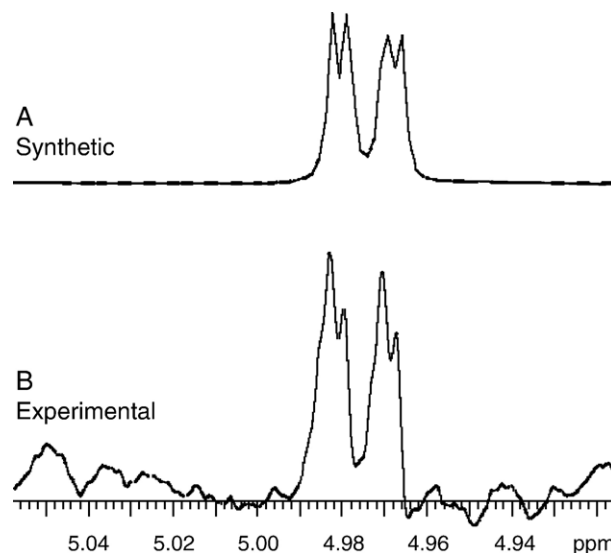


Fig. 10. The signal at 4.98 ppm produced by the proton on the anomeric (hydroxylated) carbon of the synthetic oxathianol interacting with the adjacent methylene protons frozen in axial and equatorial positions by the rigid structure of the ring (A) compared to the actual experimental result produced during the metabolism of TDG by the equine ADH (B). Again, the similarity provides strong evidence for the oxathianol as an intermediate during the action of equine liver ADH on TDG.

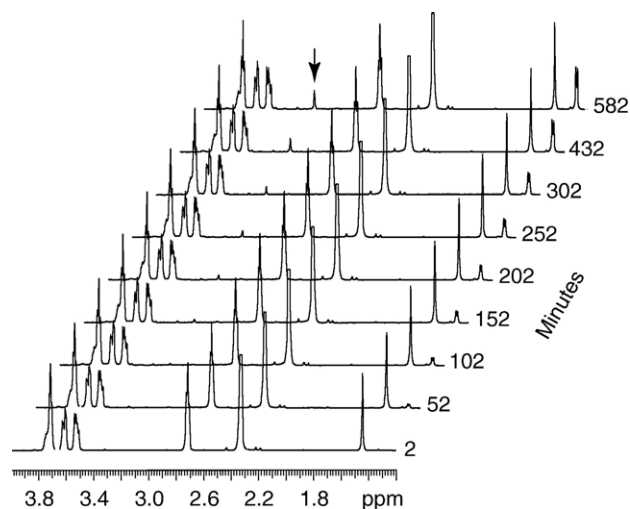


Fig. 11. Sequential spectra showing the metabolic outcome from recombinant human class I α ADH. Note the strong similarity to the results with the horse liver enzyme. The increase in the peak at 1.44 ppm over time shows the generation of lactate by LDH. The increase in the signal at 3.2 ppm (arrow) illustrates the accumulation of the methylene peak from hydroxyethylthioacetic acid over time. There is 50 min separating each spectrum.

for the hydrate and the free aldehyde appeared (Fig. 8). This spectrum did not change over the course of 21 h indicating rapid development of an equilibrium. There was evidence of the oxathianol in the experimental spectra (Figs. 9 and 10). The NMR signals indicating the presence of the hydrated aldehyde in the spectra from the original enzyme mixture are obscured by larger unrelated signals with the exception of a very small peak at 4.37 ppm (Fig. 4). We never observed a signal in any of the experimental spectra for the free aldehyde proton that appeared at 9.47 ppm (Fig. 8) in the spectrum of the synthetic product in buffer. This provided evidence of the low level at which the free aldehyde was present and reinforced the didehydration mechanism.

To test the theory that hydroxyethylthioacetic acid (Fig. 12E) evolved from the hydrated aldehyde (Henehan and Oppenheimer, 1993), we tested the oxathian-2-ol equilibrium mixture

spectrophotometrically for its ability to act as a substrate for ADH. The oxathianol, presumably after ring opening and hydration (Oppenheimer and Henehan, 1995), was a substrate for both the horse liver ADH and the human α ADH identifying it as the precursor for hydroxyethylthioacetic acid. However, the oxathianol-2-ol also has the characteristics of a secondary alcohol and could be the intermediate giving rise to the acid.

The fact that only one end of the TDG is oxidized is evident from the stoichiometry of the pyruvate to lactate conversion by the NADH recycling system. Two moles of pyruvate were converted to lactate for every mole of TDG oxidized to the acid (Fig. 5). This ratio conformed to what has been seen with other symmetric diols such as the conversion of 1,4-butanediol by ADH to 4-hydroxybutyrate (γ -hydroxybutyrate, GHB) the date rape drug (Besseman and McCabe, 1972). This consistent asymmetric attack by ADH brings into question the origin of the reported metabolite of sulfur mustard, thiodiglycolic acid (Fig. 1G), in which both ends of the molecule have been oxidized (Davison et al., 1961).

Also remarkable are the comparative rates of conversion of the oxathianol equilibrium mixture to the acid by the horse liver enzyme versus the class I human α isoform. The two enzymes, with their activity equalized toward ethanol, showed a very different reactivity toward the synthetic oxathianol mixture when the reaction was followed by monitoring NADH generation. The rate of NADH production by the human enzyme was over a hundred times that found with the horse liver ADH. This no doubt explains the lack of signals from any of the aldehyde-related intermediates in the NMR spectra made using the human α isoform. Such a large difference between isoforms and among species in the rate of oxidation for this or other aldehyde equilibrium mixtures may also explain species differences in the toxicity of alcohols.

The ultimate metabolite, TDGA (Fig. 1F), is not inhibitory to pure protein (serine/threonine) phosphatases (Brimfield, unpublished results). Testing the activity of the intermediate equilibrium mixture for its ability to inhibit pure protein (serine/threonine) phosphatases awaits the synthesis of more 1,4-oxathiane-2-ol. In the broader sense, the work has implications

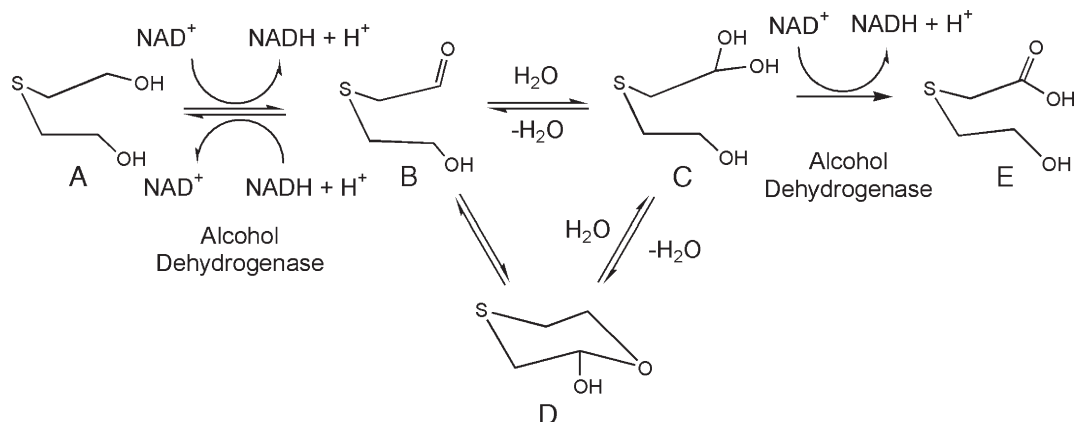


Fig. 12. The proposed generalized metabolic pathway for the conversion of TDG to TDGA by alcohol dehydrogenase: (A) TDG, (B) hydroxyethylthioacetaldehyde, (C) hydroxyethylthioacetaldehyde hydrate, (D) 1,4-oxathian-2-ol, (E) hydroxyethylthioacetic acid, TDGA. It is not clear whether the oxathianol or the hydrated aldehyde acts as the substrate for ADH during acid production. Both are secondary alcohols.

for sulfur mustard pharmacokinetics because it identifies previously unknown metabolites and describes how they arise. It sheds light on the mechanism of alcohol dehydrogenase when it is confronted with symmetrical diols and contributes to our knowledge about alcohol dehydrogenases as xenobiotic metabolizing enzymes. Additionally, we introduce a novel and very useful way to study toxicant metabolism in vitro.

Acknowledgments

This work was supported, in part, by award number DAMD 17-00-2-008 from the U.S. Army Medical Research and Materiel Command. The authors would like to thank Dr. Jonghoon Choi for purifying the recombinant human ADH isoforms from transformed *E. coli* strains; Dr. David A. Sartori acted as NMR technician in the early stages of the work, and Dr. Sunil Soni shared his extensive knowledge of the collection and interpretation of NMR data. Our thanks are due to Dr. Norman J. Oppenheimer of the University of California, San Francisco, and to Dr. Robert P. Hanzlik of the University of Kansas for thought-provoking discussions. T. David Yeung, Brendan S. Gallagher and Alexandra M. Mancebo provided excellent technical assistance.

References

- Abeles, R.H., Lee, H.A., 1960. The dismutation of formaldehyde by alcohol dehydrogenase. *J. Biol. Chem.* 274, 7106–7107.
- Bartlett, P.D., Swain, C.G., 1949. Kinetics of hydrolysis and displacement reactions of β,β' -dichlorodiethyl sulfide (mustard gas) and of β -chloro- β' -hydroxydiethyl sulfide (mustard chlorohydrin). *J. Am. Chem. Soc.* 71, 1406–1415.
- Bell, R.P., Evans, P.G., 1966. Kinetics of the dehydration of methylene glycol in aqueous medium. *Proc. R. Soc. London, Ser. A* 291, 297–323.
- Besseman, S.P., McCabe III, E.R.B., 1972. 1,4-Butanediol—A substrate for rat liver and horse liver alcohol dehydrogenases. *Biochem. Pharmacol.* 21, 1135–1142.
- Black, R.M., Brewster, K., Clark, R.J., Hambrook, J.L., Harrison, J.M., Howells, D.J., 1993. Metabolism of thiodiglycol (2,2'-thiobis-ethanol): isolation and identification of urinary metabolites following intraperitoneal administration to rat. *Xenobiotica* 23, 473–481.
- Brimfield, A.A., 1995. Possible protein phosphatase inhibition by bis(hydroxyethyl)sulfide a hydrolysis product of mustard gas. *Toxicol. Lett.* 78, 43–48.
- Brimfield, A.A., Zweig, L.M., Novak, M.J., Maxwell, D.M., 1998. In vitro oxidation of the hydrolysis product of sulfur mustard, 2,2'-thiobis-ethanol, by mammalian alcohol dehydrogenases. *J. Biochem. Mol. Toxicol.* 12, 361–369.
- Corey, E.J., Schmidt, G., 1979. Useful procedures for the oxidation of alcohols involving pyridinium dichromate in aprotic media. *Tetrahedron. Lett.* 5, 399–402.
- Choi, J., Rose, R.L., Hodgson, E., 2002. In vitro human metabolism of permethrin: the role of human alcohol and aldehyde dehydrogenases. *Pestic. Biochem. Physiol.* 73, 117–128.
- Dalziel, K., Dickerson, F.M., 1965. Aldehyde mutase. *Nature* 206, 255–257.
- Davison, C., Rozman, R.S., Smith, P.K., 1961. Metabolism of bis- β -chloroethyl sulfide (sulfur mustard gas). *Biochem. Pharmacol.* 7, 65–74.
- Dudley, B.F., Brimfield, A.A., Winston, G.W., 2000. Oxidation of 2,2'-thiodiethanol by alcohol dehydrogenase: comparison of human isozymes. *J. Biochem. Mol. Toxicol.* 14, 244–251.
- Frey, W.A., Vallee, B.L., 1979. Human liver alcohol dehydrogenase. An enzyme essential to the metabolism of digitalis. *Biochem. Biophys. Res. Commun.* 91, 1543–1548.
- Henehan, G.T.M., Kenyon, G.L., Oppenheimer, N.J., 1993. Oxidation of aldehydes by horse liver alcohol dehydrogenase. *Adv. Exp. Biol. Med.* 370, 481–491.
- Henehan, G.T.M., Oppenheimer, N.J., 1993. Horse liver alcohol dehydrogenase-catalyzed oxidation of aldehydes: dismutation precedes net production of reduced nicotinamide adenine dinucleotide. *Biochemistry* 32, 735–738.
- Henehan, G.T.M., Chang, S.H., Oppenheimer, N.J., 1995. Aldehyde dehydrogenase activity of *Drosophila melanogaster* alcohol dehydrogenase: burst kinetics at high pH and aldehyde dismutase activity at physiological pH. *Biochemistry* 34, 12294–12301.
- Hinson, J.A., Neal, R.A., 1975. An examination of octanol and octanal metabolism to octanoic acid by horse liver alcohol dehydrogenase. *Biochim. Biophys. Acta* 384, 1–11.
- Hore, P.J., 1989. Nuclear magnetic resonance. Solvent suppression. *Methods Enzymol.* 176, 64–77.
- Li, Y.-M., Casida, J.E., 1992. Cantharidin-binding protein: identification as protein phosphatase 2A. *Proc. Natl. Acad. Sci. U. S. A.* 89, 11867–11870.
- McComb, R.B., Bond, L.W., Burnette, R.W., Keech, R.C., Bowers, G.N., 1976. Determination of the molar absorptivity of NADH. *Clin. Chem.* 22, 141–150.
- Menon, K.I., Feldwick, M.G., Noaks, P.S., Mead, R.J., 2001. The mode of toxication of the pesticide Gliflor: the metabolism of 1,3-difluoroacetone to (-)-erythro-fluorocitrate. *J. Biochem. Mol. Toxicol.* 15, 47–54.
- Oppenheimer, N.J., Henehan, G.T.M., 1995. Horse liver alcohol dehydrogenase-catalyzed aldehyde oxidation. *Adv. Exp. Biol. Med.* 372, 407–415.
- Reddy, G., Major, M.A., Leach, G.J., in press. Toxicity assessment of thiodiglycol. *Int. J. Toxicol.*
- Serafini-Cessi, F., 1972. Conversion of allyl alcohol into acrolein by rat liver. *Biochem. J.* 128, 1103–1107.
- Velonia, K., Smonou, I., 2000. Dismutation of aldehydes by alcohol dehydrogenases. *J. Chem. Soc., Perkin Trans. 1*, 2283–2287.
- Yang, Y.-C., Szanfrancic, L.L., Beaudry, W.T., Ward, J.R., 1988. Kinetics and mechanisms of hydrolysis of 2-chloroethyl sulfides. *J. Org. Chem.* 53, 3293–3297.

Metabolism of Chlorpyrifos and Chlorpyrifos Oxon by Human Hepatocytes

Kyoungju Choi, Hyun Joo, Randy L. Rose, and Ernest Hodgson

Department of Environmental and Molecular Toxicology, North Carolina State University, Raleigh, NC 27695-7633, USA;
E-mail: ernest.hodgson@ncsu.edu

Received 20 September 2006

ABSTRACT: The metabolism of chlorpyrifos (CPS) and chlorpyrifos oxon (CPO) by human hepatocytes and human liver S9 fractions was investigated using LC-MS/MS. Cytochrome P450 (CYP)-dependent and phase II-related products were determined following incubation with CPS and CPO. CYP-related products, 3,5,6-trichloro-2-pyridinol (TCP), diethyl thiophosphate, and dealkylated CPS, were found following CPS treatment and dealkylated CPO following CPO treatment. Diethyl phosphate was not identified because of its high polarity and lack of retention with the chromatographic conditions employed. Phase II-related conjugates, including O- and S-glucuronides as well as 11 GSH-derived metabolites, were identified in CPS-treated human hepatocytes, although the O-sulfate of TCP conjugate was found only when human liver S9 fractions were used as the enzyme source. O-Glucuronide of TCP was also identified in CPO-treated hepatocytes. CPS and CPO were identified using HPLC-UV after CPS metabolism by the human liver S9 fraction. However, CPO was not found following treatment of human hepatocytes with either CPS or CPO. These results suggest that human liver plays an important role in detoxification, rather than activation, of CPS. © 2006 Wiley Periodicals, Inc. *J Biochem Mol Toxicol* 20:279–291, 2006; Published online in Wiley InterScience (www.interscience.wiley.com). DOI 10.1002/jbt.20145

KEYWORDS: Chlorpyrifos; Chlorpyrifos Oxon; Cytochrome P450; Phase II Metabolism; Glutathione; Glucuronide; LC-MS/MS; Human Hepatocytes; Human Liver S9 Fraction

INTRODUCTION

Chlorpyrifos (CPS, *O,O*-diethyl-*O*-3,5,6-trichloro-2-pyridyl phosphorothioate) is an organophosphorus insecticide widely used in agriculture for killing termites and in military deployments for controlling insects that act as disease vectors. The U.S. Environmental Protection Agency (EPA) has restricted its use because of concern for infants and children [1,2]. It has moderately acute oral toxicity, its lethal dose, 50% (LD₅₀) being 97–276 mg/kg in rats [3]. Metabolic biotransformation of CPS modulates its toxicity through CYP-mediated monooxygenase oxidation and/or enzymatic conjugation with glucuronide, sulfate, or glutathione in phase II metabolism [2,4]. In humans, as in other organisms, CYP-mediated desulfuration produces chlorpyrifos oxon (CPO), a potent acetylcholine esterase (AChE) inhibitor with almost three orders of magnitude higher affinity toward the active site of serine-dependent ester hydrolases such as AChE [2,5] than the parent compound, CPS. This activation reaction is catalyzed most effectively by CYP2B6 and CYP3A4. In concomitant detoxification processes, CYP3A4 and CYP2C19 produce 3,5,6-trichloro-2-pyridinol (TCP), diethyl phosphate (DEP), and diethyl thiophosphate (DETP) [2]. Studies of the phase II-mediated biotransformation of CPS have shown that the glucuronide and the sulfate of TCP are found in human urine [6]. Recently Bicker et al. [4], using LC-MS/MS, reported on GSH conjugates of CPS determined in the urine of a CPS-intoxicated woman. However, the role of phase II conjugation in human metabolism of CPS is not well understood and has not been studied *in vitro*. In the present study, *in vitro* CPS metabolism by human hepatocytes was investigated using LC-MS/MS to determine its phase I and II metabolites.

In addition to AChE, CPO interacts with carboxylesterase and A-esterases rendering it less available for cholinergic toxicity [7]. CPO also interacts with muscarinic receptors and modulates protein phosphorylation as well as causes changes in the immune

Dr. Randy L. Rose died in a tragic accident on May 23, 2006.

Correspondence to: Ernest Hodgson.

Contract Grant Sponsor: U.S. Army.

Contract Grant Number: DAMD 17-00-2-0008.

system and in the cognitive, reproductive, developmental, and sensory functions of the nervous system [8]. In addition, CPO is involved in signal transduction pathways through mitogen-activated protein kinase (MAPK) cascades and alters cellular growth and differentiation [9].

Usmani et al. [10] demonstrated that CPS inhibits the metabolism of *N,N*-diethyl-*m*-toluamide (DEET) to the ring methyl oxidation product, *N,N*-diethyl-*m*-hydroxymethyl benzamide (BALC) but does not affect the production of the *N*-deethylated metabolite of DEET, *N*-ethyl-*m*-toluamide (ET). Pre- and incubation of CPS with carbaryl and human liver microsomes reduced the formation of the CYP2B6 metabolite, carbaryl methylol [11]. In addition, CPS inhibits the human CYP-dependent metabolism of testosterone and estradiol noncompetitively and irreversibly [12,13].

Choi et al. [14] demonstrated that CPO inhibits the esterase in human liver responsible for the metabolism of transpermethrin.

MATERIALS AND METHODS

Chemicals

CPS, CPO, and TCP were purchased from Chem Service (West Chester, PA). Glutathione (GSH) was purchased from Sigma-Aldrich (St. Louis, MO), and all other chemicals, if not specified, from Fisher Scientific (Pittsburgh, PA).

Pooled Human Liver S9 Fraction

The pooled human liver (pHL) S9 fraction, pooled from 15 donors (8 males and 7 females), was purchased from BD Biosciences (Woburn, MA). Metabolic activity assays were performed by incubation of CPS, CPO, and TCP (final concentration, 50 μ M) with pHL S9 (final concentration of 0.375 mg pHL protein) in 100 mM sodium-potassium buffer (pH 7.4 at 37°C). After 5 min incubation at 37°C, reaction was started by adding phase II reaction cofactors and/or an NADPH-regenerating system consisting of 0.25 mM NADP, 2.5 mM glucose-6-phosphate, and 2 U/mL glucose-6-phosphate dehydrogenase. Cofactors for the phase II reactions were 5 mM uridine 5'-diphosphoglucuronic acid (UDPGA) (BD Biosciences, Woburn, MA), 2 μ g/mL alamethicin (BD Biosciences, Woburn, MA) for glucuronide conjugation, 0.2 mM adenosine-3'-phosphosulfate (PAPS) (Sigma, St. Louis, MO) for sulfate conjugation, and 15 mM GSH (Sigma, St. Louis, MO) for GSH conjugation. After incubation, an equal volume of acetonitrile was added to stop the reaction followed by centrifugation at 21,000 \times g for

5 min. Supernatants were collected and kept at 4°C until use. The experiments were carried out in triplicate.

Human Hepatocytes

Plates of primary human hepatocytes were supplied by ADMET technologies (Durham, NC, USA) (Table 1). 2.6×10^6 human hepatocytes were inoculated onto glass plates (60 \times 15 mm) coated with rat tail collagen type I (final concentration of 0.33 mg/cm²) from Sigma-Aldrich (St. Louis, MO). The viability of human hepatocytes was over 85%. Upon arrival, the medium was replaced with complete William's Medium E (Invitrogen, Carlsbad, CA) supplemented with 100 U/mL penicillin G sodium, 100 U/mL streptomycin sulfate, 250 ng/mL amphotericin (Invitrogen, Carlsbad, CA), 51.5 nM dexamethasone, ITS (5 μ g/mL transferrin, 9.09 μ g/mL insulin, 6.09 ng/mL selenium-A, Invitrogen, Carlsbad, CA), 5.05 mg/mL gentamycin (Sigma, St. Louis, MO), and 1% L-glutamine (Sigma, St. Louis, MO) and was acclimated for 3 days at 37°C under 5% CO₂/95% humidified air. Before treatment, the plates were rinsed with complete William's Medium E and treated with 50 μ M CPS or CPO for either 12 or 24 h at 37°C. One percent acetonitrile was used to increase the solubility of CPS or CPO. After each time point, human hepatocytes and their media were collected. Hepatocytes were detached with a scraper and resuspended in complete William's Medium E followed by sonication (30 s \times 2) and centrifugation (4000 \times g for 30 min). Supernatants were kept at 4°C until use. The experiments were duplicated.

High Performance Liquid Chromatography Analysis

A Waters high performance liquid chromatography (HPLC) system (Milford, MA) was used for analysis. This system consisted of a 2996 separation module and a 2695 photodiode array detector (PDA). A minor modification of the gradient system of Tang et al. [2] was made. The mobile phase for pump A was water/acetonitrile/phosphoric acid (89/10/1, v/v) and for pump B was acetonitrile/phosphoric acid (99/1, v/v). The gradient profile was 0–2 min (10% B), 3–15 min (to 90% B), 15–16.5 min (90% B), 16.5–17.5 min (to 100% B), 17.5–19 min (100% B), and 19–22 min (to 10% B). The flow rate was 1 mL/min, and the injection volume was 30 μ L. CPS was analyzed with a C₁₈ column (Synergi Fusion-RP 5 μ m, 150 \times 4.6 mm, Phenomenex, Rancho Palos Verdes, CA), and its maximum absorbance was 229.2 nm. Under the conditions selected, retention time and detection limit for CPS were 17.08 min and 0.02 μ M, respectively.

TABLE 1. Information on Hepatocytes Donors

ID	Age (years)	Sex	Race	Cause of Death	Smoking	Drug History	Cell Viability (%)
P1	34	Male	Caucasian	Ammonia intoxication	No	Vasopression, synthroid, zosyn, insulin, lasix, and hydrocortisone	89
P2	41	Female	Caucasian	Inner cerebral hemorrhage	Occasional	Due to OTOC No	85
P3	54	Male	Caucasian	Cerebral vascular accident	No	No	87

Solid Phase Extraction

Solid phase extraction (SPE) was performed using 1 mL Phenomenex strata-X cartridges (Phenomenex, Torrance, CA), packed with 30 mg of surface-modified styrene divinylbenzene porous copolymer beads. Cartridges were conditioned by sequential flushing with 1 mL aliquots of methanol and reagent water, and samples were loaded at 1 mL/min by vacuum aspiration. The vacuum was maintained for 30 s thereafter to dry cartridges. Cartridges were washed with 10% methanol in water, followed by eluting 0.6 mL mixture of methanol/acetonitrile/water/formic acid (60/30/10/0.1, v/v). The eluent was directly analyzed by HPLC–mass spectrometry.

Liquid Chromatography–Mass Spectrometry

Analyses were performed using a Thermo Surveyor MS pump with Surveyor autosampler and a Thermo LTQ linear ion trap mass spectrometer (MS) equipped with an Ion Max electrospray ionization (ESI) interface (Thermo Corporation, San Jose, CA). MS tuning and data acquisition and processing were performed with Xcalibur software, version 1.4. Mass Frontier 4.0 software was used to aid the prediction of fragmentation pathways. The HPLC was fitted with a Hypersil GOLD column, 3 μ m, 2.1 mm I.D. \times 50 mm (Thermo Corporation, San Jose, CA). Binary gradient elutions were used with aqueous 0.05% formic acid with pH adjusted to 3.3 with NH_4OH (A) and acetonitrile (B). The initial conditions, 95%A:5%B, were changed linearly to 5%A:95%B in 17.25 min. Conditions were held isocratic for 7.75 min and then decreased linearly to the initial conditions in 5 min. The injection volume was 5 μ L, the flow rate was 0.2 mL/min, and the column was maintained at ambient temperature ($\sim 25^\circ\text{C}$).

Initially, the liquid chromatography–mass spectrometry (LC–MS) system was run in full scan mode from m/z 150 to 770, followed by data-dependant MS/MS for potential metabolite $[\text{M} + \text{H}]^+$ or $[\text{M} - \text{H}]^-$

ions. For the ESI ion source, the flow rate of the sheath (nitrogen) gas was 60 arbitrary units. The spray voltage was set at 5 and 4 kV for positive and negative ion modes, respectively, and the heated capillary temperature was set at 300°C . In addition, a source fragmentation voltage of 10–20 V was used to eliminate adduct ions. For MS/MS experiments, normalized collision energies of 35–45% were used.

Relative Quantification of Metabolites of CPS and CPO

For semiquantitative analysis, the area under the curve (peak) (AUC) for each metabolite was divided by the sum of the total metabolites (AUC) and expressed as a percentage.

RESULTS

Pooled Human Liver S9 Fraction

Preliminary experiments were carried out using pHL S9. The data from these experiments using pHL S9 and LC–MS/MS analysis are shown in Table 2 along with other metabolites obtained from human hepatocytes. From TCP phase II reactions, the *O*-glucuronide of TCP (C5) and *O*-sulfate of TCP (S1) were found, whereas TCP-SG was not found. The *O*-Sulfate of TCP (S1) was determined in the negative ion mode, and the most abundant single fragment was $m/z = 196$ (TCP moiety), with neutral loss of SO_3 ($\Delta m = 80$ Da). In contrast to TCP, when either CPS or CPO was used, neither the glucuronide nor the sulfate conjugates were found although CPS-SG (C7) and CPO-SG (O4) conjugates were identified.

Human Hepatocytes

From LC–MS/MS analysis, 15 CPS-related and 6 CPO-related metabolites were identified and are illustrated in Figures 1 and 2, respectively. Except for

TABLE 2. The Summary of Chromatographic and Mass Spectrometric Data of Compounds, including Analytical Standards and Proposed Metabolites, in Human Hepatocytes and pHL S9 Experiment. Numbers in Parentheses Indicate the Intensity Relative to the Base Peak.

Chemical ID	Retention Time (min)	$[M - H]^-$ (m/z)	Product Ions Negative Mode (m/z)	$[M + H]^+$ (m/z)	Product Ions		Proposed Structure
					Positive Mode (m/z)		
C1 ^a	16.28			350	322 (100), 294 (18), 198 (12)		Chlorpyrifos (CPS)
C2	9.26	320	196 (100)				O-ethyl O-3,5,6-trichloropyridin-2-yl O-hydrogen phosphorothioate
C3	2.36	169	141 (100), 95 (14)				Diethyl thiophosphate (DETP)
C4	10.02	196					3,5,6-Trichloropyridin-2-ol (TCP)
C5 ^b	6.96	372	196 (100), 175 (22)				3,4,5-Trihydroxy-6-(3,5,6-trichloropyridin-2-yl)oxytetrahydro-2H-pyran-2-carboxylic acid
C6	8.28	591	573 (49), 545 (14), 467 (100), 318(11), 194(44)	593	518 (4), 469 (66), 464 (100), 451 (44), 406 (26)		2-Amino-5-(1-(carboxymethylamino)-3-(3,5-dichloro-6-(ethoxy(hydroxy)phosphorothioyl)pyridine-2-ylthio)-1-oxopropan-2-ylamino)-5-oxopentanoic acid
C7 ^b	9.65	619	601 (18), 573 (10), 495 (100), 449 (21), 194 (89)	621	546 (6), 492 (100), 389 (8)		2-Amino-5-(1-(carboxymethylamino)-3-(3,5-dichloro-6-(diethoxyphosphorothioyl)pyridin-2-ylthio)-1-oxopropan-2-ylamino)-5-oxopentanoic acid
C8	9.49	490	366 (100), 320 (75), 194 (27)	492	475 (87), 389 (62), 348 (100), 320 (20), 305 (16)		2-(2-Amino-3-(3,5-dichloro-6-(diethoxyphosphorothioyl)pyridin-2-ylthio)propanamido)acetic acid
C9	9.85	522	398 (63), 318 (7), 194 (100)	524	348 (100)		6-(3,5-Dichloro-6-(diethoxyphosphorothioyl)pyridin-2-ylthio)-3,4,5-trihydroxytetrahydro-2H-pyran-2-carboxylic acid
C10 ^c	8.08 8.23	405	318 (42), 281 (20), 194 (100)	407	390 (9), 361 (28), 283 (17), 237 (100), 220 (16), 196 (8)		2-Amino-3-(3,5-dichloro-6-(ethoxy(hydroxy)phosphorothioyl)pyridin-2-ylthio)propanoic acid
C11	7.20	467	272 (50), 194 (100)	469	394 (5), 340 (100)		2-Amino-5-(1-(carboxymethylamino)-3-[(3,5-dichloro-6-hydroxy)pyridin-2-ylthio]-1-oxopropan-2-ylamino)-5-oxopentanoic acid
C12	9.72	562	489 (71), 438 (47), 402 (92), 374 (47), 346 (36), 194 (100)	564	435 (100)		2-Amino-5-(1-carboxy-2-(3,5-dichloro-6-(diethoxyphosphorothioyl)pyridin-2-ylthio)ethylamino)-5-oxopentanoic acid

continued

TABLE 2. continued

C13	9.74	433	309 (14), 194 (100)	435	418 (100), 400 (14), 389 (93), 348 (25), 311 (19), 265 (15), 248 (20), 196 (6)	2-Amino-3-(3,5-dichloro-6-(diethoxyphosphorothioxyloxy)pyridin-2-ylthio)propanoic acid
C14	7.12	281	194 (100)	283	266 (100), 237 (28), 196 (46)	2-Amino-3-(3,5-dichloro-6-hydroxypyridin-2-ylthio)propanoic acid
C15	8.41	433	318 (75), 309 (8), 194 (100)	435	389 (30), 361 (36), 320 (16), 311 (100), 265 (59), 196 (7)	3-(3,5-Dichloro-6-hydroxypyridin-2-ylthio)-2-(diethoxyphosphorothioylamino)prop anoic acid
O1 ^a	12.65			334	306 (100), 278 (23)	Chlorpyrifos-oxon (CPO)
O2	7.58	304	196 (100)			Ethyl 3,5,6-trichloropyridin-2-yl hydrogen phosphate
O3 ^c	<1.00	153	125 (100), 79 (5)			Diethyl phosphate (DEF)
O4 ^b	8.50	603	449 (100), 194 (5)	605	476 (100), 373 (7)	2-Amino-5-(1-(carboxymethylamino)-3-(3,5-dichloro-6-(diethoxyphosphoryloxy)pyridin-2-ylthio)-1-oxopropan-2-ylamino)-5-oxopentanoic acid
O5	8.74	417	330 (13), 309 (8), 194 (100)	419	402 (8), 373 (100), 332 (5)	2-Amino-3-(3,5-dichloro-6-(diethoxyphosphoryloxy)pyridin-2-ylthio)propanoic acid
S1 ^d	7.81	276	196 (100)			3,5,6-Trichloropyridin-2-yl hydrogen sulfate
Uk#1	8.91	490	366 (100), 194 (23)	492	446 (14), 418 (9), 368 (100), 265 (10)	
Uk#2	9.10			362	344 (5), 334 (100), 316 (14), 306 (11), 208 (31)	
Uk#3	12.14			378	360 (11), 350 (75), 332 (28), 316 (18), 288 (27), 254 (61), 226 (100), 208 (25)	

^a Data obtained from analytical standards.^b Determined with reference compounds obtained from pHL S9.^c Peak splitting is observed, indicative of more than one compound.^d Determined in pHL S9 only.

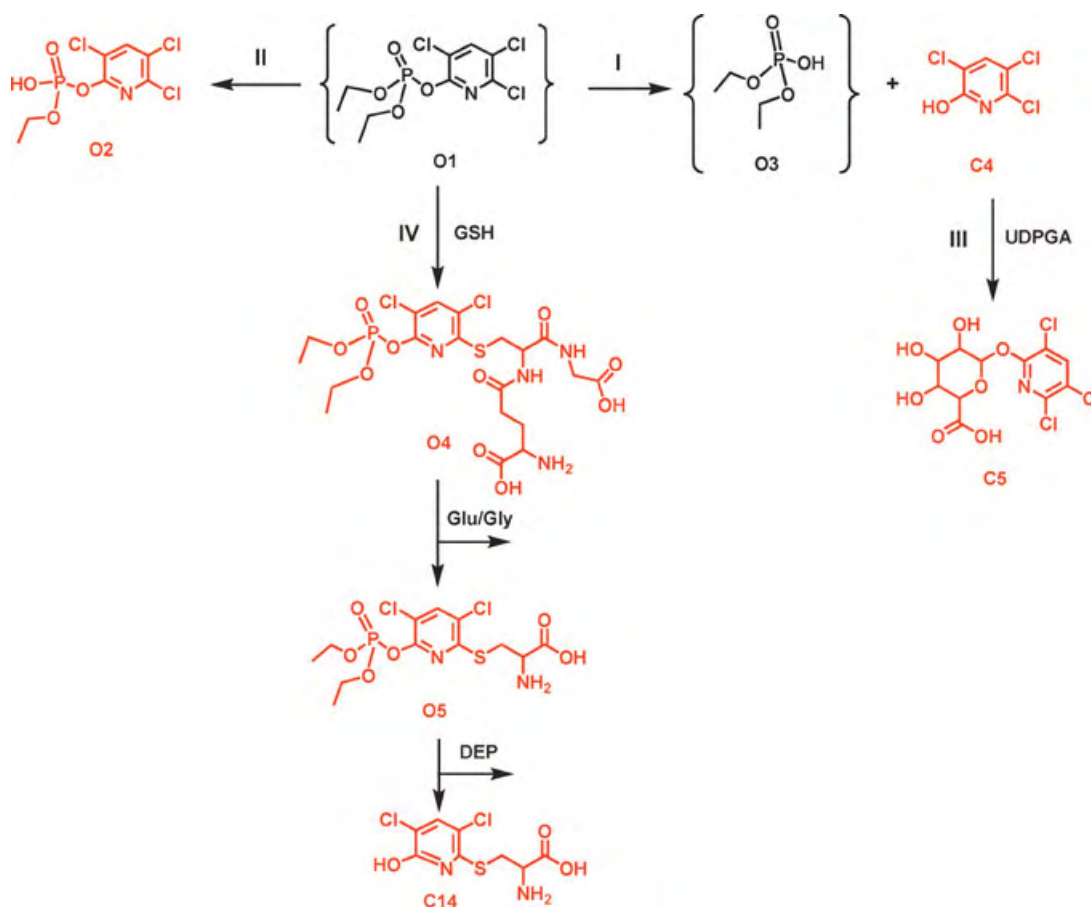


FIGURE 2. Proposed biotransformation scheme for chlorpyrifos oxon in human hepatocytes. O1 and O3 were not found. Metabolites in red were found in two donors (P2 and P3). Four possible pathways: dearylation (I), dealkylation (II), glucuronide conjugation (III), and GSH-mediated conjugation (IV).

determined from MS/MS analysis. It was determined that C3 eluted early from the reversed-phase HPLC column (i.e., RT 2.36 min), ionized only in the negative ion mode (m/z 169), and fragmented to m/z 141 (i.e., product ion formed after the McLafferty rearrangement of an ethyl group in the precursor ion) and m/z 95 (i.e., additional product ion after the subsequent neutral loss of ethanol from m/z 141) [15]. Confirming C3, both product ions were evidently reported in several publications [4,15,16]. However, it was impossible to confirm DEP (O3) because of its poor retention on reversed-phase HPLC column (i.e., RT < 1 min), even though an analytical standard of O3 was available. On the other hand, CPS was determined in HPLC–UV not in LC–MS (data not shown). This is because CPS is poorly ionized under the specified MS conditions, probably because of its highly nonpolar characteristics.

Meanwhile, in the deethylation process, one of the two aliphatic phosphoester bonds was removed at the alkylester group of CPS or CPO, resulting in C2 or O2, respectively (Figures 1 and 2). They were

visualized only in negative ion mode, and the TCP moiety (m/z 196) was the most abundant single fragment (Table 2). In addition, Figure 4 includes the spectrum of the product ion of O2. Neutral losses of ethoxy(thio)phosphoniumolate ($\Delta m = 124$ Da) and ethoxy(oxo)phosphoniumolate ($\Delta m = 108$ Da) were characteristically shown for C2 and O2, respectively. Although an analytical standard was not available for structural confirmation, O2 was determined to be the oxon-derivative of C2 since it possessed similar fragments fashion, but with a mass difference of 16 Da of the respective precursor and neutral mass losses.

In the glucuronidation of CPS, two types of metabolites were found, the *O*-glucuronide of TCP (C5) and the *S*-glucuronide of chlorine-substituted CPS (C9) (Figure 1 and Table 2). However, C5 was found only in the glucuronidation of CPO (Figure 2). C5 was identified by the negative ion mode and had two product ions, which are illustrated as one of the spectra in Figure 4. One is the TCP moiety (m/z 196) with neutral loss of anhydroglucuronic acid ($\Delta m = 176$ Da) and

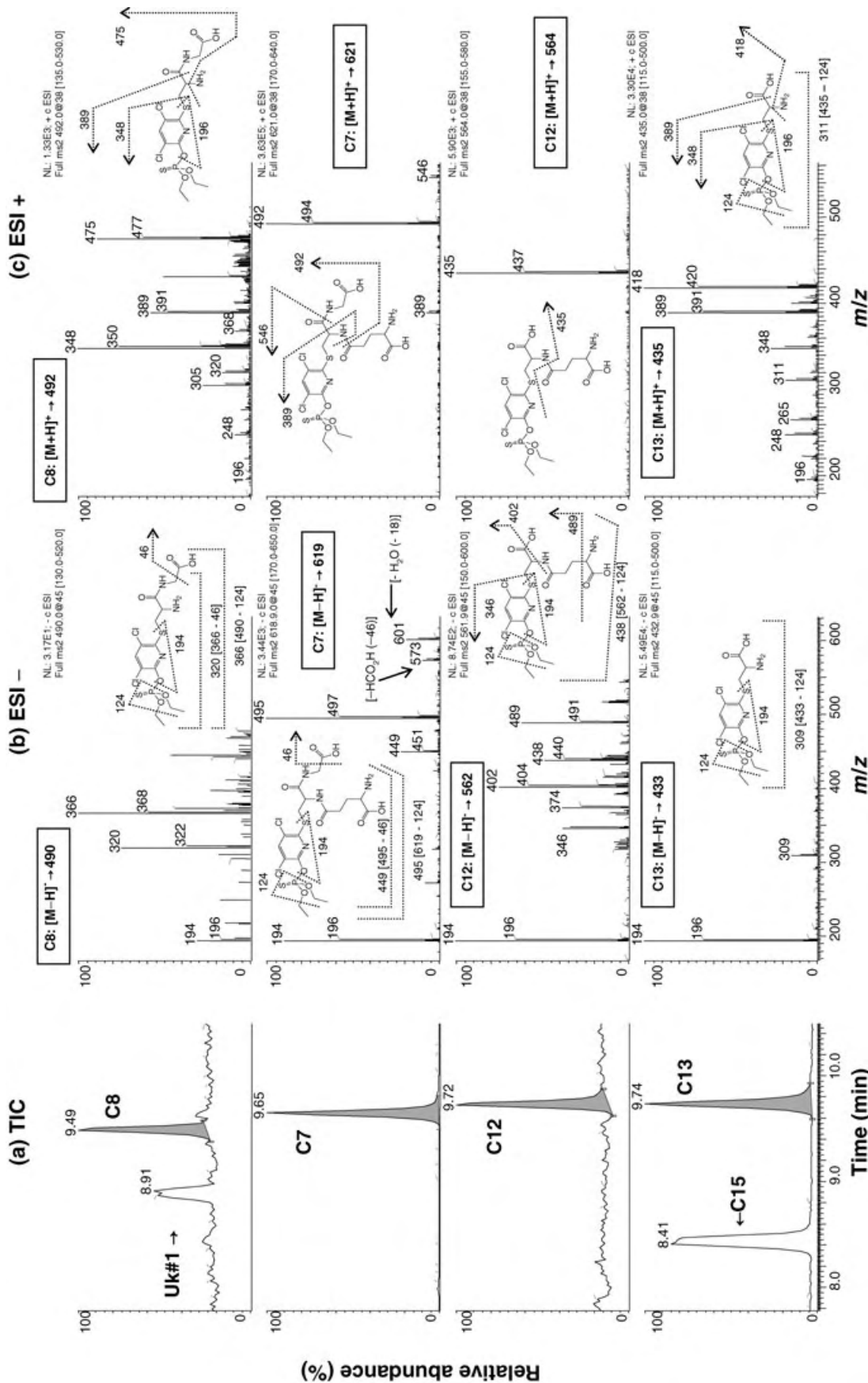


FIGURE 3. Chromatograms and proposed MS/MS fragmentation pathways for selected chlorpyrifos metabolites obtained in human hepatocytes: (a) the extracted total ion chromatogram (TIC), (b) ESI negative ion mode, and (c) ESI positive ion mode.

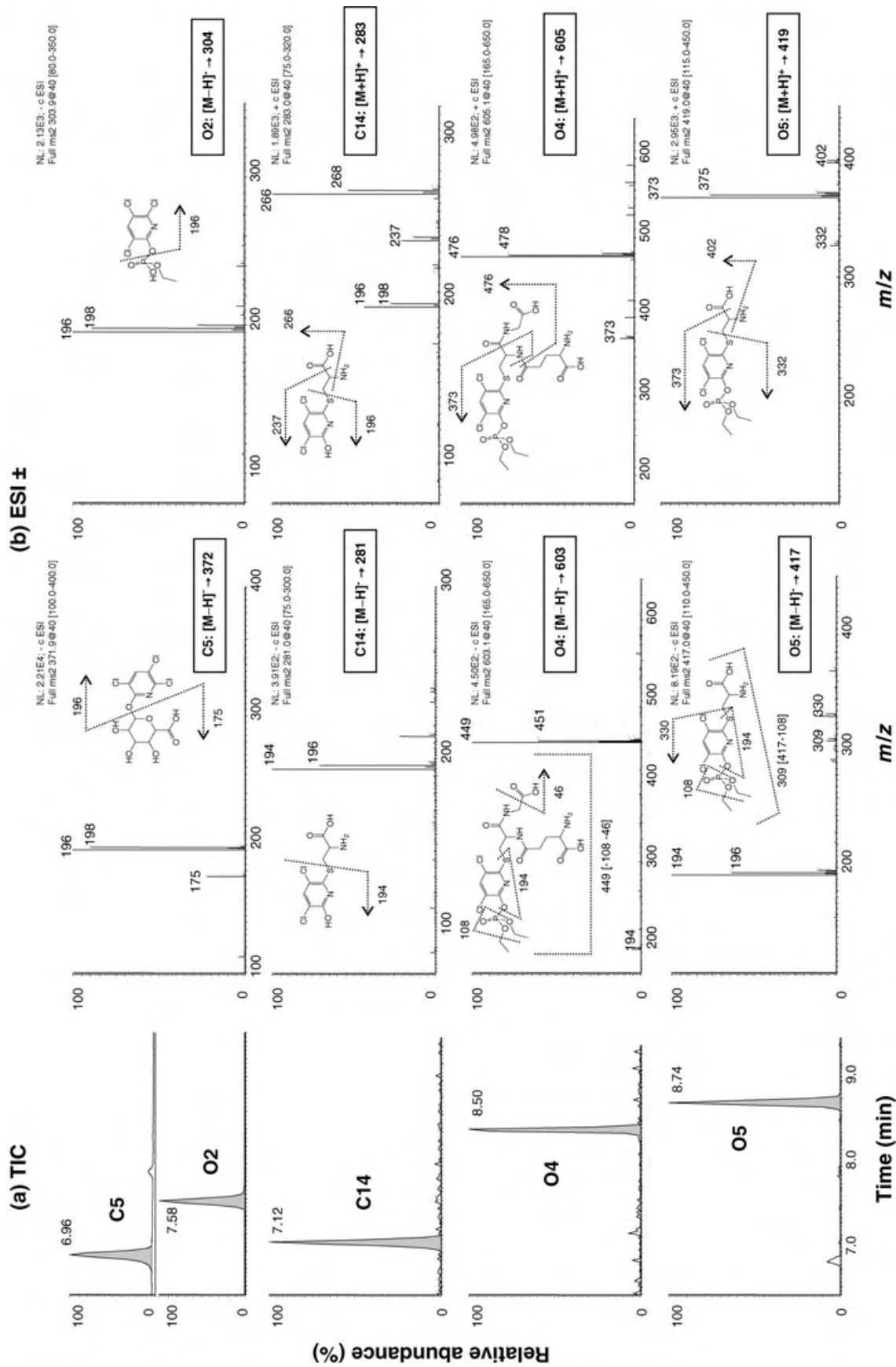


FIGURE 4. Chromatograms and proposed MS/MS fragmentation pathways for selected chlorpyrifos oxon metabolites obtained in human hepatocytes: (a) extracted ion chromatogram (XIC) and (b) ESI negative/positive ion mode, MS/MS spectra.

the other is the glucuronide moiety (m/z 175) with neutral loss of TCP ($\Delta m = 197$ Da). In the meantime, C9 was ionized in negative/positive ion mode, and the details of C9 will be explained in the GSH conjugation pathway.

As seen in Figures 1 and 2, all of the GSH-related conjugates (C6–C15 and O4 and O5) have two chlorines and sulfur-containing functional groups. Although MS/MS measurements cannot provide the position of the eliminated chlorine, chemical structures are proposed in accordance with the findings of Bicker et al. [4]. In addition, the proposed fragmentation pathways of selected metabolites are delineated in Figures 3 and 4 for CPS- and CPO-SG mediated metabolites, respectively.

Four glutathione *S*-conjugates (C6, C7, C11, and O4), probable key intermediates of the GSH conjugation pathway, were detected in human hepatocytes. The MS/MS spectra of the four metabolites were informative in both the negative/positive ion mode (Table 2 and Figures 3 and 4). However, the positive ion mode was more informative, generating more characteristic product ions for the metabolites. In the positive ESI-MS/MS, the most abundant fragments of C6, C7, C11, and O4 were m/z 464, 492, 340, and 476, respectively, with neutral loss of glutamic acid ($\Delta m = 129$ Da). Except O4, low abundance fragments (m/z 518, 546, and 394 for C6, C7, and C11, respectively) were characteristic of the neutral loss of glycine ($\Delta m = 75$ Da). In addition, C7 and O4 were definitely identified since reference products were previously determined from pHL S9 experiment. On the other hand, all four glutathione *S*-conjugates produced m/z 194 (dichloropyridinol sulfide) in negative ESI-MS/MS, ranging from 5% to 100% of the base peak. In addition, the most abundant fragments of C6 and C7 were characteristically m/z 467 and 495, respectively, with neutral loss of ethoxy(thio)phosphoniumolate ($\Delta m = 124$ Da). By a similar dissociation pattern, O4 yielded the most abundant fragment of m/z 449, which was assigned to neutral losses of ethoxy(oxo)phosphoniumolate ($\Delta m = 108$ Da) and formic acid ($\Delta m = 46$ Da). This proposed fragmentation pathway might be supported by the pathway of C7 that produced m/z 449 as well.

In a subgroup of GSH-related metabolites, C8 and C12 were also determined. In positive ion mode, C8 produced several abundant fragments such as m/z 475 by loss of ammonia ($\Delta m = 17$ Da), m/z 389 by a bond cleavage between α -carbon and carbonyl carbon in the cysteinyl moiety, and m/z 348 by a bond cleavage between the sulfur and carbon in amino acid residues (Figure 3). Meanwhile, of the probable four glutathione *S*-conjugates mentioned previously (C6, C7, C11, and O4), C12 produced a characteristic ion

(m/z 435), corresponding to neutral loss of glutamic acid ($\Delta m = 129$ Da). In the negative ion mode, C8 and C12 followed patterns similar to those found in all four glutathione *S*-conjugates determined previously, even though C12 yielded a more complicated spectrum. Both product ion spectra of C8 and C12 showed m/z 194 (dichloropyridinol sulfide) and neutral loss of ethoxy(thio)phosphoniumolate ($\Delta m = 124$ Da) as well.

For a subgroup of the cysteine *S*-conjugates, C10, C13, C14, and O5 produced similar fragmentation patterns (Figures 3 and 4 and Table 2). In the positive ion mode, all four metabolites showed loss of ammonia (17 Da) and formic acid (46 Da) as well as (excepting for C10) loss of the 2-aminopropionic acid fragment (87 Da), which resulted from a bond cleavage between the sulfur and α -carbon atom in cysteinyl moiety. In addition, C10, C13, and C14 produced product ion, m/z 196 (i.e., dichloropyridinol sulfide). The spectra of the four cysteine *S*-conjugates obtained in the negative ion mode were also characteristic. Each of the four metabolites yielded m/z 194 as the most abundant product ion. Loss of the 2-aminopropionic acid fragment (87 Da) was found in C10, C14, and O5 (i.e., m/z 318, 194, and 330, respectively). In addition, neutral loss of 124 Da was found in C10 and C13 (i.e., m/z 281 and 309, respectively), as well as loss of 108 Da in O5 (i.e., m/z 309).

For the proposed structure of C15 as seen in Figure 1, the determination was chiefly based on the report by Bicker et al. [4] and MS/MS data. They reported two identical molecular masses of 434 that corresponded to C13 and C15 in this experiment also. In the negative ion mode, C15 produced m/z 194 as the most abundant product ion, along with a neutral loss of 124 Da. However, C15 did not show loss of ammonia (17 Da) in the positive mode, implying no free amino group (Table 2). Apart from the subgroup of the cysteine *S*-conjugates, briefly mentioned in the glucuronidation pathway, C9 structure was also proposed in Figure 1. Characteristically, C9 in the positive ion mode produced a single fragment (m/z 348) with neutral loss of 176 Da, which was assumed to anhydroglucuronic acid (Table 2). This assumption was supported by the findings that C8 and C13 yielded m/z 348 as one of their major product ions. Less characteristically, in the negative ion mode, C9 produced m/z 194 as the most abundant product ion and m/z 398 with neutral loss of 124 Da as mentioned previously.

We also found three undefined metabolites, labeled as Uk#s 1, 2, and 3 (Table 2). All three appear to be one chlorine-substituted and are likely GSH-related conjugates. Interestingly, Uk#1 has identical molecular mass to C8 and shows similar fragmentation patterns in the negative ion mode. However, the information from

the positive ion mode is limited. Consequently, Uk#1 structure remains undetermined. Meanwhile, for Uk#2 and 3, MS/MS spectra were obtained from the positive ion mode only, which was not as informative. Selected major product ions generated from Uk#2 and 3 were selected for MS³ experiments. Unfortunately, the data obtained were not informative. It is assumed that Uk#2 is the oxon-derivative of Uk#3 because of similarities in fragmentation patterns (MS/MS), along with consistent *m/z* differences between the respective precursor and product ions of 16 Da. For these three unknown metabolites, further analysis and analytical methods are needed.

DISCUSSION

This study shows that CPS undergoes not only CYP-dependent phase I biotransformation but also phase II conjugation pathways in human hepatocytes. These results represent the most extensive characterization of CPS/CPO metabolism in human hepatocytes to date since most previous studies have relied on measurement of CYP-dependent products of TCP, DEP, and DETP or glucuronide conjugates using enzymatic hydrolysis. According to these earlier studies, CYP-mediated products of TCP, DETP, and DEP were very similar between species, including humans and rodents [16–22].

Pooled Human Liver S9 Fraction

Human liver S9 fraction was used as an enzyme source to analyze CYP-dependent metabolites and phase II conjugates of CPS and CPO. The results of pHL S9 experiments provided preliminary information used in subsequent studies using human hepatocytes treated with either CPS or CPO.

The finding of phase II-related products of TCP, *O*-sulfate (S1) and *O*-glucuronide (C5) found in human liver S9 fraction, was similar to an earlier study in which CPS was biotransformed in the rat, *in vivo*, into TCP and its glucuronide and sulfate conjugate [6]. The GSH conjugates of CPS (CPS-SG, C7) and CPO (CPO-SG, O4) identified are probably the primary metabolites and subsequently undergo further metabolism or degradation.

Recently, Bicker et al. [4] demonstrated, using LC-MS/MS, GSH-mediated conjugates of CPS in the urine of a CPS-intoxicated woman, although C7 and O4 were not found in this case.

Human Liver Hepatocytes

The absence of CPO in human hepatocytes exposed to CPS or CPO may be the result of hepatic

esterase-mediated hydrolysis of CPO to TCP by carboxylesterase and/or A-esterases [23,24].

Although CPS is readily metabolized to a large number of metabolites and CPO is produced by both pHLM and CYP isoforms, CPO cannot be identified as a CPS metabolite when human hepatocytes are treated with CPS. Since CPO is itself readily metabolized by human hepatocytes, it must be concluded that it does not accumulate to be released into the bloodstream and transported to the nervous system. If that is the case, the activation of CPS to CPO within the nervous system, rather than the liver, may be responsible for the cholinergic effects of CPS, whereas its metabolism in the liver will cause inhibition of CYP isoforms by the release of reactive sulfur.

From the above results, CPS appears to be extensively biotransformed in hepatocytes through four different pathways: dearylation (I), dealkylation (II), glucuronidation (III), and GSH-dependent conjugation (IV). First, CYP-mediated dearylation produced TCP (C4) and DETP (C3) in human hepatocytes exposed to CPS. However, DEP (O3) was not determined using LC-MS in CPO treatment because of its high polarity. To properly analyze O3 with LC-MS, more polar LC column materials, such as reversed-phase/weak anion exchange stationary phase, might be applicable [16], as presumably would GC-MS after derivatization.

According to early studies, CYP-dependent metabolites were considered to be major products of *in vivo* or *in vitro* metabolism of CPS [2,16–19,21,25]. Second, the monodealkylated metabolite, C2, was likely to be produced through a dealkylation process and its formation relatively minor (1.8%) compared to other metabolites. In addition, early studies reported that CPS or CPO undergo mono- or bidealkylation to produce C2 in the urine of human and catfish or TCP phosphate in the urine of rat [4,16,20,26]. Third, two glucuronide conjugates, the *O*-glucuronide of TCP (C5) and the *S*-glucuronide of chlorine-substituted CPS (C9), were found in either CPS or CPO treatment or CPS treatment alone, respectively. Based on the knowledge of substrate specificity of glucuronosyltransferase [27], C5 and C9 are presumably produced by a linkage of oxygen through hydroxyl (OH⁻) group and sulfur through sulfhydryl (SH⁻) group, respectively. C5, but not C9, was identified in the urine of human and rat and in the bile and urine of catfish [4,17,20]. In CPS-treated hepatocytes, the relative amounts of C5 and C9 were minimal (<1%). However, following CPO treatment, C5 was a relatively major metabolite (>40%), although it was minor in the P2 individual's hepatocytes at 24 h incubation. It is apparent that there is individual variation in CPS metabolism. Fourth, 11 of the CPS and 3 of the CPO metabolites were GSH-mediated conjugates (Figures 1 and 2). Glutathione (GSH) is a

major intracellular nonprotein thiol that plays a significant role in maintaining the intercellular redox state and possesses antioxidant activity. GSH with its nucleophilic cysteinyl group is involved in the interaction with electrophilic compounds such as aromatic halocompounds either noncatalytically or catalyzed by glutathione-S-transferases (GST), leading to the detoxification of reactive xenobiotics [27]. In addition, the nucleophilic GSH can substitute for chlorine at the 6-position close to the heterocyclic nitrogen of CPS [4]. As primary intermediates in the GSH-mediated pathway, CPS-SG (C7) and CPO-SG (O4) identified in pHL S9 were also found in human hepatocytes. Furthermore, mono-O-deethyl CPS-SG rather than mono-O-deethyl CPO-SG (C6) was found with CPS. Bicker et al. [4] suggested that C7 and O4 may be primary metabolites in CPS metabolism.

It is known that GSH conjugates are processed further to an acetylated cysteine S-conjugate (mercapturic acid). From the above results, C8, C10, C12, C13 or C14, and O5 identified in CPS or CPO treatment, respectively, may be the intermediates in mercapturic acid biosynthesis, although mercapturic acids themselves were not found in either treatment. Some cysteine-S conjugates are known to undergo hydrolysis by cysteine conjugate β -lyase, resulting in reactive thiols [27]. It is likely that the reactive thiol of C13 was processed to the S-glucuronide of chlorine-substituted CPS (C9). Also GSH-mediated metabolites of CPS are likely to undergo the process of dealkylation (C14) or alkylation (C15), further generating more hydrophilic compounds and facilitating the effective removal of CPS. The removal of mono- or diethyl(thio) phosphate moiety of C10, C12, and C13 was likely to produce 2-amino-3-(3,5-dichloro-6-hydroxypyridin-2-yl thio) propanoic acid (C14) (Figure 1). Presumably, C14 interacts with DETP and produces 3-(3,5-dichloro-6-hydroxypyridin-2-yl thio)-2-(diethoxyphosphorothioyl) amino propanoic acid (C15). For this compound (C15), Bicker et al. [4] mentioned that its biosynthesis was limited to high exposure to CPS.

Taken together, these results indicate that CPS and CPO undergo much more extensive metabolic detoxification than CYP-mediated activation of CPS to CPO, a more potent AChE inhibitor. Human liver efficiently performed their metabolism by both CYP-dependent reactions and also phase II conjugation. Qiao et al. [28] demonstrated that CPS was likely to increase oxidative stress in *in vitro* and *in vivo* systems, leading to developmental neurotoxicity. CPS and its metabolites cause an increase in phosphorylation of the Ca^{2+} /cAMP response element binding protein (CREB) without significant change in AChE activity, leading to changes in cognitive function or neurodevel-

opment [29]. CPO interferes with the signal transduction pathway through muscarinic acetylcholine receptors, followed by changes in protein phosphorylation or modulation of immune status [9]. In addition, the reactive atomic sulfur released in the process of CYP-activation of CPS to CPO binds to the heme iron of CYP, causing inhibition of its xenobiotic-metabolizing activity and giving rise to additional possibilities for CPS inhibition of the metabolism of the endogenous steroid hormones, testosterone, and estradiol, potentially resulting in endocrine disruption [12,13]. The results of this study suggest that CPS-induced organ toxicity needs to be further investigated and that the use of human hepatocytes will help to overcome the difficulty in extrapolation from experimental animals to humans.

ACKNOWLEDGMENTS

The authors acknowledge the invaluable role of Dr. Nigel Deighton, the director of Metabolomics and Proteomics Laboratory in NC State University, for his help in LC-MS/MS analysis and data interpretation and for his valuable comments on preparation of the manuscript.

REFERENCES

1. EPA. U.S. Memorandum of agreement between the Environmental Protection Agency and signatory registrants regarding the registration of pesticide products containing chlorpyrifos. Washington, D.C.: U.S. Environmental Protection Agency; 2000.
2. Tang J, Cao Y, Rose RL, Brimfield AA, Dai D, Goldstein JA, Hodgson E. Metabolism of chlorpyrifos by human cytochrome P450 isoforms and human, mouse and rat liver microsomes. *Drug Metab Dispos* 2001;29:1201–1204.
3. Matsumura F. Organophosphorus insecticides. In: Toxicology of insecticides. New York: Plenum; pp 62–74.
4. Bicker W, Lammerhofer M, Genser D, Kiss H, Lindner W. A case study of acute human chlorpyrifos poisoning: novel aspects on metabolism and toxicokinetics derived from liquid chromatography-tandem mass spectrometry analysis of urine samples. *Toxicol Lett* 2005;159:235–251.
5. Vittozzi L, Fabrizi L, Di Consiglio E, Testai E. Mechanistic aspects of organophosphorothionate toxicity in fish and humans. *Environ Int* 2001;26:125–129.
6. Nolan RJ, Dryzga MD, Landenberger BD, Kastl PE. Chlorpyrifos: Tissue distribution and metabolism of orally administered ^{14}C labeled chlorpyrifos in Fischer 344. Unpublished report no. HET K-044793-(76) from Dow Chemical Co., Midland, MI, USA; 1987. Submitted to WHO by Dow AgroSciences, Indianapolis, IN, USA and Dow Chemical Co., Midland, MI.
7. Karanth S, Pope C. Carboxylesterase and A-esterase activity during maturation and aging: relationship to the toxicity of chlorpyrifos and parathion in rats. *Toxicol Sci* 2000;58:282–289.

8. Richardson RJ. Assessment of the neurotoxic potential of chlorpyrifos relative to other organophosphorus compounds: A critical review of the literature. *J Toxicol Environ Health* 1995;44:135–165.
9. Bomser J, Casida JE. Activation of extracellular signal-regulated kinases (ERK 44/42) by chlorpyrifos oxon in Chinese hamster ovary cells. *J Biochem Mol Toxicol* 2000;14:346–353.
10. Usmani KA, Rose RL, Goldstein JA, Taylor WG, Brimfield AA, Hodgson E. In vitro human metabolism and interactions of repellent *N,N*-diethyl-*m*-toluamide. *Drug Metab Dispos* 2002;30:289–294.
11. Tang J, Cao Y, Rose RL, Hodgson E. In vitro metabolism of carbaryl by human cytochrome P450 and its inhibition by chlorpyrifos. *Chem-Biol Interact* 2002;141:229–241.
12. Usmani KA, Rose RL, Hodgson E. Inhibition and activation of the human liver microsomal and human cytochrome P450 metabolism of testosterone by deployment-related chemicals. *Drug Metab Dispos* 2003;31:384–391.
13. Usmani KA, Cho TM, Rose RL, Hodgson E. (2006) Inhibition of the human liver microsomal and human cytochrome P450 IA2 and 3A4 metabolism of estradiol by deployment-related and other chemicals. *Drug Metabol. Disp.* 34:1606–1614.
14. Choi J, Hodgson E, Rose RL. Inhibition of *trans*-permethrin hydrolysis in human liver fractions by chlorpyrifos oxon and carbaryl. *Drug Metab Drug Interact* 2004;20:233–245.
15. Hernandez F, Sancho J, Pozo O. Direct determination of alkyl phosphates in human urine by liquid chromatography/electrospray tandem mass spectrometry. *Rapid Commun Mass Spectrom* 2002;16:1766–1773.
16. Bicker W, Lammerhofer M, Lindner W. Determination of chlorpyrifos metabolites in human urine by reversed-phase/weak anion exchange liquid chromatography-electrospray ionisation-tandem mass spectrometry. *J Chromatogr B Anal Tech Biomed Life Sci* 2005;822:160–169.
17. Bakke JE, Feil VJ, Price CE. Rat urinary metabolites from *O,O*-diethyl-*O*-(3,5,6-Trichloro-2-pyridyl)-phosphorothioate. *J Environ Sci Health B* 1976;3:225–230.
18. Sultatos LG, Saho M, Murphy SD. The role of hepatic biotransformation in mediating the acute toxicity of the phosphorothionate insecticide chlorpyrifos. *Toxicol Appl Pharmacol* 1984;73:60–68.
19. Sunaga M, Yoshida M, Hara I. Metabolism and urinary excretion of chlorpyrifos in rats. *Jpn J Hyg* 1989;43:1124–1129.
20. Barron MG, Plakas SM, Wilga PC. Chlorpyrifos pharmacokinetics and metabolism following intravascular and dietary administration in Channel Catfish. *Toxicol Appl Pharmacol* 1991;108:474–482.
21. Vasili Ž, Drevenkar V, Rumenjak V, Štengl B, Fröbe Z. Urinary excretion of diethylphosphorus metabolites in persons poisoned by quinalphos or chlorpyrifos. *Arch Environ Contam Toxicol* 1992;22:351–357.
22. Drevenkar V, Vasilič Ž, Štengl B, Fröbe Z, Rumenjak V. Chlorpyrifos metabolites in serum and urine of poisoned persons. *Chem-Biol Interact* 1993;87:315–322.
23. Sultatos LG, Saho M, Murphy SD. The role of hepatic biotransformation in mediating the acute toxicity of the phosphorothionate insecticide chlorpyrifos. *Toxicol and Appl Pharmacol* 1984;73:60–68.
24. Clement JG. Role of aliesterase in organophosphate poisoning. *Fundam and Appl Toxicol* 1984;4:S96–S105.
25. Abdel-Rahman AA, Blumenthal GM, Abou-Donia SA, Ali FAF, Abdel-Monem AE, Abou-Donia MB. Pharmacokinetic profile and placental transfer of a single intravenous injection of [¹⁴C] chlorpyrifos in pregnant rats. *Arch Toxicol* 2002;76:452–459.
26. Smith GN, Watson BS, Fischer FS. Investigation on Dursban insecticide. Metabolism of [³⁶Cl] *O,O*-Diethyl *O*-3,5,6-Trichloro-2-pyridyl Phosphorothioate in rats. *J Agric Food Chem* 1967;15:132–138.
27. Rose RL, Hodgson E. In Rose RL, Hodgson E, editors. A textbook of modern toxicology: Metabolism of toxicants. Hoboken, NJ: Wiley; 2004. pp 111–148.
28. Qiao D, Seidler FJ, Slotkin TA. Oxidative mechanisms contributing to the developmental neurotoxicity of nicotine and chlorpyrifos. *Toxicol Appl Pharmacol* 2005;206:17–26.
29. Schuh RA, Lein PJ, Beckles RA, Jett DA. Non-cholinesterase mechanisms of chlorpyrifos neurotoxicity: altered phosphorylation of Ca²⁺/cAMP response element binding protein in cultured neurons. *Toxicol Appl Pharmacol* 2002;182:176–185.

Inhibition of Fipronil and Nonane Metabolism in Human Liver Microsomes and Human Cytochrome P450 Isoforms by Chlorpyrifos

Hyun Joo, Kyoungju Choi, Randy L. Rose,[†] and Ernest Hodgson

Department of Environmental and Molecular Toxicology, North Carolina State University, Raleigh, NC 27695, USA;
E-mail: ernest.hodgson@ncsu.edu

Received 30 January 2007; revised 1 February 2007; accepted 4 February 2007

ABSTRACT: Previous studies have established that chlorpyrifos (CPS), fipronil, and nonane can all be metabolized by human liver microsomes (HLM) and a number of cytochrome P450 (CYP) isoforms. However, metabolic interactions between these three substrates have not been described. In this study the effect of either coincubation or preincubation of CPS with HLM or CYP isoforms with either fipronil or nonane as substrate was investigated. In both co- and preincubation experiments, CPS significantly inhibited the metabolism of fipronil or nonane by HLM although CPS inhibited the metabolism of fipronil more effectively than that of nonane. CPS significantly inhibited the metabolism of fipronil by CYP3A4 as well as the metabolism of nonane by CYP2B6. In both cases, preincubation with CPS caused greater inhibition than coincubation, suggesting that the inhibition is mechanism based. © 2007 Wiley Periodicals, Inc. *J Biochem Mol Toxicol* 21:76–80, 2007; Published online in Wiley InterScience (www.interscience.wiley.com). DOI 10.1002/jbt.20161

KEYWORDS: Fipronil; Nonane; Human Liver Microsomes; Cytochrome P450; CYP2B6; CYP3A4

INTRODUCTION

In previous studies, Tang et al. [1] have demonstrated that human liver microsomes (HLM) have the ability to metabolize fipronil, an insecticide of the phenyl pyrazole family, to fipronil sulfone, the predom-

inant metabolite. It was also shown that cytochrome P450 (CYP) 3A4 was the major isoform for fipronil sulfone production in humans, although CYP2C19 contributed but was less active. In addition, nonane, a component of jet-propulsion fuel 8 (JP-8) and other fossil fuels, is metabolized to 2-nonanol and 2-nonanone by HLM, and that CYP2B6 and 2E1 are primarily responsible for this activity. In addition, CYP1A2 is also responsible for 2-nonanol production [2].

Recently, it has been established that organophosphorus insecticides containing the P=S moiety are potent inhibitors of the metabolism of both xenobiotics and endogenous substrates by HLM and by specific human CYP isoforms [3]. For example, chlorpyrifos (CPS), an organophosphorus insecticide, inhibited the metabolism of carbaryl, *N,N*-diethyl-*m*-toluamide (DEET), testosterone, and estradiol in HLM as well as by specific human CYP isoforms [4–7]. However, metabolic interactions between CPS and fipronil, as well as between CPS and nonane, have not been described previously.

The main objective of this study was to investigate the effects of CPS on fipronil or nonane metabolism in pooled HLM and by selected CYP isoforms.

MATERIALS AND METHODS

Chemicals

Fipronil, fipronil sulfone, and chlorpyrifos (CPS) were purchased from Chem Service (West Chester, PA). Nonane, 2-nonanol, and 2-nonanone were purchased from Sigma-Aldrich (St. Louis, MO). Acetonitrile, methanol, methylene chloride, and acetic acid were purchased from Fisher Scientific (Pittsburgh, PA).

Correspondence to: Ernest Hodgson.

Contract Grant Sponsor: US Army.

Contract Grant Number: DAMD 17-00-1-0008.

[†]Deceased. Dr. Rose died in a tragic accident on May 23, 2006.

© 2007 Wiley Periodicals, Inc.

Pooled Human Liver Microsomes and P450 Isoforms

Pooled HLM from 18 donors (11 males and 7 females) and cytochrome P450 (CYP) 2B6 and 3A4 SUPERSOMES™ were purchased from BD Biosciences (Woburn, MA). Final concentrations used were 1 mg protein/mL for pHLM and 20 pmol P450/mL for CYP isoforms.

Inhibition of Fipronil by Chlorpyrifos

The *in vitro* assay used by Tang et al. [1] was utilized in these experiments. Fipronil (final concentration, 80 μ M) was incubated with pHLM or CYP3A4 in 100 mM Tris buffer (pH 7.4) or 50 mM potassium-phosphate buffer, 3.3 mM MgCl₂ (pH 7.4), respectively. After 5 min of incubation at 37°C, coincubation was initiated by adding a mixture of CPS (0.25–50 μ M) and fipronil in the presence of an NADPH-regenerating system consisting of 0.25 mM NADP, 2.5 mM glucose-6-phosphate, and 2 U/mL glucose-6-phosphate dehydrogenase. After 15 min of incubation, the reaction was terminated by the addition of 250 μ L methanol, followed by centrifugation at 21,000 \times *g* for 5 min. Supernatants were collected and kept at 4°C until used. New preincubation was initiated by adding pHLM or CYP3A4 to the mixture containing varying concentrations of CPS (0.25–50 μ M or 0.25–10 μ M, respectively) and the NADPH-regenerating system. After 30 min of preincubation, fipronil was added to the reaction and incubated for 15 min. The subsequent sample preparation steps were as described in the coincubation experiments. The experiments were carried out in duplicate.

Inhibition of Nonane by Chlorpyrifos

The *in vitro* assay of Edwards et al. [2] was modified as follows: nonane (final concentration, 50 μ M) was incubated with pHLM or CYP2B6 in potassium-phosphate buffer, 3.3 mM MgCl₂ (100 or 50 mM, respectively). After 5 min of incubation at 37°C, coincubation was initiated by adding CPS (0.25–50 μ M) in the presence of the NADPH-regenerating system and incubated for 15 min. Preincubation was initiated by the addition of pHLM or CYP2B6 to the mixture containing varying concentrations of CPS (0.25–50 μ M or 0.25–10 μ M, respectively) and the NADPH-regenerating system. At the end of 30-min preincubation, nonane was added to the reaction mixture and then further incubated for 15 min. After co- or preincubation, the reaction was stopped by adding 100 μ L of methylene chloride, followed by centrifugation at 21,000 \times *g* for 5 min. The methylene chloride extracts were directly analyzed on GC/FID. The experiments were carried out in duplicate.

HPLC Analysis

A Waters HPLC system (Milford, MA) was used for analysis. This system consisted of a 2996 separation module and a 2695 photodiode array detector. Fipronil and fipronil sulfone were analyzed by a method previously reported [1]. Briefly, the isocratic system was 30% water (A) containing 0.05 M acetic acid and 70% methanol (B), the flow rate was 1 mL/min and the injection volumes were 30 μ L. A Phenomenex Synergi Polar-RP column (4 μ m, 150 \times 4.6 mm, Rancho Palos Verdes, CA) was used to separate fipronil and fipronil sulfone, which were detected at 280 and 275 nm, respectively. The retention times and method detection limits were 5.5 min and 0.048 μ M for fipronil, and 7.1 min and 0.046 μ M for fipronil sulfone, respectively.

GC Analysis

The GC/FID system consisted of a Hewlett Packard (currently Agilent Technologies) 7673 auto injector, 5890 Series II GC system, RESTEK RTX®-1701 column (30 m, 0.25 mm i.d.), and a flame ionization detector (FID). The injection port and detection temperatures were set at 250°C and 280°C, respectively. The oven temperature was programmed to rise from 40°C to 80°C at a rate of 6°C/min, from 80°C to 120°C at a rate of 3°C/min, followed by a rate of 15°C/min until a temperature of 270°C was reached. Helium was used as a carrier gas at a flow rate of 1 mL/min. Nonane, 2-nonanone, and 2-nonanol were measured at 7.5, 18.1, and 18.5 min and their method detection limits were 0.071, 0.069, and 0.096 μ M, respectively. The linear range ($r^2 > 0.99$) of the assay was 1–100 μ M for a 2- μ L injection. In addition, chlorpyrifos (CPS) was detected at 34.7 min.

Statistical Analysis

Fisher's protected least significant difference (LSD) was used to separate means at the 5% level. All statistical analyses were done with PC SAS for Windows®, version 8.2 [8].

RESULTS

Inhibition of Fipronil Metabolism in pHLM and CYP3A4 by Chlorpyrifos

The result of co- and preincubation of chlorpyrifos (CPS) with fipronil is shown in Figure 1. Coincubation of fipronil (80 μ M) with increasing concentrations of CPS (0.25–50 μ M) in pHLM resulted in decreased production of fipronil sulfone (Figure 1A). Except at 0.25 μ M CPS, all concentrations of CPS employed

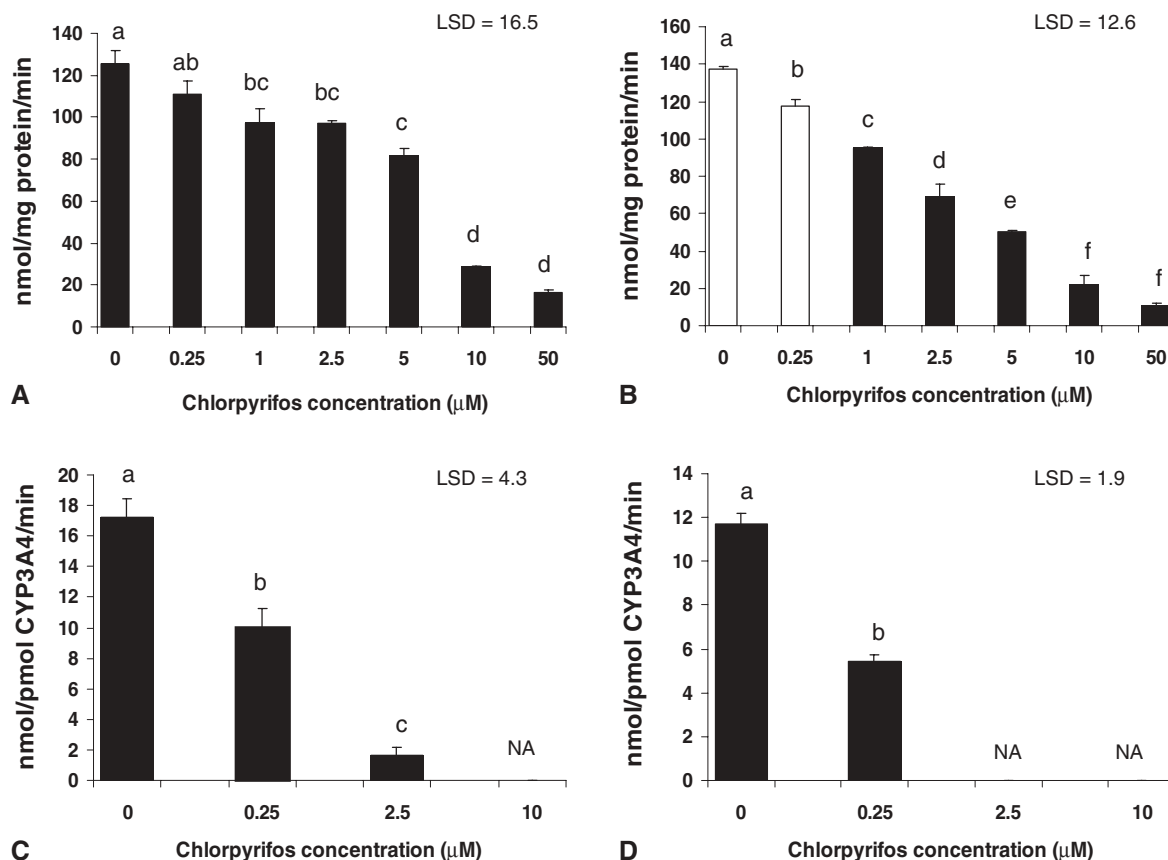


FIGURE 1. The effects of chlorpyrifos (CPS) on fipronil sulfone production in pHLM and cytochrome P450 (CYP) 3A4: (A) coincubation of chlorpyrifos with fipronil in pHLM, (B) preincubation of chlorpyrifos in pHLM before incubation with fipronil, (C) coincubation of chlorpyrifos with fipronil in CYP3A4, and (D) preincubation of chlorpyrifos in CYP3A4 before incubation with fipronil. Activities are represented as mean (nmol product/mg microsome protein per min) \pm S.E. for (A) and (B) and mean (nmol product/pmol CYP3A4 per min) \pm S.E. for (C) and (D) ($n = 2$). Means followed by the same letter are not significantly different (least significant difference [LSD] = 5%). Not available (NA).

significantly inhibited the metabolism of fipronil in pHLM. At the two highest concentrations of CPS (10 and 50 μM), the production of fipronil sulfone was decreased by approximately 77% and 87%, respectively. The ability of pHLM to metabolize fipronil was also reduced by preincubation of pHLM with CPS (Figure 1B), which showed significant inhibition of fipronil metabolism at all concentrations of CPS (0.25–50 μM), demonstrating that preincubation with CPS caused more significant inhibition than coincubation with CPS.

As also shown in Figures 1C and 1D, metabolism of fipronil was significantly inhibited by both co- and preincubations of CYP3A4 with CPS (0.25–10 μM). The role of CYP3A4 in the metabolism of fipronil was verified by co- and preincubations of CPS with fipronil. At the lowest concentration of 0.25 μM CPS, the production of fipronil decreased by 43% and 54% in co- and preincubations of CYP3A4, respectively. Preincubation with CPS caused greater inhibition than coincubation since fipronil sulfone was not found at 2.5 and 10 μM

CPS, probably because it was below the method detection limit.

Inhibition of Nonane Metabolism in pHLM and CYP2B6 by Chlorpyrifos

Figure 2 shows the results for co- and preincubations of chlorpyrifos (CPS) with 50 μM nonane. For the co- and preincubations in pHLM with CPS (Figures 2A and 2B, respectively), a significant inhibition of nonane metabolism is shown in both cases, throughout all CPS concentrations employed (0.25–50 μM), although preincubation with CPS caused greater inhibition than coincubation. The production of 2-nonanol and 2-nonanone indicates that there was no statistically significant difference in the increase in inhibition from 2.5 to 50 μM CPS and 0.25 to 50 μM CPS for co- and preincubation, respectively.

CPS also significantly inhibited the metabolism of nonane by CYP2B6. In coincubation of CYP2B6 with CPS, the production of 2-nonanol and 2-nonanone

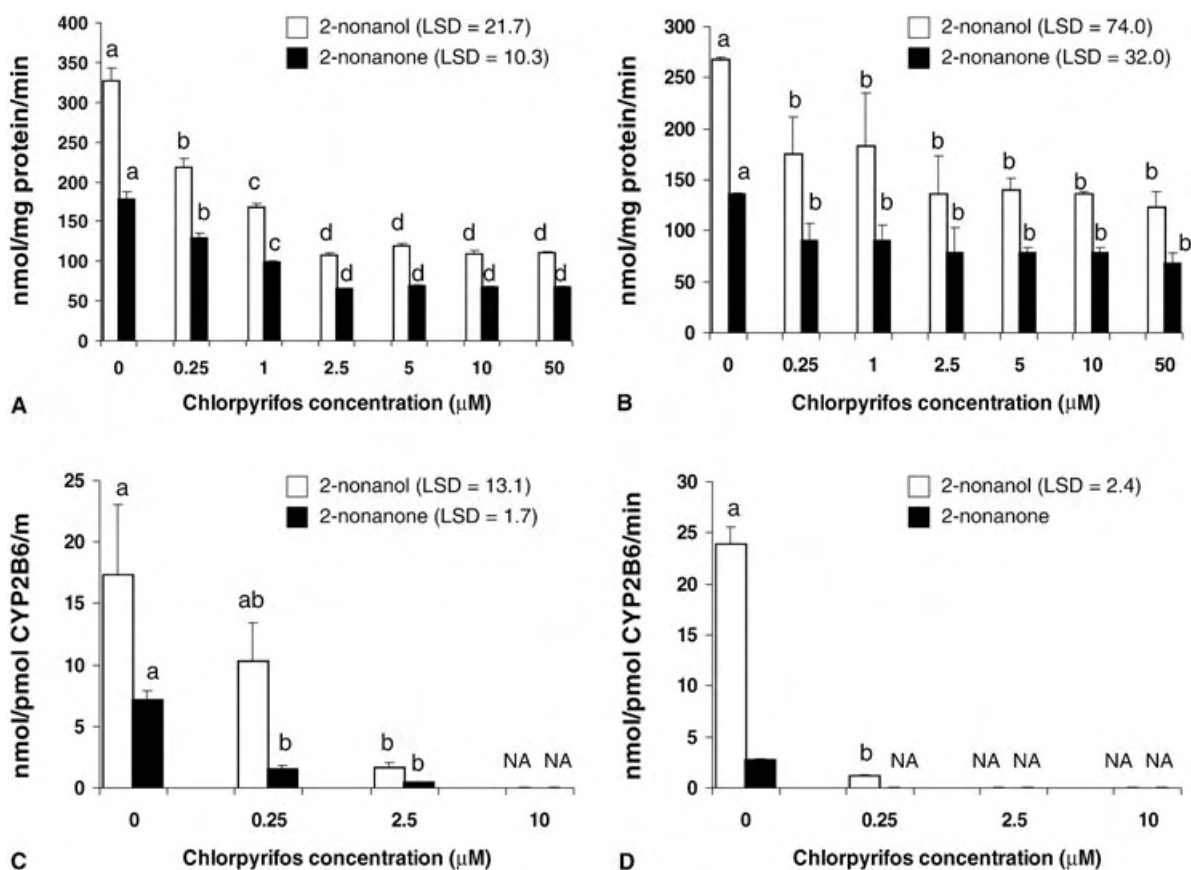


FIGURE 2. The effects of chlorpyrifos (CPS) on 2-nonanol and 2-nonanone production in pHLM and cytochrome P450 (CYP) 2B6: (A) coincubation of chlorpyrifos with nonane in pHLM, (B) preincubation of chlorpyrifos in pHLM before incubation with nonane, (C) coincubation of chlorpyrifos with nonane in CYP2B6, and (D) preincubation of chlorpyrifos in CYP2B6 before incubation with nonane. Activities are represented as mean (nmol product/mg microsomal protein per min) \pm S.E. for (A) and (B) and mean (nmol product/pmol CYP2B6 per min) \pm S.E. for (C) and (D) ($n=2$). Means followed by the same letter are not significantly different for each metabolite (least significant difference [LSD]=5%). Not available (NA).

decreased with increasing concentrations of CPS (Figure 2C). Furthermore, neither metabolite was found at 10 μ M CPS. At 2.5 μ M CPS, the production of 2-nonanol and 2-nonanone decreased by 91% and 94%, respectively. Preincubation of CYP2B6 with CPS showed more significant inhibition of nonane metabolism than coincubation (Figure 2D). Except for 5% production of 2-nonanol at 0.25 μ M CPS in the preincubation experiments, 2-nonanol and 2-nonanone were not found at concentrations of 0.25, 2.5, and 10 μ M CPS.

DISCUSSION

Chlorpyrifos (CPS), fipronil, and nonane can all be metabolized by HLM and specific CYP isoforms [1,2,9]. In this study, metabolic interactions between CPS and fipronil, and CPS and nonane, were investigated. In both co- and preincubation experiments, CPS significantly inhibited the metabolism of fipronil

by pHLM as well as by CYP3A4, a result that is not surprising since CYP3A4 is the major CYP isoform metabolizing fipronil [1] and CPS is an irreversible noncompetitive inhibitor of human CYP isoforms [6,7,10]. This result is also correlated with the finding that CPS inhibits the formation of the CYP3A4-mediated metabolite 3-hydroxycarbofuran from carbofuran in HLM [10]. The importance of CYP3A4 in the metabolism of fipronil was further verified by co- and preincubation of CYP3A4 with CPS, which showed a significant inhibition by CPS in both cases, although preincubation caused greater inhibition than coincubation.

The effect of CPS on nonane metabolism was also investigated. When compared to controls, the production of 2-nonanol and 2-nonanone, followed by both co- and preincubation of pHLM with CPS, was decreased by more than 50% at a concentration of 2.5 μ M. However, further inhibition was not achieved with increasing CPS concentrations up to 50 μ M. Because nonane is readily metabolized to 2-nonanol and

2-nonanone in pHLM and by CYP isoforms, including 1A2, 2B6, 2E1 and alcohol dehydrogenase [2], it is likely that CPS inhibited CYP2B6 predominantly but is less effective as an inhibitor of other nonane-metabolizing enzymes. As further verification of the role of CYP2B6 in the metabolism of nonane, co- and preincubation of CYP2B6 with CPS was also carried out and, as shown in Figures 2C and 2D, CPS significantly inhibited the ability of CYP2B6 to metabolize nonane in both cases. This correlates with the finding that CYP2B6-mediated production of carbaryl methylol is inhibited by CPS. These results are most likely due to the release of reactive sulfur from CPS during activation to CPS oxon binding to the heme of CYP and inhibiting its activity [4,6,11,12].

In both co- and preincubation experiments, CPS significantly inhibited the metabolism of fipronil or nonane by pHLM although CPS inhibited the metabolism of fipronil more effectively than that of nonane. CPS also inhibited CYP3A4 and 2B6, the primary metabolizing enzymes of fipronil and nonane, respectively. In both cases, preincubation with CPS caused greater inhibition than coincubation, suggesting that the inhibition is time dependent and mechanism based.

ACKNOWLEDGMENTS

The authors thank Dr. Damian Shea for the use of GC/FID and Dr. Gail Mahnken for her technical assistance in the analysis of nonane.

REFERENCES

1. Tang J, Usmani KA, Hodgson E, Rose RL. In vitro metabolism of fipronil by human and rat cytochrome P450 and its interactions with testosterone and diazepam. *Chem Biol Interact* 2004;147:319–329.
2. Edwards JE, Rose RL, Hodgson E. The metabolism of nonane, a JP-8 jet fuel component, by human liver microsomes, P450 isoforms and alcohol dehydrogenase and inhibition of human P450 isoforms by JP-8. *Chem Biol Interact* 2005;151:203–211.
3. Hodgson E, Rose RL. Organophosphorus chemicals: Potent inhibitors for the human metabolism of steroid hormones and xenobiotics. *Drug Metab Rev* 2006;38:149–162.
4. Tang J, Cao Y, Rose RL, Hodgson E. In vitro metabolism of carbaryl by human cytochrome P450 and its inhibition by chlorpyrifos. *Chem Biol Interact* 2002;141:229–241.
5. Usmani KA, Rose RL, Goldstein JA, Taylor WG, Brimfield AA, Hodgson E. In vitro human metabolism and interactions of repellent, *N,N*-diethyl-*m*-toluamide (DEET). *Drug Metab Dispos* 2002;30:289–294.
6. Usmani KA, Rose RL, Hodgson E. Inhibition and activation of the human liver microsomal and human cytochrome P450 3A4 metabolism of testosterone by deployment-related chemicals. *Drug Metab Dispos* 2003;31:384–391.
7. Usmani KA, Cho TM, Rose RL, Hodgson E. Inhibition of the human liver microsomal and human cytochrome P450 1A2 and 3A4 metabolism of estradiol by deployment-related and other chemicals. *Drug Metab Dispos* 2006;34:1606–1614.
8. SAS. Procedures guide. Release 8.2. Cary, North Carolina: SAS Institute; 2001.
9. Tang J, Cao Y, Rose RL, Brimfield AA, Dai D, Goldstein JA, Hodgson E. Metabolism of chlorpyrifos by human cytochrome P450 isoforms and human, mouse, and rat liver microsomes. *Drug Metab Dispos* 2001;29:1201–1204.
10. Usmani KA, Hodgson E, Rose RL. In vitro metabolism of carbofuran by human, mouse, and rat cytochrome P450 and interactions with chlorpyrifos, testosterone, and estradiol. *Chem Biol Interact* 2004;150:221–232.
11. Neal RA. Microsomal metabolism of thiono-sulfur compounds: Mechanisms and toxicological significance. *Rev Biochem Toxicol* 1980;2:131–171.
12. Neal RA, Halpert J. Toxicology of thiono-sulfur compounds. *Annu Rev Pharmacol Toxicol* 1982;22:321–339.

Identification of Variants of CYP3A4 and Characterization of Their Abilities to Metabolize Testosterone and Chlorpyrifos

DIANA DAI, JUN TANG, RANDY ROSE, ERNEST HODGSON, RACHELLE J. BIENSTOCK, HARVEY W. MOHRENWEISER and JOYCE A. GOLDSTEIN

National Institute of Environmental Health Sciences, National Institutes of Health, Research Triangle Park, North Carolina (D.D., R.J.B., J.A.G.); Department of Toxicology, North Carolina State University, Raleigh, North Carolina (J.T., R.R., E. H.); and Lawrence Livermore National Laboratory, Livermore, California (H.W.M.)

Received June 22, 2001; accepted September 12, 2001 This paper is available online at <http://jpet.aspetjournals.org>

ABSTRACT

CYP3A4 is the most abundant isoform of cytochrome P450 (CYP) in adult human liver. It metabolizes numerous clinically, physiologically, and toxicologically important compounds. The expression of CYP3A4 varies 40-fold in individual human livers, and metabolism of CYP3A4 substrates varies at least 10-fold in vivo. Single nucleotide polymorphisms (SNPs) in *CYP3A4* were identified by direct sequencing of genomic DNA in 72 individuals from three different ethnic groups, including Caucasians, Blacks (African-Americans and African pygmies), and Asians. A total of 28 SNPs were identified, including five which produced coding changes M445T (*CYP3A4*3*), R162Q (*CYP3A4*15*), F189S (*CYP3A4*17*), L293P (*CYP3A4*18*), and P467S (*CYP3A4*19*). The latter four represent new allelic variants. Racial variability was observed for the frequency of individual SNPs. CYP3A R162Q was identified only in Black populations

with an allelic frequency of 4%. CYP3A4 F189S and CYP3A4 M445T were identified in Caucasians with allelic frequencies 2% and 4%, respectively. L293P and P467S were only observed in Asians at allelic frequencies of 2%. The cDNAs for the F189S, L293P, M445T, and P467S mutant alleles were constructed by site-directed mutagenesis and expressed in an *Escherichia coli* expression system. Testosterone and the insecticide chlorpyrifos were used to assess the catalytic activities of the most common CYP3A4 allele (*CYP3A4*1*) and its allelic variants. CYP3A4 F189S exhibited lower turnover numbers for testosterone and chlorpyrifos, while CYP3A4 L293P had higher turnover numbers for both substrates. The turnover numbers of the CYP3A4 M445T and P467S alleles to metabolize these compounds were not significantly different from those of wild-type CYP3A4.

The *CYP3A* genes encode the most abundant CYP enzymes in humans including CYP3A4, CYP3A5, CYP3A7, and CYP3A43 (de Wildt et al., 1999; Gellner et al., 2001). Hepatic CYP3A4 has been estimated to metabolize ~50% of currently used drugs as well as a number of steroids, environmental chemicals, and carcinogens (Aoyama et al., 1989; Shimada et al., 1994; Thummel et al., 1996; Rebbeck et al., 1998; Guengerich, 1999). CYP3A4 is considered to be the predominant form in adult human liver. CYP3A5, a polymorphic form, is present to a variable extent in adult livers. CYP3A5 is believed to be present in the livers of approximately 20% of Caucasians, but a recent study suggests that CYP3A5 is

expressed and may predominate in more than 50% of African-Americans (Lown et al., 1994; de Wildt et al., 1999; Wandel et al., 2000; Kuehl et al., 2001). Both CYP3A4 and CYP3A5 are distributed in multiple tissues including not only liver, but also intestine and kidney (Thummel and Wilkinson, 1998; Guengerich, 1999). CYP3A7 is an isoform found in intestine, reproductive organs, and infant liver but is also present in some adult livers (Kitada et al., 1985; Schuetz et al., 1994). Recently, a new CYP3A member (CYP3A43) has been identified. CYP3A43 mRNA is found predominantly in adult prostate and is also present in multiple tissues, including liver, where it is inducible by rifampicin (Gellner et al., 2001). However, Westlind et al. (2001) using heterologous expression systems including yeast, COS-1 cells, mouse hepatic H2.35 cells, and human embryonic kidney 293 cells suggested that CYP3A43 was a non-functional isoform.

CYP3A levels fluctuate in the liver throughout the life span of an individual (Shimada et al., 1994; Oesterheld,

Work at Lawrence Livermore National Laboratory was performed under the auspices of the U.S. Department of Energy by Lawrence Livermore National Laboratory; contract No. W-7405-ENG-48 and supported by interagency agreement Y1-ES-8054-05 from the National Institute of Environmental Health Sciences (H.W.M.). The work at North Carolina State University (J.T., R.R., and E.H.) was supported, in part, by the North Carolina Department of Agriculture Pesticide Environmental Trust Fund and U.S. Army Grant DAMD 17-00-2-0008.

ABBREVIATIONS:CYP, cytochrome P450; SNP, single nucleotide polymorphism; OPs, organophosphorus; TLC, thin layer chromatography; TCP, trichloropyridinol; CPO, chlorpyrifos-oxon; PCR, polymerase chain reaction; HPLC, high-pressure liquid chromatography; NADPH, β -nicotinamide adenine dinucleotide phosphate, reduced form; CHAPS, 3-[(3-cholamidopropyl)dimethylammonio]-1-propanesulfonic acid.

1998). Up to 40-fold interindividual variations in expression levels of CYP3A4 have been observed in human liver. There is an approximately 10-fold variation in metabolism of CYP3A4 substrates in vivo including the antibiotics rifampicin and ketoconazole, the calcium blocker nifedipine, and the immunosuppressant cyclosporine (Thummel and Wilkinson, 1998; Guengerich, 1999). This variation can affect drug efficacy and toxicity. CYP3A4 is inducible by drugs such as rifampicin (Kolars et al., 1992). The variable expression of CYP3A4 is at least partially due to multiple factors, including induction by drugs, endogenous compounds, and environmental chemicals, but also includes genetic factors. Recent evidence suggests that the coding region of CYP3A4 is also genetically variable (Sata et al., 2000; Eiselt et al., 2001).

CYP3A4 has also been shown to be important in the metabolism of organophosphate pesticides (OPs), such as chlorpyrifos (Tang et al., 2001) and parathion (Butler and Murray, 1997; Eaton, 2000). Chlorpyrifos is a widely used broad-spectrum OP insecticide that elicits toxicity through inhibition of acetylcholinesterase (Chambers, 1992). OPs inhibit acetylcholinesterase and exert their toxicity by causing the accumulation of the neurotransmitter acetylcholine at nerve synapses and neuromuscular junctions. These OPs are used as the phosphorothioate ($P = S$), which is a very weak inhibitor of acetylcholinesterase. However, OPs are converted in vivo from ($P = S$) to an active phosphate ester or oxon ($P = O$), which is a potent acetylcholinesterase inhibitor (Chambers, 1992) by CYP enzymes.

Genetic variations of CYP3A4 have recently been reported. A mutation in the 5'-upstream region termed *CYP3A4*1B* (A290G) was observed in 52% of African-Americans and 9.6% of Caucasians, but has not been identified in Asians (Ball et al., 1999; Rebbeck, 2000; Sata et al., 2000; Gellner et al., 2001). It was suggested to be associated with advanced stage prostate cancer in men (Rebbeck et al., 1998), yet has protective effects for secondary cancer caused by chemotherapeutic drugs for leukemia metabolized by CYP3A4, such as epipodophyllotoxins (Felix et al., 1998). However, this polymorphism does not appear to affect constitutive levels of CYP3A4 (Wandel et al., 2000). Gonzales and coworkers (Sata et al., 2000) have described two coding SNPs including *CYP3A4*2* (S222P) found only in Finnish Caucasians with an allelic frequency of 2.7%, and a single case of *CYP3A4*3* (M445T) in a Chinese population of 178 individuals. Baculovirus expressed *CYP3A4*2* protein exhibited an increase in the K_m for nifedipine but not for testosterone compared with *CYP3A4*1*. There has been limited information about the effects of a new M445T allele on metabolism (Sata et al., 2000). *CYP3A4*4* (I118V), *CYP3A4*5* (P218R), and *CYP3A4*6* (a stop codon at 285) were reported in a Chinese population with allelic frequencies of 1.4%, 0.98%, and 0.5%, and all of these variant alleles were associated with lower ratios of 6 β -hydroxycortisol to free cortisol in an in vivo study (Hsieh et al., 2001). A very recent study has identified seven new polymorphisms in European Caucasians (Eiselt et al., 2001).

To identify *CYP3A4* polymorphisms, we screened for single nucleotide polymorphisms among 72 individuals from three different racial groups including ethnically diverse Caucasians, Blacks (African-Americans and African pygmies) and ethnically diverse Asians. We identified four new coding polymorphisms in *CYP3A4*. A bacterial cDNA expression system was used. Catalytic activities of wild-type CYP3A4

and allelic variants were compared using testosterone and the insecticide chlorpyrifos as prototypic 3A4 substrates.

Materials and Methods

Testosterone, β -nicotinamide adenine dinucleotide phosphate, reduced form (NADPH), isopropyl β -D-thiogalactopyranoside, δ -aminolevulinic acid, phenylmethylsulfonyl fluoride, phosphatidylcholine, and leupeptin were purchased from Sigma Chemical Co. (St. Louis, MO). 14 C-Testosterone was purchased from Invitrogen (Boston, MA). Chlorpyrifos, chlorpyrifos-oxon (CPO), and 3,5,6-trichloro-2-pyridinol (TCP) were purchased from ChemService (West Chester, PA). HPLC grade acetonitrile and methanol were purchased from Fisher Scientific (Fair Lawn, NJ). Human NADPH reductase was obtained from Oxford Biomedical Research (Oxford, MI). All restriction enzymes were obtained from New England Biolabs (Beverly, MA). *Taq* polymerase was purchased from QIAGEN (Valencia, CA). Anti-CYP3A4 antibody was obtained from GENTEST (Woburn, MA).

Direct Sequencing. Genomic DNA was obtained from 72 different human lymphoblastoid cell lines (Cornell Institute, Camden, NJ). The individuals contain the following varied racial and ethnic ancestries: 24 Africans (16 African-Americans and 8 African pygmies), 24 Asians (5 native Taiwanese, 5 mainland Chinese, 4 Melanesian, 4 Indo-Pakistani, 3 Cambodian, and 3 Japanese), and 24 Caucasians (9 from Utah, 5 Druze [Lebanon], 5 eastern European, and 5 from Moscow).

Variant Identification. The exons plus splice junctions and the 5' and 3' regions of CYP3A4 were sequenced as previously described by Shen et al. (1998). Briefly, PCR primers were located so that amplification of the genomic sequence is initiated approximately 50 nucleotides from each intron-exon boundary. This is sufficient distance for high quality sequence data to be obtained before reaching the intron/exon splice site. Appended to the 5'-end of each of the PCR primers were sequences containing the primer binding sites for the forward or reverse energy transfer DNA sequencing primers (Amersham Pharmacia Biotech, Cleveland, OH). The amplification products are directly sequenced according to the manufacturer's instructions using the DYEnamic Direct cycle sequencing kit with the DYEnamic energy transfer primers (Amersham Pharmacia Biotech). The denatured products are loaded onto ABI Prism 377 stretch DNA sequencers (Foster City, CA). "PolyPhred" (version 2.1), a software package that utilizes the output from Phred, Phrap, and Consed, was used to identify single nucleotide substitutions in heterozygous individuals (Nickerson et al., 1997; Rieder et al., 1998). A nucleotide sequence analysis program (<http://genomic.sanger.ac.uk/gf/gftl.html>) was used to predict possible new splice sites introduced by any new mutations.

Modification of CYP3A4 cDNA. CYP3A4 wild-type cDNA in the vector pUC19 was generously supplied by Frank Gonzales (National Cancer Institute, National Institute of Health). N-Terminal modification of CYP3A4 cDNA included removal of the initial 10 amino acids and conversion of the first eight amino acids of CYP3A4 into those of bovine 17 α -hydroxylase (MALLLAVF). This was accomplished by PCR using sense primer: 5'-TTAGGAGGTCATATG-GCTCTGTTATTAGCAGTTTTTCTGGTGCTCCTCTAT-3', which introduced a unique restriction site for *NdeI*. The antisense primer (5'-AGCAGAAGTCTCTAGAAAAATTCAGGCTCCACTTACGGTGC-3') was used to introduce an *EcoRI* site. *NdeI* and *EcoRI* sites are unique for the expression vector pCW. Amplification of CYP3A4 ORF was accomplished by PCR with Pfu polymerase using primers described above. PCR products containing an open reading frame of CYP3A4 were digested by *NdeI* and *EcoRI* and then were subcloned into pCW. Fidelity of PCR was verified by complete sequencing of CYP3A4. Sequentially, the plasmids were transformed into *E. coli* XL1 Blue cells.

Site-Directed Mutagenesis. Five mutations containing R162Q, F189S, L293P, M445T, and P467S were made using site-directed mutagenesis. A Chameleon double-stranded site-directed mutagen-

esis kit from Stratagene (La Jolla, CA) was used to introduce single nucleotide changes (indicated in lower case and boldface): primer 5'-GGTGAGAAATCTGAGGC**Ca**GGAAGCAGAGACAGG-3', was used to produce the substitution R162Q. The primer 5'-GTGATCACTAG-CACATCAT**c**TGGAGTGAACATCGACTC-3' was used to substitute individual nucleotide changes coding for the F189S substitution in exon 7. Primer 5'-CAAAGCTCTGTCCGATC**c**GGAGCTCGTG-GCCCAATC-3' introduced the substitution L293P in exon 10. Primer 5'-CTGCATTGGC**Ac**GAGGTTTGCTCTC-3' introduced M445T in exon 12. Primer 5'-CAGA**ACTT**CTCCTTCAA**At**CTTGTA-AAGAAACACAGATCCC-3' introduces P467S in exon 12. The entire coding region, including the mutated sites, was verified by sequencing with an ABI PRISM 377 DNA sequencer (PerkinElmer Life Sciences, Foster City, CA). The entire cDNA was then excised and subcloned into a new pCW plasmid to avoid any accidental mutations in the plasmid caused by the mutagenesis procedure and expressed in *E. coli* XL1 Blue.

Expression and Partial Purification of CYP3A4s. Wild-type and variant CYP3A4 alleles were expressed in *E. coli* XL1 Blue and the allelic proteins were purified as previously described (Dai et al., 2001). Cytochrome P450 content was monitored by the reduced CO spectrum using a DW-2000 Spectrophotometer. Protein concentration was determined by the method of Lowry (Dawson and Heatlie, 1984).

Western Blot Analysis. SDS-polyacrylamide gel electrophoresis was used to separate the recombinant proteins, followed by transferring the proteins onto nitrocellulose membranes. Nonspecific binding was blocked by 10% nonfat milk for 1 h. The membranes were incubated with anti-CYP3A4 primary antibody for 1 h at room temperature. An enhanced chemiluminescent kit (Pierce, Rockford, IL) was used for immunodetection.

Testosterone Metabolism. Metabolism of testosterone by the recombinant wild-type and mutant CYP3A4 alleles was characterized. The purified recombinant CYP3A4 proteins (10 pmol) were reconstituted in with 0.4% CHAPS, 1 μ g of dioleoylphosphatidylcholine, and 40 pmol of human NADPH reductase (Oxford Biomedical Research, Oxford MI) and 20 pmol of cytochrome b_5 in 1 \times HEPES buffer, pH 7.6 (50 mM HEPES, 15 mM MgCl₂, and 0.1 mM EDTA) a 10- μ l volume. The reconstitution mixture was preincubated at 37°C for 5 min and then diluted to a final volume of 100 μ l with 1 \times HEPES containing 10 μ g of dioleoylphosphatidylcholine. The optimal conditions for this substrate were generously provided by Drs. Halpert and He at the University of Texas Medical School in Galveston Texas. The reaction mixture was preincubated at 37°C for 5 min, and the reaction initiated by addition of 10 μ l of 10 mM NADPH and terminated with 50 μ l of tetrahydrofuran. All incubations were performed in triplicate. Samples were analyzed by thin layer chromatography (TLC) using a solvent system of dichloromethane/acetone (4:1, v/v). Finally, the TLC plate was exposed to radioautography and analyzed. Turnover numbers for CYP3A4*1 and mutants were determined by counting the radioactivity of the TLC spots.

Chlorpyrifos Metabolism. CYP3A4s (100 pmol) were reconstituted with dioleoylphosphatidylcholine (3 μ g/10 pmol P450), NADPH reductase (400 pmol), and cytochrome b_5 (200 pmol) added in this order. The reaction was initiated by adding 100 μ M chlorpyrifos in 100 mM potassium phosphate buffer with 3.3 mM MgCl₂ (pH 7.4) with the NADPH generating system (the final concentration was 0.25 mM NADP, 2.5 mM glucose 6-phosphate, and 2 U/ml glucose-6-phosphate dehydrogenase). The final assay volume was 500 μ l. The 30-min incubation was terminated by the addition of 500 μ l of ice-cold acetonitrile and vortexing. After 5 min of centrifugation at 15,000 rpm, the supernatant was analyzed for chlorpyrifos-oxon and trichloropyridinol concentrations by HPLC. The HPLC system used in this study consisted of two Shimadzu pumps (LC-10AT; Kyoto, Japan) and a Shimadzu auto injector (SIL-10AD VP). The mobile phase for pump A was 10% acetonitrile, 89% water, and 1% phosphoric acid, whereas for pump B it was 99% acetonitrile and 1% phosphoric acid. A gradient system was initiated at 20% pump B and increased to 100% pump B in 20 min. The flow rate was 1 ml/min.

Metabolites were separated by a C₁₂ column (Synergi Max 4 μ , 150 \times 4.6 mm, Phenomenex, Rancho Palos Verdes, CA) and detected at 230 nm by a Waters 486 tunable absorbance detector (Milford, MA). Concentrations of metabolites were obtained by extrapolation of peak height from a standard curve.

Statistical Analysis. All enzymatic data were analyzed by analysis of variance followed by Student's *t* test. *N* is the number of samples used in study. Differences were considered significant at *P* < 0.05.

Molecular Modeling. A molecular model was developed for the human CYP 3A4 wild-type protein using the technique of comparative/homology modeling. The polymorphism residue side chains were identified and modified in the completed wild-type model. The template structure used for development of the homology model was the solved mammalian microsomal rabbit cytochrome P450 2C5/2C3 chimeric structure (protein database entry: 1DT6) (Williams et al., 2000). The Molecular Simulations homology modeling package was used in a manual mode for development of the homology model. All molecular dynamics studies of the protein were performed using the Discover, Lifson and Hagler, Consistent Valence Force Field. The model was developed based on a multiple sequence alignment (Fig. 4) of the solved crystal structure (protein database: 1DT6) sequence with human cytochrome P450 2C8, 2C9, 2C18, 2C19, and 3A4 sequences. The multiple sequence alignment was performed manually based on the published P450 alignments of Gotoh (1992; Lewis, 1998) and D. Nelson (<http://drnelson.utmem.edu>). The model required insertion of seven small loops ranging from three to nine residues inserted using the loop generation program present within the Molecular Simulations homology program. There were no deletions. Discontinuities, steric bumps, and overlaps were resolved with molecular dynamics.

Results

Direct Sequencing. Genomic sequencing of all exons and intron-exon junctions was performed on DNA from 72 different human lymphoblastoid cell lines selected from individuals of varied racial and ethnic ancestries [24 individuals with African ancestry (16 African-Americans and 8 African pygmies), 24 Asians (5 Indo-Pakistani, 5 native Taiwanese, 5 mainland Chinese, 3 Cambodians, 3 Japanese, 3 Melanesian) and 24 Caucasians (10 from Utah in the United States, 5 Druze (Lebanon), 5 eastern Europeans, and 5 Russians)]. Twenty-eight SNPs were identified in these regions of CYP3A4 (Table 1). Eight SNPs were located in the exonic regions: R162Q, F189S, I193L, L293P, A297A, T346T, M445T, and P467S. The remaining SNPs were distributed in the 5'-upstream, introns, and 3'-flanking region. Sequencing results showed that R162Q was only detected in Black populations with an allelic frequency of 4% (African-Americans 7.1%, pygmies 0%). F189S was detected only in Caucasians with an allelic frequency of 2% (ethnic frequencies 10% in Eastern Europeans, not found in other Caucasian groups). Two SNPs were only found in Asians. L293 was found in Asians with a frequency of 2% (ethnic frequencies of 10% in Chinese, 0% in other Asian groups). P467S was also found in Asians with an allelic frequency of 2% (ethnic frequencies were 12% in Indo-Pakistani and 0% in other Asian ethnic groups). M445T was only detected in Caucasians in our study with an allelic frequency of 4% (Eastern Europeans: frequency of 10%, Caucasians from Utah 5.6%, not detected in other Caucasian ethnic groups). None of the samples was homozygous for the coding SNPs. No new putative splice sites were introduced by any of these coding, noncoding, or intron SNPs.

TABLE 1
CYP3A4 SNPs^a

SNPs	Site	Amino Acid Substitution	Nucleotide Substitution	Allelic Frequencies			Location in CYP3A4 Genome
				Africans 24	Caucasians 24	Asians 24	
				%			
1	5'-UTR		aatcc(A/G)acagc	0	0	2.1	148874
2	Intron 2		tttca(T/C)tgget	14.6	0	0	154915
3	Intron 3		agctc(T/A)tgca	0	0	2.1	155157
4	Intron 4		aactg(A/T)tgtag	0	0	2.1	162802
5	Intron 5		tggtg(T/G)tgtgt	0	0	2.1	163198
6	Intron 6		ccagc(T/G)gcctg	0	4.2	0	163355
7	Exon 6	R162Q	gaggc(G/A)ggaag	4.2	0	0	163267
8	Intron 7		atctt(T/G)ctctc	50.0	2.1	2.2	164751
9	Intron 7		tgaga(T/C)ataaa	8.7	0	0	164781
10	Intron 7		attca(T/G)ccaact	2.2	0	0	164802
11	Intron 7		tgtag(T/C)acatt	6.5	0	0	164835
12	Exon 7	F189S	atcat(T/C)tgagag	0	2.1	0	164613
13	Exon 7	Silent	aacat(C/T)gactc	4.2	0	0	164626
14	Intron 9		gacac(AT/-)gtttg ^b	0	0	4.2	166813
15	Intron 10		ggatg(G/A)tacat	73	14.6	37.5	169228
16	Intron 10		cttag(C/T)aaaaa	8.3	0	0	169263
17	Intron 10		aaaaa(G/C)cataa	10.4	0	0	169307
18	Intron 10		gttte(G/A)ttctt	2.1	0	0	170793
19	Exon 10	L293P	cgatc(T/C)ggagc	0	0	2.1	169068
20	Exon 10	Silent	gtggc(C/T)caatc	2.1	0	0	169081
21	Intron 11		aagaa(A/G)cccta	0	2.1	0	172022
22	Intron 11		accaa(C/T)gtgga	21	0	2.1	172079
23	Exon 11	Silent	cccac(C/A)tatga	0	0	2.1	170821
24	Exon 12	M445T	tgcca(T/C)gaggt	0	4.2	0	172170
25	Exon 12	P467S	tcaaa(C/T)cttgt	0	0	2.1	172235
26	3'-UTR		aaata(A/T)ccggg	4.2	0	0	175065
27	3'-UTR		gtaca(T/G)gcatt	2.1	0	0	175082
28	3'-UTR		ctgca(C/T)attaa	2.1	0	0	175416

UTR, untranslated region.

^a Accession number of CYP3A4 genomic DNA in GenBank is NG_000004.^b Deletion 2 bases (AT).

Expression and Enzymatic Assay of CYP3A4 Recombinant Alleles. The CYP3A4 alleles were inserted into the pCW expression vector, expressed in *E. coli*, and partially purified with the exception of the newly discovered R162Q allele, which we are currently attempting to express. Comparison of Western blotting (data not shown) and CO spectra of the mutants indicated that all were present as the holo-protein. Both CYP3A4*1 and all mutant CYP3A4s metabolized radioactive testosterone into 6 β -OH testosterone as the only detectable metabolite (Fig. 1). CYP3A4-P189S exhibited a lower turnover number (1.9 nmol/min/nmol) than CYP3A4*1 (7.03 nmol/min/nmol) ($P < 0.05$). Conversely, CYP3A4-L293P metabolized testosterone at a higher rate

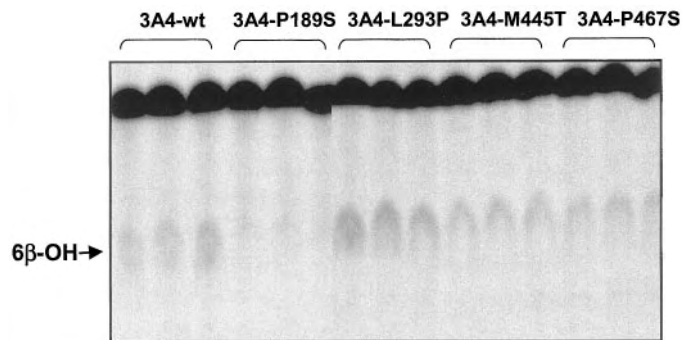


Fig. 1. Metabolism of testosterone by CYP3A4s. TLC profile of testosterone hydroxylation assay. Purified recombinant CYP3A4 wild-type and mutant proteins (10 pmol) were reconstituted and incubated with ¹⁴C-testosterone (25 μ M) for 5 min as described under *Materials and Methods*. Each assay was run in triplicate. 6 β -OH testosterone was the only metabolite detected in significant amounts.

(12.4 nmol/min/nmol) than CYP3A4*1 ($P < 0.05$) (Fig. 2). The turnover numbers for M445T and P457S were 5.8 and 5.9 nmol/min/nmol, respectively.

Chlorpyrifos Metabolism. The active metabolite chlorpyrifos-oxon and the inactive product trichloropyridinol were the major metabolites of chlorpyrifos by CYP3A4 (Figs. 3 and 4). The mutant allele L293P exhibited an increased turnover number for both metabolites ($P < 0.01$). In contrast, the F189S allele exhibited a lower turnover number for formation of both CPO

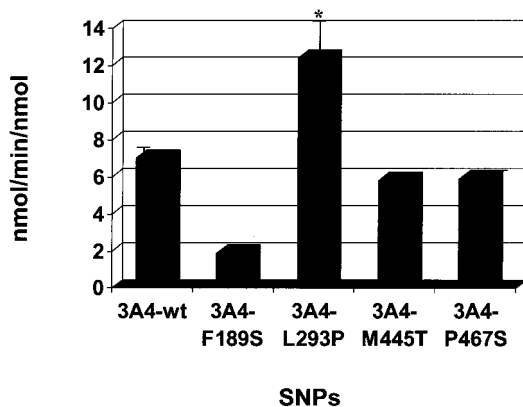


Fig. 2. Metabolism of testosterone. 6 β -OH-testosterone is the principle metabolite produced by CYP3A4*1 and its allelic variants. Purified recombinant CYP3A4 wild-type and mutant proteins (10 pmol) were reconstituted and incubated with testosterone (25 μ M) for 5 min as described under *Materials and Methods*. The turnover numbers for CYP3A4*1, F189S, L293P, M445T, and P457S are 7.03, 1.9 ($P < 0.05$), 12.4 ($P < 0.05$), 5.8, and 5.9 nmol/min/nmol, respectively.

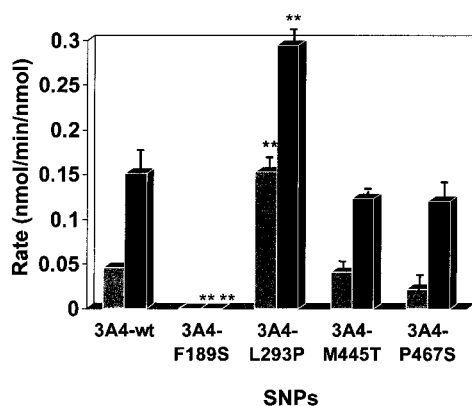


Fig. 3. Metabolism of chlorpyrifos CYP3A4 metabolizes chlorpyrifos into TCP (□) and CPO (■). CYP3A4s (100 pmol) were reconstituted and were then incubated with 100 μ M chlorpyrifos in 100 mM potassium phosphate buffer with 3.3 mM $MgCl_2$ (pH 7.4) with the NADPH generating system (the final concentration was 0.25 mM NADP, 2.5 mM glucose 6-phosphate, and 2 U/ml glucose-6-phosphate dehydrogenase) for 30 min. The metabolites of chlorpyrifos-oxon (CPO) and trichloropyridinol (TCP) were analyzed by HPLC.

and TCP. The remaining two alleles did not significantly change the turnover numbers for either metabolite.

Model of CYP3A4. CYP3A4 was aligned with rabbit CYP2C5. Figure 5 shows the results of modeling CYP3A4 based on the known crystal structure of CYP2C5 (protein database entry: 1DT6). Mutations are indicated in blue. The heme is indicated in purple and the substrate testosterone in gray. The identified variants are predicted from the model to be located near the following identified structural features; R162Q is located at the end of helix D, F189S at the end of helix E, L293P is at the beginning of helix I, M445T at the beginning at helix L and P467S in a β -sheet near the C terminus of the protein. The M445T SNP is located on the other side of the heme from the ligand binding site and helix I. Side chains of residues F189, L292, and P467 are largely buried and packed into the interior of the protein. Side chains of residues R162 and M445 are largely surface exposed.

Discussion

CYP3A4 is known to metabolize many clinically important drugs, such as rifampicin, cyclosporine, and ritonavir (Kolars et al., 1992; Boxenbaum, 1999; Guengerich, 1999; Hesse et al., 2001) as well as endogenous compounds such as testosterone (Wang et al., 1997). The distribution of metabolism of CYP3A substrates is unimodal but metabolism of these sub-

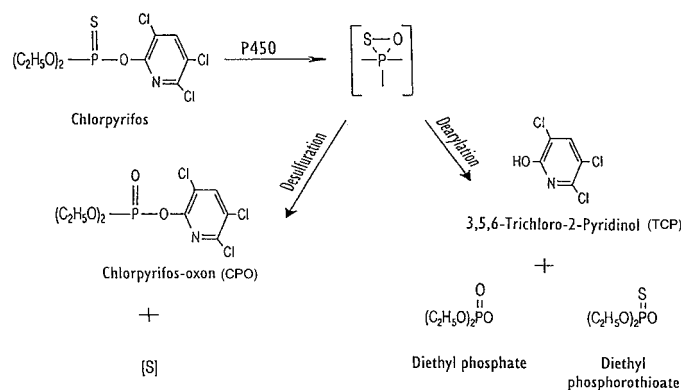


Fig. 4. Metabolic pathway of chlorpyrifos by P450.

strates shows at least a 10-fold variability in vivo (Thummel et al., 1996). Some variability may be due to the inducibility of the CYP3A4 gene by drugs and environmental chemicals. However, some of this variability is believed to be due to genetic factors. A previous study found a S222P allele in Finnish Caucasians and a M445T allele in Chinese (Sata et al., 2000). A very recent study identified seven new polymorphisms in European Caucasians (Eiselt et al., 2001). Two of these alleles, S222P and L373F, have been reported to affect catalytic activities toward certain substrates (Sata et al., 2000; Eiselt et al., 2001).

In the present study, we sequenced the coding regions and intron-exon junctions of CYP3A4 in DNAs from three different racial groups. Each racial group had been selected to represent ethnic diversity. A total of 28 SNPs in CYP3A4 were detected. Five SNPs produced amino acid substitutions including R162Q in exon 6; F189S in exon 7; L293P in exon 10; M445T in exon 12; and P467S in exon 12. Four of these are newly described alleles. Only the M445T allele had previously been reported (Sata et al., 2000; Eiselt et al., 2001). P189S and M445T were detected only in Caucasians in our study with frequencies of 2% and 4%, respectively. However, M445T has also been reported in Asians (Sata et al., 2000), indicating it is of ancient ancestry. The L293P and P467S alleles were found only in Asians, both at frequencies of 2% (L293 occurred in Chinese with a frequency of 10% while P467S occurred in Indo-Pakistani with a frequency of 12.5%). The coding change R162Q occurred only in African-Americans. In both individuals, this SNP was associated with an SNP in intron 10 (bp 169228) of the gene, in intron 7 (bp 164751), and in intron 11 (bp 172079). However, these intron SNPs were more frequent than the R162Q SNP in Africans. Interestingly, all alleles in African pygmies, and the majority (19/28) of alleles in African-Americans carried the SNP in intron 10 (bp 169228), which was not frequent in Caucasians. This SNP was also frequent in Asians (37.5%), indicating that it is associated with an ancient allele. The intron 7 SNP was also frequent in Africans (50% of the samples).

Testosterone and the OP insecticide chlorpyrifos were used as two examples of substrates for CYP3A4 to test effects of the coding mutations on function. The CYP3A4 active site is large (He et al., 1997), which explains its ability to metabolize a wide group of structurally diverse pharmacores (Elkins et al., 1999). Testosterone was selected as an example of a spatially large molecule that is metabolized by CYP3A4. Coding polymorphisms might potentially affect orientation of large substrates preferentially over their effects on binding of smaller substrates. Interestingly, the F189S and L293P mutations affected metabolism of both substrates in a similar fashion. The F189S allele exhibited significantly lower turnover numbers for both testosterone and chlorpyrifos than wild-type CYP3A4, while the L293P allele exhibited higher turnover numbers for both substrates. These results indicated that individuals might potentially have alterations in their ability to metabolize not only testosterone but potentially other pharmacores. Future studies will address metabolism of clinically important drugs.

Based on comparisons of the model of CYP3A4 with the crystal structure of CYP2C5, we would predict that the mutation at L293P is at the beginning of the I helix while residue F189S is at the end of helix E. These residues are not predicted to reside in the active-site cavity where they would

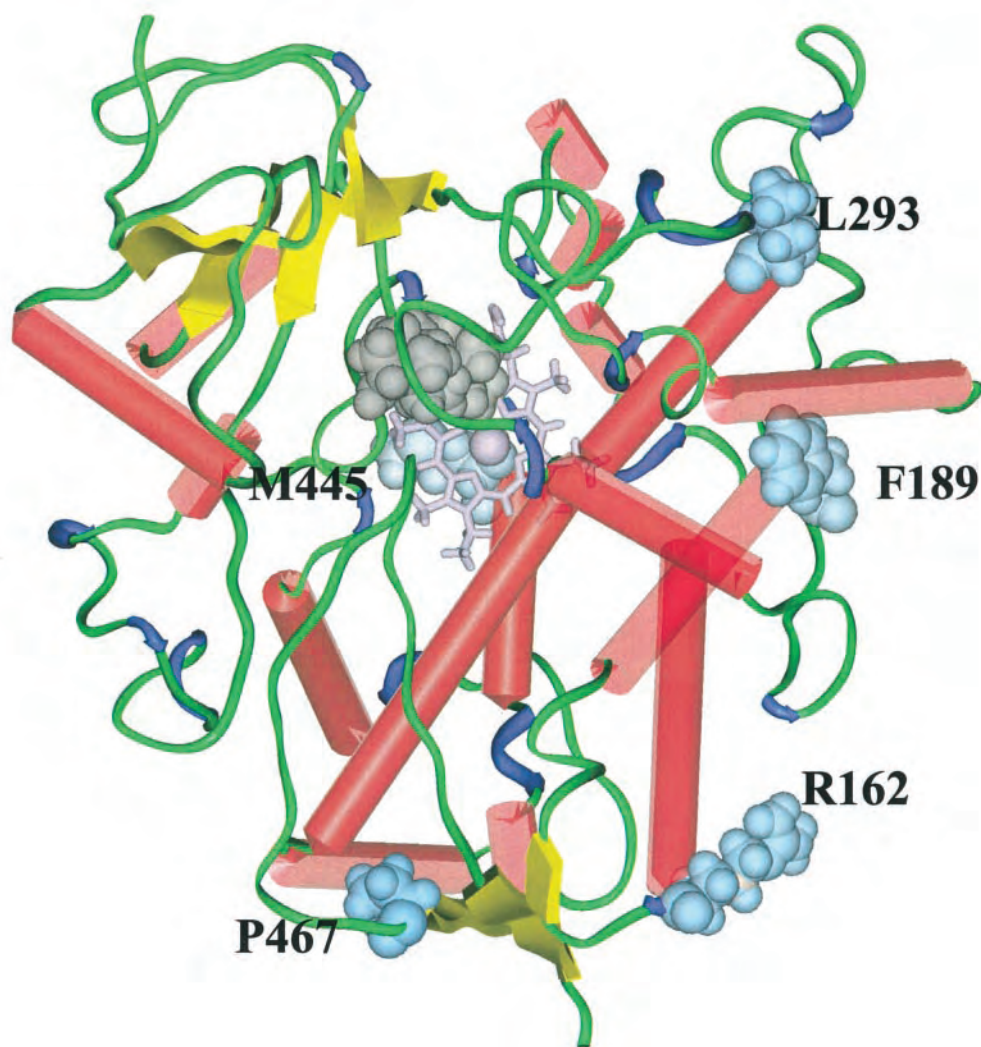


Fig. 5. Crystal structure of CYP3A4 showing locations of amino acid variants. Ribbon diagram of the molecular model of the human cytochrome P450 3A4 based on the solved x-ray crystal structure of the rabbit microsomal cytochrome P450 2C5 (protein database entry: 1DT6) (Williams et al., 2000). Complete side chains are shown in blue for the identified SNPs. The substrate testosterone is shown in gray docked in the enzyme active site. The heme is shown in purple.

directly interact with the substrate. However, the residues are nonconservative mutations in tightly packed regions, which could conceivably affect the conformation of the protein, substrate access, and/or catalytic activity. Our results indicating that the M445T mutation has no effect on testosterone or chlorpyrifos metabolism are consistent with the very recent report by Eiselt et al. (2001) using testosterone and progesterone as substrates. Modeling based on the crystal structure of CYP2C5 predicts that the M445T SNP is located in close proximity to the heme, but it is on the opposite side of the heme from the ligand binding site on helix I. This is consistent with the data indicating that this mutation may not affect catalytic activity.

CYP3A4 is important in the metabolism of environmental compounds as well as clinically important drugs. CYP3A4 is known to activate the OP insecticides parathion and chlorpyrifos into oxons that are neurotoxicants (Butler and Murray, 1997; Tang et al., 2001) (Fig. 5). CYP3A4 also inactivates chlorpyrifos into 2,3,5-trichloro-2-pyridinol. The relative rates of activation and inactivation are critical to the toxicity of the compound. The L293P allele could possibly increase

the toxicity of OP insecticides to individuals carrying this allele. Interestingly, the F189S allele decreased both activation and inactivation of chlorpyrifos and could also potentially affect toxicity after exposure to OP insecticides. In addition, CYP3A4 can activate aflatoxin B₁ into the reactive form, aflatoxin B₁-8, 9-epoxide, which is a mutagen (Gallagher et al., 1996; Chen et al., 1998). Thus polymorphisms of CYP3A4 could potentially influence the risk of different populations from various environmental compounds.

In summary, five coding polymorphisms in *CYP3A4* were identified as M445T (*CYP3A4**3), R162Q(*CYP3A4**15), F189S (*CYP3A4**16), L293P(*CYP3A4**17), and P467S (*CYP3A4**18) by resequencing 72 individuals from three diverse racial groups.¹ Four of these represent newly described *CYP3A4* alleles. Two SNPs occurred in Caucasians (F189S

¹New CYP3A4 alleles were submitted to the CYP allele web page (www.imm.ki.se/CYPalleles). The names designated by the international nomenclature committee are *CYP3A4**17 (F189S) and *CYP3A4**18 (L292P and *CYP23A4**19 (P467S)). R162Q was submitted to the CYP3A4 allele web page by another laboratory while this work was in progress and was designated *CYP3A4**15 but has not yet been published otherwise.

and M445T), while two occurred in Asians (L293P and P467S). M445T has also been reported previously in Asians. One coding SNP R162Q was detected only in African-Americans. Testosterone and the OP insecticide chlorpyrifos were selected to assess their catalytic activities of four new alleles. The F189L allele exhibited significantly a lower turnover number for both substrates than CYP3A4*1, while the L293P allele metabolized both substrates with a higher turnover number. Potentially, these alleles may contribute to the known variability in metabolism of clinically used drugs and environmental compounds that are CYP3A4 substrates. Future studies will examine a wider range of CYP3A4 substrates including clinically used drugs.

Acknowledgments

We thank Dr. F. J. Gonzalez for supplying the CYP3A4 cDNA. We also thank Drs. J. R. Halpert and Y. A. He for the detailed methods for testosterone metabolism. We thank Dr. Eric Johnson for helpful discussions on the location of the two mutations that affect catalytic activity. Dr. Stephen Ferguson, Dr. Cheng-Chung Tsao, and Joyce A. Blaisdell contributed helpful comments, and Dr. L Wojnowski provided a preprint of the paper by Eiselt and coworkers.

References

- Aoyama T, Yamano S, Waxman DJ, Lapenson DP, Meyer UA, Fischer V, Tyndale R, Inaba T, Kalow W, Gelboin HV, et al. (1989) Cytochrome P-450 hPCN3, a novel cytochrome P-450 IIIA gene product that is differentially expressed in adult human liver. cDNA and deduced amino acid sequence and distinct specificities of cDNA-expressed hPCN1 and hPCN3 for the metabolism of steroid hormones and cyclosporine. *J Biol Chem* **264**:10388–10395.
- Ball SE, Scatina J, Kao J, Ferron GM, Frunzillo R, Mayer P, Weinryb I, Guida M, Hopkins PJ, Warner N, and Hall J (1999) Population distribution and effects on drug metabolism of a genetic variant in the 5' promoter region of CYP3A4. *Clin Pharmacol Ther* **66**:288–294.
- Boxenbaum H (1999) Cytochrome P450 3A4 in vivo ketoconazole competitive inhibition: determination of Ki and dangers associated with high clearance drugs in general. *J Pharm Pharm Sci* **2**:47–52.
- Butler AM and Murray M (1997) Biotransformation of parathion in human liver: participation of CYP3A4 and its inactivation during microsomal parathion oxidation. *J Pharmacol Exp Ther* **280**:966–973.
- Chambers HW (1992) Organophosphorus compounds: an overview, in *Organophosphates: Chemistry, Fate and Effects* (Chambers JE and Levi PE eds) p 317, Academic Press, San Diego, CA.
- Chen Q, Wu J, and Yu Y (1998) [Establishment of transgenic cell line CHL-3A4 and its metabolic activation]. *Zhonghua Yu Fang Yi Xue Za Zhi* **32**:281–284.
- Dai D, Zeldin D, Blaisdell JA, Coulter SJ, Ghanayem BI, and Goldstein JA (2001) Genetic polymorphisms of CYP2C8 decrease the metabolism of the anticancer drug taxol and arachidonic acid. *Pharmacogenetics* **11**:597–607.
- Dawson JM and Heatlie PL (1984) Lowry method of protein quantification: evidence for photosensitivity. *Anal Biochem* **140**:391–393.
- de Wildt SN, Kearns GL, Leeder JS, and van den Anker JN (1999) Cytochrome P450 3A: ontogeny and drug disposition. *Clin Pharmacokinet* **37**:485–505.
- Eaton DL (2000) Biotransformation enzyme polymorphism and pesticide susceptibility. *Neurotoxicology* **21**:101–111.
- Eiselt R, Domanski TL, Zibat A, Mueller R, Presecan-Siedel E, Hustert E, Zanger UM, Brockmoller J, Klenk HP, Meyer UA, et al. (2001) Identification and functional characterization of eight CYP3A4 protein variants. *Pharmacogenetics* **11**:447–458.
- Ekins S, Bravi G, Wikel JH, and Wrighton SA (1999) Three-dimensional-quantitative structure activity relationship analysis of cytochrome P-450 3A4 substrates. *J Pharmacol Exp Ther* **291**:424–433.
- Felix CA, Walker AH, Lange BJ, Williams TM, Wimick NJ, Cheung NK, Lovett BD, Nowell PC, Blair IA, and Rebbeck TR (1998) Association of CYP3A4 genotype with treatment-related leukemia. *Proc Natl Acad Sci USA* **95**:13176–13181.
- Gallagher EP, Kunze KL, Stapleton PL, and Eaton DL (1996) The kinetics of aflatoxin B1 oxidation by human cDNA-expressed and human liver microsomal cytochromes P450 1A2 and 3A4. *Toxicol Appl Pharmacol* **141**:595–606.
- Gellner K, Eiselt R, Hustert E, Arnold H, Koch I, Haberl M, Deglmann CJ, Burk O, Buntfuss D, Escher S, et al. (2001) Genomic organization of the human CYP3A locus: identification of a new, inducible CYP3A gene. *Pharmacogenetics* **11**:111–121.
- Gotoh O (1992) Substrate recognition sites in cytochrome P450 family 2 (CYP2)

- proteins inferred from comparative analyses of amino acid and coding nucleotide sequences. *J Biol Chem* **267**:83–90.
- Guengerich FP (1999) Cytochrome P-450 3A4: regulation and role in drug metabolism. *Annu Rev Pharmacol Toxicol* **39**:1–17.
- He YA, He YQ, Szklarz GD, and Halpert JR (1997) Identification of three key residues in substrate recognition site 5 of human cytochrome P450 3A4 by cassette and site-directed mutagenesis. *Biochemistry* **36**:8831–8839.
- Hesse LM, Venkatakrisnan K, von Moltke LL, Shader RI, and Greenblatt DJ (2001) CYP3A4 is the major CYP isoform mediating the in vitro hydroxylation and demethylation of flunitrazepam. *Drug Metab Dispos* **29**:133–140.
- Hsieh KP, Lin YY, Cheng CL, Lai ML, Lin MS, Siest JP, and Huang JD (2001) Novel mutations of CYP3A4 in Chinese. *Drug Metab Dispos* **29**:268–273.
- Kitada M, Kamataki T, Itahashi K, Rikihisa T, Kato R, and Kanakubo Y (1985) Purification and properties of cytochrome P-450 from homogenates of human fetal livers. *Arch Biochem Biophys* **241**:275–280.
- Kolars JC, Schmiedlin-Ren P, Schuetz JD, Fang C, and Watkins PB (1992) Identification of rifampin-inducible P450III A4 (CYP3A4) in human small bowel enterocytes. *J Clin Invest* **90**:1871–1878.
- Kuehl P, Zhang J, Lin Y, Lamba J, Assem M, Schuetz J, Watkins PB, Daly A, Wrighton SA, Hall SD, et al. (2001) Sequence diversity in CYP3A promoters and characterization of the genetic basis of polymorphic CYP3A5 expression. *Nat Genet* **27**:383–391.
- Lewis DF (1998) The CYP2 family: models, mutants and interactions. *Xenobiotica* **28**:617–661.
- Lown KS, Kolars JC, Thummel KE, Barnett JL, Kunze KL, Wrighton SA, and Watkins PB (1994) Interpatient heterogeneity in expression of CYP3A4 and CYP3A5 in small bowel. Lack of prediction by the erythromycin breath test. *Drug Metab Dispos* **22**:947–955.
- Nickerson DA, Tobe VO, and Taylor SL (1997) PolyPhred: automating the detection and genotyping of single nucleotide substitutions using fluorescence-based resequencing. *Nucleic Acids Res* **25**:2745–2751.
- Oesterheld JR (1998) A review of developmental aspects of cytochrome P450. *J Child Adolesc Psychopharmacol* **8**:161–174.
- Rebbeck TR (2000) More about: modification of clinical presentation of prostate tumors by a novel genetic variant in CYP3A4. *J Natl Cancer Inst* **92**:76.
- Rebbeck TR, Jaffe JM, Walker AH, Wein AJ, and Malkowicz SB (1998) Modification of clinical presentation of prostate tumors by a novel genetic variant in CYP3A4. *J Natl Cancer Inst* **90**:1225–1229.
- Rieder MJ, Taylor SL, Tobe VO, and Nickerson DA (1998) Automating the identification of DNA variations using quality-based fluorescence re-sequencing: analysis of the human mitochondrial genome. *Nucleic Acids Res* **26**:967–973.
- Sata F, Sapone A, Elizondo G, Stocker P, Miller VP, Zheng W, Raunio H, Crespi CL, and Gonzalez FJ (2000) CYP3A4 allelic variants with amino acid substitutions in exons 7 and 12: evidence for an allelic variant with altered catalytic activity. *Clin Pharmacol Ther* **67**:48–56.
- Schuetz JD, Beach DL, and Guzelian PS (1994) Selective expression of cytochrome P450 CYP3A mRNAs in embryonic and adult human liver. *Pharmacogenetics* **4**:11–20.
- Shen MJ, Jones I, and Mohrenweiser HW (1998) Non-conservative amino acid substitutions exist at polymorphic frequency in DNA repair genes. *Cancer Res* **58**:604–608.
- Shimada T, Gillam EM, Sandhu P, Guo Z, Tukey RH, and Guengerich FP (1994) Activation of procarcinogens by human cytochrome P450 enzymes expressed in *Escherichia coli*. Simplified bacterial systems for genotoxicity assays. *Carcinogenesis* **15**:2523–2529.
- Tang J, Cao Y, Rose RL, Brimfield AA, Dai D, Goldstein JA, and Hodgson E (2001) Metabolism of chlorpyrifos by human cytochrome p450 isoforms and human, mouse, and rat liver microsomes. *Drug Metab Dispos* **29**:1201–1204.
- Thummel KE, O'Shea D, Paine MF, Shen DD, Kunze KL, Perkins JD, and Wilkinson GR (1996) Oral first-pass elimination of midazolam involves both gastrointestinal and hepatic CYP3A-mediated metabolism. *Clin Pharmacol Ther* **59**:491–502.
- Thummel KE and Wilkinson GR (1998) In vitro and in vivo drug interactions involving human CYP3A. *Annu Rev Pharmacol Toxicol* **38**:389–430.
- Wandel C, Witte JS, Hall JM, Stein CM, Wood AJ, and Wilkinson GR (2000) CYP3A activity in African-American and European American men: population differences and functional effect of the CYP3A4*1B5' promoter region polymorphism. *Clin Pharmacol Ther* **68**:82–91.
- Wang RW, Newton DJ, Scheri TD, and Lu AY (1997) Human cytochrome P450 3A4-catalyzed testosterone 6 beta-hydroxylation and erythromycin N-demethylation. Competition during catalysis. *Drug Metab Dispos* **25**:502–507.
- Westlind A, Malmbo S, Johansson I, Otter C, Andersson TB, Ingelman-Sundberg M, and Oscarson M (2001) Cloning and tissue distribution of a novel human cytochrome p450 of the cyp3a subfamily, cyp3a43. *Biochem Biophys Res Commun* **281**:1349–1355.
- Williams PA, Cosme J, Sridhar V, Johnson EF, and McRee DE (2000) Mammalian microsomal cytochrome P450 monooxygenase: structural adaptations for membrane binding and functional diversity. *Mol Cell* **5**:121–131.

Address correspondence to: Dr. Joyce A. Goldstein, Laboratory of Pharmacology and Chemistry, National Institute of Environmental Health Sciences, P.O. Box 12233, Research Triangle Park, NC 27709. E-mail: goldst1@niehs.nih.gov

Inhibition of Fipronil and Nonane Metabolism in Human Liver Microsomes and Human Cytochrome P450 Isoforms by Chlorpyrifos

Hyun Joo, Kyoungju Choi, Randy L. Rose,[†] and Ernest Hodgson

Department of Environmental and Molecular Toxicology, North Carolina State University, Raleigh, NC 27695, USA;
E-mail: ernest.hodgson@ncsu.edu

Received 30 January 2007; revised 1 February 2007; accepted 4 February 2007

ABSTRACT: Previous studies have established that chlorpyrifos (CPS), fipronil, and nonane can all be metabolized by human liver microsomes (HLM) and a number of cytochrome P450 (CYP) isoforms. However, metabolic interactions between these three substrates have not been described. In this study the effect of either coincubation or preincubation of CPS with HLM or CYP isoforms with either fipronil or nonane as substrate was investigated. In both co- and preincubation experiments, CPS significantly inhibited the metabolism of fipronil or nonane by HLM although CPS inhibited the metabolism of fipronil more effectively than that of nonane. CPS significantly inhibited the metabolism of fipronil by CYP3A4 as well as the metabolism of nonane by CYP2B6. In both cases, preincubation with CPS caused greater inhibition than coincubation, suggesting that the inhibition is mechanism based. © 2007 Wiley Periodicals, Inc. *J Biochem Mol Toxicol* 21:76–80, 2007; Published online in Wiley InterScience (www.interscience.wiley.com). DOI 10:1002/jbt.20161

KEYWORDS: Fipronil; Nonane; Human Liver Microsomes; Cytochrome P450; CYP2B6; CYP3A4

INTRODUCTION

In previous studies, Tang et al. [1] have demonstrated that human liver microsomes (HLM) have the ability to metabolize fipronil, an insecticide of the phenyl pyrazole family, to fipronil sulfone, the predom-

inant metabolite. It was also shown that cytochrome P450 (CYP) 3A4 was the major isoform for fipronil sulfone production in humans, although CYP2C19 contributed but was less active. In addition, nonane, a component of jet-propulsion fuel 8 (JP-8) and other fossil fuels, is metabolized to 2-nonanol and 2-nonanone by HLM, and that CYP2B6 and 2E1 are primarily responsible for this activity. In addition, CYP1A2 is also responsible for 2-nonanol production [2].

Recently, it has been established that organophosphorus insecticides containing the P=S moiety are potent inhibitors of the metabolism of both xenobiotics and endogenous substrates by HLM and by specific human CYP isoforms [3]. For example, chlorpyrifos (CPS), an organophosphorus insecticide, inhibited the metabolism of carbaryl, *N,N*-diethyl-*m*-toluamide (DEET), testosterone, and estradiol in HLM as well as by specific human CYP isoforms [4–7]. However, metabolic interactions between CPS and fipronil, as well as between CPS and nonane, have not been described previously.

The main objective of this study was to investigate the effects of CPS on fipronil or nonane metabolism in pooled HLM and by selected CYP isoforms.

MATERIALS AND METHODS

Chemicals

Fipronil, fipronil sulfone, and chlorpyrifos (CPS) were purchased from Chem Service (West Chester, PA). Nonane, 2-nonanol, and 2-nonanone were purchased from Sigma-Aldrich (St. Louis, MO). Acetonitrile, methanol, methylene chloride, and acetic acid were purchased from Fisher Scientific (Pittsburgh, PA).

Correspondence to: Ernest Hodgson.

Contract Grant Sponsor: US Army.

Contract Grant Number: DAMD 17-00-1-0008.

[†]Deceased. Dr. Rose died in a tragic accident on May 23, 2006.

© 2007 Wiley Periodicals, Inc.

Pooled Human Liver Microsomes and P450 Isoforms

Pooled HLM from 18 donors (11 males and 7 females) and cytochrome P450 (CYP) 2B6 and 3A4 SUPERSOMES™ were purchased from BD Biosciences (Woburn, MA). Final concentrations used were 1 mg protein/mL for pHLM and 20 pmol P450/mL for CYP isoforms.

Inhibition of Fipronil by Chlorpyrifos

The *in vitro* assay used by Tang et al. [1] was utilized in these experiments. Fipronil (final concentration, 80 μ M) was incubated with pHLM or CYP3A4 in 100 mM Tris buffer (pH 7.4) or 50 mM potassium-phosphate buffer, 3.3 mM MgCl₂ (pH 7.4), respectively. After 5 min of incubation at 37°C, coincubation was initiated by adding a mixture of CPS (0.25–50 μ M) and fipronil in the presence of an NADPH-regenerating system consisting of 0.25 mM NADP, 2.5 mM glucose-6-phosphate, and 2 U/mL glucose-6-phosphate dehydrogenase. After 15 min of incubation, the reaction was terminated by the addition of 250 μ L methanol, followed by centrifugation at 21,000 \times *g* for 5 min. Supernatants were collected and kept at 4°C until used. New preincubation was initiated by adding pHLM or CYP3A4 to the mixture containing varying concentrations of CPS (0.25–50 μ M or 0.25–10 μ M, respectively) and the NADPH-regenerating system. After 30 min of preincubation, fipronil was added to the reaction and incubated for 15 min. The subsequent sample preparation steps were as described in the coincubation experiments. The experiments were carried out in duplicate.

Inhibition of Nonane by Chlorpyrifos

The *in vitro* assay of Edwards et al. [2] was modified as follows: nonane (final concentration, 50 μ M) was incubated with pHLM or CYP2B6 in potassium-phosphate buffer, 3.3 mM MgCl₂ (100 or 50 mM, respectively). After 5 min of incubation at 37°C, coincubation was initiated by adding CPS (0.25–50 μ M) in the presence of the NADPH-regenerating system and incubated for 15 min. Preincubation was initiated by the addition of pHLM or CYP2B6 to the mixture containing varying concentrations of CPS (0.25–50 μ M or 0.25–10 μ M, respectively) and the NADPH-regenerating system. At the end of 30-min preincubation, nonane was added to the reaction mixture and then further incubated for 15 min. After co- or preincubation, the reaction was stopped by adding 100 μ L of methylene chloride, followed by centrifugation at 21,000 \times *g* for 5 min. The methylene chloride extracts were directly analyzed on GC/FID. The experiments were carried out in duplicate.

HPLC Analysis

A Waters HPLC system (Milford, MA) was used for analysis. This system consisted of a 2996 separation module and a 2695 photodiode array detector. Fipronil and fipronil sulfone were analyzed by a method previously reported [1]. Briefly, the isocratic system was 30% water (A) containing 0.05 M acetic acid and 70% methanol (B), the flow rate was 1 mL/min and the injection volumes were 30 μ L. A Phenomenex Synergi Polar-RP column (4 μ m, 150 \times 4.6 mm, Rancho Palos Verdes, CA) was used to separate fipronil and fipronil sulfone, which were detected at 280 and 275 nm, respectively. The retention times and method detection limits were 5.5 min and 0.048 μ M for fipronil, and 7.1 min and 0.046 μ M for fipronil sulfone, respectively.

GC Analysis

The GC/FID system consisted of a Hewlett Packard (currently Agilent Technologies) 7673 auto injector, 5890 Series II GC system, RESTEK RTX®-1701 column (30 m, 0.25 mm i.d.), and a flame ionization detector (FID). The injection port and detection temperatures were set at 250°C and 280°C, respectively. The oven temperature was programmed to rise from 40°C to 80°C at a rate of 6°C/min, from 80°C to 120°C at a rate of 3°C/min, followed by a rate of 15°C/min until a temperature of 270°C was reached. Helium was used as a carrier gas at a flow rate of 1 mL/min. Nonane, 2-nonanone, and 2-nonanol were measured at 7.5, 18.1, and 18.5 min and their method detection limits were 0.071, 0.069, and 0.096 μ M, respectively. The linear range ($r^2 > 0.99$) of the assay was 1–100 μ M for a 2- μ L injection. In addition, chlorpyrifos (CPS) was detected at 34.7 min.

Statistical Analysis

Fisher's protected least significant difference (LSD) was used to separate means at the 5% level. All statistical analyses were done with PC SAS for Windows®, version 8.2 [8].

RESULTS

Inhibition of Fipronil Metabolism in pHLM and CYP3A4 by Chlorpyrifos

The result of co- and preincubation of chlorpyrifos (CPS) with fipronil is shown in Figure 1. Coincubation of fipronil (80 μ M) with increasing concentrations of CPS (0.25–50 μ M) in pHLM resulted in decreased production of fipronil sulfone (Figure 1A). Except at 0.25 μ M CPS, all concentrations of CPS employed

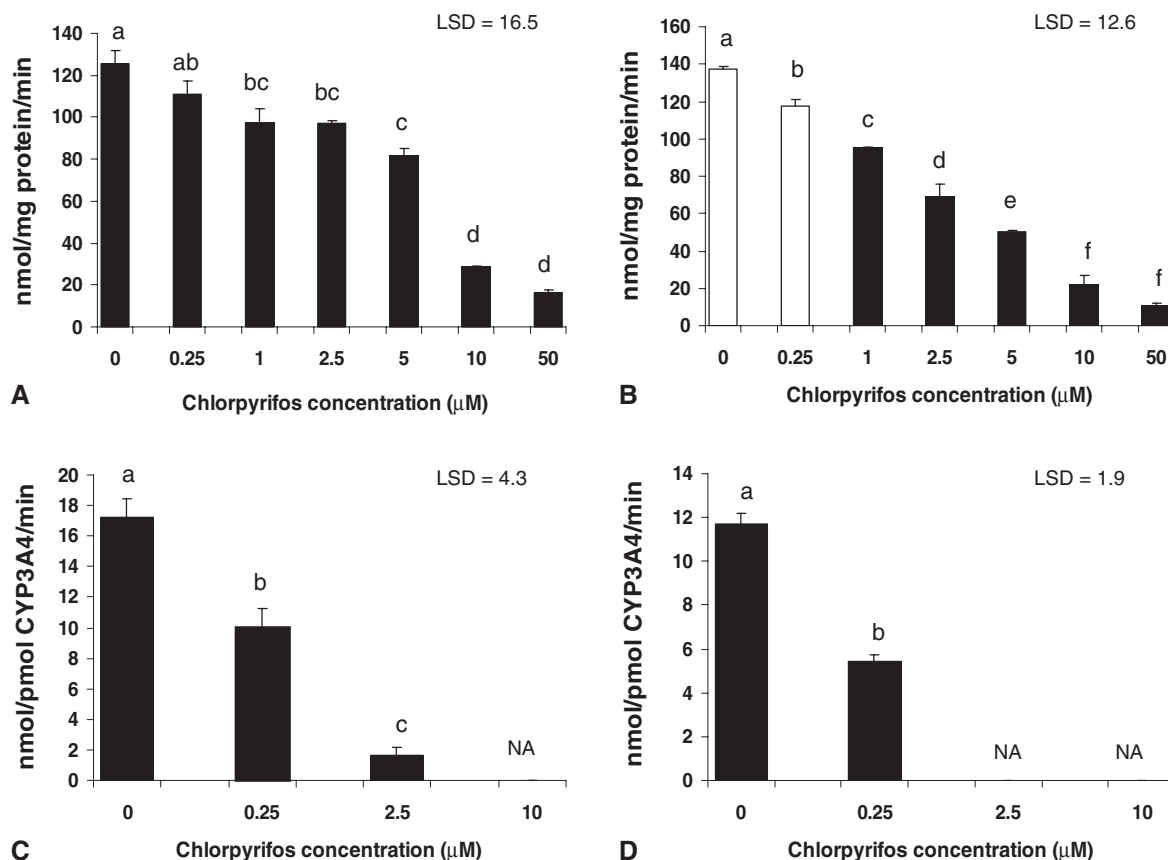


FIGURE 1. The effects of chlorpyrifos (CPS) on fipronil sulfone production in pHLM and cytochrome P450 (CYP) 3A4: (A) coincubation of chlorpyrifos with fipronil in pHLM, (B) preincubation of chlorpyrifos in pHLM before incubation with fipronil, (C) coincubation of chlorpyrifos with fipronil in CYP3A4, and (D) preincubation of chlorpyrifos in CYP3A4 before incubation with fipronil. Activities are represented as mean (nmol product/mg microsome protein per min) \pm S.E. for (A) and (B) and mean (nmol product/pmol CYP3A4 per min) \pm S.E. for (C) and (D) ($n = 2$). Means followed by the same letter are not significantly different (least significant difference [LSD] = 5%). Not available (NA).

significantly inhibited the metabolism of fipronil in pHLM. At the two highest concentrations of CPS (10 and 50 μM), the production of fipronil sulfone was decreased by approximately 77% and 87%, respectively. The ability of pHLM to metabolize fipronil was also reduced by preincubation of pHLM with CPS (Figure 1B), which showed significant inhibition of fipronil metabolism at all concentrations of CPS (0.25–50 μM), demonstrating that preincubation with CPS caused more significant inhibition than coincubation with CPS.

As also shown in Figures 1C and 1D, metabolism of fipronil was significantly inhibited by both co- and preincubations of CYP3A4 with CPS (0.25–10 μM). The role of CYP3A4 in the metabolism of fipronil was verified by co- and preincubations of CPS with fipronil. At the lowest concentration of 0.25 μM CPS, the production of fipronil decreased by 43% and 54% in co- and preincubations of CYP3A4, respectively. Preincubation with CPS caused greater inhibition than coincubation since fipronil sulfone was not found at 2.5 and 10 μM

CPS, probably because it was below the method detection limit.

Inhibition of Nonane Metabolism in pHLM and CYP2B6 by Chlorpyrifos

Figure 2 shows the results for co- and preincubations of chlorpyrifos (CPS) with 50 μM nonane. For the co- and preincubations in pHLM with CPS (Figures 2A and 2B, respectively), a significant inhibition of nonane metabolism is shown in both cases, throughout all CPS concentrations employed (0.25–50 μM), although preincubation with CPS caused greater inhibition than coincubation. The production of 2-nonanone and 2-nonanol indicates that there was no statistically significant difference in the increase in inhibition from 2.5 to 50 μM CPS and 0.25 to 50 μM CPS for co- and preincubation, respectively.

CPS also significantly inhibited the metabolism of nonane by CYP2B6. In coincubation of CYP2B6 with CPS, the production of 2-nonanol and 2-nonane

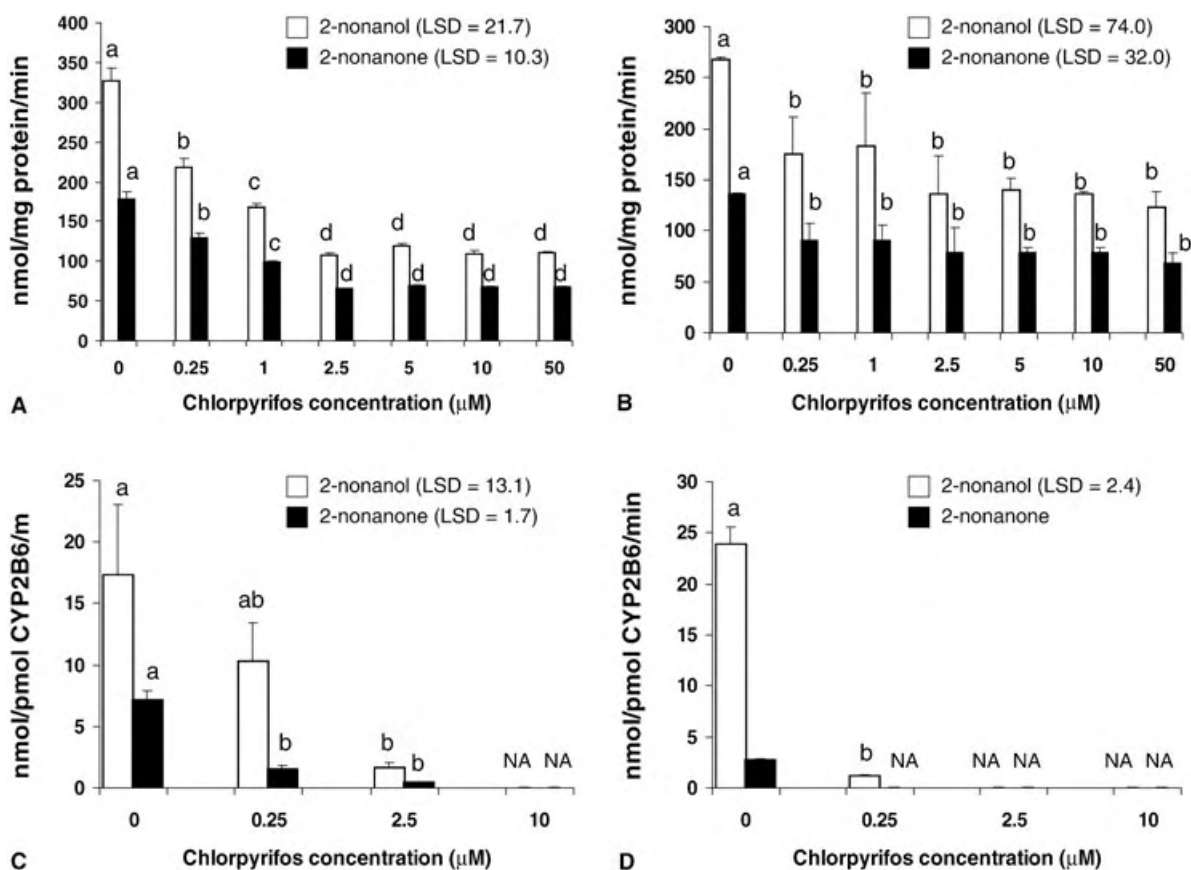


FIGURE 2. The effects of chlorpyrifos (CPS) on 2-nonanol and 2-nonanone production in pHLM and cytochrome P450 (CYP) 2B6: (A) coincubation of chlorpyrifos with nonane in pHLM, (B) preincubation of chlorpyrifos in pHLM before incubation with nonane, (C) coincubation of chlorpyrifos with nonane in CYP2B6, and (D) preincubation of chlorpyrifos in CYP2B6 before incubation with nonane. Activities are represented as mean (nmol product/mg microsomal protein per min) \pm S.E. for (A) and (B) and mean (nmol product/pmol CYP2B6 per min) \pm S.E. for (C) and (D) ($n=2$). Means followed by the same letter are not significantly different for each metabolite (least significant difference [LSD]=5%). Not available (NA).

decreased with increasing concentrations of CPS (Figure 2C). Furthermore, neither metabolite was found at 10 μ M CPS. At 2.5 μ M CPS, the production of 2-nonanol and 2-nonanone decreased by 91% and 94%, respectively. Preincubation of CYP2B6 with CPS showed more significant inhibition of nonane metabolism than coincubation (Figure 2D). Except for 5% production of 2-nonanol at 0.25 μ M CPS in the preincubation experiments, 2-nonanol and 2-nonanone were not found at concentrations of 0.25, 2.5, and 10 μ M CPS.

DISCUSSION

Chlorpyrifos (CPS), fipronil, and nonane can all be metabolized by HLM and specific CYP isoforms [1,2,9]. In this study, metabolic interactions between CPS and fipronil, and CPS and nonane, were investigated. In both co- and preincubation experiments, CPS significantly inhibited the metabolism of fipronil

by pHLM as well as by CYP3A4, a result that is not surprising since CYP3A4 is the major CYP isoform metabolizing fipronil [1] and CPS is an irreversible noncompetitive inhibitor of human CYP isoforms [6,7,10]. This result is also correlated with the finding that CPS inhibits the formation of the CYP3A4-mediated metabolite 3-hydroxycarbofuran from carbofuran in HLM [10]. The importance of CYP3A4 in the metabolism of fipronil was further verified by co- and preincubation of CYP3A4 with CPS, which showed a significant inhibition by CPS in both cases, although preincubation caused greater inhibition than coincubation.

The effect of CPS on nonane metabolism was also investigated. When compared to controls, the production of 2-nonanol and 2-nonanone, followed by both co- and preincubation of pHLM with CPS, was decreased by more than 50% at a concentration of 2.5 μ M. However, further inhibition was not achieved with increasing CPS concentrations up to 50 μ M. Because nonane is readily metabolized to 2-nonanol and

2-nonanone in pHLM and by CYP isoforms, including 1A2, 2B6, 2E1 and alcohol dehydrogenase [2], it is likely that CPS inhibited CYP2B6 predominantly but is less effective as an inhibitor of other nonane-metabolizing enzymes. As further verification of the role of CYP2B6 in the metabolism of nonane, co- and preincubation of CYP2B6 with CPS was also carried out and, as shown in Figures 2C and 2D, CPS significantly inhibited the ability of CYP2B6 to metabolize nonane in both cases. This correlates with the finding that CYP2B6-mediated production of carbaryl methylol is inhibited by CPS. These results are most likely due to the release of reactive sulfur from CPS during activation to CPS oxon binding to the heme of CYP and inhibiting its activity [4,6,11,12].

In both co- and preincubation experiments, CPS significantly inhibited the metabolism of fipronil or nonane by pHLM although CPS inhibited the metabolism of fipronil more effectively than that of nonane. CPS also inhibited CYP3A4 and 2B6, the primary metabolizing enzymes of fipronil and nonane, respectively. In both cases, preincubation with CPS caused greater inhibition than coincubation, suggesting that the inhibition is time dependent and mechanism based.

ACKNOWLEDGMENTS

The authors thank Dr. Damian Shea for the use of GC/FID and Dr. Gail Mahnken for her technical assistance in the analysis of nonane.

REFERENCES

1. Tang J, Usmani KA, Hodgson E, Rose RL. In vitro metabolism of fipronil by human and rat cytochrome P450 and its interactions with testosterone and diazepam. *Chem Biol Interact* 2004;147:319–329.
2. Edwards JE, Rose RL, Hodgson E. The metabolism of nonane, a JP-8 jet fuel component, by human liver microsomes, P450 isoforms and alcohol dehydrogenase and inhibition of human P450 isoforms by JP-8. *Chem Biol Interact* 2005;151:203–211.
3. Hodgson E, Rose RL. Organophosphorus chemicals: Potent inhibitors for the human metabolism of steroid hormones and xenobiotics. *Drug Metab Rev* 2006;38:149–162.
4. Tang J, Cao Y, Rose RL, Hodgson E. In vitro metabolism of carbaryl by human cytochrome P450 and its inhibition by chlorpyrifos. *Chem Biol Interact* 2002;141:229–241.
5. Usmani KA, Rose RL, Goldstein JA, Taylor WG, Brimfield AA, Hodgson E. In vitro human metabolism and interactions of repellent, *N,N*-diethyl-*m*-toluamide (DEET). *Drug Metab Dispos* 2002;30:289–294.
6. Usmani KA, Rose RL, Hodgson E. Inhibition and activation of the human liver microsomal and human cytochrome P450 3A4 metabolism of testosterone by deployment-related chemicals. *Drug Metab Dispos* 2003;31:384–391.
7. Usmani KA, Cho TM, Rose RL, Hodgson E. Inhibition of the human liver microsomal and human cytochrome P450 1A2 and 3A4 metabolism of estradiol by deployment-related and other chemicals. *Drug Metab Dispos* 2006;34:1606–1614.
8. SAS. Procedures guide. Release 8.2. Cary, North Carolina: SAS Institute; 2001.
9. Tang J, Cao Y, Rose RL, Brimfield AA, Dai D, Goldstein JA, Hodgson E. Metabolism of chlorpyrifos by human cytochrome P450 isoforms and human, mouse, and rat liver microsomes. *Drug Metab Dispos* 2001;29:1201–1204.
10. Usmani KA, Hodgson E, Rose RL. In vitro metabolism of carbofuran by human, mouse, and rat cytochrome P450 and interactions with chlorpyrifos, testosterone, and estradiol. *Chem Biol Interact* 2004;150:221–232.
11. Neal RA. Microsomal metabolism of thiono-sulfur compounds: Mechanisms and toxicological significance. *Rev Biochem Toxicol* 1980;2:131–171.
12. Neal RA, Halpert J. Toxicology of thiono-sulfur compounds. *Annu Rev Pharmacol Toxicol* 1982;22:321–339.



The metabolism of nonane, a JP-8 jet fuel component, by human liver microsomes, P450 isoforms and alcohol dehydrogenase and inhibition of human P450 isoforms by JP-8

Jeffrey E. Edwards, Randy L. Rose, Ernest Hodgson*

Environmental and Molecular Toxicology, North Carolina State University, Box 7633, Raleigh, NC 27695, USA

Accepted 9 December 2004

Available online 19 January 2005

Abstract

Nonane, a component of jet-propulsion fuel 8 (JP-8), is metabolized to 2-nonanol and 2-nonanone by pooled human liver microsomes (pHLM). Cytochrome P450 (CYP) isoforms 1A2, 2B6 and 2E1 metabolize nonane to 2-nonanol, whereas alcohol dehydrogenase, CYPs 2B6 and 2E1 metabolize 2-nonanol to 2-nonanone. Nonane and 2-nonanol showed no significant effect on the metabolism of testosterone, estradiol or *N,N*-diethyl-*m*-toluamide (DEET), but did inhibit carbaryl metabolism. JP-8 showed modest inhibition of testosterone, estradiol and carbaryl metabolism, but had a more significant effect on the metabolism of DEET. JP-8 was shown to inhibit CYPs 1A2 and 2B6 mediated metabolism of DEET, suggesting that at least some of the components of JP-8 might be metabolized by CYPs 1A2 and/or 2B6.

© 2004 Elsevier Ireland Ltd. All rights reserved.

Keywords: Nonane; JP-8; Metabolism; Cytochrome P450; Alcohol dehydrogenase

1. Introduction

Military personnel are exposed to a variety of chemicals, including pesticides, insect repellents, prophylactic drugs and jet fuel, collectively known as deployment-related chemicals. Understanding the

human metabolism of deployment-related chemicals has become increasingly important due to the incidence of adverse health effects in military personnel during the first Gulf-War [1]. One potential hazard of deployment-related chemicals involves their potential interaction with the metabolism of endogenous compounds including hormones such as testosterone and estradiol. While the metabolism of many deployment-related chemicals, including carbaryl, DEET, permethrin and chlorpyrifos, has been

* Corresponding author. Tel.: +1 919 515 5295;
fax: +1 919 515 7169.

E-mail address: ernest.hodgson@ncsu.edu (E. Hodgson).

studied [2–5], there is little information concerning the metabolism and interactions of JP-8 components.

Military personnel may be exposed to JP-8 from incomplete combustion and the handling and transport of JP-8 during normal activities. JP-8 consists of a mixture of hydrocarbons including *n*-alkanes, isoalkanes, olefins, naphthenes and aromatics [6]. JP-8 has been shown to affect many organ systems including the liver, skin, immune, nervous, respiratory and reproductive systems [7–20]. Since JP-8 is a complex mixture of hydrocarbons, it is not feasible to study the metabolism of all JP-8 components, rather, nonane was chosen as a model hydrocarbon since *n*-alkanes and isoalkanes make up 33–61% of JP-8 [6].

Nonane has been shown to interact with rat liver microsomes suggesting that nonane undergoes phase I metabolism [21]. *In vivo*, rats metabolize nonane to γ -valerolactone, δ -hexanolactone, 2,4-hexanedione, δ -heptanolactone, 1-heptanol, 2-nonanol, 3-nonanol, 4-nonanol, 4-nonanone and 5-methyl-2-(3-oxobutyl) furan [22]. Nonane has also been shown to accumulate in rodent metabolizing organs including the liver and kidney after atmospheric exposure to nonane [23]. The objective of this investigation is to determine the human metabolism of nonane, a surrogate marker for alkanes and isoalkanes in JP-8, and which cytochrome P450 isoforms are responsible for the phase I metabolism of nonane. Furthermore, the metabolism of 2-nonanol, a metabolite of nonane, by human liver microsomes, cytochrome P450 isoforms, human liver cytosol and human alcohol dehydrogenase was also investigated. Finally, the effects of nonane, 2-nonanol and JP-8 on the metabolism of hormones (testosterone and estradiol) and military deployment related chemicals (DEET and carbaryl) were also investigated.

2. Materials and methods

2.1. Chemicals

N,N-Diethyl-*m*-toluamide (DEET) and carbaryl were purchased from ChemService (West Chester, PA). *N,N*-Diethyl-*m*-hydroxymethylbenzamide (BALC) was a generous gift from Dr. WG Taylor. Acetonitrile, methanol, methylene chloride and acetic acid were purchased from Fisher Scientific (Pittsburg, PA). Tetrahydrofuran was purchased from Mallinckrodt

Baker, Inc. (Paris, KY). All other chemicals were purchased from Sigma–Aldrich (St. Louis, MO).

2.2. Metabolism of nonane and 2-nonanol by human liver microsomes, cytosol and P450 isoforms

Pooled human liver microsomes (pHLM), human liver cytosol, insect cell control membranes and cytochrome P450 (CYP) 1A1, 1A2, 2B6, 3A4, 3A5, 3A7, 4A11, 2B6, 2C8, 2A6, 2C9*1 (Arg₁₁₄), 2C9*2 (Cys₁₄₄), 2C9*3 (Leu₃₅₉), 2C18, 2C19, 2D6*1 (Val₃₇₄) and 2E1 were purchased from BD Gentest Corporation (Bedford, MA). Either nonane or 2-nonanol (25–500 μ M) was incubated for 5 min at 37 °C in 100 mM potassium phosphate or Tris–buffer at pH 7.4 containing an NADPH regenerating system (2.5 mM glucose-6-phosphate, 3.3 mM MgCl₂, 0.25 mM NADP and 2 U ml⁻¹ glucose-6-phosphate dehydrogenase). The potassium phosphate buffer was used for pHLM, CYPs 1A1, 1A2, 2E1, 2C8, 2D6*1 (Val₃₇₄), 3A4, 3A7, 2B6, 2C18, 2C19 and insect control membranes. Tris–buffer was used for cytosol, CYPs 2C9*1 (Arg₁₁₄), 2C9*2 (Cys₁₄₄), 2C9*3 (Leu₃₅₉), 4A11, 2A6 and insect control membranes. After the preincubation period, pHLM (1 mg ml⁻¹) or CYP isoform (0.04 pmol ml⁻¹) was added and incubated for 30 min at 37 °C. The reaction was stopped by adding 250 μ l of methylene chloride. All metabolism studies were performed in a closed eppendorf tube to minimize any loss of the hydrocarbons. New peaks that were observed after the incubation of nonane with pHLM were compared to standards for nonane, 1-nonanol, 2-nonanol, 2-nonanone, 3-nonanol, 4-nonanol, 4-nonanone and γ -valerolactone, known metabolites of nonane in rats.

2.3. Determination of Michaelis–Menten kinetic parameters

Nonane (25–500 μ M) or 2-nonanol (25–500 μ M) was incubated with pHLM (1 mg ml⁻¹), CYPs 1A2, 2B6, 2E1, or control insect cell control membranes (0.04 pmol ml⁻¹ or an equal volume of control membrane) at 37 °C. For the human liver cytosolic fraction, 2-nonanol (25–500 μ M) was incubated in phosphate buffer at pH 7.4 with 7.5 mM NAD. Individual experimental parameters (i.e., concentration of enzymes

Table 1
Parameters for the metabolism of nonane and 2-nonanol by pHLM, cytosol and CYPs 1A2, 2B6 and 2E1

	Quantity of enzyme	Incubation time (min)
(A) Nonane		
pHLM	1.0 ^a	10
1A2	40 ^b	6
2B6	40 ^b	4
2E1	40 ^b	5
(B) 2-Nonanol		
Cytosol	0.8	2
2B6	8.0 ^a	4
2E1	40 ^b	5

^a mg ml⁻¹.

^b pmol P450 ml⁻¹.

and incubation time for linearity) for the metabolism of nonane and 2-nonanol are listed in Table 1.

2.4. Metabolism of 2-nonanol by alcohol dehydrogenase

Previously purified subunits of alcohol dehydrogenase (α , β I, β II and δ , 0.6 mg ml⁻¹) [5] were incubated with 2-nonanol (500 μ M) containing 7.5 mM NAD at pH 7.4 for 30 min at 37 °C.

2.5. Inhibition of testosterone, estradiol, DEET and carbaryl metabolism by nonane, 2-nonanol, 2-nonanone and JP-8

Nonane (50 μ M), 2-nonanol (50 μ M), 2-nonanone (50 μ M), or JP-8 (10⁻² to 10⁻⁵%, v/v) was incubated with pHLM (1 mg ml⁻¹) containing an NADPH regenerating system for 5 min at 37 °C. Following the incubation of nonane or 2-nonanol, either DEET, carbaryl, chlorpyrifos, testosterone or estradiol (50 μ M) was added and incubated for 10–20 min. In order to further characterize the inhibition by JP-8 of DEET metabolism, the apparent K_m and V_{max} for the formation of BALC were determined by co-incubating DEET (0–600 μ M) with JP-8 (5 \times 10⁻³ to 5 \times 10⁻⁴%, v/v) for 10 min. Reactions were stopped with 250 μ l of either ice-cold methanol or acetonitrile, briefly vortexed and then centrifuged (21,000 RCF). The degree of inhibition of metabolite formation for each substrate was determined by HPLC analysis as described below.

2.6. GC–MS assay

The GC–MS system consisted of an Agilent 7683 auto-injector, 6890 GC system, RESTEK Rtx-5MS column (30 m, 0.25 mm i.d.) and a 5973 network mass selective detector (Electron Impact, 70 V). The initial temperature of the column was set at 35 °C. The column was heated at a rate of 10 °C min⁻¹ until a temperature of 200 °C was reached, followed by a rate of 25 °C min⁻¹ until a temperature of 300 °C was reached. Helium was used as a carrier gas at a flow rate of 1 ml min⁻¹. For qualitative analysis of nonane metabolites, the mass selective detector was set in full scan mode. For the quantitative analysis of nonane, 2-nonanol and 2-nonanone, the detector was set for selective ion mode (SIM) for ions 41.1, 43.1, 47.1 for nonane and 41.1, 43.1, 45.1, 58.1, 69.1 and 71.1 for 2-nonanol and 2-nonanone. The retention times of nonane, 2-nonanone and 2-nonanol were 7.7, 10.8 and 10.9 min, respectively. The linear range ($r^2 > 0.99$) of the assay was 1–100 μ M for a 2 μ l injection.

2.7. HPLC assays

The HPLC system consisted of a Shimadzu SIL-10ADVP auto-injector, SCL-10AVP controller, SPD-10AVP UV–vis detector and 2 LC-10AT VP pumps, with the exception of the estradiol assay, which consisted of a Waters 2690 separation module and a Waters 2296 UV photodiode array detector. A 50 μ l sample was injected onto the HPLC system and chromatograms were analyzed using Shimadzu Class VP 7.2 or Waters Empower software.

2.8. HPLC analysis of DEET and BALC

DEET and BALC were analyzed using a previously reported HPLC assay [3]. Briefly, a gradient system consisting of 3.5% tetrahydrofuran:96.5% water (mobile phase A) and 100% acetonitrile (mobile phase B) with a flow rate of 1 ml min⁻¹ was used to separate DEET and BALC. The gradient system used was 10% mobile phase B from 0 to 3 min, with a linear increase or decrease of mobile phase B from 10 to 60% from 3 to 30 min, 60 to 10% from 30 to 32 min and 10% mobile phase B from 32 to 35 min. A Phenomenex Prodigy column (3 μ M, 100 A, 150 mm \times 4.6 mm) was used to separate DEET and BALC, which were detected at

230 nm. BALC and DEET had retention times of 13.3 and 24.5 min, respectively. The linear range ($r^2 > 0.99$) of the assay was 10–100 μM .

2.9. HPLC analysis of testosterone and 6 β -hydroxy testosterone

A previously reported HPLC assay was used to analyze testosterone and 6 β -hydroxy testosterone [24]. Briefly, a gradient system using 5% tetrahydrofuran:95% water (mobile phase A) and 100% methanol (mobile phase B) at a flow rate of 0.5 ml min⁻¹ was used to separate 6 β -hydroxy testosterone and testosterone. The gradient system used was 30% mobile phase B from 0 to 1 min, followed by a linear increase or decrease of mobile phase B from 30 to 60% from 1 to 10 min, 60 to 65% from 10 to 20 min, 80 to 90% from 28 to 30 min, 90% from 30 to 32 min, 90 to 30% from 32 to 34 min and 30% from 34 to 36 min. A Phenomenex Prodigy (3 μM , ODS(3), 150 mm \times 4.6 mm) column was used to separate testosterone and 6 β -hydroxy testosterone and they were detected at 247 nm. 6 β -Hydroxy testosterone and testosterone had retention times of 21.5 and 35.1 min, respectively. The linear range ($r^2 > 0.99$) of the assay was 0.2–100 μM .

2.10. HPLC analysis of carbaryl, 4-hydroxy carbaryl and carbaryl methylol

A previously reported HPLC assay was used to analyze carbaryl and its P450 dependent metabolites 4-hydroxycarbaryl and carbaryl methylol [2]. Briefly, a gradient system consisting of 10% acetonitrile:10% methanol:80% 3.5 mM tetrabutyl ammonium buffer (mobile phase A) and 90% acetonitrile:10% methanol (mobile phase B) at a flow rate of 1 ml min⁻¹ was used to separate carbaryl and its metabolites. The gradient system consisted of a linear increase or decrease of mobile phase B from 10 to 15% from 0 to 15 min, 15 to 35% from 15 to 25 min, 35% mobile phase B from 25 to 35 min and 35 to 10% from 35 to 40 min. A Phenomenex Synergi column (4 μM , 80 A, 150 mm \times 4.60 mm) was used to separate carbaryl, 4-hydroxy carbaryl and carbaryl methylol and they were detected at 290 nm. 4-Hydroxy carbaryl, carbaryl methylol and carbaryl had retention times of 17.1, 19.3 and 27.6 min, respectively. The linear range ($r^2 > 0.99$) of the assay was 0.05–50 μM .

2.11. HPLC analysis of estradiol and 2-hydroxy estradiol

A previously reported HPLC assay was used to analyze estradiol and 2-hydroxy estradiol [25]. Briefly, a gradient system consisting of acetonitrile (solvent A), 0.1% acetic acid in water (solvent B) and 0.1% acetic acid in methanol (solvent C) with a flow rate of 1.2 ml min⁻¹ was used to separate estradiol and 2-hydroxy estradiol. The gradient (solvent A:solvent B:solvent C) consisted of 16:68:16 from 0 to 8 min, concave gradient to 18:64:18 from 8 to 15 min, concave gradient to 20:59:21 from 15 to 28 min, convex gradient to 22:57:21 from 28 to 38 min, concave gradient to 58:21:21 from 38 to 51 min, a linear gradient to 92:5:3 from 51.0 to 51.1 min, an isocratic period of 92:5:3 from 51.1 to 55 min, 16:68:16 isocratic period from 55 to 60 min. Estradiol and 2-hydroxy estradiol were separated using a Phenomenex Ultracarb column (150 mm \times 4.6 mm, 5 ODS) at 30 °C and they were detected at 280 nm. Estradiol and 2-hydroxy estradiol had retention times of 34.3 and 46.8 min, respectively. The linear range ($r^2 > 0.99$) of the assay was 0.2–20 μM .

2.12. Statistics

Enzyme kinetic parameters (K_m and V_{max}) and the inhibition constant (K_i) for JP-8 were determined using non-linear regression assuming one binding site and competitive inhibition, respectively. A one-way analysis of variance with a Tukey's post hoc test was used to determine significant differences for the inhibition of testosterone, DEET, carbaryl and estradiol metabolism by nonane, 2-nonanol and 2-nonanone. A Student's *t*-test was used to determine significant differences for the inhibition of testosterone, DEET, carbaryl and estradiol metabolism by JP-8. A *p*-value of <0.05 was considered statistically significant.

3. Results

Two metabolites, 2-nonanol and 2-nonanone, were formed when nonane was incubated with pHLM (Fig. 1). Of the CYP isoforms studied, CYPs 1A2, 2B6 and 2E1 metabolized nonane to 2-nonanol (Fig. 2). The apparent K_m and V_{max} values for the formation of 2-

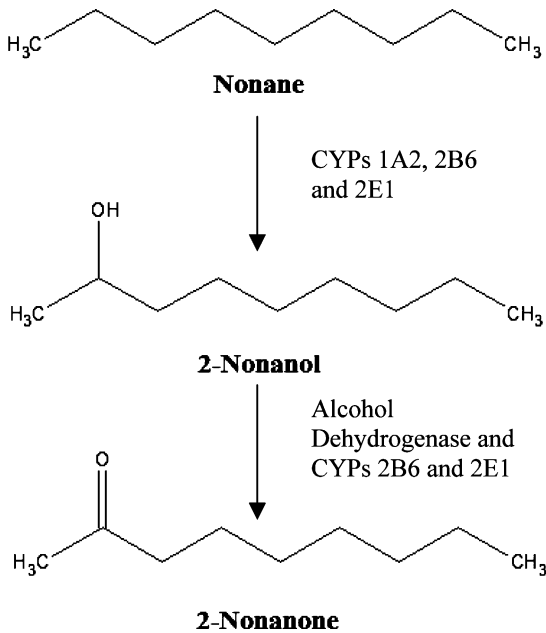


Fig. 1. Metabolism of nonane.

nonanol from nonane by pHLM and CYPs 1A2, 2B6 and 2E1 are shown in Table 2. The CYP isoforms and pHLM showed similar affinity for nonane with the apparent K_m values ranging from 44.7 to 65.0 μM . There was a wide range in the V_{max} values for the CYP isoforms for the formation of 2-nonanol, with the V_{max} values for CYPs 1A2 and 2B6 being over 11- and 31-fold higher than CYP 2E1, respectively. The apparent intrinsic clearance (Cl_{int}) for human liver microsomes

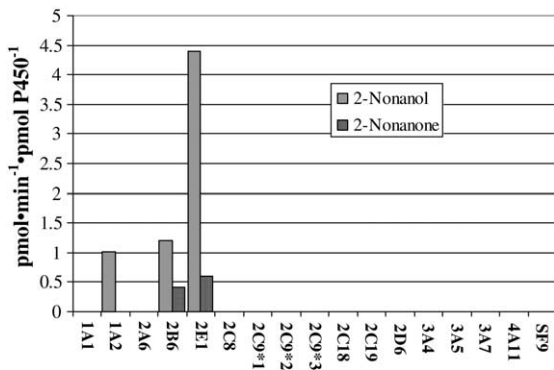


Fig. 2. Metabolism of nonane by P450 isoforms. Nonane (500 μM) was incubated with individual P450 isoforms (10 pmol) for 30 min ($n = 2$ for each isoform).

Table 2
Enzyme kinetic parameters for the formation of 2-nonanol from nonane by HLM and CYP isoforms

	K_m (mean \pm S.E., μM)	V_{max} (mean \pm S.E.)	Cl_{int}
pHLM	62.5 \pm 17.5	429 \pm 37 ^a	0.412 ^c
1A2	65.0 \pm 23.7	28.2 \pm 3.0 ^b	26.0 ^d
2B6	79.0 \pm 13.1	76.0 \pm 4.0 ^b	57.7 ^d
2E1	44.7 \pm 21.4	2.41 \pm 0.32 ^b	3.23 ^d

^a nmol min⁻¹ mg protein⁻¹.

^b pmol min⁻¹ pmol P450⁻¹.

^c l h⁻¹ mg protein⁻¹.

^d $\mu\text{l h}^{-1}$ pmol P450⁻¹ ($n = 3$ for each time point).

and CYPs 1A2, 2B6 and 2E1 for the metabolism of nonane to 2-nonanol are listed in Table 2.

pHLM and CYPs 2B6 and 2E1 not only produced 2-nonanol when incubated with nonane, but also the ketone, 2-nonanone. Interestingly, the liver cytosolic fraction, which does not contain CYP, also metabolized 2-nonanol to 2-nonanone. This would indicate that enzymes other than CYP (e.g., alcohol dehydrogenase) are also responsible for the metabolism of 2-nonanol to 2-nonanone. In order to determine the potential role of alcohol dehydrogenase in the metabolism of 2-nonanol, individual subunits of alcohol dehydrogenase (α , βI , βII and δ) were incubated with 2-nonanol. All four subunits metabolized 2-nonanol to 2-nonanone, proving that alcohol dehydrogenase is also capable of metabolizing 2-nonanol (Fig. 3). The apparent K_m and V_{max} values for the metabolism of 2-nonanol to 2-nonanone by pHLM, human liver cytosol and CYPs 2B6 and 2E1 are shown in Table 3. The liver cytosolic fraction and pHLM had similar apparent K_m values for 2-nonanol (97.7 and 145 μM , respectively). The apparent K_m of 2-

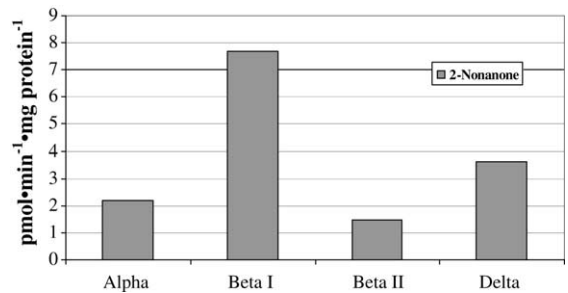


Fig. 3. Metabolism of 2-nonanol to 2-nonanone by alcohol dehydrogenase subunits. 2-Nonanol (500 μM) was incubated with alcohol dehydrogenase subunits (0.6 mg ml⁻¹) α , βI , βII and δ 30 min ($n = 2$ for each subunit).

Table 3
Enzyme kinetic parameters for the formation of 2-nonanone from 2-nonanol by HLM, cytosol and CYP isoforms

	K_m (mean \pm S.E., μM)	V_{\max} (mean \pm S.E.)
HLM	97.7 \pm 12.4	2.43 \pm 0.11 ^a
Cytosol	145 \pm 33	8.34 \pm 0.74 ^a
2B6	35.0 \pm 1.2	72.8 \pm 0.6 ^b
2E1	71.6 \pm 10.4	7.53 \pm 0.34 ^b

^a nmol min⁻¹ mg protein⁻¹.

^b pmol min⁻¹ pmol P450⁻¹.

nonanol for CYP 2B6 ($K_m = 35 \mu\text{M}$) was slightly lower than the apparent K_m for CYP 2E1 ($K_m = 71.6 \mu\text{M}$), whereas the V_{\max} value for 2B6 was over nine times higher than the V_{\max} value for 2E1.

Nonane did not significantly inhibit ($p > 0.05$) the in vitro metabolism of testosterone, estradiol, or DEET. 2-Nonanol also did not significantly inhibit ($p > 0.05$) the in vitro metabolism of testosterone or estradiol, but did significantly inhibit the metabolism of DEET to BALC (55% inhibition, $p < 0.001$). Both nonane and 2-nonanol significantly inhibited ($p < 0.01$) the in vitro metabolism of carbaryl to carbaryl methylol (21 and 27%, respectively); however, nonane showed no effect on the in vitro metabolism of carbaryl to 4-hydroxy carbaryl ($p > 0.05$), whereas, 2-nonanol significantly inhibited ($p < 0.001$) the formation of 4-hydroxy carbaryl (36% inhibition). 2-Nonanone showed similar inhibition on testosterone, estradiol, DEET and carbaryl metabolism compared to 2-nonanol (data not shown).

JP-8, as low as 0.01% (v/v), significantly inhibited the metabolism of testosterone (16% inhibition, $p = 0.009$) and estradiol (19% inhibition, $p = 0.008$) by pHLM (Fig. 4). JP-8 also significantly inhibited the metabolism of carbaryl to 4-hydroxy carbaryl (43% inhibition, $p < 0.001$) and carbaryl methylol (56% inhibition, $p < 0.001$) by pHLM (Fig. 4). Interestingly, JP-8 showed the greatest effect on the metabolism of DEET to BALC (73% inhibition, $p < 0.001$) by pHLM, suggesting that at least some of the components of JP-8 might be metabolized by CYPs 1A2 and/or 2B6 (Fig. 4), which is consistent with the metabolism of nonane. In order to determine what type of effect JP-8 has on DEET metabolism (e.g., competitive or non-competitive inhibition), the apparent K_m and V_{\max} values for the formation of BALC from DEET were determined in the absence and presence of JP-8. JP-8 was shown to competitively inhibit the metabolism of

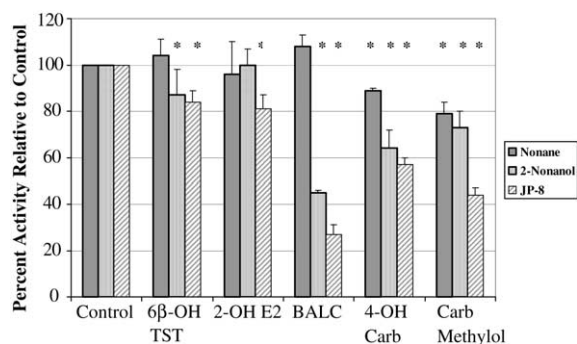


Fig. 4. Inhibition of testosterone, estradiol, DEET and carbaryl metabolism by nonane, 2-nonanol and JP-8. Testosterone, estradiol, DEET and carbaryl (50 μM) were incubated with pHLM in the absence and presence of nonane (50 μM), 2-nonanol (50 μM), or JP-8 (0.01%, v/v). The formation rate of 6 β -hydroxy testosterone (6 β -OH TST), 2-hydroxy estradiol (2-OH E2), BALC and 4-hydroxy carbaryl (4-OH Carb) or carbaryl methylol (Carb Methylol) were measured. Data are represented as the activity (formation rate of each metabolite) corrected for the activity of the control samples (mean \pm S.D., $n = 3$ for each group). (*) Statistically different ($p = 0.05$) from control.

DEET to BALC by pHLM, with an apparent K_i of 0.003% JP-8 (v/v) (Fig. 5). In order to further understand the effects of JP-8 on CYP, the apparent K_m and V_{\max} for the formation of BALC were determined for the CYP isoforms 1A2 and 2B6. JP-8 significantly inhibited CYPs 1A2 and 2B6 metabolism of DEET in a dose-dependent manner, which is consistent with the inhibition of DEET metabolism by JP-8 when using pHLM (Table 4). However, unlike the pHLM, JP-8 not only changed the apparent K_m of DEET for CYPs 1A2

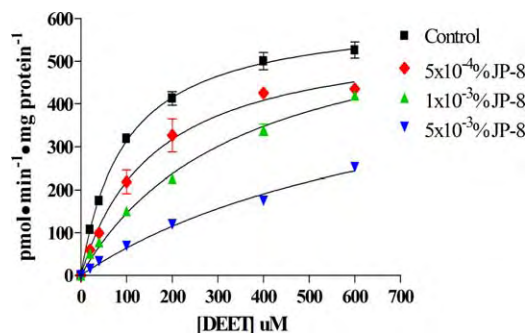


Fig. 5. The formation of BALC from DEET by pHLM in the presence and absence of JP-8. DEET (25–600 μM) was incubated with pHLM (1 mg ml⁻¹) for 10 min in the presence and absence of JP-8. Data are presented as the mean \pm S.D. ($n = 3$ for each time point) for the formation of BALC.

Table 4

Enzyme kinetic parameters for the formation of BALC from DEET by CYPs 1A2 and 2B6 in the presence and absence of JP-8

%JP-8 (v/v)	CYP 1A2		CYP 2B6	
	K_m	V_{max}	K_m	V_{max}
0	88.4 ± 8.9	33.0 ± 1.0	46.2 ± 7.0	34.7 ± 1.3
5 × 10 ⁻⁴	139 ± 54.4	23.9 ± 3.3	58.2 ± 26.7	22.2 ± 2.7
1 × 10 ⁻³	176 ± 49	22.9 ± 2.4	221 ± 93	22.7 ± 3.9
5 × 10 ⁻³	289 ± 105	17.2 ± 2.9	702 ± 491	15.8 ± 6.9

DEET (25–600 μM) was incubated with either CYPs 1A2 or 2B6 isoform (10 pmol) for 10 min in the presence and absence of JP-8. K_m and V_{max} values are presented as mean (μM) ± S.E. and mean (pmol min⁻¹ P450⁻¹) ± S.E., respectively.

and 2B6, but it also changed the V_{max} value for both isoforms, although the increase in K_m was much greater than the reduction in V_{max} .

4. Discussion

The metabolism of nonane by pHLM is consistent with literature reports that have shown nonane to interact with rat liver microsomes [21]. In vivo, rats metabolize nonane to γ -valerolactone, 2-nonanol, 3-nonanol, 4-nonanone, δ -heptanolactone, 1-heptanol, 4-nonanol, 5-methyl-2-(3-oxobutyl) furan, δ -hexanolactone and 2,5-hexanedione [22], but interestingly, nonane was only metabolized to 2-nonanol and 2-nonanone by pHLM. It is important to note that the previously mentioned metabolism study was performed in vivo [22], where nonane would be exposed to metabolizing enzymes not only in the liver but also throughout the body including the lungs, intestine and kidneys.

CYPs 1A2, 2B6 and 2E1 showed similar affinity for nonane; however, CYPs 1A2 and 2B6 had significantly higher V_{max} values compared to CYP 2E1. In the human liver, CYPs 1A2 and 2E1 have considerably higher protein expression levels compared to CYP 2B6 [26]. This suggests that CYP1A2 is the most relevant CYP isoform for the metabolism of nonane, since CYP1A2 protein expression level is much greater (>30 times) than CYP 2B6 and the V_{max} of CYP 1A2 is over 10 times higher than that of CYP 2E1. However, since CYPs 1A2, 2B6 and 2E1 are highly inducible, the overall contribution of each isoform may vary from individual to individual [27–29]. CYP 2E1 has been shown to metabolize ethanol [30], so it is not surprising that pHLM and individual CYP isoforms (CYPs 2B6 and 2E1) are able to metabolize 2-nonanol to 2-nonanone. As with ethanol metabolism, alcohol dehydrogenase

was also able to metabolize 2-nonanol to 2-nonanone. Since the relative amount of alcohol dehydrogenase is presumably much higher than CYPs 2E1 and 2B6 in the liver, alcohol dehydrogenase is probably the most significant pathway for the metabolism of 2-nonanol to 2-nonanone in the liver.

It is not surprising that nonane or 2-nonanol did not inhibit the metabolism of testosterone or estradiol, which is predominately metabolized by CYP3A4, since neither nonane or 2-nonanol is metabolized by CYP 3A4 [24,31]. It was surprising that nonane did not inhibit the metabolism of DEET to BALC, since both DEET and nonane are metabolized by CYPs 2B6 and 1A2. Interestingly, 2-nonanol did inhibit the metabolism of DEET, which is metabolized by CYP 2B6 [3]. The mixed effects of nonane on the metabolism of carbaryl to 4-hydroxy carbaryl and carbaryl methylol might be explained by the relative contribution of each CYP isoform (CYPs 1A1, 1A2, 2B6, 2C19 and 3A4) responsible for the overall metabolism of carbaryl [2]. Since nonane is metabolized by CYPs 1A2 and 2B6, but not by CYPs 1A1, 2C19, or 3A4, it is possible that the overall contribution of CYPs 1A2 and/or 2B6 is more important in the metabolism of carbaryl to carbaryl methylol than for the formation of 4-hydroxy carbaryl.

It is not feasible to determine the metabolism of all the components of JP-8. However, since the inhibition profiles of nonane and 2-nonanol were similar to JP-8, with the exception of the modest inhibition of testosterone and estradiol metabolism, this would suggest that the CYPs responsible for the metabolism of nonane and 2-nonanol are likely be important for the metabolism of the other JP-8 components. Unfortunately, there is little information on the metabolism of other aliphatic hydrocarbons found in JP-8. Although JP-8 is mainly composed of aliphatic hydrocarbons,

some aromatic hydrocarbons are also found in JP-8 including benzene, naphthalene, toluene and xylene. Benzene has been shown to be metabolized primarily by CYP2E1 in human liver microsomes [32]. CYP 2E1 has also been shown to be the primary pathway in the metabolism of toluene and xylene, with a minor contribution from CYP 1A2 [33]. The CYPs responsible for the metabolism of benzene, toluene and xylene are similar to nonane and consistent with the strong inhibition of JP-8 on BALC formation, which is dependent on CYPs 1A2 and 2B6 metabolism. This would suggest that inadvertent systemic exposure to JP-8 components could potentially inhibit CYPs 1A2 and/or 2B6 metabolism *in vivo*. A better understanding of the exposure levels to JP-8 and the systemic concentrations of JP-8 components after exposure would help in assessing the risk of JP-8 to military personnel.

In conclusion, nonane, a surrogate marker of alkanes and isoalkanes found in JP-8, is metabolized to 2-nonanol by cytochrome P450 enzymes found in the liver. CYPs 1A2, 2B6 and 2E1 are the most relevant isoforms responsible for the metabolism of nonane to 2-nonanol. 2-Nonanol is further metabolized to 2-nonanone by alcohol dehydrogenase and by CYPs 2B6 and 2E1. JP-8 significantly inhibited the metabolism of DEET and to a lesser extent carbaryl.

Acknowledgements

We would like to thank Dr. Damian Shea and Peter Lazaro for their help in the analysis of nonane, as well as Dr. Usmani Amin for his help in the analysis of estradiol. We would also like to thank Dr. Wesley Taylor for supplying BALC. This work was supported by US Army Grant DAMD 17-00-2-008.

References

- [1] D.G. Upshall, Gulf related illness—current perspectives, *J. R. Army Med. Corps* 146 (2000) 13–17.
- [2] J. Tang, Y. Cao, R.L. Rose, E. Hodgson, *In vitro* metabolism of carbaryl by human cytochrome P450 and its inhibition by chlorpyrifos, *Chem. Biol. Interact.* 141 (2002) 229–241.
- [3] K.A. Usmani, R.L. Rose, J.A. Goldstein, W.G. Taylor, A.A. Brimfield, E. Hodgson, *In vitro* human metabolism and interactions of repellent *N,N*-diethyl-*m*-toluamide, *Drug Metab. Dispos.* 30 (2002) 289–294.
- [4] J. Tang, Y. Cao, R.L. Rose, A.A. Brimfield, D. Dai, J.A. Goldstein, E. Hodgson, Metabolism of chlorpyrifos by human cytochrome P450 isoforms and human, mouse, and rat liver microsomes, *Drug Metab. Dispos.* 29 (2001) 1201–1204.
- [5] J. Choi, R. Rose, E. Hodgson, *In vitro* human metabolism of permethrin: the role of human alcohol and aldehyde dehydrogenase, *Pestic. Biochem. Physiol.* 73 (2002) 117–128.
- [6] National Research Council, *Toxicologic Assessment of Jet-Propulsion Fuel 8*, The National Academies Press, Washington, 2003, p. 207.
- [7] D.G. Allen, J.E. Riviere, N.A. Monteiro-Riviere, Identification of early biomarkers of inflammation produced by keratinocytes exposed to jet fuels jet A, JP-8, and JP-8(100), *J. Biochem. Mol. Toxicol.* 14 (2000) 231–237.
- [8] D.G. Allen, J.E. Riviere, N.A. Monteiro-Riviere, Cytokine induction as a measure of cutaneous toxicity in primary and immortalized porcine keratinocytes exposed to jet fuels, and their relationship to normal human epidermal keratinocytes, *Toxicol. Lett.* 119 (2001) 209–217.
- [9] J.R. Cooper, D.R. Mattie, Developmental toxicity of JP-8 jet fuel in the rat, *J. Appl. Toxicol.* 16 (1996) 197–200.
- [10] A.C. Dudley, M.M. Peden-Adams, J. EuDaly, R.S. Pollenz, D.E. Keil, An aryl hydrocarbon receptor independent mechanism of JP-8 jet fuel immunotoxicity in Ah-responsive and Ah-nonresponsive mice, *Toxicol. Sci.* 59 (2001) 251–259.
- [11] D.T. Harris, D. Sakiestewa, R.F. Robledo, R.S. Young, M. Witten, Effects of short-term JP-8 jet fuel exposure on cell-mediated immunity, *Toxicol. Ind. Health* 16 (2000) 78–84.
- [12] M.B. Kabbur, J.V. Rogers, P.G. Gunasekar, C.M. Garrett, K.T. Geiss, W.W. Brinkley, J.N. McDougal, Effect of JP-8 jet fuel on molecular and histological parameters related to acute skin irritation, *Toxicol. Appl. Pharmacol.* 175 (2001) 83–88.
- [13] N. Kanikkannan, B.R. Locke, M. Singh, Effect of jet fuels on the skin morphology and irritation in hairless rats, *Toxicology* 175 (2002) 35–47.
- [14] N. Monteiro-Riviere, A. Inman, J. Riviere, Effects of short-term high-dose and low-dose dermal exposure to Jet A, JP-8 and JP-8 + 100 jet fuels, *J. Appl. Toxicol.* 21 (2001) 485–494.
- [15] G. Ramos, D.X. Nghiem, J.P. Walterscheid, S.E. Ullrich, Dermal application of jet fuel suppresses secondary immune reactions, *Toxicol. Appl. Pharmacol.* 180 (2002) 136–144.
- [16] G.D. Ritchie, K.R. Still, W.K. Alexander, A.F. Nordholm, C.L. Wilson, J. Rossi III, D.R. Mattie, A review of the neurotoxicity risk of selected hydrocarbon fuels, *J. Toxicol. Environ. Health B Crit. Rev.* 4 (2001) 223–312.
- [17] R.F. Robledo, R.S. Young, R.C. Lantz, M.L. Witten, Short-term pulmonary response to inhaled JP-8 jet fuel aerosol in mice, *Toxicol. Pathol.* 28 (2000) 656–663.
- [18] S.E. Ullrich, H.J. Lyons, Mechanisms involved in the immunotoxicity induced by dermal application of JP-8 jet fuel, *Toxicol. Sci.* 58 (2000) 290–298.
- [19] B. Rhyne, J. Pirone, J. Riviere, N. Monteiro-Riviere, The use of enzyme histochemistry in detecting cutaneous toxicity of three topically applied jet fuel mixtures, *Toxicol. Mech. Methods* 12 (2002) 17–34.

- [20] G.M. Grant, K.M. Shaffer, W.Y. Kao, D.A. Stenger, J.J. Pan-crazio, Investigation of in vitro toxicity of jet fuels JP-8 and Jet A, *Drug Chem. Toxicol.* 23 (2000) 279–291.
- [21] A.Y. Lu, H.W. Strobel, M.J. Coon, Properties of a solubilized form of the cytochrome P-450-containing mixed-function oxidase of liver microsomes, *Mol. Pharmacol.* 6 (1970) 213–220.
- [22] M.P. Serve, D.D. Bombick, T.M. Baughman, B.M. Jarnot, M. Ketcha, D.R. Mattie, The metabolism of *n*-nonane in male Fischer 344 rats, *Chemosphere* 31 (1995) 2661–2668.
- [23] K. Zahlse, A.M. Nilsen, I. Eide, O.G. Nilsen, Accumulation and distribution of aliphatic (*n*-nonane), aromatic (1,2,4-trimethylbenzene) and naphthenic (1,2,4-trimethylcyclohexane) hydrocarbons in the rat after repeated inhalation, *Pharmacol. Toxicol.* 67 (1990) 436–440.
- [24] K.A. Usmani, R.L. Rose, E. Hodgson, Inhibition and activation of the human liver microsomal and human cytochrome P4503A4 metabolism of testosterone by deployment-related chemicals, *Drug Metab. Dispos.* 31 (2003) 384–391.
- [25] L.A. Suchar, R.L. Chang, R.T. Rosen, J. Lech, A.H. Conney, High-performance liquid chromatography separation of hydroxylated estradiol metabolites: formation of estradiol metabolites by liver microsomes from male and female rats, *J. Pharmacol. Exp. Ther.* 272 (1995) 197–206.
- [26] T. Shimada, H. Yamazaki, M. Mimura, Y. Inui, F.P. Guengerich, Interindividual variations in human liver cytochrome P-450 enzymes involved in the oxidation of drugs, carcinogens and toxic chemicals: studies with liver microsomes of 30 Japanese and 30 Caucasians, *J. Pharmacol. Exp. Ther.* 270 (1994) 414–423.
- [27] I. Kessova, A.I. Cederbaum, CYP2E1: biochemistry, toxicology, regulation and function in ethanol-induced liver injury, *Curr. Mol. Med.* 3 (2003) 509–518.
- [28] D.L. Eaton, E.P. Gallagher, T.K. Bammler, K.L. Kunze, Role of cytochrome P4501A2 in chemical carcinogenesis: implications for human variability in expression and enzyme activity, *Pharmacogenetics* 5 (1995) 259–274.
- [29] H. Wang, M. Negishi, Transcriptional regulation of cytochrome p4502B genes by nuclear receptors, *Curr. Drug Metab.* 4 (2003) 515–525.
- [30] H. Matsumoto, Y. Fukui, Pharmacokinetics of ethanol: a review of the methodology, *Addict. Biol.* 7 (2002) 5–14.
- [31] T. Satoh, K.I. Fujita, H. Munakata, S. Itoh, K. Nakamura, T. Kamataki, I. Yoshizawa, Studies on the interactions between drugs and estrogen: analytical method for prediction system of gynecomastia induced by drugs on the inhibitory metabolism of estradiol using *Escherichia coli* coexpressing human CYP3A4 with human NADPH-cytochrome P450 reductase, *Anal. Biochem.* 286 (2000) 179–186.
- [32] M.W. Powley, G.P. Carlson, Cytochromes P450 involved with benzene metabolism in hepatic and pulmonary microsomes, *J. Biochem. Mol. Toxicol.* 14 (2000) 303–309.
- [33] W. Tassaneeyakul, D.J. Birkett, J.W. Edwards, M.E. Veronese, R.H. Tukey, J.O. Miners, Human cytochrome P450 isoform specificity in the regioselective metabolism of toluene and *o*-, *m*- and *p*-xylene, *J. Pharmacol. Exp. Ther.* 276 (1996) 101–108.



ELSEVIER

Chemico-Biological Interactions 141 (2002) 229–241

Chemico-Biological
Interaction

www.elsevier.com/locate/chembiont

In vitro metabolism of carbaryl by human cytochrome P450 and its inhibition by chlorpyrifos

Jun Tang, Yan Cao, Randy L. Rose, Ernest Hodgson*

Department of Environmental and Molecular Toxicology, North Carolina State University, Box 7633, Raleigh, NC 27695, USA

Received 28 May 2002; received in revised form 28 June 2002; accepted 29 June 2002

Abstract

Carbaryl is a widely used anticholinesterase carbamate insecticide. Although previous studies have demonstrated that carbaryl can be metabolized by cytochrome P450 (CYP), the identification and characterization of CYP isoforms involved in metabolism have not been described either in humans or in experimental animals. The in vitro metabolic activities of human liver microsomes (HLM) and human cytochrome P450 (CYP) isoforms toward carbaryl were investigated in this study. The three major metabolites, i.e. 5-hydroxycarbaryl, 4-hydroxycarbaryl and carbaryl methylol, were identified after incubation of carbaryl with HLM or individual CYP isoforms and analysis by HPLC. Most of the 16 human CYP isoforms studied showed some metabolic activity toward carbaryl. CYP1A1 and 1A2 had the greatest ability to form 5-hydroxycarbaryl, while CYP3A4 and CYP1A1 were the most active in generation of 4-hydroxycarbaryl. The production of carbaryl methylol was primarily the result of metabolism by CYP2B6. Differential activities toward carbaryl were observed among five selected individual HLM samples with the largest difference occurring in the production of carbaryl methylol. Co-incubations of carbaryl and chlorpyrifos in HLM greatly inhibited carbaryl metabolism. The ability of HLM to metabolize carbaryl was also reduced by pre-incubation of HLM with chlorpyrifos. Chlorpyrifos inhibited the generation of carbaryl methylol, catalyzed predominately by CYP2B6, more than other pathways, correlating with an earlier observation that chlorpyrifos is metabolized to its oxon primarily by CYP2B6. Therefore, carbaryl metabolism in humans and its interaction with other chemicals is reflected by the concentration of CYP isoforms in HLM and their activities in the metabolic pathways

* Corresponding author. Tel.: +1-919-515-5295; fax: +1-919-513-1012

E-mail address: ernest_hodgson@ncsu.edu (E. Hodgson).

for carbaryl. (Supported by NCDA Environmental Trust Fund)

© 2002 Elsevier Science B.V. All rights reserved.

Keywords: Carbaryl; Human liver microsomes; Metabolism

1. Introduction

Carbaryl (1-naphthol *N*-methylcarbamate, CAS No. 63-25-2) is a broad spectrum carbamate insecticide with a variety of agricultural and non-agricultural applications. Due to its wide use, humans may be exposed to its residues through food and other routes [1]. The mechanism underlying the toxicity of carbamate pesticides is its anticholinesterase activity [2], the inhibition of cholinesterase causing accumulation of acetylcholine in synapses, resulting in malfunction of the nervous system. The inhibition of cholinesterase by carbamates is reversible and less persistent than that by organophosphates.

Early studies of carbamate metabolism focused on hydrolysis because of the assumption that the ester linkage was susceptible to esterase attack as well as limitations of the analytical techniques then available [3]. However, the importance of oxidative pathways had been shown earlier with the demonstration of NADPH-dependent metabolic activity toward carbamates in rat liver microsomes [4,5]. Like many other carbamates, carbaryl can be hydrolyzed by esterases and oxidized by cytochrome P450-mediated monooxygenases (CYP) to form both hydrolysis and hydroxylation products, respectively, which are subject to further conjugation, such as sulfate and glucuronic acid conjugates of 1-naphthol and 4-hydroxycarbaryl [6]. The major hydroxylation products include 5-hydroxycarbaryl (5-hydroxy 1-naphthyl *N*-methylcarbamate, CAS No. 5721-72-2), 4-hydroxycarbaryl (4-hydroxy 1-naphthyl *N*-methylcarbamate, CAS No. 5266-97-7) and carbaryl methylol (1-naphthyl *N*-(hydroxymethyl)carbamate, CAS No. 5266-96-6) [7–9] (Fig. 1). Although the contributions of hydrolysis and hydroxylation toward total metabolism of carbaryl have yet to be elucidated, it has been suggested that hydroxylation by CYP is the more important route of carbaryl metabolism [10,11]. It has been shown [11] that chickens had higher clearance rate for carbaryl than rats although they have lower carboxylesterase and A-esterase activities than rats, suggesting that these esterases did not contribute to the difference between chickens and rats. An inhibition study in rats and humans showed that the CYP inhibitor cimetidine reduced the metabolism of carbaryl, again suggesting that CYP play a major role in carbaryl metabolism [10].

Although carbaryl itself is an anticholinesterase, some hydroxylation products have been shown to be more active than the parent compound. It has been shown [12] that while pretreatment with cimetidine increased the plasma concentration of carbaryl in man, the inhibition of blood cholinesterase activity was reduced, suggesting that cimetidine is blocking the production of active metabolites generated by CYP. 5-Hydroxycarbaryl has been reported to be more toxic than carbaryl [3,13].

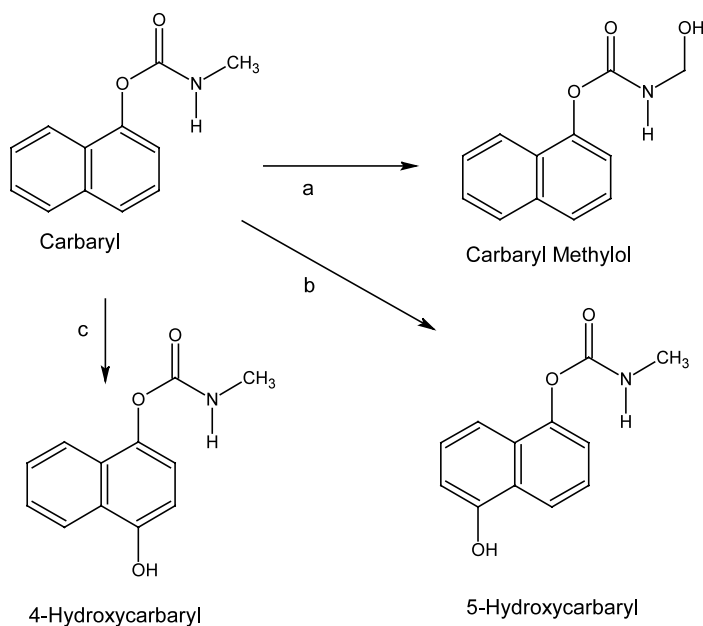


Fig. 1. Cytochrome P450-dependent metabolism of carbaryl: (a) methyl hydroxylation, (b) 5-hydroxylation, (c) 4-hydroxylation.

Both carbamate and organophosphorus insecticides are metabolized by CYP [6] and act as anticholinesterases [2]. It is possible, therefore, they may interact in metabolic pathways as well as in target sites. One important group of organophosphorus insecticides is the phosphorothionates, such as chlorpyrifos and malathion. Bioactivation of this group by CYP causes suicide inhibition of CYP activity [14], resulting in a reduction of CYP activity. A significant increase in carbaryl toxicity in red-legged partridges following malathion administration has been attributed to inhibition of carbaryl metabolism [15].

Although the hepatic metabolism of carbaryl in humans has been previously investigated *in vitro* [9,16], contributions of CYP isoforms to the metabolic pathways have not been elucidated. Knowledge of the varying contributions of CYP isoforms to carbaryl metabolism will enable better understanding of differences in metabolism among individuals as well as among ethnic groups or populations and will provide important information relative to metabolic interactions of carbaryl with other chemicals. The present *in vitro* study was designed to examine: (1) oxidation activities toward carbaryl in pooled human liver microsomes (HLM); (2) human cytochrome P450 (CYP) isoforms responsible for metabolism of carbaryl; (3) potential differences in oxidation activities among individual HLMs; and (4) effects of pre- or co-incubation of chlorpyrifos on carbaryl metabolism.

2. Materials and methods

2.1. Chemicals

Carbaryl was purchased from ChemService (West Chester, PA). 5-Hydroxycarbaryl, 4-hydroxycarbaryl, carbaryl methylol and desmethylcarbaryl were obtained from the late Dr W.C. Dauterman. HPLC grade acetonitrile and methanol were purchased from Fisher Scientific (Fair Lawn, NJ). All other chemicals, if not specified, were purchased from Sigma (St. Louis, MO).

3. HLM and human CYP isoforms

Pooled and individual HLM and human CYP1A1, 1A2, 2A6, 2B6, 2C8, 2C9*1, 2C9*2, 2C9*3, 2C18, 2C19, 2D6*1, 2D6*10, 2E1, 3A4, 3A5, and 4A11 Super-somesTM were purchased from Gentest, a BD Biosciences Company (Woburn, MA). Individual HLM obtained from Gentest were from donors HG6, HG23, HG42, HG43 and HG112. CYP1A2, 2B6, 2C19, and 3A4 activities (pmol product/mg protein per min, represented by phenacetin *O*-deethylase, (*S*)-mephenytoin *N*-demethylase, (*S*)-mephenytoin 4'-hydroxylase, and testosterone 6 β -hydroxylase catalytic activities, respectively) in these individuals are 770, 3.1, 36, 2990 in HG6 (16-year-old male), 770, 12.2, 78.1, 4050 in HG23 (25-year-old male), 550, 140, 3.5, 14530 in HG42 (48-year-old female), 356, 7.4, 212, 3408 in HG43 (23-year-old female), 244, 59.1, 260, 17519 in HG112 (2-year-old female) (data were provided by GENTEST). Data for activity of CYP1A1 in these individuals were not available.

3.1. *In vitro* assay of carbaryl metabolism

Activity assays were performed by incubation of a single concentration of carbaryl (final concentration 500 μ M) with microsomal enzymes (1 mg protein for HLM, 18–50 pmol P450 for CYP isoforms) in the presence of an NADPH-generating system (final concentrations: 0.25 mM NADP, 2.5 mM glucose-6-phosphate, and 2 U/ml glucose-6-phosphate dehydrogenase) for 15 min. The buffer used for HLM was 100 mM Tris (pH 7.4) containing 5 mM MgCl₂. Buffers used for CYP isoforms were those recommended by Gentest, i.e. 100 mM potassium phosphate (pH 7.4) with 3.3 mM magnesium chloride for CYP1A1, 1A2, 2D6*1, 2D6*10, 3A4, 3A5; 50 mM Tris (pH 7.4) with 3.3 mM magnesium chloride for CYP2A6; 50 mM potassium phosphate (pH 7.4) with 3.3 mM magnesium chloride for CYP2B6, 2C8, 2C19, 2E1; 100 mM Tris (pH 7.5) with 3.3 mM magnesium chloride for CYP2C9*1, 2C9*2, 2C9*3, 2C18, 4A11.

Kinetic assays were performed by incubation of a series of concentrations of carbaryl (final concentrations 10–1000 μ M) with enzymes for 15 min under the same conditions described above. Preliminary experiments indicated that the 15 min was the most appropriate incubation time.

Reactions were initiated by the addition of the enzyme. Controls were performed in the absence of the NADPH-generating system. The reaction was terminated by the addition of ice-cold acetonitrile followed by vortexing. The supernatant after centrifugation (10 min at $21\,000 \times g$) was analyzed by HPLC.

To determine the potential role of esterase enzymes in carbaryl metabolism, incubations of carbaryl (final concentration $125\ \mu\text{M}$) were conducted in buffer only (0.1 M Tris-HCl/5 mM MgCl₂, pH 7.4), pooled HLM (1 mg protein) in buffer, or pooled human liver cytosol (2 mg protein) in buffer for 15 min (assay volume 500 μl). No cofactors were added to these incubations.

3.2. Assay of carbaryl metabolism in the presence of chlorpyrifos

Varying concentrations of chlorpyrifos (0.25–125 μM) were added to one of two concentrations of carbaryl (10 and 500 μM) to assess the ability of chlorpyrifos to inhibit metabolism. Co-incubation was initiated by the addition of enzyme into a reaction mixture containing both chlorpyrifos and carbaryl in the presence of the NADPH-generating system and terminated after 15 min incubation.

Pre-incubation was initiated by the addition of enzyme into a reaction mixture containing chlorpyrifos in the presence of the NADPH-generating system. After 30 min pre-incubation, the reaction was started by the addition of carbaryl. The reaction was terminated after 15 min incubation.

3.3. Analysis of metabolites by HPLC

Carbaryl and its metabolites were separated by a Synergi Max C12 column (Phenomenex, Rancho Palos Verdes, CA) using a gradient HPLC system containing two pumps (Shimadzu LC-10AT). The mobile phase for pump A was 10% acetonitrile, 10% methanol and 80% water containing 3.5 mM tetrabutyl ammonium, for pump B 90% acetonitrile and 10% methanol. The flow rate was 1 ml/min. The gradient system was initiated at 10% of pump B and increased linearly as follow: 15% of pump B in 15 min, 35% of pump B through 25 min, and 35% of pump B till 35 min.

Using this gradient, carbaryl and its metabolites were well separated with baseline separation. Retention times for 5-hydroxycarbaryl, 4-hydroxycarbaryl, carbaryl methylol, desmethyl carbaryl, carbaryl, and 1-naphthol were 14, 16, 18, 22, 27, and 29.5 min, respectively. The limit of detections were 0.1, 0.6 and 0.9 pmol for 5-hydroxycarbaryl, 3-hydroxycarbaryl and carbaryl methylol, respectively. The concentration ranges used for calibration were 0.039–5 μM for 5-hydroxycarbaryl and 0.156–20 μM for 3-hydroxycarbaryl, carbaryl methylol and 1-naphthol.

In incubations containing chlorpyrifos, the gradient was the same as described above before 35 min and then increased from 35% pump B at 35 min to 100% pump B at 36 min and maintained at 100% pump B until 50 min for elution of trichloropyridinal, chlorpyrifos oxon and chlorpyrifos at retention times of 30, 40 and 41 min.

Carbaryl, chlorpyrifos and their metabolites were detected by a Waters 486 Tunable Absorbance Detector at 290 nm (the maximal absorption for carbaryl and its metabolites produced) and identified by comparing retention times with standards. Concentrations of metabolites were obtained by extrapolation of peak area from a standard curve.

3.4. Enzyme kinetic calculations and statistics

Apparent K_m and V_{max} were determined by non-linear regression using a GRAPHPAD PRISM software and K_i was determined using a Dixon plot [17]. All values are expressed as mean \pm S.E.M. ($n = 3$ determinations). Significant differences between data sets were determined by one-way analysis of variance using an SAS program [18].

4. Results

Four metabolites were detected after incubation of carbaryl with pooled HLM in the presence of an NADPH regenerating system: 5-hydroxycarbaryl, 4-hydroxycarbaryl, carbaryl methylol, and 1-naphthol. The first three metabolites were generated only in the presence of an NADPH regenerating system and, therefore, were products of CYP-mediated reactions. The enzyme kinetics of CYP-mediated carbaryl metabolism indicates that 4-hydroxylation had the highest V_{max} , followed by methyl hydroxylation, while 5-hydroxylation had much lower V_{max} (Fig. 2 and Table 1). Methyl hydroxylation had the lowest K_m , while both ring hydroxylation had similar K_m , and, thus, methyl hydroxylation had the highest clearance rate (Table 1).

1-Naphthol, the fourth metabolite, was a product of hydrolysis because there were no significant differences in its generation in pooled HLM either in the presence or absence of the NADPH regenerating system. In the absence of the NADPH

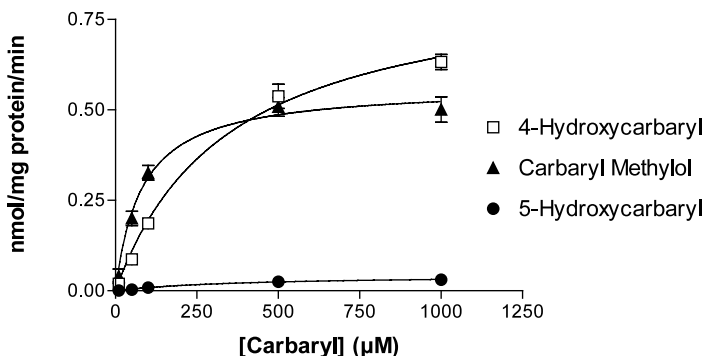


Fig. 2. Reaction velocities of carbaryl metabolism in HLM. Values are expressed as mean \pm S.E.M. ($n = 3$ determinations).

Table 1

Apparent K_m (μM) and V_{max} (nmol/mg protein per min) for carbaryl metabolism in pooled HLM (pooled from ten donors)

Metabolites	V_{max}	K_m	V_{max}/K_m
5-Hydroxycarbaryl	0.04 ± 0.01	349 ± 65	0.0001
4-Hydroxycarbaryl	0.87 ± 0.05	349 ± 57	0.0025
Carbaryl methylol	0.57 ± 0.03	81 ± 15	0.0070

Values are expressed as mean \pm S.E.M. ($n = 3$ determinations). V_{max}/K_m is expressed as ml/mg protein per min.

regenerating system, 1-naphthol was generated at a rate of 0.034 ± 0.006 nmol/mg protein per min after incubation of $125 \mu\text{M}$ carbaryl with pooled HLM. The potential hydrolysis of carbaryl by esterases in the cytosolic fraction was also examined. 1-Naphthol was the only carbaryl metabolite detected and was generated at a rate of 0.008 ± 0.001 nmol/mg protein per min at $125 \mu\text{M}$ carbaryl.

From five selected individual HLM, differences in generating 5-hydroxycarbaryl or 4-hydroxycarbaryl were only 2-fold among individuals and did not correlate with any single CYP isoform activity. The differences in generating carbaryl methylol were 5-fold between the lowest and the highest in these five individuals and were, apparently, correlated with the activity of CYP2B6 (Table 2).

Activities of CYP isoforms in metabolizing carbaryl are shown in Fig. 3. Of 16 CYP isoforms investigated (i.e. CYP1A1, 1A2, 2A6, 2B6, 2C8, 2C9*1, 2C9*2, 2C9*3, 2C18, 2C19, 2D6*1, 2D6*10, 2E1, 3A4, 3A5, 4A11), only CYP2D6*10 and 4A11 had no detectable activity toward carbaryl. All the other CYP isoforms were active in generating all three metabolites, although the extent of metabolism and the ratios of metabolites varied widely among isoforms. CYP1A1, 1A2, 2B6, 2C19, and 3A4 were among those most active in carbaryl metabolism. Their role toward carbaryl metabolism in microsomes may be estimated based on their clearance values (V_{max}/K_m) (Table 3) and their concentrations in liver microsomes.

The metabolism of carbaryl was inhibited by both co- and pre-incubation with chlorpyrifos (Fig. 4). Methyl hydroxylation (generating carbaryl methylol) was the pathway inhibited most significantly by chlorpyrifos while there was little effect of chlorpyrifos on 5-hydroxylation (generating 5-hydroxycarbaryl). Use of the Dixon

Table 2

Metabolic activity (nmol/mg protein per min) toward carbaryl in individual HLM

Individuals	5-Hydroxycarbaryl	4-Hydroxycarbaryl	Carbaryl methylol
HG6	0.02 ± 0.01	0.40 ± 0.02	0.17 ± 0.01
HG23	0.03 ± 0.01	0.48 ± 0.03	0.21 ± 0.02
HG42	0.04 ± 0.01	0.48 ± 0.12	0.93 ± 0.19
HG43	0.03 ± 0.01	0.31 ± 0.03	0.18 ± 0.02
HG112	0.05 ± 0.01	0.63 ± 0.05	0.72 ± 0.06

Activities are expressed as mean \pm S.E.M. ($n = 3$ determinations).

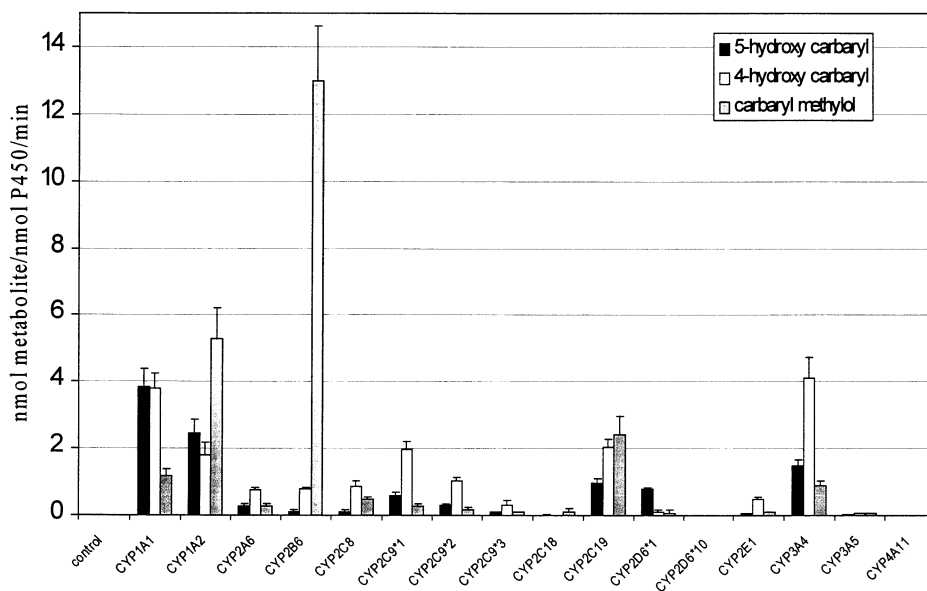


Fig. 3. Metabolic activities (nmol of product/nmol cytochrome P450/min \pm S.E.M., $n = 3$ determinations) toward carbaryl in human cytochrome P450 isoform SupersomesTM.

plot produced a K_i of 149.9 μM for chlorpyrifos inhibition of 4-hydroxylation of carbaryl and a K_i of 2.17 μM for inhibition of methyl hydroxylation (Fig. 5).

5. Discussion

In this *in vitro* study, 5-hydroxy-, 4-hydroxycarbaryl and carbaryl methylol were identified as the major metabolites of carbaryl produced by HLM. 1-Naphthol was not, apparently, a major product of CYP-catalyzed reactions because there was no significant difference in the small amount of 1-naphthol production in the presence or absence of the NADPH-generating system. Other hydroxylation products of carbaryl have been reported previously in non-human species [19]. Presumably they represent minor products or are not formed in HLM since only the three metabolites discussed were found in the current study. Production of 1-naphthol in the absence of NADPH-generating system is minimal, suggesting hydrolysis of carbaryl in both microsomes and cytosol is not the major pathway of carbaryl metabolism. This result is consistent with the suggestion that hydrolysis is not favored in carbaryl metabolism because of generating a more lipophilic product (1-naphthol) [6].

Our data show that CYP isoforms are differentially active in metabolic pathways of carbaryl, CYP1A1, 1A2, 2B6, 2C19, and 3A4 being the most active isoforms in human metabolism of carbaryl. CYP1A1 and 1A2 had the greatest ability to form 5-hydroxy carbaryl, while CYP3A4 and CYP1A1 were the most active in generation of 4-hydroxy carbaryl. The production of carbaryl methylol was primarily the result of

Table 3
 Apparent K_m (μM) and V_{\max} (nmol/nmol P450/min) for carbaryl metabolism in several human CYP isoforms

CYP isoforms	5-Hydroxycarbaryl			4-Hydroxycarbaryl			Carbaryl methylol		
	V_{\max}	K_m	V_{\max}/K_m	V_{\max}	K_m	V_{\max}/K_m	V_{\max}	K_m	V_{\max}/K_m
1A1	4.81 ± 0.33	15 ± 5	0.32	3.89 ± 0.19	20 ± 5	0.19	1.19 ± 0.20	51 ± 31	0.02
1A2	2.62 ± 0.13	89 ± 15	0.03	1.72 ± 0.08	58 ± 11	0.03	4.80 ± 0.20	36 ± 7	0.13
2B6	0.29 ± 0.05	110 ± 47	0.01	0.80 ± 0.05	11 ± 3	0.07	15.54 ± 0.94	45 ± 10	0.35
2C19	0.99 ± 0.09	62 ± 22	0.02	2.21 ± 0.17	44 ± 16	0.05	3.46 ± 0.24	15 ± 5	0.23
3A4	2.34 ± 0.34	281 ± 98	0.01	5.81 ± 0.50	235 ± 57	0.02	1.47 ± 0.28	156 ± 91	0.01

Values are expressed as mean \pm S.E.M. ($n = 3$ determinations). V_{\max}/K_m is expressed as ml/mg protein per min.

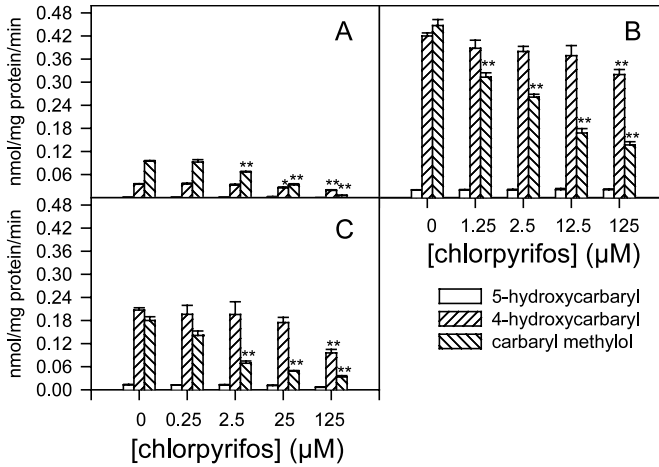


Fig. 4. Activities of carbaryl metabolism in the presence of chlorpyrifos: (A) co-incubation of chlorpyrifos with 10 μM carbaryl, (B) co-incubation of chlorpyrifos with 500 μM carbaryl, (C) pre-incubation of chlorpyrifos before incubation with 500 μM carbaryl. Activities were expressed as nmol product/mg microsome protein per min \pm S.E.M. ($n = 3$ determinations). Significant differences from correspondent control (i.e. 0 μM chlorpyrifos) were indicated by *, $P < 0.05$; or **, $P < 0.01$.

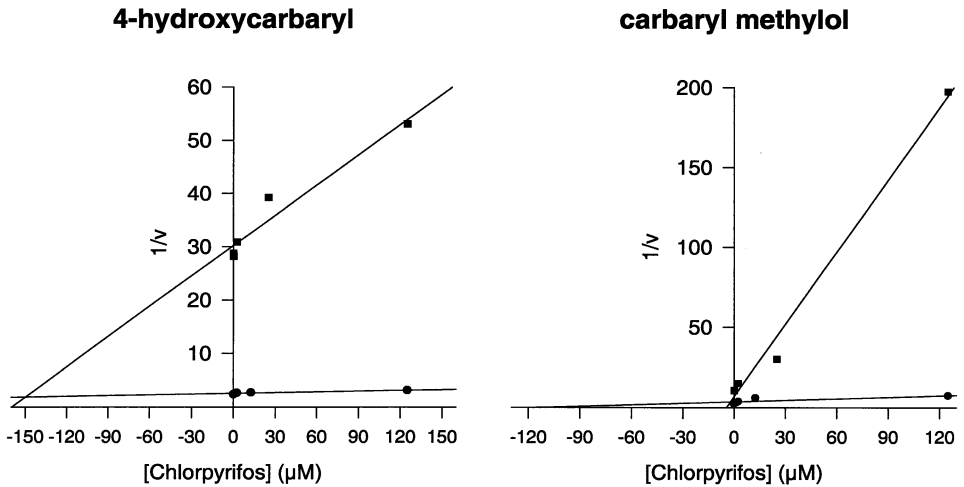


Fig. 5. Dixon plot of co-incubation of variant concentrations of chlorpyrifos with 10 μM carbaryl (■) and 500 μM chlorpyrifos (●).

metabolism by CYP2B6. The kinetic parameters as well as concentrations of these isoforms in HLM may explain the relative activities in microsomes of these carbaryl metabolic pathways, i.e. the low activity of 5-hydroxylation in HLM may result from low concentrations of CYP1A1, while high activities of 4-hydroxylation and methyl hydroxylation may result from high concentrations of CYP3A4 in HLM and high

activity of CYP2B6 in methyl hydroxylation, respectively. However, the relatively low activity of 5-hydroxylation may be enhanced after a period of chronic exposure to carbaryl because previous studies have shown that carbaryl can induce CYP1A1 activity [20–22].

Differential metabolic activities toward carbaryl by variants of CYP2C9 and 2D6 were observed in this study. CYP2C9*1 (Arg₁₄₄, Ile₃₅₉), the most common form of CYP2C9, is more active in carbaryl metabolism than CYP2C9*2 (Cys₁₄₄) and CYP2C9*3 (Leu₃₅₉). CYP2D6*10 did not show any detectable activity toward carbaryl while CYP2D6*1 displayed some activity toward carbaryl, especially in the generation of 5-hydroxycarbaryl.

Variation in carbaryl metabolism among individual HLMs was observed in this study. Differences in 5- and 4-hydroxylation among 5 selected individuals were only 2-fold, while the difference in methyl hydroxylation was about 5-fold. Two or more CYP isoforms are involved in these ring hydroxylation with high activity. For example, both CYP1A1 and 1A2 are very active in 5-hydroxylation and CYP3A4, 1A1 and 2C19 are all involved in 4-hydroxylation with high activity. Thus, a change in a single isoform may not greatly affect the total activity of microsomes. Greater differences of ring hydroxylation activity may only be observed between individuals with low or high activities for all CYP1A1, 1A2, 2C19 and 3A4.

Methyl hydroxylation is a pathway that is predominately catalyzed by a single isoform, CYP2B6. Thus, changes in CYP2B6 activity are not thoroughly compensated for by other isoforms in the methyl hydroxylation pathway, and greater differences in methyl hydroxylation occur between individuals with low and high CYP2B6 (HG6 and HG42, respectively).

The effect of chlorpyrifos on carbaryl metabolism was investigated. Chlorpyrifos, a phosphorothionate insecticide, is activated to chlorpyrifos-oxon through a CYP-catalyzed desulfuration reaction [2]. The sulfur atom released from chlorpyrifos in this reaction is highly reactive and is believed to bind immediately to the heme iron of CYP and inhibit its activity [14]. CYP2B6 has been shown to have the highest chlorpyrifos desulfuration activity among all CYP isoforms [23]. A decrease in CYP2B6 activity after incubation with chlorpyrifos should, therefore, occur because of immediate binding to CYP2B6 of the sulfur atom released in the desulfuration reaction. CYP2B6 was also found in this study to have a predominant role in the generation of carbaryl methylol, thus carbaryl would also compete with chlorpyrifos for the active site of CYP2B6. Therefore, it is not surprising that the methyl hydroxylation pathway is the pathway of carbaryl metabolism most affected by chlorpyrifos, either co-incubation or pre-incubation.

In summary, carbaryl can be metabolized by CYP oxidation in HLM to form 5-hydroxycarbaryl, 4-hydroxycarbaryl, and carbaryl methylol. Most CYP isoforms responsible for xenobiotic metabolism have some activity toward carbaryl. The highest activity was observed in CYP1A1 for 5-hydroxylation, CYP3A4 for 4-hydroxylation, and CYP2B6 for methyl hydroxylation. Differential activities among carbaryl metabolic pathways in HLM may be attributed to different concentrations of these most active CYP isoforms in HLM. Likewise, the varying concentrations of CYP isoforms among individuals may contribute to the differences in carbaryl

metabolism among human populations. Metabolism of carbaryl by CYP oxidation is inhibited by chlorpyrifos. The most affected pathway is methyl hydroxylation, catalyzed predominately by CYP2B6, which is also the most active isoform for chlorpyrifos desulfuration.

References

- [1] M.F. Cranmer, Carbaryl: a toxicological review and risk analysis, *Neurotoxicology* 7 (1986) 247–332.
- [2] T.R. Fukuto, Mechanism of action of organophosphorus and carbamate insecticides, *Environ. Health Perspect.* 87 (1990) 245–254.
- [3] H.W. Dorough, Metabolism of insecticidal methylcarbamates in animals, *J. Agric. Food Chem.* 18 (1970) 1015–1022.
- [4] E. Hodgson, J.E. Casida, Biological oxidation of *N,N*-dialkyl carbamates, *Biochim. Biophys. Acta* 42 (1960) 184–186.
- [5] E. Hodgson, J.E. Casida, Metabolism of *N,N*-dialkyl carbamates and related compounds by rat liver, *Biochem. Pharmacol.* 8 (1961) 179–191.
- [6] F. Matsumura, Metabolism of carbamate insecticides, in: F. Matsumura (Ed.), *Toxicology of Insecticides*, Plenum Press, New York, 1975, pp. 228–239.
- [7] H.W. Dorough, N.C. Leeling, J.E. Casida, Nonhydrolytic pathway in metabolism of *N*-methylcarbamate insecticides, *Science* 140 (1963) 170–171.
- [8] H.W. Dorough, J.E. Casida, Nature of certain carbamate metabolites of the insecticide Sevin, *J. Agric. Food Chem.* 12 (1964) 294–304.
- [9] A. Strother, In vitro metabolism of methylcarbamate insecticides by human and rat liver fraction, *Toxicol. Appl. Pharmacol.* 21 (1972) 112–129.
- [10] S.A. Ward, D.G. May, A.J. Heath, R.A. Branch, Carbaryl metabolism is inhibited by cimetidine in the isolated perfused rat liver and in man, *Clin. Toxicol.* 26 (1988) 269–281.
- [11] M. Ehrlich, L. Correll, J. Strait, W. McCain, J. Wilcke, Toxicity and toxicokinetics of carbaryl in chickens and rats: a comparative study, *J. Toxicol. Environ. Health* 36 (1992) 411–423.
- [12] D.G. May, R.J. Naukam, J.R. Kambam, R.A. Branch, Cimetidine-carbaryl interaction in humans: evidence for an active metabolite of carbaryl, *J. Pharmacol. Exp. Ther.* 262 (1992) 1057–1061.
- [13] E.S. Oonithan, J.E. Casida, Oxidation of methyl- and dimethylcarbamate insecticide chemicals by microsomal enzymes and anticholinesterase activity of the metabolites, *J. Agric. Food Chem.* 16 (1968) 28–44.
- [14] R.A. Neal, Microsomal metabolism of thiono-sulfur compounds: mechanisms and toxicological significance, *Rev. Biochem. Toxicol.* 2 (1980) 131–171.
- [15] G. Johnston, The study of interactive effects of pollutants—a biomarker approach, *Sci. Total Environ.* 171 (1995) 205–212.
- [16] B.H. Chin, J.M. Eldridge, L.J. Sullivan, Metabolism of carbaryl by selected human tissues using an organ-maintenance technique, *Clin. Toxicol.* 7 (1974) 37–56.
- [17] I.H. Segel, *Biochemical Calculations*, Wiley, New York, 1975.
- [18] SAS, *JMP User's Guide*, SAS Institute, Cary, NC, (1989).
- [19] T.R. Roberts, D.H. Hutson, Carbaryl, in: T.R. Roberts, D.H. Hutson (Eds.), *Metabolic Pathways of Agrochemicals, Part 2: Insecticides and Fungicides*, The Royal Society of Chemistry, Cambridge, UK, 1999, pp. 15–24.
- [20] G. de Sousa, F. Fontaine, M. Pralavorio, D. Botta-Fridlund, Y. Letrent, R. Rahmani, Insecticide cytotoxicity and CYP1A1/2 induction in primary human and rat hepatocyte cultures, *Toxicol. Vitro* 11 (1997) 451–457.
- [21] N. Ledirac, C. Deleschuse, G. de Sousa, M. Pralavorio, P. Lesca, M. Amichot, J.B. Berge, R. Rahmani, Carbaryl induces CYP1A1 gene expression in HepG2 and HaCat cells but is not a ligand of the human hepatic Ah receptor, *Toxicol. Appl. Pharmacol.* 144 (1997) 177–182.

- [22] M.S. Denison, D. Phelan, G.M. Winter, M.H. Ziccardi, Carbaryl, a carbamate insecticide, is a ligand for the hepatic Ah (Dioxin) receptor, *Toxicol. Appl. Pharmacol.* 152 (1998) 406–414.
- [23] J. Tang, Y. Cao, R.L. Rose, A.A. Brimfield, D. Dai, J.A. Goldstein, E. Hodgson, Metabolism of chlorpyrifos by human cytochrome P450 isoforms and human, mouse, and rat liver microsomes, *Drug Metab. Dispos.* 29 (2001) 1201–1204.



In vitro metabolism of fipronil by human and rat cytochrome P450 and its interactions with testosterone and diazepam

Jun Tang, K. Amin Usmani, Ernest Hodgson, Randy L. Rose*

Department of Environmental and Molecular Toxicology, North Carolina State University, Raleigh, NC 27695, USA

Accepted 5 March 2004

Abstract

Fipronil (5-amino-1-[2,6-dichloro-4-(trifluoromethyl)phenyl]-4-[(trifluoromethyl)sulfinyl]-1H-pyrazole-3-carbonitrile) is a highly active, broad spectrum insecticide from the phenyl pyrazole family, which targets the γ -amino butyric acid (GABA) receptor. Although fipronil is presently widely used as an insecticide and acaricide, little information is available with respect to its metabolic fate and disposition in mammals. This study was designed to investigate the in vitro human metabolism of fipronil and to examine possible metabolic interactions that fipronil may have with other substrates. Fipronil was incubated with human liver microsomes (HLM) and several recombinant cytochrome P450 (CYP) isoforms obtained from BD Biosciences. HPLC was used for metabolite identification and quantification. Fipronil sulfone was the predominant metabolite via CYP oxidation. The K_m and V_{max} values for human liver microsomes are 27.2 μ M and 0.11 nmol/mg protein min, respectively; for rat liver microsomes (RLM) the K_m and V_{max} are 19.9 μ M and 0.39 nmol/mg protein min, respectively. CYP3A4 is the major isoform responsible for fipronil oxidation in humans while CYP2C19 is considerably less active. Other human CYP isoforms have minimal or no activity toward fipronil. Co-expression of cytochrome b_5 (b_5) is essential for CYP3A4 to manifest high activity toward fipronil. Ketoconazole, a specific inhibitor of CYP3A4, inhibits 78% of the HLM activity toward fipronil at a concentration of 2 μ M. Oxidative activity toward fipronil in 19 single-donor HLMs correlated well with their ability to oxidize testosterone. The interactions of fipronil and other CYP3A4 substrates, such as testosterone and diazepam, were also investigated. Fipronil metabolism was activated by testosterone in HLM but not in CYP3A4 Supersomes®. Testosterone 6 β -hydroxylation in HLM was inhibited by fipronil. Fipronil inhibited diazepam demethylation but had little effect on diazepam hydroxylation. The results suggest that fipronil has the potential to interact with a wide range of xenobiotics or endogenous chemicals that are CYP3A4 substrates and that fipronil may be a useful substrate for the characterization of CYP3A4 in HLM.

© 2004 Elsevier Ireland Ltd. All rights reserved.

Keywords: Fipronil; Metabolism; Human liver microsomes; Cytochrome P450; CYP3A4; Interaction

1. Introduction

Fipronil (5-amino-1-[2,6-dichloro-4-(trifluoromethyl)phenyl]-4-[(trifluoromethyl)sulfinyl]-1H-pyrazole-3-carbonitrile) is a highly active, broad spectrum insecticide from the phenyl pyrazole family, which

* Corresponding author. Tel.: +1-919-515-4378;

fax: +1-919-515-7169.

E-mail address: randy_rose@ncsu.edu (R.L. Rose).

targets the γ -amino butyric acid (GABA) receptor [1–5]. Agriculturally, this pesticide has been used on pests of a wide variety of food crops [6–8]. In non-agricultural applications, fipronil is used to control veterinary pests [9] and has also been designated by EPA as one of alternatives to the organophosphates (OP) for termite and fire ant control [10]. Concerns for fipronil effects on public health have been raised because of the wide range of uses of this pesticide [9,11].

Fipronil is moderately toxic to rats and mice with oral LD₅₀'s ranging from ca. 40 to 100 mg/kg [12,13], but is much more toxic toward insects than toward mammals [1,12]. Fipronil selectivity is due to its greater potency in blocking insect GABA-gated chloride channels than their mammalian counterparts [12,14]. Limited metabolic studies indicate that the predominant pathway of fipronil metabolism is S-oxidation to form the sulfone (Fig. 1). Fipronil sulfone is the only metabolite reported in mice [12] and *in vitro* studies suggest that fipronil sulfone is more potent as an antagonist of the GABA receptor than fipronil [14]. In addition to neurotoxicity, fipronil has been reported to have the potential to induce thyroid cancer in rodents by enhancing the hepatic metabolism and excretion of thyroid hormone [15].

Metabolism may be an important determinant of toxicity. Studies of metabolic stability and pathways of pesticide metabolism in humans can provide important information on differences between humans and laboratory animals in metabolism and potential interactions with endogenous chemicals and other

xenobiotics. This study was designed to compare the metabolism of fipronil in human and rat liver microsomes (RLM), to identify enzymes responsible for the metabolism of fipronil and to examine potential interactions with chemicals that are substrates for the same enzymes.

2. Materials and methods

2.1. Chemicals

Fipronil was purchased from ChemService (West Chester, PA). Testosterone and 6 β -hydroxy testosterone were purchased from Steraloids (Newport, RI). Fipronil sulfone was a gift from the Rhône-Poulenc Company (Research Triangle Park, NC). HPLC grade methanol was purchased from Fisher Scientific (Fair Lawn, NJ). All other chemicals, unless specified otherwise, were purchased from Sigma (St. Louis, MO).

2.2. Liver microsomes and cytochrome P450 isoforms

Rat liver microsomes were prepared from adult male Long-Evans rats (Charles River Laboratories, Raleigh, NC), according to the method of Cook and Hodgson [16].

Pooled and single-donor human liver microsomes (HLM), human cytochrome P450 (CYP) isoforms and human cytochrome b₅ (b₅) were purchased from BD Biosciences (Woburn, MA). CYP isoforms in Supersomes[®] obtained were CYP2A6, 2B6, 2C8, 2C9*1, 2C19, 2E1, 3A4, and 3A7, all of which are co-expressed with b₅. Also obtained were CYP1A1, 1A2, 2C9*2, 2C9*3, 2C18, 2D6*1, 2D6*10, 3A4, 3A5, and 4A11 Supersomes[®], which are not co-expressed with b₅. All human CYP isoforms in Supersomes[®] are co-expressed with human CYP reductase.

2.3. *In vitro* fipronil metabolism

The general method for the *in vitro* assay was described by Tang et al. [17]. Preliminary experiments determined that incubation times and enzyme amounts were within a linear range. Enzyme kinetics in pooled HLM (1 mg protein), RLM (0.75 mg protein), and

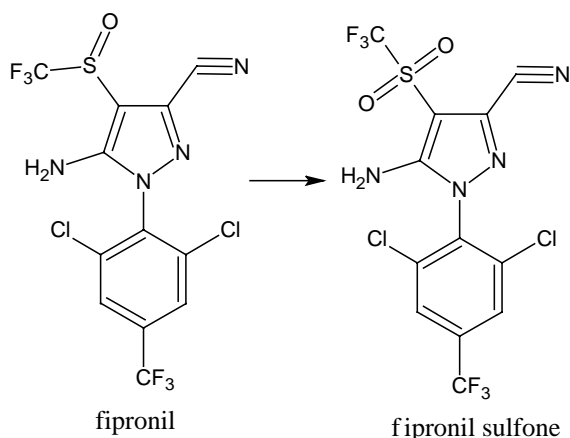


Fig. 1. Cytochrome P450-dependent metabolism of fipronil.

CYP3A4 (20 pmol P450) were assayed by incubation of serial concentrations of fipronil (final concentrations 1.25–80 μM). Activities in single-donor HLM (1 mg protein) or CYP isoforms (18–100 pmol P450) were assayed by incubation of a single concentration of fipronil (final concentration 80 μM). The NADPH-regenerating system used contained NADP (final concentration 0.25 mM), glucose-6-phosphate (final concentration 2.5 mM) and glucose-6-phosphate dehydrogenase (final concentration 2 U/ml).

Reactions were initiated by the addition of the enzyme. Controls were performed in the absence of the NADPH-regenerating system. The reaction was terminated after 30 min of incubation by the addition of ice-cold acetonitrile followed by vortexing. After centrifugation (5 min at $21\,000 \times g$), the supernatant was analyzed by HPLC.

To determine the role of CYP3A4 in fipronil metabolism in HLM (0.5 mg protein), a CYP3A4 specific inhibitor, ketoconazole (final concentrations 0–20 μM), was added to the reaction mixture simultaneously with 10 μM fipronil.

To determine the role of b_5 in CYP3A activities, exogenous b_5 was pre-mixed at room temperature with CYP3A4 and 3A5 Supersomes[®] that were not co-expressed with b_5 . The amount of b_5 added to CYP3A4 or 3A5 was the same b_5 /CYP3A4 ratio as that in CYP3A4 co-expressed with b_5 . Studies involving the pre-mixing of CYP3A4 with b_5 for different times (from 0 to 30 min at room temperature) before the addition of substrate showed that the effect was not time dependent (data not shown). Metabolic activity toward fipronil was compared between CYP3As with and without b_5 .

2.4. Interaction with testosterone

The effect of testosterone on fipronil metabolism was assayed in HLM (0.4 mg protein) or CYP3A4 Supersomes[®] (10 pmol CYP) by co-incubation of fipronil (final concentration 1.25, 5 or 20 μM) with testosterone (final concentrations 0–200 μM) for 15 min. The effect of fipronil on testosterone 6 β -hydroxylation was assayed in HLM (0.4 mg protein) by co-incubation of testosterone (final concentration 4, 20 or 100 μM) with fipronil (final concentrations 0–160 μM) for 10 min. Metabolic effects of fipronil and testosterone on each others metabolism

were determined by monitoring fipronil sulfone and 6 β -hydroxy testosterone (Steraloids, Newport, RI) levels by HPLC, respectively.

2.5. Interaction with diazepam

The effect of diazepam on fipronil metabolism was assayed in HLM (0.4 mg protein) by co-incubation of fipronil (final concentration 5, 20, or 80 μM) with diazepam (final concentrations 0–400 μM) for 15 min. The effect of fipronil on diazepam metabolism was assayed in HLM (0.4 mg protein) by co-incubation of diazepam (final concentration 6.25, 25 or 100 μM) with fipronil (final concentrations 0–160 μM) for 15 min.

2.6. HPLC methods for analysis of fipronil, testosterone and diazepam

The HPLC method to separate fipronil and its metabolite, fipronil sulfone, was modified from Ngim et al. [18]. Briefly, a Synergi Max C12 column (Phenomenex, Rancho Palos Verdes, CA) was used with an isocratic mobile phase (70% methanol and 30% water containing 0.005 M acetic acid). A Shimadzu (Kyoto, Japan) HPLC system (LC-10AT VP pump, SPD-10A VP UV-VIS detector, SIL-10AD VP auto injector, and SCL-10A VP system controller) was used. The flow rate and detection wavelength were set at 1 ml/min and 275 nm, respectively. Retention times for fipronil and fipronil sulfone were 12 and 18 min, respectively. Peak areas of fipronil and its sulfone metabolite were integrated using Shimadzu Class-VP 7.0 program. The limit of detection was 0.02 pmol for either compound. Concentrations of fipronil sulfone were obtained by extrapolation of peak area from a standard curve ranging from 0.25 to 32 μM . Testosterone and its metabolites eluted several minutes before fipronil and fipronil sulfone.

Testosterone and its metabolites were separated using the method described by Usmani et al. [19]. Fipronil and its metabolite eluted after 6 β -hydroxy testosterone and testosterone.

Diazepam and its metabolites were separated by a Synergi Max C12 column using a method modified from Shou et al. [20]. Briefly, a gradient system containing two pumps was used. From 0 to 30 min, pump A (20% acetonitrile, 30% methanol and 50% water) was maintained at 100% to separate diazepam and its

metabolites. After that, the ratio of pump B (70% acetonitrile and 30% methanol) was increased to 100% in 1 min and maintained for 8 min to elute fipronil and its metabolite. The retention times for diazepam, desmethyl diazepam, temazepam and oxazepam were 28, 19, 16, and 11 min, respectively.

2.7. Enzyme kinetic calculations and statistics

All values were expressed as mean \pm S.E. ($n = 2$ –3 determination). Enzyme kinetic parameters were determined using SigmaPlot Enzyme Kinetics Module 1.1 (SPSS Inc., Chicago, IL).

3. Results

3.1. Enzyme kinetics of fipronil metabolism in liver microsomes

Fipronil sulfone was the only metabolite detected following incubation of fipronil with either RLM or pooled HLM. While K_m values in human and rat liver microsomes were similar (19.9 and 27.2 μM , respectively), the V_{max} in RLM was 3.8-fold higher than that observed in HLM (0.39 and 0.11 nmol/mg protein min, respectively) (Fig. 2). It should be noted that unless otherwise stated, studies involving human liver microsomes utilized pooled human liver microsomes from BD Biosciences. These preparations have been formulated to be representative of the catalytic activities for an average of many individuals.

3.2. Fipronil metabolism by human CYP isoforms

In a comparison of 15 different CYP isoforms and three polymorphic variants, only CYP2C19 and CYP3A4 showed substantial activity toward fipronil (Fig. 3). The activity of CYP3A4 toward fipronil was five times greater than that of CYP2C19. Kinetic studies of CYP3A4 activity toward fipronil showed that its K_m value was close to that obtained in liver microsomes (Fig. 2).

The high activity of CYP3A4 depended on co-expression of b_5 (Table 1). In the absence of co-expressed b_5 the activity of CYP3A4 toward fipronil is dramatically decreased. The addition of exogenous b_5 to CYP3A4 Supersomes[®] in which

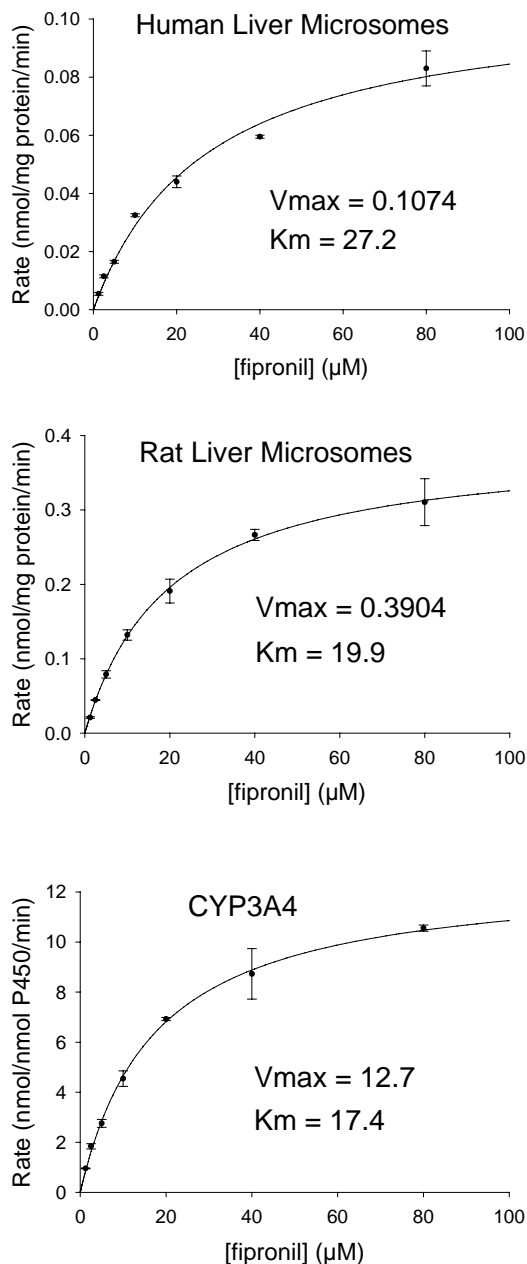


Fig. 2. Kinetic plots of fipronil metabolism in human liver, rat liver and baculovirus-expressed CYP3A4 microsomes. Data points represent the mean of three separate determinations and error bars represent S.E.

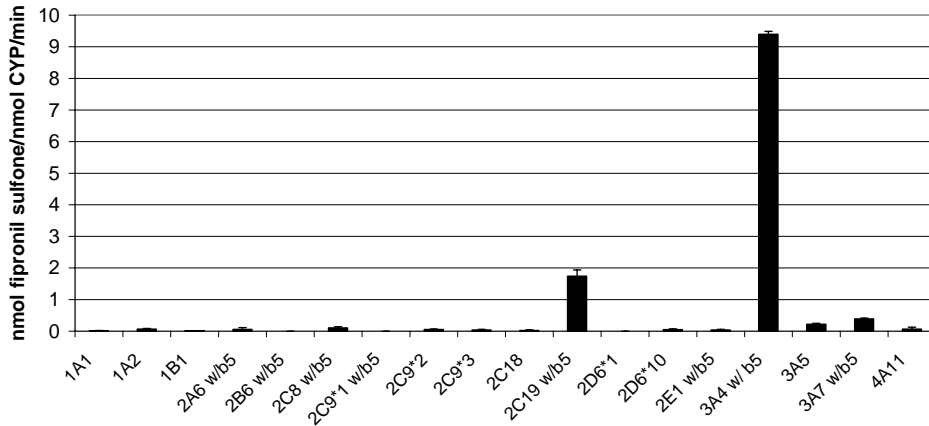


Fig. 3. Metabolic activities (nmol of product/nmol cytochrome P450 min) toward fipronil in human cytochrome P450 Supersomes®. Columns represent the mean of three separate determinations and error bars represent S.E.

Table 1
Effect of cytochrome b₅ (b₅) on CYP3A activity (mean ± S.E., n = 2–3 determinations)

	Activity (nmol/nmol CYP min)
CYP3A4 co-expressed with b ₅	9.40 ± 0.09
CYP3A4	0.38 ± 0.03
CYP3A4 pre-mixed with b ₅	1.27 ± 0.15
CYP3A5	0.22 ± 0.02
CYP3A5 pre-mixed with b ₅	0.36 ± 0.01
CYP3A7 co-expressed with b ₅	0.39 ± 0.02

b₅ was not co-expressed increased activity of these preparations ca. 3.5-fold, although it must be noted that these activities were still significantly lower than preparations where b₅ was co-expressed. CYP3A5

was less active than CYP3A4 even with the addition of exogenous b₅ (Table 1). CYP3A7 was not very active toward fipronil even though b₅ was co-expressed.

3.3. Fipronil metabolism in single-donor HLM

Fipronil metabolism was analyzed in 19 single-donor HLM. The difference in fipronil metabolism between different individuals is over 40-fold (Fig. 4). Correlation analyses between fipronil sulfoxidase activities and CYP-specific metabolic activities among these individuals (BD Biosciences) demonstrated that the best correlations were for CYP3A4 ($r^2 = 0.81$) and CYP2B6 ($r^2 = 0.66$) (Fig. 5). All other

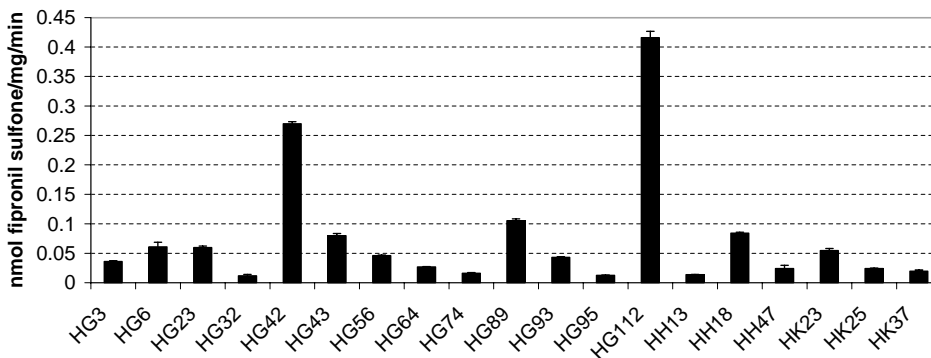
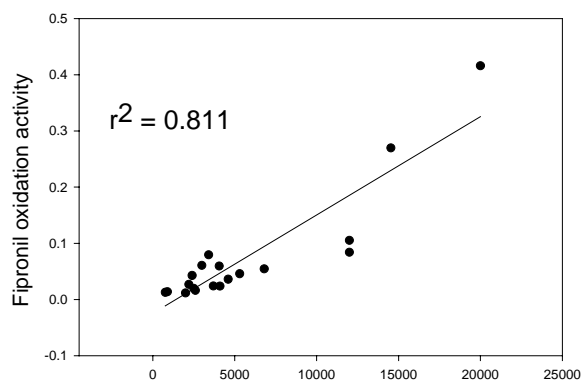
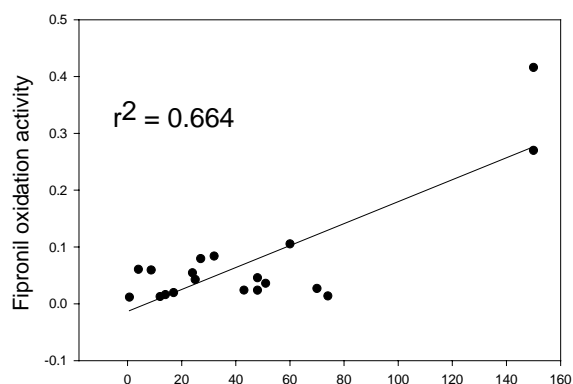
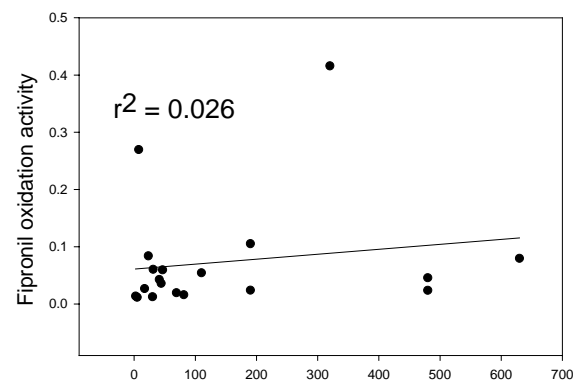


Fig. 4. Metabolic activities (nmol of product/mg protein min) toward fipronil in single-donor HLM. Columns represent the mean of three separate determinations and error bars represent S.E.

(A) Testosterone 6 β -hydroxylation activity of CYP3A4

(B) (S)-Mephenytoin N-Demethylation activity of CYP2B6



(C) (S)-Mephenytoin 4'-Hydroxylation Activity of CYP2C19

Fig. 5. Correlation analyses of fipronil sulfoxidation activity with CYP isoforms. Substrate-specific activity levels for each individual were reported by BD Biosciences for (A) CYP3A4 using testosterone 6 β -hydroxylation, (B) CYP2B6 using mephenytoin *N*-demethylation, and (C) CYP2C19 using mephenytoin 4'-hydroxylation.

correlations between sulfoxidation activity and specific CYP isoforms were less than 0.17.

3.4. Inhibition of fipronil metabolism in HLM by ketoconazole

The role of CYP3A4 in the metabolism of fipronil was verified by co-incubations of ketoconazole, a specific CYP3A4 inhibitor, with fipronil. In pooled HLM, increasing concentrations of ketoconazole significantly inhibited metabolism of 10 μ M fipronil, resulting in 78% inhibition at 2 μ M ketoconazole. The IC₅₀ at this concentration of fipronil for ketoconazole inhibition was 0.16 μ M. In similar experiments involving ketoconazole inhibition of CYP3A4-mediated testosterone 6 β -hydroxylation, 50 μ M concentrations of testosterone were inhibited by 95% with 2 μ M ketoconazole.

3.5. Metabolic interactions of fipronil and testosterone or diazepam in HLM

Co-incubations of varying concentrations of fipronil with increasing concentrations of testosterone in pooled HLM resulted in increased fipronil sulfone production at all three fipronil substrate concentrations tested (Fig. 6). The greatest level of activation was observed at the lowest fipronil concentration (1.25 μ M) in combination with a 20 μ M concentration of testosterone (ca. 2.3-fold). Incubations of 20 μ M fipronil were not as readily activated by increasing testosterone concentrations (control levels for fipronil sulfone production at fipronil concentrations of 1.25, 5 and 20 μ M were 0.005 \pm 0.000, 0.020 \pm 0.002, and 0.042 \pm 0.003 nmol/mg protein min, respectively). In contrast with HLM preparations, the activation of fipronil metabolism by testosterone was not observed when using CYP3A4 Supersomes[®] as the enzyme source (data not shown).

In contrast to the fipronil results, testosterone metabolism was inhibited by increasing concentrations of fipronil at all three dose levels examined (Fig. 7). At the two lowest concentrations of testosterone (4 and 20 μ M) fipronil concentrations of 100 μ M resulted in approximately 50% inhibition of the 6 β hydroxy-testosterone product (control values for 6 β -hydroxy testosterone metabolite production at testosterone substrate concentrations were 0.050 \pm

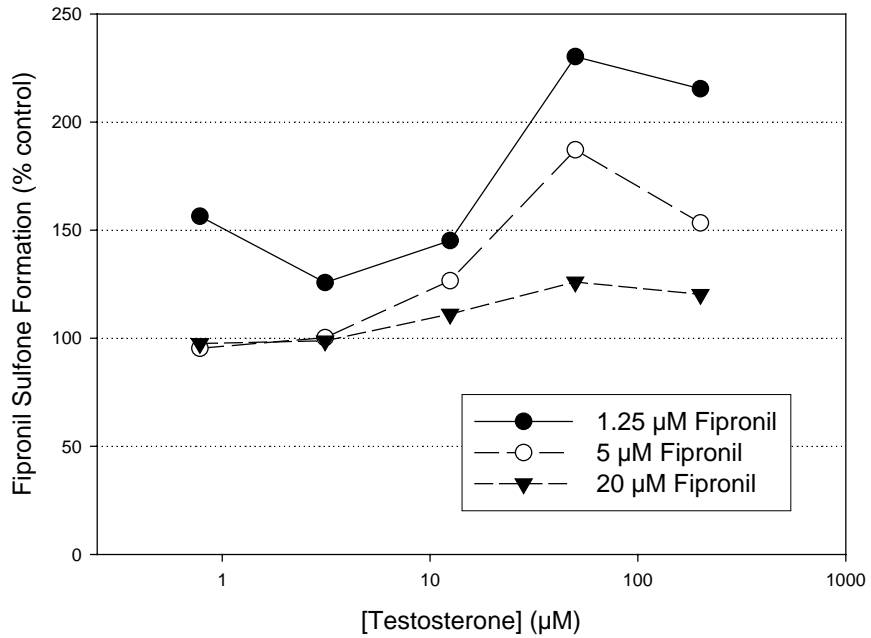


Fig. 6. The effects of testosterone on fipronil sulfone formation in HLM. Data presented is based on the percent of fipronil sulfone formation when compared to control (0 μM testosterone) with each data point representing the mean of two separate determinations.

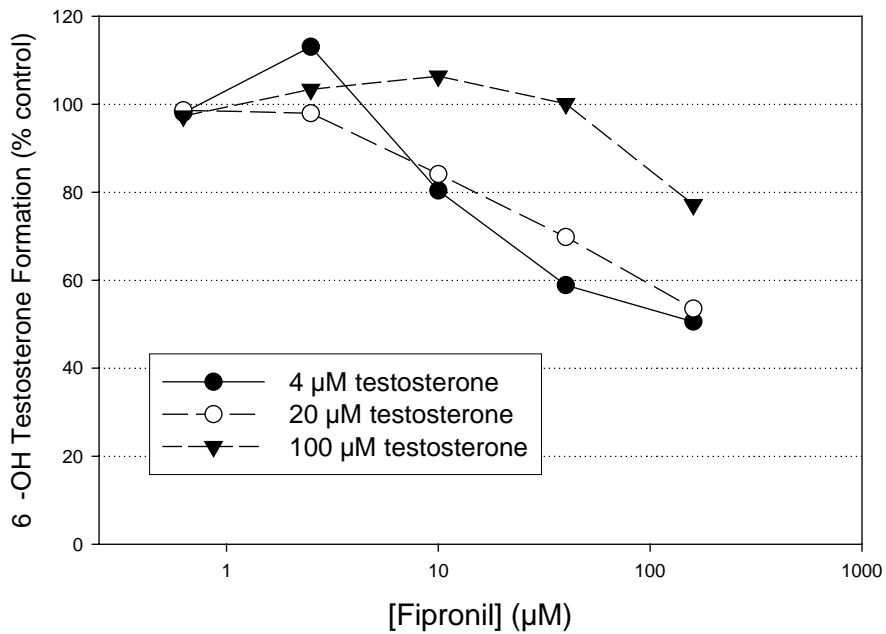
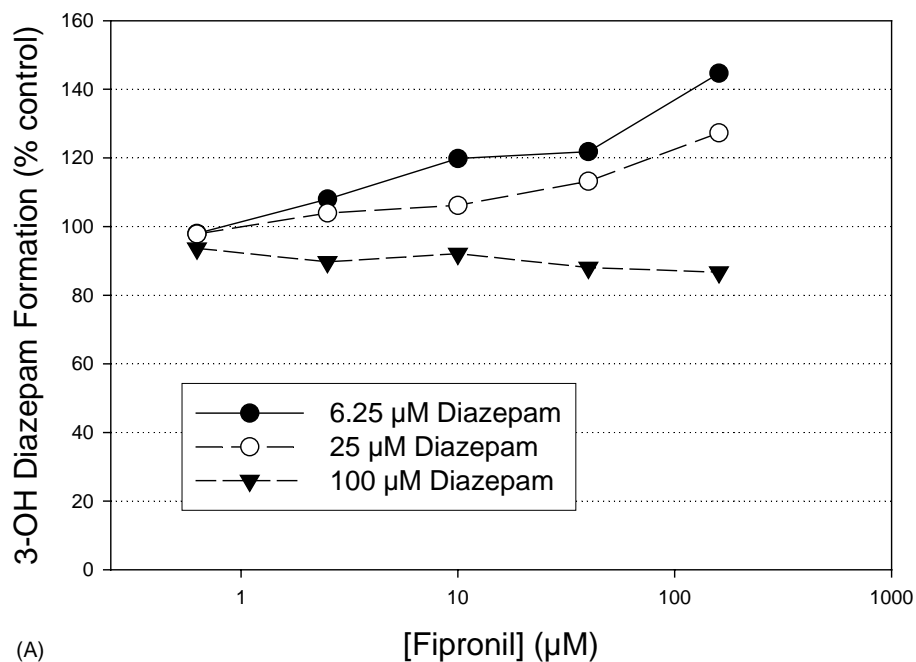
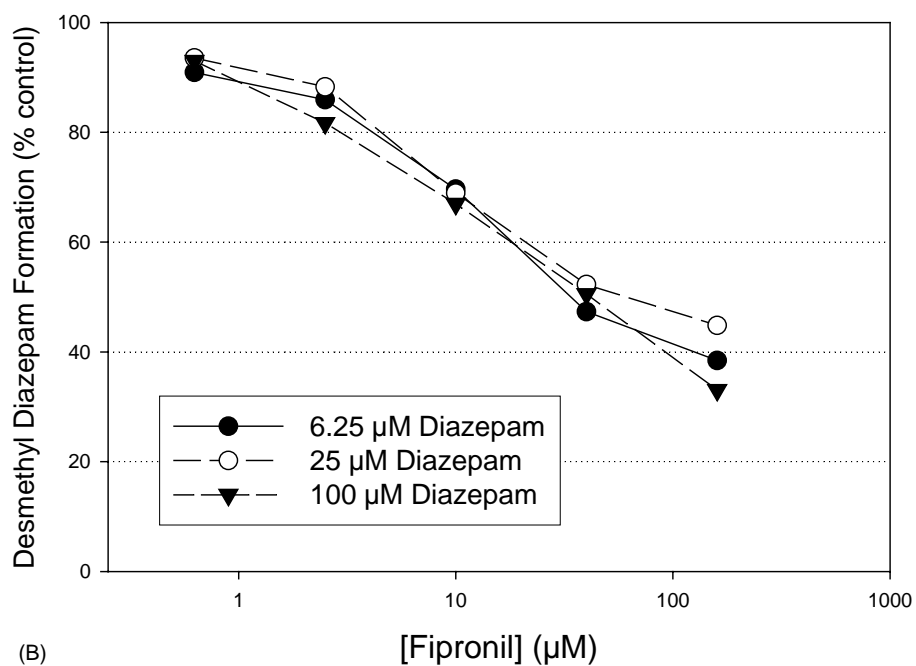


Fig. 7. The effects of fipronil on 6β-OH testosterone formation in HLM. Data presented is based on the percent of 6β-OH testosterone formation when compared to control (0 μM fipronil) with each data point representing the mean of two separate determinations.



(A)



(B)

Fig. 8. The effects of fipronil on diazepam metabolism in HLM. (A) The percent of 3-hydroxy diazepam formation when compared to control (0 μM fipronil) with increasing fipronil concentrations; data points represent the mean of two separate determinations. (B) The percent of desmethyl diazepam formation when compared to control (0 μM fipronil) with increasing fipronil concentrations; data points represent the mean of two separate determinations.

0.002, 0.980 ± 0.018 , and 2.680 ± 0.169 nmol/mg protein min, respectively).

Co-incubations of HLM with varying concentrations of diazepam, a known CYP3A4 substrate, in the presence of three doses of fipronil only slightly increased fipronil sulfone levels at the higher dose levels examined, but had small effects on lower concentrations of fipronil (data not shown). The opposite experiment, in which increasing concentrations of fipronil were incubated with three dose levels of diazepam produced different results depending on the diazepam metabolite examined (Fig. 8). At the two lower concentrations of diazepam, increasing concentrations of fipronil slightly increased levels of the 3-OH metabolite, while at the highest diazepam concentration there was slight inhibition (Fig. 8A). For the desmethylated product, increasing concentrations of fipronil consistently inhibited diazepam metabolism, with approximately 60% inhibition reported for all three diazepam concentrations examined. Control values for 3-hydroxy diazepam formation at diazepam concentrations of 6.25, 25, or 100 μM in the absence of fipronil were 0.008 ± 0.001 , 0.043 ± 0.004 , and 0.298 ± 0.057 nmol/mg protein min, respectively. Desmethyl diazepam formation in the absence of fipronil from these same concentrations of diazepam were 0.027 ± 0.002 , 0.100 ± 0.004 , and 0.340 ± 0.028 nmol/mg protein min, respectively.

4. Discussion

The predominant metabolic pathway for fipronil in both HLM and RLM is the oxidation of the thioether group to generate fipronil sulfone, as was previously reported in mice [12]. The enzyme kinetic studies indicated that K_m values for fipronil metabolism are similar in HLM and RLM, but RLM has higher V_{\max} values than HLM, suggesting a higher intrinsic clearance of fipronil in rats than in humans. Fipronil sulfone is more toxic than fipronil to birds but not to mice although in both cases the sulfone is more persistent than the parent compound in the GABA receptor [14]. It is not known whether sulfone production enhances toxicity of fipronil in humans.

These studies provide strong evidence that CYP3A4 is the predominant isoform responsible for S-oxidation

of fipronil. Of the 15 isoforms screened for activity, only CYP3A4 and 2C19 significantly metabolized fipronil. Correlation analysis conducted on 19 single-donor HLM samples revealed significant correlations for CYP3A4 and CYP2B6. Examination of isoform levels as reported by BD Biosciences for this group of individuals indicated that those with high levels of CYP2B6 were often the same individuals with high CYP3A4 activity and vice versa. Further verification of the importance of CYP3A4 in the metabolism of fipronil was obtained by demonstrating 78% inhibition of fipronil sulfone production in HLM by 2 μM ketoconazole, a specific CYP3A4 inhibitor. In similar experiments with testosterone, a known CYP3A4 substrate, the same concentration of ketoconazole inhibited up to 95% of testosterone 6 β -hydroxylation. The remaining fipronil sulfone activity following ketoconazole inhibition may be attributed to either incomplete inhibition or to CYP2C19 activity, the only other CYP isoform with significant fipronil metabolizing activity.

As demonstrated previously with some, but not all substrates, CYP3A4 activity based on fipronil sulfone production requires the presence of b_5 [21–23]. Co-expression of b_5 has much greater impact than the addition of equivalent amounts of exogenous b_5 on CYP3A4 activity toward fipronil. The length of exogenous b_5 pre-incubation time with CYP3A4 has little effect on CYP3A4 activity. Co-expressed b_5 is likely better integrated into the microsomal membrane with CYP3A4 than exogenous b_5 to facilitate the function of CYP3A4. Although CYP3A7 also was co-expressed with b_5 it apparently is not effective in the oxidation of fipronil. It is unclear whether co-expression of b_5 would have such dramatic effects on fipronil metabolism by CYP3A5 as it has on CYP3A4, however, if not fipronil may be a great substrate to differentiate between CYP3A4 and CYP3A5 activities.

CYP3A4 is usually the most abundant isoform in human liver and has broad substrate specificity. Because fipronil is predominantly metabolized by CYP3A4, it could potentially interact metabolically with many other CYP3A4 substrates, both endogenous and exogenous, such as testosterone and diazepam. The usual interaction between two different substrates for the same enzyme is competitive inhibition. However, interactions between CYP3A4

substrates are complicated because of the allosteric characteristics of CYP3A4 [20,24,25].

Kenworthy et al. [26] proposed multisite kinetic models for the interaction of testosterone and diazepam in CYP3A4. The interaction between fipronil and testosterone in HLM that we observed displays a similar pattern as observed for the interaction between diazepam and testosterone [26], i.e., testosterone activated fipronil metabolism while increasing doses of fipronil inhibited testosterone metabolism. Although in our study, 2.3-fold levels of activation of fipronil metabolism by testosterone in HLM were similar in nature to activation levels reported for diazepam and testosterone in lymphoblast-expressed CYP3A4 microsomes [26] the same phenomenon was not observed when using CYP3A4 Supersomes[®] as the enzyme source. This difference between HLM and CYP3A4 Supersomes[®] needs further scrutiny. It is postulated that the human lymphoblast-expressed CYP3A4 has a greater similarity to CYP3A4 in HLM than the insect baculovirus-expressed CYP3A4 Supersomes[®] used in this study.

Because fipronil and diazepam display the same pattern in their interactions with testosterone, we also examined the interactions between these two compounds. When examining fipronil sulfone production at low fipronil substrate concentrations co-incubation of diazepam had little effect, but at high fipronil concentrations there was a slight activation of metabolism. This is different from the interactions with testosterone, where low substrate concentrations are more sensitive to the modifier. Also, the two pathways of diazepam metabolism [20] respond differently to the presence of fipronil. In the case of the 3-OH diazepam metabolite, increasing concentrations of fipronil resulted in small increases in metabolism, while for desmethyl diazepam high concentrations of fipronil caused up to 60% inhibition. Differences in the response of these two diazepam metabolites are likely the result of conformational changes in the active site brought about by increasing concentrations of fipronil.

In conclusion, CYP3A4 is the major enzyme responsible for fipronil metabolism. Co-expression of b₅ is essential for CYP3A4 to have high activity toward fipronil. Interactions between fipronil and other CYP3A4 substrates display activation, inhibition and regio-selectivity effects, in agreement with previously

reported multisite kinetic analysis of atypical interactions of CYP3A4 [26,27].

Acknowledgements

This project was supported by NIOSH Grant OH07551-ECU.

References

- [1] L.M. Cole, R.A. Nicholson, J.E. Casida, Action of phenylpyrazole insecticides at the GABA-gated chloride channel, *Pestic. Biochem. Physiol.* 46 (1993) 47–54.
- [2] A.S. Moffat, New chemicals seek to outwit insect pests, *Science* 261 (1993) 550–551.
- [3] A.M. Hosie, H.A. Baylis, S.D. Buckingham, D.B. Sattelle, Action of the insecticide fipronil, on dieldrin-sensitive and dieldrin-resistant GABA receptors of *Drosophila-melanogaster*, *Br. J. Pharmacol.* 115 (1995) 909–912.
- [4] G.S. Ratra, S.G. Kamita, J.E. Casida, Role of human GABA(A) receptor beta 3 subunit in insecticide toxicity, *Toxicol. Appl. Pharmacol.* 172 (2001) 233–240.
- [5] G.S. Ratra, B.E. Erkkila, D.S. Weiss, J.E. Casida, Unique insecticide specificity of human homomeric rho 1 GABA(C) receptor, *Toxicol. Lett.* 129 (2002) 47–53.
- [6] M.E. Scharf, B.D. Siegfried, Toxicity and neurophysiological effects of fipronil and fipronil sulfone on the western corn rootworm (Coleoptera:Chrysomelidae), *Arch. Insect Biochem.* 40 (1999) 150–156.
- [7] K.K. Ngim, D.G. Crosby, Abiotic processes influencing fipronil and desethiofipronil dissipation in California, USA, rice fields, *Environ. Toxicol. Chem.* 20 (2001) 972–977.
- [8] G.E. Wilde, R.J. Whitworth, M. Claassen, R.A. Shufman, Seed treatment for control of wheat insects and its effect on yield, *J. Agr. Urban Entomol.* 18 (2001) 1–11.
- [9] K.A. Jennings, R.J. Keller, B.H. Atieh, R.B. Doss, R.C. Gupta, Human exposure to fipronil from dogs treated with Frontline, *Vet. Hum. Toxicol.* 44 (2002) 303–303.
- [10] EPA, Expediting the review of alternatives to the Organophosphates (OPs). US EPA Committee to Advise on Reassessment and Transition CARAT 2–2, 2000.
- [11] C.C. Tingle, J.A. Rother, C.F. Dewhurst, S. Lauer, W.J. King, Fipronil: Environmental fate, ecotoxicology, and human health concerns, *Rev. Environ. Contam. Toxicol.* 176 (2003) 1–66.
- [12] D. Hainzl, J.E. Casida, Fipronil insecticide: novel photochemical desulfinylation with retention of neurotoxicity, *Proc. Natl. Acad. Sci. U.S.A.* 93 (1996) 12746–12767.
- [13] R.L. Rose, E. Hodgson, R.M. Roe, Pesticides, in: H. Marquardt, S.G. Schafer, R. McClellan, F. Welsch (Eds.), *Toxicology*, Academic, San Diego, CA, 1999. pp. 663–697.
- [14] D. Hainzl, L.M. Cole, J.E. Casida, Mechanisms for selective toxicity of fipronil insecticide and its sulfone metabolite and

- desulfinyl photoproduct, *Chem. Res. Toxicol.* 11 (1998) 1529–1535.
- [15] P.M. Hurley, R.N. Hill, R.J. Whiting, Mode of carcinogenic action of pesticides inducing thyroid follicular cell tumors in rodents, *Environ. Health Perspect.* 106 (1998) 437–445.
- [16] J.C. Cook, E. Hodgson, Induction of Cytochrome P-450 by methylenedioxyphenyl compounds: importance of the methylene carbon, *Toxicol. Appl. Pharmacol.* 68 (1983) 131–139.
- [17] J. Tang, Y. Cao, R.L. Rose, E. Hodgson, In vitro metabolism of carbaryl by human cytochrome P450 and its inhibition by chlorpyrifos, *Chem-Biol. Interact.* 141 (2002) 229–241.
- [18] K.K. Ngim, S.A. Mabury, D.G. Crosby, Elucidation of fipronil photodegradation pathways, *J. Agric. Food Chem.* 48 (2000) 4661–4665.
- [19] K.A. Usmani, R.L. Rose, E. Hodgson, Inhibition and activation of the human liver microsomal and human cytochrome P450 3A4 metabolism of testosterone by deployment-related chemicals, *Drug Metab. Dispos.* 31 (2003) 384–391.
- [20] M. Shou, Q. Mei, M.R. Ettore, R. Dai, T.A. Baillie, T.H. Rushmore, Sigmoidal kinetic model for two co-operative substrate-binding sites in a cytochrome P450 3A4 active site: an example of the metabolism of diazepam and its derivatives, *Biochem. J.* 340 (1999) 845–853.
- [21] M.S. Shet, C.W. Fisher, F.P. Holmans, R.W. Estabrook, Human cytochrome P450 3A4: enzymatic properties of a purified recombinant fusion protein containing NADPH-P450 reductase, *Proc. Natl. Acad. Sci. U.S.A.* 90 (1993) 11748–11752.
- [22] H. Yamazaki, Y.-F. Ueng, T. Shimada, F.P. Guengerich, Role of divalent metal ions in oxidations catalyzed by recombinant cytochrome P450 3A4 and replacement of NADPH-cytochrome P450 reductase with other flavoproteins, ferredoxin, and oxygen surrogates, *Biochemistry* 34 (1995) 8380–8389.
- [23] J.B. Schenkman, I. Jansson, The many roles of cytochrome b5, *Pharmacol. Ther.* 97 (2003) 139–152.
- [24] R.W. Wang, D.J. Newton, N. Liu, W.M. Atkins, A.Y.H. Lu, Human cytochrome P-450 3A4: in vitro drug–drug interaction patterns are substrate-dependent, *Drug Metab. Dispos.* 28 (2000) 360–366.
- [25] W. Tang, R.A. Stearns, Heterotropic cooperativity of cytochrome P450 3A4 and potential drug–drug interactions, *Curr. Drug Metab.* 2 (2001) 185–198.
- [26] K.E. Kenworthy, S.E. Clarke, J. Andrews, J.B. Houston, Multisite kinetic models for CYP3A4: simultaneous activation and inhibition of diazepam and testosterone metabolism, *Drug Metab. Dispos.* 29 (2001) 1644–1651.
- [27] A. Galetin, S.E. Clark, J.B. Houston, Multisite kinetic analyses of interactions between prototypical CYP3A4 subgroup substrates: midazolam, testosterone, and nifedipine, *Drug Metabol Disp.* 31 (2003) 1108–1116.